Technische Universität München
TUM School of Natural Sciences

Catalyst Design for the Precise Synthesis of Polyester Materials

Jonas Bruckmoser

Vollständiger Abdruck der von der TUM School of Natural Sciences der Technischen

Universität München zur Erlangung eines

Doktors der Naturwissenschaften (Dr. rer. nat.)

genehmigten Dissertation.

Vorsitz: apl. Prof. Dr. Wolfgang Eisenreich

Prüfer der Dissertation:

1.   Prof. Dr. Dr. h.c. Bernhard Rieger
2.   Prof. Dr. Torben Gädt
3.   Prof. Dr. Carmine Capacchione

Die Dissertation wurde am 05.01.2023 bei der Technischen Universität München eingereicht

und durch die TUM School of Natural Sciences am 23.03.2023 angenommen.

Non quia difficilia sunt non audemus, sed quia non audemus difficilia sunt.

Lucius Annaeus Seneca the Younger

Alles Wissen und alle Vermehrung unseres Wissens endet nicht mit einem Schlusspunkt, sondern mit Fragezeichen.

Hermann Hesse

Acknowledgements

Mein besonderer Dank gilt meinem Doktorvater,

Herrn Prof. Dr. Dr. h.c. Bernhard Rieger

für die herzliche Aufnahme in seinen Lehrstuhl und die Möglichkeit, meine Doktorarbeit unter seiner Betreuung anfertigen zu dürfen. Ihre Begeisterung für den Kunststoff PHB hat mich angesteckt und ich danke Ihnen für die äußerst interessante und auch herausfordernde Themenstellung, die wertvollen Diskussionen und die mir gewährten Freiräume. Es hat mir große Freude bereitet, dass wir viele Projekte erfolgreich abschließen konnten und es freut mich sehr, dass das PHB-Projekt fortgeführt wird.

Dr. Carsten Troll möchte ich danken, dass er mir immer mit Tat und Rat zur Seite stand und bei technischen Problemen an jeglichem Laborgerät stets eine Lösung parat hatte. Weiterhin gebührt *Dr. Sergei Vagin* großer Dank für eine Vielzahl an spannenden, wissenschaftlichen Diskussionen, die mich immer sehr voran gebracht haben.

Meinen Masteranden, Bacheloranden und Forschungspraktikanten *Sebastian Remke, Simon Bodesheim, Stefan Frei, Miriam Jänchen* und *Max Müller* möchte ich für ihre engagierte Mitarbeit an meinen Forschungsthemen danken. Meiner Nachfolgerin *Stefanie Pongratz* danke ich für ihre Mitarbeit beim PHB-Projekt; auch wenn dieses Projekt für mich bereits so mancherlei Überraschungen bereithielt, wächst man hierbei schnell mit seinen Aufgaben und kann in diesem großen Puzzle ein Teil nach dem anderen zusammensetzen. Ich bin überzeugt, dass hier noch viel Potential schlummert und wünsche dir bei der Fortsetzung des PHB-Projekts weiterhin viel Erfolg.

Dass das Arbeiten im Labor eine Menge Spaß gemacht hat, lag vor allem an der guten Atmosphäre in unserer Laborreihe und hierfür möchte ich mich besonders bei *Lucas Stieglitz* und *Philipp Weingarten* bedanken. Ebenso zur Bereicherung des Laboralltags, zu geselligen Abenden, schönen Konferenzbesuchen und lustigen Erinnerungen haben im Laufe der Jahre besonders *Brigita Bratic*, *Paula Großmann, Kerstin Halama, Lena Kleybolte, Moritz Kränzlein,* (und erneut *Lucas Stieglitz*) beigetragen. Dem ganzen Wacker-Lehrstuhl danke ich für die sehr angenehme und kollegiale Arbeitsatmosphäre und Zusammenarbeit.

Über den Lehrstuhl hinaus gebührt *Alex Böth* und *Daniel Döllerer* besonderer Dank, dass wir auch über unser gemeinsames Studium hinfort (und trotz der örtlichen Entfernung) stets eng in Kontakt geblieben sind und aus unseren abendlichen Skype-Sessions so manch gute Idee für die Problembehebung im Labor entstanden ist. Ihr habt somit auch sehr zum erfolgreichen

Gelingen dieser Arbeit beigetragen. Auch wenn wir nun keine Laborgeschichten mehr zu bereden haben, bin ich mir sicher, dass unsere Freundschaft genauso rege bestehen bleiben wird.

Mein größter Dank gilt abschließend meiner Familie. Dafür, dass ihr mich immer bei all meinen Vorhaben unterstützt, mir Rückhalt und Motivation gebt, und das ermöglicht habt, dass ich stehe, wo ich jetzt bin.

List of Publications

1. Bruckmoser, J.; Henschel, D.; Vagin, S.; Rieger, B.; Combining high activity with broad monomer scope: indium salan catalysts in the ring-opening polymerization of various cyclic esters. *Catal. Sci. Technol.* **2022**, *12*, 3295–3302.

2. Bruckmoser, J.; Rieger, B.; Simple and Rapid Access toward AB, BAB and ABAB Block Copolyesters from One-Pot Monomer Mixtures Using an Indium Catalyst. *ACS Macro Lett.* **2022**, *11*, 1067–1072.

3. Bruckmoser, J.[‡]; Remke, S.[‡]; Rieger, B.; Ring-Opening Polymerization of a Bicyclic Lactone: Polyesters Derived from Norcamphor with Complete Chemical Recyclability. *ACS Macro Lett.* **2022**, *11*, 1162–1166. [‡]These authors contributed equally.

4. Bruckmoser, J.; Rieger, B.; High-Throughput Approach in the Ring-Opening Polymerization of *β*-Butyrolactone Enables Rapid Evaluation of Yttrium Salan Catalysts. *Manuscript in preparation.*

5. Bruckmoser, J.; Pongratz, S.; Stieglitz, L.; Rieger, B.; Highly Isoselective Ring-Opening Polymerization of *rac-β*-Butyrolactone: Access to Synthetic Poly(3-hydroxybutyrate) with Polyolefin-like Material Properties. *Manuscript in preparation.*

Publications beyond the scope of this thesis:

6. Boström, H. L. B.; Bruckmoser, J.; Goodwin, A. L.; Ordered B-Site Vacancies in an ABX_3 Formate Perovskite. *J. Am. Chem. Soc.* **2019**, *141*, 17978–17982.

7. Koch, M.; Bruckmoser, J.; Scholl, J.; Hauf, W.; Rieger, B.; Forchhammer, K.; Maximizing PHB content in *Synechocystis* sp. PCC 6803: a new metabolic engineering strategy based on the regulator PirC. *Microb. Cell Fact.* **2020**, *19*, 231.

8. Kränzlein, M.[‡]; Pongratz, S.[‡]; Bruckmoser, J.; Bratić, B.; Breitsameter, J. M.; Rieger, B.; Polyester synthesis based on 3-carene as renewable feedstock. *Polym. Chem.*, **2022**, *13*, 3726–3732. [‡]These authors contributed equally.

Conference contribution:

9. Bruckmoser, J.; Rieger, B.; Indium salan catalysts: Very high activities in the ring-opening polymerization of various cyclic esters and synthesis of well-defined copolymers from monomer mixtures. ACS Spring 2022 – Bonding Through Chemistry, **2022**, San Diego, oral presentation.

List of Abbreviations

bdsa	bis(dimethylsilyl)amide
BEMP	2-*tert*-butylimino-2-diethylamino-1,3-dimethyl-perhydro-1,3,2-diaza-phosphorine
Bn	benzyl
BnOH	benzyl alcohol
CHO	cyclohexene oxide
CMVL	4-carbomethoxylated δ-valerolactone
CRM	chemical recycling to monomer
$Đ$	polydispersity index (M_w/M_n)
DBU	1,8-diazabicyclo[5.4.0]undec-7-ene
DFT	density functional theory
DL	cyclic diolide, formally 4,8-dimethyl-1,5-dioxocane-2,6-dione
DPP	diphenyl phosphate
DSC	differential scanning calorimetry
Et	ethyl
ΔG_p	Gibbs free energy of polymerization
HDPE	high density polyethylene
HPPO	hydrogen peroxide to propylene oxide
IR	infrared
i-PP	isotactic polypropylene
^{i}Pr	*iso*-propyl
^{i}PrOH	*iso*-propanol
k_A	polymerization rate of monomer A
k_B	polymerization rate of monomer B
k_i	rate of initiation
k_p	rate of propagation
k_{tr}	rate of transfer reactions
L_n	ligand framework
LA	lactide
L-LA	L-lactide
Ln	lanthanide
m	*meso*-linkage
M	metal center
M_n	number-average molecular weight
M_w	weight-average molecular weight

Me	methyl
MLABe	benzyl-β-malolactone
Mt	million metric tons
MTP	methanol to propylene
^{n}Bu	n-butyl
NCL	norcamphorlactone, formally 2-oxabicyclo[3.2.1]octan-3-one
NHC	N-heterocyclic carbene
NMR	nuclear magnetic resonance
Nu	nucleophile
P_m	probability of *meso*-linkages
P_r	probability of *racemic*-linkages
PCL	poly(ε-caprolactone)
PDL	poly(ε-decalactone)
PE	polyethylene
PET	poly(ethylene terephthalate)
PGBL	poly(γ-butyrolactone)
Ph	phenyl
PHA	poly(hydroxyalkanoate)
PHB	poly(3-hydroxybutyrate)
PLA	poly(lactide)
PMLA	poly(β-malic acid)
PNCL	poly(norcamphorlactone)
PP	polypropylene
PS	polystyrene
PUR	poly(urethane)
PVC	poly(vinyl chloride)
r	*racemic*-linkage
rac-β-BL	*racemic*-β-butyrolactone
rac-DL	*racemic* diolide
rac-LA	*racemic* lactide
REM	rare-earth metal
ROCOP	ring-opening copolymerization
ROP	ring-opening polymerization
Sn(Oct)$_2$	tin bis(2-ethylhexanoate)
T	temperature
T_c	ceiling temperature
T_d	decomposition temperature

$T_{d,max}$	maximum rate decomposition temperature
T_g	glass transition temperature
T_m	melting temperature
TBD	1,5,7-triazabicyclo[4.4.0]-dec-5-ene
^tBu	*tert*-butyl
TGA	thermal gravimetric analysis
THF	tetrahydrofuran
TOF	turn-over-frequency
α-MVL	α-methylene-δ-valerolactone
β-BL	β-butyrolactone
β-MVL	β-methyl-δ-valerolactone
β-PL	β-propiolactone
γ-BL	γ-butyrolactone
δ-CL	δ-caprolactone
δ-VL	δ-valerolactone
ε-CL	ε-caprolactone
ε-DL	ε-decalactone
$ε_B$	elongation at break

Table of Contents

Abstract

Ring-opening polymerization (ROP) of lactones is a valuable method for the synthesis of aliphatic polyesters with promising material properties comparable to current commodity plastics. Besides their (bio)degradability, these polymers offer the potential of chemical recyclability as a consequence of the monomer–polymer equilibrium present in ROP. In this thesis, catalyst and monomer design studies were performed to unlock the full potential of ROP. Catalyst design focused on the utilization of tunable and flexible salan-type frameworks for group 3 and 13 initiators. An indium salan alkoxide catalyst was tested in the ROP of various cyclic esters including β-butyrolactone, γ-butyrolactone, ε-caprolactone, ε-decalactone and lactide. In contrast to a related but more constrained indium catam-type initiator, the salan-type species combined high catalytic activity with broad monomer scope, demonstrating its versatility. The indium salan all-rounder catalyst was subsequently employed in the copolymerization of one-pot monomer mixtures. Here, it showed monomer-selective polymerization behavior in the ROP of β-butyrolactone and ε-decalactone, generating well-defined AB-, BAB-, and ABAB-type block copolymers. The ROP of β-butyrolactone is particularly promising as it gives access to poly(3-hydroxybutyrate) (PHB). While naturally produced, bacterial PHB has an isotactic stereomicrostructure and represents an auspicious biodegradable alternative to current commodity plastics, the chemical synthesis via ROP additionally enables atactic and syndiotactic stereomicrostructures. Hence, catalyst design is crucial for a stereocontrolled ROP of β-butyrolactone and a high-throughput approach was developed for that. The *in situ* catalyst generation, in combination with rational tuning of electronic and steric parameters of the salan ligand framework, allowed for the rapid identification of structure-property relationships in the yttrium-catalyzed ROP of β-butyrolactone. Using this high-throughput approach, a novel yttrium salan catalyst platform was found to give access to highly isotactic PHB with polyolefin-like thermomechanical properties. Expanding ROP beyond synthesis of (bio)degradable polymers, monomer design studies within this work focused on the generation of polyesters with intrinsic chemical recyclability. The ROP of a hybridized, bicyclic lactone with 6-membered ring core structure derived from norcamphor was investigated. High molecular weight alicyclic polyesters were obtained and thermolysis furnished selective and quantitative depolymerization to the pristine monomer, thus closing the monomer–polymer loop.

Zusammenfassung

Die Ringöffnungspolymerisation (ROP) von Lactonen ist eine wertvolle Methode, um aliphatische Polyester mit vielversprechenden Materialeigenschaften, vergleichbar mit denen gegenwärtiger Massenkunststoffe, zu synthetisieren. Neben ihrer (Bio-)Abbaubarkeit bieten diese Polymere das Potenzial von chemischem Recycling aufgrund des vorhandenen Monomer–Polymer-Equilibriums in ROP. In dieser Arbeit wurden Studien zum Katalysator- und Monomerdesign durchgeführt, um das volle Potential der ROP zu entfalten. Das Katalysatordesign fokussierte sich auf die Verwendung abstimmbarer und flexibler Ligandengerüststrukturen des Salan-Typs für Initiatoren der Gruppe 3 und 13. Ein Indium-Salan-Alkoxid Katalysator wurde in der ROP verschiedener cyclischer Ester, einschließlich β-Butyrolacton, γ-Butyrolacton, ε-Caprolacton, ε-Decalacton und Lactid, getestet. Im Gegensatz zu einem verwandten, aber weniger flexibleren Indium Initiator vom Catam-Typ zeigte die Salan-Spezies ihre Vielseitigkeit durch eine hohe katalytische Aktivität kombiniert mit einem breiten Monomerspektrum. Anschließend wurde der Indium-Salan Allrounder-Katalysator in der Copolymerisation von Monomermischungen verwendet. Hier zeigte dieser in der ROP von β-Butyrolacton und ε-Decalacton ein monomerselektives Polymerisations-verhalten und generierte definierte Blockcopolymere vom AB-, BAB- und ABAB-Typ. Die ROP von β-Butyrolacton ist besonders vielversprechend, da sie Zugang zu Poly(3-hydroxybutyrat) (PHB) ermöglicht. Während natürlich hergestelltes, bakterielles PHB eine isotaktische Stereostruktur aufweist und eine erfolgsversprechende biologisch abbaubare Alternative zu gängigen Massenkunststoffen darstellt, lässt die chemische Synthese mittels ROP zusätzlich ataktische und syndiotaktische Stereomikrostrukturen zu. Aufgrund dessen ist das Katalysatordesign für eine stereokontrollierte ROP von β-Butyrolacton unverzichtbar und es wurde dafür ein Hochdurchsatzverfahren entwickelt. Die *in situ* Katalysatorbildung erlaubte im Zusammenspiel mit der rationalen Feinabstimmung der elektronischen und sterischen Parameter des Salan-Ligandengerüsts die rasche Identifizierung von Struktur-Eigenschafts-Beziehungen in der Yttrium-katalysierten ROP von β-Butyrolacton. Mittels dieses Hochdurchsatzverfahrens wurde eine neuartige Yttrium-Salan-Katalysatorplattform gefunden, welche Zugang zu hochisotaktischem PHB mit polyolefinartigen thermomechanischen Eigenschaften gewährt. Um die ROP über (bio-)abbaubare Polymere hinaus zu erweitern, fokussierten sich in dieser Arbeit die Studien zum Monomerdesign auf die Entwicklung von Polyestern mit intrinsischer chemischer Recycelbarkeit. Die ROP eines hybridisierten, bicyclischen Lactons mit 6-gliedriger Ringkernstruktur, abgeleitet von Norcampher, wurde untersucht. Hochmolekulare, alicyclische Polyester wurden erhalten und mittels Thermolyse eine selektive sowie quantitative Depolymerisation zum ursprünglichen Monomer erzielt – und somit der Monomer–Polymer Kreislauf geschlossen.

1 Introduction – Polymers for the Second Century of Polymer Chemistry

The year 2020 marked the beginning of the second century of polymer chemistry and based on the successful first century with rapid developments in the field, the scientific contributions of polymer chemists within the next 100 years will help to overcome major global challenges society is facing.[1] It was in 1920 that Hermann Staudinger published his seminal work 'Über Polymerisation'.[2,3] While polymeric materials have already been used prior to that, their molecular structure was unknown and controversially discussed by scientists at that time. Staudinger correctly proposed that polymers are in fact long chains of covalently linked building blocks, so called macromolecules, and not colloidal structures or aggregates, which was the prevailing opinion of many researchers.[1,2,4,5] Nowadays, he is considered as the father of polymer chemistry and most likely, by then, he could not have imagined the enormous positive impact polymers would have on our daily life today.[4] It was the work of Karl Ziegler and Giulio Natta on ethylene and propylene polymerization catalysis in the early 1950s that laid the foundation for the industrial mass production of polyolefins.[6] While 2 million metric tons (Mt) of plastics were produced in 1950, the global production increased to 407 Mt of primary plastics in 2015 and polyolefins make up the largest share of all plastics produced today (Figure 1).[7] The reasons for this drastic increase in plastic production are the outstanding properties of this material class and the plethora of applications it has found, considerably improving daily life from food packaging to light-weight materials for construction or engineering applications to biomedicine solutions to consumer goods.[4,6]
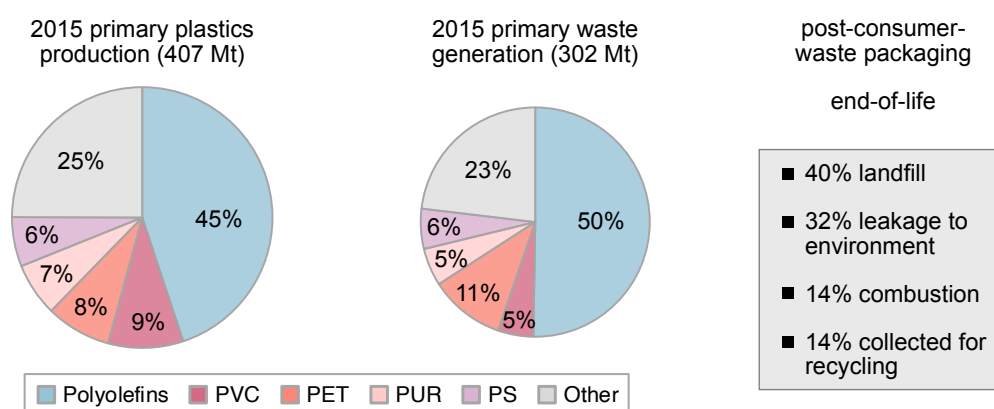

Figure 1. Share of different polymers in the total plastics production and waste generation in 2015, and end-of-life fates of post-consumer-waste plastics packaging. PVC, poly(vinyl chloride); PET, poly(ethylene terephthalate); PUR, poly(urethane)s; PS, polystyrene. Other includes produced fibers.[7-9]

However, when it comes to the end-of-life fate of these materials, their strength and durability, which is one of their benefits during lifetime, becomes a major drawback and results in the accumulation of plastic waste in the environment with severe side effects.[7,10-13] In 2017, it was estimated that 8300 Mt of virgin plastics has been manufactured from 1950 to 2015, and

6300 Mt of plastic waste has been generated. An estimated 407 Mt of plastics were produced in 2015 while 302 Mt of plastic waste was generated in the same year (Figure 1). Most of this waste (79%) is accumulated in landfills or in the environment, and only a small fraction has been recycled (9%). Very similar numbers have been estimated for single-use post-consumer-waste plastic packaging.[7,8] The persistence of current commodity plastics in the environment and the loss of material value if plastics are not recycled but simply discarded has become a pressing global issue that requires urgent action.[14] Single-use packaging waste accounts for 47% of the total plastic waste and the loss in material value is estimated at US\$ 80–120 billion annually.[7,8] Additionally, scenarios show that by 2050, the oceans could contain more plastic than fish by weight if no changes are made.[8] Materials with similar or even enhanced properties compared to today's commodity plastics but with beneficial end-of-life options such as biodegradability or chemical recyclability are thus highly needed. Fortunately, polymer chemists do have the right tools at hand and the research areas of non-fossil fuel based, biodegradable as well as recyclable polymers are rapidly developing.[9,15-21] Within this field, aliphatic polyesters have gained considerable attention due to their comparable properties to commodity plastics such as polyethylene (PE), polypropylene (PP) or polystyrene (PS).[15,19,22,23] In contrast to PE, PP or PS, which only possess stable, nonpolar carbon–carbon linkages in their polymer chain, the polar carbonyl units in the backbone of aliphatic polyesters comprise a point of attack and enable simple chain scission. Consequently, these polyesters are degradable or even biodegradable in the environment, and recycling approaches such as chemical recycling to monomer or to value-added chemicals becomes feasible.[19,23,24] While the current production volumes of biobased and/or biodegradable polymers are still very low in comparison to traditional commodity plastics, they are expected to grow substantially within the next few years.[25] The second century of polymer chemistry will most likely be a tremendous success story for this specific class of polymers.

2 Ring-Opening Polymerization as Convenient Method for the Synthesis of Aliphatic Polyesters

2.1. General Remarks and Thermodynamics of Ring-Opening Polymerization

Aliphatic polyesters are a class of materials with promising properties that can be produced via different methods, yet three main routes have been established (Scheme 1).[22,23,26,27] The polycondensation of diacids or diesters with diols is a well-studied process and traditionally applied for the industrial synthesis of current commodity polyesters such as poly(ethylene terephthalate) (PET). Similarly, the self-condensation polymerization of hydroxy acids gives access to polyester materials. These methods have the advantage of a broad range of monomers that are available and enable the synthesis of polyesters with diverse structural features. However, for these processes, harsh polymerization conditions are required, control over the molecular weight is limited and sophisticated polymer structures such as block copolymers are difficult to access.[26] Ring-opening polymerization (ROP) of cyclic esters overcomes these issues and is the most promising and efficient method for the synthesis of aliphatic polyesters. ROP enables the production of polyesters with very narrow polydispersities (Đ), tunable molecular weights and high end-group fidelity under mild reaction conditions while maintaining high polymerization rates. Additionally, ROP can be performed as living-type polymerization when metal-based catalysts or organocatalysts are employed and thus, the control over the polymerizations is usually excellent and allows for the synthesis of polymers with defined molecular weight and defined microstructures such as block copolymers.[22,23,28,29]
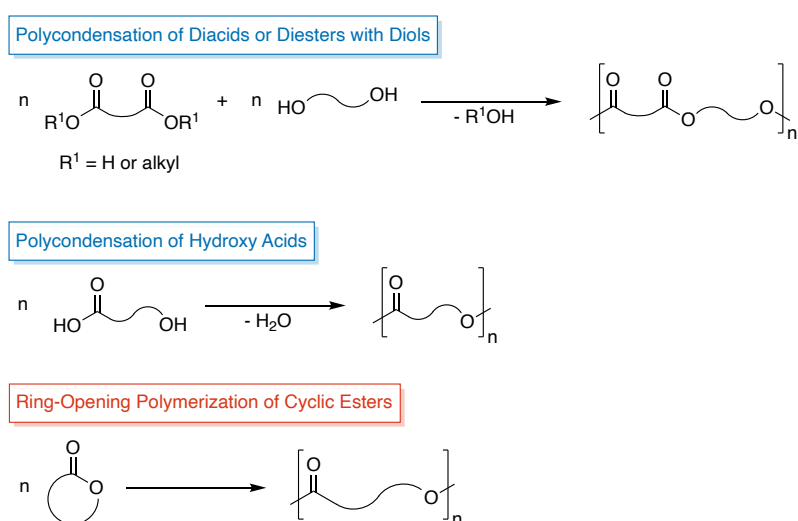
Scheme 1 Schematic representation of main synthesis routes for the production of aliphatic polyesters: polycondensation of diacids or diesters with diols (top), polycondensation of hydroxy acids (middle) and ring-opening polymerization of cyclic esters (bottom).[22,23,26,27]

Concerning the structural variety of aliphatic polyesters accessible via ROP, limitations only exist in the (simple) availability of cyclic monomers. Within the last few decades, the scope of monomers has been remarkably broadened and a plethora of lactones and cyclic diesters from 4-membered up to 17-membered rings have been reported for ROP.[22,23,27,30,31] Additionally, ROP of O-carboxyanhydrides is another promising strategy for accessing polyester materials.[32] Besides these methods, radical ROP of cyclic ketene acetals is an additional route towards aliphatic polyesters, albeit less commonly employed and more restricted in terms of monomer scope.[33] The alternating ring-opening copolymerization (ROCOP) of epoxides and cyclic anhydrides has gained increasing attention in recent years since the wide range of available epoxides and anhydrides substantially broadens the structural diversity of accessible aliphatic polyesters. This specific field of ROP is beyond the scope of this thesis and detailed overviews of current advances can be found in excellent review articles.[34,35]

Focusing on the ROP of cyclic esters, distinctions have to be made between small-sized (up to 6-membered rings), medium-sized (7- to 11-membered rings) and large-sized lactones (12-membered rings and higher, i.e. macrolactones). The ROP of small- and medium-sized lactones is enthalpically driven by the release of the ring strain, whereas macrolactones exhibit minimal ring strain and therefore their polymerization is entropically driven by a less-hindered chain rotation in the polymer than in the monomer. Consequently, the ROP of macrolactones requires higher reaction temperatures compared to small- and medium-sized lactones.[31,36] Besides this general classification, the monomer structure such as ring size and degree of substitution strongly influences polymerizability, and the equilibrium polymerization behavior of a lactone is also affected by the monomer concentration. The ceiling temperature (T_c) is a measure for the polymerization behavior of the monomer and is the temperature at which the polymerization rate equals the depolymerization rate. This equilibrium behavior is of utmost practical importance when novel monomers are designed and rapid and high conversion of monomer to polymer is desired (polymerization temperature well below T_c) or when chemical recycling of polymers back to monomer is targeted (depolymerization temperature well above T_c).[36,37] The magnitude of Gibbs free energy of polymerization (ΔG_p) correlates with the polymerization equilibrium behavior. For the highly strained 4-membered β-propiolactone (β-PL) and 7-membered ε-caprolactone (ε-CL), ΔG_p is very low and thus polymerization highly favored at ambient temperatures (Figure 2).[28,36,38,39] For the "nonstrained" 5-membered γ-butyrolactone (γ-BL), ΔG_p is >0 at ambient temperatures.[28,38] This has led to the widespread assumption that γ-BL is non-polymerizable.[28,40] However, performing the polymerization at very low temperatures ($T = -40°C$) enabled the successful ROP of γ-BL towards poly(γ-butyrolactone) (PGBL), demonstrating the importance of thermodynamic pre-synthetic considerations and polymerization conditions in ROP.[40] Substitutions such as cyclohexyl rings fused to the γ-BL core strongly increased T_c and polymerization of such lactones became

feasible even at room temperature, highlighting the strong influence of substitutions on the polymerizability of a certain monomer.[41-43] Similarly, 6-membered rings show a strong dependence of polymerization behavior on substitutions but are generally easier polymerized than γ-BL and its derivatives.[36] ROP of δ-valerolactone (δ-VL) is thermodynamically favored ($\Delta G_p \approx -6.0$ kJ mol^{-1}), whereas the T_c is drastically reduced with increasing length of alkyl chain substitution.[28,36,38,39] In contrast to that, L-lactide (L-LA), a disubstituted 6-membered diester, has beneficial polymerization thermodynamics ($\Delta G_p \approx -15.5$ kJ mol^{-1}) and is conveniently polymerized to high conversion even at high reaction temperatures (Figure 2).[28,44]
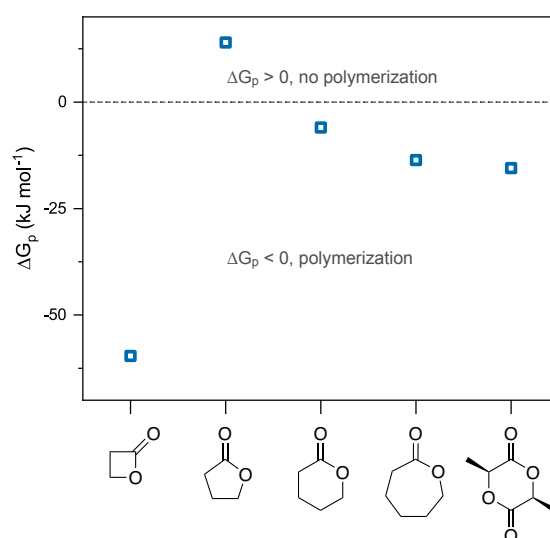

Figure 2. Correlation of ΔG_p with ring size. ΔG_p of lactones β-PL, γ-BL, δ-VL, ε-CL, and cyclic diester L-LA for polymerization conditions at 298 K and ambient pressure.[28,36,38,39,44]

If the thermodynamics for a specific monomer are favorable, its efficient polymerization is nonetheless not guaranteed.[36] Catalysts are essential for ROP and the specific type of catalyst used highly influences polymerization outcome.[22,27,29] Mechanistically, ROP proceeds via either a coordination-insertion, anionic, cationic, or activated monomer mechanism.[28] Homogeneous metal-based catalysts are most widely applied in the field of ROP and typically follow a coordination-insertion mechanism (*vide infra*). They have shown remarkable activity, control over the polymerization and, in the specific case of *racemic* monomers, stereoselectivity. The central metal atom as well as the coordination geometry and electronic influence of the ligand framework play a crucial role.[22,27-29] A detailed overview of the most prominent metal-based catalysts is provided in chapter 2.3. Besides metal catalysts, organocatalysts have demonstrated promising results in ROP as these types of catalysts provide polymers without metal residues, which is an important advantage for applications in microelectronic devices or in biomedicine.[45,46] The use of organocatalysts is often considered as sustainable alternative to conventional metal catalysts in terms of toxicity, however, this has to be viewed with caution as the toxicity of novel organocatalysts is often unknown and needs to be further investigated.[47]

2.2. Scope of Monomers in Ring-Opening Polymerization and Polymer Properties

As a consequence of the strongly increasing academic and industrial interest in ROP, a plethora of monomers have been explored within the last few decades and these span various ring sizes from 4- to 17-membered lactones as well as diverse substitutions (Figure 3). Lactide (LA), *β*-butyrolactone (*β*-BL) and *ε*-CL are among the best studied monomers in the field (Figure 3, highlighted in bold) as the resulting polyesters have comparable material properties to some commodity plastics. *β*-PL, *δ*-VL and glycolide are also commonly used as well as ω-pentadecalactone in the field of macrolactones.
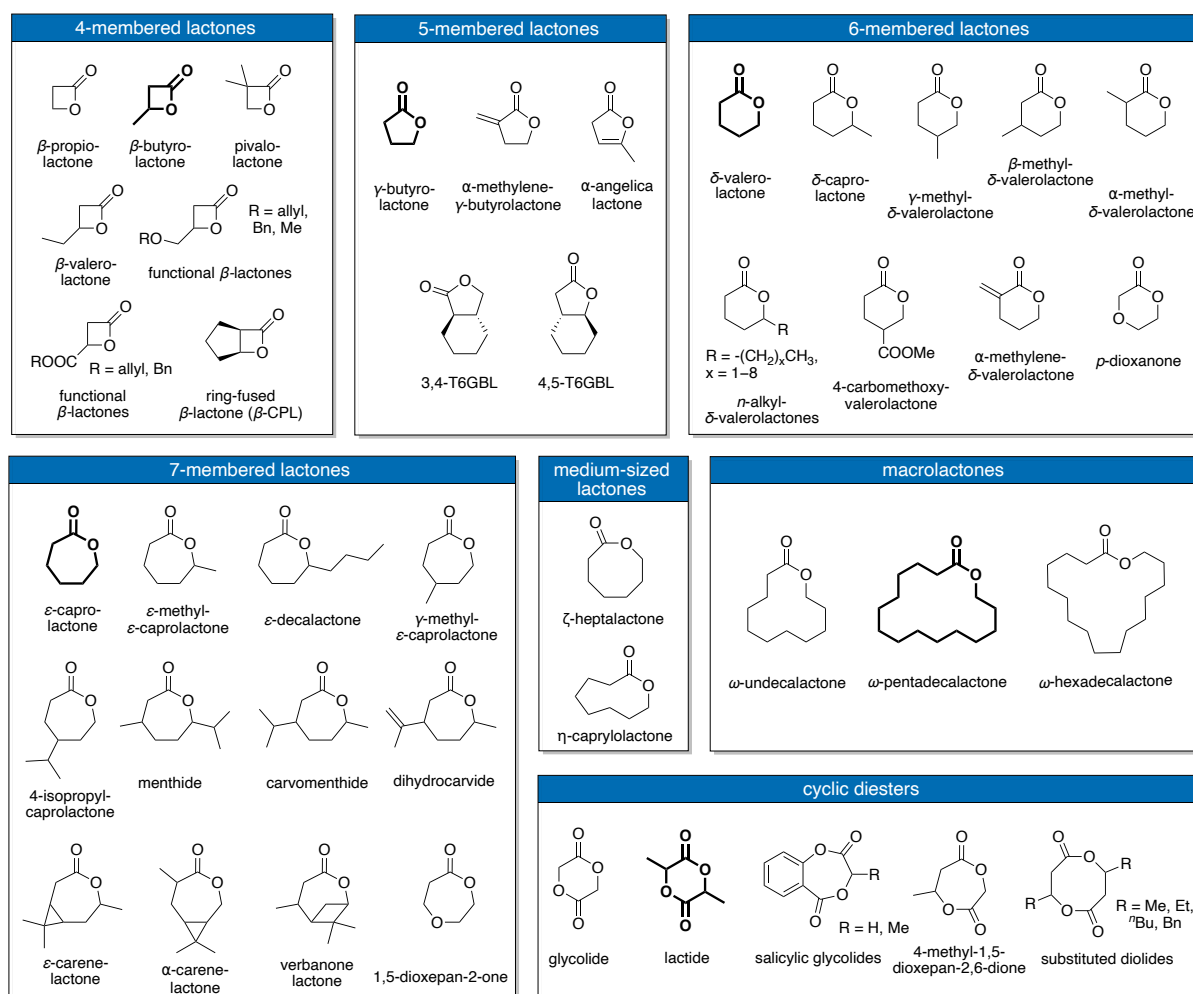

Figure 3. Overview of diverse lactones and cyclic diesters with various ring sizes for ring-opening polymerization. Most prominent monomers of each class are highlighted in bold.[19,22,23,27-29,31,37,48-62]

Numerous catalysts have been reported to date for these monomers and those will be covered in detail in chapter 2.3. Using LA, *β*-BL or *ε*-CL as benchmark monomers allows for a thorough understanding of parameters influencing ROP and for establishing structure-property relationships in catalyst design.[22,27-29,31,48] In the case of *β*-BL and LA, where one or two stereocenters, respectively, are present in the molecule, various stereomicrostructures

(tacticities) of the resulting polyester exist.[22,27,29] Generally, the tacticity gives information about the relation of adjacent stereocenters along the polymer main chain. At the diad level, the relation of two successive stereocenters is examined, whereas at the triad level, three successive stereocenters are assessed (Scheme 2). Based on this, a classification into isotactic polymers with *meso*-linkages (*mm*), syndiotactic polymers with *racemic*-linkages (*rr*) and heterotactic polymers with alternating linkages (*mr*) can be made. The probability of *meso*-linkages is defined as P_m whereas the probability of *racemic*-linkages is defined as P_r. For perfectly isotactic polymers $P_m = 1$ and for perfectly syndiotactic polymers $P_r = 1$. P_m and P_r are interrelated via $P_m = 1 - P_r$. If the stereocenters are randomly configured, an atactic polymer is present and $P_m = P_r = 0.5$. The tacticity of a polymer strongly influences its crystallinity and thus, has a strong impact on its thermal and mechanical properties.[27,63]
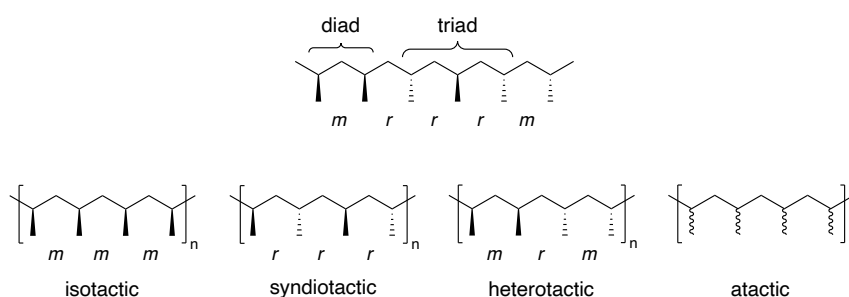
**Scheme 2.** Polymer stereochemistry. *r* = *racemic*-linkage, *m* = *meso*-linkage.[63]

Poly(3-hydroxybutyrate) (PHB), the most prominent member of biodegradable poly(hydroxyalkanoates) (PHAs), can be synthesized chemically via ROP of *β*-BL but is also naturally produced by bacteria and various other living microorganisms as energy storage material. Naturally occurring PHB is perfectly isotactic with all stereocenters in (*R*)-configuration, resulting in a semi-crystalline, high-melting, thermoplastic material. Its properties can compete with current commodity plastics and especially resemble those of isotactic polypropylene (*i*-PP) regarding thermal properties and mechanical properties such as Young's modulus, tensile strength and impact strength (Table 1). Additionally, it has a high resistance against ultraviolet radiation and high oxygen barrier.[23,29,64,65] Bacterial PHB shows a melting temperature (T_m) of around 177°C, glass transition temperature (T_g) of around 5°C, and high Young's modulus and tensile strength of 1.6 GPa and 38 MPa, respectively. These properties render biodegradable PHB an ideal candidate for the replacement of commodity plastics such as *i*-PP or high density polyethylene (HDPE) and reveals great promise in packaging applications, which are the main contributor to single-use plastics waste.[23,66] Nevertheless, various challenges for the successful commercialization of PHB are still existing. The high crystallinity of perfectly isotactic PHB results in a stiff and brittle material with very low elongation at break (ε_B = 5%).[66] The high melting temperature of PHB which is relatively

close to its decomposition temperature ($T_d \approx 250°C$) hampers melt processing and in combination with its brittleness the potential of PHB for industrial application is currently limited.[23,67,68] Additionally, the fermentative production of PHB is cost-intensive and restricted in scalability, thus, incapable of competing with cheap fossil fuel-based polyolefin production.[23,65]

Table 1. Comparison of thermal and mechanical material properties of aliphatic polyesters PHB and PLA with current commodity plastics [23,24,66,69]

polymer	T_g (°C)	T_m (°C)	Young's modulus (GPa)	tensile strength (MPa)	elongation at break (%)
bacterial PHB	5	177	1.6	38	5
isotactic PLA	55–65	170–200	3.5	60	<10
i-PP	−10	170–176	1.0–1.7	29.3–38.6	500–900
HDPE	−95	112–132	0.4–1.0	17.9–33.1	12–700
PET	75	250–265	2.2–2.9	56–70	100–7300
PS	100	237	3.0–3.1	50	3–4

The chemical synthesis of PHB via ROP of β-BL has the potential to overcome these challenges (Scheme 3A). β-BL is a commercially available monomer and can be easily synthesized from an inexpensive and abundant propylene oxide feedstock via atom-efficient carbon monoxide insertion.[23,29,70] This route can be realized from established fossil fuel-based chemistry but the CO_2-based propylene production via methanol is a valuable alternative option for a sustainable feedstock synthesis, as well (Scheme 3B).[23,71,72] Very recently, the synthesis of PHB via ROP of an 8-membered diolide has been reported (Scheme 3A).[55] While this is an elegant approach and demonstrates the potential of synthetic PHB production, the elaborate multi-step monomer synthesis is a severe drawback when it comes to industrial applicability.[55-57]
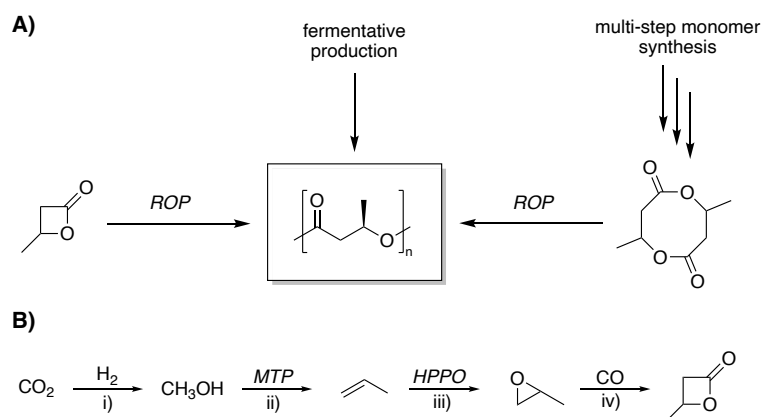
Scheme 3. A) Synthesis pathways towards isotactic PHB. Fermentative production, ROP of β-BL and ROP of 8-membered diolide. B) Monomer synthesis of β-BL starting from CO_2. i) Catalytic hydrogenative conversion, ii) methanol to propylene process (MTP), iii) hydrogen peroxide to propylene oxide process (HPPO), iv) carbonylative ring expansion.[23,29,55,70-72]

Considering the ROP of β-BL, an industrial process demands the use of cheap *racemic* β-BL instead of expensive enantiopure monomers.[29,66,73,74] Thus, controlling the stereoregularity is crucial as atactic PHB has an amorphous nature with poor polymer characteristics and syndiotactic PHB is not biodegradable.[29,66,75] Specifically designed metal-based catalysts are required that enable the synthesis of isotactic PHB and allow for a subtle adjustment of their stereocontrol. The chemical synthesis via ROP of β-BL facilitates the production of PHB with reduced degree of isotacticity that is otherwise inaccessible via biotechnological routes. Reducing the isotacticity of the polymer lowers its crystallinity and as a consequence melting temperature and brittleness are decreased, ultimately enabling melt processing of the polymer and improving the properties for industrial applications.[29,63] Early work by Doi et al. showed that the T_m of (*R*)-PHB with certain amount of (*S*)-stereo errors is reduced from 177°C (P_m = 1) to 132°C (P_m = 0.84) to 107°C (P_m = 0.76) to 92°C (P_m = 0.68), and inversely, the elongation at break increases from 5% to 740% (Table 2).[66,73] The authors also investigated the biodegradation behavior of those samples and found that synthetic (*R*)-PHB with reduced isotacticity is degraded faster than biological PHB (P_m = 1), due to the larger amorphous regions in the polymer that are easier attacked by degrading bacteria than the highly crystalline domains.[24,66,75]

Table 2. Thermal and mechanical properties of PHBs with variable degrees of isotacticity [66]

P_m	T_g (°C)	T_m (°C)	degree of crystallinity X_c (%)	Young's modulus (MPa)	tensile strength (MPa)	elongation at break (%)
1.00	5	177	62 ± 5	1560	38	5
0.84	6	132	49 ± 5	1190	15	7
0.76	6	107	45 ± 5	310	11	10
0.68	5	92	40 ± 5	90	11	740

Apart from its beneficial biodegradation properties, PHB offers chemical recyclability as an additional end-of-life option. While the material value of the polymer is lost when it is biodegraded to CO_2, H_2O and other small molecules, chemical recycling is a promising alternative where the material value is retained and polymers with virgin properties can be (re)produced, closing the loop in polymer economy.[9,19,76] Under acidic, Lewis acidic or basic conditions, PHB is easily depolymerized to 3-hydroxybutyrate and crotonic acid.[76-78] Decarboxylation of crotonic acid yields propylene, the starting material for β-BL production, and thus closes the material loop.[79] Additionally, processes such as the hydrothermal depolymerization of PHB have demonstrated access to propylene in an one-step route.[80] The selective depolymerization towards β-BL has not been reported so far and is thermodynamically highly unfavorable due to the high ring strain of β-BL. Instead, cyclic trimers and higher oligomers of 3-hydroxybutyrate were obtained upon dilute acidic reaction

conditions. The polymerization of the cyclic trimer is however challenging and only gave PHB in low yields with low molecular weights.[81,82] Alcoholysis of PHB yields valuable small molecule precursors and provides alternative starting points for regeneration of embedded polymer material value, among other processes.[76,83-87]

In contrast to PHB, the synthesis of poly(lactide) (PLA) via ROP of L-LA is already performed at the commercial level and PLA is by now one of the most widely used bioplastics today.[25] Its thermal and mechanical properties are comparable to those of PET and PS (Table 1). Similarly to PHB, isotactic PLA is a very stiff and brittle material with an elongation at break below 10% and requires plasticizers for its specific applications.[23,24] Academic research also focusses on the utilization of *rac*-LA for the production of PLA, where the properties of the generated polyesters are strongly dependent on the degree of stereoregularity.[22,27,63] PLA shows relatively fast degradation rates under industrial composting conditions ($T > 60°C$) and slow hydrolysis in the natural environment at land. However, PLA biodegradation is negligible in marine environments and its resistance against degradation is as high as its petrochemical counterparts, which is a strong disadvantage compared to sea water degradable PHB.[88,89] Industrial depolymerization of PLA in order to retain the material value shows great promise and the ring-closing depolymerization to selectively recover L-LA monomer has already been demonstrated at the laboratory scale.[76,90]

Beyond those commonly applied cyclic esters such as *β*-BL and LA, novel monomers sourced from renewable feedstocks are gaining increased attention as well as lactones which can be used for the synthesis of functional polymers (Figure 3). Lactones as well as cyclic diesters reported for ROP span various ring sizes and show a broad structural diversity regarding their substitution patterns.[19,22,23,27-29,31,48,49] Monomers with alkyl substitutions are frequently investigated in ROP as the substituent allows for subtle tuning of material properties of the resulting polyester. Methyl-substituted *ε*-caprolactones, for example, are sustainable monomers based on cresols derived from renewable lignin bio-oil.[50] Another prominent class of biobased monomers are lactones on a terpene basis such as 4-isopropyl-caprolactone, menthide, carvomenthide, dihydrocarvide or carene and verbanone lactones.[36,51-54] While the monomer synthesis often consists of multiple steps and still demands for further improvements in terms of sustainability, terpenes are a promising feedstock furnishing the synthesis of a highly diverse set of aliphatic polyesters.[18,53] Besides alkyl substitutions, monomers bearing functional groups such as *β*-malolactones or methylene substituted lactones provide advanced polymers for use as smart materials or options for additional post-polymerization functionalization.[62,91,92] Another strategy is the use of cyclic diesters that give access to structurally diverse polymers.[55-61] The ROP of macrolactones has found interest as polyesters with large linear segments of carbon–carbon linkages are obtained, thus being similar to PE,

but degradation is facilitated by the ester units.[31] Fusion of cyclopentyl or cyclohexyl rings with lactones to generate bicyclic monomers has become a promising strategy in monomer design for enabling chemically recyclable polymers and is discussed in detail in chapter 2.5.[9,37] Those examples demonstrate the versatility of cyclic esters available for ROP and the structural diversity of the resulting aliphatic polyesters. With specifically designed monomers at hand, ROP is a highly valuable method that gives simple and rapid access to (bio)degradable and/or chemically recyclable polymers.

2.3 Catalysts for Ring-Opening Polymerization

2.3.1 Mechanisms, Side Reactions and Immortal Ring-Opening Polymerization

Catalysts play a vital role in the ROP of cyclic esters and most commonly the ROP proceeds either via a cationic, anionic, coordination-insertion or activated monomer mechanism. Anionic and coordination-insertion polymerizations are the prevalent types in the field and the former is observed with nucleophilic reagents such as metal alkoxides as initiators. The alkoxide attacks the carbonyl of the monomer followed by ring-opening via acyl–oxygen bond cleavage. The newly generated alkoxide then ring-opens the next monomer and the polymer chain is propagating (Scheme 4A).[23,28] In the specific case of β-lactones such as β-BL two mechanistic pathways have been observed, which includes an alkyl–oxygen bond cleavage in addition to acyl–oxygen bond cleavage. In case of cleavage of the acyl–oxygen bond, an alkoxide is the propagating chain end and retention of the stereoconfiguration is observed, whereas for the alkyl–oxygen pathway, a carboxy end-group is present and the configuration of the stereocenter is inverted (Scheme 4B).[29]
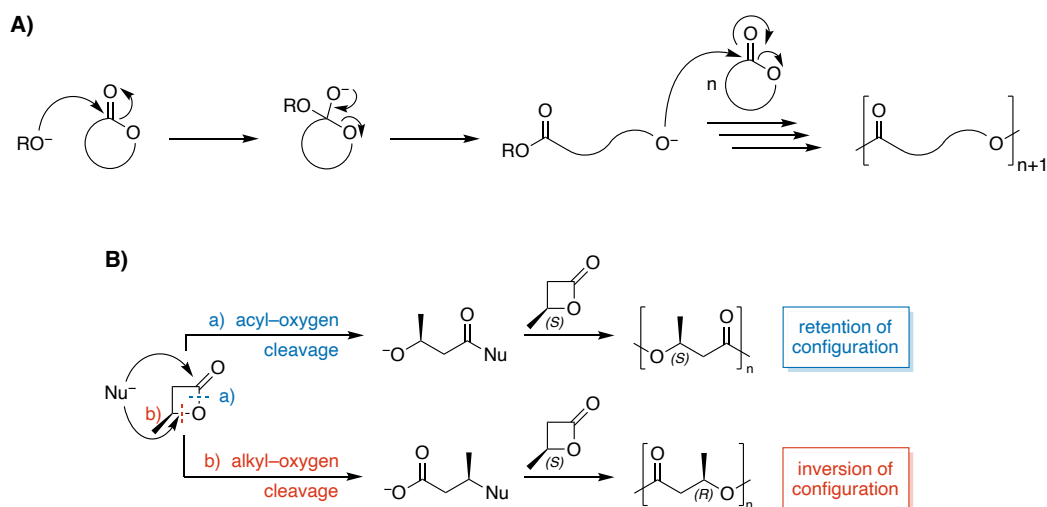
Scheme 4. A) Mechanism of anionic ring-opening polymerization and B) mechanistic pathways in the particular case of β-lactones including acyl–oxygen or alkyl–oxygen bond cleavage.[23,28,29]

The anionic ROP of lactones is a living-type polymerization yet control over the molecular weight and end-group of the polymer is often lost due to side reactions such as inter- and intramolecular transesterifications or β-hydride elimination (Scheme 5). While intermolecular transesterifications result in a broadening of the polymers' dispersity, intramolecular transesterifications generate cyclic oligomers or polymers as side product. β-hydride eliminations are particularly observed in ROP of β-BL and lead to crotonate as well as carboxylate chain-ends which are capable of deactivating the metal catalyst. The extent to

which these side reactions are observed is strongly dependent on the applied initiator and the reaction conditions.[23,28,93,94]

A) *Transesterification Side Reactions*
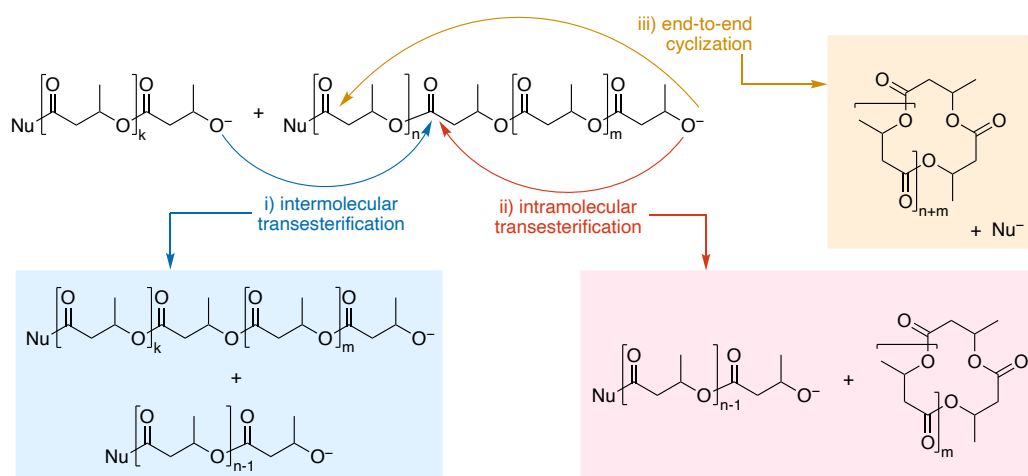

B) *β-H-Elimination*
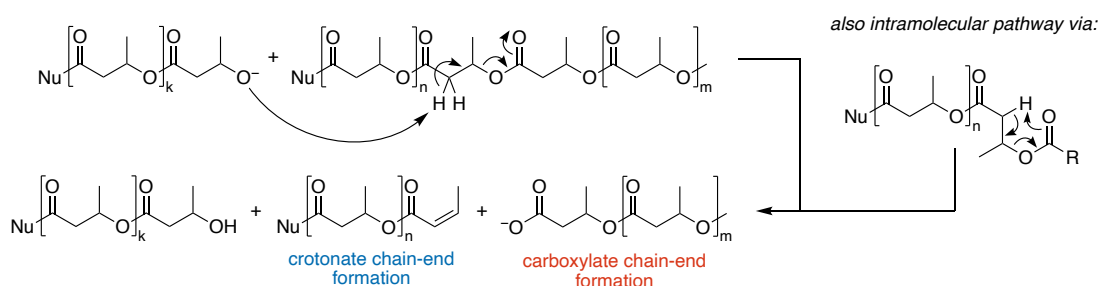
Scheme 5. A) Transesterification side reactions observed in ROP of cyclic esters exemplarily shown for *β*-BL polymerization towards PHB. B) *β*-H-elimination during ROP of *β*-BL is often observed and generates crotonate as well as carboxylate chain-ends.[23,28,93,94]

Contrary to this, coordination-insertion polymerization using defined single-site metal catalysts overcomes these limitations and shows increased polymerization control. The first generation of metal catalysts for ROP was based on homoleptic metal complexes such as tin bis(2-ethylhexanoate) [Sn(Oct)$_2$], zinc lactate, diethyl zinc (ZnEt$_2$) or aluminum isopropoxide [Al(O^{i}Pr)$_3$]. Further development led to today's catalytic systems where the central metal atom is coordinated by one or more multidentate ligands that allow for precise adjustment of electronic and steric parameters, and by at least one nucleophilic ligand such as an alkoxide or amido group that is initiating the polymerization.[22,27,29,48,95] The coordination–insertion mechanism for the ROP of cyclic esters employing these catalysts proceeds via coordination of the monomer to the metal center and subsequent addition of the nucleophilic initiating group of the catalyst to the carbonyl of the monomer (Scheme 6). This is followed by insertion into the metal–alkoxide bond via a 4-membered transition state and acyl–oxygen ring-opening,

resulting in a new metal–alkoxide species with a free coordination site that promotes further monomer coordination and propagation.[22,23,28]
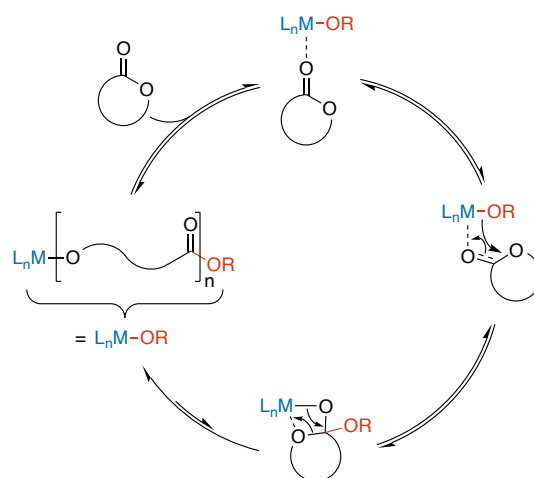
Scheme 6. Coordination-insertion mechanism for ROP of cyclic esters using metal-based catalysts with ligand framework L_n and nucleophilic (alkoxide) initiating group.[22,23]

In metal-mediated coordination–insertion polymerization, catalysts are capable of inducing stereoselectivity when monomers with chiral centers such as *β*-BL or LA are used (Figure 4), either via i) a chain-end control mechanism where the chirality of the last inserted monomer determines the chirality of the next monomer to be incorporated or via ii) an enantiomorphic site-control mechanism where the chirality of the catalyst determines the enantiomer which is inserted next.[27,29] Both mechanisms generate polymers with distinct stereochemical errors: in a chain-end-control mechanism, a misinsertion results in a propagation of the error, while in an enantiomorphic site control mechanism the error is corrected by the catalytic species (Figure 4, bottom panel, left). This leads to a different distribution of triads as for chain-end control the number of *mr* and *rm* triads is equal, but higher than either the *rr* or *mm* triad (Figure 4, bottom panel, right). Contrary, enantiomorphic site control exhibits an equal distribution of *mr*, *rm* and either the *rr* or *mm* triad.[27]

In the classical living ROP each catalyst molecule is initiating one polymer chain and protic sources are capable of terminating the polymerization. In the immortal ROP however, which is considered a special subtype, such protic sources do not deactivate the catalyst but act as chain transfer agent and initiator (Scheme 7). Commonly used chain transfer agents include alcohols such as *iso*-propanol (^{i}PrOH) or benzyl alcohol (BnOH). The number of growing polymer chains is equal to the amount of initial chain transfer agent used. Prerequisites for this behavior are a faster rate of initiation than propagation ($k_i \gg k_p$) and the absence of termination reactions as for classical living ROP. Additionally, for successful immortal ROP, the transfer reactions between the dormant (OH-terminated) polymer chain and the active catalyst species bearing the growing polymer chain have to be faster than propagation ($k_{tr} \gg k_p$). Besides this

major difference, the mechanism of immortal ROP with organometallic catalysts typically follows a coordination–insertion mechanism (*vide supra*).[96-98] The amount of catalyst used can be drastically reduced with this technique and thus ensures cheaper and more sustainable processes. Moreover, the predefined amount of chain transfer agent applied gives high control over the molecular weight of the polymers. Practical limitations have been observed regarding the stability of some organometallic catalysts and developing catalysts with high tolerance against chain transfer agents remains an important goal in the field of ROP catalysis.[96-103]
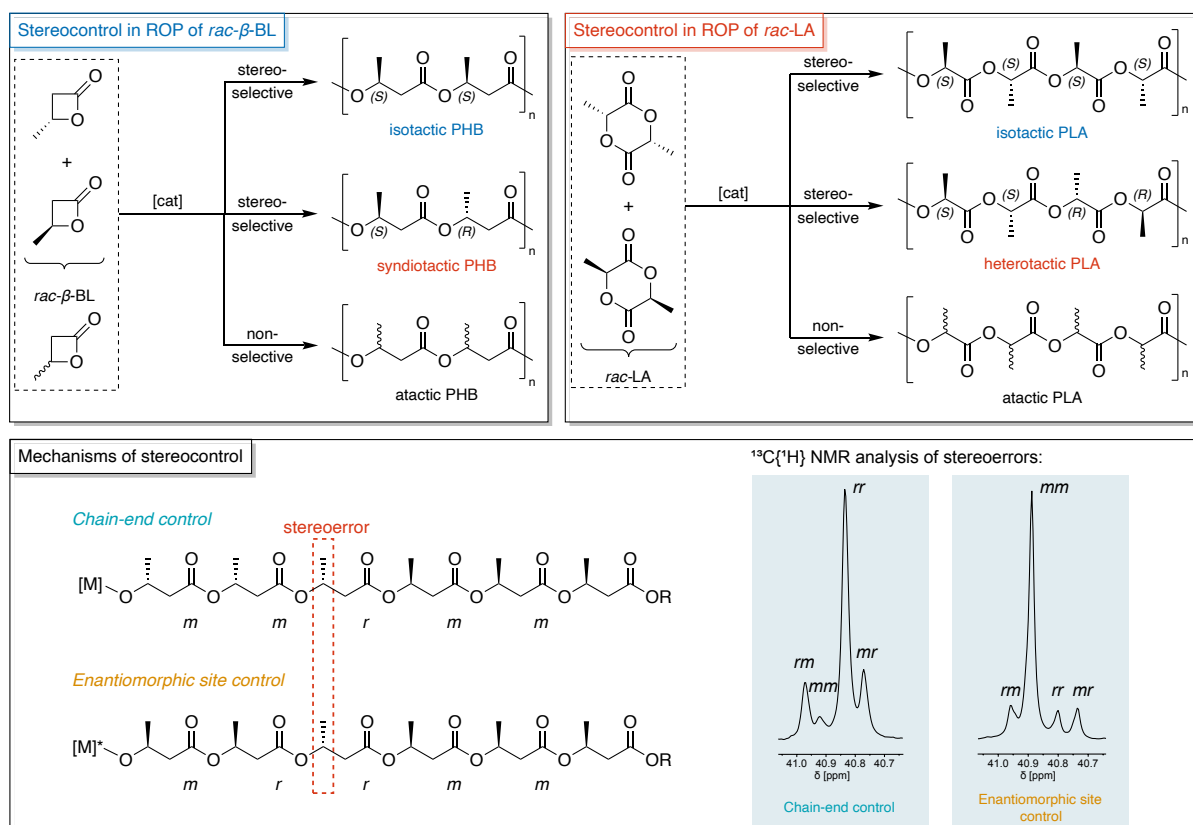
Figure 4. Stereomicrostructures of PHB and PLA accessible via ROP of *rac-β*-BL and *rac*-LA, respectively (top panels). Bottom panel: mechanisms of stereocontrol (left) and exemplary analysis of the triads of PHB via $^{13}C\{^1H\}$ NMR analysis in the methylene region (right). The NMR spectra show syndiotactic PHB produced via chain-end control mechanism and isotactic PHB produced via enantiomorphic site control mechanism (note the distribution of signal intensity of triads *rm, mm, mr* and *rm, rr, mr,* respectively).[27,29,104]
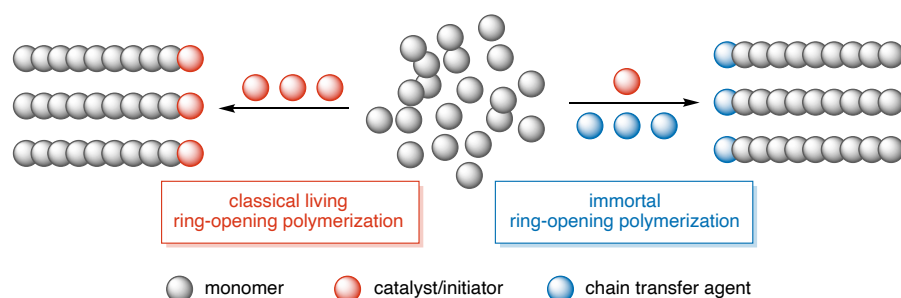
Scheme 7. Schematic illustration of differences between classical living ROP (left) and immortal ROP (right).[97]

2.3.2 All-Rounder Catalysts in the Ring-Opening Polymerization of Cyclic Esters

In chapter 2.1 the broad differences in polymerizability of cyclic esters depending on ring size and substitutions have been outlined. Given the variety of monomers that are available for ROP, it is highly desirable having catalysts at hand that show a high rate of polymerization for various lactones. Such initiators not only enable the simple and rapid synthesis of copolymers with tailored properties, but are also an important starting point for polymer chemists who focus on monomer design or polymer properties, and are interested in facile access toward the polymer without conducting elaborate catalyst screening studies. Here, all-rounder catalysts are the first choice in polymerization tests of novel monomers as previous successful ROP of related monomers usually indicates a high chance for efficient ROP of the new derivative (and is often observed empirically in the laboratory). Despite the ever-growing reports of catalysts for ROP of cyclic esters, the number of initiators combining a broad monomer scope with high polymerization activity for "benchmark" monomers β-BL, LA and ε-CL is fairly limited.[22,23,27-29,95] It is worth noting here, that some catalysts exhibit ultrahigh polymerization rates for one specific monomer yet activity for other lactones is strongly reduced.[105-107] Similarly, initiators that have shown high stereocontrol in the ROP of rac-LA are non-stereoselective when rac-β-BL is the monomer (and $vice$ $versa$).[106,108-118] Polymerization parameters such as activity and stereocontrol of a catalyst are thus not (necessarily) transferable to different monomers even though the mechanism of their ROP is identical. Despite the high ring strain of β-BL, its polymerization is particularly challenging due to its tendency for side reactions ($vide$ $supra$).[29] Sn(Oct)$_2$ is used in the industrial production of PLA and poly(ε-caprolactone) (PCL), and is commonly applied for a variety of lactones. Similarly, titanium tetraisopropoxide [Ti(O^{i}Pr)$_4$] and ZnEt$_2$ have found widespread application. These initiators however often require high reaction temperatures and are prone to severe transesterification side reactions, usually revealing poor molecular weight control.[22,28,48,59,119,120] The most prominent all-rounder catalysts for controlled ROP of a variety of cyclic esters are the β-diiminate zinc and yttrium amino-alkoxy-bis(phenolate) systems developed by Coates et al. and Carpentier et al. (Figure 5 **A** and **E**). In the ROP of β-BL, LA and ε-CL, moderate to high turn-over-frequencies (TOFs) from 156 to 154 440 h^{-1} were achieved.[108,109,121-123] The zinc complex showed high stereocontrol in the ROP of rac-LA giving heterotactic PLA while in the ROP of rac-β-BL only atactic PHB was generated.[108,109] Highly heterotactic PLA was also obtained by the yttrium initiator but high syndioselectivity was likewise observed in the ROP of rac-β-BL.[122,123] Various steric and electronic substitutions at the ligand framework and variations of the nucleophilic initiating group have been explored in those two systems after their initial discovery.[98,124] Beyond investigating catalyst design, they have found widespread applications such as in the ROP of challenging lactones,[40] in the synthesis of polycarbonates via ROP of cyclic carbonates or

ROCOP of epoxides and CO_2,[125-127] and in the production of sophisticated copolymer structures.[128]

Based on these promising results much research focused on zinc- and rare-earth metal-based (REM-based) complexes for ROP of lactones and the field is still dominated by catalysts utilizing these central metal atoms today.[27,68,95] For example, a simple catalyst generated *in situ* from Zn[N(SiMe$_3$)$_2$] and BnOH showed very high activity in LA and ε-CL polymerization, yet activity was reduced for β-BL, highlighting again the challenging nature of this monomer (Figure 5 **B**).[83] Initiators **C** and **D** showed similar ROP behaviors (Figure 5).[129,130] Regarding REM-based allrounder catalysts for cyclic ester ROP, La(O^{i}Pr)$_3$ revealed very high activity for LA and ε-CL, and reasonable polymerization rates for β-BL (Figure 5 **F**).[39] Even higher rates were achieved using cerium(III)–NHC complex **G** which interestingly produced high molar mass cyclic PLA. While activity was ultrahigh for ROP of LA (TOF = 270 000 h^{-1}), it was reduced for β-BL and ε-CL, albeit still high (TOF = 219 and 4440 h^{-1}, respectively), and the polymerizations exhibited good control.[107]
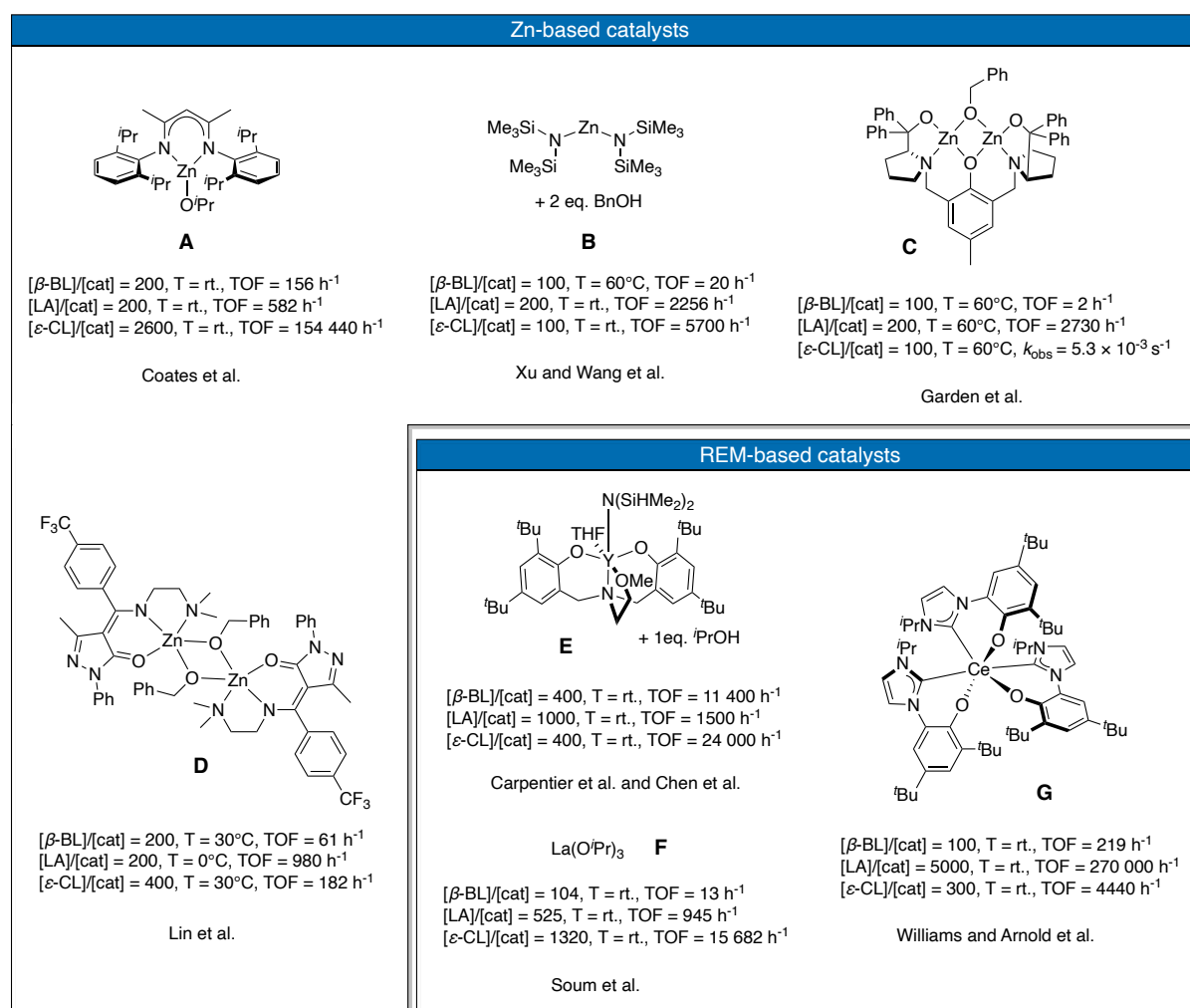
Figure 5. Highly active zinc and rare-earth metal all-rounder catalysts for the ROP of β-BL, ε-CL and LA.[39,83,107-109,121-123,129,130] Adapted from ref. 131 with permission from the Royal Society of Chemistry.

Besides zinc- and REM-based initiators, a plethora of catalysts with different metal centers as diverse as the periodic table has been reported but group 13 catalysts have shown particular potential. The interest in aluminum catalysts for ROP of cyclic esters is high as aluminum is an abundant, non-toxic metal. However, catalytic activity is often limited and high reaction temperatures are required. In contrast to most gallium compounds which are also hampered by low conversion, indium species have shown high potential in ROP catalysis and gained increasing research interest in recent years, mostly due to their strongly increased activity, higher air and moisture stability as well as tolerance against functional groups.[132,133] This is demonstrated by a simple and robust catalyst system based on InCl$_3$, BnOH and triethylamine (NEt$_3$) which was found to efficiently catalyze the heteroselective ROP of *rac*-LA (Figure 6 **H**).[134,135] It was further used in polymerizations of *ε*-CL and *ε*-decalactone (*ε*-DL), which is a biobased alternative to *ε*-CL, and here even showed tolerance for primary amines as initiators besides typical alcohol derivatives.[136] Mehrkhodavandi et al. reported a highly active dinuclear ONN-type indium catalyst for the ROP of *β*-BL and LA (Figure 6 **I**). The catalyst also exhibited high control over the polymerization under immortal ROP conditions using ethanol or hydroxy-terminated poly(ethylene glycol) as chain transfer agents.[102,137]
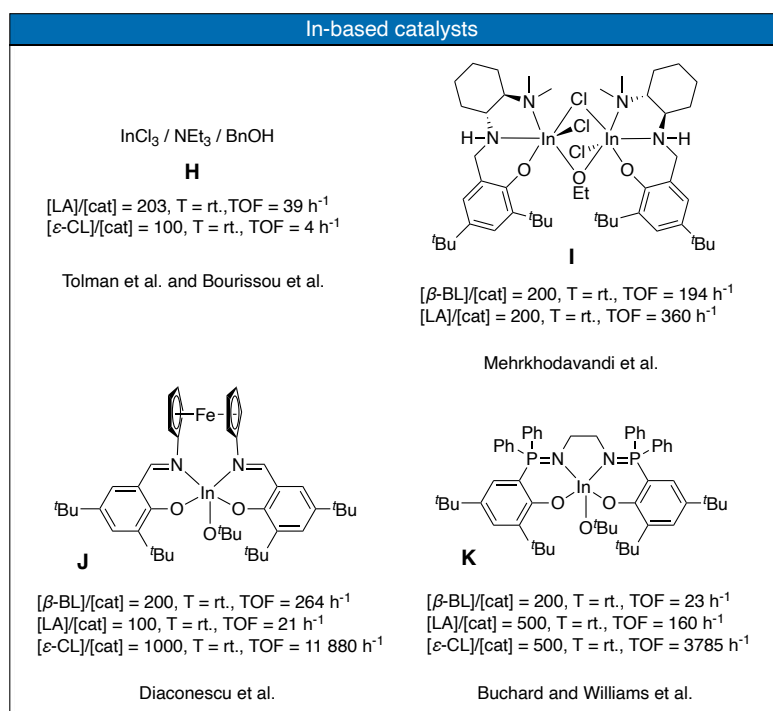
Figure 6. Highly active indium all-rounder catalysts for the ROP of *β*-BL, *ε*-CL and LA.[102,111,134-138] Adapted from ref. 131 with permission from the Royal Society of Chemistry.

Promising results were achieved with salen-type and phosphasalen-type complexes (Figure 6 **J** and **K**). Compound **J** showed high activity for 4- to 7-membered monomers including *β*-BL, *δ*-VL, LA, *ε*-CL as well as trimethylene carbonate.[138] A library of phosphasalen complexes was

reported by Williams et al. which are capable of efficiently producing highly isotactic PLA (P_m up to 0.92) via a chain-end control mechanism. In ROP of *rac-β*-BL however no stereocontrol was observed and only atactic PHB isolated. These initiators also exhibited a broad monomer scope combined with high activity for *ε*-CL, *ε*-DL, and *δ*-caprolactone, highlighting the potential of indium-based initiators in ROP.[111,139]

2.3.3 Catalysts for Stereoselective Ring-Opening Polymerization of Cyclic Esters

Besides catalysts showing broad monomer scope, their capability of inducing stereoselectivity in ROP is also of crucial importance as material properties of PHB and PLA are strongly dependent on their tacticity (see chapter 2.2).[22,27,29,63] Initiators that combine monomer scope with high activity and high stereoselectivity are exceptionally rare, and catalyst design often focuses on achieving high stereocontrol for one particular monomer. An exceptional case are the yttrium bis(phenolate) systems (Figure 5 **E** and derivatives; and Figure 7) with high stereoselectivity for *rac-β*-BL as well as *rac*-LA.[122,123] Here, detailed investigations have shown the striking influence of the *ortho*-phenolic substituent R^1 on stereoselectivity. The larger the steric demand of the substituent, the higher the heterotacticity of the PLA obtained was (Figure 7).[140,141]

R^1		-*t*Bu	-CMe$_2$Ph	-CMe$_2$*t*Bu	-CPh$_3$	-CMe$_2$(4-CF$_3$Ph)
R^2		*t*Bu	Me	Me	Me	Me
rac-LA	P_r	0.81	0.91	0.95	0.95	-
rac-β-BL	P_r	0.80	0.91	0.70	0.94	0.83
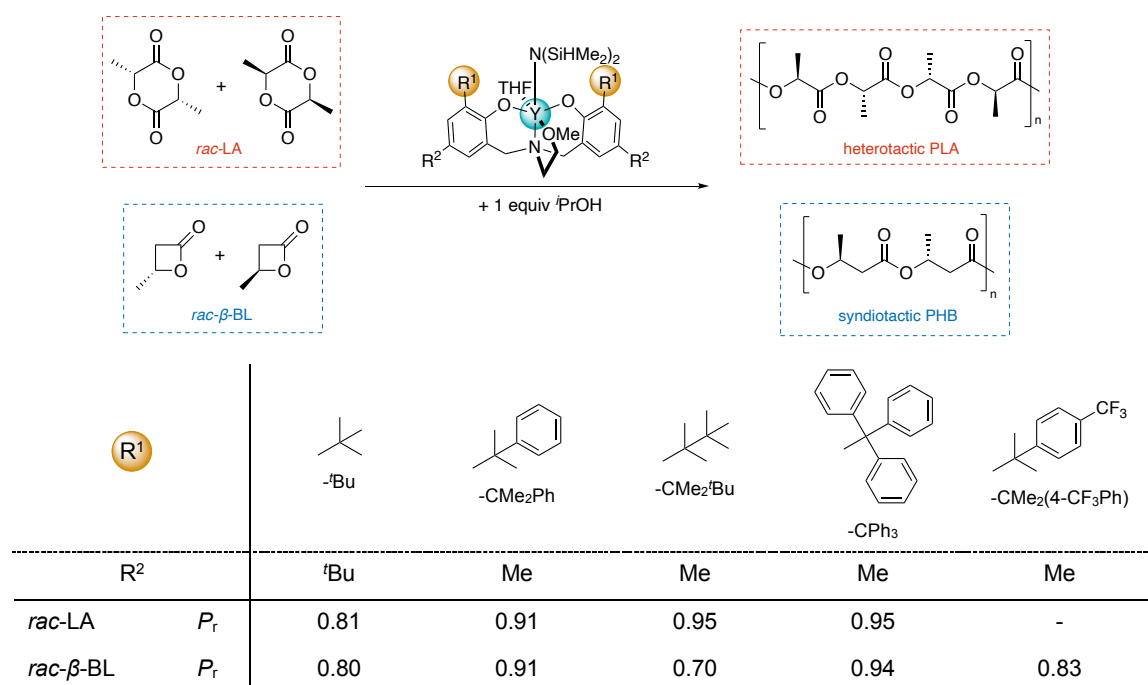
Figure 7. Correlation of stereoselectivity in ROP of *rac*-LA and *rac-β*-BL with *ortho*-phenolic position R^1 using yttrium bis(phenolate) systems. Adapted from ref. 140 with permission from the Royal Society of Chemistry.

A similar trend in the ROP of *rac-β*-BL was observed as syndioselectivity increased from -CMe$_3$ to -CMe$_2$Ph to -CPh$_3$ (P_r = 0.80, 0.91 and 0.94, respectively). The stereoselectivity however was not purely dependent on the steric demand as a sterically comparable -CMe$_2$^{t}Bu group resulted in a decline (P_r = 0.70). The additional importance of electronic factors was demonstrated by a trifluoro methyl substituted -CMe$_2$Ph group (i.e. -CMe$_2$(4-CF$_3$Ph)) which led to a substantial drop in syndioselectivity from P_r = 0.91 to 0.83 (Figure 7).[140-142] Density functional theory (DFT) calculations further highlighted these electronic factors and suggested C–H···π interactions between the methylene protons of the growing polymer chain and the phenyl ring of the *ortho*-substituent, stabilizing the active species by 5–10 kcal mol^{-1}. Analogous DFT calculations for these initiators revealed the absence of such interactions in the ROP of *rac*-LA, explaining the strict dependence of stereoselectivity on bulkiness of the *ortho*-substituent observed. Nevertheless, in both cases the mechanism of stereocontrol was chain-end control.[140,141]

While the synthesis of heterotactic PLA from *rac*-LA is relatively easily achieved with defined organometallic catalysts (often via a chain-end control mechanism), its isotactic microstructure has turned out to be far more difficult to access.[22,27] Pioneering work was conducted by Spassky et al. using salen-type aluminum complexes capable of kinetic resolution polymerization of *rac*-LA via an enantiomorphic site control mechanism affording highly isotactic PLA (Figure 8 **L**).[143] Gibson et al. investigated aluminum salan complexes with various ligand substitution patterns and were able to establish structure-property relationships in the ROP of *rac*-LA. Salan complexes with an unsubstituted *ortho*-phenolic position, for example, demonstrated strong isoselectivity (P_m = 0.79) while chloro substitution afforded highly heterotactic PLA (P_r = 0.96) (Figure 8 **M**).[144] Similarly, catalysts sharing the same ligand platform but showing a switch in stereocontrol based on their ligand backbone substitution were reported by Auffrant and Williams et al. (Figure 8 **N**). While yttrium phosphasalen initiators with an ethylene backbone were extremely active in ROP of *rac*-LA (TOF up to 158 000 h^{-1}) and produced highly heterotactic PLA (P_r up to 0.90), their counterparts with an additional NH–donor ligand in the backbone gave highly isotactic PLA (P_m up to 0.84) with excellent control over the polymerization. In both cases a chain-end control mechanism governed the stereocontrol.[145] Further studies with respective lutetium and lanthanum complexes revealed a metal-size dependent stereoselectivity and additionally indium derivatives were found to promote the isoselective ROP of *rac*-LA (*vide supra*).[111,115,139] Apart from those selected examples, the number of isoselective catalysts for the ROP of *rac*-LA has been constantly growing within the last two decades and today not only diverse metal-based initiators have shown high potential but also an increasing number of stereoselective organocatalysts.[27]
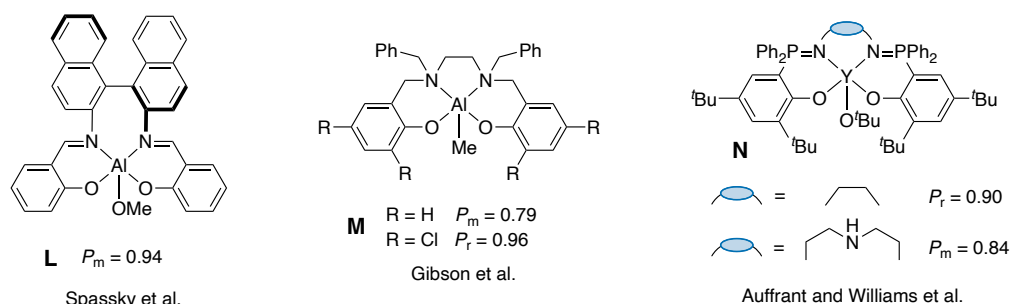
Figure 8. Catalysts for the highly stereoselective ROP of *rac*-LA.[143-145]

When it comes to the ROP of *rac*-β-BL, achieving stereocontrol is much more difficult compared to *rac*-LA due to the challenging nature of this monomer. Nevertheless, a syndiotactic microstructure of PHB is overall easier to access than an isotactic one (something the monomer has yet in common with *rac*-LA).[22,27,29,68,91] Apart from the previously discussed prominent yttrium bis(phenolate) system by Carpentier et al.,[98,140] various other REM-based catalysts demonstrated high syndioselectivity in the ROP of *rac*-β-BL such as bis(guanidinate) complexes **O** or yttrium salan complex **P** (Figure 9).[68,99,146-148] Magnesium and zinc complexes bearing a chiral aminophenolate framework produced syndiotactic-enriched PHB (P_r up to 0.75, Figure 9 **Q** and **R**) and tin-based catalysts showed a similar degree of stereocontrol, yet activity was comparably poor.[68,106,149]
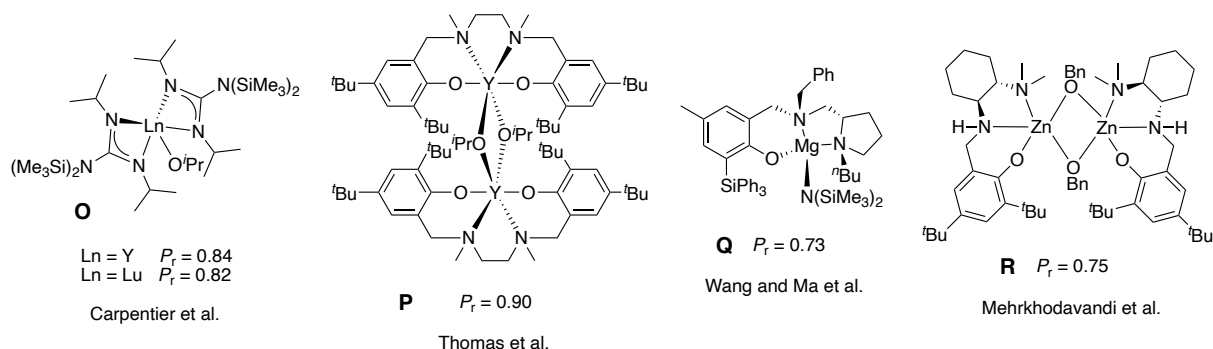
Figure 9. Catalysts for the syndioselective ROP of *rac*-β-BL.[99,106,147-149]

In contrast to that, catalysts enabling the synthesis of isotactic PHB, which has superior material properties compared to atactic or syndiotactic PHB, remain particularly scarce in literature despite intensive research efforts since the 1960s.[23,29,68] Pioneering work by Agostini, Tani and others in the 1970s revealed that partially hydrolyzed aluminum alkyl species produce PHB with a major atactic fraction and only a minor fraction of isotactic polymer ($P_m \approx 0.8$). The isotacticity of the crude samples reached up to $P_m = 0.65$. Another drawback of these catalyst systems besides the PHB product mixture generated (most likely due to ill-defined and various catalytically active species present) was their poor catalytic activity.[104,150-155] Improvements were made by Spassky et al. using a catalyst system based on $ZnEt_2$ and

(R)-3,3-dimethylbutane-1,2-diol that allowed for the kinetic resolution polymerization of *rac-β*-BL yielding isotactic (R)-PHB and enriched unreacted (S)-enantiomer in 46%ee (Figure 10 **S**). A higher activity compared to the aluminum systems was observed, yet the product again consisted of a mixture of atactic methanol-soluble and isotactic-enriched insoluble ($P_m \approx 0.8$, ≈ 25 wt%) fractions. Replacing $ZnEt_2$ in this system for $AlEt_3$ or $CdMe_2$ resulted in an almost complete loss of stereoselectivity.[156]

The first discrete metal complexes for the synthesis of isotactic-enriched PHB were reported by Rieger et al. in 2008. These chromium salophen catalysts generated high-molecular weight PHB (M_w up to 780 kg mol^{-1}, $Đ > 5.2$) with an isotacticity of P_m up to 0.67 and melting temperatures within a range of 116 to 149°C (Figure 10 **T**). Besides the broad dispersity of the obtained material, control over the molecular weight was also limited. Activity of the catalysts was positively influenced by substitution with electron withdrawing halogen substituents at the phenyl backbone but stereoselectivity was almost unaffected thereof. Strongly electron withdrawing groups such as -CF_3 or -CN as well as alkyl substitutions however resulted in a loss of isotacticity.[157,158] A stereocontrol mechanism based on bimetallic cooperation of two achiral catalyst centers was initially suggested, however, later studies have shown a complex mechanism to be present which involves the generation of heterogeneous catalytically active species.[157,159] Related conformationally flexible dimeric chromium salophen complexes showed an increased activity in ROP of *rac-β*-BL but stereocontrol was lost in this case.[160]
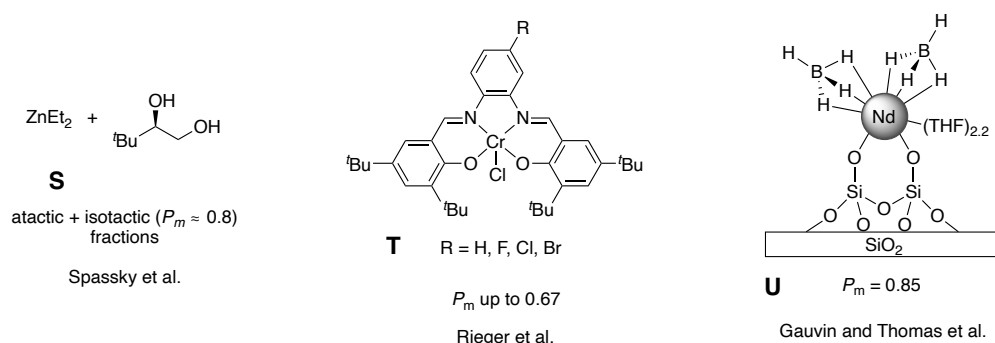
Figure 10. Catalysts for the isoselective ROP of *rac-β*-BL reported by the groups of Spassky, Rieger, and Gauvin and Thomas.[156,157,161]

A heterogenous catalyst system based on silica-supported neodymium borohydrides for the isoselective polymerization of *rac-β*-BL was reported by Gauvin, Thomas and co-workers. While the unsupported compound $Nd(BH_4)_3THF_3$ only generated atactic PHB, grafting of this precursor onto non-porous dehydroxylated silica gave a well-defined bis(borohydride) surface species that was capable of producing highly isotactic PHB ($P_m = 0.85$) with high control over the polymerization (Figure 10 **U**). This represents the highest isoselectivity in ROP of *rac-β*-BL achieved to date. Despite these promising results, the poor activity of the catalyst and the

limitation in achieving high molecular weight (TOF = 6 h^{-1}, M_n < 12 kg mol^{-1}) hamper the industrial application of this system. The respective silica-supported lanthanum catalysts surprisingly showed no stereocontrol and additionally demonstrate the complexity of the grafting approach and understanding its relevant parameters.[161]

Two very recent reports by Yao et al. and Robinson et al. highlighted the potential of homogeneous REM-based catalysts: the first group developed yttrium and ytterbium salan-type complexes while the latter used a lanthanum complex with a bis(phenolate) framework.[94,162] Particularly interesting in the case of the salan complexes was the stereoselectivity-dependent substitution of the tertiary amine in the ligand framework (Figure 11). An *N*-phenyl substitution led to an isotactic stereomicrostructure (P_m = 0.66–0.72), whereas *N*-cyclohexyl gave a syndiotactic one (P_m = 0.22–0.23) and *N-tert*-butyl an atactic one (P_m = 0.52–0.54). This switch in selectivity was unprecedented and the authors speculated that the reason for this was rather an electronic than a steric effect of the substituents at the ligand. The influence of the metal center was small as both yttrium and ytterbium complexes followed the same trend. Reducing the polymerization temperature from 25 to 0°C further enabled a higher stereocontrol and PHB with a P_m of 0.77 was obtained. The polymers were characterized by a relatively high molecular weight (M_n up to 81 kg mol^{-1}) and slightly broadened dispersity (*Đ* = 1.2–2.2). Polymerization control could be increased by addition of *i*PrOH to the catalyst prior to ROP, albeit at the expense of reduced stereocontrol. The variety of stereomicrostructures accessible with these catalysts highlights the potential of the highly tunable salan framework regarding steric and electronic factors.[162]
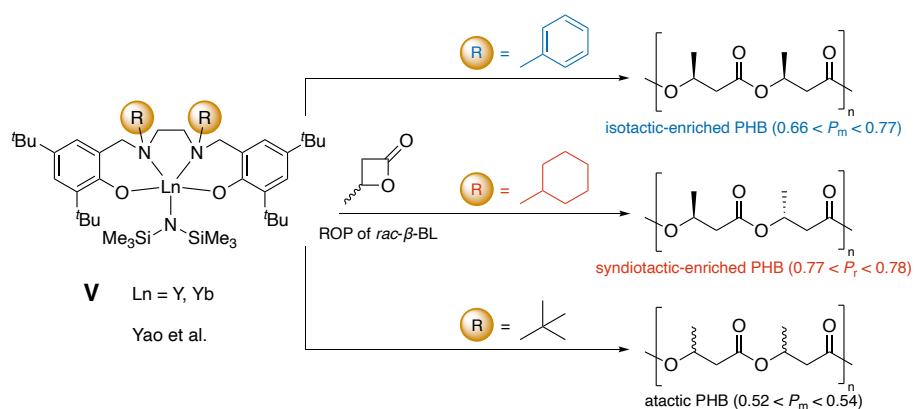
Figure 11. Yttrium and ytterbium salan complexes reported by Yao et al. showed a high sensitiveness on the stereoselectivity in ROP of *rac-β*-BL depending on the *N*-substituent.[162]

The catalyst developed by the group of Robinson is based on a tridendate amino-bis(phenolate) framework closely related to initiator **E** but without a coordinating donor fragment and instead with a non-coordinating benzyl substituent (Figure 12). While this lanthanum catalyst produced basically atactic PHB (P_m = 0.57), the addition of neutral achiral

donor ligands such as phosphine oxides (OPR$_3$) was crucial for boosting isoselectivity. When trioctylphosphine oxide was used, ROP of *rac-β*-BL became isoselective and stereocontrol could be enhanced even more by reducing the polymerization temperature from 25 to 0°C (P_m = 0.75 and 0.80, respectively). A reduction to –30°C did not result in any further improvements. Molecular weight of the synthesized PHB was limited to 19 kg mol^{-1} as crotonyl chain-end formation and catalyst inactivation were occurring as side reactions. Mechanistic investigations revealed chain-end control as the present stereocontrol mechanism.[94] Follow-up work showed that the class of donor ligands used in this catalyst system is not limited to phosphine oxides but also *N*-oxides can be used. With this donor class, the highest isoselectivity obtained was P_m = 0.73 at room temperature (similar to phosphine oxides) and P_m = 0.82 at –30°C, which is the highest isoselectivity in ROP of *rac-β*-BL achieved to date with homogenous catalysts. Apart from the slight increase in isotacticity, *N*-oxides considerable amplified the reactivity of the catalyst compared to phosphine oxide donor ligands (TOF = 1900 vs. 190 h^{-1}, respectively).[163]
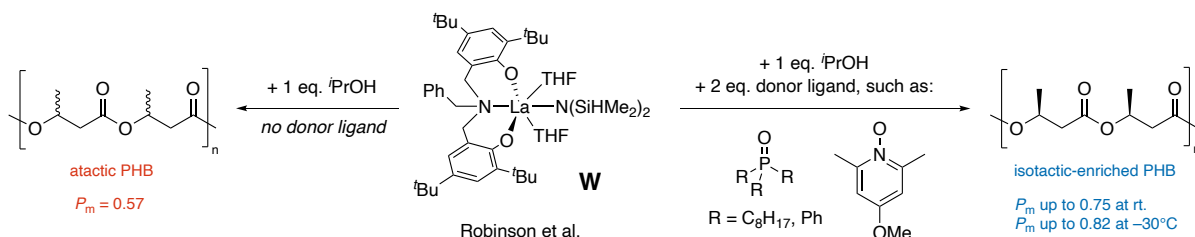
Figure 12. Isoselective ROP of *rac-β*-BL with a lanthanum bis(phenolate) catalyst in the presence of phosphine oxide or *N*-oxide donor ligands. The absence of donor ligands results in loss of stereocontrol.[94,163]

The current catalytic systems available in literature for the isoselective ROP of *rac-β*-BL are all limited by either poor activity, inaccessibility of high molecular weight, low degree of isotacticity (particularly at room temperature) or combinations thereof, highlighting the importance of designing catalysts that fulfill all these factors in order to achieve the replacement of commodity plastics such as *i*-PP by biodegradable and chemically recyclable PHB.[23,68]

The tedious search for isoselective catalysts in ROP of *rac-β*-BL and the relatively little progress achieved over the decades inspired Chen and co-workers to adapt a different approach by developing a new synthetic route towards PHB. Based on the fact that the dimer of L-lactic acid (i.e. L-LA) is used in the ROP process for commercial PLA production, the authors hypothesized that using the dimer of 3-hydroxybutyric acid (i.e. an 8-membered cyclic diolide (DL)) instead of the cyclic monomer (i.e. *β*-BL) might facilitate simple access towards PHB. The strongly increased steric demand of DL compared to *β*-BL might be additionally beneficial for synthesizing isotactic PHB from *racemic*-diolide (*rac*-DL). Indeed, employing a series of yttrium salen-type complexes, highly isotactic, high-molecular weight PHB was

obtained with excellent control over the polymerizations (M_n up to 154 kg mol^{-1}, $Đ < 1.1$).[55] Similarly to the yttrium bis(phenolate) systems reported by Carpentier et al. for the synthesis of syndiotactic PHB (Figure 5 **E**),[98,140] the yttrium salen catalysts showed a dependence of stereoselectivity on the steric demand of the *ortho*-phenolic position. Increasing the substituent from -CMe$_3$ to -CMe$_2$Ph enhanced isoselectivity (P_m = 0.91 and 0.96, respectively) and perfectly isotactic PHB was obtained when even bulkier -CPh$_3$ groups were in place ($P_m > 0.99$, Figure 13).[55] Using these catalysts operating via an enantiomorphic site control mechanism also enabled a kinetic resolution polymerization where the enantiomerically pure salen catalysts with cyclohexyl backbones (*S,S* or *R,R*) polymerized the contrary enantiomer of *rac*-DL, i.e. *R,R* or *S,S* and left the other enantiomer untouched, thus giving access to pure (*R*)-PHB or (*S*)-PHB.[55,57] Subsequent works showed that copolymerization of *rac*-DL with *meso*-DL (a side product during *rac*-DL synthesis) or with other 8-membered diolides having different alkyl side chains (Et, ^{n}Bu) yields polymers with polyolefin-like thermomechanical properties.[56,57] However, considering the industrial applicability of this elegant novel approach, the multistep monomer synthesis is currently limiting its commercialization[55] and the most viable pathway towards isotactic PHB from an industrial point of view is still the ROP of *rac-β*-BL due to its atom-efficient preparation from commercially available large-scale feedstocks (see chapter 2.2).[23]
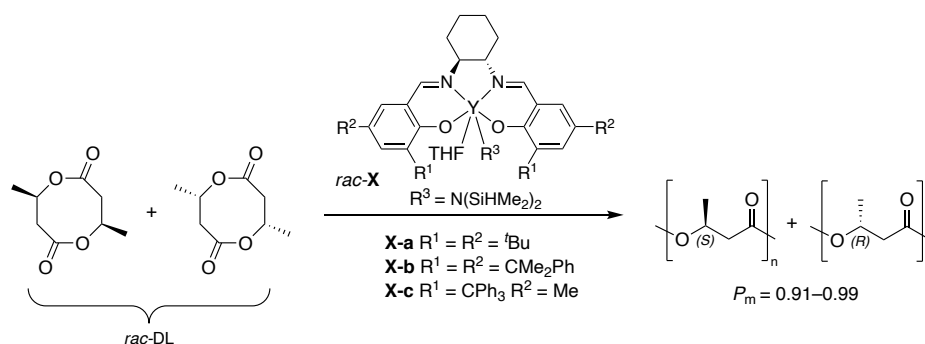
Figure 13. ROP of *rac*-DL to access highly isotactic PHB using yttrium salen catalysts.[55]

2.4 Synthesis of Oxygenated Copolymers

2.4.1 General Remarks

Apart from improving the properties of polymers by tuning their stereochemistry such as previously described for PLA or PHB, copolymerization offers an important pathway for synthesizing polymeric materials with defined physical and chemical properties. These characteristics can be precisely adjusted by a plethora of comonomers available, and thus tailored for specific applications.[23,28,30,164-166] For instance, toughening of PLA and PHB has been achieved by copolymerization with ε-CL.[167,168] The thermal, mechanical and also degradation behaviors of a copolymer are not only strongly influenced by its different comonomers and their relative molar composition but also by its macromolecular architecture such as random, gradient, alternating or block structure, as well as linear, graft, or star/dendritic structure (Scheme 8, left).[23,28,30,164-166] Attempting the ROCOP of lactones and related monomers requires a catalyst that is capable of efficient initiation and propagation for each specific monomer used, otherwise only homopolymers yet no copolymers are generated. Here, all-rounder catalysts (see chapter 2.3.2) combining a broad monomer scope with high catalytic activity are extremely beneficial in order to rapidly access defined copolymers. The synthesis of block copolymers has attracted particular attention, for example the synthesis of ABA triblock copolyesters with hard "A" blocks and soft "B" block for use as thermoplastic elastomers,[169] or the sequence control from mixed-monomer feedstocks in order to access sophisticated block copolymer structures with the ultimate goal of imitating Nature's sequence control in biological macromolecular syntheses.[170-172] Generally, common synthesis routes towards block copolymers include sequential monomer addition, kinetic control as well as switchable catalysis from one-pot monomer mixtures (Scheme 8, right).[30,173]
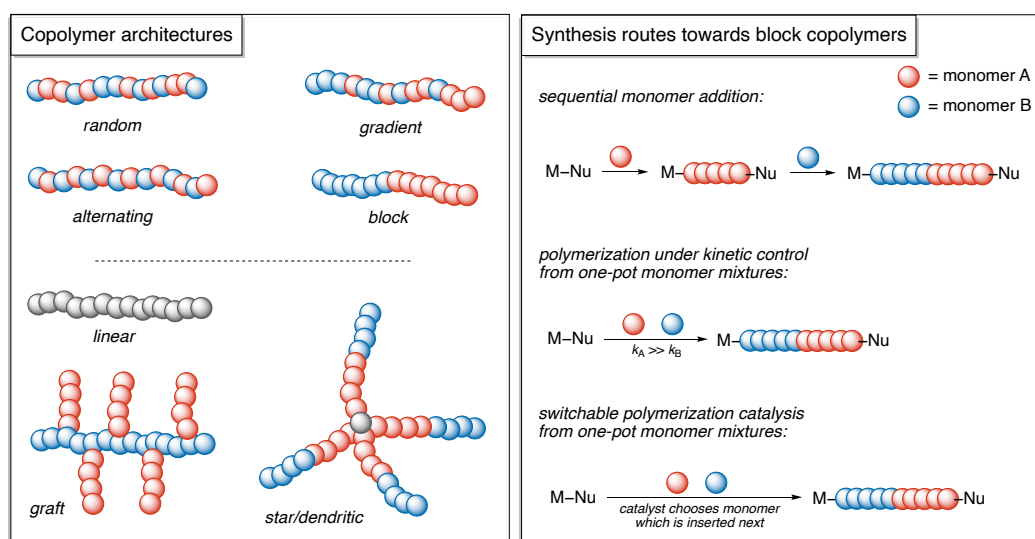
Scheme 8. General architectures of copolymers (left) and synthesis routes towards block copolymers (right).[23,28,30,165,173]

2.4.2 Synthesis of Block Copolyesters via Sequential Monomer Addition

The sequential addition approach is the most typically applied synthesis route towards block copolyesters. The scope of lactones applicable for this method is only limited by the prerequisite that the catalyst has to show activity in ROP towards all co-monomers and exhibit a living-type polymerization mechanism. After full consumption of monomers and synthesis of the first block, the second monomer is added to the reaction mixture, generating the second block of the polymer. Further sequential additions allow for the production of tri-, tetra-, or pentablock copolymers (and so on), however, representing a rather elaborate synthesis strategy with some limitations. The living character of the polymerization has to be sustained otherwise only homopolymers or mixtures of homo- and block copolymers are obtained, and transesterification side reactions have to be absent as those would result in a scrambling of the block structure and would ultimately give random copolymers. Additionally, some catalysts have shown limitations regarding the order of monomer addition such that reversing the order resulted in unsuccessful copolymerization.[28,30] For example, the sequential addition copolymerization of β-BL with benzyl-β-malolactone (MLABe) using a β-diiminate zinc complex **A** (Figure 5) was successful when β-BL was introduced first and then MLABe, however, when MLABe was added first, subsequent β-BL polymerization was very sluggish. Using organocatalysts 1,8-diazabicyclo[5.4.0]undec-7-ene (DBU), 1,5,7-triazabicyclo[4.4.0]-dec-5-ene (TBD) and 2-*tert*-butylimino-2-diethylamino-1,3-dimethyl-perhydro-1,3,2-diaza-phosphorine (BEMP), successful blockcopolymer synthesis of β-BL and MLABe was achieved regardless of monomer order. Remarkably, in simultaneous copolymerization approaches, BEMP polymerized MLABe faster than β-BL despite similar rates in homopolymerizations, thus demonstrating a monomer-selective behavior even though very long reaction times were required and relatively poor polymerization control was observed.[174] Subsequent hydrogenolysis of the benzyloxycarbonyl of these copolyesters afforded amphiphilic poly(β-malic acid)-*b*-PHB (PMLA-*b*-PHB) which formed nanoparticles with promising characteristics for potential drug delivery systems.[175] Dinuclear indium catalyst **I** (Figure 6) was employed by Mehrkhodavandi et al. in the synthesis of elastomeric PLA-PHB-PLA triblock copolymers which demonstrated significantly improved elongation at break, albeit at the expense of poor tensile strength.[176] The same catalyst was also capable of producing star-shaped PLA-PHB block copolymers when a trifunctional alcohol was used as chain transfer agent in a sequential addition approach.[177] Later, air- and moisture stable indium salan-type catalysts were reported by the same group for block copolymerization of β-BL and LA showing excellent control over the ROCOP (Figure 14).[103] A simple catalyst system based on InCl$_3$, NEt$_3$ and BnOH that was previously found to catalyze the stereoselective ROP of *rac*-LA (*vide supra*) was also efficiently producing PCL-*b*-poly(ε-decalactone) (PCL-*b*-PDL) or PDL-*b*-PCL copolymers via sequential addition of monomers (Figure 14).[136] Similarly, di- and triblock

copolyesters PDL-*b*-PHB and PDL-*b*-PHB-*b*-PDL were obtained in a sequential synthetic protocol using a yttrium salan-type catalyst, whereas, approaches of simultaneously copolymerizing β-BL and ε-DL monomer mixtures failed (Figure 14). Due to the immiscibility of the crystalline, syndiotactic PHB block and the amorphous PDL block, microphase separation was observed.[178] The idea of tuning the material properties of PHB by introducing a soft block was also revisited by Rieger et al. who demonstrated that yttrium bis(phenolate) catalyst **E** and a derivative with a bifunctional initiator are capable of efficiently copolymerizing β-BL and (–)-menthide, a sustainable lactone sourced from the cyclic terpene (–)-menthone (Figure 14). Di- and triblock copolymers were accessible and their thermomechanical properties characterized in detail. The ABA copolyester showed microphase separation, similarly to the PDL-*b*-PHB-*b*-PDL material, and increased elongation at break compared to bacterial PHB, albeit at the expense of a strongly reduced Young's modulus.[179] Those selected examples not only highlight the tunability of material properties by block copolymerization via sequential addition of monomers but also the potential of indium and yttrium catalysis in ROCOP.
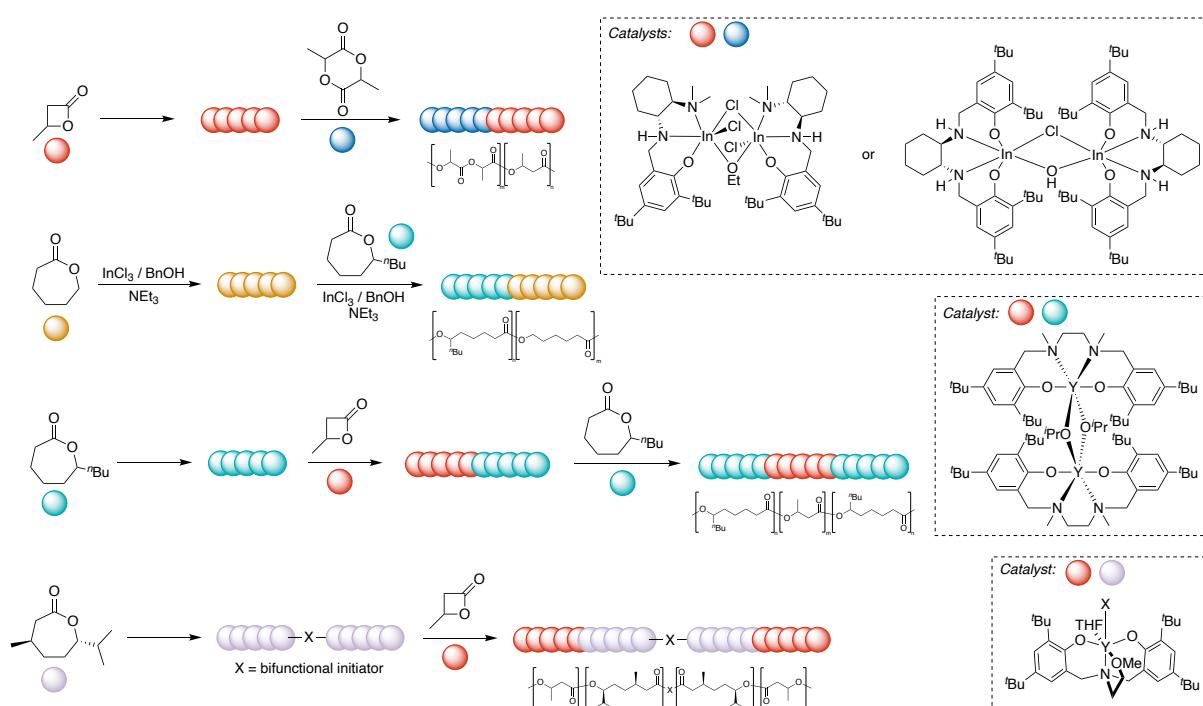
Figure 14. Sequential copolymerizations of cyclic esters with a focus on β-BL as well as indium and yttrium catalysis.[103,136,176-179]

2.4.3 Synthesis of Block Copolyesters via Kinetic Control

Another method of synthesizing block copolyesters is the ROCOP of a one-pot lactone monomer mixture under kinetic control. Here, block copolymers are generated based on the

considerably higher polymerization rate for monomer A (k_A) than for monomer B (k_B). The extent of the tapering region in the block copolymer is strongly depending on the k_A/k_B-ratio: the higher the ratio, the smaller the tapering phase. While this is a more elegant approach compared to the sequential addition of monomers from a synthetic point of view, some issues are still present such as large tapering regions when the k_A/k_B-ratio is not as high. Contrary, a very high k_A/k_B-ratio is beneficial for only very small tapering to occur, but long reaction times are needed to generate the B-block of the copolymer as the polymerization rate for monomer B has to be low by definition in this specific case.[30] The latter was exploited by Jones et al. using a hafnium tris(phenolate) complex for the copolymerization of a LA and β-BL one-pot monomer mixture. Consumption of β-BL was much slower than that of LA, and even after long reaction times (>10 h) conversion of β-BL was below 15%.[180] An elegant work combined the simultaneous copolymerization of a macrolactone, ω-pentadecalactone, with small-sized lactones ε-CL or δ-VL exploiting the different polymerizability of the monomers, i.e. entropically vs. enthalpically driven. The catalyst system based on an N-heterocyclic olefin and Lewis acidic metal chlorides readily polymerized ε-CL or δ-VL, followed by ω-pentadecalactone. However, transesterifications ultimately resulted in randomized structures and no block copolymers were obtained, highlighting the importance of control over the ROCOP in order to retain the macromolecular architecture.[181] Guided by the hypothesis that the high ductility of PCL homopolymer could reduce the brittleness of PHB, Chen et al. attempted the copolymerization of 8-membered rac-DL with ε-CL. The lanthanum and yttrium salen-type catalysts successfully generated PHB-b-PCL copolymers via kinetic control such that rac-DL was rapidly consumed, followed by slower ε-CL polymerization. Most importantly, the defined block copolymer showed a high ultimate tensile strength and Young's modulus combined with a much increased elongation at break compared to initial PHB homopolymer, demonstrating the vast potential of copolymerizations for improving material properties.[167]

2.4.4 Switchable Catalysis for the Generation of Oxygenated Block Copolymers from One-Pot Monomer Mixtures

Previously described approaches for the synthesis of block copolymers have severe drawbacks such as synthetic complexity (sequential addition approach), or long reaction times or large tapered regions in the polymer (kinetic control approach). These have consequently inspired researchers to develop simpler protocols for the generation of precise block copolymers via ROP. In recent years, switchable catalysis showing chemoselectivity in monomer mixtures has been developed in the field of ROP and is receiving ever-increasing research interest.[171,173,182,183] Early work by Coates et al. demonstrated that the terpolymerization of cyclohexene oxide (CHO), diglycolic anhydride and CO_2 using a

β-diiminate zinc complex produced a highly resolved polyester-*b*-polycarbonate block copolymer. Monitoring the reaction progress via *in situ* infrared (IR) spectroscopy revealed that the ROCOP of CHO and the anhydride occurs first, generating the polyester block, and only after complete consumption of the anhydride, ROCOP of CHO with CO_2 begins and leads to a polycarbonate block (Figure 15A). The mechanism includes two distinct catalytic cycles, a polyester and a polycarbonate cycle (Figure 15B).[184] In 2014, Williams et al. were the first to extend the concept of chemoselective polymerizations to the ROCOP of epoxides/CO_2 and lactones, also giving polyester-*b*-polycarbonate block copolymers.[185]
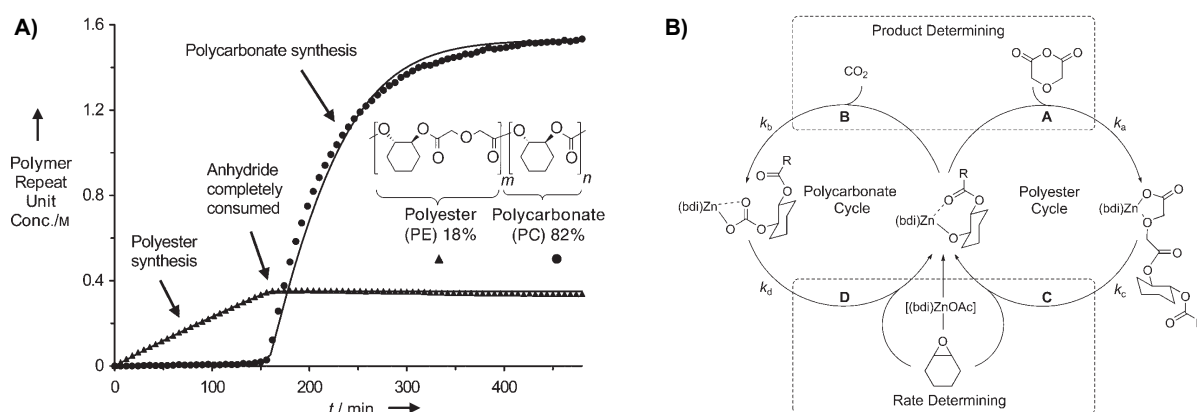
Figure 15. A) Concentration of repeat units vs. time plot in the terpolymerization of CHO, diglycolic anhydride and CO_2 using a *β*-diiminate zinc complex and B) proposed mechanism for the switchable catalysis producing polyester-*b*-polycarbonate block copolymers. Reprinted with permission from ref. 184. Copyright 2008 John Wiley & Sons.

Later, the monomer scope was further broadened beyond epoxides/CO_2, anhydrides/epoxides and lactones to *O*-carboxyanhydrides.[173,183,186-189] A plethora of catalysts has been reported to successfully provide block copolymers via switchable catalysis from this large monomer feedstock since then.[128,173,183,190-199] In these instances, the generation of copolymers is based on the capability of the catalyst to combine different catalytic cycles such as the ROP of lactones and the ROCOP of epoxides/CO_2. The macromolecular block structure is obtained as a consequence of the distinct reactivity differences of the diverse monomer classes: the descending order of reactivity is *O*-carboxyanhydrides > anhydrides/epoxides > epoxides/CO_2 > cyclic esters. Thus, after consumption of the most reactive monomer class in the one-pot mixture, the catalyst automatically switches to the next monomer class.[173,183]

Besides the utilization of monomer reactivity in switchable ROP catalysis, another approach for the generation of sequence-controlled polymers includes polymerization catalysts that can be switched between two or more states by external stimuli such as redox or electrochemical stimuli.[171,182,200-202] Here, much progress has been achieved in the context of reversible "on/off" switching of polymerizations, triggered by switching the catalyst from one state to the other (and back).[203-207] More complex strategies comprised redox-switchable catalysts that show high selectivity towards one specific monomer class such as cyclic esters in the reduced state

and high selectivity towards another monomer class such as epoxides in the oxidized state (while not showing polymerization activity for the other monomer in the respective state).[208,209] In this context, redox-switchable catalysts demonstrating monomer-selective behavior within *one* class of monomers are extremely rarely reported in literature due to challenges associated with similar monomer reactivity.[201,202] The most prominent example showing such an orthogonal reactivity for two different lactones is a redox-switchable titanium catalyst developed by Diaconescou et al. (Figure 16). From a one-pot monomer mixture consisting of LA and ε-CL, the initiator in its reduced form polymerized LA, while showing almost no activity for ε-CL. Oxidation of the catalyst resulted in ROP of ε-CL with almost no conversion of LA in this step, ultimately yielding PLA-*b*-PCL block copolymers. However, detailed characterization revealed that tapering indeed occurred and the copolymer is in fact best described as poly[block(LA-minor-CL)-block(CL-minor-LA)], highlighting the highly challenging task of creating sequence-controlled copolymers from one-pot mixtures of the *same* monomer class.[210]
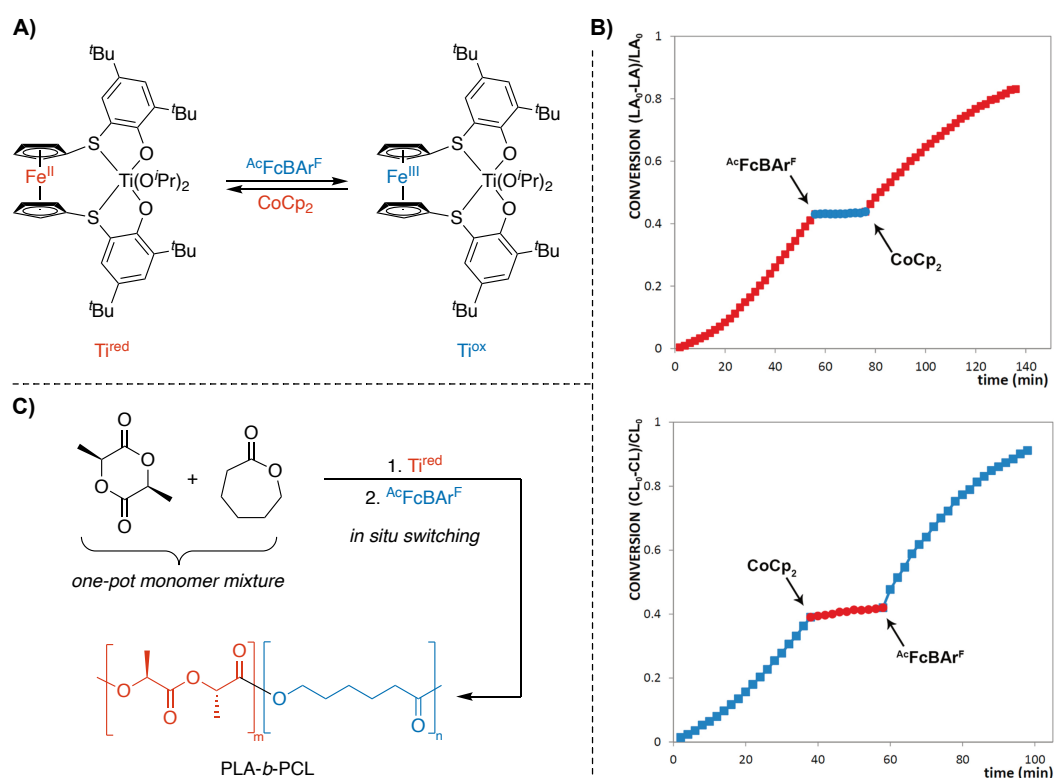
Figure 16. A) Redox-switchable titanium catalyst. B) Conversion vs. time plots for the homopolymerization of LA (top) or ε-CL (bottom) using a closely related zirconium salfan catalyst. The reduced catalyst is active for the ROP of LA while its oxidized form is active for ROP of ε-CL. C) PLA-*b*-PCL block copolymers generated from one-pot monomer mixtures by *in situ* redox switching of titanium catalyst shown in panel A).[210] Panel B): reprinted with permission from ref. 210. Copyright 2014 American Chemical Society.

2.5 Chemically Recyclable Polyesters – An Approach Towards a Circular Polymer Economy

While biodegradable polymers offer a solution to the rapidly increasing amount of persistent plastic waste in the environment caused by current commodity plastics, their degradation to CO_2, H_2O and other small molecules results in a complete loss of material value combined with the need for extracting virgin raw materials. From an economic and sustainable perspective, this represents a huge drawback and reuse and recycling of plastics is a superior option.[20,21,211] When it comes to the end-of-life fate of plastics, alternatives to common landfilling and incineration are highly needed. In this respect, chemical recycling to monomer (CRM) has emerged as a promising strategy to tackle the detrimental end-of-life options of current commodity plastics and to achieve a circular polymer economy where the intrinsic material value is preserved. A major advantage of CRM are the virgin material properties of recycled and reprocessed polymers even after various cycles as pristine monomer is recovered and used for each (re)polymerization, in contrast to mechanical recycling where a steady degradation of material properties is occurring due to heat stress in the recycling process.[9,211] ROP of cyclic esters is a particularly promising method for establishing CRM due to the thermodynamic equilibrium between monomer and resulting polymer.[9,19,37,49,212] In that case, the monomer equilibrium concentration and ceiling temperature are highly important for achieving successful CRM (see chapter 2.1). ROP only proceeds below the T_c of the system whereas depolymerization is only achieved well above the T_c, illustrating the practical importance of the level of T_c (Scheme 9).[9,36]

Polymerization

$T < T_c$

$T > T_c$
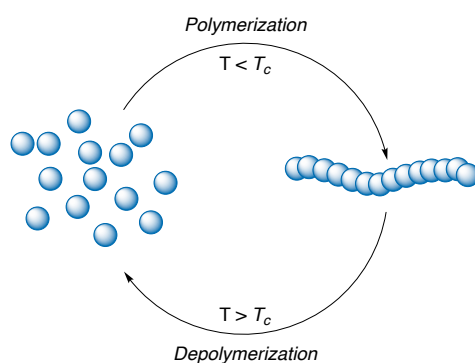
Depolymerization

Scheme 9. Concept of chemical recycling of polymers back to monomer (CRM) based on the monomer–polymer equilibrium in the system.[9,37]

Early work on the depolymerization of PHB to cyclic oligomers (mainly trimer and higher oligomers) and repolymerization of the trimer has been conducted by Höcker and co-workers. The polymerization however was very sluggish and only low molecular weight PHB was obtained, strongly limiting this specific approach for chemical recycling of PHB.[81,82] Despite the knowledge of reversibility of ROP and some reports of relatively low equilibrium monomer

conversions for monomers such as δ-decalactone or p-dioxanone,[212-214] the positive consequences of these results in terms of polymer sustainability had been largely overlooked. It was until 2016, when the pioneering work by Chen et al. demonstrated the huge potential of ROP for CRM approaches and its implications on achieving a circular polymer economy: while ROP of 5-membered, "nonstrained" γ-BL is not feasible at room temperature due to its low T_c, successful polymerization towards PGBL was achieved at very low temperatures (–40°C). Heating the obtained polymer at high temperatures (>220°C) selectively recovered γ-BL, proving the complete chemical recyclability back to the monomer of this material (Figure 17).[40] The relatively poor material properties of PGBL, aside from its chemical recyclability, such as low melting temperature and low thermostability, inspired the same group to design monomers for CRM approaches with a 5-membered γ-BL core and trans-fused cyclohexyl rings, namely 3,4-T6GBL and 4,5-T6GBL (Figure 17). 3,4-T6GBL showed considerably improved polymerizability with up to 88% conversion at room temperature, and the respective polymers exhibited high melting temperatures (T_m = 126°C, stereocomplexed polymer even showed a T_m of 199°C), high decomposition temperatures (T_d > 300°C) and mechanical properties competitive to some commodity plastics. Quantitative depolymerization to monomer was achieved by heating the polymer in bulk at temperatures >300°C, or at 120°C when a catalytic amount of $ZnCl_2$ was used. Hence, this elegant monomer–polymer system successfully tackled three major tasks at once: polymerizability, depolymerizability, and material properties.[41,43] Similarly, closely related 4,5-T6GBL furnished the synthesis of completely chemically recyclable polymers, yet, no melting transition was observed for this material but a T_g of 75°C.[42]
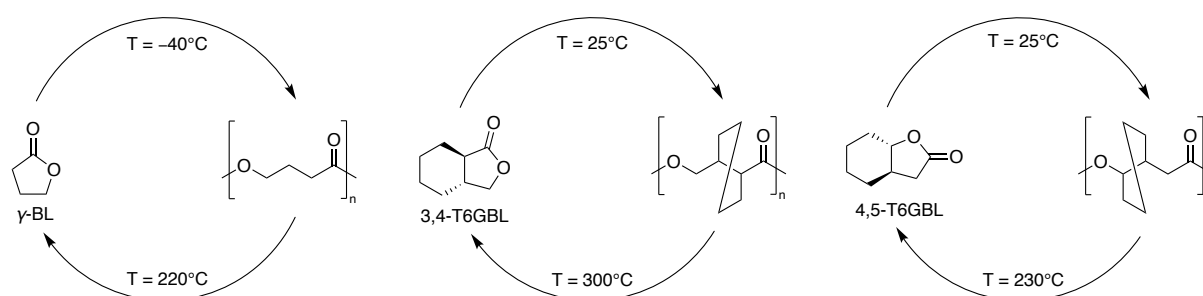
Figure 17. Completely chemically recyclable polyesters based on a 5-membered backbone structure. γ-BL and its corresponding polymer (left), and cyclohexyl trans-fused γ-BL-based monomers 3,4-T6GBL and 4,5-T6GBL with corresponding polymers (middle and right). Depolymerization temperatures correspond to bulk thermolysis without catalyst added.[40-42]

These works indicated that a 5-membered backbone structure of the polyester and thus γ-BL-based monomers are thermodynamically beneficial for successful CRM approaches. Chen and co-workers further expanded this concept to bicyclic lactones using a monomer design strategy where γ-BL is hybridized with ε-CL (Figure 18, left). This monomer easily underwent ROP and the resulting polyester was completely depolymerized back to the bicyclic monomer due to its

5-membered backbone structure. In addition to the good polymerizability as well as depolymerizability, the polyesters showed promising material properties such as high T_g or T_m and high thermal stability.[215] Thiolactones based on a 5-membered ring core structure hybridized with a 6-membered ring were also reported for CRM and the polythioesters achieved excellent thermomechanical properties, highlighting the potential of sulfur-based polymers (Figure 18, middle and right).[216,217] In this context, even a 4-membered thiolactone furnished the synthesis of chemically recyclable polythioesters facilitated by subtle monomer design including a geminal dimethyl substitution.[218]
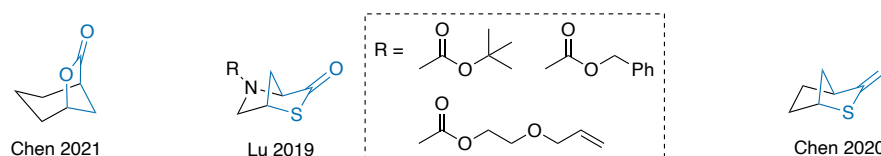
Figure 18. Bicyclic (thio)lactones for CRM approaches utilizing a hybridization of a 5-membered ring core structure (highlighted in blue) with a 7-membered ring (left) or with a 6-membered ring (middle and right).[215-217]

The monomer design strategy of using bicyclic structures in order to produce polyesters capable of selective depolymerization back to monomer has also been studied with lactones based on a 7-membered ring core structure with an additional heteroatom and additionally bearing an aromatic unit (Figure 19). The initial report by Shaver et al. in 2016 focused on a purely oxygen containing monomer,[219,220] whereas later studies by Du and Li et al. as well as Cai and Zhu et al. explored the effect of sulfur as heteroatom, alkyl substitution as well as fusion position of the aromatic unit.[221-223] Upon these substitutions, positive influences were observed such as enhanced thermal stability or tunability of T_g or T_m, and some of the materials exhibited good mechanical performance.[221-223]
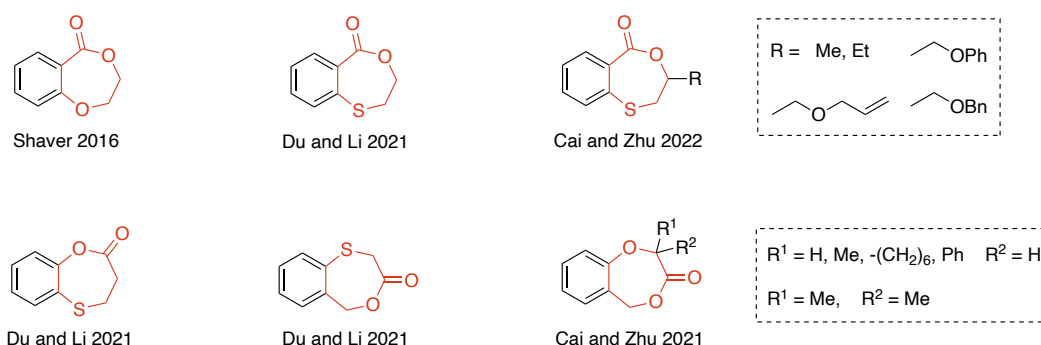
Figure 19. Bicyclic monomers reported for CRM approaches utilizing a 7-membered ring core structure (highlighted in red) with additional heteroatom, and an aromatic unit fused to the ring.[219-223]

In general, bicyclic monomer structures have shown great potential in CRM approaches in order to combine three usually conflicting parameters: polymerizability, depolymerizability and material properties (*vide supra*). When it comes to bicyclic monomers with 6-membered ring

core structure, their ROP has been reported, albeit not their depolymerization to the monomers.[37,224-227] A few examples of (non-bicyclic) 6-membered lactones for CRM approaches can be found in the literature such as a 4-carbomethoxylated δ-valerolactone (CMVL, Figure 20A). ROP was furnished at room temperature using diphenyl phosphate (DPP) as organocatalyst with a high equilibrium monomer conversion of 98%. A semi-crystalline material with two T_m's at 68 and 86°C was obtained. Heating a bulk sample of the polymer at 150°C and 0.05 Torr in the presence of Sn(Oct)$_2$ as depolymerization catalyst recovered CMVL in 87% yield.[228] β-Methyl-δ-valerolactone (β-MVL) polyols were employed for the synthesis of thermoplastic polyurethanes. The polyester block of these polyurethane networks could then be depolymerized to β-MVL monomer at high reaction temperatures (T = 200–250°C, Sn(Oct)$_2$) while the polyurethane block remained intact (Figure 20B).[229]
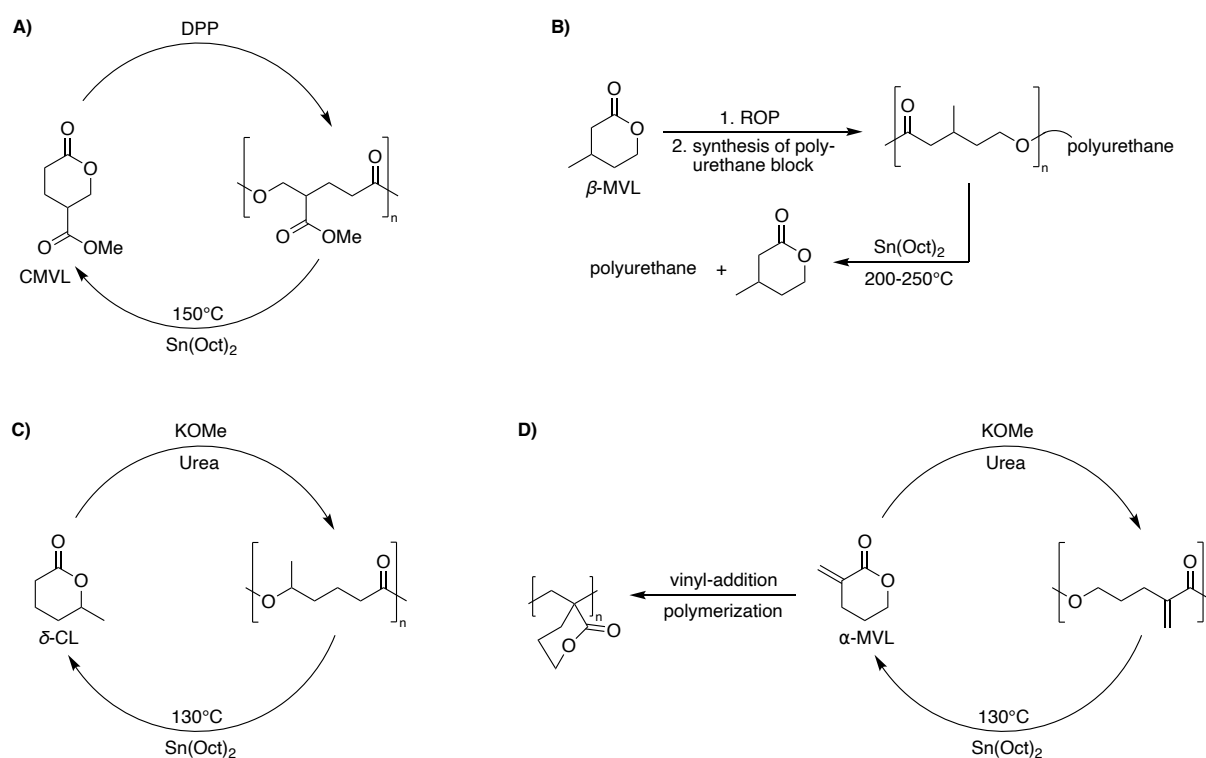
Figure 20. Monomer–polymer systems for CRM approaches based on a 6-membered ring structure.[62,228-230]

Another 6-membered monomer for CRM is δ-caprolactone (δ-CL) which was rapidly polymerized with excellent control using a binary catalyst system consisting of KOMe and urea organocatalysts. The obtained polymer was selectively and quantitatively depolymerized under thermolysis conditions at 130°C with Sn(Oct)$_2$ as catalyst and distillation under reduced pressure (Figure 20C). Additionally, the polyester was also chemically recyclable under dilute conditions at room temperature in the presence of an organophosphazene superbase. δ-CL and LA were then used for the generation of triblock copolymers, revealing promising mechanical properties and elastic behavior.[230] Later, the same group reported a closely related

monomer yielding functionalizable and chemically recyclable thermoplastics. The monomer, α-methylene-δ-valerolactone (α-MVL), enabled access to two polymerization pathways due to both α-methylene and ester unit: vinyl-addition polymerization gave $PMVL_{VAP}$ whereas ROP produced $PMVL_{ROP}$ with an intact vinyl unit for post-polymerization functionalization (Figure 20D). Similarly to δ-CL, ROP was achieved using KOMe and urea organocatalysts, and pristine monomer was recovered almost quantitatively when the polyester was treated in bulk in the presence of $Sn(Oct)_2$ at 130°C. The material properties of $PMVL_{ROP}$ were promising, including high tensile strength and Young's modulus, as well as high elongation at break.[62] These examples demonstrate that the field of chemically recyclable polyesters is extremely rapidly developing and holds large potential for future investigations in order to obtain materials enabling a circular polymer industry.

3 Objective

ROP of cyclic esters is a highly efficient approach for the production of aliphatic polyesters that show (bio)degradability in combination with promising material properties comparable to current commodity plastics such as PP, PE or PS, thus illustrating the future potential of this material class.[22,23,27,28] Additionally, the monomer–polymer equilibrium in ROP enables the synthesis of polymers with intrinsic chemical recyclability back to the monomer, enabling a circular polymer economy.[9,19,37] While these two major goals, (bio)degradable polymers and polymer recycling, can be addressed via ROP, catalysts as well as monomer/polymer structure play a crucial role in unleashing the full potential of ROP and in advancing its industrial applicability. In this work, both catalyst and monomer design studies are performed: i) catalyst design focuses on group 3 and 13 initiators bearing specifically tailored ligand frameworks for the ROP of well-known lactones in order to establish all-rounder and/or stereoselective catalysts for tailoring materials, and ii) monomer design is utilized to achieve the synthesis of novel polyesters with complete chemical recyclability.

Early work in ROP of typical monomers such as β-BL, LA or ε-CL has focused on zinc- and REM-based catalysts with some of them showing very high activity for a range of cyclic esters.[22,28,29,48] In recent years, group 13 based initiators have found increasing attention and particularly indium complexes are an interesting target due to their high catalytic activity at mild temperatures, enhanced air and moisture stability as well as tolerance against functional groups.[132,133] Indium salen and phosphasalen complexes have shown promising results in the ROP of cyclic esters,[111,138,139,231] and in the first part of this work, related indium salan complexes are targeted. Salan ligands are the reduced derivatives of salens, thus a tertiary amine instead of an imine moiety is present in the backbone, resulting in an increased flexibility of the framework and in an additional position for electronic and steric tuning of the ligand (Scheme 10).[232,233] The related catam framework also bears tertiary amines but lacks the methylene bridges, giving a more constrained scaffold in comparison to the salan type (Scheme 10).[234]
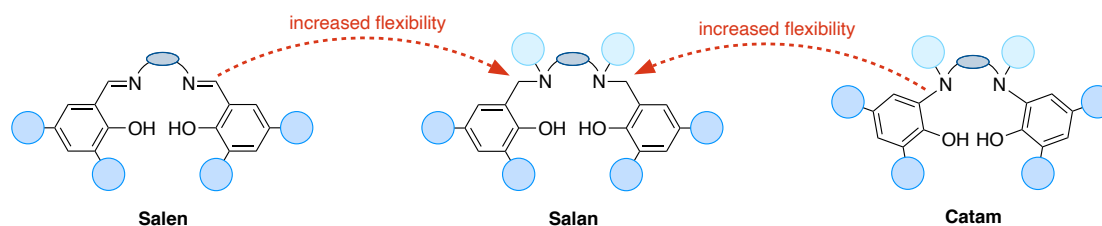
Scheme 10. Structural comparison of salen-, salan-, and catam-type ligand frameworks. Potential substitution positions are highlighted in blue.[232,234]

Compared to their salen counterparts, salan complexes are less commonly reported in literature and indium salan complexes are particularly rare.[133,232] Indium salan complex **1** (Figure 21) is targeted in this work as the low steric demand of the backbone and amine substituents combined with the overall increased flexibility of the salan framework might favor coordination of lactones of various ring sizes as well as propagation due to feasible structural ligand rearrangement, eventually resulting in increased polymerization rates.[235] The chloro complex of **1** is literature known but was only tested in the ROP of LA and showed very poor activities even at high reaction temperatures (TOF < 4 h^{-1}).[236] Thus, the importance of the initiating group (chloro vs. alkoxy) will also be elucidated. Moreover, the synthesis of the first indium catam-type complex (**2**) is targeted (Figure 21). Both complexes are to be tested in the ROP of various cyclic esters including β-BL, γ-BL, ε-CL, ε-DL and LA. By comparing the catalytic activity of both catalysts, conclusions on the importance of the ligands' flexibility for achieving high polymerization rates might be drawn.
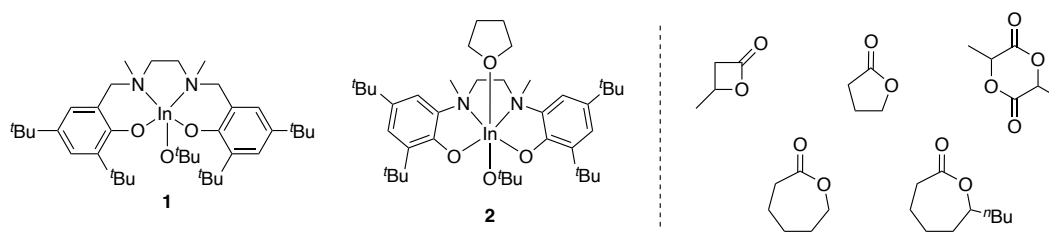
Figure 21. Indium salan and catam catalysts (left) studied in this thesis for the ROP of various cyclic esters (right).

Once a highly active all-rounder catalyst is established, the synthesis of copolymers from one-pot monomer mixtures is investigated. Block copolymers are particularly interesting targets and achieving sequence control from mixed monomer feedstocks is a challenging goal. While an increasing number of catalysts is available in literature for the one-pot synthesis of defined block copolymers from *different* monomer classes (such as epoxides/CO_2 and lactones), the synthesis of block structures from one-pot feedstocks of the *same* monomer class (such as two different lactones) is particularly challenging due to very similar reactivity of the monomers.[170,173,183] Here, it is hypothesized that monomer selectivity is obtained if a small-sized lactone is combined with a sterically demanding lactone as the catalyst potentially favors ROP of the small-sized one for steric reasons (before switching to the bulkier monomer). Thus, the copolymerization of β-BL with ε-CL or ε-DL will give interesting insights into the potential sequence control of indium catalysts. Using ε-DL might provide an additional advantage of a large *n*-butyl group in close proximity to the metal-coordinating carbonyl group, potentially further favoring the ROP of β-BL over ε-DL in comparison to ε-CL lacking such an additional steric demand (Figure 22).

A) *Monomer differentiation of the catalyst based on the steric demand of the monomer feasible?*
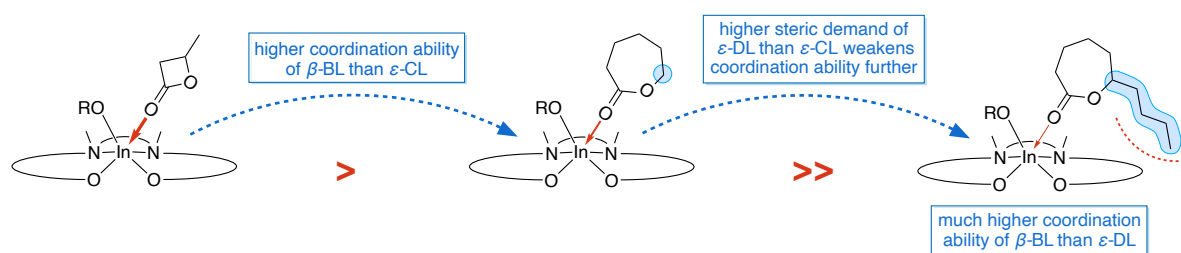
B) *Synthesis of block copolymers from one-pot mixtures of same-class-monomers feasible?*
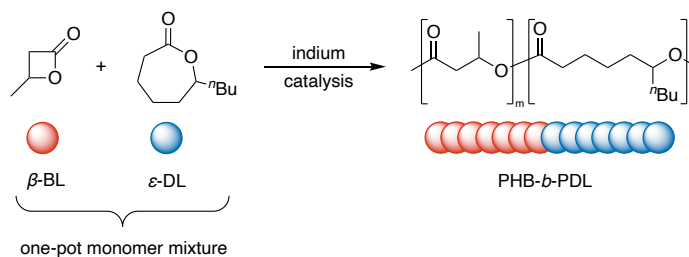
Figure 22. A) Hypothesized monomer differentiation of the catalyst via different steric demand of *β*-BL, *ε*-CL and *ε*-DL (the catalyst is shown schematically), and B) block copolymer synthesis from a one-pot lactone mixture as a consequence thereof.[237]

As previously mentioned, rare-earth metal complexes have found widespread application in the field of ROP catalysis and particularly yttrium initiators have shown high reaction rates and good stereocontrol.[22,27,29,146] Salan ligands are also suitable frameworks for REM complexes and in contrast to indium species various REM salan-type initiators have already been reported in literature.[147,148,238-249] A very interesting example represents the work of Yao et al. on yttrium and ytterbium salan-type complexes where a switch in stereoselectivity in ROP of *β*-BL from syndioselective to isoselective was observed in dependence on the *N*-substituent of the ligand (cyclohexyl vs. phenyl, see chapter 2.3.3).[162] Control of the stereomicrostructure of PHB is of utmost importance: atactic and syndiotactic PHB are materials with low application potential due to their amorphous nature or non-biodegradability, respectively, whereas isotactic PHB has an enormous industrial potential as it shows material properties comparable to *i*-PP.[23,29] Establishing structure-property relationships in ROP of *β*-BL is thus highly important, however, the synthesis and isolation of catalyst libraries for that purpose is a time-consuming and elaborate task. This thesis also aims for the development of a high-throughput approach that generates yttrium salan complexes *in situ* by conveniently treating a suitable yttrium precursor with the respective salan pro-ligand. *β*-BL is then directly added to the reaction mixture, circumventing the isolation of the catalytically active species and allowing for the rapid screening of a library of yttrium salan complexes (Figure 23).
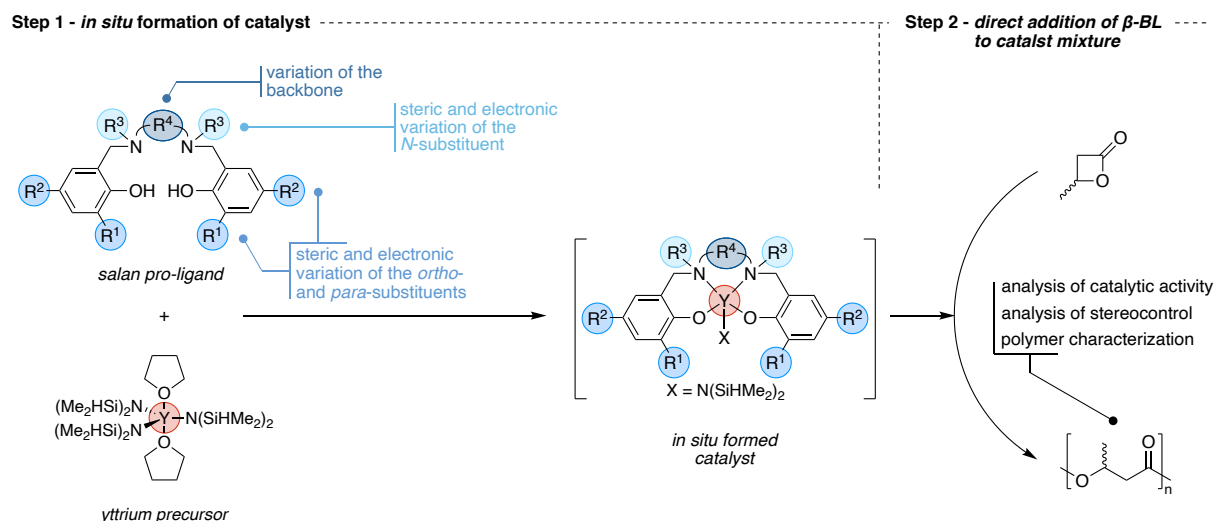
Figure 23. Concept of the high-throughput approach for the screening of salan-type catalyst libraries: *in situ* formation of the catalyst (step 1) and direct addition of the monomer to the catalyst mixture (step 2).

The salan ligands might be modified according to the substituents on the amine position (phenyl vs. alkyl and steric vs. electronic influences) as well as steric and electronic influences on the phenolic positions and the effect of the ligand backbone (Figure 23). This approach will allow for a rapid correlation of activity and stereocontrol data and enable the identification of structure-property relationships in the ROP of β-BL. Furthermore, the *in situ* protocol will most likely give access to PHB with various tacticities, i.e. atactic, syndiotactic or isotactic PHB, similarly to the REM salan complexes reported by Yao and co-workers.[162] PHB with a reduced isotacticity in the range of $P_m \approx 0.8–0.9$ is targeted as the introduced stereoerrors are expected to reduce its crystallinity and thus result in improved material properties (Scheme 11). Once a promising ligand/yttrium combination is identified via high-throughput screening, further experiments should follow for optimization studies regarding catalyst structure and polymerization, overall gaining for a deeper understanding. Beyond catalyst design studies, the thermal and mechanical properties of the material should be investigated in detail. These analyses are expected to reveal whether synthetic PHB with a reduced tacticity has the potential to overcome current limitations of bacterial PHB, in particular its brittleness and low thermostability.[23,68] If these challenges are overcome, synthetic PHB represents a highly promising biodegradable alternative to current commodity plastics such as *i*-PP.
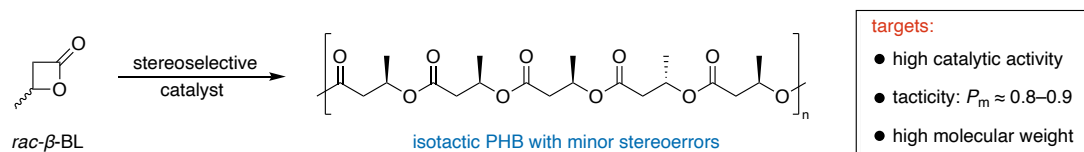
Scheme 11. Synthesis of isotactic PHB with minor stereoerrors incorporated for improving material properties.

A further aim of this work is the sophisticated design of novel monomers for chemical recycling approaches. ROP of bicyclic lactones with a 5- or 7-membered ring core structure has previously generated polymers with promising properties that can be easily depolymerized to the pristine monomer (Figure 24).[37,41,42,215,219,221-223] Despite very recent examples of (monocyclic) 6-membered lactones for CRM approaches,[62,228-230] bicyclic 6-membered lactones have not yet been explored for this concept. The hybridization approach of fusing two different lactones in order to obtain a novel monomer with the best properties of each original one has shown high potential for combining polymerizability, depolymerizability and material properties.[215] Herein, the ROP of a hybridized bicyclic lactone with a 6-membered ring core structure and its depolymerization behavior will be investigated (Figure 24). This will provide valuable insights whether the hybridization approach in monomer design for chemically recyclable polymers is applicable beyond the typical 5-membered ring structures reported so far. Of particular interest is a simple monomer synthesis: the one-step Baeyer-Villiger oxidation of commercially available norcamphor represents a promising starting point for the generation of a 6-membered bicyclic lactone, i.e. norcamphorlactone (NCL, formally 2-oxabicyclo-[3.2.1]octan-3-one, Figure 24).[250] Screening of various all-rounder catalysts should allow for establishing suitable polymerization conditions and successfully obtained polyesters will be studied regarding their thermal properties and their chemical recyclability back to the monomer. Therefore, this work on CRM approaches complements the catalyst studies for tailoring (bio)degradable polyesters and intends to demonstrate the full potential of ROP.
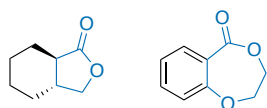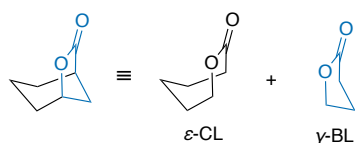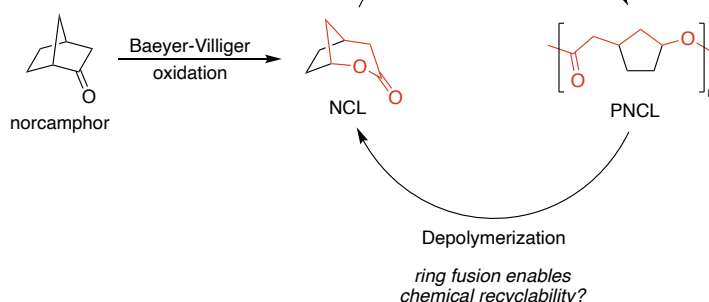
Figure 24. Examples of previous works on the ROP of bicyclic lactones (left) and overview of this work (right).[41,215,219,250]

4 Indium All-Rounder Catalysts for the Ring-Opening Polymerization of Various Cyclic Esters

4.1 Bibliographic Data

- highly active catalyst
- broad monomer scope
- excellent control over ROP
- immortal ROP conditions
- air-stable chloro precatalyst
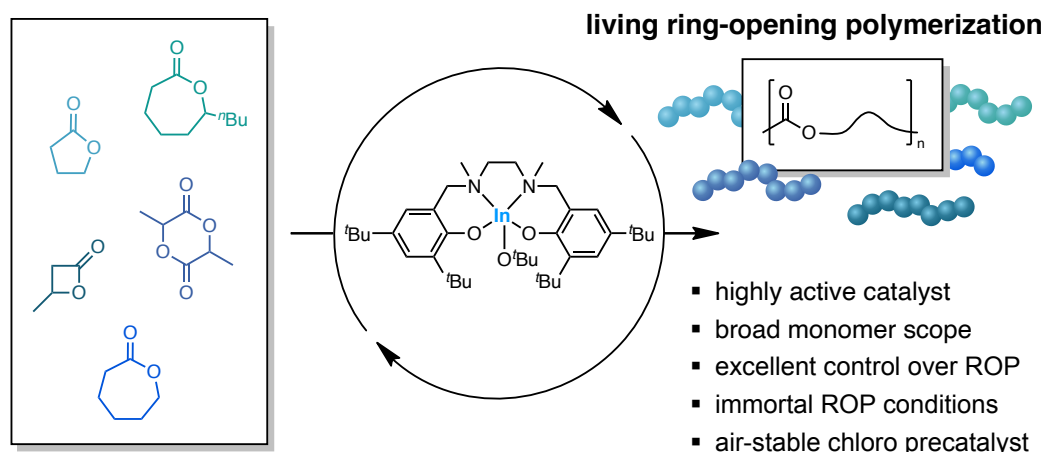
Title:	Combining high activity with broad monomer scope: indium salan catalysts in the ring-opening polymerization of various cyclic esters
Status:	Full paper, published online March 31, 2022
Journal:	Catalysis Science & Technology, 2022, 12, 3295–3302.
Publisher:	Royal Society of Chemistry
DOI:	10.1039/d2cy00436d
Authors:	Jonas Bruckmoser, Daniel Henschel, Sergei Vagin, Bernhard Rieger

4.2 Content

All-rounder catalysts showing high activity and broad monomer scope are appealing targets in polymerization catalysis, yet examples of such initiators are surprisingly rare in the ROP of lactones. In this work, the synthesis and characterization of indium alkoxide salan- and catam-type complexes, and their application in the ROP of various cyclic esters including β-BL, γ-BL, LA, ε-CL and ε-DL were reported. The indium salan complex showed very high activities for all of these monomers, maintained excellent control over the polymerizations, and yielded high molecular weight (bio)degradable polyesters with narrow dispersities. The initiator was also operable under immortal ROP conditions using BnOH as chain transfer agent and allowed for a precise adjustment of molecular weights. Additionally, the use of an impure lactide feedstock under industrially relevant conditions was tolerated and gave identical polymerization results compared to purified monomers. Detailed kinetic investigations in the ROP of β-BL revealed a first-order dependence on monomer and catalyst concentration. Together with the results of the end-group analysis, the kinetic experiments pointed towards a mononuclear coordination-insertion mechanism in the polymerizations. Air-stable (but poorly active) indium chloro pre-catalyst[236] could be conveniently converted *in situ* into a highly active alkoxide species by using propylene oxide as polymerization solvent and activation reagent. A comprehensive comparison against the literature revealed that the indium salan catalyst strongly outperforms current leading group 13 catalysts in the field and is one of the top-performing all-rounders in ROP catalysis in a broader context. In addition to the initiator supported by a relatively flexible salan-type framework, a more constrained indium catam complex was tested in the ROP of afore-mentioned monomers and showed generally reduced reaction rates, indicating that framework flexibility plays a subtle but crucial role in achieving high activity in ROP catalysis over a wide range of substrates spanning 4- to 7-membered ring sizes.

4.3 Manuscript

PAPER

Check for updates

Combining high activity with broad monomer scope: indium salan catalysts in the ring-opening polymerization of various cyclic esters†

Jonas Bruckmoser, Daniel Henschel, Sergei Vagin and Bernhard Rieger [iD] *

Combining high catalytic activity with broad monomer scope is an appealing yet challenging task in polymerization catalysis. Examples of such all-rounder catalysts in the ring-opening polymerization (ROP) of lactones are rare. Herein we report an indium alkoxide complex supported by a salan-type framework that shows very high rates, excellent control and high tolerance against chain transfer agents in the ROP of several cyclic esters yielding high molecular weight (bio)degradable polymers. Additionally, by using propylene oxide as solvent, poorly active but air-stable indium chloro pre-catalyst can be converted *in situ* into a catalytically active species with drastically enhanced polymerization rates. In contrast to the salan-type initiator, a related indium alkoxide catam-type complex shows reduced activity in ROP of β-butyrolactone, ε-caprolactone, ε-decalactone and lactide, highlighting the importance of framework flexibility in catalyst design.

Introduction

Plastic contamination of the environment has become a global problem with an estimated 19 to 23 million metric tons of plastics leaking out of waste management systems and entering aquatic ecosystems annually.[1] Reducing global plastic emissions into the environment requires tremendous and combined efforts of the plastics economy, governments and society.[1–4] Polymer chemists play an important role in shaping the future of plastics and do have the right tools at hand. Besides current mechanical and chemical recycling approaches for polymer waste,[5–7] (bio)degradable polyesters are one part of the solution to the plastic waste crisis and have attracted much research attention in both academia and industry.[8,9] Ring-opening polymerization (ROP) of cyclic esters offers simple access to these materials and among the best studied monomers within the field are lactide (LA), β-butyrolactone (β-BL) and ε-caprolactone (ε-CL).[8,10,11] Isotactic poly(lactide) (PLA) has similar material properties compared to petroleum-derived commodity polymers such as polystyrene, and is currently the most widely, commercially produced biobased and compostable polyester, while

poly(hydroxybutyrate) (PHB) prepared *via* ROP of β-BL holds great potential as a replacement for isotactic polypropylene.[9,12,13] Apart from these commercially relevant polyesters, research also focuses on novel and easily accessible, biobased monomers for ROP such as ε-decalactone (ε-DL),[14] (−)-menthide[15] or 4-isopropyl-caprolactone[16] and chemically recyclable polymers based on γ-butyrolactone (γ-BL).[17,18]

Besides novel, specifically designed polymers for depolymerization to monomers,[6,7,18] aliphatic polyesters are also promising materials for catalytic chemical recycling in order to achieve a circular polymer economy.[19,20] For example, methanolysis of PLA affords methyl lactate that can be converted back to lactide.[20] Depolymerization strategies for PHB to propylene (the starting material for β-BL production) exist as well.[21] Consequently, simple and rapid access to such promising polyester materials is of great importance.

Numerous metal-based catalysts for the ROP of cyclic esters have been reported to date, however, it still remains a challenge to combine high catalytic activity with control over polymerization and broad monomer scope of the catalyst.[8,10,11] In this context, it is worth noting that some initiators have shown ultrahigh polymerization rates for one specific monomer such as lactide, but activity for other lactones is strongly reduced.[22–24] Such a narrow monomer scope is disadvantageous when targeting more complex polymer structures such as copolymers or when attempting switchable polymerization catalysis. The ROP of β-BL, which is a rather reluctant monomer, is particularly challenging

Paper

despite its high internal ring strain. Many initiators suffer from low reaction rates and are prone to side-reactions.[10] Tin bis(2-ethylhexanoate) [Sn(Oct)$_2$] is used in the industrial synthesis of PLA and poly(ε-caprolactone) and generally finds widespread application in ROP of lactones.[8,11,25] However, high reaction temperatures are required, and transesterifications as well as poor molecular weight control are usually observed. The most prominent examples of highly active catalysts for the controlled ROP of a range of cyclic esters are the β-diiminate zinc and yttrium amino-alkoxy-bis(phenolate) systems developed by Coates *et al.* and Carpentier *et al.* These initiators show very high activities in the ROP of β-BL, LA and ε-CL with turnover frequencies (TOFs) ranging from 156 to 154 440 h^{-1}.[26–30] Due to their versatility, these catalysts are often considered as the catalysts of choice in ROP of lactones. Based on these early reports, zinc and rare-earth metal catalysts have found widespread applications in the field of ROP.[24,31–36]

In recent years, indium compounds have shown great potential in ROP catalysis due to their exceptionally higher activity compared to aluminum and gallium derivatives, their generally higher air and moisture stability as well as functional group tolerance.[37–39] A simple catalyst system consisting of InCl$_3$/BnOH/NEt$_3$ showed broad substrate scope, albeit polymerization rates were only moderate.[40–42] Increased activities in ROP for a range of cyclic esters were realized by using a dinuclear indium catalyst supported by chiral, tridentate diaminophenolate ligands as well as mononuclear ferrocenyl-salen- or phosphasalen-type indium alkoxide complexes.[43–46]

It was in this context that we sought to explore the activity of indium salan complexes **1** and **2** (Scheme 1) in the ROP of various cyclic esters including β-BL, γ-BL, ε-CL, ε-DL and LA. Salan ligands are the reduced derivatives of salen ligands bearing tertiary amine instead of imine groups.[47] We hypothesized that the increased flexibility of the salan framework compared to salen-type scaffolds favors coordination of (several different-sized) monomers as well as propagation due to feasible structural ligand rearrangement, thus resulting in overall increased reaction rates. Additionally, a comparison is made to a related indium catam-type complex **3** (Scheme 1) which also bears tertiary amine groups but is characterized by a more constrained geometry around the metal center, highlighting the importance of ligand framework flexibility in catalyst design for achieving high polymerization rates.

Results and discussion

The synthesis of indium complex **1** was achieved by deprotonation of salan ligand **L1** with KH and subsequent salt metathesis with InCl$_3$ as reported previously in the literature.[48] We observed that in solid state, **1** is air- and moisture-stable for at least 3 months with no signs of decomposition (Fig. S7 and S8†), albeit in solution the moisture stability is reduced (Fig. S9 and S10†). Treatment of **1** with KO^{t}Bu in THF overnight, removal of salt by-products and washing with pentane gave analytically pure **2** in 74% yield. Additionally, **2** is also accessible in a one-pot procedure starting from **L1** in 64% yield without the need to isolate any intermediates (Scheme 1). In contrast to **1**, the air and moisture stability of **2** is reduced, showing signs of decomposition after exposure to air for 24 h (Fig. S13†). Indium catam complex **3** was accessible in a one-pot route similar to **2** in 32% yield. Complexes **1–3** were fully characterized by ^{1}H and ^{13}C{^{1}H} NMR spectroscopy and elemental analysis.

Crystals of compound **2** suitable for X-ray crystallography were obtained by slow evaporation from toluene (Fig. 1). **2** is monomeric in the solid state and the indium center is penta-coordinate in a distorted square-based pyramidal geometry ($\tau = 0.32$). Selected bond lengths and angles are given in Table S2 in the ESI.† Diffusion-ordered NMR spectroscopy (DOSY) indicated that **2** and **3** are monomeric in solution (Fig. S31 and S32†).
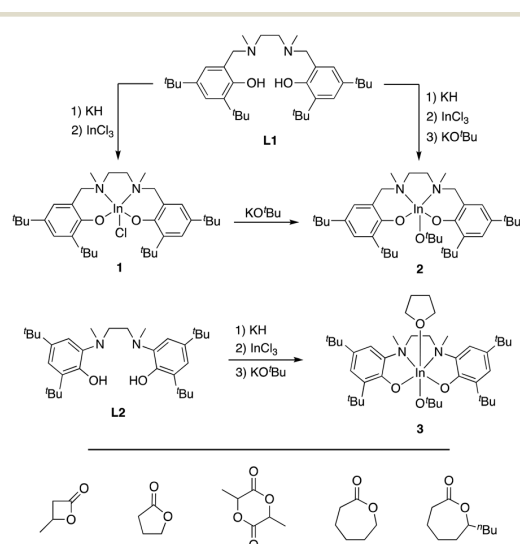
Scheme 1 Synthesis of indium salan complexes **1** and **2**, and indium catam complex **3** (top). Bottom: Scope of monomers investigated in this study.
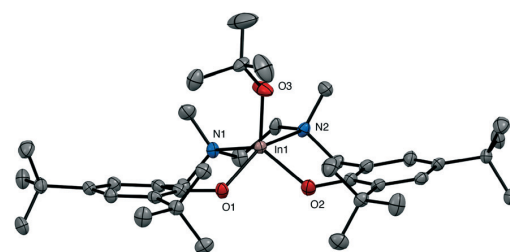

Fig. 1 Molecular structure of initiator **2** with thermal ellipsoids set at 50% probability. Hydrogen atoms are omitted for clarity.

Catalysis Science & Technology

First, we tested initiators **1** and **2** in the ROP of β-BL. While **1** was reported to show moderate activity in the ROP of *rac*-LA,[48] we observed only traces of conversion of β-BL at room temperature (Table S1,† entry 1). Raising the temperature to 50 °C improved activity but overall, the polymerization was still rather sluggish (TOF = 5 h^{-1}; Table S1,† entry 2). We hypothesized that the low activity was a result of the poor ability of the chloro group to initiate the polymerization and the more polarized character of the In–O^{t}Bu bond as in **2** might facilitate efficient initiation. Excitingly, **2** rapidly polymerized 200 equiv of β-BL to near-quantitative conversion within 15 min at room temperature to give atactic PHB (TOF = 776 h^{-1}; Table 1, entry 1; Fig. S23†). Further increasing the [β-BL]/[**2**] ratio to 400/1 led to a molecular weight of the polymer twice as high and eventually PHB with a M_n = 187.5 kg mol^{-1} ($Đ$ = 1.09) could be obtained when the [β-BL]/[**2**] ratio was as high as 2000/1 (Table 1, entries 2 and 3). Electrospray ionization mass spectrometry (ESI-MS) and ^{1}H NMR analysis of oligomeric PHB revealed high end-group fidelity (Fig. S29 and S30†). Initiator **2** exhibited excellent control over the polymerizations ($Đ$ = 1.03–1.10) and the linear evolution of M_n values with increasing [β-BL]/[**2**] ratio indicated high control over the molecular weight (Fig. S17†). Additionally, the molecular weight of PHB increased linearly with increasing monomer conversion suggesting a living-type polymerization (Fig. S18†). A chain extension experiment, in which an additional 200 equiv of monomer were added after near-quantitative conversion of 200 equiv of β-BL, was carried out to further support the living-type behavior (Table 1, entry 4). As expected, the molecular weight of the obtained polymer after the second monomer addition was almost exactly twice as high (M_n = 24.5 *vs.* 48.0 kg mol^{-1}) while dispersity remained very narrow. The ROP of β-BL could also be carried out in the presence of benzyl alcohol (BnOH) as chain transfer agent. We tested ratios of 1–20 equiv of BnOH at a catalyst loading of 0.1 mol% and observed a high tolerance of **2** against chain

transfer agent without any decrease in activity and control over the polymerization (Table 1, entries 5–9). As expected, the molecular weight of the resulting PHB decreased linearly with increasing amount of BnOH (Fig. S19†).

Polymerization kinetics with different [β-BL]/[**2**] ratios ranging from 100/1 to 400/1 at constant initial monomer concentrations ([β-BL]$_0$ = 2.0 M) were performed. In all cases, first-order dependence on monomer concentration was found as evident by the linear semi-logarithmic plots (Fig. 2A). The rate constants were determined as k_{obs} = 0.526 ± 0.006 min^{-1} (100/1), 0.361 ± 0.013 min^{-1} (150/1), 0.244 ± 0.008 min^{-1} (200/1), 0.151 ± 0.007 min^{-1} (300/1) and 0.118 ± 0.003 min^{-1} (400/1). First-order dependence with respect to catalyst concentration was confirmed by linear relationship of ln(k_{obs}) *vs.* ln[**2**] with a slope of 1.11 ± 0.04 (Fig. 2B). The propagation rate constant was determined as k_p = 27.9 ± 0.9 L mol^{-1} min^{-1} (Fig. S20†). Together with the results of the end-group analysis (*vide supra*), the findings of the kinetic experiments support that the polymerization follows a mononuclear coordination-insertion mechanism.

The importance of the initiating group is clearly demonstrated by the differences in catalytic activity of **1** and **2**. Consequently, we were interested whether an indium alkoxide complex could be conveniently generated *in situ* by using air-stable pre-catalyst **1**. Such a suitable activation method was previously reported by Thomas *et al.* where a salen-type aluminum chloro complex was transformed *in situ* into an alkoxide complex by stirring it in neat propylene oxide (PO) in the presence of an onium salt as cocatalyst.[49] This method is gaining increasing attention for chloro complexes, and despite some minor mechanistic distinctions for different catalytic systems (*e.g.*, addition of cocatalyst required or not),[49,50] it is generally accepted that PO is ring-opened by the chloro group to form a chloropropoxy species.[49–54] Stirring **1** in neat PO for 24 h and subsequent addition of 200 equiv of β-BL led to rapid monomer consumption without any sign of polyether formation

Table 1 Ring-opening polymerization of β-BL using initiators **1**–**3**[a]

Entry	Catalyst	[M]/[I]	Time (min)	Conv.[b] (%)	$M_{n,theo.}$[c] (kg mol^{-1})	$M_{n,GPC}$[d] (kg mol^{-1})	$Đ$[d]
1	**2**	200	15	97	16.7	22.7	1.10
2	**2**	400	30	95	32.7	43.9	1.03
3	**2**	2000	1440	>99	172.2	187.5	1.09
4[e]	**2**	200 + 200	15 + 30	97/96	16.7/33.1	24.5/48.0	1.05/1.06
5[f]	**2**	1000	480	>99	43.0	56.8	1.07
6[g]	**2**	1000	480	>99	21.5	31.6	1.08
7[h]	**2**	1000	480	>99	14.3	22.4	1.06
8[i]	**2**	1000	480	>99	7.8	11.9	1.06
9[j]	**2**	1000	480	98	4.0	5.4	1.05
10[k]	**1**	200	120	87	15.0	19.2	1.10
11	**3**	200	60	80	13.8	19.0	1.09

[a] Polymerizations were performed in toluene at room temperature, [β-BL] = 2.0 M. Reaction times not necessarily optimized. Additional polymerization data can be found in the ESI,† Table S1. [b] Conversion determined by ^{1}H NMR spectroscopy. [c] Theoretical molecular weights were determined from the [M]/[I] ratio and monomer conversion data. [d] Determined by GPC in CHCl$_3$ at room temperature relative to polystyrene standards. [e] Sequential addition of 200 equiv β-BL after near-quantitative conversion of first 200 equiv β-BL. [f] 1 equiv BnOH added. [g] 3 equiv BnOH added. [h] 5 equiv BnOH added. [i] 10 equiv BnOH added. [j] 20 equiv BnOH added. [k] Propylene oxide (PO) used as solvent. Preactivation time of catalyst in PO prior to monomer addition was 24 h.
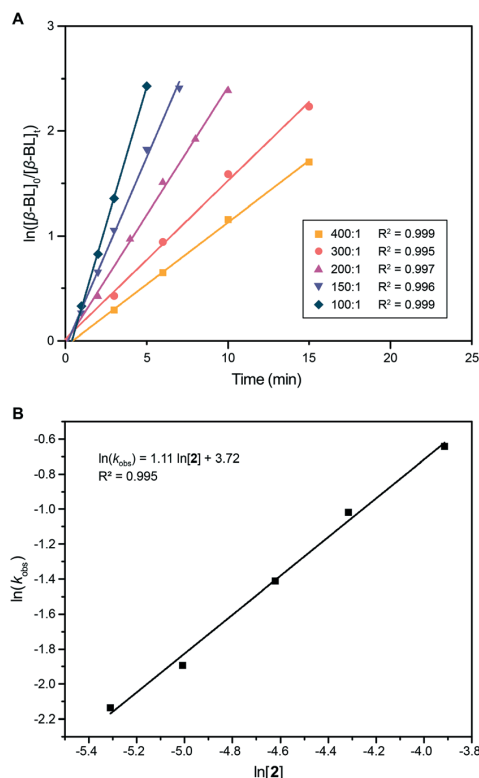
Paper

Fig. 2 A) Semi-logarithmic first-order plots for the polymerization of β-BL at different [β-BL]/[**2**] ratios. B) Plot of ln(k_{obs}) vs. ln[**2**] for ROP of β-BL.

dependence on monomer concentration was observed (Fig. S22†) indicating a well-controlled polymerization behavior. These results suggest that **1** can be *in situ* transformed into an alkoxide species, albeit polymerization activity is somewhat reduced compared to **2**. This might be attributed to an incomplete formation of catalytically active alkoxide species or the difference in initiation efficiency of *tert*-butoxy *vs.* chloropropoxy. When the preactivation time of **1** in PO was reduced to 15 min, no conversion of β-BL was observed after 1 h (Table S1,† entry 3). Additionally, large excess of PO was needed to form the catalytically active species since stirring **1** in toluene with 10 equiv of PO for 24 h and subsequent monomer addition gave no polymer (Table S1,† entry 4). Nevertheless, our results show that polymerization rates of air-stable **1** can be drastically increased when performing the ROP of β-BL in neat PO as activation reagent.

These initial results in the ROP of β-BL prompted us to investigate the activity of **2** in the ROP of various cyclic esters including ε-CL, ε-DL, LA and γ-BL. In the ROP of ε-CL, ultrahigh activities were observed while low catalyst loadings of **2** (0.2–0.05 mol%) could be used. 72% of 500 equiv ε-CL were converted in just 20 s with gelation of the reaction mixture (Table 2, entry 1). The outstanding polymerization activity was still maintained when increasing the [ε-CL]/[**2**] ratio to 1000/1 and 2000/1 leading to TOFs as high as 71 100 h^{-1} (Table 2, entries 2 and 3). In all cases, slightly broadened polymer distributions are evident, typically observed in ε-CL ROP due to transesterification side reactions at high conversions.[11] Additionally, high polymerization viscosities and a higher rate of propagation compared to the rate of initiation might explain the broadening as well as the higher experimental molecular weights compared to those theoretically calculated. Moving forward, we turned to ε-DL, a related seven-membered lactone that attracts increasing

(Table 1, entry 10). The molecular weight of PHB increased linearly with increasing conversion (Fig. S21†) and first-order

Table 2 Ring-opening polymerization of various cyclic esters using initiators **2** and **3**[a]

Entry	Catalyst	Monomer	[M]/[I]	T (°C)	Time (min)	Conv.[b] (%)	TOF (h^{-1})	$M_{n,theo.}$[c] (kg mol^{-1})	$M_{n,GPC}$[d] (kg mol^{-1})	Đ[d]
1	2	ε-CL	500	rt	20 s	72	64 800	41.1	117.1	1.48
2	2	ε-CL	1000	rt	40 s	79	71 100	90.2	214.8	1.42
3	2	ε-CL	2000	rt	90 s	82	65 600	187.2	318.8	1.49
4	2	ε-DL	100	rt	60	84	84	14.3	33.8	1.12
5	2	ε-DL	200	rt	120	90	90	30.6	50.8	1.13
6	2	ε-DL	500	rt	360	84	70	71.5	87.5	1.10
7	2	*rac*-LA	500	130	10	94	2820	67.7	26.8	1.15
8	2	*rac*-LA	1000	130	10	78	4680	112.4	31.8	1.17
9[e]	2	*rac*-LA	1000	130	10	83	4980	119.6	35.1	1.16
10[e]	2	*rac*-LA	2000	130	15	79	6320	227.7	47.0	1.19
11[e]	2	ʟ-LA	1000	130	10	46	2760	66.3	18.4	1.16
12[e]	2	ʟ-LA	1000	170	3	42	8400	60.5	12.8	1.18
13	2	γ-BL	200	−35	1440	28	2	4.8	21.2	1.80
14	2	γ-BL	400	−35	1440	20	3	6.9	21.6	1.88
15	3	ε-CL	500	rt	5	37	2220	21.1	41.0	1.33
16	3	ε-DL	100	rt	60	69	69	11.7	19.9	1.22
17	3	*rac*-LA	500	130	10	51	1530	36.8	57.8	3.26

[a] Polymerizations were performed in toluene, [M] = 2.0 M, except entries 7–14 and 17, which were performed in bulk. Reaction times not necessarily optimized. [b] Conversion determined by ^{1}H NMR spectroscopy. [c] Theoretical molecular weights were determined from the [M]/[I] ratio and monomer conversion data. [d] Determined by GPC in THF at 40 °C relative to polystyrene standards. Molecular weights of PεCL and PLA were corrected with a factor of 0.56 and 0.58, respectively.[35] [e] Impure, commercial grade monomer used.

3298 | *Catal. Sci. Technol.*, 2022, **12**, 3295–3302

This journal is © The Royal Society of Chemistry 2022

49

Catalysis Science & Technology

Paper

research attention as a biobased substituent for low-T_g-polymers and shows promising performance as soft segment in copolymers for adhesives and thermoplastic elastomers.[55,56] In contrast to ε-CL, ε-DL is a more reluctant monomer in ROP and usually requires prolonged reaction times or elevated temperatures for high conversions.[14,55–57] We decided to perform the ROP of ε-DL at room temperature and observed 84% conversion within 1 h at a [ε-DL]/[**2**] ratio of 100/1 (Table 2, entry 4). Increasing the monomer to catalyst ratio required longer reaction times to achieve high conversions (Table 2, entries 5 and 6). Nevertheless, initiator **2** showed high degrees of polymerization control, as poly(ε-decalactone) with high molecular weight and narrow dispersity could be obtained (M_n = 87.5 kg mol^{-1}, Đ = 1.10).

We were then interested in the ROP of *rac*-LA at industrially relevant bulk conditions at 130 °C. At the outset, sublimed *rac*-LA was used and **2** proved to be highly active converting 500 equiv of monomer almost quantitatively into PLA within 10 min (Table 2, entry 7). Despite the high reaction temperatures, the resulting PLA had narrow dispersity (Đ = 1.15), even though the molecular weight was only half than expected. When increasing the [*rac*-LA]/[**2**] ratio to 1000/1, **2** was still highly active (TOF = 4680 h^{-1}, Table 2, entry 8). Inspired by the work of Mehrkhodavandi *et al.*,[58] we tested the robustness of **2** against water and impurities using as received, commercial grade *rac*-LA. Strikingly, almost identical polymerization outcomes compared to purified *rac*-LA were observed in respect to activity, molecular weight and dispersity (Table 2, entries 8 *vs.* 9). When further lowering the catalyst loading to 0.05 mol%, 79% conversion was realized within 15 min, highlighting the exceptional tolerance of initiator **2** against unpurified monomer (Table 2, entry 10). In all LA polymerization experiments, lower experimental than expected molar masses were observed indicating chain scission processes at these high reaction temperatures. All polymers were slightly heterotactic enriched (P_r = 0.60–0.63; Fig. S25†). Using as received, commercial grade L-LA, the activity of **2** is reduced but still high (TOF = 2760 h^{-1}) and affords PLA with M_n = 18.4 kg mol^{-1}, Đ = 1.16 (Table 2, entry 11). The polymerization of L-LA proceeds with almost no sign of epimerization, even when the polymerization temperature is further raised to 170 °C (Table 2, entry 12; P_m > 0.97, Fig. S26 and S27†).

Finally, γ-BL was chosen for polymerization tests with **2** since γ-BL is a very challenging monomer requiring low reaction temperatures and only few metal-based catalysts have been reported to accomplish the synthesis of chemically recyclable poly(γ-butyrolactone) (PγBL).[18] Under bulk conditions at −35 °C, initiator **2** demonstrated its versatility producing PγBLs with relatively high molecular weights (Table 2, entries 13 and 14). Due to precipitation of the polymers from the reaction mixture, the M_n values are indifferent of initial [γ-BL]/[**2**] ratios and dispersities were broadened (M_n ≈ 21 kg mol^{-1}, Đ ≈ 1.8).[17]

Using catam complex **3**, the ROP of β-BL proceeded significantly slower compared to the salan derivative (TOF = 160 h^{-1}; Table 1, entry 11), albeit slightly isotactic enriched PHB with narrow dispersity was obtained (P_m = 0.61; Fig. S24†). Moreover, initiator **3** showed lower reaction rates in the ROP of ε-CL and ε-DL but displayed generally good polymerization control (Table 2, entries 15 and 16). In addition to lower catalytic activity, ROP of *rac*-LA was accompanied by severe transesterification side reactions (Table 2, entry 17). Although the catalytic activity of **3** is still high in the broader context, these results indicate that the methylene bridge in the framework of salan complex **2** is a favorable design criterion in ROP catalysis. Generally, salan ligands are considered more flexible than salen derivatives and less constrained than related catam ligands.[47] The improved ability of framework distortion in the case of salan ligands might favor coordination of (several different-sized) monomers as well as rapid propagation. A combined experimental and theoretical study showed that backbone linker flexibility in salen-type aluminum complexes reduces the energy cost of framework distortion, ultimately leading to improved reaction rates in ROP.[59] These results might also be applicable to indium complexes. Furthermore, useful comparisons can be drawn with related indium all-rounder catalysts (Fig. 3C and D, *vide infra*). Here, our work gives additional support for the importance of framework flexibility in order to achieve very high rates in the ROP of cyclic esters spanning various ring sizes (4- to 7-membered).

When compared to the literature, initiator **2** substantially outperforms reported group 13 catalysts (Fig. 3).[37,38] The respective aluminum salan complex requires several days to achieve moderate conversions in the ROP of β-BL and *rac*-LA even at elevated temperatures.[60,61] A simple catalyst system based on InCl$_3$/NEt$_3$/BnOH showed broad monomer scope but TOFs were generally low.[40–42] High activities were observed with leading group 13 catalysts **B–D**.[43–46] The overall higher rates of salan complex **2** in comparison to more rigid (phospha)salen-type complexes **C** and **D** supports again the relevance of framework flexibility in catalyst design. When comparing **2** against a broader context of catalysts showing high rates as well as diverse monomer scope (Fig. 3), leading zinc catalysts **E–G** are outperformed.[31,33,34] Catalytic activity is similar to β-diiminate zinc system **H**, one of the superior catalysts in the field of ROP.[26,27] Besides catalysts based on zinc, several rare earth-metal complexes exhibit the highest rates for ROP of various lactones.[36] TOFs of yttrium species **I** are in the same order of magnitude as those of **2** except β-BL polymerization, while La(O^{i}Pr)$_3$ (**K**) is generally less active.[28–30,35] Ultrahigh rates were observed with initiator **J** for the ROP of *rac*-LA but strongly reduced rates for other lactones.[24] This again emphasizes the challenge in catalyst design of achieving high activity in combination with diverse monomer scope. Here, indium salan complex **2** shows very high activities for a remarkably broad range of cyclic esters, thus representing it as one of the leading all-rounder catalysts in ROP of cyclic esters. Putting **2** in an industrial context, the rates of commercially used Sn(Oct)$_2$ (**L**) are higher for PLA production albeit in the same order of

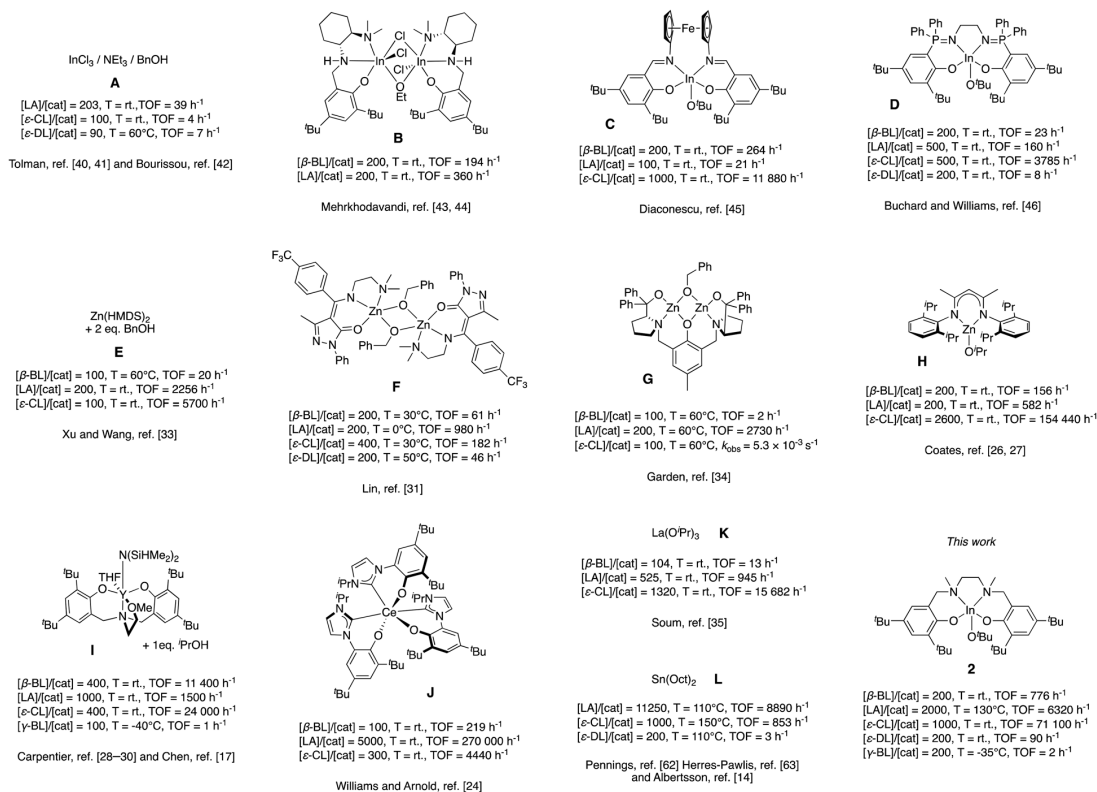This journal is © The Royal Society of Chemistry 2022

Catal. Sci. Technol., 2022, **12**, 3295–3302 | **3299**

50

Catalysis Science & Technology

Fig. 3 Catalysts showing high activity and broad monomer scope in ROP (**A–K**), including this work (**2**). Sn(Oct)$_2$ (**L**) is shown as an example of an industrially relevant catalyst.

magnitude.[62] High temperatures are required for the ROP of ε-CL and ε-DL,[14,63] whereas **2** provides substantially faster access to the respective polyesters already at room temperature.

Conclusions

In summary, an indium salan alkoxide complex with excellent performance in the ROP of β-BL, γ-BL, ε-CL, ε-DL and LA was described, showing the high versatility of this complex. The polymerizations were well controlled, operable under immortal conditions and yielded high molecular weight polyesters with narrow dispersities. Additionally, the use of an impure lactide feedstock under industrially relevant conditions gave identical polymerization results compared to a purified monomer feedstock, demonstrating the outstanding robustness of catalyst **2**. The polymerization rates of poorly active but air-stable chloro pre-catalyst **1** could be drastically enhanced by *in situ* activation with propylene oxide. In comparison with the indium salan alkoxide catalyst featuring flexible methylene bridges in the ligand framework, a more constrained indium catam alkoxide initiator **3** (lacking these methylene bridges) showed reduced activity for this range of monomers. These results indicate the benefit of

introducing framework flexibility in catalyst design in order to achieve highly active all-rounder catalysts such as **2**. Additionally, salan complex **2** highlights the remarkable potential of indium initiators in ROP catalysis, a research area, that is traditionally dominated by zinc and rare-earth metal compounds in terms of leading catalytic activities. Versatile catalysts that show high activity across a broad substrate range, as reported herein, are appealing and provide various opportunities in the rapid and precise synthesis of copolymers. Future work will focus on exploiting these indium complexes in other polymerizations such as CO$_2$ and epoxide copolymerization. Combined with the broad substrate scope in ROP of cyclic esters established in this work, using one simple, versatile all-rounder catalyst opens access to sophisticated copolymer architectures with tailored properties.

Author contributions

J. B. conducted all experimental work, D. H. conducted the crystallographic analysis, S. V. and B. R. supervised the research. The final version of the manuscript was written with contributions from all authors.

51

Catalysis Science & Technology

Paper

Conflicts of interest

There are no conflicts to declare.

Acknowledgements

Notes and references

1 S. B. Borrelle, J. Ringma, K. L. Law, C. C. Monnahan, L. Lebreton, A. McGivern, E. Murphy, J. Jambeck, G. H. Leonard and M. A. Hilleary, *Science*, 2020, **369**, 1515–1518.
2 N. Simon, K. Raubenheimer, N. Urho, S. Unger, D. Azoulay, T. Farrelly, J. Sousa, H. van Asselt, G. Carlini, C. Sekomo, M. L. Schulte, P.-O. Busch, N. Wienrich and L. Weiand, *Science*, 2021, **373**, 43–47.
3 J. R. Jambeck, R. Geyer, C. Wilcox, T. R. Siegler, M. Perryman, A. Andrady, R. Narayan and K. L. Law, *Science*, 2015, **347**, 768–771.
4 W. W. Lau, Y. Shiran, R. M. Bailey, E. Cook, M. R. Stuchtey, J. Koskella, C. A. Velis, L. Godfrey, J. Boucher and M. B. Murphy, *Science*, 2020, **369**, 1455–1461.
5 J. M. Garcia and M. L. Robertson, *Science*, 2017, **358**, 870–872.
6 X. Tang and E. Y. X. Chen, *Chem*, 2019, **5**, 284–312.
7 G. W. Coates and Y. D. Y. L. Getzler, *Nat. Rev. Mater.*, 2020, **5**, 501–516.
8 C. M. Thomas, *Chem. Soc. Rev.*, 2010, **39**, 165–173.
9 B. Rieger, A. Künkel, G. W. Coates, R. Reichardt, E. Dinjus and T. A. Zevaco, *Synthetic biodegradable polymers*, Springer-Verlag, Berlin, Heidelberg, 2012.
10 J. F. Carpentier, *Macromol. Rapid Commun.*, 2010, **31**, 1696–1705.
11 M. Labet and W. Thielemans, *Chem. Soc. Rev.*, 2009, **38**, 3484–3504.
12 J. C. Worch, H. Prydderch, S. Jimaja, P. Bexis, M. L. Becker and A. P. Dove, *Nat. Rev. Chem.*, 2019, **3**, 514–535.
13 Bioplastics market data 2021. European Bioplastics. **https://www.european-bioplastics.org/market/**.
14 P. Olsen, T. Borke, K. Odelius and A. C. Albertsson, *Biomacromolecules*, 2013, **14**, 2883–2890.
15 D. Zhang, M. A. Hillmyer and W. B. Tolman, *Biomacromolecules*, 2005, **6**, 2091–2095.
16 H. C. Quilter, M. Hutchby, M. G. Davidson and M. D. Jones, *Polym. Chem.*, 2017, **8**, 833–837.
17 M. Hong and E. Y. Chen, *Nat. Chem.*, 2016, **8**, 42–49.
18 Y. Liu, J. Wu, X. Hu, N. Zhu and K. Guo, *ACS Macro Lett.*, 2021, **10**, 284–296.
19 E. Feghali, L. Tauk, P. Ortiz, K. Vanbroekhoven and W. Eevers, *Polym. Degrad. Stab.*, 2020, **179**, 109241.
20 J. Payne and M. D. Jones, *ChemSusChem*, 2021, **14**, 4041–4070.

21 Y. Li and T. J. Strathmann, *Green Chem.*, 2019, **21**, 5586–5597.
22 V. Poirier, T. Roisnel, J. F. Carpentier and Y. Sarazin, *Dalton Trans.*, 2009, 9820–9827.
23 H. Wang, J. Guo, Y. Yang and H. Ma, *Dalton Trans.*, 2016, **45**, 10942–10953.
24 R. W. F. Kerr, P. M. D. A. Ewing, S. K. Raman, A. D. Smith, C. K. Williams and P. L. Arnold, *ACS Catal.*, 2021, **11**, 1563–1569.
25 A.-C. Albertsson and I. K. Varma, *Biomacromolecules*, 2003, **4**, 1466–1486.
26 B. M. Chamberlain, M. Cheng, D. R. Moore, T. M. Ovitt, E. B. Lobkovsky and G. W. Coates, *J. Am. Chem. Soc.*, 2001, **123**, 3229–3238.
27 L. R. Rieth, D. R. Moore, E. B. Lobkovsky and G. W. Coates, *J. Am. Chem. Soc.*, 2002, **124**, 15239–15248.
28 C.-X. Cai, L. Toupet, C. W. Lehmann and J.-F. Carpentier, *J. Organomet. Chem.*, 2003, **683**, 131–136.
29 A. Amgoune, C. M. Thomas, T. Roisnel and J. F. Carpentier, *Chem. – Eur. J.*, 2006, **12**, 169–179.
30 A. Amgoune, C. M. Thomas, S. Ilinca, T. Roisnel and J. F. Carpentier, *Angew. Chem., Int. Ed.*, 2006, **45**, 2782–2784.
31 H.-J. Chuang, H.-L. Chen, B.-H. Huang, T.-E. Tsai, P.-L. Huang, T.-T. Liao and C.-C. Lin, *J. Polym. Sci., Part A: Polym. Chem.*, 2013, **51**, 1185–1196.
32 T. Ebrahimi, D. C. Aluthge, S. G. Hatzikiriakos and P. Mehrkhodavandi, *Macromolecules*, 2016, **49**, 8812–8824.
33 R. Yang, G. Xu, C. Lv, B. Dong, L. Zhou and Q. Wang, *ACS Sustainable Chem. Eng.*, 2020, **8**, 18347–18353.
34 W. Gruszka, L. C. Walker, M. P. Shaver and J. A. Garden, *Macromolecules*, 2020, **53**, 4294–4302.
35 M. Save, M. Schappacher and A. Soum, *Macromol. Chem. Phys.*, 2002, **203**, 889–899.
36 D. M. Lyubov, A. O. Tolpygin and A. A. Trifonov, *Coord. Chem. Rev.*, 2019, **392**, 83–145.
37 S. Dagorne, M. Normand, E. Kirillov and J.-F. Carpentier, *Coord. Chem. Rev.*, 2013, **257**, 1869–1886.
38 K. M. Osten and P. Mehrkhodavandi, *Acc. Chem. Res.*, 2017, **50**, 2861–2869.
39 Z. L. Shen, S. Y. Wang, Y. K. Chok, Y. H. Xu and T. P. Loh, *Chem. Rev.*, 2013, **113**, 271–401.
40 A. Pietrangelo, M. A. Hillmyer and W. B. Tolman, *Chem. Commun.*, 2009, 2736–2737.
41 A. Pietrangelo, S. C. Knight, A. K. Gupta, L. J. Yao, M. A. Hillmyer and W. B. Tolman, *J. Am. Chem. Soc.*, 2010, **132**, 11649–11657.
42 S. Thongkham, J. Monot, B. Martin-Vaca and D. Bourissou, *Macromolecules*, 2019, **52**, 8103–8113.
43 A. F. Douglas, B. O. Patrick and P. Mehrkhodavandi, *Angew. Chem., Int. Ed.*, 2008, **47**, 2290–2293.
44 C. Xu, I. Yu and P. Mehrkhodavandi, *Chem. Commun.*, 2012, **48**, 6806–6808.
45 S. M. Quan and P. L. Diaconescu, *Chem. Commun.*, 2015, **51**, 9643–9646.
46 N. Yuntawattana, T. M. McGuire, C. B. Durr, A. Buchard and C. K. Williams, *Catal. Sci. Technol.*, 2020, **10**, 7226–7239.

Paper

Catalysis Science & Technology

47 J. C. Pessoa and I. Correia, *Coord. Chem. Rev.*, 2019, **388**, 227–247.

48 J. Beament, M. F. Mahon, A. Buchard and M. D. Jones, *New J. Chem.*, 2017, **41**, 2198–2203.

49 C. Robert, T. E. Schmid, V. Richard, P. Haquette, S. K. Raman, M. N. Rager, R. M. Gauvin, Y. Morin, X. Trivelli, V. Guerineau, I. Del Rosal, L. Maron and C. M. Thomas, *J. Am. Chem. Soc.*, 2017, **139**, 6217–6225.

50 A. J. Gaston, G. Navickaite, G. S. Nichol, M. P. Shaver and J. A. Garden, *Eur. Polym. J.*, 2019, **119**, 507–513.

51 A. J. Gaston, Z. Greindl, C. A. Morrison and J. A. Garden, *Inorg. Chem.*, 2021, **60**, 2294–2303.

52 R. Duan, C. Hu, X. Li, X. Pang, Z. Sun, X. Chen and X. Wang, *Macromolecules*, 2017, **50**, 9188–9195.

53 S. Impemba, F. Della Monica, A. Grassi, C. Capacchione and S. Milione, *ChemSusChem*, 2020, **13**, 141–145.

54 W. Xia, S. I. Vagin and B. Rieger, *Chem. – Eur. J.*, 2014, **20**, 15499–15504.

55 L. P. Carrodeguas, T. T. D. Chen, G. L. Gregory, G. S. Sulley and C. K. Williams, *Green Chem.*, 2020, **22**, 8298–8307.

56 G. S. Sulley, G. L. Gregory, T. T. D. Chen, L. Pena Carrodeguas, G. Trott, A. Santmarti, K. Y. Lee, N. J. Terrill and C. K. Williams, *J. Am. Chem. Soc.*, 2020, **142**, 4367–4378.

57 M. P. F. Pepels, M. Bouyahyi, A. Heise and R. Duchateau, *Macromolecules*, 2013, **46**, 4324–4334.

58 T. Ebrahimi, D. C. Aluthge, B. O. Patrick, S. G. Hatzikiriakos and P. Mehrkhodavandi, *ACS Catal.*, 2017, **7**, 6413–6418.

59 E. E. Marlier, J. A. Macaranas, D. J. Marell, C. R. Dunbar, M. A. Johnson, Y. DePorre, M. O. Miranda, B. D. Neisen, C. J. Cramer, M. A. Hillmyer and W. B. Tolman, *ACS Catal.*, 2016, **6**, 1215–1224.

60 P. Hormnirun, E. L. Marshall, V. C. Gibson, A. J. White and D. J. Williams, *J. Am. Chem. Soc.*, 2004, **126**, 2688–2689.

61 J. Fagerland, A. Finne-Wistrand and D. Pappalardo, *New J. Chem.*, 2016, **40**, 7671–7679.

62 A. Nijenhuis, D. Grijpma and A. Pennings, *Macromolecules*, 1992, **25**, 6419–6424.

63 A. Hermann, S. Hill, A. Metz, J. Heck, A. Hoffmann, L. Hartmann and S. Herres-Pawlis, *Angew. Chem., Int. Ed.*, 2020, **59**, 21778–21784.

53

5 Monomer-Selective Indium Catalyst for the Synthesis of Block Copolyesters from One-Pot Monomer Mixtures

5.1 Bibliographic Data
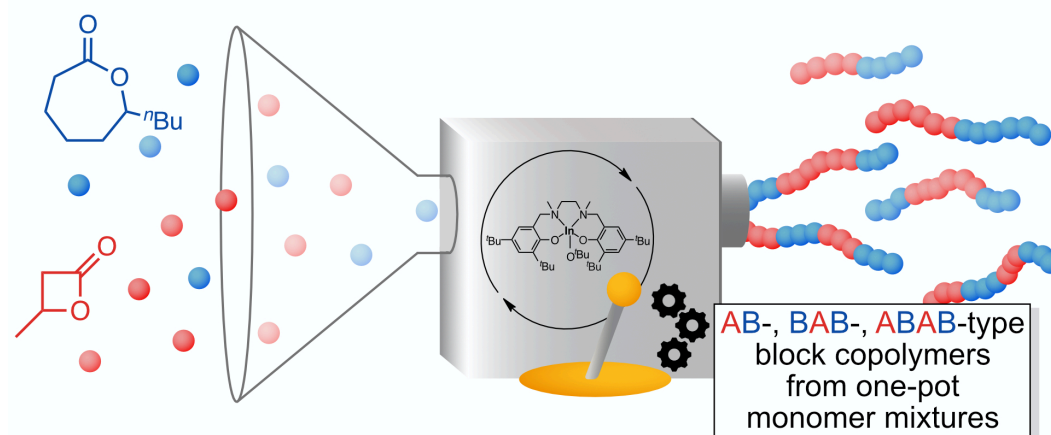
Title:	Simple and Rapid Access toward AB, BAB and ABAB Block Copolyesters from One-Pot Monomer Mixtures Using an Indium Catalyst
Status:	Letter, published online August 17, 2022
Journal:	ACS Macro Letters, 2022, 11, 1067–1072.
Publisher:	American Chemical Society
DOI:	10.1021/acsmacrolett.2c00468
Authors:	Jonas Bruckmoser, Bernhard Rieger

Article reproduced with permission from the American Chemical Society.

5.2 Content

In this work, the indium salan initiator described previously in chapter 4[131] was employed to demonstrate the potential of all-rounder catalysts in the ROCOP of various lactones for generating defined copolymers. Block copolymers combine properties of their homopolymers and can be prepared by sequential addition protocols. However, the synthesis of such polymers from monomer mixtures is more appealing as it reduces synthetic efforts and is one step forward into the direction of mimicking Nature's sequence control. Previously, the synthesis of oxygenated block copolymers from monomer mixtures has been achieved by exploiting distinct reactivities of *different* monomer classes such as the combination of lactones with epoxides/CO_2 or carboxyanhydrides.[173,183] Herein, the precise synthesis of AB-, BAB- and ABAB-type block copolymers from same-class monomer mixtures using an indium salan-type catalyst was described. An unexpected switch in reactivity was observed in one-pot copolymerizations of β-BL and ε-CL, reversing monomer reactivity expected from homopolymerization results and highlighting the high affinity of the indium initiator towards β-BL. Instead of a PCL-*b*-PHB block copolymer, PHB-*co*-PCL gradient copolymers were obtained. Increasing the difference in steric demand between the 4-membered and 7-membered lactone even further by introduction of a bulky *n*-butyl side chain (i.e. using ε-DL instead of ε-CL as monomer), resulted in an even more pronounced monomer-selective behavior of the catalyst. This enabled the simple synthesis of sequence-controlled AB copolymers from β-BL/ε-DL monomer mixtures. Kinetic analysis showed that ε-DL conversion was very low as long as β-BL was present in the reaction mixture, however, after full consumption of β-BL, ε-DL polymerization rate increased by a factor of 4.9. These results demonstrated that the catalyst successfully differentiates between the comonomers in the mixture. This synthetic protocol in combination with the indium salan initiator also enabled the simple and rapid synthesis of ABAB block copolymers when an additional portion of β-BL was added to a β-BL/ε-DL monomer mixture after 50% conversion of ε-DL. Similarly, starting with a homopolymerization of ε-DL and adding β-BL after 50% conversion conveniently generated BAB block copolymers. The structure of these defined AB-, BAB-, and ABAB-type block copolymers was unambiguously identified by ^{1}H and ^{13}C{^{1}H} NMR analysis, DSC and TGA measurements. In the ^{13}C{^{1}H} NMR spectra, heterodyads from tapering regions were almost completely absent, DSC curves showed two distinct T_g values and a two-step decomposition process was evident in the TGA. Thus, it could be demonstrated that sequence control in copolymerizations is not only feasible by combination of *different* monomer classes but also within *one* class of *similarly* reactive monomers.

5.3 Manuscript

ACS *Macro* Letters

Letter

Simple and Rapid Access toward AB, BAB and ABAB Block Copolyesters from One-Pot Monomer Mixtures Using an Indium Catalyst

Jonas Bruckmoser and Bernhard Rieger*

Cite This: *ACS Macro Lett.* 2022, 11, 1067−1072

Read Online

ACCESS | 📊 Metrics & More | 📄 Article Recommendations | ⓢ Supporting Information

ABSTRACT: The synthesis of well-defined block copolymers from one-pot monomer mixtures is particularly challenging when monomers are from the same class and show similar reactivity. Herein, an indium-based catalyst that shows comparable rates in the ring-opening homopolymerization of β-butyrolactone (β-BL) and ε-decalactone (ε-DL), demonstrates monomer-selective behavior in one-pot copolymerizations of β-BL and ε-DL. This provides simple and rapid access to well-defined di-, tri-, or tetra-block copolyesters from monomer mixtures. The sequence-controlled nature of these polymers was confirmed by kinetic analysis, $^{13}C\{^{1}H\}$ NMR spectroscopy, DSC, and TGA measurements.

AB-, BAB-, ABAB-type block copolymers from one-pot monomer mixtures
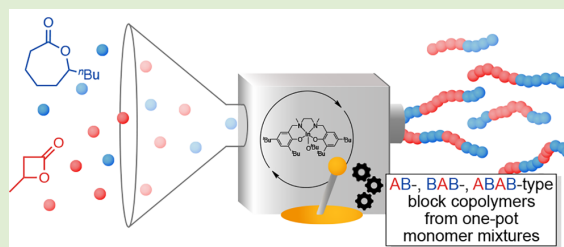
While sequence-controlled polymers are ubiquitous in Nature, the synthetic production of polymers with a defined order of building blocks remains highly challenging.[1] The scope of artificial catalytic polymerization methods is far away from such sophisticated systems, yet imitation of Nature has led to innovative catalyst design where, for example, allosteric control enables different reactivity of the catalyst.[2] Similarly, polymerization catalysts that can be switched between two or more states by external stimuli such as redox, electrochemical, or photochemical stimuli have emerged to give access to sequence-controlled polymers.[3−5]

Switchable catalysis is gaining increased research attention in the field of ring-opening polymerization (ROP) of cyclic esters.[6,7] ROP gives simple access to (bio)degradable polyesters with high control over molecular weight and polydispersity, however, the precise control of polymer sequence still remains a major challenge. When different monomer classes, such as lactones, epoxides/CO₂, or carboxyanhydrides, are combined in ring-opening copolymerizations,[8,9] distinct reactivity differences of the metal chain end group in the respective catalytic cycles enable high chemoselectivity and simple access to block copolymers.[10−15] In contrast to that, sequence control from one-pot mixtures of the same monomer class is highly challenging due to similar reactivity.[16] Redox-controlled "on/off" switching in ROP of one specific cyclic ester monomer is achieved with an increasing number of catalysts,[17−23] yet, establishing orthogonal monomer reactivity for two different lactones to generate block copolyesters is rarely reported.[7,24] For example, the synthesis of a block copolymer microstructure from an L-lactide (L-LA)/ε-caprolactone (ε-CL) feedstock has been

achieved with a redox-switchable titanium catalyst.[25] Using a different approach, stereoselective polymerization catalysts allowed for the synthesis of alternating sequence-controlled polyesters when mixed monomers of opposite stereochemistry were employed.[26,27] However, the addition of oxidants and reductants or the use of enantiopure monomer mixtures makes these approaches experimentally challenging.

Achieving the goal of a defined polymer sequence, such as block copolymers, in ROP of lactone mixtures can in general be relatively simple if large reactivity differences of the catalyst are observed in the homopolymerization of different monomers, and these are retained in copolymerizations (i.e., kinetic control).[16,28−32] Nevertheless, the drawbacks of this method are long reaction times or large tapered regions in the polymer, potential transesterification side reactions that lead to randomization of the initial block architecture and inactivity of the catalyst for different monomer combinations.[16,33−35]

In this context, catalysts that show high chemoselectivity for one specific monomer in one-pot mixtures and give rapid access to block copolymer structures, similarly to ring-opening copolymerization of different monomer classes, are an appealing target. Herein, we report on the simple and rapid synthesis of well-defined AB-, BAB-, and ABAB-type block copolymers from

1067
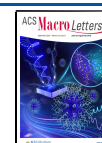
one-pot monomer mixtures using an indium salan-type catalyst that demonstrates monomer-selective behavior (Scheme 1).

Scheme 1. Copolymerization of β-BL with ε-CL and ε-DL to Access Gradient or AB-, BAB-, and ABAB-Type Block Copolymers from One-Pot Monomer Mixtures Using Indium Catalyst 1
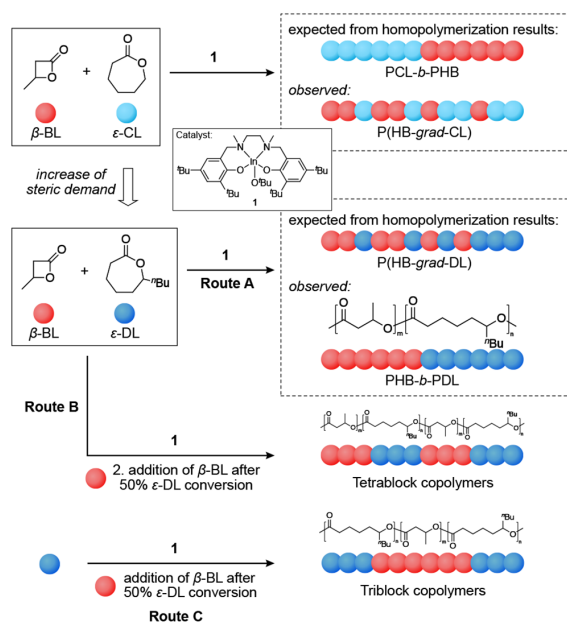
For the synthesis of sequence-controlled polymers, a catalyst with high control over the polymerization is required, otherwise inter- and intramolecular transesterifications lead to scrambling of the polymer sequence. Indium catalyst **1** (Scheme 1) was recently reported by our group and showed very high activity in ROP across a broad range of lactone monomers.[36] Besides its high activity, the catalyst showed excellent polymerization control with minimal transesterification side reactions, rendering it an ideal candidate to approach copolymers with defined microstructure. Aiming for block copolyesters from monomer mixtures via kinetic control, we performed copolymerization experiments of β-BL and ε-CL. Considering the ultrahigh activity of **1** in ROP of ε-CL (turnover frequency (TOF) = 64800 h^{-1} vs TOF = 776 h^{-1} for β-BL; Table S1, entries 1 and 2), we expected rapid conversion of ε-CL to form a PCL-block followed by slower polymerization of β-BL giving PCL-*b*-PHB. To our surprise, when 500 equiv of each monomer were used in a one-pot mixture, β-BL conversion was twice as high as ε-CL conversion after a polymerization time of 15 min (Table 1, entry 1). Reducing the β-BL/ε-CL ratio to 200/500 equiv revealed that β-BL was still consumed faster than ε-CL, albeit ε-CL conversion was strongly increased (Table 1, entry 2). Consequently, these results indicated that the polymerization of ε-CL is limited by the amount of β-BL present in the monomer mixture when catalyst **1** is employed. A kinetic study of the copolymerization monitored by ^{1}H NMR spectroscopy further corroborated these findings. The polymerization rate of β-BL was significantly higher than that of ε-CL, and while consumption of β-BL follows a first-order behavior, conversion of ε-CL follows a zero-order rate law (Figures S2−S4). These observations suggest that the addition of ε-CL to the propagating chain end is rapid, while the ROP of β-BL is the rate-limiting step. However, coordination strength of β-BL toward **1** is higher than that of ε-CL, thus, overall limiting ε-CL ROP (Figure S8). The obtained polymers exhibited unimodal gel permeation chromatography (GPC) traces and very narrow polydispersities ($Đ \leq 1.07$). The synthesis of copolymers was additionally confirmed by diffusion-ordered NMR spectroscopy (DOSY) showing a single diffusion coefficient for the polymer samples (Figures S27 and S28).

Having identified that catalyst **1** shows a high selectivity toward β-BL in monomer mixtures, we hypothesized that increasing the steric demand of the comonomer might favor affinity of **1** for polymerizing sterically less demanding β-BL even further. We therefore chose ε-DL as a related comonomer to ε-CL but having a large *n*-butyl side chain in close proximity to the metal-coordinating carbonyl group. Homopolymerization experiments revealed a high activity of **1** in ROP of ε-DL (TOF up to 168 h^{-1}, Table S1, entry 4).

Previous reports have shown that the copolymerization of β-BL and ε-DL is highly challenging, as only sequential copolymerization approaches were successful, but one-pot approaches failed.[37] We first tested the sequential block copolymerization of β-BL and ε-DL using catalyst **1** (Table 1, entry 3). A well-defined copolymer with $M_{n,AB} = 51.0$ kg mol^{-1}

Table 1. Ring-Opening Copolymerization of β-BL with ε-CL or ε-DL Using Indium Catalyst 1[a]

entry	monomer A	monomer B	[A]/[B]/[1]	route[b]	t (min)	conv. A[c] (%)	conv. B[c] (%)	$M_{n,theo}$[d] (kg mol^{-1})	$M_{n,GPC}$[e] (kg mol^{-1})	$Đ$[e]	T_g[f] (°C)
1	β-BL	ε-CL	500:500:1	A	15	51	24	35.6	48.6	1.07	−30
2	β-BL	ε-CL	200:500:1	A	15	86	68	53.6	88.9	1.07	−55
3[g]	β-BL	ε-DL	200:200:1	seq. add.	140	>99	82	45.0	51.0	1.08	−53/−2
4	β-BL	ε-DL	100:100:1	A	90	>99	93	24.4	31.8	1.06	−52/−9
5	β-BL	ε-DL	200:200:1	A	180	>99	87	46.7	49.7	1.08	−53/−6
6	β-BL	ε-DL	300:300:1	A	240	>99	70	61.3	58.9	1.07	−54/−6
7	β-BL	ε-DL	200:200:1	C	60/180	−/>99	40/77	43.3	45.8	1.20[h]	n.d.
8[i]	β-BL	ε-DL	200:200:1	C	45/180	−/>99	51/81	22.3	23.8	1.11	−53/−16
9[j]	β-BL	ε-DL	200:200:1	B	90/240	>99/>99	52/82	45.0	50.2	1.09	−50/−15

[a]Polymerizations were performed in toluene at room temperature, $[\beta\text{-BL}] = [M_B] = 2.0$ M. [b]Reaction pathway according to Scheme 1. [c]Conversion determined by ^{1}H NMR spectroscopy. [d]Theoretical molecular weights were determined from the $[M]/[I]$ ratio and monomer conversion data. [e]Determined by GPC in THF at 40 °C relative to polystyrene standards. [f]Determined by DSC, second heating scan. [g]Sequential addition, ε-DL was added after full conversion of β-BL (20 min). [h]Bimodal distribution. [i]2 equiv of BnOH added. [j]Initial monomer mixture 100:200:1, additional 100 equiv of β-BL added after 90 min.
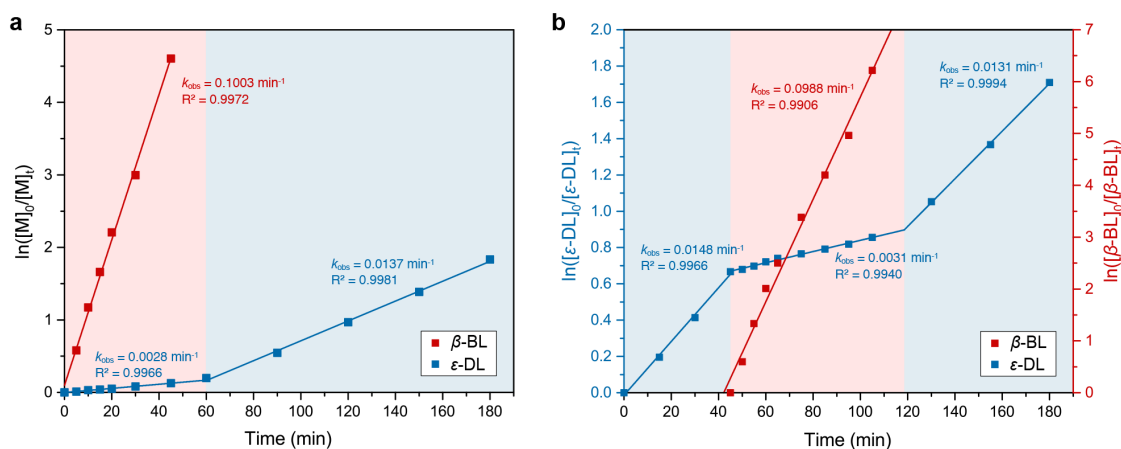
Figure 1. Semilogarithmic plots of monomer concentration over time for the copolymerization of β-BL and ε-DL mediated by complex **1**. (a) One-pot monomer mixture, [β-BL]/[ε-DL]/**1** = 200/200/1 (Route A, Scheme 1). (b) ε-DL ROP and addition of β-BL after 45 min, [β-BL]/[ε-DL]/[BnOH]/**1** = 200/200/2/1 (Route C, Scheme 1).

and $Đ$ = 1.08 was obtained ($M_{n,A}$ = 24.3 kg mol^{-1}, $Đ$ = 1.03). DOSY NMR spectroscopy confirmed the synthesis of a copolymer (Figure S29), and the ^{13}C{^{1}H} NMR spectrum showed only two resonances in the carbonyl region, as expected for block formation (the carbonyl resonance of PHB is split due to the atactic nature of the polymer, Figure S43). The absence of heterodyads resulting from transesterifications highlights the excellent polymerization control of **1**. Additionally, differential scanning calorimetry (DSC) revealed two distinct glass transition temperatures (T_g) at −53 and −2 °C, which are in good agreement with the respective T_g values of pure PDL and PHB, further supporting the successful synthesis of a block copolymer (Figure S13). Thermal gravimetric analysis (TGA) revealed a two-step decomposition process of the copolymer with maximum decomposition rates at 284 and 341 °C (Figure S22).

Based on these results, we aimed for the synthesis of copolymers from one-pot monomer mixtures, potentially resulting in interesting polymer microstructures based on aforementioned hypothesis regarding steric differentiation of monomers by the catalyst. A 100/100/1 mixture of β-BL and ε-DL was rapidly converted by **1** yielding a polymer with M_n = 31.8 kg mol^{-1} and $Đ$ = 1.06 (Table 1, entry 4). Increasing the monomer-to-catalyst ratio to 200/200/1 and 300/300/1 resulted in the successful synthesis of polymers with increased molecular weights while dispersity remained very narrow (Table 1, entries 5 and 6). Experimental molecular weights were agreeing well with those theoretically calculated and the content of β-BL and ε-DL in the isolated polymers was in accordance with respective monomer conversions (Figures S44−S49). Importantly, the successful copolymer formation was confirmed by DOSY NMR (Figures S30−S32).

In order to gain further insights into the copolymerization of β-BL/ε-DL monomer mixtures via Route A, we performed a kinetic analysis. Aliquots were withdrawn from a β-BL/ε-DL/**1** (200/200/1) reaction mixture and the samples analyzed by ^{1}H NMR and GPC analysis. A linear increase of M_n with conversion was observed while dispersity of the growing polymer chains remained very narrow (Figure S5), evident of a living-type polymerization. While consumption of β-BL follows a first-order behavior with k_{obs} = 0.1003 min^{-1}, ε-DL conversion showed an

unprecedented result (Figure 1a). During the presence of β-BL in the polymerization mixture, the rate of ε-DL polymerization is very low (k_{obs} = 0.0028 min^{-1}). However, once all β-BL is consumed the ε-DL rate increases by a factor of 4.9 (k_{obs} = 0.0137 min^{-1}), indicating that the catalyst successfully differentiates between the two comonomers in the mixture. Thus, the self-switchable behavior of **1** in ROP of β-BL/ε-DL allows for the synthesis of well-defined diblock copolymers with minimal tapering from one-pot mixtures, as further supported by ^{13}C{^{1}H} NMR (Figure 2). To the best of our knowledge, such
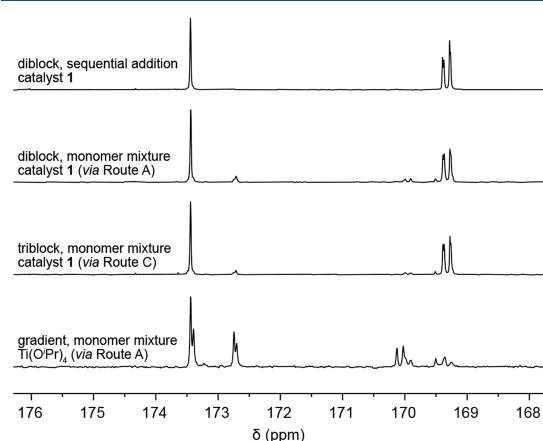
Figure 2. Comparison of ^{13}C{^{1}H} NMR spectra (carbonyl region) of PHB-*co*-PDL copolymers prepared via different synthesis routes and catalysts.

a chemoselective behavior has previously only been observed in phosphazene-catalyzed ROP of β-BL with benzyl β-malolactone, but required very long reaction times and showed relatively poor polymerization control.[38] The polymer microstructure of synthesized PHB-*b*-PDLs (Table 1, entries 4−6) was additionally verified by the presence of two T_g values in the DSC traces with values close to their homopolymers (Figures 3 and S14−S16) and a two-step decomposition process in the TGA (Figures S23−S25). Overall, analytical data of PHB-*b*-PDLs prepared
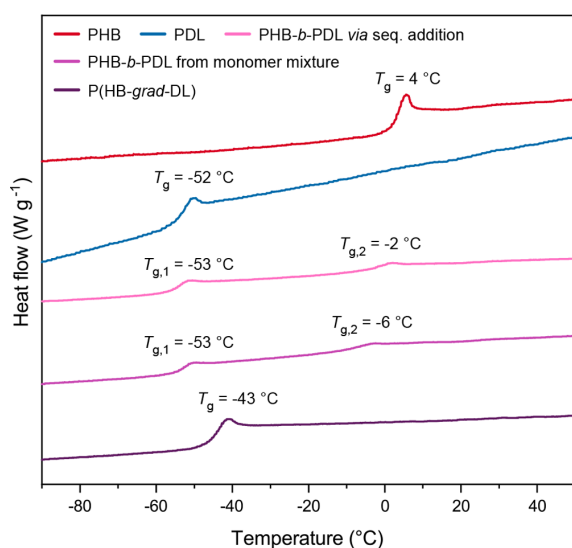
Figure 3. Comparison of DSC curves (exo down) of PHB and PDL homopolymers with PHB-co-PDL block and gradient copolymers.

from monomer mixtures was in close resemblance to those of PHB-b-PDL prepared via sequential addition (Figures 2 and 3).

Attempting the copolymer synthesis from one-pot mixtures with an yttrium bisphenolate catalyst that has shown broad monomer scope for a range of cyclic esters,[39] only gave copolymers with a limited amount of ε-DL incorporated into the polymer chain (Table S1, entries 6 and 7). Using organocatalyst 1,5,7-triazabicyclo[4.4.0]dec-5-ene (TBD) did not result in the formation of copolymers while tin(II) 2-ethylhexanoate [Sn-(Oct)$_2$] only afforded oligomeric materials (Table S1, entries 8 and 9). Ti(O^{i}Pr)$_4$ was capable of accessing PHB-co-PDL copolymers, albeit long reaction times and high temperatures were required (Table S1, entry 10). ^{13}C{^{1}H} NMR analysis of the copolymer revealed a gradient microstructure (Figure 2) and accordingly, a single thermal transition was observed in the DSC curve (Figure 3). These results clearly show the challenge of synthesizing defined (block) copolymers from monomer mixtures and highlight the potential of catalyst **1**.

On the basis of the exceptional monomer-selective polymerization behavior of initiator **1**, we became interested in the synthesis of more complex polymer architectures such as tri- or tetrablock copolymers. We reasoned that starting the polymerization with ε-DL and adding β-BL at ~50% conversion of ε-DL should result in preferential consumption of β-BL from that point on while ROP of ε-DL should be effectively halted. After full conversion of β-BL, ε-DL polymerization is expected to resume, ultimately yielding a triblock copolymer (Scheme 1, Route C). Testing this approach, 200 equiv of ε-DL were polymerized until 40% conversion using **1**, then, 200 equiv of β-BL were added to the reaction mixture, and the polymerization allowed to resume until high conversion of β-BL (>99%) and ε-DL (77%) was achieved (Table 1, entry 7). However, the isolated polymer exhibited a bimodal GPC trace indicating that the formation of a defined multiblock copolymer failed. GPC analysis of reaction aliquots and the fact that unimodal GPC traces were observed for tetrablock copolymers prepared via a similar approach (*vide infra*), led us to conclude that the poor initiation efficiency of **1** in ROP of ε-DL was the reason for the

bimodal polymer distribution (see SI, Section 2.1). In order to achieve a high initiation efficiency in ROP of ε-DL, **1** was activated *in situ* by the addition of 2 equiv of benzyl alcohol (BnOH). Following aforementioned copolymerization protocol, copolymers with a unimodal GPC trace and a single diffusion coefficient in DOSY NMR measurements could be successfully isolated (Table 1, entry 8; Figures S7 and S33). The triblock polymer microstructure was verified by kinetic analysis of the copolymerization (Figure 1b). After β-BL addition, the rate of ε-DL polymerization is drastically reduced (k_{obs} = 0.0031 min^{-1} vs k_{obs} = 0.0148 min^{-1}) and β-BL is 32-fold more likely incorporated into the polymer chain than ε-DL. The highly resolved nature of the triblock copolymer was further confirmed by ^{13}C{^{1}H} NMR spectroscopy (Figure 2) and DSC (Figure S17). Expanding this approach, the simple synthesis of an ABAB tetrablock copolymer was feasible when starting from a β-BL/ε-DL monomer mixture and adding a second portion of β-BL monomer after ~50% conversion of ε-DL (Scheme 1, Route B; Table 1, entry 9). Again, the structure of the tetrablock copolyester was unambiguously identified by DOSY and ^{13}C{^{1}H} NMR spectroscopy (Figures S34 and S53), DSC (Figure S18), and TGA (Figure S26).

In summary, copolymerizations of ε-CL and β-BL using an indium salan-type catalyst **1** revealed that **1** shows a strong affinity toward β-BL in monomer mixtures. PHB-co-PCL gradient copolymers were obtained instead of block copolymers, reversing monomer reactivity expected from homopolymerization results. Switching to a related but sterically more demanding comonomer compared to ε-CL, namely, ε-DL, allowed for the simple and rapid synthesis of well-defined AB, BAB, and ABAB block copolymers from β-BL/ε-DL monomer mixtures. Previously, switchable catalysis has focused on exploiting distinct reactivities of different monomer classes such as lactones, epoxides/CO$_2$ or carboxyanhydrides in order to achieve block copolymers from monomer mixtures. Our work shows that monomer differentiation by the catalyst is feasible not only within different monomer classes, but also within one class of similarly reacting monomers, and thus gives access to even more complex sequence-controlled polymer architectures.

■ ASSOCIATED CONTENT

ⓢ Supporting Information

The Supporting Information is available free of charge at https://pubs.acs.org/doi/10.1021/acsmacrolett.2c00468.

Experimental procedures, additional polymerization data, and analytical and characterization data of polymers (PDF)

■ AUTHOR INFORMATION

Corresponding Author

Bernhard Rieger − *WACKER-Chair of Macromolecular Chemistry, Catalysis Research Center, Department of Chemistry, Technical University of Munich, 85748 Garching, Germany;* ⊙ orcid.org/0000-0002-0023-884X; Email: rieger@tum.de

Author

Jonas Bruckmoser − *WACKER-Chair of Macromolecular Chemistry, Catalysis Research Center, Department of Chemistry, Technical University of Munich, 85748 Garching, Germany*

Complete contact information is available at:

Notes
The authors declare no competing financial interest.

■ REFERENCES

(1) Badi, N.; Lutz, J. F. Sequence control in polymer synthesis. *Chem. Soc. Rev.* **2009**, *38*, 3383−3390.

(2) Yoon, H. J.; Kuwabara, J.; Kim, J.-H.; Mirkin, C. A. Allosteric supramolecular triple-layer catalysts. *Science* **2010**, *330*, 66−69.

(3) Leibfarth, F. A.; Mattson, K. M.; Fors, B. P.; Collins, H. A.; Hawker, C. J. External regulation of controlled polymerizations. *Angew. Chem., Int. Ed.* **2013**, *52*, 199−210.

(4) Teator, A. J.; Lastovickova, D. N.; Bielawski, C. W. Switchable Polymerization Catalysts. *Chem. Rev.* **2016**, *116*, 1969−1992.

(5) Doerr, A. M.; Burroughs, J. M.; Gitter, S. R.; Yang, X.; Boydston, A. J.; Long, B. K. Advances in Polymerizations Modulated by External Stimuli. *ACS Catal.* **2020**, *10*, 14457−14515.

(6) Guillaume, S. M.; Kirillov, E.; Sarazin, Y.; Carpentier, J. F. Beyond stereoselectivity, switchable catalysis: some of the last frontier challenges in ring-opening polymerization of cyclic esters. *Chem.— Eur. J.* **2015**, *21*, 7988−8003.

(7) Chen, C. Redox-Controlled Polymerization and Copolymerization. *ACS Catal.* **2018**, *8*, 5506−5514.

(8) Deacy, A. C.; Gregory, G. L.; Sulley, G. S.; Chen, T. T. D.; Williams, C. K. Sequence Control from Mixtures: Switchable Polymerization Catalysis and Future Materials Applications. *J. Am. Chem. Soc.* **2021**, *143*, 10021−10040.

(9) Hu, C.; Pang, X.; Chen, X. Self-Switchable Polymerization: A Smart Approach to Sequence-Controlled Degradable Copolymers. *Macromolecules* **2022**, *55*, 1879−1893.

(10) Romain, D. C.; Williams, C. K. Chemoselective polymerization control: from mixed-monomer feedstock to copolymers. *Angew. Chem., Int. Ed.* **2014**, *53*, 1607−1610.

(11) Zhu, Y.; Romain, C.; Williams, C. K. Selective polymerization catalysis: controlling the metal chain end group to prepare block copolyesters. *J. Am. Chem. Soc.* **2015**, *137*, 12179−12182.

(12) Romain, C.; Zhu, Y.; Dingwall, P.; Paul, S.; Rzepa, H. S.; Buchard, A.; Williams, C. K. Chemoselective Polymerizations from Mixtures of Epoxide, Lactone, Anhydride, and Carbon Dioxide. *J. Am. Chem. Soc.* **2016**, *138*, 4120−4131.

(13) Kernbichl, S.; Reiter, M.; Adams, F.; Vagin, S.; Rieger, B. CO₂-Controlled One-Pot Synthesis of AB, ABA Block, and Statistical Terpolymers from β-Butyrolactone, Epoxides, and CO₂. *J. Am. Chem. Soc.* **2017**, *139*, 6787−6790.

(14) Sulley, G. S.; Gregory, G. L.; Chen, T. T. D.; Pena Carrodeguas, L.; Trott, G.; Santmarti, A.; Lee, K. Y.; Terrill, N. J.; Williams, C. K. Switchable catalysis improves the properties of CO₂-derived polymers: poly(cyclohexene carbonate-*b*-ε-decalactone-*b*-cyclohexene carbonate) adhesives, elastomers, and toughened plastics. *J. Am. Chem. Soc.* **2020**, *142*, 4367−4378.

(15) Yang, Z.; Hu, C.; Cui, F.; Pang, X.; Huang, Y.; Zhou, Y.; Chen, X. One-Pot Precision Synthesis of AB, ABA and ABC Block Copolymers via Switchable Catalysis. *Angew. Chem., Int. Ed.* **2022**, *61*, No. e202117533.

(16) Diaz, C.; Mehrkhodavandi, P. Strategies for the synthesis of block copolymers with biodegradable polyester segments. *Polym. Chem.* **2021**, *12*, 783−806.

(17) Gregson, C. K.; Gibson, V. C.; Long, N. J.; Marshall, E. L.; Oxford, P. J.; White, A. J. Redox control within single-site polymerization catalysts. *J. Am. Chem. Soc.* **2006**, *128*, 7410−7411.

(18) Broderick, E. M.; Guo, N.; Vogel, C. S.; Xu, C.; Sutter, J.; Miller, J. T.; Meyer, K.; Mehrkhodavandi, P.; Diaconescu, P. L. Redox control of

a ring-opening polymerization catalyst. *J. Am. Chem. Soc.* **2011**, *133*, 9278−9281.

(19) Broderick, E. M.; Guo, N.; Wu, T.; Vogel, C. S.; Xu, C.; Sutter, J.; Miller, J. T.; Meyer, K.; Cantat, T.; Diaconescu, P. L. Redox control of a polymerization catalyst by changing the oxidation state of the metal center. *Chem. Commun.* **2011**, *47*, 9897−9899.

(20) Biernesser, A. B.; Li, B.; Byers, J. A. Redox-controlled polymerization of lactide catalyzed by bis(imino)pyridine iron bis(alkoxide) complexes. *J. Am. Chem. Soc.* **2013**, *135*, 16553−16560.

(21) Qi, M.; Dong, Q.; Wang, D.; Byers, J. A. Electrochemically Switchable Ring-Opening Polymerization of Lactide and Cyclohexene Oxide. *J. Am. Chem. Soc.* **2018**, *140*, 5686−5690.

(22) Hern, Z. C.; Quan, S. M.; Dai, R.; Lai, A.; Wang, Y.; Liu, C.; Diaconescu, P. L. ABC and ABAB Block Copolymers by Electrochemically Controlled Ring-Opening Polymerization. *J. Am. Chem. Soc.* **2021**, *143*, 19802−19808.

(23) de Vries, F.; Otten, E. Reversible On/Off Switching of Lactide Cyclopolymerization with a Redox-Active Formazanate Ligand. *ACS Catal.* **2022**, *12*, 4125−4130.

(24) Wei, J.; Diaconescu, P. L. Redox-Switchable Ring-Opening Polymerization with Ferrocene Derivatives. *Acc. Chem. Res.* **2019**, *52*, 415−424.

(25) Wang, X.; Thevenon, A.; Brosmer, J. L.; Yu, I.; Khan, S. I.; Mehrkhodavandi, P.; Diaconescu, P. L. Redox control of group 4 metal ring-opening polymerization activity toward L-lactide and ε-caprolactone. *J. Am. Chem. Soc.* **2014**, *136*, 11264−11267.

(26) Kramer, J. W.; Treitler, D. S.; Dunn, E. W.; Castro, P. M.; Roisnel, T.; Thomas, C. M.; Coates, G. W. Polymerization of enantiopure monomers using syndiospecific catalysts: a new approach to sequence control in polymer synthesis. *J. Am. Chem. Soc.* **2009**, *131*, 16042−16044.

(27) Jia, Z.; Jiang, J.; Zhang, X.; Cui, Y.; Chen, Z.; Pan, X.; Wu, J. Isotactic-Alternating, Heterotactic-Alternating, and ABAA-Type Sequence-Controlled Copolyester Syntheses via Highly Stereoselective and Regioselective Ring-Opening Polymerization of Cyclic Diesters. *J. Am. Chem. Soc.* **2021**, *143*, 4421−4432.

(28) Basko, M.; Duda, A.; Kazmierski, S.; Kubisa, P. Cationic copolymerization of racemic-β-butyrolactone with L,L-lactide: One-pot synthesis of block copolymers. *J. Polym. Sci., Part A: Polym. Chem.* **2013**, *51*, 4873−4884.

(29) Wilson, J. A.; Hopkins, S. A.; Wright, P. M.; Dove, A. P. Synthesis and Postpolymerization Modification of One-Pot ω-Pentadecalactone Block-like Copolymers. *Biomacromolecules* **2015**, *16*, 3191−3200.

(30) Wilson, J. A.; Hopkins, S. A.; Wright, P. M.; Dove, A. P. Dependence of Copolymer Sequencing Based on Lactone Ring Size and ε-Substitution. *ACS Macro Lett.* **2016**, *5*, 346−350.

(31) Pothupitiya, J. U.; Dharmaratne, N. U.; Jouaneh, T. M. M.; Fastnacht, K. V.; Coderre, D. N.; Kiesewetter, M. K. H-Bonding Organocatalysts for the Living, Solvent-Free Ring-Opening Polymerization of Lactones: Toward an All-Lactones, All-Conditions Approach. *Macromolecules* **2017**, *50*, 8948−8954.

(32) Tang, X.; Shi, C.; Zhang, Z.; Chen, E. Y. X. Toughening Biodegradable Isotactic Poly(3-hydroxybutyrate) via Stereoselective Copolymerization of a Diolide and Lactones. *Macromolecules* **2021**, *54*, 9401−9409.

(33) Kramer, J. W.; Coates, G. W. Fluorinated β-Lactones and Poly(β-hydroxyalkanoate)s: Synthesis via Epoxide Carbonylation and Ring-Opening Polymerization. *Tetrahedron* **2008**, *64*, 6973−6978.

(34) Jasinska-Walc, L.; Hansen, M. R.; Dudenko, D.; Rozanski, A.; Bouyahyi, M.; Wagner, M.; Graf, R.; Duchateau, R. Topological behavior mimicking ethylene-hexene copolymers using branched lactones and macrolactones. *Polym. Chem.* **2014**, *5*, 3306−3310.

(35) Walther, P.; Naumann, S. N-Heterocyclic Olefin-Based (Co)-polymerization of a Challenging Monomer: Homopolymerization of ω-Pentadecalactone and Its Copolymers with γ-Butyrolactone, δ-Valerolactone, and ε-Caprolactone. *Macromolecules* **2017**, *50*, 8406−8416.

(36) Bruckmoser, J.; Henschel, D.; Vagin, S.; Rieger, B. Combining high activity with broad monomer scope: indium salan catalysts in the

ring-opening polymerization of various cyclic esters. *Catal. Sci. Technol.* **2022**, *12*, 3295−3302.

(37) Kiriratnikom, J.; Robert, C.; Guerineau, V.; Venditto, V.; Thomas, C. M. Stereoselective Ring-Opening (Co)polymerization of *β*-Butyrolactone and *ε*-Decalactone Using an Yttrium Bis(phenolate) Catalytic System. *Front. Chem.* **2019**, *7*, 301.

(38) Jaffredo, C. G.; Carpentier, J.-F.; Guillaume, S. M. Poly-(hydroxyalkanoate) Block or Random Copolymers of *β*-Butyrolactone and Benzyl *β*-Malolactone: A Matter of Catalytic Tuning. *Macromolecules* **2013**, *46*, 6765−6776.

(39) Carpentier, J.-F. Rare-Earth Complexes Supported by Tripodal Tetradentate Bis(phenolate) Ligands: A Privileged Class of Catalysts for Ring-Opening Polymerization of Cyclic Esters. *Organometallics* **2015**, *34*, 4175−4189.

6 Monomer Design for the Synthesis of Chemically Recyclable Polyesters

6.1 Bibliographic Data
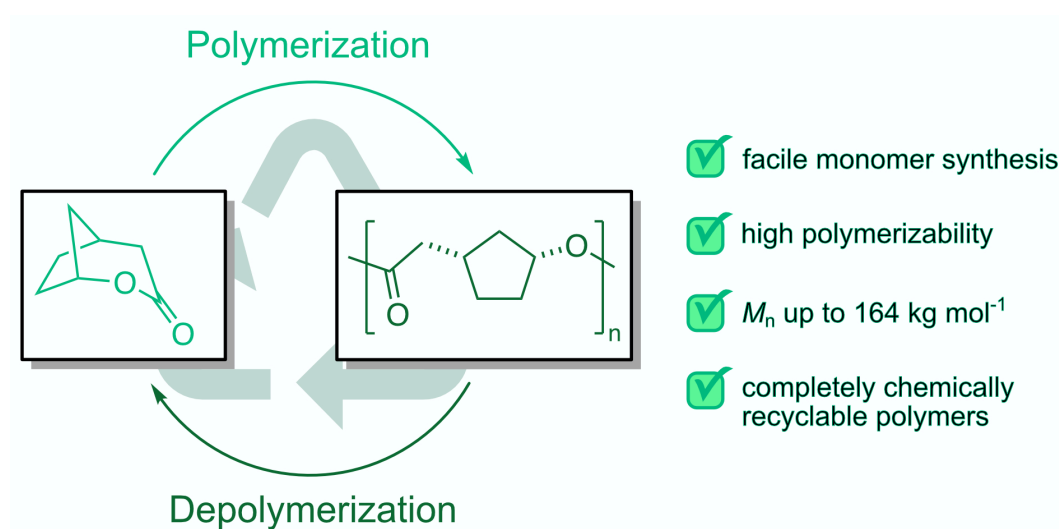
Title:	Ring-Opening Polymerization of a Bicyclic Lactone: Polyesters Derived from Norcamphor with Complete Chemical Recyclability
Status:	Letter, published online September 8, 2022
Journal:	ACS Macro Letters, 2022, 11, 1162–1166.
Publisher:	American Chemical Society
DOI:	10.1021/acsmacrolett.2c00445
Authors:	Jonas Bruckmoser,[‡] Sebastian Remke,[‡] Bernhard Rieger

Article reproduced with permission from the American Chemical Society.

6.2 Content

Polymers are a class of materials that have found immense use in various applications and have a significant positive impact on our daily lives. However, when it comes to the end-of-life fate of today's commodity plastics, their durability and persistence are a major drawback. Plastic contamination of the environment is nowadays considered as one of the urging, global challenges calling for innovations from polymer chemists. Chemical recycling approaches in order to achieve a circular plastics economy have gained significant attention in recent years. Particularly promising are novel, specifically designed polymer systems that can be depolymerized back to monomer, thus closing the loop and enabling the synthesis of recycled polymers with virgin material properties. In this study, the ROP of a bicyclic lactone (NCL) derived from norcamphor was described and the chemical recyclability of the resulting polyesters investigated. Previously, several bicyclic lactones based on a 5- or 7-membered ring core structure have enabled the synthesis of chemically recyclable polyesters. Herein, this strategy of ring-fusion in monomer design was expanded to a 6-membered ring core structure. A catalyst screening including tin-, titanium-, yttrium and zinc-based catalysts, revealed $ZnEt_2$ as the most potent catalyst for ROP of NCL. It was shown that NCL is highly polymerizable (even at high polymerization temperatures of 110°C) and high molecular weight polyesters can be obtained (M_n up to 164 kg mol^{-1}). The thermal properties of this novel polyester were studied by means of DSC and TGA, displaying an amorphous nature of PNCL with a maximum rate decomposition temperature $T_{d,max}$ of 234°C. Most importantly, the obtained materials could be completely recycled back to monomer in quantitative yield within 4 h under thermolysis conditions (T = 220°C). Additionally, NCL could be recovered under chemolysis conditions when a lanthanum catalyst was used. Thus, it was demonstrated that the ring-fusion/hybridization approach in monomer design is also applicable for 6-membered rings and is eminently suitable to overcome typically conflicting parameters in monomer–polymer systems, i.e. high polymerizability and high depolymerizability.

6.3 Manuscript

ACS *Macro Letters*

Letter

Ring-Opening Polymerization of a Bicyclic Lactone: Polyesters Derived from Norcamphor with Complete Chemical Recyclability

Jonas Bruckmoser,[‡] Sebastian Remke,[‡] and Bernhard Rieger*

Cite This: *ACS Macro Lett.* 2022, 11, 1162−1166

Read Online

ACCESS | Metrics & More | Article Recommendations | Supporting Information

ABSTRACT: Chemical recycling of polymers is an elegant approach to achieve a circular economy and address the sustainability and end-of-life issues of plastics. Herein, we report the ring-opening polymerization of a bicyclic lactone that is easily accessible from norcamphor. High molecular weight polyesters (M_n up to 164 kg mol^{-1}) are obtained using ZnEt$_2$ as catalyst, while the polymerizability of the monomer is good even at high temperatures. More importantly, the polymers can be completely depolymerized under thermolysis conditions to selectively recover the pristine monomer. Thus, the monomer design strategy of using ring-fused/hybridized lactones enables an innovative monomer−polymer system that shows both high polymerizability and high depolymerizability.

Polymerization / Depolymerization

- facile monomer synthesis
- high polymerizability
- M_n up to 164 kg mol^{-1}
- completely chemically recyclable polymers
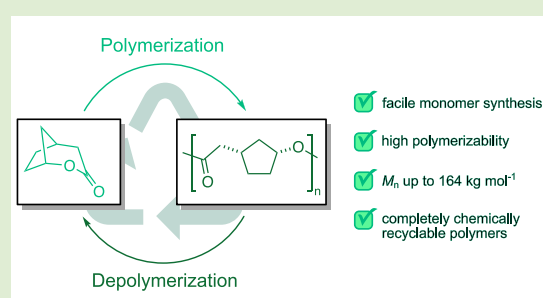
Current commodity plastics are extremely useful materials that have found a plethora of applications and are present in everyday life. Within the past decades, an estimated 8300 million metric tons (Mt) of virgin plastics have been produced.[1] However, when it comes to the end-of-life fate of these materials, various issues arise. Most of these plastics have been discarded or incinerated, and only a fraction (600 Mt) have been recycled since.[1,2] Besides major issues arising from the persistence of current commodity plastics in the environment, the loss of material value, together with the need for extraction of virgin raw materials, is a severe drawback.[2−4]

In recent years, chemical recycling to monomer (CRM) has emerged as a promising strategy to tackle these challenges and enable a circular polymer economy.[5−8] Ring-opening polymerization (ROP) of cyclic esters is a valuable method for enabling such polymerization−depolymerization systems due to the thermodynamic equilibrium between the monomer and resulting polymer.[8,9] Chen et al. exploited this behavior in their pioneering work on the ROP of "nonstrained" γ-butyrolactone (GBL). ROP was performed at low temperatures (−40 °C), and complete chemical recyclability back to the monomer was achieved when heating the obtained polymer at high temperatures (>220 °C).[10] However, the poor polymerizability yet good depolymerizability demonstrate the trade-off commonly observed in such systems and illustrate the need for delicate monomer design.

In order to balance polymerizability/depolymerizability and achieve promising material properties, approaches of using bicyclic monomers have emerged (Scheme 1). ROP of *trans*-cyclohexyl-ring-fused GBLs delivered materials with improved thermal and mechanical properties yet retained their full recyclability due to the GBL-based core.[11−13] Further

Scheme 1. Bicyclic Monomers Based on Five- or Seven-Membered Rings as the Core Structure Enabling the Synthesis of Chemically Recyclable Polymers and This Work

5-membered ring core structure

Chen 2018 Chen 2018 Chen 2021 X = N-R Lu 2019
X = CH$_2$ Chen 2020

6-membered ring core structure

this work

ring fusion enables chemical recyclability?

7-membered ring core structure with heteroatom

X = O Shaver 2016
X = S Du and Li 2021
X = S Cai and Zhu 2022

Du and Li 2021

X = O Cai and Zhu 2021
X = S Du and Li 2021
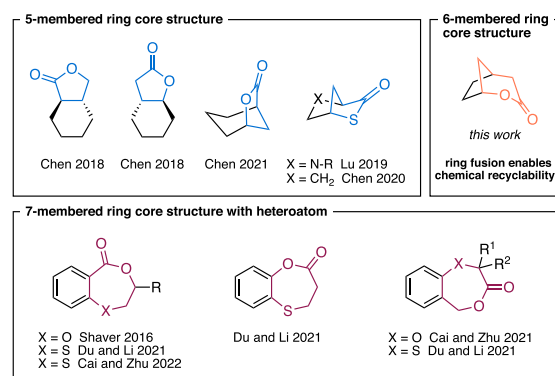
expanding this concept, Chen and co-workers used the structural hybridization of ε-caprolactone and GBL to create a bicyclic lactone that affords polyester materials with high

1162
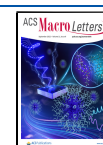
glass transition temperature (T_g) or melting point (T_m), high thermal stability, and complete chemical recyclability.[14] Similarly, clean depolymerization to the monomer was achieved with polythioesters based on bicyclic thiolactones.[15,16]

Apart from those bicyclic monomers with a five-membered ring core structure, seven-membered lactones with aromatic units have emerged as a promising monomer class for the synthesis of chemically recyclable polymers with beneficial material properties (Scheme 1). Since the initial report of Shaver et al.,[17,18] various substitution patterns and their influence on polymerization/depolymerization as well as polymer characteristics have been studied.[19−21]

Inspired by the strategy of using ring-fused monomers for CRM and especially the hybridization approach of Chen et al., we were interested in whether this concept could be expanded to bicyclic lactones with a six-membered ring core structure and still yield chemically recyclable polyesters (Scheme 1). ROP of six-membered bicyclic lactones is rarely reported in the literature,[22−26] and CRM has not yet been described. While δ-valerolactone has a relatively high ceiling temperature (T_c), alkyl substitution strongly influences T_c and monomer equilibrium concentration.[27] For instance, early work has shown that poly(β-methyl-δ-valerolactone)-based polyurethanes and carbomethoxylated polyvalerolactone are chemically recyclable.[28,29] δ-Methyl and α-methylene-substituted six-membered lactones have been very recently explored for CRM.[30,31] Based on this, we set out to investigate the ROP of a bicyclic lactone with a six-membered ring core structure derived from norcamphor and study the depolymerization behavior of the resulting alicyclic polyester.

The synthesis of norcamphor lactone (**NCL**), formally 2-oxabicyclo[3.2.1]octan-3-one, was achieved by a facile one-step Baeyer−Villiger oxidation from commercially available norcamphor (Scheme 2).[32] While various procedures for the

Scheme 2. Monomer Synthesis Starting from Norcamphor and Subsequent Ring-Opening Polymerization[a]
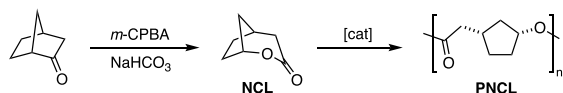
[a]($\pm$)-Norcamphor was employed in the synthesis of **NCL**. For clarity, only one enantiomer is shown.

synthesis of this lactone exist, its polymerization has surprisingly been only attempted twice in the literature, but either the polymerization failed or the molecular weight of the polymers was limited to <2 kg mol^{-1}.[33,34] Keeping in mind the depolymerizability of related polyesters bearing cyclic fragments in the polymer backbone, we were initially interested in whether high molecular weight polyesters can be obtained in the ROP of **NCL** or if thermodynamic equilibria limit the synthesis thereof.

At the outset of our catalyst screening, we attempted the ROP of **NCL** using the established catalyst tin octoate [Sn(oct)$_2$]. However, no conversion was observed at a [**NCL**]/[cat] ratio of 100:1 despite the high reaction temperatures (Table 1, entry 1). Switching to a discrete yttrium-based catalyst **Y1** (Figure S1) that has shown superior performance in ROP for a range of monomers[35] resulted in the successful isolation of poly(norcamphor lactone) (**PNCL**).

High conversions were obtained at room temperature when 20 equiv of **NCL** was used (Table 1, entry 2). However, further increasing the [**NCL**]/[cat] ratio to 100:1 led to a drastic decrease in activity, and only 37% of monomer was converted after 48 h (Table 1, entry 3). Using Ti(O^{i}Pr)$_4$ as catalyst, conversion was low at reaction temperatures of 80 °C under both solvent and bulk conditions (Table 1, entries 4 and 5). Increasing the temperature to 110 °C resulted in high conversion in bulk polymerizations, and activity was still moderate when performing the polymerization under solvent conditions (Table 1, entries 6 and 7). However, in all polymerization runs using Ti(O^{i}Pr)$_4$, only low molecular weight polymers were obtained (M_n < 4 kg mol^{-1}).

Finally, we arrived at ZnEt$_2$ as a potent ROP catalyst and obtained **PNCL** with high molecular weight and narrow dispersity (M_n = 22.3 kg mol^{-1}, Đ = 1.2) at a [**NCL**]/[cat] ratio of 100:1 at 80 °C (Table 1, entry 8). Performing the polymerization in bulk at 110 °C gave high monomer conversions (83%) in only 3 h, albeit at the expense of broadened dispersity due to transesterifications (Table 1, entry 9). Increasing the [**NCL**]/[cat] ratio to 200:1 nearly doubled the molecular weight of **PNCL** (Table 1, entry 10). Similar ROP performance in terms of activity and molecular weight control was observed when the catalyst loading was decreased even further to 400:1 (Table 1, entry 11). Eventually, **PNCL** with a molecular weight of 163.7 kg mol^{-1} (Đ = 1.7) could be obtained when the [**NCL**]/[cat] ratio was as high as 1500:1 (Table 1, entry 12).

^{1}H NMR analysis of the resulting polymers revealed that the ROP of **NCL** takes place with retention of its *cis*-configuration, and no epimerization was observed as evidenced by the absence of a second set of resonances expected for a *trans*-stereoconfiguration (Figure S4).[14] The tacticity of **PNCL** was investigated by means of ^{13}C{^{1}H} NMR spectroscopy. Some signals, including the carbonyl resonance, showed a splitting with identical intensity, indicating an atactic polymer structure (Figure S5).

The thermal properties of obtained **PNCL** were investigated by thermal gravimetric analysis (TGA) and differential scanning calorimetry (DSC). TGA revealed a $T_{d,5\%}$ of 183 °C and a maximum rate decomposition temperature $T_{d,max}$ of 234 °C (Figure 1a). Comparing the decomposition temperature of **PNCL** to literature known polyesters bearing cyclic fragments in the backbone, its thermal stability is reduced.[11,12,14,24−26,36] Decomposition temperatures of **PNCL** are similar to poly(2-(2-hydroxyethoxy)benzoate) (Scheme 1, Shaver 2016).[18] Subsequent work has shown that the thermal stability can be improved by O to S as well as alkyl substitution in the backbone.[19,21] Such strategies might also be promising for increasing the decomposition temperature of **NCL**-based polymers in the future. **PNCL** is an amorphous material as evidenced by DSC (Figure 1b). The T_g of **PNCL** (T_g = −9 °C) is increased more than 50 °C in relation to poly(δ-valerolactone).[37] In comparison to polyesters bearing purely cyclopentyl or cyclohexyl backbones that often exhibit high T_g or T_m values,[14,24,26,36] the CH$_2$ group in α-position to the carbonyl of **PNCL** presumably enables a higher chain flexibility.[11,12]

Curious whether the ring-fusion approach in our monomer design enabled the synthesis of recyclable polymers, we first attempted thermolysis experiments. **PNCL** with a molecular weight of 42.4 kg mol^{-1} was heated in bulk at 280 °C. Depolymerization conversion reached 75% after 0.5 h and was

1163

Table 1. Ring-Opening Polymerization of NCL Using Various Catalysts[a]

entry	catalyst	solvent	[M]/[cat]	T (°C)	time (h)	conv. (%)[b]	M_n (kg mol^{-1})[c]	Đ[c]
1	Sn(oct)$_2$	Tol	100	110	24	0	n.d.	n.d.
2	**Y1**	Tol	20	rt	24	89	7.0	1.6
3	**Y1**	Tol	100	rt	48	37	8.4	1.4
4	Ti(O^{i}Pr)$_4$	Tol	100	80	24	3	n.d.	n.d.
5	Ti(O^{i}Pr)$_4$	bulk	100	80	24	14	2.1	1.2
6	Ti(O^{i}Pr)$_4$	Tol	100	110	24	53	1.9	1.5
7	Ti(O^{i}Pr)$_4$	bulk	100	110	24	80	3.8	1.3
8	ZnEt$_2$	Tol	100	80	24	72	22.3	1.2
9	ZnEt$_2$	bulk	100	110	3	83	22.2	2.1
10	ZnEt$_2$	bulk	200	110	24	83	35.4	1.8
11	ZnEt$_2$	bulk	400	110	24	81	86.8	1.9
12	ZnEt$_2$	bulk	1500	110	24	41	163.7	1.7

[a]Polymerizations were performed under solvent or bulk conditions (Tol = toluene), for solvent conditions [**NCL**] = 3.4 M, except entries 2 and 3, [**NCL**] = 2.4 M. n.d. = not determined. [b]Conversion determined by ^{1}H NMR spectroscopy. [c]Determined by GPC in CHCl$_3$ at room temperature relative to polystyrene standards.
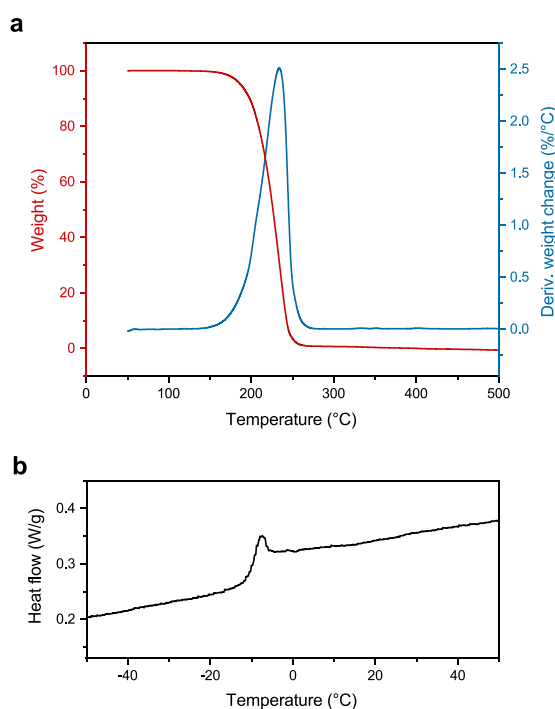
Figure 1. Analysis of thermal properties. (a) TGA curve for **PNCL**. (b) DSC curve for **PNCL** (second heating scan, exo down).

Figure 2. Complete chemical recyclability of **PNCL**. ^{1}H NMR spectra (CDCl$_3$, 25 °C) of pristine monomer (bottom), **PNCL** obtained by ROP (middle), and recovered monomer from the thermolysis of **PNCL** at 220 °C (top) (*grease).

quantitative within 2 h. ^{1}H NMR spectroscopy revealed that the **NCL** monomer is recovered; however, the high temperatures also promoted an elimination to give 2-cyclopentene-1-acetic acid as a side product in a ratio of 1:2 (Figures S6 and S7). By reducing the temperature to 220 °C, **NCL** is selectively and quantitatively recovered within 4 h (Figure 2). The high purity of recycled **NCL** was additionally confirmed by gas chromatography (Figure S11). The chemical recycling behavior of **PNCL** was further investigated using ZnCl$_2$ as the catalyst. However, bulk depolymerization at 180 °C occurred unselectively without generation of monomer. In contrast to that, pure **NCL** can be recovered by using La[N(SiMe$_3$)$_2$]$_3$. At catalyst loadings of 50:1 (respective to the

polymer repeating unit, M_n = 42.4 kg mol^{-1}), >90% of pure **NCL** was obtained within 2 h in bulk depolymerizations at 220 °C. Investigating the chemolysis under dilute conditions at 120 °C (25 mg mL^{-1} **PNCL** in toluene), monomer could also be selectively recovered (43% conversion after 3 h). It is worth noting that polyesters obtained via ROP of a closely related bicyclic lactone with five-membered ring core structure were not chemically recyclable.[38] Hence, the introduction of a CH$_2$ group in α-position to the carbonyl in the **PNCL** backbone has a vast positive effect and facilitates clean recovery of monomer.

In summary, the ROP of a norcamphor-derived bicyclic lactone was described, and high molecular weight polyesters were obtained. **NCL** was readily polymerized even at high temperatures, and for the first time, a bicyclic lactone with six-membered core structure furnished the synthesis of polymeric materials with complete chemical recyclability to monomer under thermolysis or chemolysis conditions. Thus, the hybridization approach in monomer design could be successfully expanded to structures beyond the typical γ-butyrolactone-based core. This strategy enabled the combination of excellent polymerizability with facile depolymerizability. Given the simplicity of this approach, the material properties of such polymers based on six-membered rings could be easily

1164

pubs.acs.org/macroletters

tuned in the future by specifically designed monomer modifications.

ASSOCIATED CONTENT

Supporting Information

The Supporting Information is available free of charge at https://pubs.acs.org/doi/10.1021/acsmacrolett.2c00445.

Experimental procedures, analytical and characterization data of polymers (PDF)

AUTHOR INFORMATION

Corresponding Author

Bernhard Rieger − WACKER-Chair of Macromolecular Chemistry, Catalysis Research Center, Department of Chemistry, Technical University of Munich, 85748 Garching, Germany; orcid.org/0000-0002-0023-884X; Email: rieger@tum.de

Authors

Jonas Bruckmoser − WACKER-Chair of Macromolecular Chemistry, Catalysis Research Center, Department of Chemistry, Technical University of Munich, 85748 Garching, Germany

Sebastian Remke − WACKER-Chair of Macromolecular Chemistry, Catalysis Research Center, Department of Chemistry, Technical University of Munich, 85748 Garching, Germany; orcid.org/0000-0002-8471-0477

Complete contact information is available at: https://pubs.acs.org/10.1021/acsmacrolett.2c00445

Author Contributions

‡J.B. and S.R. contributed equally.

Notes

The authors declare no competing financial interest.

REFERENCES

(1) Geyer, R.; Jambeck, J. R.; Law, K. L. Production, use, and fate of all plastics ever made. *Sci. Adv.* **2017**, *3*, No. e1700782.

(2) Borrelle, S. B.; Ringma, J.; Law, K. L.; Monnahan, C. C.; Lebreton, L.; McGivern, A.; Murphy, E.; Jambeck, J.; Leonard, G. H.; Hilleary, M. A.; et al. Predicted growth in plastic waste exceeds efforts to mitigate plastic pollution. *Science* **2020**, *369*, 1515−1518.

(3) Jambeck, J. R.; Geyer, R.; Wilcox, C.; Siegler, T. R.; Perryman, M.; Andrady, A.; Narayan, R.; Law, K. L. Plastic waste inputs from land into the ocean. *Science* **2015**, *347*, 768−771.

(4) Korley, L. T. J.; Epps, T. H.; Helms, B. A.; Ryan, A. J. Toward polymer upcycling—adding value and tackling circularity. *Science* **2021**, *373*, 66−69.

(5) Hong, M.; Chen, E. Y. X. Chemically recyclable polymers: a circular economy approach to sustainability. *Green Chem.* **2017**, *19*, 3692−3706.

(6) Lu, X. B.; Liu, Y.; Zhou, H. Learning Nature: Recyclable Monomers and Polymers. *Chem. Eur. J.* **2018**, *24*, 11255−11266.

(7) Coates, G. W.; Getzler, Y. D. Y. L. Chemical recycling to monomer for an ideal, circular polymer economy. *Nat. Rev. Mater.* **2020**, *5*, 501−516.

(8) Xu, G.; Wang, Q. Chemically recyclable polymer materials: polymerization and depolymerization cycles. *Green Chem.* **2022**, *24*, 2321−2346.

(9) Tang, X.; Chen, E. Y. X. Toward infinitely recyclable plastics derived from renewable cyclic esters. *Chem.* **2019**, *5*, 284−312.

(10) Hong, M.; Chen, E. Y. Completely recyclable biopolymers with linear and cyclic topologies via ring-opening polymerization of γ-butyrolactone. *Nat. Chem.* **2016**, *8*, 42−49.

(11) Zhu, J.-B.; Watson, E. M.; Tang, J.; Chen, E. Y.-X. A synthetic polymer system with repeatable chemical recyclability. *Science* **2018**, *360*, 398−403.

(12) Zhu, J. B.; Chen, E. Y. X. Living Coordination Polymerization of a Six-Five Bicyclic Lactone to Produce Completely Recyclable Polyester. *Angew. Chem., Int. Ed.* **2018**, *57*, 12558−12562.

(13) Zhu, J. B.; Chen, E. Y. Catalyst-Sidearm-Induced Stereo-selectivity Switching in Polymerization of a Racemic Lactone for Stereocomplexed Crystalline Polymer with a Circular Life Cycle. *Angew. Chem., Int. Ed.* **2019**, *58*, 1178−1182.

(14) Shi, C.; Li, Z.-C.; Caporaso, L.; Cavallo, L.; Falivene, L.; Chen, E. Y. X. Hybrid monomer design for unifying conflicting polymer-izability, recyclability, and performance properties. *Chem.* **2021**, *7*, 670−685.

(15) Yuan, J.; Xiong, W.; Zhou, X.; Zhang, Y.; Shi, D.; Li, Z.; Lu, H. 4-Hydroxyproline-Derived Sustainable Polythioesters: Controlled Ring-Opening Polymerization, Complete Recyclability, and Facile Functionalization. *J. Am. Chem. Soc.* **2019**, *141*, 4928−4935.

(16) Shi, C.; McGraw, M. L.; Li, Z.-C.; Cavallo, L.; Falivene, L.; Chen, E. High-performance pan-tactic polythioesters with intrinsic crystallinity and chemical recyclability. *Sci. Adv.* **2020**, *6*, No. eabc0495.

(17) MacDonald, J. P.; Shaver, M. P. An aromatic/aliphatic polyester prepared via ring-opening polymerisation and its remarkably selective and cyclable depolymerisation to monomer. *Polym. Chem.* **2016**, *7*, 553−559.

(18) Lizundia, E.; Makwana, V. A.; Larrañaga, A.; Vilas, J. L.; Shaver, M. P. Thermal, structural and degradation properties of an aromatic-aliphatic polyester built through ring-opening polymerisation. *Polym. Chem.* **2017**, *8*, 3530−3538.

(19) Li, L.-G.; Wang, Q.-Y.; Zheng, Q.-Y.; Du, F.-S.; Li, Z.-C. Tough and Thermally Recyclable Semiaromatic Polyesters by Ring-Opening Polymerization of Benzo-thia-caprolactones. *Macromolecules* **2021**, *54*, 6745−6752.

(20) Tu, Y. M.; Wang, X. M.; Yang, X.; Fan, H. Z.; Gong, F. L.; Cai, Z.; Zhu, J. B. Biobased High-Performance Aromatic-Aliphatic Polyesters with Complete Recyclability. *J. Am. Chem. Soc.* **2021**, *143*, 20591−20597.

(21) Fan, H. Z.; Yang, X.; Chen, J. H.; Tu, Y. M.; Cai, Z.; Zhu, J. B. Advancing the Development of Recyclable Aromatic Polyesters by Functionalization and Stereocomplexation. *Angew. Chem., Int. Ed.* **2022**, *61*, No. e202117639.

(22) Hall Jr, H. Polymerization and ring strain in bridged bicyclic compounds. *J. Am. Chem. Soc.* **1958**, *80*, 6412−6420.

(23) Ceccarelli, G.; Andruzzi, F.; Paci, M. Nmr spectroscopy of polyesters from bridged bicyclic lactones. *Polymer* **1979**, *20*, 605−610.

(24) Okada, M.; Sumitomo, H.; Yamada, S.; Atsumi, M.; Hall, H., Jr; Chan, R. J.; Ortega, R. Synthesis and ring opening polymerization of bicyclic lactones containing a tetrahydropyran ring. 2,5-Dioxabicyclo [2.2.2] octan-3-one. *Macromolecules* **1986**, *19*, 953−959.

(25) Xu, Y.; Sucu, T.; Perry, M. R.; Shaver, M. P. Alicyclic polyesters from a bicyclic 1,3-dioxane-4-one. *Polym. Chem.* **2020**, *11*, 4928−4932.

(26) Zhou, T.; Guo, Y.-T.; Du, F.-S.; Li, Z.-C. Ring-opening Polymerization of 2-Oxabicyclo[2.2.2]octan-3-one and the Influence of Stereochemistry on the Thermal Properties of the Polyesters. *Chin. J. Polym. Sci.* **2022**, DOI: 10.1007/s10118-022-2725-1.

(27) Olsen, P.; Odelius, K.; Albertsson, A. C. Thermodynamic Presynthetic Considerations for Ring-Opening Polymerization. *Biomacromolecules* **2016**, *17*, 699−709.

(28) Schneiderman, D. K.; Vanderlaan, M. E.; Mannion, A. M.; Panthani, T. R.; Batiste, D. C.; Wang, J. Z.; Bates, F. S.; Macosko, C. W.; Hillmyer, M. A. Chemically Recyclable Biobased Polyurethanes. *ACS Macro Lett.* **2016**, *5*, 515−518.

(29) Fahnhorst, G. W.; Hoye, T. R. A Carbomethoxylated Polyvalerolactone from Malic Acid: Synthesis and Divergent Chemical Recycling. *ACS Macro Lett.* **2018**, *7*, 143−147.

(30) Li, C.; Wang, L.; Yan, Q.; Liu, F.; Shen, Y.; Li, Z. Rapid and Controlled Polymerization of Bio-sourced δ-Caprolactone toward Fully Recyclable Polyesters and Thermoplastic Elastomers. *Angew. Chem., Int. Ed.* **2022**, *61*, No. e202201407.

(31) Li, J.; Liu, F.; Liu, Y.; Shen, Y.; Li, Z. Functionalizable and Chemically Recyclable Thermoplastics from Chemoselective Ring-Opening Polymerization of Bio-renewable Bifunctional α-Methylene-δ-valerolactone. *Angew. Chem., Int. Ed.* **2022**, No. e202207105.

(32) Tani, K.; Stoltz, B. M. Synthesis and structural analysis of 2-quinuclidonium tetrafluoroborate. *Nature* **2006**, *441*, 731−734.

(33) Farhat, W.; Stamm, A.; Robert-Monpate, M.; Biundo, A.; Syren, P. O. Biocatalysis for terpene-based polymers. *Z. Naturforsch. C* **2019**, *74*, 91−100.

(34) Hall Jr, H. Mechanisms of Hydrolysis of Several Atom-Bridged Bicyclic Anhydrides, N-Methylimides, and Lactones. *J. Org. Chem.* **1963**, *28*, 2027−2029.

(35) Carpentier, J.-F. Rare-Earth Complexes Supported by Tripodal Tetradentate Bis(phenolate) Ligands: A Privileged Class of Catalysts for Ring-Opening Polymerization of Cyclic Esters. *Organometallics* **2015**, *34*, 4175−4189.

(36) Li, Y.-T.; Yu, H.-Y.; Li, W.-B.; Liu, Y.; Lu, X.-B. Recyclable Polyhydroxyalkanoates via a Regioselective Ring-Opening Polymerization of α,β-Disubstituted β-Lactone Monomers. *Macromolecules* **2021**, *54*, 4641−4648.

(37) Abe, H. Thermal degradation of environmentally degradable poly(hydroxyalkanoic acid)s. *Macromol. Biosci.* **2006**, *6*, 469−486.

(38) In ref 16, chemically recyclable polythioesters are described (see Scheme 1, Chen 2020). In a follow-up work (ref 14), the authors added a statement in the introduction that the respective O-analogon of this polythioester was not chemically recyclable.

7 Yttrium Salan Catalysts for the Production of PHB with Variable Tacticity

7.1 Bibliographic Data
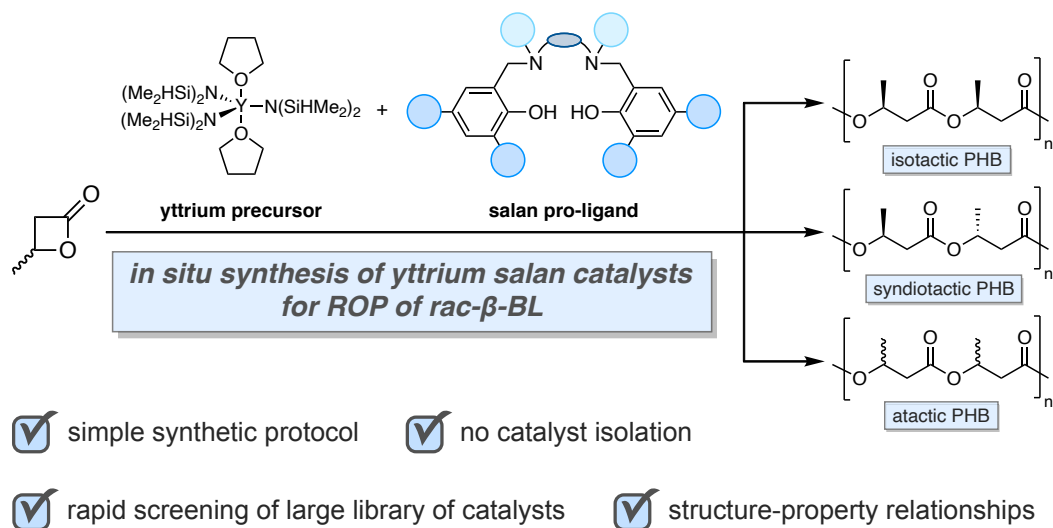
Title:	High-Throughput Approach in the Ring-Opening Polymerization of β-Butyrolactone Enables Rapid Evaluation of Yttrium Salan Catalysts
Status:	Manuscript in preparation
Authors:	Jonas Bruckmoser, Bernhard Rieger

J. Bruckmoser had the initial idea, planned and performed all experiments, and wrote the manuscript. All work was supervised by B. Rieger.

7.2 Content

PHB is produced naturally by bacteria but its synthesis via ROP of β-BL represents a promising synthetic pathway. Here, catalysts play a crucial role since they are capable of controlling the stereomicrostructure of PHB (isotactic, syndiotactic, atactic), which is eventually a crucial factor in determining the properties of the polymer. Establishing structure-property relationships in ROP catalysis is therefore highly important in order to understand the parameters influencing activity and stereocontrol of a catalyst. In this work, a high-throughput approach for the ROP of β-BL enabling the rapid evaluation of a large library of yttrium salan catalysts and revealing structure-property relationships was reported. Typically, synthesizing large libraries of catalysts for this purpose is an elaborate and time-consuming task. Therefore, an approach where the catalyst is conveniently generated *in situ* by treating a suitable catalyst precursor ($Y[N(SiHMe_2)_2]_3(THF)_2$) with the respective salan pro-ligand was developed. Then, monomer was directly added to the *in situ* formed catalyst, circumventing catalyst isolation and allowing for the rapid screening of various catalysts. Comparison of isolated vs. *in situ* generated catalysts revealed identical polymerization results in ROP of β-BL with regard to catalytic activity, degree of stereocontrol and polymer characteristics, thus, verifying the synthetic procedure of the *in situ* approach. Guided by previous reports on yttrium salan catalysts,[147,148,162] the focus was set on two salan ligand sub-types. The first set consisted of *N*-aryl-based and the second set of *N*-alkyl-based salan ligands. With these pro-ligands at hand, the respective *in situ* generated yttrium catalysts were able to access isotactic (*N*-aryl-based) as well as syndiotactic PHB (*N*-alkyl-based), which are both interesting semi-crystalline materials (in contrast to amorphous atactic PHB). Rational steric and electronic modifications of the ligands, in combination with the developed *in situ* catalyst synthesis and polymerization procedure, allowed for the rapid evaluation of these catalysts in the ROP of β-BL and for establishing structure-property relationships in order to obtain polymers with tailored material properties.

7.3 Manuscript Draft

High-Throughput Approach in the Ring-Opening Polymerization of *β*-Butyrolactone Enables Rapid Evaluation of Yttrium Salan Catalysts

Jonas Bruckmoser, and Bernhard Rieger*

WACKER-Chair of Macromolecular Chemistry, Catalysis Research Center, Department of Chemistry, Technical University of Munich, 85748 Garching, Germany

1

ABSTRACT: Poly(3-hydroxybutyrate) (PHB) is a material produced naturally by bacteria but is also chemically accessible *via* ring-opening polymerization (ROP) of β-butyrolactone (β-BL). In ROP, catalyst design plays a key role in the production of PHB with different stereomicrostructures, i.e. syndiotactic, isotactic or atactic PHB. In this work, we demonstrate a simple procedure for generating the catalysts *in situ* by conveniently combining a suitable yttrium precursor with the respective salan pro-ligand. This approach circumvents the elaborate isolation of the catalyst and enables the high-throughput screening of a library of yttrium salan catalysts for the ROP of β-BL. Electronic and steric influences of the ligand framework on stereoselectivity and activity of the catalyst as well as limitations could be determined, and structure-property relationships established. Depending on the substitution pattern, these *in situ* generated catalysts produced syndiotactic-enriched, isotactic-enriched or atactic PHB with high activity.

Introduction.

Polyhydroxyalkanoates (PHAs) are an intriguing class of biodegradable aliphatic polyesters that are naturally produced by a various number of microorganisms and have attracted considerable research attention due to promising applications in the biomedical, pharmaceutical and packaging sector.[1, 2] The most extensively studied PHA is poly(3-hydroxybutyrate) (PHB), naturally existing strictly in its (*R*)-configuration and thus, being an isotactic, semi-crystalline thermoplastic material.[1-3] Its properties resemble those of isotactic polypropylene, thus, demonstrating the vast potential of PHB as a future commodity plastic.[3]

However, the fermentative production of PHB is an elaborate process and industrial production costs remain high.[1, 2] A more convenient route towards PHB constitutes the ring-opening

2

polymerization (ROP) of *rac*-*β*-butyrolactone (*β*-BL). *β*-BL can be easily accessed *via* carbon monoxide insertion into propylene oxide, and its polymerization enables the synthesis of materials with diverse microstructure that are otherwise inaccessible *via* fermentative approaches (i.e. atactic or syndiotactic PHB).[3-5] Control over the microstructure is highly important as material properties are strongly influenced by the tacticity of the polymer. Isotactic- or syndiotactic-enriched PHB is a semi-crystalline polymer with promising material properties whereas atactic PHB has an amorphous nature with relatively poor polymer characteristics for applications.[3, 6]

Keeping this in mind, the search for highly active catalysts exhibiting pronounced stereocontrol is a crucial yet very challenging goal in the ROP of *β*-BL. Despite its high ring strain, *β*-BL is a rather reluctant monomer and side reactions are frequently observed during its polymerization.[4] Additionally, the stereoselective ROP of *β*-BL has proven to be highly challenging. *β*-Diiminate zinc complexes developed by Coates et al. have shown high activity but yielded only atactic PHB.[7] The lack of stereocontrol in ROP of *β*-BL is also in stark contrast to the highly heterotactic polylactide (PLA) obtained, when these complexes were applied in the ROP of *rac*-lactide (LA).[8] Such a behavior has similarly been observed with other catalysts showing high stereocontrol in ROP of LA but diminishing stereoselectivity in ROP of *β*-BL (or vice versa).[9-19]

Syndioselective polymerization of *β*-BL is much more commonly observed than isoselective enchainment.[4] For example, highly syndiotactic PHB can be accessed by yttrium amino-alkoxy-bis(phenolate) systems reported by Carpentier et al.[20] Detailed studies have shown that electronics and sterics of the catalyst have a profound influence on the syndioselectivity. Increasing the steric demand of the phenolic *ortho*-substituents from *tert*-butyl to cumyl to trityl

3

resulted in an increase of the observed syndiotacticity up to $P_r = 0.94$.[20-22] Apart from this prominent catalyst system, various other rare-earth metal-based catalysts enabled the syndioselective ROP of β-BL.[23-28] Chiral aminophenolate magnesium and zinc complexes could also produce syndiotactic-enriched PHB with P_r up to 0.75.[12, 29] Tin-based catalysts showed a similar degree of stereocontrol, albeit activity was relatively poor.[30, 31]

In contrast to that, examples of discrete, isoselective initiators in the ROP of β-BL remain very scarce. Chromium salen catalysts yielding isotactic-enriched PHB with P_m up to 0.67 were reported by our group in 2008.[32-34] A heterogenous neodymium-based catalyst achieved high stereocontrol ($P_m = 0.85$)[35] as well as lanthanum bis(phenolate) systems resembling those of Carpentier et al.[20] in combination with neutral donor ligands (P_m up to 0.82).[36, 37] Very interestingly, Luo, Wang and Yao et al. showed recently that rare-earth metal salan-type catalysts are capable of either producing syndiotactic- or isotactic-enriched PHB ($P_r = 0.78$, $P_m = 0.77$) depending on the ligand substitution.[38]

Scheme 1. Comparison of salen and salan ligand framework. Positions of interest for potential substitutions are highlighted
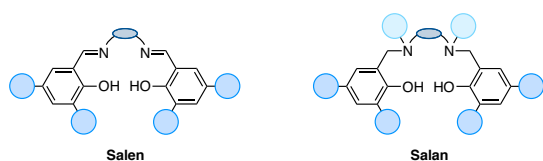
It was in this context, that we became interested in understanding the factors influencing activity as well as stereocontrol in catalyst design for ROP of β-BL. Salan-type ligands are less commonly employed in literature compared to their salen-type counterparts, yet they possess the

4

advantage of a tertiary amine in the backbone of the framework that is in close proximity to the metal center and can be precisely tuned regarding electronic and steric factors (Scheme 1). Additionally, their synthesis is easily accomplished *via* Mannich-type reactions in a one-step procedure (Scheme 2, Route A).[39] This renders salan-type frameworks excellent candidates for establishing structure-property-relationships. While a plethora of catalysts has been reported for ROP of LA and structure-property-relationships could be established,[40] these results are unfortunately not transferrable to ROP of β-BL, and such a detailed understanding is barely present for β-BL polymerization. Most importantly, the synthesis of libraries of catalysts with different ligand substitutions is highly elaborate and time-consuming, and catalyst targets are likely not achieved due to the challenging nature of β-BL polymerization. Hence, a simpler procedure would be highly valuable for boosting efficiency and saving synthesis resources.

Herein, we report a high-throughput approach that enables the rapid generation of structure-property-relationships in the ROP of β-BL. The catalysts are conveniently formed *in situ* prior to the addition of monomer by reacting a rare-earth metal precursor with the respective salan-type pro-ligand. A comparison of isolated catalysts with the respective *in situ* generated catalyst demonstrated that identical results regarding activity and stereoselectivity in the ROP of β-BL are obtained, thus obviating the need for experimentally challenging catalyst synthesis and isolation. Following this synthetic protocol, a plethora of salan-type catalysts could be rapidly tested and influences from the ligand framework on activity as well as stereoselectivity identified.

Scheme 2. Synthesis routes for salan pro-ligands

5

Route **A** – Mannich condensation
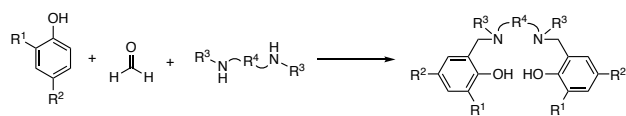
Route **B** – Nucleophilic substitution
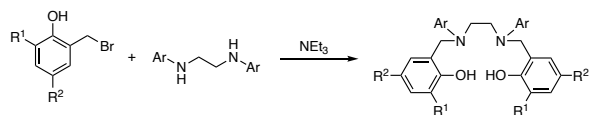
Results and Discussion.

Synthesis of Salan Pro-Ligands. A library of salan pro-ligands was prepared in accordance to literature known procedures.[38, 39] The fundamental structure of the first set of pro-ligands is based on the previously reported *N*-phenyl substituted version (Figure 1, **L1**). Due to the fact that the respective yttrium and ytterbium complexes catalyzed the isoselective ROP of β-BL,[38] we hypothesized that variation of electronic and steric motifs will give more detailed insights in accessing isotactic-enriched PHB (**L2–L6**). The second set featured *N*-methylated and related pro-ligands. Syndiotactic-enriched PHB was produced by an **L7**-based yttrium complex,[24] and **L7** was consequently chosen as the basic framework structure for investigating the syndioselective ROP in more detail (Figure 1). Within this scaffold, the steric influence of the *N*-alkyl substituent (**L7–L10**), electronic influences at the phenolic positions (**L11** and **L12**) and backbone variations (**L13** and **L14**) were studied. Importantly, comparing activity and stereoselectivity of those two previously reported complexes (basic ligand structure **L1** and **L7**) to the herein prepared *in situ* versions, allows for simple verification of our *in situ* approach. Besides those previously reported complexes, several novel pro-ligands and initiators were synthesized. High to moderate yields were achieved when the pro-ligands were prepared *via* a Mannich-type reaction (Scheme 2, Route A and Figure 1, **L7–L14**). This procedure is not applicable in the case of aryl-substituted amines, and successful synthesis was instead achieved

6

via nucleophilic substitution of (bromomethyl)phenols in good yields (Scheme 2, Route B and Figure 1, **L1**–**L6**).
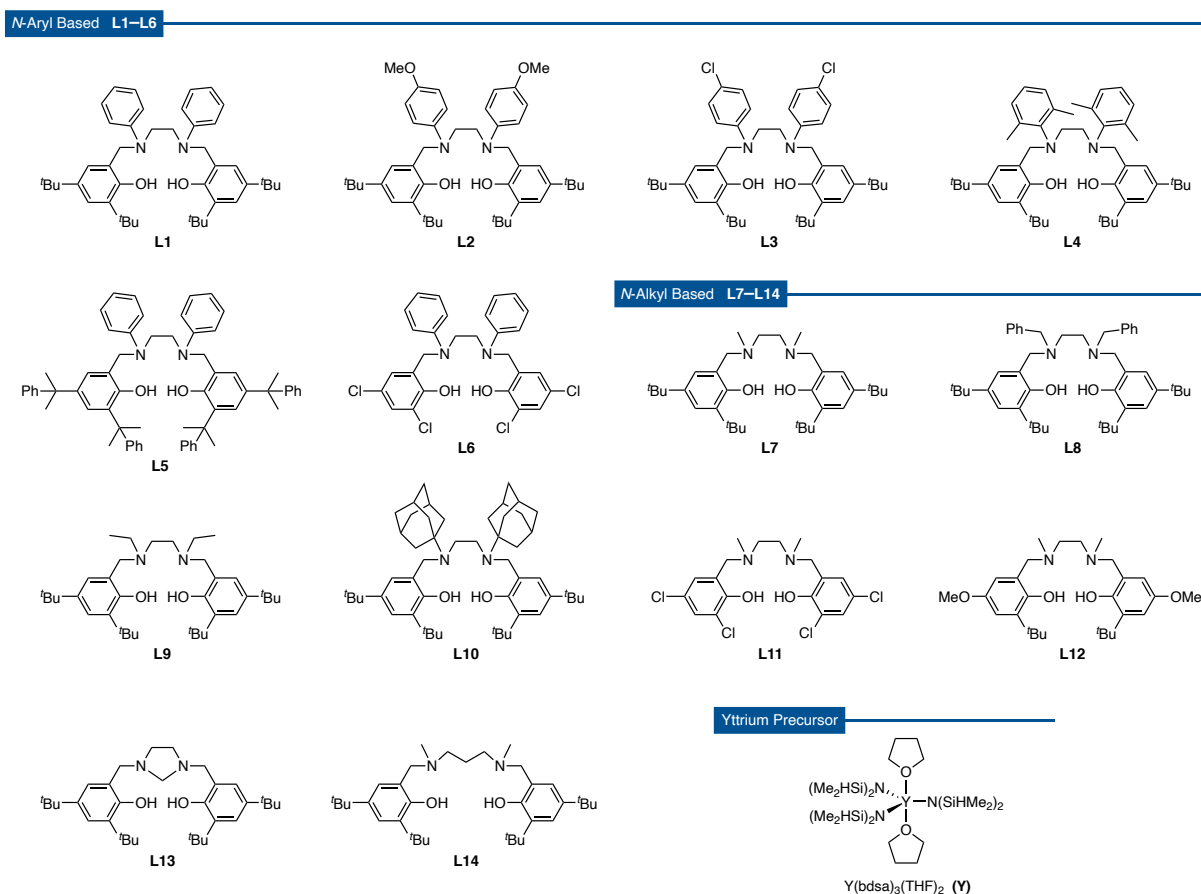
Figure 1. Overview of salan pro-ligands **L1**–**L14** and the corresponding yttrium precursor **Y** studied in this work.

***In Situ* Generated vs. Isolated Catalysts.** We aimed for the rapid evaluation of the influences of the ligand framework on activity and stereoselectivity in the ROP of β-BL catalyzed by yttrium-based initiators. Y[N(SiHMe$_2$)$_2$]$_3$(THF)$_2$ (**Y**) is a commonly employed precursor for the synthesis of yttrium-based catalysts due to its selective reactions with protic pro-ligands and its

7

readily eliminated bis(dimethylsilyl)amide ligands.[41] We hypothesized that the simple elimination enables the selective preparation of the catalyst species *in situ* and thus, elaborate isolation of the catalyst is not necessary for high-throughput polymerization screenings. The reaction of 1 equiv of **Y** precursor with 1 equiv of salan pro-ligand **L1** in toluene-d_8 at room temperature was followed by ^{1}H NMR spectroscopy. Within less than 30 min, the reaction showed complete conversion. Comparison of the ^{1}H NMR spectrum with the respective isolated, recrystallized catalyst **Y1** revealed identical signals (Figure 2). This demonstrates that salan catalysts can be easily generated *in situ* by combining the yttrium precursor with an equimolar amount of pro-ligand and stirring at room temperature for a short period of time. Further proof for the generation of an identical catalyst species (*in situ* vs. isolated) was obtained by polymerization experiments of β-BL. Here, the catalyst was prepared *in situ* according to the aforementioned protocol. Then, β-BL was directly added to this reaction mixture and the polymerization initiated by the *in situ* generated catalyst (Scheme 3). Two independent polymerization runs showed nearly identical results and further confirm the simplicity and reproducibility of the approach (Table 1, entries 1 and 2). Most importantly, comparing these results to those obtained by the isolated catalyst species **Y1** revealed almost identical outcomes (Table 1, entries 1 and 2 vs. entry 3). This emphasizes the applicability of the *in situ* approach and allows for a high-throughput testing of conveniently *in situ* generated catalysts. Comparison of literature known **Y2** (Scheme S1),[38] which bears the identical salan framework but differs in the initiating ligand (-N(SiHMe$_2$)$_2$ for **Y1** vs. -N(SiMe$_3$)$_2$ for **Y2**) showed the same degree of stereocontrol, as expected (Table 1, entry 4). Activity of **Y2** is reduced due to the poorer initiating efficiency of -N(SiMe$_3$)$_2$. Control experiments testing solely the **Y** precursor or **L1** in the ROP of β-BL resulted in very poor or no conversion, respectively (Table 1, entries 5 and 6).

8
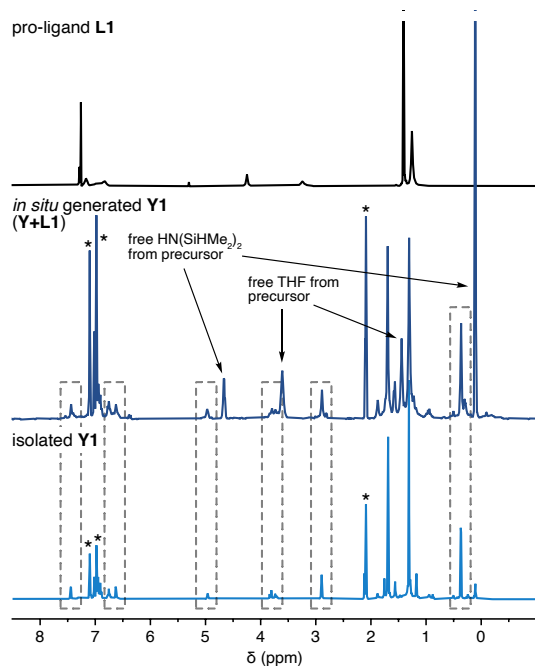
Figure 2. Comparison of ^{1}H NMR spectra of salan pro-ligand **L1** (top), *in situ* generated **Y1** from precursor **Y** and pro-ligand **L1** (middle) and isolated catalyst **Y1** (bottom). * = residual proton signals of deuterated toluene.

Table 1. Comparison of *In Situ* Generated and Isolated Catalysts in the Ring-Opening Polymerization of β-BL [a]

entry	approach	precursor	pro-ligand	[M]/[I]	t (min)	conv.[b] (%)	M_n [c] (kg mol^{-1})	$Đ$ [c]	P_m [d]
1	in situ	**Y**	**L1**	200:1	15	59	23.0	1.5	0.63
2	in situ	**Y**	**L1**	200:1	15	57	25.0	1.5	0.63
3	isolated	**Y1**		200:1	15	61	23.4	1.5	0.63
4[e]	isolated	**Y2**		200:1	180	89	52.4	1.5	0.63
5	-	**Y**	-	200:1	1440	8	n.d.	n.d.	n.d.

9

6	-	-	**L1**	200:1	1440	0	n.d.	n.d.	n.d.

[a]Polymerizations were performed in toluene at room temperature, [β-BL] = 2.0 M. *In situ* approach: precursor **Y** and salan pro-ligand **L1** (1:1) were stirred for 1 h at room temperature prior to monomer addition. [b]Conversion determined by ^{1}H NMR spectroscopy. [c]Determined by GPC in THF at 40°C relative to polystyrene standards. [d]Tacticity determined by ^{13}C{^{1}H} NMR spectroscopy, integration of the carbonyl signal. [e]Literature catalyst, ref 38. n.d. = not determined.

ROP of β-BL Using *In Situ* Generated Catalysts. The successful implementation of the *in situ* approach inspired us to investigate a library of salan catalysts (**Y** + **L2–L14**) in the ROP of β-BL. In general, the *in situ* approach was carried out under identical conditions for all polymerizations and consisted of two steps. First, the catalyst was formed *in situ* by stirring the yttrium precursor complex and respective salan pro-ligand for 1 h at room temperature in toluene and then, β-BL was directly added to the catalyst mixture (Scheme 3). All polymerization runs were independently repeated in duplicate to ensure high reproducibility.

Scheme 3. Concept of the *in situ* approach for ROP of β-BL. 1) *In situ* formation of salan catalyst and 2) direct addition of monomer to this catalyst mixture
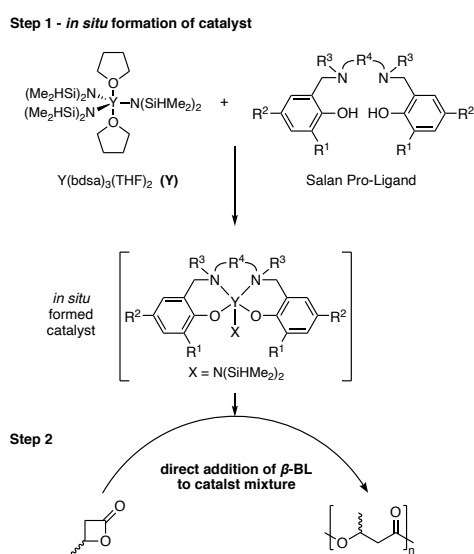
Table 2. Ring-Opening Polymerization of β-BL Using *In Situ* Generated Salan Catalysts [a]

entry	precursor	pro-ligand	[M]/[I]	t (min)	conv.[b] (%)	TOF (h^{-1})	M_n[c] (kg mol^{-1})	$Đ$[c]	P_m[d]
1	**Y**	**L1**	200:1	15	59	472	23.0	1.5	0.63
2	**Y**	**L2**	200:1	15	86	688	29.8	1.4	0.63
3	**Y**	**L3**	200:1	1440	28	2	9.7	1.6	0.62
4	**Y**	**L4**	200:1	1440	14	1	n.d.	n.d.	0.47
5	**Y**	**L5**	200:1	30	76	304	24.4	1.4	0.67
6	**Y**	**L6**	200:1	1440	6	<1	n.d.	n.d.	0.51
7	**Y**	**L7**	400:1	2	62	7440	20.3	1.7	0.21
8	**Y**	**L8**	400:1	2	69	8280	27.1	1.6	0.27
9	**Y**	**L9**	400:1	2	60	7200	25.7	1.3	0.33
10	**Y**	**L10**	200:1	1440	30	3	11.1	1.2	0.46
11	**Y**	**L11**	200:1	1440	3	<1	n.d.	n.d.	n.d.
12	**Y**	**L12**	400:1	2	36	4320	25.7	1.9	0.26
13	**Y**	**L13**	200:1	1440	13	1	4.8	1.7	0.46
14	**Y**	**L14**	200:1	10	73	876	23.2	1.2	0.55

[a]Polymerizations were performed in toluene at room temperature, [β-BL] = 2.0 M. Initiator was generated *in situ*: precursor **Y** and salan pro-ligand (1:1) were stirred for 1 h at room temperature prior to monomer addition. All polymerization runs were performed in duplicate. [b]Conversion determined by ^{1}H NMR spectroscopy. [c]Determined by GPC in THF at 40°C relative to polystyrene standards. [d]Tacticity determined by ^{13}C{^{1}H} NMR spectroscopy, integration of the carbonyl signal. $P_r = 1–P_m$. n.d. = not determined.

Para-methoxy substituted aryls at the *N*-substituent (**L2**) in the salan framework increased catalytic activity in respect to **Y+L1**, whereas chloro substituents at the aryl group (**L3**) strongly hampered polymerization of β-BL (Table 2, entries 1 vs. 2 and 3). Consequently, the electronic variation at the *N*-substituent has a profound influence on catalytic activity, however,

11

stereoselectivity was not affected by such variations and remained unchanged at $P_m = 0.63$. Increasing the steric demand of the *N*-aryl substituent with two additional methyl substituents in *ortho* positions (**L4**) revealed a negative influence as activity and stereoselectivity was drastically decreased and only atactic PHB was produced (Table 2, entry 4 and Figure 3c). Next, the importance of the steric demand as well as electronics at the *ortho* and *para* phenolic positions was tested while the *N*-substituent was left unchanged as *N*-phenyl (**L5** and **L6**). In previous works on distantly related aminoalkoxy bis(phenolate) systems, a strong dependence of stereoselectivity on the *ortho* phenolic substituent was observed.[20-22] Surprisingly, for the yttrium salan-based catalysts, such a behavior was not evident and isotacticity only increased slightly to $P_m = 0.67$ when a bulky cumyl group was introduced (Table 2, entry 5 and Figure 3b). Activity of the catalyst was slightly reduced in line with hindered monomer coordination due to increased steric bulk (TOF = 304 h^{-1} vs. 472 h^{-1}). Chloro substituents again drastically reduced activity and the catalyst showed only 6% conversion after 24 h (Table 2, entry 6). Additionally, the polymerization was non-stereoselective ($P_m = 0.51$), presumably caused by the low steric demand of the chloro groups. The polymers generated by catalysts with *N*-aryl ligand substitutions showed monomodal but slightly broadened GPC traces ($Đ = 1.4–1.6$), typically observed for rare-earth metal-based salan catalysts.[27, 38] The mechanism of stereocontrol for the isoselective polymerizations was analyzed based on the stereoerrors of the polymers. In the methylene region of the ^{13}C{^{1}H} NMR spectra, the intensity of the *rr* triad was significantly reduced compared to the *mr* and *rm* triads, indicative of a chain-end control mechanism (Figure S34).[36, 40]

Having identified structure-property relationships in the ROP of *β*-BL for the first set of salan catalysts based on *N*-aryl substituted versions, we turned to the second set of catalysts based on

12

N-alkyl salan pro-ligands (Figure 1). Catalyst system **Y+L7** was extremely active in the polymerizations of β-BL that we decided to increase the monomer-to-initiator ratio to 400:1. Within 2 min, conversion reached 62% (TOF = 7440 h^{-1}, Table 2, entry 7). Strikingly, the low steric demand of the N-methyl substituents enabled a highly syndioselective polymerization (P_m = 0.21, Figure 3d). This is also in line with the previously tested, isolated version of **Y+L7**,[24] further supporting the synthetic protocol of *in situ* generation and obviating elaborate catalyst isolation. We were then interested whether increasing the steric demand at the amine results in a more pronounced stereoselectivity. For this, benzyl-, ethyl- and adamantyl-substituted salan catalysts were investigated (**L8–L10**). The N-benzyl and N-ethyl substitution had no negative impact on the activity of the catalysts and was as high as for the related N-methyl based catalyst (TOF > 7000 h^{-1}, Table 2, entries 8 and 9). In contrast to that, the very high steric demand of the adamantyl substituent in catalyst system **Y+L10** drastically reduced activity (TOF = 3 h^{-1}), even at a lower monomer-to-initiator ratio of 200:1 (Table 2, entry 10). Analyzing the tacticity of the produced PHBs revealed that the benzyl substitution reduces the syndioselectivity of the catalyst to P_m = 0.27. Surprisingly, the syndiotacticity of PHB was even further reduced when ethyl substituents were in place (P_m = 0.33, Figure 3e). These results are unexpected as a higher steric demand in close proximity to the metal center was anticipated to result in a more constraint geometry and therefore in an improved stereoselectivity. However, if the steric demand is too high, polymerizations become sluggish and non-stereoselective due to hindered and unselective monomer coordination.[38, 42] This was noticeably observed with catalyst **Y+L10**, where in addition to its poor activity a completely atactic and amorphous material was generated (P_m = 0.46, Figure 3f). Besides the N-substitution, electronic and backbone effects of the salan catalysts in the ROP of β-BL were investigated (**L11–L14**). As previously observed for **L6**, chloro substituents in

13

ortho and *para* phenolic positions are highly detrimental for efficient polymerization (Table 2, entry 11). While methoxy groups at the *N*-aryl position (**L2**) increased the activity of the catalyst, such an effect was not present in the case for **Y+L12**, yet activity was even slightly reduced (Table 2, entry 12). The lower steric demand of the methoxy group in contrast to the *tert*-butyl group of **L7** might explain the reduced syndiotacticity of the polymer (P_m = 0.26 vs. 0.21). The introduction of a cyclic ligand backbone (**L13**) resulted in a drastic decrease in activity as well as complete loss of stereoselectivity (Table 2, entry 13). Similarly, increasing the linker length of the backbone from ethyl (**L7**) to propyl (**L14**) gave an atactic polymer (Table 2, entry 14). Catalytic activity of **Y+L14** was also drastically reduced (TOF = 7440 h^{-1} vs. 876 h^{-1}), albeit still high in a broader context. These experiments highlight the strong influence of the ligand backbone on both the activity and stereocontrol of the catalyst in ROP of *β*-BL. In the case of syndioselective polymerizations, analysis of the methylene region in the $^{13}C\{^1H\}$ NMR spectra of the obtained PHBs revealed that stereoselectivity is achieved *via* a chain-end control mechanism (Figure S35).
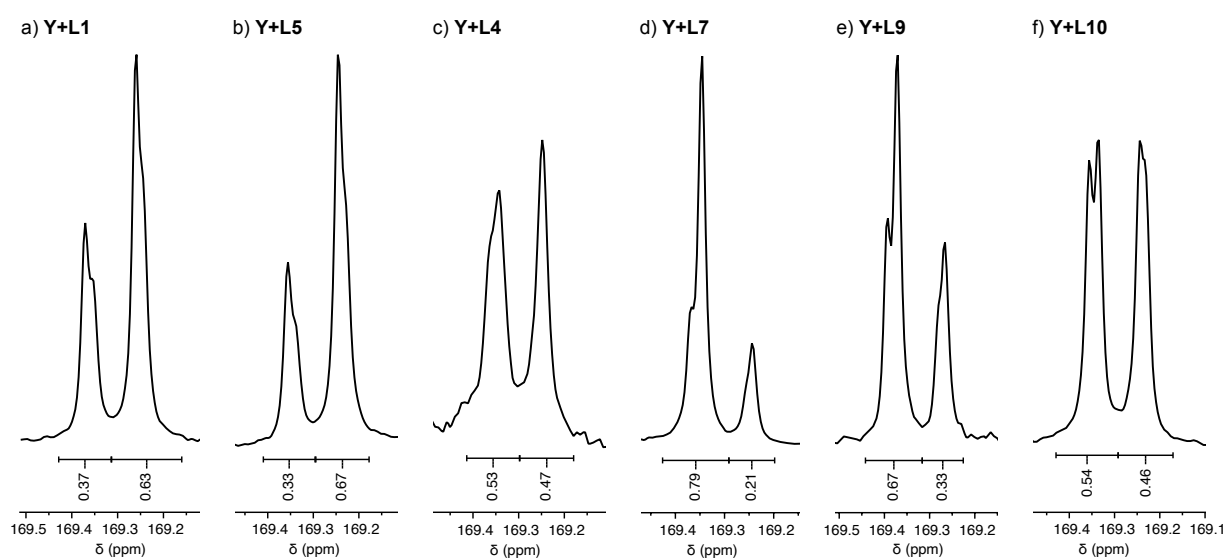
14

Figure 3. $^{13}C\{^1H\}$ NMR spectra (carbonyl region) of PHBs with variable tacticity produced by salan catalyst systems. Isotactic-enriched PHB: a) **Y+L1**, $P_m = 0.63$, b) **Y+L5**, $P_m = 0.67$. Atactic PHB: c) **Y+L4**, $P_m = 0.47$. Syndiotactic-enriched PHB: d) **Y+L7**, $P_m = 0.21$, e) **Y+L9**, $P_m = 0.33$. Atactic PHB: f) **Y+L10**, $P_m = 0.46$.

Discussion of Activity and Stereocontrol Data. The *in situ* approach allowed for a rapid generation of a relatively large dataset of activity/stereocontrol parameters of yttrium salan catalysts (Figure 4). Both *N*-aryl and *N*-alkyl supported catalysts could show high activity in the ROP of *β*-BL if substituents were carefully chosen. However, the challenging nature of *β*-BL polymerization is highlighted by the large proportion of catalysts that were inactive or only poorly active (6 of 14 catalysts, TOF < 5 h^{-1}). Especially electron withdrawing chloro groups on either phenolic- (**L6** and **L11**) or *N*-positions (**L3**) had a large detrimental effect on catalytic activity. Electron donating methoxy groups in *N*-aryl position (**L2**) increased activity considerably whereas the effect was ambiguous and presumably superimposed by steric influences if such groups were installed at the phenolic *para* position (**L12**). Since the substituent

15

of the tertiary amine is in close proximity to the metal center, it strongly influences activity as well as stereoselectivity (Figure 4). If the amine bears an aryl group, isotactic-enriched PHB is obtained (**L1–L3**). Sterically more demanding *ortho-* and *para*-phenolic substituents (**L5**) in this framework only slightly increase the stereoselectivity (P_m up to 0.67). Increasing the steric demand of the aryl group is detrimental for both activity and stereoselectivity (**L4**). Similar observations regarding the amine substituent could be observed for the catalysts based on **L7**. A higher steric demand at the *N*-position decreases stereoselectivity (**L7–L9**) and if the steric demand is too high, activity and stereocontrol of the catalyst drop significantly (**L11**). Such observations reveal that these salan catalysts are capable of producing PHB with relatively high stereoselectivity *via* chain-end control if the close coordination sphere around the metal center is not too crowded. Otherwise, monomer coordination and stereocontrol is hampered. A relatively open ligand backbone enables high activity due to simple monomer coordination, however, it is not able of introducing stereocontrol (**L14**). In contrast to that, a rigid, cyclic backbone has a strongly negative effect on the ROP of β-BL (**L13**), further highlighting the need for subtle tuning of the steric demand of the ligand framework.

16
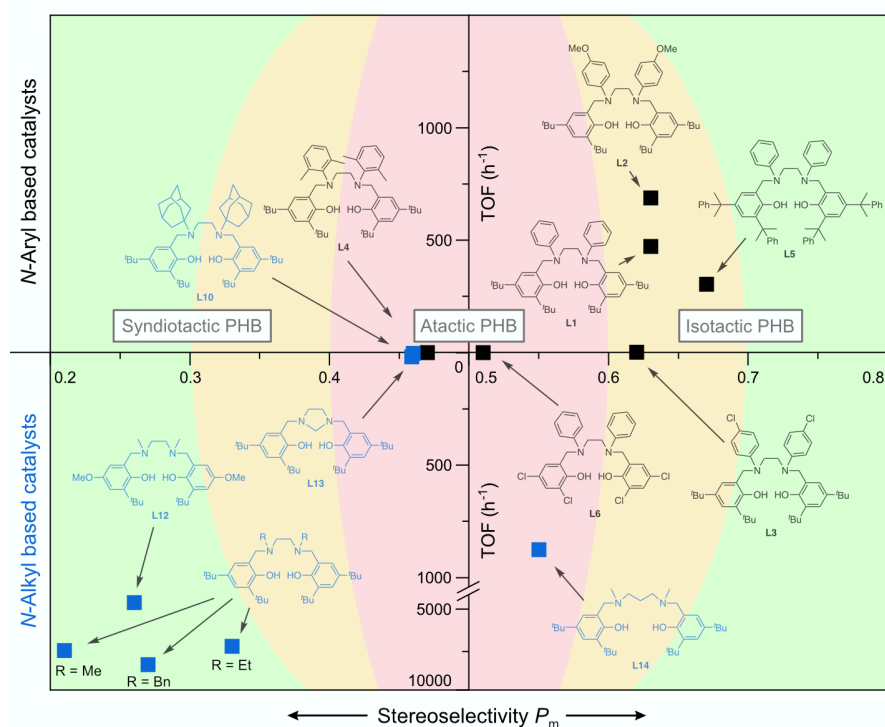
Figure 4. Correlation of activity/stereoselectivity in the ROP of β-BL using the respective yttrium salan catalysts (note: only the ligand framework is shown for clarity). *N*-Aryl based catalysts (black) are mapped in the upper half and *N*-alkyl based catalysts (blue) in the lower half. Background colors indicate favored regions of high stereoselectivity and activity.

Conclusions.

In summary, we have established a synthetic protocol that allows for the simple *in situ* synthesis of various yttrium salan-based catalysts and their use in the ROP of β-BL. To this end, precursor complex Y[N(SiHMe$_2$)$_2$]$_3$(THF)$_2$ is stirred with the respective salan pro-ligand for a short period of time, followed by direct addition of the monomer to the reaction mixture. Comparison of an *in situ* generated catalyst with a literature known, isolated example demonstrated that the isolated and *in situ* prepared catalysts are identical species. This could be

17

additionally verified by identical polymerization outcomes of isolated versus *in situ* generated catalysts regarding activity, degree of stereocontrol and polymer characteristics. Following this synthetic protocol, a plethora of salan pro-ligands with various steric and electronic variations and their influence on activity and stereoselectivity in the yttrium-catalyzed ROP of β-BL could be conveniently and rapidly tested. This allowed for the facile generation of structure-property relationships in the iso- as well as syndioselective PHB production and also revealed current limitations of these yttrium salan-based catalyst systems.

Our *in situ* approach renders challenging and time consuming catalyst isolation redundant and enables the rapid identification of promising catalyst design criterions. Given the simplicity of this approach, it might also find application for various other ligand systems. In ROP of β-BL, stereocontrol is crucial for obtaining PHB materials with interesting properties, similarly, for example, to PLA synthesis. Thus, the *in situ* generation of catalysts has further potential in the ROP of various cyclic esters and could also be a facile high-throughput screening method for the identification of promising catalyst candidates for successful copolymerizations.

18

ASSOCIATED CONTENT

Supporting Information.

The following files are available free of charge.

Experimental procedures and characterization data of polymers (PDF)

AUTHOR INFORMATION

Corresponding Author

*rieger@tum.de

Notes

The authors declare no competing financial interest.

REFERENCES

1.   Kumar, M.; Rathour, R.; Singh, R.; Sun, Y.; Pandey, A.; Gnansounou, E.; Andrew Lin, K.-Y.; Tsang, D. C. W.; Thakur, I. S., Bacterial polyhydroxyalkanoates: Opportunities, challenges, and prospects. *J. Clean. Prod.* **2020,** *263*, 121500.

19

2.   Muhammadi; Shabina; Afzal, M.; Hameed, S., Bacterial polyhydroxyalkanoates-eco-friendly next generation plastic: production, biocompatibility, biodegradation, physical properties and applications. *Green Chem. Lett. Rev.* **2015,** *8*, 56-77.

3.   Rieger, B.; Künkel, A.; Coates, G. W.; Reichardt, R.; Dinjus, E.; Zevaco, T. A., *Synthetic biodegradable polymers*. Springer-Verlag: Berlin, Heidelberg: 2012.

4.   Carpentier, J. F., Discrete metal catalysts for stereoselective ring-opening polymerization of chiral racemic β-lactones. *Macromol. Rapid Commun.* **2010,** *31*, 1696-1705.

5.   Li, H.; Shakaroun, R. M.; Guillaume, S. M.; Carpentier, J. F., Recent Advances in Metal-Mediated Stereoselective Ring-Opening Polymerization of Functional Cyclic Esters towards Well-Defined Poly(hydroxy acid)s: From Stereoselectivity to Sequence-Control. *Chem. Eur. J.* **2020,** *26*, 128-138.

6.   Worch, J. C.; Prydderch, H.; Jimaja, S.; Bexis, P.; Becker, M. L.; Dove, A. P., Stereochemical enhancement of polymer properties. *Nat. Rev. Chem.* **2019,** *3*, 514-535.

7.   Rieth, L. R.; Moore, D. R.; Lobkovsky, E. B.; Coates, G. W., Single-site β-diiminate zinc catalysts for the ring-opening polymerization of β-butyrolactone and β-valerolactone to poly (3-hydroxyalkanoates). *J. Am. Chem. Soc.* **2002,** *124*, 15239-15248.

8.   Chamberlain, B. M.; Cheng, M.; Moore, D. R.; Ovitt, T. M.; Lobkovsky, E. B.; Coates, G. W., Polymerization of lactide with zinc and magnesium β-diiminate complexes: stereocontrol and mechanism. *J. Am. Chem. Soc.* **2001,** *123*, 3229-3238.

9.   Cross, E. D.; Allan, L. E. N.; Decken, A.; Shaver, M. P., Aluminum salen and salan complexes in the ring-opening polymerization of cyclic esters: Controlled immortal and

copolymerization of rac-β-butyrolactone and rac-lactide. *J. Polym. Sci., Part A: Polym. Chem.* **2013,** *51*, 1137-1146.

10. Yuntawattana, N.; McGuire, T. M.; Durr, C. B.; Buchard, A.; Williams, C. K., Indium phosphasalen catalysts showing high isoselectivity and activity in racemic lactide and lactone ring opening polymerizations. *Catal. Sci. Technol.* **2020,** *10*, 7226-7239.

11. Bruckmoser, J.; Henschel, D.; Vagin, S.; Rieger, B., Combining high activity with broad monomer scope: indium salan catalysts in the ring-opening polymerization of various cyclic esters. *Catal. Sci. Technol.* **2022,** *12*, 3295-3302.

12. Wang, H.; Guo, J.; Yang, Y.; Ma, H., Diastereoselective synthesis of chiral aminophenolate magnesium complexes and their application in the stereoselective polymerization of rac-lactide and rac-β-butyrolactone. *Dalton Trans.* **2016,** *45*, 10942-10953.

13. Abbina, S.; Du, G., Zinc-Catalyzed Highly Isoselective Ring Opening Polymerization of rac-Lactide. *ACS Macro Lett.* **2014,** *3*, 689-692.

14. Shaik, M.; Peterson, J.; Du, G., Cyclic and Linear Polyhydroxylbutyrates from Ring-Opening Polymerization of β-Butyrolactone with Amido-Oxazolinate Zinc Catalysts. *Macromolecules* **2018,** *52*, 157-166.

15. Saha, T. K.; Ramkumar, V.; Chakraborty, D., Salen complexes of zirconium and hafnium: synthesis, structural characterization, controlled hydrolysis, and solvent-free ring-opening polymerization of cyclic esters and lactides. *Inorg. Chem.* **2011,** *50*, 2720-2722.

16. Bakewell, C.; White, A. J.; Long, N. J.; Williams, C. K., Metal-size influence in iso-selective lactide polymerization. *Angew. Chem. Int. Ed.* **2014,** *53*, 9226-9230.

21

17.   Bakewell, C.; White, A. J.; Long, N. J.; Williams, C. K., Scandium and yttrium phosphasalen complexes as initiators for ring-opening polymerization of cyclic esters. *Inorg. Chem.* **2015,** *54*, 2204-2212.

18.   Nie, K.; Gu, W.; Yao, Y.; Zhang, Y.; Shen, Q., Synthesis and Characterization of Salalen Lanthanide Complexes and Their Application in the Polymerization of rac-Lactide. *Organometallics* **2013,** *32*, 2608-2617.

19.   Tian, T.; Feng, C.; Wang, Y.; Zhu, X.; Yuan, D.; Yao, Y., Synthesis of N-Methyl-o-phenylenediamine-Bridged Bis(phenolato) Lanthanide Alkoxides and Their Catalytic Performance for the (Co)Polymerization of rac-Butyrolactone and l-Lactide. *Inorg. Chem.* **2022,** *61*, 9918-9929.

20.   Amgoune, A.; Thomas, C. M.; Ilinca, S.; Roisnel, T.; Carpentier, J. F., Highly active, productive, and syndiospecific yttrium initiators for the polymerization of racemic β-butyrolactone. *Angew. Chem. Int. Ed.* **2006,** *45*, 2782-2784.

21.   Ajellal, N.; Bouyahyi, M.; Amgoune, A.; Thomas, C. M.; Bondon, A.; Pillin, I.; Grohens, Y.; Carpentier, J.-F., Syndiotactic-enriched poly(3-hydroxybutyrate)s via stereoselective ring-opening polymerization of racemic β-butyrolactone with discrete yttrium catalysts. *Macromolecules* **2009,** *42*, 987-993.

22.   Bouyahyi, M.; Ajellal, N.; Kirillov, E.; Thomas, C. M.; Carpentier, J. F., Exploring electronic versus steric effects in stereoselective ring-opening polymerization of lactide and β-butyrolactone with amino-alkoxy-bis(phenolate)-yttrium complexes. *Chem. Eur. J.* **2011,** *17*, 1872-1883.

23.   Ajellal, N.; Lyubov, D. M.; Sinenkov, M. A.; Fukin, G. K.; Cherkasov, A. V.; Thomas, C. M.; Carpentier, J. F.; Trifonov, A. A., Bis(guanidinate) alkoxide complexes of lanthanides: synthesis, structures and use in immortal and stereoselective ring-opening polymerization of cyclic esters. *Chem. Eur. J.* **2008,** *14*, 5440-5448.

24.   Kramer, J. W.; Treitler, D. S.; Dunn, E. W.; Castro, P. M.; Roisnel, T.; Thomas, C. M.; Coates, G. W., Polymerization of enantiopure monomers using syndiospecific catalysts: a new approach to sequence control in polymer synthesis. *J. Am. Chem. Soc.* **2009,** *131*, 16042-16044.

25.   Grunova, E.; Kirillov, E.; Roisnel, T.; Carpentier, J.-F., Group 3 metal complexes supported by tridentate pyridine-and thiophene-linked bis (naphtholate) ligands: synthesis, structure, and use in stereoselective ring-opening polymerization of racemic lactide and β-butyrolactone. *Dalton Trans.* **2010,** *39*, 6739-6752.

26.   Nie, K.; Fang, L.; Yao, Y.; Zhang, Y.; Shen, Q.; Wang, Y., Synthesis and characterization of amine-bridged bis(phenolate)lanthanide alkoxides and their application in the controlled polymerization of rac-lactide and rac-β-butyrolactone. *Inorg. Chem.* **2012,** *51*, 11133-11143.

27.   Zeng, T.; Qian, Q.; Zhao, B.; Yuan, D.; Yao, Y.; Shen, Q., Synthesis and characterization of rare-earth metal guanidinates stabilized by amine-bridged bis(phenolate) ligands and their application in the controlled polymerization of rac-lactide and rac-β-butyrolactone. *RSC Advances* **2015,** *5*, 53161-53171.

28.   Liu, H.; Shi, X., Phosphasalalen Rare-Earth Complexes for the Polymerization of rac-Lactide and rac-β-Butyrolactone. *Inorg. Chem.* **2021,** *60*, 705-717.

29.   Ebrahimi, T.; Aluthge, D. C.; Hatzikiriakos, S. G.; Mehrkhodavandi, P., Highly Active Chiral Zinc Catalysts for Immortal Polymerization of β-Butyrolactone Form Melt Processable Syndio-Rich Poly(hydroxybutyrate). *Macromolecules* **2016,** *49*, 8812-8824.

30.   Kemnitzer, J. E.; McCarthy, S. P.; Gross, R. A., Preparation of predominantly syndiotactic poly(β-hydroxybutyrate) by the tributyltin methoxide catalyzed ring-opening polymerization of racemic-β-butyrolactone. *Macromolecules* **1993,** *26*, 1221-1229.

31.   Kricheldorf, H. R.; Eggerstedt, S., Polylactones. 41. Polymerizations of β-d, l-Butyrolactone with Dialkyltinoxides as Initiators. *Macromolecules* **1997,** *30*, 5693-5697.

32.   Zintl, M.; Molnar, F.; Urban, T.; Bernhart, V.; Preishuber-Pflugl, P.; Rieger, B., Variably isotactic poly(hydroxybutyrate) from racemic β-butyrolactone: microstructure control by achiral chromium(III) salophen complexes. *Angew. Chem. Int. Ed.* **2008,** *47*, 3458-3460.

33.   Reichardt, R.; Vagin, S.; Reithmeier, R.; Ott, A. K.; Rieger, B., Factors Influencing the Ring-Opening Polymerization of Racemic β-Butyrolactone Using CrIII(salphen). *Macromolecules* **2010,** *43*, 9311-9317.

34.   Vagin, S.; Winnacker, M.; Kronast, A.; Altenbuchner, P. T.; Deglmann, P.; Sinkel, C.; Loos, R.; Rieger, B., New Insights into the Ring-Opening Polymerization of β-Butyrolactone Catalyzed by Chromium(III) Salphen Complexes. *ChemCatChem* **2015,** *7*, 3963-3971.

35.   Ajellal, N.; Durieux, G.; Delevoye, L.; Tricot, G.; Dujardin, C.; Thomas, C. M.; Gauvin, R. M., Polymerization of racemic β-butyrolactone using supported catalysts: a simple access to isotactic polymers. *Chem. Commun.* **2010,** *46*, 1032-1034.

36. Dong, X.; Robinson, J. R., The role of neutral donor ligands in the isoselective ring-opening polymerization of rac-β-butyrolactone. *Chem. Sci.* **2020,** *11*, 8184-8195.

37. Dong, X.; Brown, A. M.; Woodside, A. J.; Robinson, J. R., N-Oxides amplify catalyst reactivity and isoselectivity in the ring-opening polymerization of rac-β-butyrolactone. *Chem. Commun.* **2022,** *58*, 2854-2857.

38. Zhuo, Z.; Zhang, C.; Luo, Y.; Wang, Y.; Yao, Y.; Yuan, D.; Cui, D., Stereo-selectivity switchable ROP of rac-β-butyrolactone initiated by salan-ligated rare-earth metal amide complexes: the key role of the substituents on ligand frameworks. *Chem. Commun.* **2018,** *54*, 11998-12001.

39. Tshuva, E. Y.; Gendeziuk, N.; Kol, M., Single-step synthesis of salans and substituted salans by Mannich condensation. *Tetrahedron Lett.* **2001,** *42*, 6405-6407.

40. Tschan, M. J.; Gauvin, R. M.; Thomas, C. M., Controlling polymer stereochemistry in ring-opening polymerization: a decade of advances shaping the future of biodegradable polyesters. *Chem. Soc. Rev.* **2021,** *50*, 13587-13608.

41. Carpentier, J.-F., Rare-Earth Complexes Supported by Tripodal Tetradentate Bis(phenolate) Ligands: A Privileged Class of Catalysts for Ring-Opening Polymerization of Cyclic Esters. *Organometallics* **2015,** *34*, 4175-4189.

42. Hormnirun, P.; Marshall, E. L.; Gibson, V. C.; White, A. J.; Williams, D. J., Remarkable stereocontrol in the polymerization of racemic lactide using aluminum initiators supported by tetradentate aminophenoxide ligands. *J. Am. Chem. Soc.* **2004,** *126*, 2688-2689.

25

8 Chemical Synthesis of PHB with Reduced Isotacticity Using Yttrium Salan Catalysts – Accessing a Material with Polyolefin-like Properties

8.1 Bibliographic Data
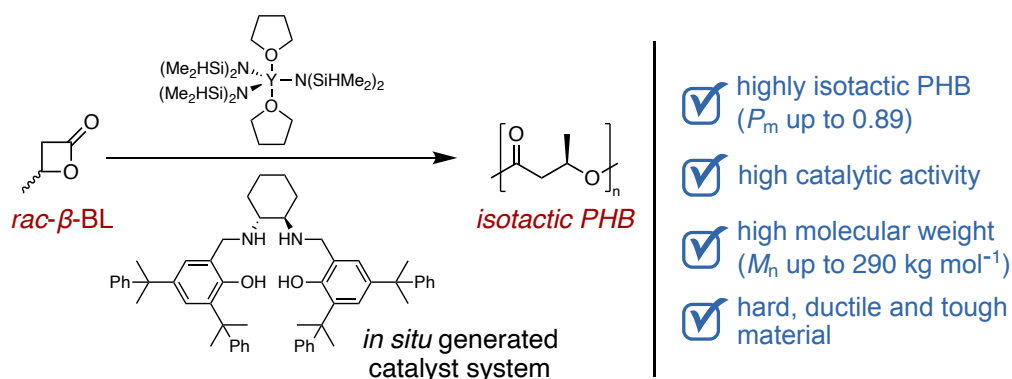
synthetic PHB with improved properties over bacterial PHB

Title:	Highly Isoselective Ring-Opening Polymerization of *rac-β*-Butyrolactone: Access to Synthetic Poly(3-hydroxybutyrate) with Polyolefin-like Material Properties
Status:	Manuscript in preparation
Authors:	Jonas Bruckmoser, Stefanie Pongratz, Lucas Stieglitz, Bernhard Rieger

---

J. Bruckmoser had the initial idea, planned all experiments, performed most of the experiments, and wrote the manuscript. S. Pongratz performed some polymerization experiments and the polymer end-group analysis. L. Stieglitz and J. Bruckmoser conducted the stress-strain measurements. S. Pongratz and L. Stieglitz gave advice on the manuscript. All work was supervised by B. Rieger.

8.2 Content

Polyolefins account for the largest share of industrial plastics production and have found a plethora of applications due to their excellent properties. However, when it comes to the end-of-life fate of these materials, their strength and durability, which is one of their benefits during lifetime, becomes a major drawback and results in the accumulation of plastic waste in the environment. Isotactic PHB is a particularly promising candidate as substitute for current commodity plastics since it shows comparable material properties to *i*-PP but features biodegradability. Nonetheless, catalysts for the synthesis of isotactic PHB via ROP of *β*-BL are extremely scarce in literature and current systems are limited by either poor activity, inaccessibility of high molecular weight, low degree of isotacticity or combinations thereof. In this study, the high-throughput approach described previously in chapter 7 was applied to identify a platform of *in situ* generated catalysts for the highly isoselective ROP of *β*-BL. $Y[N(SiHMe_2)_2]_3(THF)_2$ was used as a precursor complex, and the salan pro-ligands had an N–H substitution motif in common while the backbone was modified from a chiral cyclohexyl to an achiral phenyl, ethyl or propyl version. Irrespective of the ligand backbone of the initiator, they all produced highly isotactic PHB starting from a *racemic β*-BL feedstock (P_m up to 0.89). The yttrium catalyst bearing a cyclohexyl substituted backbone showed the highest catalytic activity with a remarkable TOF of up to 32 000 h^{-1} and was capable of yielding high molecular weight PHB (M_n up to 290 kg mol^{-1}). In comparison to perfectly isotactic, bacterial PHB, the synthetic PHB with reduced isotacticity generated in this work demonstrated superior material properties. Two main challenges that are hampering the commercialization of PHB were overcome, namely the low thermostability and the brittleness of the material. Due to the reduced isotacticity and therefore reduced crystallinity of the synthetic PHB, the melting temperature was lowered by ~35°C while still being high ($T_m ≈ 140$°C), thus, substantially increasing the window for melt processing without material decomposition. Additionally, the brittleness of the material was drastically reduced, showing a remarkably high elongation at break in stress-strain measurements of $ε_B$ = 392%, in stark contrast to bacterial PHB with an $ε_B$ = 2%. Overall, the obtained synthetic PHB using *in situ* generated yttrium salan catalysts demonstrated enhanced polyolefin-like material properties, highlighting the outstanding future potential of PHB as a sustainable substitute for current commodity plastics.

8.3 Manuscript Draft

Highly Isoselective Ring-Opening Polymerization of *rac-β*-Butyrolactone: Access to Synthetic Poly(3-hydroxybutyrate) with Polyolefin-like Material Properties

Jonas Bruckmoser, Stefanie Pongratz, Lucas Stieglitz, and Bernhard Rieger*

WACKER-Chair of Macromolecular Chemistry, Catalysis Research Center, Department of Chemistry, Technical University of Munich, 85748 Garching, Germany

ABSTRACT: We report the highly isoselective ring-opening polymerization (ROP) of *racemic β*-butyrolactone (*β*-BL) using *in situ* generated catalysts based on Y[N(SiHMe$_2$)$_2$]$_3$(THF)$_2$ and salan-type pro-ligands. The catalyst system produces isotactic poly(3-hydroxybutyrate) (PHB) with record productivity (TOF up to 32 000 h^{-1}) and highest isoselectivity (P_m up to 0.89) in ROP of *β*-BL achieved to date. In contrast to bacterial PHB, the chemically synthesized PHB has beneficial material properties, such as increased melt processing window by a lowered melting temperature (T_m ~140°C) and drastically reduced brittleness. The produced PHB showed an elongation at break of 392%, thus demonstrating promising polyolefin-like thermomechanical material properties.

Poly(3-hydroxybutyrate) (PHB) is the most prominent member of poly(hydroxyalkanoates), a class of biodegradable aliphatic polyesters that are naturally produced by bacteria and other living microorganisms.[1,2] Bacterial PHB is a perfectly isotactic polymer with (*R*)-configuration and therefore a semi-crystalline, high-melting, thermoplastic material. The thermal and mechanical properties of PHB resemble those of isotactic polypropylene (*i*-PP), rendering it a promising future commodity plastic with beneficial end-of-life options (i.e. degradability or chemical recyclability).[1-3]

However, the current industrial application of PHB is limited for several reasons. In contrast to chemical *i*-PP synthesis, the fermentative production costs of PHB are high and restricted in scalability.[2,3] As bacterial PHB is perfectly isotactic ($P_m = 1$), its high crystallinity leads to a stiff and brittle material, and, additionally, its high melting temperature near the decomposition temperature hampers processing via common routes such as melt processing.[3-5] The chemical synthesis of PHB provides solutions for these challenges and the ring-opening polymerization (ROP) of cyclic esters is the most promising approach.[6,7] Chen et al. very recently reported an elegant work in which the synthesis of perfectly isotactic PHB was achieved via ROP of an 8-membered diolide.[8-10] However, the multi-step synthesis of the monomer is elaborate and limiting its industrial potential. With regard to monomer availability, ROP of 4-membered *β*-butyrolactone (*β*-BL) is the most convenient and promising approach toward PHB synthesis.[3,6] The use of enantiopure (*R*)-*β*-BL (mixed with a certain amount of (*S*)-*β*-BL) gives PHB with reduced isotacticity (such as P_m ~0.8–0.9) that is not accessible via biotechnological routes.[4] This reduced stereoregularity substantially lowers the crystallinity of the polymer and thus results in a material with reduced brittleness and decreased melting temperature (but still >100°C), generally enabling industrial applications.[4,11] Nevertheless, using enantiopure monomers for producing isotactic PHB is expensive[4,11,12] and a cost-effective approach demands the use of cheap *racemic β*-BL. This monomer is commercially available and easily produced from an inexpensive propylene oxide feedstock via atom-efficient carbon monoxide insertion.[13] However, when it comes to ROP of *β*-BL, the synthesis of iso-enriched or isotactic PHB from a *racemic* feedstock has been a challenge since the early 1960s.[3,6,8,14]

While atactic or syndiotactic PHB can be easily accessed via ROP of *β*-BL using metal-based catalysts, the amorphous nature of atactic and the lack of biodegradability of syndiotactic PHB diminish the value of these materials.[4,6,15] Catalyst systems inducing isoselectivity in the ROP of *β*-BL remain scarce. Early work by Agostini, Tani and others revealed that partially hydrolyzed aluminum alkyl species produce PHB with a minor fraction of isotactic polymer (P_m ~0.8) and a major atactic fraction.[16-22] Synthesis of iso-enriched PHB was achieved using a catalyst system consisting of ZnEt$_2$ and a chiral diol.[23] However, the product also consisted of a mixture of methanol-soluble atactic and insoluble (~25%) isotactic (P_m ~0.8) fractions. Chromium salophen complexes reported by our group gave access to high-molecular-weight PHB with modest isotactic bias (P_m up to 0.67, Figure 1A).[24-26] In 2010, Thomas and Gauvin et al. obtained isotactic PHB ($P_m = 0.85$) using neodymium borohydrides supported on silica, and this heterogeneous catalyst system still accounts for the highest isoselectivity in ROP of *β*-BL reported to date (Figure 1B).[27]

1

Recently, phenyl-substituted yttrium and ytterbium salan complexes gave access to iso-enriched PHB (P_m = 0.66–0.77, Figure 1C).[28] Robinson and co-workers very recently showed that the isoselectivity in ROP of β-BL is strongly increased up to P_m = 0.75 at room temperature (up to 0.82 at -30°C) by addition of neutral donor ligands to a lanthanum amino bis(phenolate) catalyst (Figure 1D).[29,30]
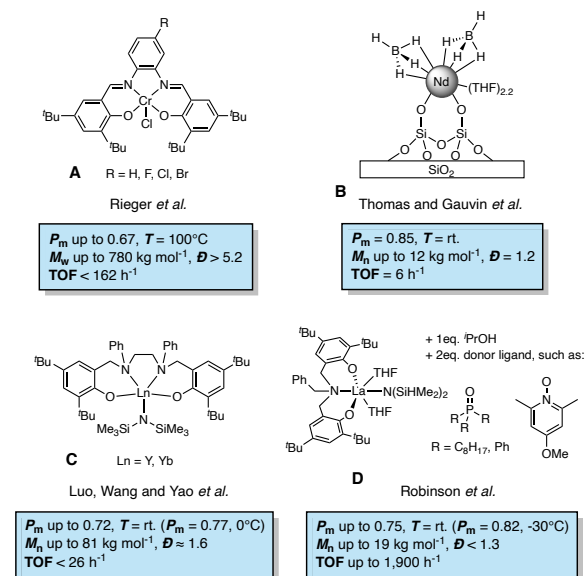
Figure 1. Discrete catalysts reported in literature for the isoselective ROP of β-BL.

In the context of replacing *i*-PP by biodegradable PHB, current catalytic systems for the production of this aliphatic polyester are limited by either poor activity, inaccessibility of high molecular weight, low degree of isotacticity or combinations thereof. Herein, we report a novel catalyst system that shows very high activities in the ROP of *racemic* β-BL and produces high-molecular-weight isotactic PHB (P_m up to 0.89) with drastically enhanced material properties.

Inspired by the simple *in situ* formation of catalysts often carried out in enantioselective catalysis,[31-35] we set out to investigate an *in situ* generated catalyst system consisting of Y[N(SiHMe$_2$)$_2$]$_3$(THF)$_2$ (**Y**) and a salan-type pro-ligand (**L1**) bearing a chiral cyclohexyl backbone for the ROP of β-BL (Figure 2). Excitingly, **Y+L1** showed high activity and produced iso-enriched PHB (P_m = 0.63, Table 1, entry 1 and Figure 3a). Increasing the steric demand of the phenolic *ortho*-position from *tert*-butyl to cumyl (**Y+L2**) gave a catalytic system that converted 200 equiv of β-BL within 1 min, and most strikingly, the generated PHB was highly isotactic (P_m = 0.82, Table 1, entry 2). Increasing the [β-BL]/[**Y+L2**] ratio to 400/1 led to a molecular weight of the polymer twice as high and eventually high-molecular-weight isotactic PHB (P_m = 0.84, M_n = 290 kg mol^{-1}) could be obtained with record productivity (turnover frequency, TOF = 32 000 h^{-1}) when the [β-BL]/[**Y+L2**] ratio was as high as 2000/1 (Table 1, entries 3 and 4, and Figure 3b). The stereoregularity of the polymer was even further pronounced when the polymerization was carried out at -35°C (Table 1, entry 5). The produced PHB showed a P_m of 0.89, which is the highest isoselectivity in ROP of β-BL reported to date (Figure 3c). Catalyst system **Y+L2** generated

polymers with unimodal GPC traces but relatively broad polydispersities ($Đ$ ~2.0). Nevertheless, the molecular weight could be controlled by the [β-BL]/[**Y+L2**] ratio (Figure S11). Scale-up of the polymerization to a 10 g scale was also feasible using a 250 mL double-walled Büchi steel autoclave (Table S1, entry 6).
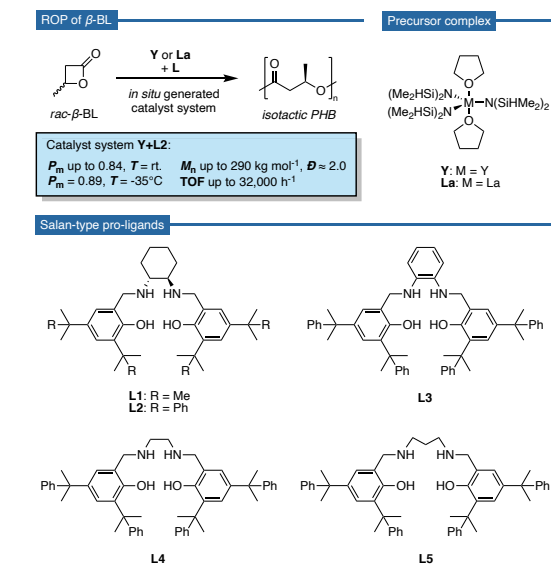
Figure 2. Overview of this work. Isoselective ROP of β-BL using *in situ* generated salan catalysts based on yttrium or lanthanum. **L1** and **L2** were used as racemic mixtures.

Curious whether the stereocontrol of the catalytic system is induced by the chiral cyclohexyl backbone of the ligand framework, we tested pro-ligand **L3** bearing a phenyl backbone in combination with **Y** (Figure 2). Surprisingly, even an achiral pro-ligand enabled a highly isoselective ROP of β-BL, albeit with strongly reduced activity (Table 1, entry 6). When the backbone of the pro-ligand was further reduced to an ethylene- or propylene-linker (**L4** and **L5**), the generated PHB showed an even increased isotacticity with P_m = 0.85 and 0.88, respectively (Table 1, entries 7 and 8). Yet, molecular weight control of catalyst systems **Y+L3–L5** was reduced in comparison to **Y+L2**. While the ultra-fast polymerization mediated by **Y+L2** was beyond the limit to be monitored via collecting aliquots from the reaction mixture, the reduced activity of **Y+L5** made kinetic analysis possible. Conversion vs time data indicated a first-order dependence of the polymerization rate on β-BL concentration after a short initiation period of ~0.7 min (Figure S12). The rate constant was determined as k_{obs} = 0.415 ± 0.019 min^{-1} (0.5 mol%, [β-BL] = 2.0 M). Electrospray ionization mass spectrometry (ESI-MS) of oligomers showed that the polymerization is initiated by the silylamido group and the polymer chains are hydroxyl- or crotonate-terminated (Figure S13). A preliminary result revealed that the platform of salan pro-ligands is also capable of introducing stereoselectivity in ROP of β-BL when a lanthanum precursor is used instead of the corresponding yttrium species (Table 1, entry 9). Stereocontrol is reduced due to the larger ionic radius of lanthanum in comparison to yttrium, in line with previous works in the field of ROP that have demonstrated the profound influence of the metal size on stereoselectivity.[28,36-38]

2

Table 1. Ring-Opening Polymerization of *rac-β*-BL Using Yttrium and Lanthanum Salan Catalysts [a]

entry	catalytic system	[M]/[Y+L]	T (°C)	time (min)	conv.[b] (%)	M_n [c] (kg mol^{-1})	$Đ$ [c]	P_m [d]	T_m [e] (°C)
1	**Y+L1**	200	rt.	120	83	35	1.9	0.63	n.d.
2	**Y+L2**	200	rt.	1	98	41	2.2	0.82	123/138
3	**Y+L2**	400	rt.	2	99	85	2.0	0.83	126/139
4	**Y+L2**	2000	rt.	3	80	290	2.0	0.84	126/140
5	**Y+L2**	200	-35	60	>99	130	3.2	0.89	154
6	**Y+L3**	200	rt.	30	52	103	1.8	0.82	n.d.
7	**Y+L4**	200	rt.	3	91	77	2.1	0.85	n.d.
8	**Y+L5**	200	rt.	3	55	184	1.9	0.88	146
9	**La+L2**	200	rt.	30	32	11	1.8	0.61	n.d.

[a]Polymerizations were performed in toluene, [*β*-BL] = 2.0 M. Catalyst was prepared *in situ* by treatment of **Y** or **La** with salan pro-ligand **L** (1 eq.) in toluene at room temperature for 1 h prior to monomer addition. [b]Conversion determined by ^{1}H NMR spectroscopy. [c]Determined by GPC in CHCl$_3$ at room temperature relative to polystyrene standards. [d]Tacticity determined by ^{13}C{^{1}H} NMR spectroscopy, integration of the carbonyl signal. [e]Determined by DSC, second heating cycle. n.d. = not determined.
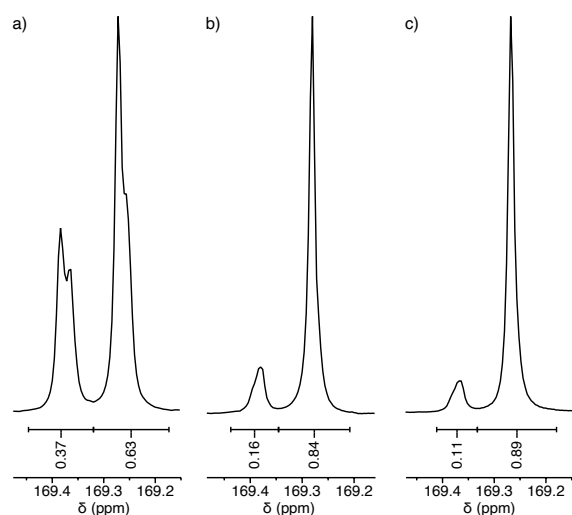
Figure 3. ^{13}C{^{1}H} NMR spectra (carbonyl region) of isotactic PHBs produced by a) **Y+L1** (Table 1, entry 1), b) **Y+L2** at rt. (Table 1, entry 4) and c) **Y+L2** at -35°C (Table 1, entry 5).

Figure 4. DSC curve (exo down) of PHB with P_m = 0.88 (Table 1, entry 8). T_g = glass transition temperature, T_c = crystallization temperature.

The yttrium salen catalysts employed by Chen et al. for the highly isoselective ROP of 8-membered diolide toward PHB are closely related to the yttrium salan-type catalyst systems reported herein. But notably, the most stereoselective salen catalyst for ROP of the diolide was not stereoselective in the ROP of *β*-BL.[8] We have tested *in situ* generated yttrium salen catalysts (**Y+L'1-3**) for *β*-BL polymerization and similarly observed that these initiators are poorly active and only generate atactic PHB (Table S2). The distinct difference between the ligand frameworks is the N–H substituted, tertiary amine and hence increased flexibility in salans, instead of the rigid imine moiety in salens. However, this subtle change has drastic implications for the stereoselectivity. Detailed mechanistic investigations in the future will help to understand the specific reason of stereocontrol such as potential non-covalent interactions with the N–H moieties[39] or the potentially beneficial increase in framework flexibility.[40]

The brittleness and high melting temperature of bacterial PHB currently limit its broad commercialization. Guided by our hypothesis that a reduced isotacticity should result in beneficial material properties, we set out to investigate the properties of the chemically synthesized PHBs. Differential scanning calorimetry (DSC) revealed that the samples with a P_m of 0.82–0.89 have melting transitions (T_m) within the range of 123–154°C (Figure 4). Thermal gravimetric analysis (TGA) showed a 5% weight loss ($T_{d,5\%}$) at 239°C and maximum decomposition rate ($T_{d,max}$) at 273°C. Comparing the chemically synthesized PHBs with bacterial PHB demonstrates that the decomposition of both material occurs at similar temperatures (Figures S21 and S22), but synthetic PHB with reduced isotacticity shows a T_m which is ~35°C lowered and thus, provides a substantially increased window for melt processing. Analysis of the mechanical properties was carried out by tensile testing of dog-bone-shaped specimens prepared by compression molding. The stress-strain curve of bacterial PHB showed an ultimate tensile strength (σ_B) of 30.3 MPa, Young's modulus (E) of 1.6 GPa, and elongation at break (ε_B) of 2%, in line with literature reported values (Figure 5).[4] Contrary to this, synthet-

3

ic PHB with a P_m of 0.84 revealed a markedly different stress-strain behavior. In comparison to bacterial PHB, the ultimate tensile strength and Young's modulus were slightly reduced to σ_B = 21.1 MPa and E = 762 MPa. But most strikingly, the reduced stereoregularity of the synthetic PHB resulted in a drastically enhanced elongation at break (ε_B = 392%, Figure 5). Thus, the PHB produced via ROP of β-BL using catalyst system **Y+L2** is a hard, ductile, and tough material, much like i-PP.
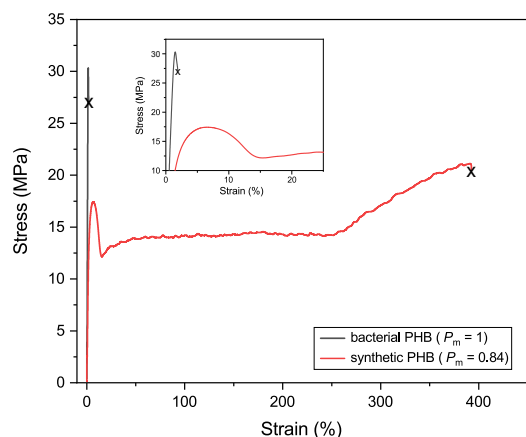
Figure 5. Stress-strain curves of bacterial PHB (M_n = 247 kg mol^{-1}, Đ = 2.3) and synthetic PHB with reduced isotacticity (M_n = 259 kg mol^{-1}, Đ = 2.5). Inset: zoom in of curves at low strain. Break point indicated by "x".

In conclusion, we have introduced a novel catalyst platform based on *in situ* generated yttrium salan catalysts for the highly isoselective ROP of β-BL. Catalytic system **Y+L2** is the most isoselective initiator for the ROP of β-BL reported to date (P_m up to 0.89) and showed an unprecedented high activity (TOF up to 32 000 h^{-1}). In comparison to brittle and high-melting bacterial PHB, the synthetic isotactic PHB with reduced stereoregularity has a lower melting temperature (T_m ~140°C) that is advantageous for polymer processing, and a drastically enhanced elongation at break (ε_B = 392%). These polyolefin-like thermomechanical material properties are highly beneficial and overcome current limitations of naturally produced PHB.

ASSOCIATED CONTENT

Supporting Information

The Supporting Information is available free of charge on the ACS Publications website.
Experimental procedures, additional polymerization data, analytical and characterization data of polymers (PDF)

AUTHOR INFORMATION

Corresponding Author

*rieger@tum.de
Notes
J.B. and B.R. are inventors on a patent application covering the methods in this paper. The remaining authors declare no competing financial interest.

REFERENCES

1. Muhammadi; Shabina; Afzal, M.; Hameed, S., Bacterial polyhydroxyalkanoates-eco-friendly next generation plastic: production, biocompatibility, biodegradation, physical properties and applications. *Green Chem. Lett. Rev.* **2015**, *8*, 56-77.
2. Kumar, M.; Rathour, R.; Singh, R.; Sun, Y.; Pandey, A.; Gnansounou, E.; Andrew Lin, K.-Y.; Tsang, D. C. W.; Thakur, I. S., Bacterial polyhydroxyalkanoates: Opportunities, challenges, and prospects. *J. Clean. Prod.* **2020**, *263*, 121500.
3. Rieger, B.; Künkel, A.; Coates, G. W.; Reichardt, R.; Dinjus, E.; Zevaco, T. A., *Synthetic biodegradable polymers*. Springer-Verlag: Berlin, Heidelberg, **2012**.
4. Abe, H.; Matsubara, I.; Doi, Y.; Hori, Y.; Yamaguchi, A., Physical properties and enzymic degradability of poly(3-hydroxybutyrate) stereoisomers with different stereoregularities. *Macromolecules* **1994,** *27*, 6018-6025.
5. Gogolewski, S.; Jovanovic, M.; Perren, S.; Dillon, J.; Hughes, M., The effect of melt-processing on the degradation of selected polyhydroxyacids: polylactides, polyhydroxybutyrate, and polyhydroxybutyrate-co-valerates. *Polym. Degrad. Stab.* **1993,** *40*, 313-322.
6. Carpentier, J. F., Discrete metal catalysts for stereoselective ring-opening polymerization of chiral racemic β-lactones. *Macromol. Rapid Commun.* **2010,** *31*, 1696-1705.
7. Li, H.; Shakaroun, R. M.; Guillaume, S. M.; Carpentier, J. F., Recent Advances in Metal-Mediated Stereoselective Ring-Opening Polymerization of Functional Cyclic Esters towards Well-Defined Poly(hydroxy acid)s: From Stereoselectivity to Sequence-Control. *Chem. Eur. J.* **2020**, *26*, 128-138.
8. Tang, X.; Chen, E. Y., Chemical synthesis of perfectly isotactic and high melting bacterial poly(3-hydroxybutyrate) from bio-sourced racemic cyclic diolide. *Nat. Commun.* **2018, 9**, 2345.
9. Tang, X.; Westlie, A. H.; Watson, E. M.; Chen, E. Y.-X., Stereosequenced crystalline polyhydroxyalkanoates from diastereomeric monomer mixtures. *Science* **2019**, *366*, 754-758.
10. Tang, X.; Westlie, A. H.; Caporaso, L.; Cavallo, L.; Falivene, L.; Chen, E. Y., Biodegradable Polyhydroxyalkanoates by Stereoselective Copolymerization of Racemic Diolides: Stereocontrol and Polyolefin-Like Properties. *Angew. Chem. Int. Ed.* **2020,** *59*, 7881-7890.
11. Tanahashi, N.; Doi, Y., Thermal properties and stereoregularity of poly(3-hydroxybutyrate) prepared from optically active β-butyrolactone with a zinc-based catalyst. *Macromolecules* **1991,** *24*, 5732-5733.
12. Hori, Y.; Suzuki, M.; Yamaguchi, A.; Nishishita, T., Ring-opening polymerization of optically active β-butyrolactone using distannoxane catalysts: Synthesis of high-molecular-weight poly(3-hydroxybutyrate). *Macromolecules* **1993,** *26*, 5533-5534.
13. Getzler, Y. D.; Mahadevan, V.; Lobkovsky, E. B.; Coates, G. W., Synthesis of β-lactones: a highly active and selective catalyst for epoxide carbonylation. *J. Am. Chem. Soc.* **2002**, *124*, 1174-1175.
14. Inoue, S.; Tomoi, Y.; Tsuruta, T.; Furukawa, J., Organometallic-catalyzed polymerization of propiolactone. *Makromol. Chem.* **1961,** *48*, 229-233.
15. Abe, H.; Doi, Y., Enzymatic and environmental degradation of racemic poly(3-hydroxybutyric acid)s with different stereoregularities. *Macromolecules* **1996,** *29*, 8683-8688.
16. Agostini, D.; Lando, J.; Shelton, J. R., Synthesis and characterization of poly-β-hydroxybutyrate. I. Synthesis of crystalline DL-poly-β-hydroxybutyrate from DL-β-butyrolactone. *J. Polym. Sci., Part A: Polym. Chem.* **1971,** *9*, 2775-2787.

4

17. Teranishi, K.; Iida, M.; Araki, T.; Yamashita, S.; Tani, H., Stereospecific polymerization of β-alkyl-β-propiolactone. *Macromolecules* **1974,** *7*, 421-427.

18. Iida, M.; Araki, T.; Teranishi, K.; Tani, H., Effect of substituents on stereospecific polymerization of β-alkyl-and β-chloroalkyl-β-propiolactones. *Macromolecules* **1977,** *10*, 275-284.

19. Gross, R. A.; Zhang, Y.; Konrad, G.; Lenz, R. W., Polymerization of β-monosubstituted-β-propiolactones using trialkylaluminum-water catalytic systems and polymer characterization. *Macromolecules* **1988,** *21*, 2657-2668.

20. Bloembergen, S.; Holden, D. A.; Bluhm, T. L.; Hamer, G. K.; Marchessault, R. H., Stereoregularity in synthetic β-hydroxybutyrate and β-hydroxyvalerate homopolyesters. *Macromolecules* **1989,** *22*, 1656-1663.

21. Jaimes, C.; Arcana, M.; Brethon, A.; Mathieu, A.; Schue, F.; Desimone, J., Structure and morphology of poly([R,S]-β-butyrolactone) synthesized from aluminoxane catalyst. *Eur. Polym. J.* **1998,** *34*, 175-186.

22. Wu, B.; Lenz, R. W., Stereoregular Polymerization of [R, S]-3-Butyrolactone Catalyzed by Alumoxane− Monomer Adducts. *Macromolecules* **1998,** *31*, 3473-3477.

23. Le Borgne, A.; Spassky, N., Stereoelective polymerization of β-butyrolactone. *Polymer* **1989,** *30*, 2312-2319.

24. Zintl, M.; Molnar, F.; Urban, T.; Bernhart, V.; Preishuber-Pflugl, P.; Rieger, B., Variably isotactic poly(hydroxybutyrate) from racemic β-butyrolactone: microstructure control by achiral chromium(III) salophen complexes. *Angew. Chem. Int. Ed.* **2008,** *47*, 3458-3460.

25. Reichardt, R.; Vagin, S.; Reithmeier, R.; Ott, A. K.; Rieger, B., Factors Influencing the Ring-Opening Polymerization of Racemic β-Butyrolactone Using CrIII(salphen). *Macromolecules* **2010,** *43*, 9311-9317.

26. Vagin, S.; Winnacker, M.; Kronast, A.; Altenbuchner, P. T.; Deglmann, P.; Sinkel, C.; Loos, R.; Rieger, B., New Insights into the Ring-Opening Polymerization of β-Butyrolactone Catalyzed by Chromium(III) Salphen Complexes. *ChemCatChem* **2015,** *7*, 3963-3971.

27. Ajellal, N.; Durieux, G.; Delevoye, L.; Tricot, G.; Dujardin, C.; Thomas, C. M.; Gauvin, R. M., Polymerization of racemic β-butyrolactone using supported catalysts: a simple access to isotactic polymers. *Chem. Commun.* **2010,** *46*, 1032-1034.

28. Zhuo, Z.; Zhang, C.; Luo, Y.; Wang, Y.; Yao, Y.; Yuan, D.; Cui, D., Stereo-selectivity switchable ROP of rac-β-butyrolactone initiated by salan-ligated rare-earth metal amide complexes: the key role of the substituents on ligand frameworks. *Chem. Commun.* **2018,** *54*, 11998-12001.

29. Dong, X.; Robinson, J. R., The role of neutral donor ligands in the isoselective ring-opening polymerization of rac-β-butyrolactone. *Chem. Sci.* **2020,** *11*, 8184-8195.

30. Dong, X.; Brown, A. M.; Woodside, A. J.; Robinson, J. R., N-Oxides amplify catalyst reactivity and isoselectivity in the ring-opening polymerization of rac-β-butyrolactone. *Chem. Commun.* **2022,** *58*, 2854-2857.

31. Blaser, H.-U.; Federsel, H.-J., *Asymmetric Catalysis on Industrial Scale*. Wiley-VCH Verlag: Weinheim, **2010**.

32. Trost, B. M., Asymmetric catalysis: an enabling science. *Proc. Natl. Acad. Sci. U.S.A.* **2004,** *101*, 5348-5355.

33. Lefort, L.; Boogers, J. A.; de Vries, A. H.; de Vries, J. G., Instant ligand libraries. Parallel synthesis of monodentate phosphoramidites and in situ screening in asymmetric hydrogenation. *Org. Lett.* **2004,** *6*, 1733-1735.

34. Matsumoto, K.; Oguma, T.; Katsuki, T., Highly enantioselective epoxidation of styrenes catalyzed by proline-derived C1-symmetric titanium(salan) complexes. *Angew. Chem. Int. Ed.* **2009,** *48*, 7432-7435.

35. Egami, H.; Oguma, T.; Katsuki, T., Oxidation catalysis of Nb(salan) complexes: asymmetric epoxidation of allylic alcohols using aqueous hydrogen peroxide as an oxidant. *J. Am. Chem. Soc.* **2010,** *132*, 5886-5895.

36. Bakewell, C.; White, A. J.; Long, N. J.; Williams, C. K., Metal-size influence in iso-selective lactide polymerization. *Angew. Chem. Int. Ed.* **2014,** *53*, 9226-9230.

37. Altenbuchner, P. T.; Kronast, A.; Kissling, S.; Vagin, S. I.; Herdtweck, E.; Pothig, A.; Deglmann, P.; Loos, R.; Rieger, B., Mechanistic Investigations of the Stereoselective Rare Earth Metal-Mediated Ring-Opening Polymerization of β-Butyrolactone. *Chem. Eur. J.* **2015,** *21*, 13609-13617.

38. Grunova, E.; Kirillov, E.; Roisnel, T.; Carpentier, J.-F., Group 3 metal complexes supported by tridentate pyridine-and thiophene-linked bis (naphtholate) ligands: synthesis, structure, and use in stereoselective ring-opening polymerization of racemic lactide and β-butyrolactone. *Dalton Trans.* **2010,** *39*, 6739-6752.

39. Gesslbauer, S.; Savela, R.; Chen, Y.; White, A. J. P.; Romain, C., Exploiting Noncovalent Interactions for Room-Temperature Heteroselective rac-Lactide Polymerization Using Aluminum Catalysts. *ACS Catal.* **2019,** *9*, 7912-7920.

40. Marlier, E. E.; Macaranas, J. A.; Marell, D. J.; Dunbar, C. R.; Johnson, M. A.; DePorre, Y.; Miranda, M. O.; Neisen, B. D.; Cramer, C. J.; Hillmyer, M. A.; Tolman, W. B., Mechanistic Studies of ε-Caprolactone Polymerization by (salen)AlOR Complexes and a Predictive Model for Cyclic Ester Polymerizations. *ACS Catal.* **2016,** *6*, 1215-1224.

5

9 Summary and Outlook

In this thesis, ROP was utilized as an efficient method for the synthesis of (bio)degradable and chemically recyclable polyesters. Catalyst and monomer design studies were performed to unlock the full potential of ROP for the generation of materials with sophisticated and promising properties. In the first part, novel indium salan and catam complexes were synthesized, characterized, and employed as initiators for the ROP of various cyclic esters including β-BL, γ-BL, ε-CL, ε-DL and LA (Figure 25). The indium salan alkoxide complex revealed excellent performance for all these monomers, highlighting its versatility. The polymerizations were well controlled, could be carried out under immortal ROP conditions and gave high molecular weight polyesters with narrow dispersities. Detailed kinetic investigations in the ROP of β-BL were performed and indicated a mononuclear coordination-insertion mechanism. The robustness of this initiator was demonstrated by its tolerance of an impure lactide feedstock without any loss of activity or control over the ROP. Applying an *in situ* activation protocol, the air-stable (but poorly active) indium chloro pre-catalyst was conveniently converted into a catalytically active species with drastically enhanced polymerization rates. Whilst the indium salan complex is one of the top all-rounder catalysts in ROP of cyclic esters, the respective indium catam complex showed generally reduced reaction rates. These results suggested that the more constrained geometry of the catam-type initiator compared to the salan-type derivative is detrimental. The introduction of framework flexibility (such as the flexible methylene bridges in the salan-type complex) thus seems to be a promising approach in catalyst design in order to achieve highly active all-rounder catalysts.

The indium salan complex was subsequently chosen for demonstrating the advantages of such all-rounder catalysts. In copolymerizations, such initiators enable rapid and simple access towards sophisticated copolymer structures. More specifically, the copolymerization of two lactones with large difference in their steric demand was studied with the goal of achieving sequence control from one-pot monomer mixtures (Figure 25). Simultaneous copolymerization of small-sized β-BL and relatively large-sized ε-CL revealed a strong affinity of the indium catalyst towards β-BL, as evidenced by a surprisingly reversed monomer reactivity compared to homopolymerization results. PHB-*co*-PCL gradient copolymers instead of PCL-*b*-PHB block copolymers were obtained. Switching to a related but sterically more demanding comonomer, namely ε-DL, a monomer-selective polymerization behavior of the initiator in one-pot copolymerizations with β-BL was observed. Hence, this catalyst was capable of the simple and rapid synthesis of AB-, BAB-, and ABAB-type block copolymers from monomer mixtures. While switchable catalysis has previously focused on combining *different* monomer classes such as lactones with epoxides/CO_2 or carboxyanhydrides for generating block copolymers,[173,183] this study demonstrated that sequence control in copolymerizations is also feasible within *one*

class of *similarly* reactive monomers. Such a monomer-selective behavior might also be observed for other catalysts in the future and has important implications for the synthesis of even more sophisticated copolymer structures from one-pot monomer mixtures. For example, applying the indium salan catalyst to a mixture of two different lactones in the presence of epoxide and CO_2 has the potential to generate conveniently polyester-*b*-polyester-*b*-polycarbonate triblock copolymers. Combining such monomer- or chemoselective polymerization approaches holds great potential for the future as promising material properties could be obtained given the tunability of the different polymer blocks. Block copolymers can be prepared by sequential addition protocols, however, the generation of such polymers from monomer mixtures is more appealing as it reduces synthetic efforts by allowing the use of premixed feedstocks with adjustable ratios. The synthesis of sequence-controlled polymers is an extraordinary challenge and the perfection of temporal and spatial control of Nature (such as DNA or polypeptide synthesis) is the ultimate paragon. Having monomer-selective and switchable catalysts at hand is one step closer toward imitation of Nature's perfection.
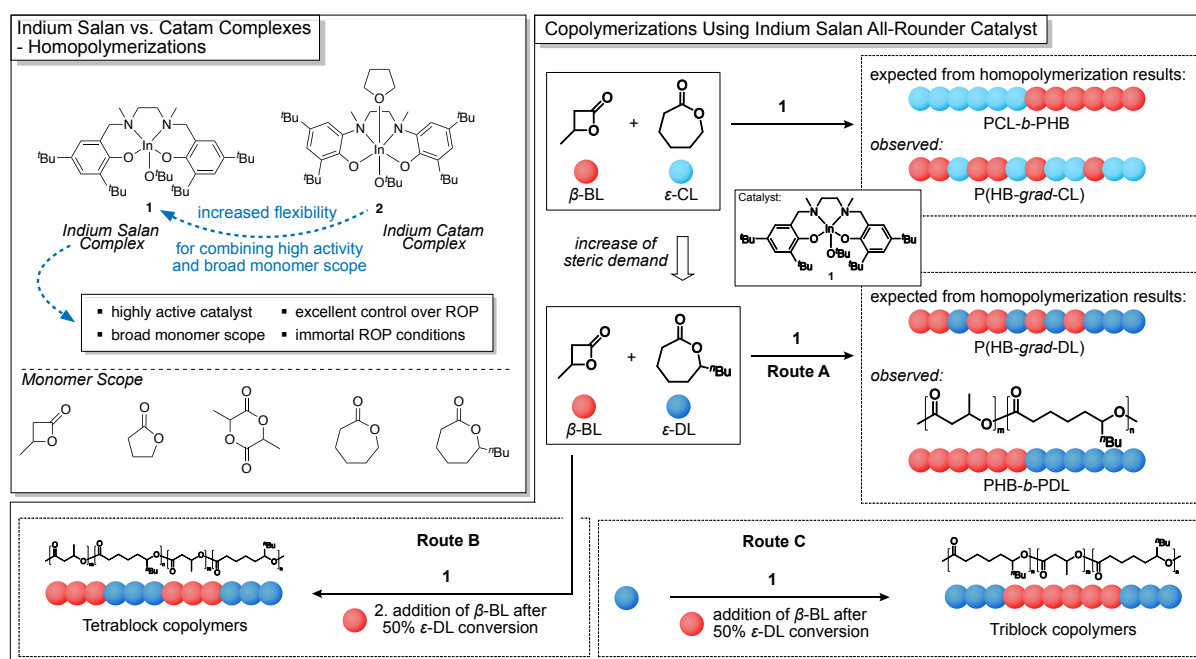
Figure 25. Homopolymerization of various cyclic esters using indium salan and catam complexes (left). Synthesis of block copolymers from one-pot monomer mixtures using monomer-selective indium salan catalyst (right).[131,237]

The second approach in catalyst design focused on yttrium salan catalysts for the ROP of *rac-β*-BL. Since the control over the polymer's microstructure is highly important, ultimately influencing its properties, the development of stereoselective initiators is crucial. For understanding structure-property relationships in catalyst design, the elaborate and time-consuming synthesis of large catalyst libraries is necessary. Herein, a high-throughput

approach was developed, enabling the rapid screening of various yttrium salan catalysts and the establishment of structure-property relationships (Figure 26). The initiators were prepared conveniently *in situ* by combining an yttrium precursor complex with a salan pro-ligand, followed by direct addition of monomer to the catalyst mixture. The applicability of the *in situ* approach was verified by identical polymerization results of isolated vs. *in situ* generated catalysts. Subsequently, various modifications of the ligand framework at the backbone, the *N*-substituent and the phenolic *ortho-* and *para*-positions and their influence on activity as well as stereoselectivity in the ROP of *rac-β*-BL were studied. *N*-aryl-based salan catalysts were capable of accessing isotactic-enriched PHB (P_m up to 0.67) whereas *N*-alkyl-based derivatives yielded syndiotactic-enriched PHB (P_r up to 0.79). While the innovative high-throughput approach enabled understanding of catalyst design parameters that affect the ROP of *rac-β*-BL, it is not restricted to this particular monomer. The properties of PLA for example are likewise to PHB strongly dependent on its stereomicrostructure and the *in situ* approach might lead to promising results here as well.[22,27] Besides structure-property relationships, the identification of suitable copolymerization catalysts for various combinations of monomers is considerably less time-consuming when the initiators are easily prepared *in situ* and immediately tested. Thus, using this high-throughput approach is highly valuable for spending less time on catalyst synthesis but focusing more on the polymer and material chemistry itself.
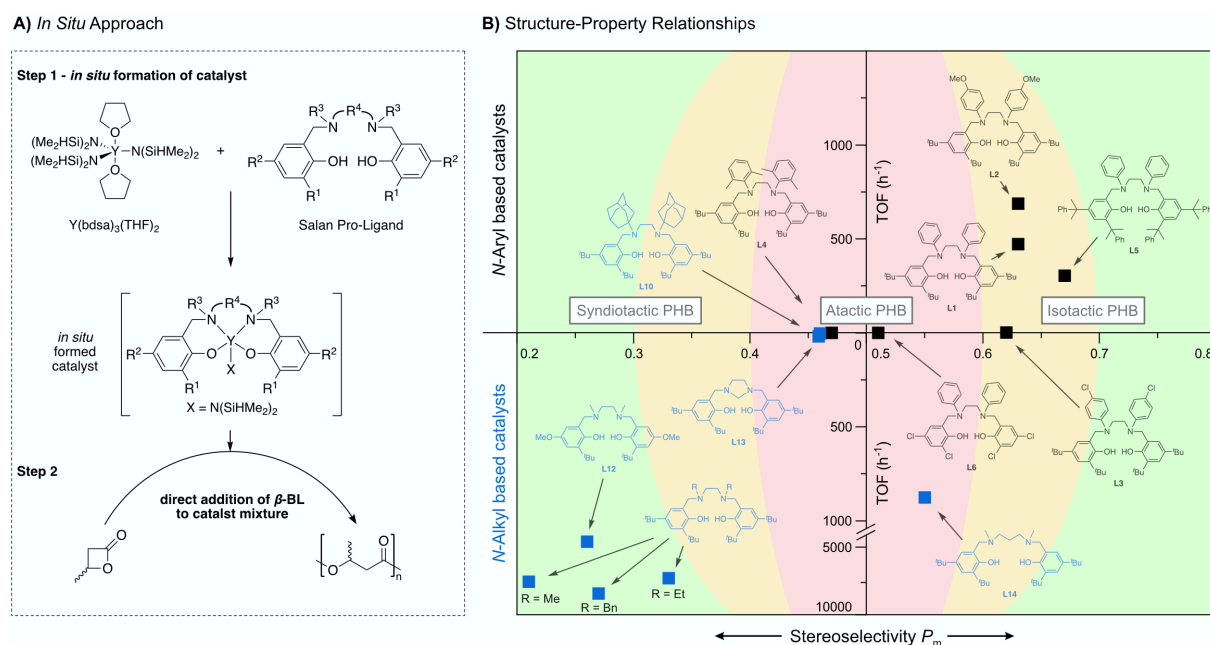
Figure 26. A) Schematic overview of the developed *in situ* approach for the synthesis of yttrium salan catalysts and B) structure-property relationships obtained using this approach in the ROP of *rac-β*-BL. Note: only the ligand framework is shown for clarity.

PHB is also produced naturally by bacteria, however, only in an isotactic microstructure. Bacterial PHB shows promising material properties comparable to *i*-PP but features

biodegradation or chemical recyclability as favorable end-of-life options. Contrary, non-biological syndiotactic and atactic PHB are materials of lower value as the syndiotactic conformation is not biodegradable and in case of atacticity it is an amorphous material with poor characteristics. The synthesis of isotactic PHB starting from a cheap *racemic β*-BL feedstock is thus a highly appealing target.[23,29,64,68] The previously described high-throughput approach facilitated the identification of a novel yttrium salan catalyst platform (Figure 27). While *N*-aryl-based salan initiators were limited to relatively poor isotacticity (P_m up to 0.67), various derivatives bearing an N–H substitution gave highly isotactic PHB (P_m up to 0.89). This represents the highest isoselectivity in ROP of *rac-β*-BL achieved to date. Additionally, the catalysts were remarkably active showing TOFs of up to 32 000 h^{-1} and capable of producing high molecular weight PHB (M_n up to 290 kg mol^{-1}).
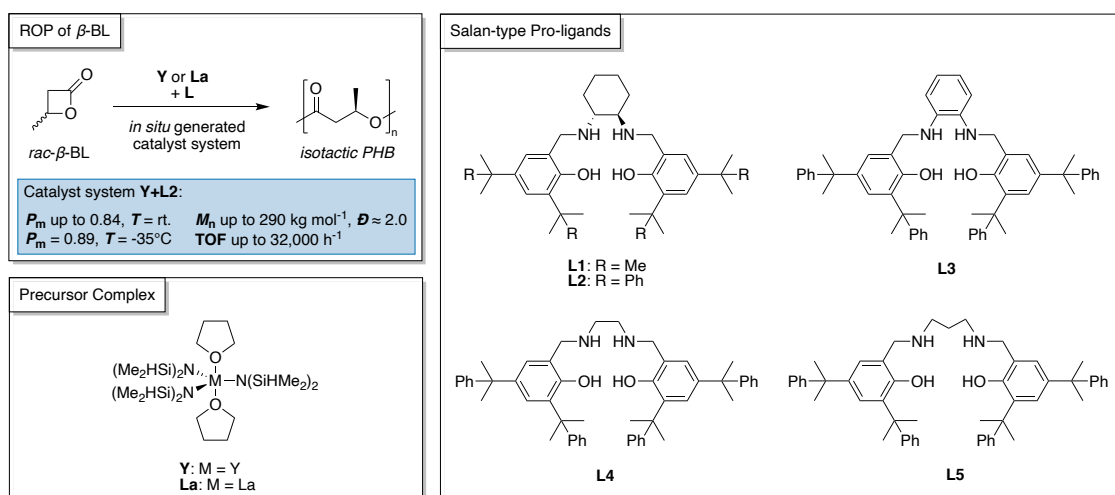
Figure 27. Synthesis of highly isotactic PHB from *rac-β*-BL using yttrium and lanthanum catalysts bearing a salan framework with N–H moieties in the backbone.

The commercialization of bacterial PHB is currently limited by two major challenges: first, the melting temperature of the polymer is close to its decomposition temperature, hampering melt processing and, secondly, its high crystallinity results in a very brittle material.[23,68] The synthetic isotactic PHB produced by *in situ* generated yttrium salan catalysts successfully overcame these challenges: due to its reduced isotacticity, its crystallinity is reduced. This consequently results in a lowered melting temperature ($T_m \approx 140°C$) and significantly increased elongation at break (ε_B = 392%, bacterial PHB: ε_B = 2%). These novel yttrium salan catalysts tackled previous challenges in the ROP of *rac-β*-BL at once, namely high isoselectivity, high productivity and high molecular weight. Combined with the extraordinary polyolefin-like material properties of the generated PHB, this constitutes a major paradigm shift. Early mechanistic studies revealed that the N–H moiety and/or the flexibility of the salan framework might be the reason for the observed isotacticity as respective yttrium salen initiators featuring a rigid imine moiety only gave atactic PHB. Future investigations should focus on

understanding the polymerization mechanism of this class of catalysts in detail as it will allow for the rational design of further isoselective catalysts in the ROP of *rac-β*-BL. Another interesting target constitute salalen catalysts as they combine the salan and salen framework in one ligand.[117,233] This will also allow for further conclusions on the mechanism as one half of the catalyst framework is rigid while the other half remains flexible. Considering the commercialization of synthetic isotactic PHB, heterogenization of the initiators, upscaling of the process and early application tests of the material are important targets in the future.

Apart from efficient production of biodegradable polyesters, ROP is a convenient method for designing innovative monomer–polymer loops in order to achieve a circular polymer chemistry. Chemical recycling of polymers has gained ever-increasing interest as a sustainable solution for the plastic waste issue and in contrast to biodegradation, the intrinsic material value is preserved.[9,19,37] Monomer design plays an important role in accessing chemically recyclable polyesters and the ring-fusion/hybridization approach has previously shown high potential. It was reported that the ROP of bicyclic lactones combines typically conflicting parameters, i.e. polymerizability, depolymerizability and material properties. Bicyclic monomers were previously based on a 5- or 7-membered ring core structure.[37,215] Within this thesis, the strategy of ring-fusion/hybridization was expanded to a bicyclic monomer with 6-membered ring core structure (Figure 28). The monomer NCL was easily accessible via a one-step Baeyer-Villiger oxidation of commercially available norcamphor. It was found that ZnEt$_2$ as low-cost catalyst successfully promotes the ROP of NCL to a high equilibrium monomer conversion even at elevated polymerization temperatures of 110°C. High molecular weight PNCL was obtained (M_n up to 164 kg mol^{-1}). Thermolysis of the material at 220°C selectively and quantitatively recovered pristine monomer, thus closing the monomer–polymer loop. For the first time, a bicyclic lactone with 6-membered ring core structure furnished the synthesis of polyesters with complete chemical recyclability to monomer under thermolysis or chemolysis conditions. The hybridization strategy in monomer design was thus demonstrated to be applicable beyond the typical *γ*-butyrolactone-based core structure. High polymerizability was combined with high depolymerizability, albeit material properties were still somewhat inferior to top-performing chemically recyclable polymers in literature.[215,222] Given the simplicity of this approach, specifically designed monomer modifications will enable various promising NCL-based polymers with targeted properties and full chemical recyclability in the future. ROP of the respective thiolactone derivative might give a material with improved properties yet retained recyclability.[217,219,221,223] Investigating various alkyl substitutions might also give interesting insights into the polymerization and depolymerization behavior as well as material properties of such bicyclic lactones/alicyclic polyesters and contribute to a more detailed understanding of relevant monomer design parameters. ROP as method for the generation of chemically

recyclable polymers besides (bio)degradable polymers reveals the extensive potential of this valuable toolbox.
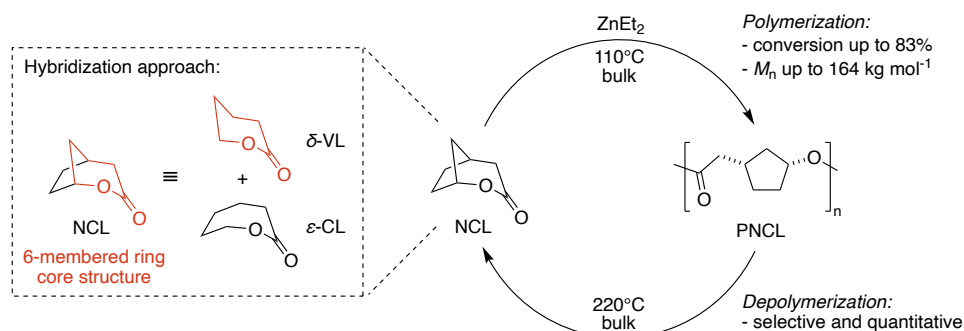
Figure 28. Utilizing the hybridization approach for designing a bicyclic lactone with 6-membered ring core structure that enables the synthesis of completely recyclable polyesters.[251]

This thesis has described specifically designed catalysts and monomers that enable the production of materials with promising properties and sustainable built-in end-of-life options. While the first century of polymer chemistry focused on generating materials and on ever-improving their properties, this work made its contribution to the incipient second century of polymers – a century where degradation or recycling of the material will be as important as its properties.

10 Appendix

10.1 Supporting Information for Chapter 4

Supporting Information

For

Combining High Activity with Broad Monomer Scope: Indium Salan Catalysts in the Ring-Opening Polymerization of Various Cyclic Esters

Jonas Bruckmoser, Daniel Henschel, Sergei Vagin, Bernhard Rieger[*]

WACKER-Chair of Macromolecular Chemistry, Catalysis Research Center
Technical University of Munich
Lichtenbergstraße 4, 85748 Garching bei München, Germany.

[*]Corresponding Author; email: rieger@tum.de

Table of Contents

1. Experimental Section

Materials and Methods

All manipulations were carried out under argon atmosphere using standard Schlenk or glovebox techniques. Glassware was flame-dried under vacuum prior to use. Unless otherwise stated, all chemicals were purchased from Sigma-Aldrich, TCI Chemicals or ABCR and used as received. Solvents were obtained from an MBraun MB-SPS 800 solvent purification system and stored over 3 Å molecular sieves prior to use. β-BL was treated with BaO, dried over CaH_2 and distilled prior to use. ε-CL, ε-DL and γ-BL were distilled from CaH_2 prior to use. *rac*-LA was sublimed once prior to use. Deuterated chloroform ($CDCl_3$) and toluene (C_7D_8) were obtained from Sigma-Aldrich and dried over 3 Å molecular sieves. Proligand **L3** was prepared according to the literature.[1]

Nuclear magnetic resonance (NMR) spectra were recorded on a Bruker AV-III-500 spectrometer equipped with a QNP-Cryoprobe, AV-III-300 or AV-III-400 spectrometers at ambient temperature (298 K). ^{1}H and $^{13}C\{^{1}H\}$ NMR spectroscopic chemical shifts δ are reported in ppm relative to tetramethylsilane and were referenced internally to the relevant residual solvent resonances. The following abbreviations are used: br, broad; s, singlet; d, doublet; m, multiplet.

The tacticity of PHB was determined by integration of the carbonyl region of the $^{13}C\{^{1}H\}$ NMR spectrum whereas for PLA, the tacticity was calculated from the peak deconvoluted methine region of the $^{1}H\{^{1}H\}$ NMR spectrum.[2, 3]

Elemental analyses were measured with a EURO EA instrument from HEKAtech at the Laboratory for Microanalysis, Catalysis Research Center, Technical University of Munich.

Electrospray ionization mass spectrometry (ESI-MS) was measured with a Thermo Fisher Scientific Exactive Plus Orbitrap in the positive mode in acetonitrile.

Polymer weight-average molecular weight (M_w), number-average molecular weight (M_n) and polydispersity indices ($Đ = M_w/M_n$) were determined *via* gel permeation chromatography (GPC) relative to polystyrene standards on PL-SEC 50 Plus instruments from Polymer Laboratories. For PHB the analysis was performed at ambient temperatures using chloroform as the eluent at a flow rate of 1.0 mL min^{-1}. For PεCL, PεDL, PLA and PγBL the analysis was performed at

S2

40°C using THF as the eluent at a flow rate of 1.0 mL min^{-1}. Molecular weights of PεCL and PLA were corrected with a Mark–Houwink factor of 0.56 and 0.58, respectively.[4]

General Polymerization Procedures

Typical polymerization of β-BL: In a glove box, initiator **2** (13.0 mg, 18.3 μmol) was dissolved in 1.55 mL of toluene and β-BL (300 μL, 315 mg, 3.66 mmol) was injected into the reaction, such that the overall concentration of β-BL was 2.0 M. After 15 min the polymerization was quenched by addition of 0.5 mL MeOH and conversion was determined by ^{1}H NMR spectroscopy of an aliquot. The mixture was precipitated into excess diethyl ether/pentane (1:1), filtered, washed with additional diethyl ether/pentane and dried under vacuum.

Typical immortal ROP of β-BL: In a glove box, initiator **2** was dissolved in toluene and the respective amount of a BnOH stock solution in toluene (0.080 M) was added. After 15 min of stirring, β-BL was injected into the reaction, such that the overall concentration of β-BL was 2.0 M. The rest of the procedure followed the general polymerization procedure.

Kinetic experiments of β-BL polymerization: In a glove box, the respective amount of initiator **2**, toluene and β-BL were mixed, such that the overall concentration of β-BL was 2.0 M. After certain time intervals, aliquots were taken from the reaction mixture, quenched with 0.4 mL hydrous CDCl$_3$ and conversion determined by ^{1}H NMR spectroscopy. The crude products were additionally analyzed by GPC.

Polymerization of β-BL with PO-activated **1**: In a glove box, initiator **1** (10.0 mg, 14.9 μmol) was dissolved in 1.24 mL of propylene oxide (PO) and the mixture stirred for 24 h at room temperature. After this preactivation time, β-BL (244 μL, 256 mg, 2.97 mmol) was injected into the reaction, such that the overall concentration of β-BL was 2.0 M. After certain time intervals, aliquots were taken from the reaction mixture, quenched with 0.4 mL hydrous CDCl$_3$ and conversion determined by ^{1}H NMR spectroscopy. The polymerization was quenched by addition of 0.5 mL MeOH, precipitated into excess diethyl ether/pentane (1:1), filtered, washed with additional diethyl ether/pentane and dried under vacuum. The isolated polymer and crude products were analyzed by GPC.

Typical polymerization of ε-CL: In a glove box, initiator **2** (4.0 mg, 5.6 μmol) was dissolved in 1.09 mL of toluene and ε-CL (312 μL, 321 mg, 2.81 mmol) was rapidly injected into the reaction, such that the overall concentration of ε-CL was 2.0 M. After 20 s the polymerization was quenched by rapid addition of 1.0 mL hydrous CDCl$_3$ and conversion was determined by

^{1}H NMR spectroscopy of an aliquot. The mixture was precipitated into excess methanol, filtered, washed with additional methanol and dried under vacuum.

Typical polymerization of ε-DL: In a glove box, initiator **2** (5.0 mg, 7.0 μmol) was dissolved in 0.46 mL of toluene and ε-DL (245 μL, 240 mg, 1.41 mmol) was injected into the reaction, such that the overall concentration of ε-DL was 2.0 M. After 2 h the polymerization was quenched by addition of 0.2 mL MeOH and conversion was determined by ^{1}H NMR spectroscopy of an aliquot. The mixture was precipitated into excess methanol, filtered, washed with additional methanol and dried under vacuum.

Typical polymerization of γ-BL: In a glove box, γ-BL (107 μL, 121 mg, 1.41 mmol) was added to initiator **2** (5.0 mg, 7.0 μmol) and the reaction mixture cooled to -35°C. After 24 h at -35°C the polymerization was quenched by addition of a cold solution of 1.0 mL benzoic acid in CHCl$_3$ (10 mg mL^{-1}) and conversion was determined by ^{1}H NMR spectroscopy of an aliquot. The mixture was precipitated into excess cold methanol, filtered and dried under vacuum.

Typical polymerization of purified *rac*-LA: In a glove box, sublimed *rac*-LA (406 mg, 2.81 mmol) was added to initiator **2** (4.0 mg, 5.6 μmol). The vial was sealed, removed from the glove box and placed in a preheated aluminum block at 130°C. After 10 min the polymerization was quenched by addition of 0.2 mL MeOH and conversion was determined by ^{1}H NMR spectroscopy of an aliquot. The mixture was dissolved in a minimal amount of dichloromethane and precipitated into excess pentane, filtered, washed with additional pentane and dried under vacuum.

Polymerization of unpurified *rac*-LA: The polymerization procedure was as described above but commercial grade *rac*-LA (99%, Sigma-Aldrich) was used as received instead of sublimed *rac*-LA.

Polymerization of unpurified *L*-LA: The polymerization procedure was as described above but commercial grade *L*-LA (98%, Sigma-Aldrich) was used as received instead of sublimed *rac*-LA.

Synthesis of Compounds
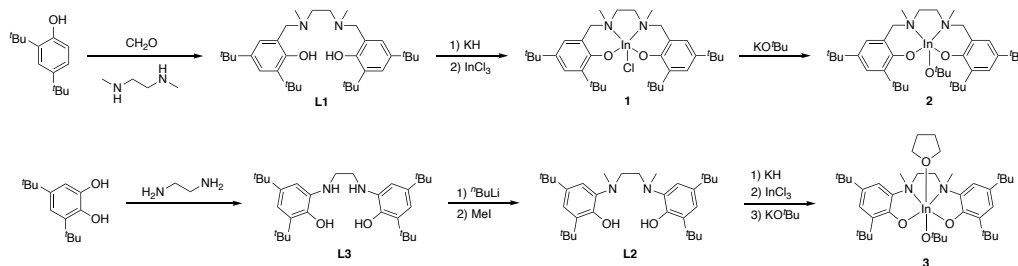
Scheme S1. Synthesis of indium complexes **1 – 3**. Complex **2** can also be prepared in a one-pot route starting from ligand **L1** (not shown).

Synthesis of Salan Ligand L1.

The synthesis followed a reported literature procedure.[5] 2,4-di-*tert*-butylphenol (8.25 g, 40.0 mmol) was dissolved in 20 mL of methanol and 15 mL aqueous formaldehyde solution (37 wt.%) and *N,N'*-dimethylethylenediamine (2.15 mL, 1.76 g, 20.0 mmol) were added. The reaction mixture was refluxed for 16 h. After cooling to room temperature, the colorless precipitate was filtered off, washed with 30 mL of methanol and dried *in vacuo* to give 9.09 g (87%) of **L1**.

^{1}H NMR (400 MHz, CDCl$_3$): δ 10.68 (br s, 2H, OH), 7.20 (d, J = 2.4 Hz, 2H, Ar-H), 6.80 (d, J = 2.4 Hz, 2H, Ar-H), 3.66 (s, 4H, Ar-CH$_2$), 2.63 (s, 4H, N-CH$_2$), 2.26 (s, 6H, N-Me), 1.40 (s, 18H, ^{t}Bu), 1.27 (s, 18H, ^{t}Bu). ^{13}C{^{1}H} NMR (101 MHz, CDCl$_3$): δ 154.3, 140.7, 135.8, 123.5, 123.1, 121.1, 62.9, 53.9, 41.8, 35.0, 34.3, 31.9, 29.8.

Synthesis of Catam Ligand L2.

The synthesis followed a reported literature procedure.[6] A solution of **L3** (1.87 g, 4.0 mmol) in 25 mL of THF was cooled to -78°C and *n*-butyllithium (2.5 M in hexane, 3.20 mL, 0.51 g, 8.0 mmol) was added dropwise. After stirring at -78°C for 15 min, the reaction mixture was allowed to warm to room temperature and stirred for an additional 2 h. Subsequently, methyl iodide (0.50 mL, 1.14 g, 8.0 mmol) was added, the solution stirred for 16 h at room temperature and then refluxed for an additional 5 h. The solvent was removed under reduced pressure, water (25 mL) added and the mixture extracted with dichloromethane (3×20 mL). The combined organic phases were washed with brine (20 mL), dried over MgSO$_4$ and the solvent removed under reduced pressure. The residue was recrystallized from methanol/dichloromethane (2:1) to give an off-white solid (1.37 g, 69%).

S5

^{1}H NMR (400 MHz, CDCl$_3$): δ 8.37 (br s, 2H, OH), 7.13 (d, J = 2.4 Hz, 2H, Ar-H), 7.07 (d, J = 2.4 Hz, 2H, Ar-H), 2.87 (s, 4H, N-CH$_2$), 2.73 (s, 6H, N-Me), 1.42 (s, 18H, ^{t}Bu), 1.30 (s, 18H, ^{t}Bu). ^{13}C{^{1}H} NMR (101 MHz, CDCl$_3$): δ 148.6, 141.1, 138.6, 135.1, 120.7, 115.6, 57.1, 43.1, 35.2, 34.7, 31.9, 29.7.

Synthesis of Indium Complexes 1 – 3

Compound 1. The synthesis followed a reported literature procedure.[7] To a suspension of KH (0.24 g, 6.0 mmol) in 10 mL of THF, a solution of **L1** (1.57 g, 3.0 mmol) in 10 mL of THF was added dropwise. The resulting solution was stirred for 20 h at room temperature and then cooled to -78°C. A solution of InCl$_3$ (0.66 g, 3.0 mmol) in 10 mL of THF was added dropwise and after complete addition the reaction mixture was allowed to slowly warm to room temperature within 2 h and was then stirred for one additional hour. The reaction mixture was evaporated to dryness, the residue resuspended in 20 mL of dichloromethane, filtered over Celite and the solvent removed *in vacuo*. After washing with 5 mL of pentane, a colorless solid was obtained (1.45 g, 72%).

^{1}H NMR (400 MHz, CDCl$_3$): δ 7.30 (d, J = 2.5 Hz, 2H, Ar-H), 6.79 (d, J = 2.5 Hz, 2H, Ar-H), 4.84 (d, J = 12.0 Hz, 2H, Ar-CH$_2$), 3.28 – 3.17 (m, 4H, Ar-CH$_2$ and N-CH$_2$), 2.99 – 2.89 (m, 2H, N-CH$_2$), 2.42 (s, 6H, N-Me), 1.50 (s, 18H, ^{t}Bu), 1.27 (s, 18H, ^{t}Bu). ^{13}C{^{1}H} NMR (101 MHz, CDCl$_3$): δ 160.5, 139.9, 138.2, 125.3, 125.1, 119.9, 64.2, 55.6, 44.0, 35.4, 34.2, 31.9, 30.0. Anal. Calc. for C$_{34}$H$_{54}$N$_2$O$_2$ClIn: C, 60.67; H, 8.09; N, 4.16. Found: C, 61.21; H, 8.32; N, 4.16%.

Characterization data for compound **1** after being stored under air at room temperature for 3 months: ^{1}H NMR data as stated above; no decomposition was observed (Figure S7, S8). Anal. Calc. for C$_{34}$H$_{54}$N$_2$O$_2$ClIn: C, 60.67; H, 8.09; N, 4.16. Found: C, 61.41; H, 8.30; N, 4.17%. Hydrolytic stability tests of compound **1** in solution: ca. 10 mg of **1** were dissolved in 0.5 ml hydrous CDCl$_3$ (water content: 110 ppm) and ^{1}H NMR spectra of the sample measured in regular intervals. Signals corresponding to free salan ligand **L1** were increasing steadily and after 20 h at room temperature 31% of **1** was decomposed (Figure S9).

Compound 2. KO^{t}Bu (67 mg, 0.6 mmol) was added to a solution of **1** (404 mg, 0.6 mmol) in 10 mL of THF. The resulting suspension was stirred for 16 h at room temperature, subsequently

S6

filtered using a 0.45 μm PTFE syringe filter and the solvent removed *in vacuo*. The residue was washed with pentane (2×2 mL) to give a colorless solid (315 mg, 74%). Single crystals of **2** suitable for X-ray diffraction measurements were obtained by slow evaporation from a saturated toluene solution at room temperature.

^{1}H NMR (400 MHz, CDCl$_3$): δ 7.27 (d, *J* = 2.6 Hz, 2H, Ar-H), 6.74 (d, *J* = 2.6 Hz, 2H, Ar-H), 4.49 (d, *J* = 12.1 Hz, 2H, Ar-CH$_2$), 3.24 (d, *J* = 12.3 Hz, 2H, Ar-CH$_2$), 3.06 – 2.97 (m, 2H, N-CH$_2$), 2.90 – 2.81 (m, 2H, N-CH$_2$), 2.51 (s, 6H, N-Me), 1.45 (s, 18H, Ar-*t*Bu), 1.27 (s, 18H, Ar-*t*Bu), 1.24 (s, 9H, O-*t*Bu). ^{13}C{^{1}H} NMR (101 MHz, CDCl$_3$): δ 161.6, 139.1, 136.8, 125.3, 124.6, 119.4, 63.8, 55.1, 44.0, 35.5, 35.4, 34.1, 31.9, 31.9, 30.2. Anal. Calc. for C$_{38}$H$_{63}$N$_2$O$_3$In: C, 64.22; H, 8.93; N, 3.94. Found: C, 64.33; H, 9.06; N, 3.82%.

Compound 2 – One-Pot-Route. To a suspension of KH (160 mg, 4.0 mmol) in 7 mL of THF, a solution of **L1** (1050 mg, 2.0 mmol) in 8 mL of THF was added dropwise. The resulting solution was stirred for 17 h at room temperature and then cooled to -78°C. A solution of InCl$_3$ (442 mg, 2.0 mmol) in 10 mL of THF was added dropwise and after complete addition the reaction mixture was allowed to slowly warm to room temperature within 2 h and was then stirred for an additional 2 h. Subsequently, KO*t*Bu (224 mg, 2.0 mmol) was added to the reaction mixture and stirring continued for 23 h at room temperature. After filtration using a 0.45 μm PTFE syringe filter, removal of volatiles *in vacuo* and washing the residue with pentane (2×5 mL) a colorless solid was obtained (909 mg, 64%).

^{1}H and ^{13}C{^{1}H} NMR data as stated above. Anal. Calc. for C$_{38}$H$_{63}$N$_2$O$_3$In: C, 64.22; H, 8.93; N, 3.94. Found: C, 63.99; H, 9.04; N, 3.96%.

Compound 3. To a suspension of KH (64 mg, 1.6 mmol) in 3 mL of THF, a solution of **L2** (397 mg, 0.8 mmol) in 4 mL of THF was added dropwise. The resulting solution was stirred for 16 h at room temperature and then cooled to -78°C. A solution of InCl$_3$ (177 mg, 0.8 mmol) in 5 mL of THF was added dropwise and after complete addition the reaction mixture was allowed to slowly warm to room temperature within 2 h and was then stirred for an additional 2 h. Subsequently, KO*t*Bu (90 mg, 0.8 mmol) was added to the reaction mixture and stirring continued for 21 h at room temperature. The cloudy solution was filtered using a 0.45 μm PTFE syringe filter and the solvent removed *in vacuo*. Recrystallization from pentane and additional washing with a minimal amount of cold pentane gave **3** as a colorless solid (193 mg, 32%). Multiple attempts for the isolation of single crystals of **3** suitable for X-ray diffraction measurements were unsuccessful.

S7

^{1}H NMR (400 MHz, C$_7$D$_8$): δ 7.42 (d, J = 2.5 Hz, 2H, Ar-H), 6.94 (d, J = 2.5 Hz, 2H, Ar-H), 3.93 – 3.83 (m, 4H, THF), 2.71 (s, 6H, N-Me), 2.48 (d, J = 10.1 Hz, 2H, N-CH$_2$), 2.00 (d, J = 10.1 Hz, 2H, N-CH$_2$), 1.77 (s, 18H, Ar-^{t}Bu), 1.46 (s, 9H, O-^{t}Bu), 1.34 (s, 18H, Ar-^{t}Bu), 1.30 – 1.26 (m, 4H, THF). ^{13}C{^{1}H} NMR (101 MHz, C$_7$D$_8$): δ 157.7, 138.2, 136.1, 134.8, 122.3, 114.5, 69.8, 69.0, 58.3, 46.2, 35.9, 35.4, 34.5, 32.0, 30.0, 25.3. Anal. Calc. for C$_{40}$H$_{67}$N$_2$O$_4$In: C, 63.65; H, 8.95; N, 3.71. Found: C, 63.49; H, 9.16; N, 3.72%.

S8

NMR Spectra of Compounds
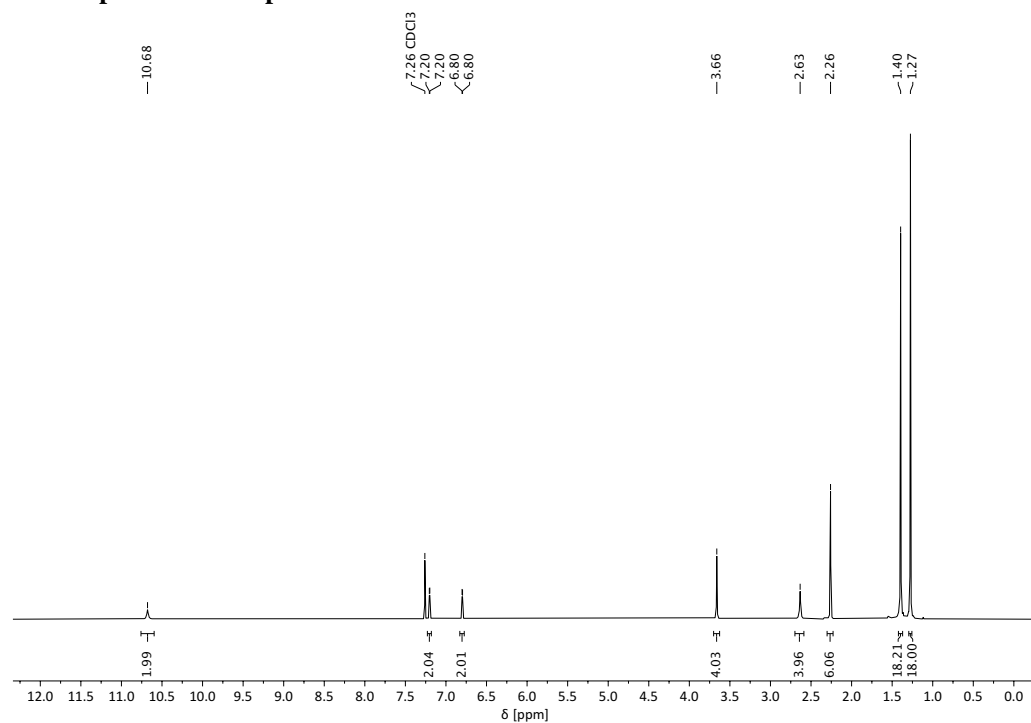
Figure S1. ¹H NMR spectrum (CDCl₃) of salan ligand **L1**.

Figure S2. ¹³C{¹H} NMR spectrum (CDCl₃) of salan ligand **L1**.

S9
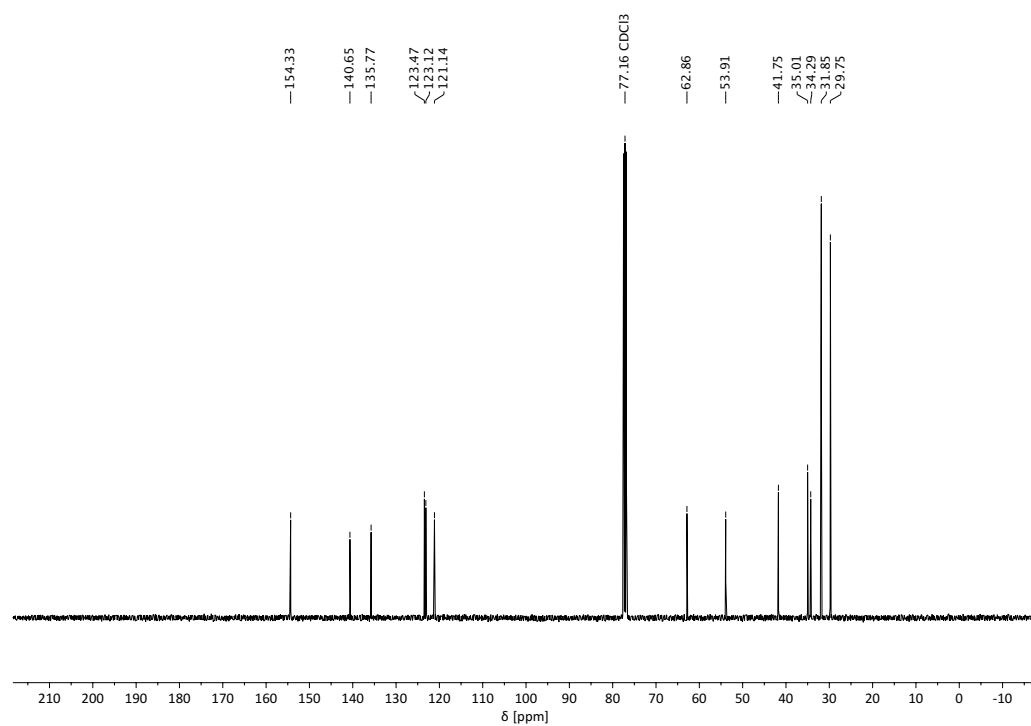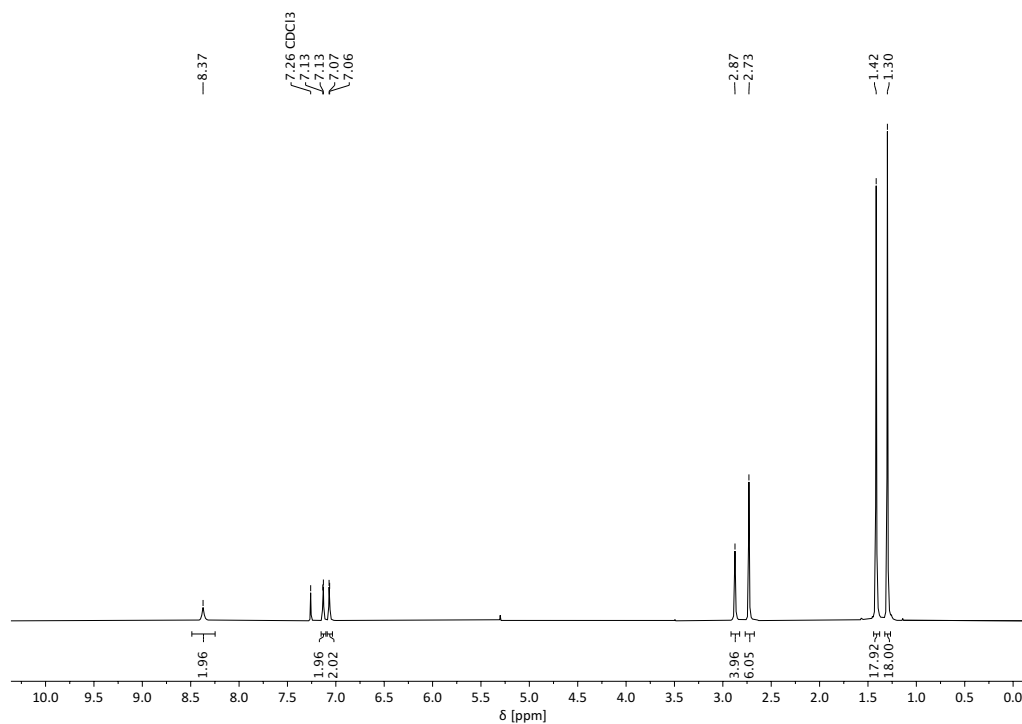
Figure S3. ^{1}H NMR spectrum (CDCl$_3$) of catam ligand **L2**.

Figure S4. ^{13}C{^{1}H} NMR spectrum (CDCl$_3$) of catam ligand **L2**.

S10
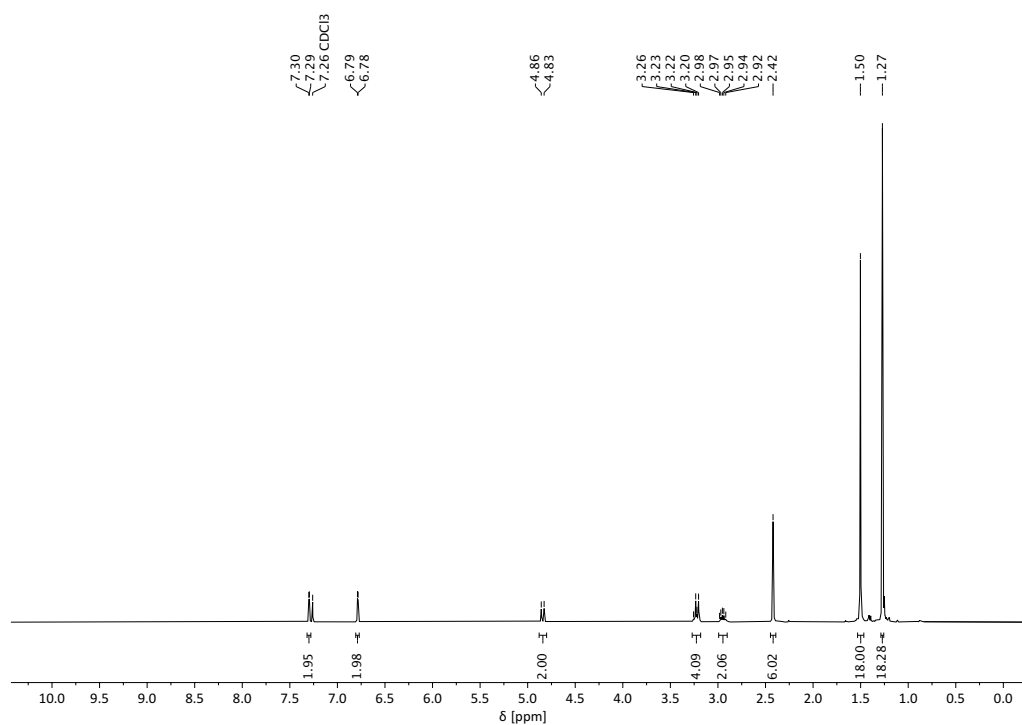
7.30
7.29
7.26 CDCl3
6.79
6.78
4.86
4.83
3.26
3.23
3.22
3.20
2.98
2.97
2.95
2.94
2.92
2.42
1.50
1.27

1.95
1.98
2.00
4.09
2.06
6.02
18.00
18.28

10.0 9.5 9.0 8.5 8.0 7.5 7.0 6.5 6.0 5.5 5.0 4.5 4.0 3.5 3.0 2.5 2.0 1.5 1.0 0.5 0.0
δ [ppm]

Figure S5. ^{1}H NMR spectrum (CDCl$_3$) of indium complex **1**.

160.51
139.88
138.24
125.26
125.12
119.94
77.16 CDCl3
64.16
55.58
44.00
35.44
34.16
31.93
30.04

210 200 190 180 170 160 150 140 130 120 110 100 90 80 70 60 50 40 30 20 10 0 -10
δ [ppm]
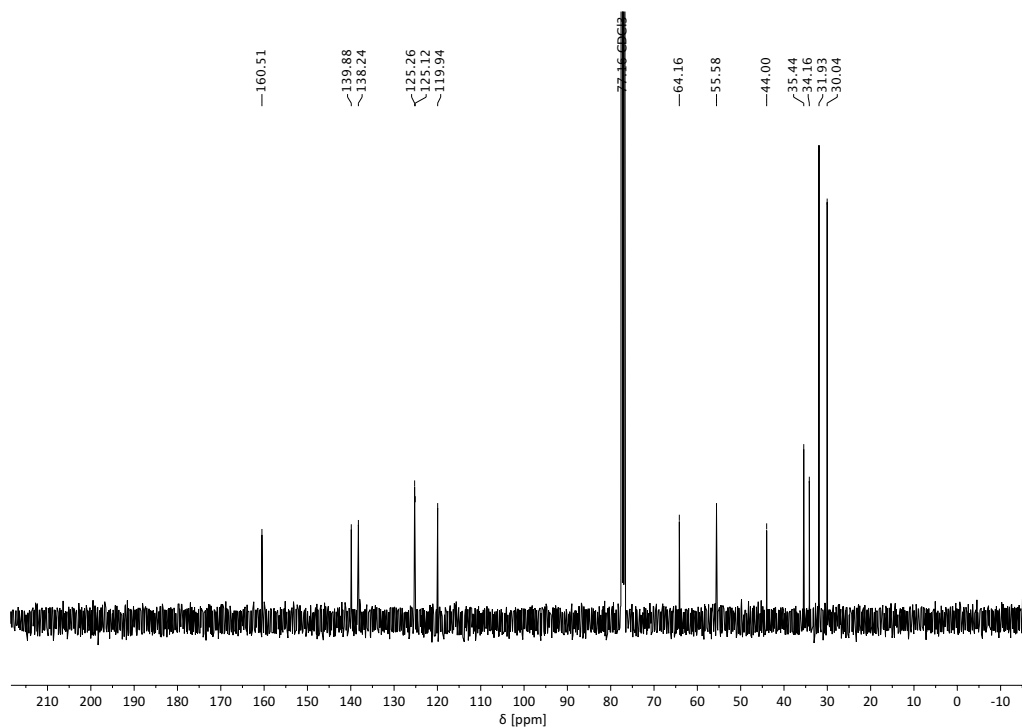
Figure S6. ^{13}C{^{1}H} NMR spectrum (CDCl$_3$) of indium complex **1**.

S11
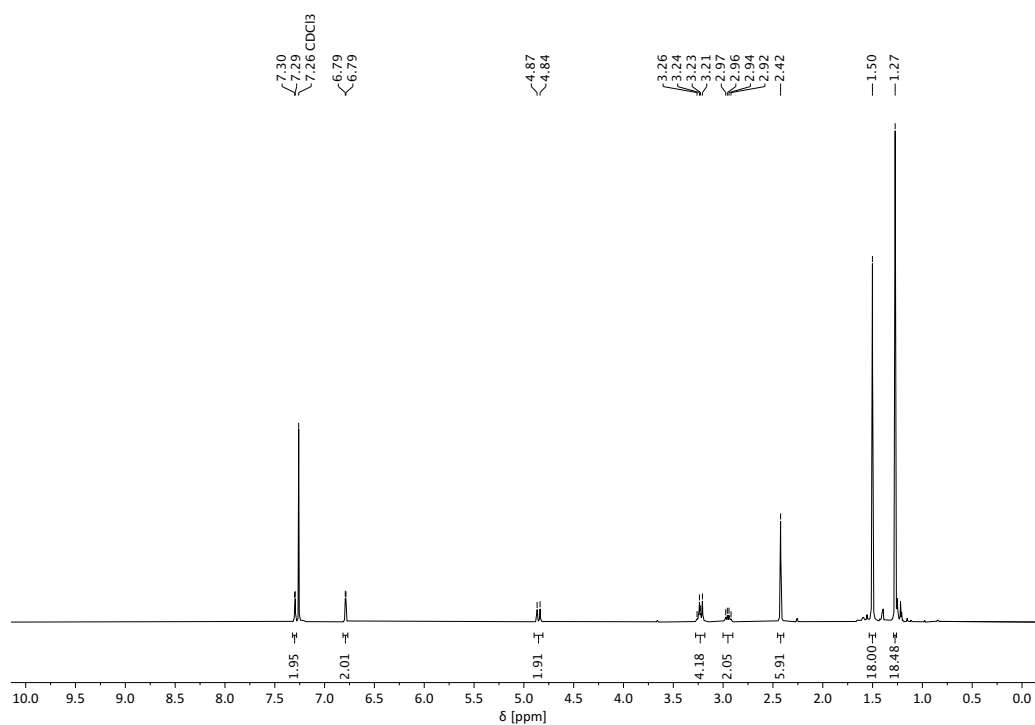
Figure S7. ^{1}H NMR spectrum (CDCl$_3$) of indium complex **1** stored under air at room temperature for 3 months.
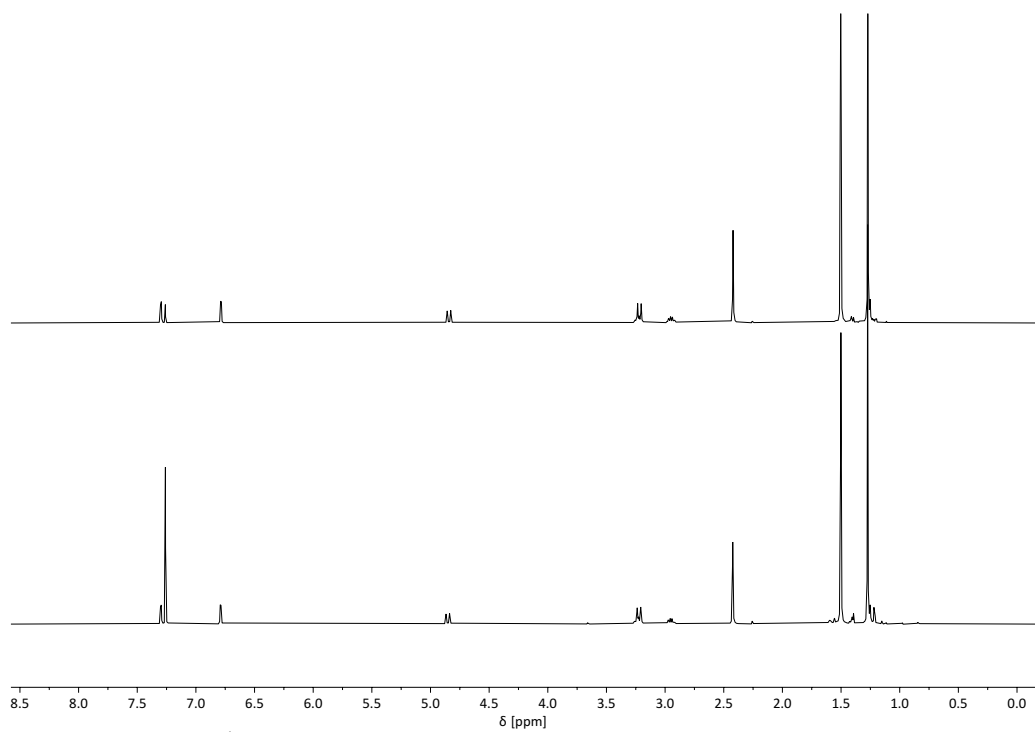
Figure S8. Comparison of ^{1}H NMR spectra (CDCl$_3$) of indium complex **1** stored under argon (top) and stored under air (bottom) at room temperature for 3 months.

S12
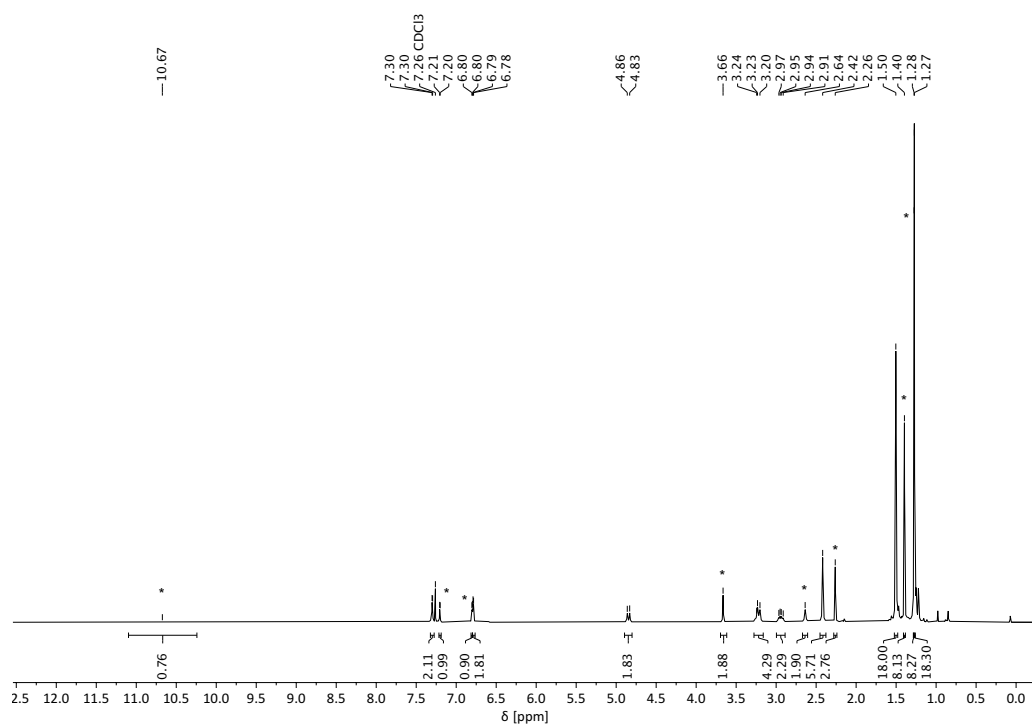
Figure S9. ^{1}H NMR spectrum (CDCl$_3$) of indium complex **1** after 20 h at room temperature in 0.5 ml hydrous CDCl$_3$ (water content: 110 ppm). Signals denoted with an asterisk belong to free salan ligand **L1**.
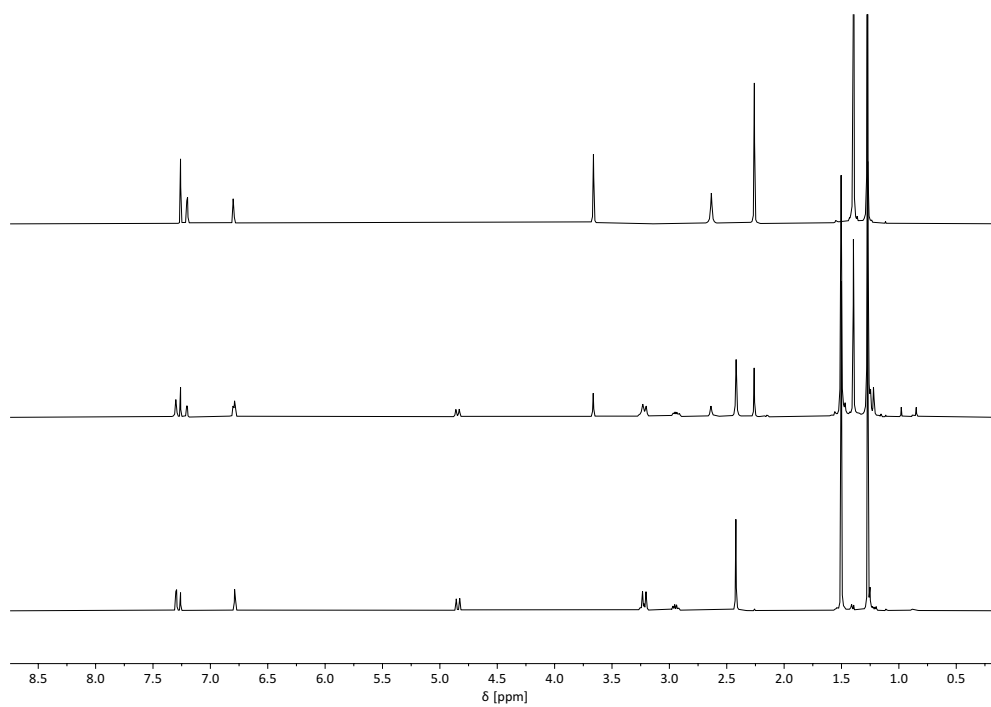
Figure S10. Comparison of ^{1}H NMR spectra (CDCl$_3$) of i) salan ligand **L1** (top), ii) indium complex **1** after 20 h at room temperature in 0.5 ml hydrous CDCl$_3$ (water content: 110 ppm) (middle), iii) indium complex **1** in dry CDCl$_3$ (bottom).

S13
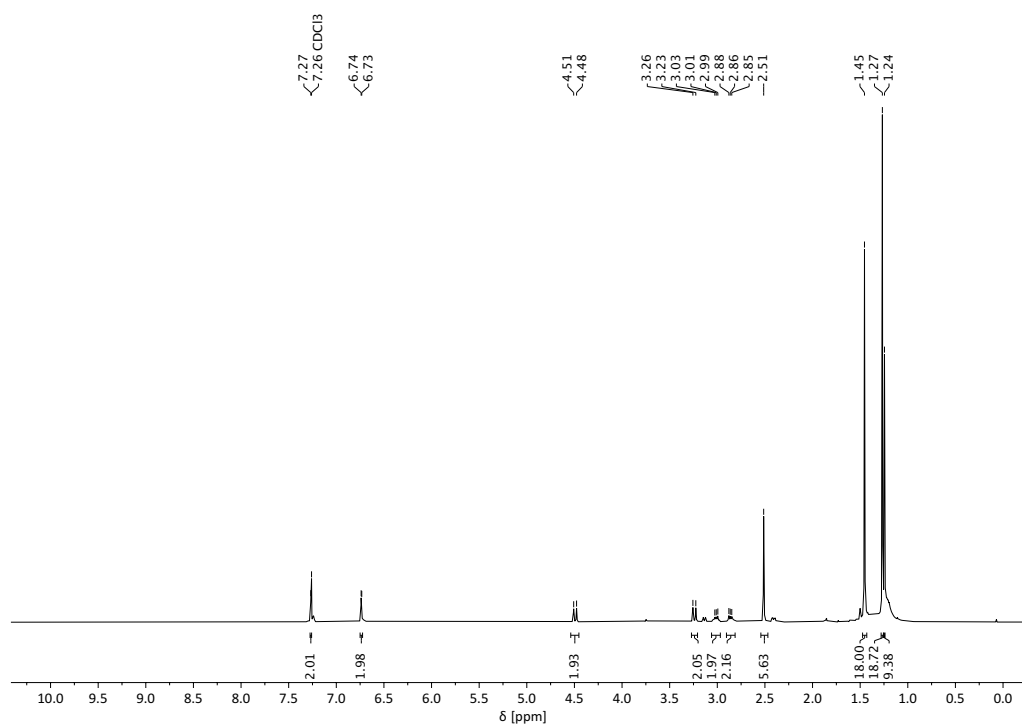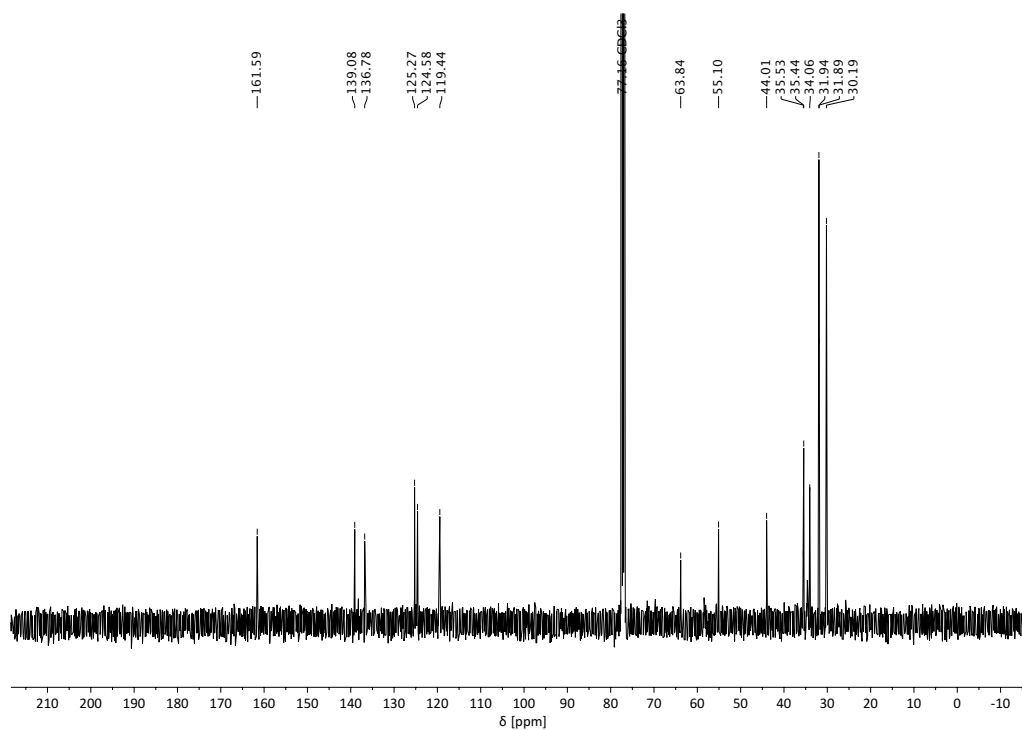
Figure S11. ^{1}H NMR spectrum (CDCl$_3$) of indium complex **2**.

Figure S12. ^{13}C{^{1}H} NMR spectrum (CDCl$_3$) of indium complex **2**.

S14
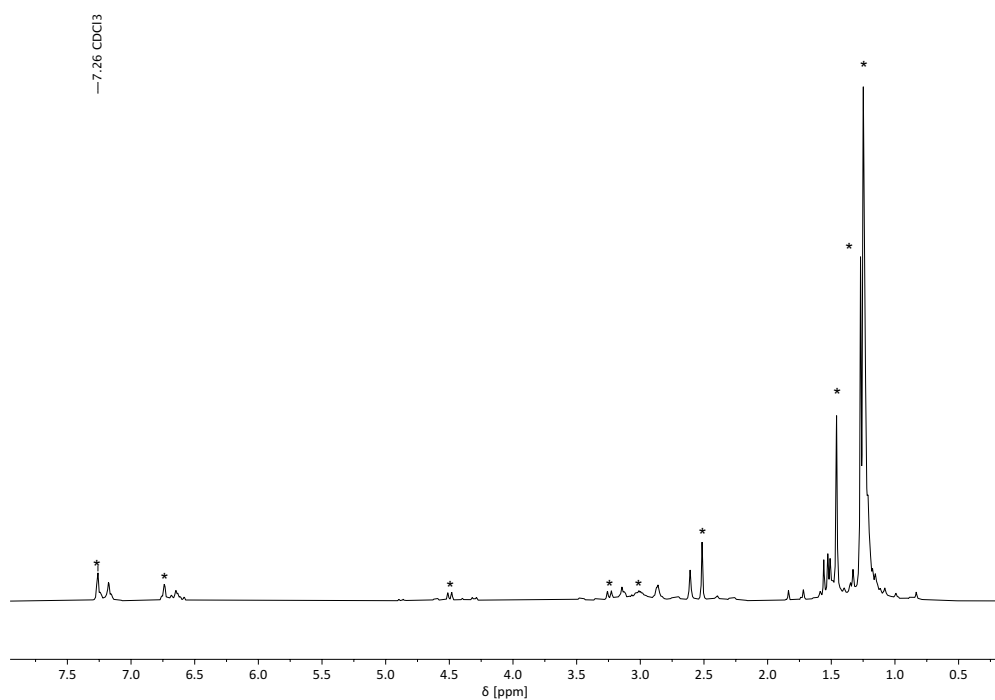
Figure S13. ^{1}H NMR spectrum (CDCl$_3$) of indium complex **2** stored under air at room temperature for 24 h. Signals denoted with an asterisk belong to complex **2**.
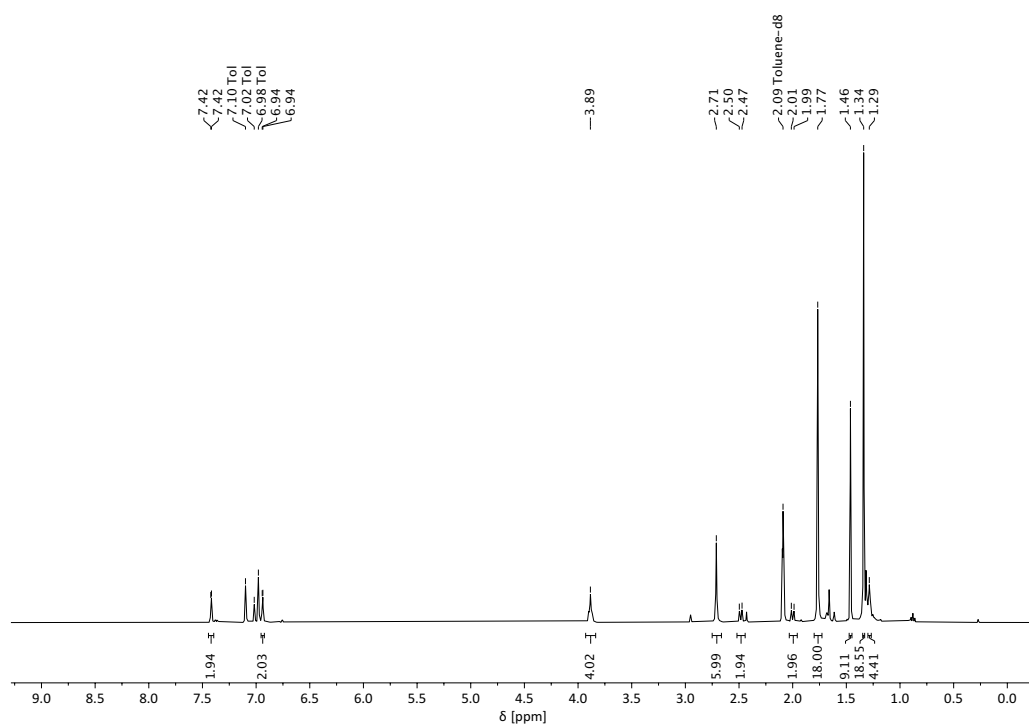
Figure S14. ^{1}H NMR spectrum (C$_7$D$_8$) of indium complex **3**.

S15

Figure S15. $^{13}C\{^1H\}$ NMR spectrum (C_7D_8) of indium complex **3**.

S16
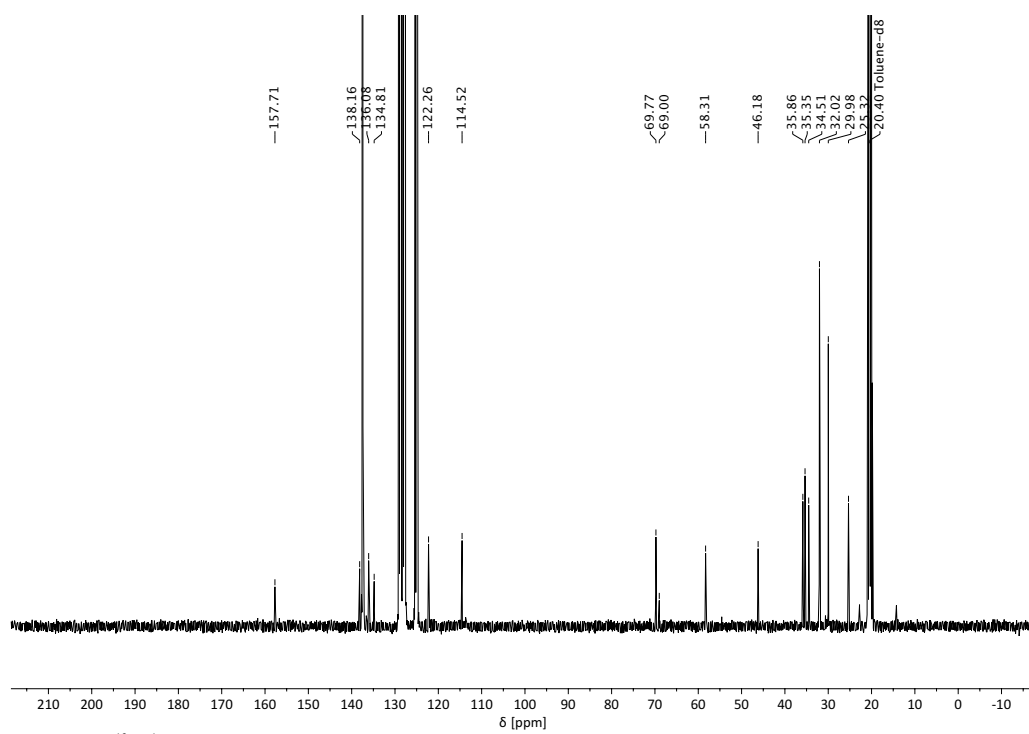
2. Polymerization Kinetics and Polymer Characterization Data

Table S1. Additional polymerization data [a]

entry	catalyst	monomer	[M]/[I]	time (min)	conv.[b] (%)	TOF (h^{-1})	M_n (theo.)[c] (kg mol^{-1})	M_n (GPC)[d] (kg mol^{-1})	$Đ$[d]
1	**1**	β-BL	200	1440	3	<1	n.d.	n.d.	n.d.
2[e]	**1**	β-BL	200	1440	63	5	10.8	32.5	1.39
3[f]	**1**	β-BL	200	60	0	0	n.d.	n.d.	n.d.
4[g]	**1**	β-BL	200	120	0	0	n.d.	n.d.	n.d.
5[h]	**2**	β-BL	200	30	97	388	16.7	26.7	1.07
6[i]	**2**	β-BL	200	30	73	292	12.6	18.5	1.05
7	**2**	β-BL	100	7	96	823	8.3	13.9	1.05
8	**2**	β-BL	150	10	96	864	12.4	19.9	1.04
9	**2**	β-BL	300	30	98	588	25.3	38.1	1.04
10	**2**	β-BL	400	15	82	1312	28.2	35.3	1.04
11	**2**	β-BL	800	60	60	480	41.3	56.5	1.05
12	**2**	β-BL	800	240	95	190	65.4	91.9	1.05

[a]Polymerizations were performed in toluene at room temperature, [β-BL] = 2.0 M. n.d. = not determined. [b]Conversion determined by ^{1}H NMR spectroscopy. [c]Theoretical molecular weights were determined from the [M]/[I] ratio and monomer conversion data. [d]Determined by GPC in CHCl$_3$ at room temperature relative to polystyrene standards. [e]T = 50°C. [f]Propylene oxide (PO) used as solvent. Preactivation time of catalyst in PO prior to monomer addition was 15 min. [g]10 equiv PO added. Preactivation time of catalyst prior to monomer addition was 24 h. [h]THF used as solvent. [i]CH$_2$Cl$_2$ used as solvent.
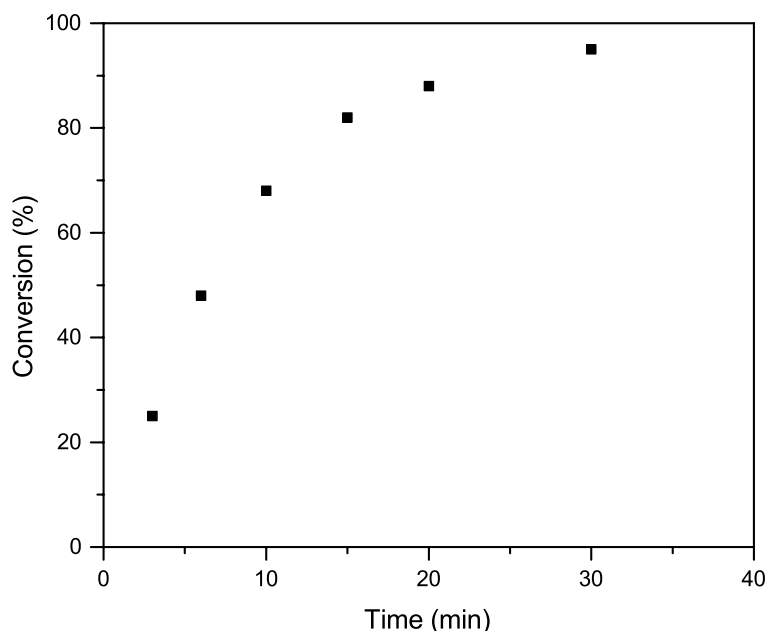
Figure S16. Conversion vs time plot for the ROP of β-BL using **2** as catalyst ([β-BL]/[**2**] = 400/1, T = rt., [β-BL] = 2.0 M).
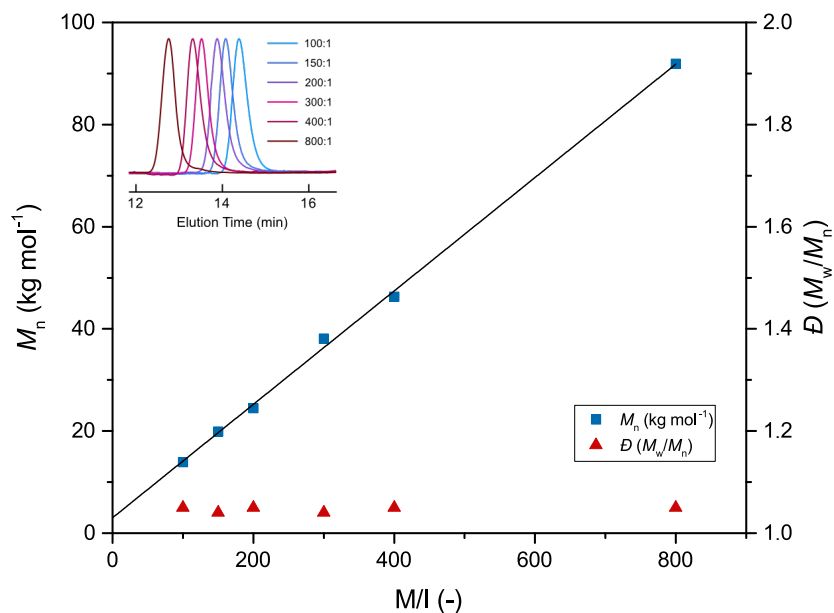
Figure S17. Plot of molecular weight and dispersity vs monomer-to-initiator ratio for the ROP of β-BL mediated by catalyst **2**. Inset: GPC traces of the polymers for different monomer-to-initiator ratios.
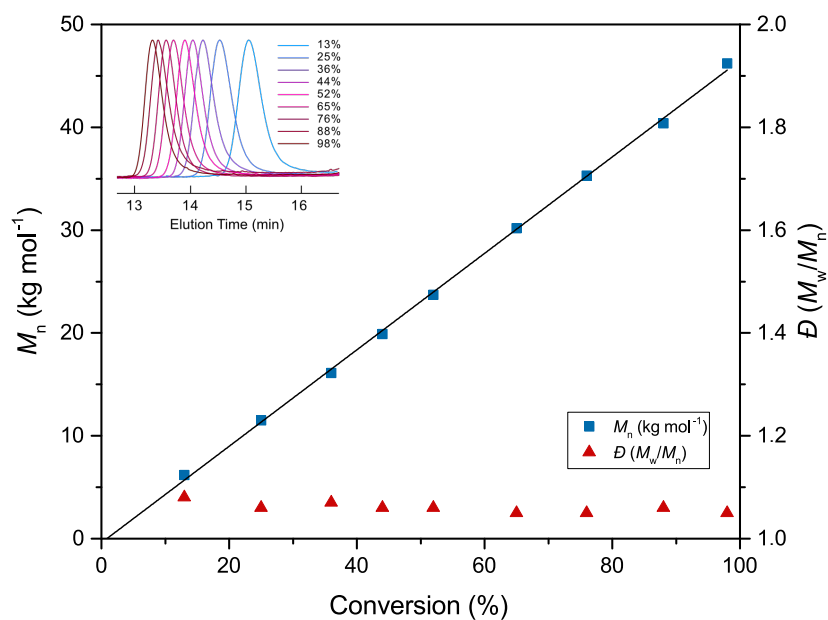
Figure S18. Evolution of molecular weight and dispersity with conversion for the ROP of β-BL mediated by catalyst **2**. Inset: GPC traces of the polymers at respective conversions.

S18
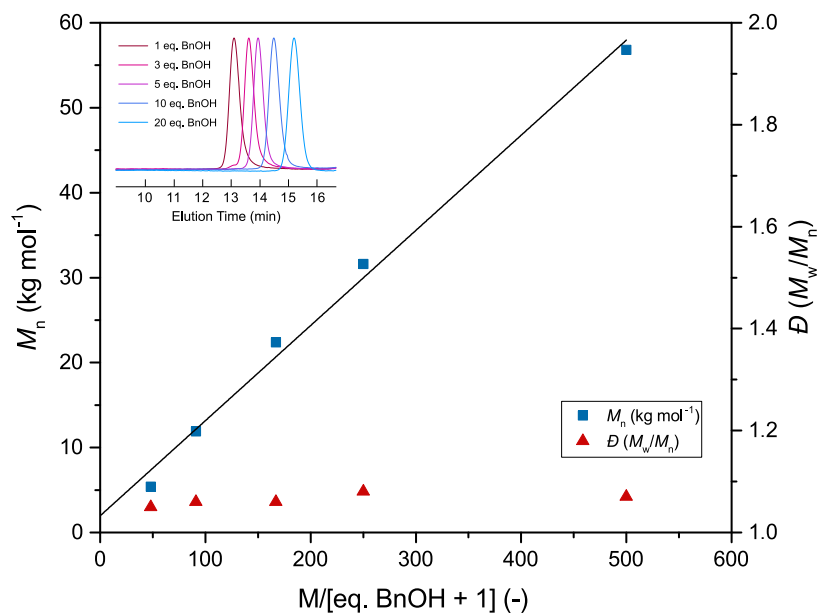
Figure S19. Immortal ROP of β-BL using catalyst **2** and BnOH as chain transfer agent. Plot of molecular weight and dispersity vs monomer-to-(BnOH + 1) ratio. Inset: GPC traces of the polymers with various amounts of chain transfer agent used in the ROP of β-BL.
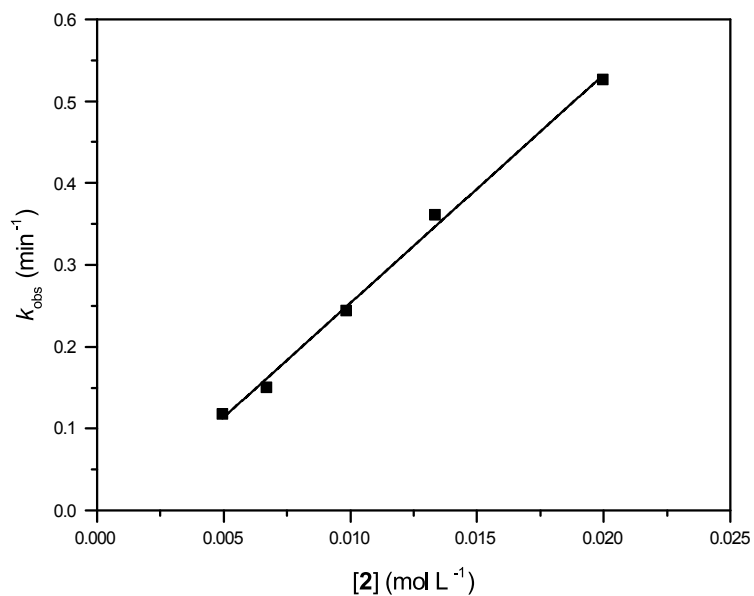
Figure S20. Plot of k_{obs} vs [**2**] for determination of propagation rate constant k_p. $k_p = 27.9 \pm 0.9$ L mol^{-1} min^{-1}, $R^2 = 0.997$.

S19
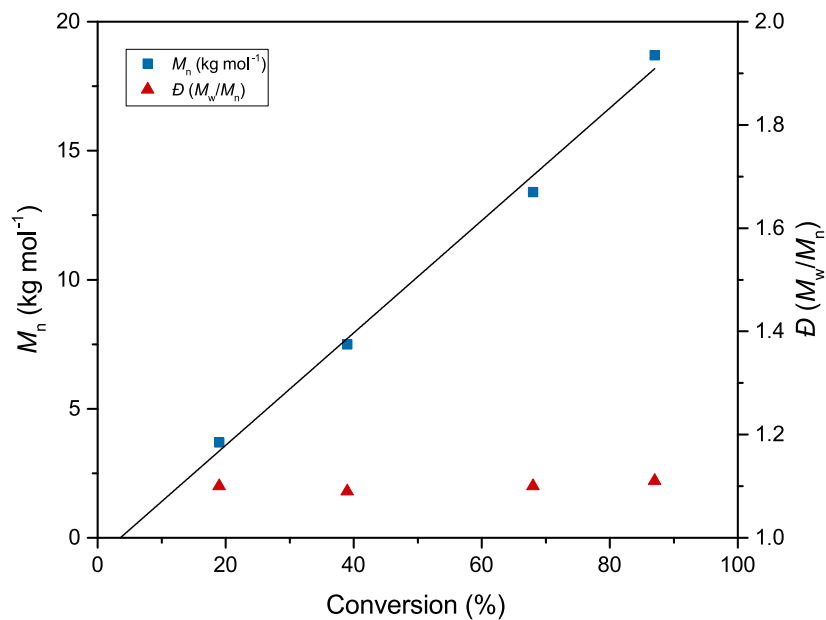
Figure S21. Evolution of molecular weight and dispersity with conversion for the ROP of β-BL mediated by complex **1** (activated for 24 h in PO prior to addition of β-BL).
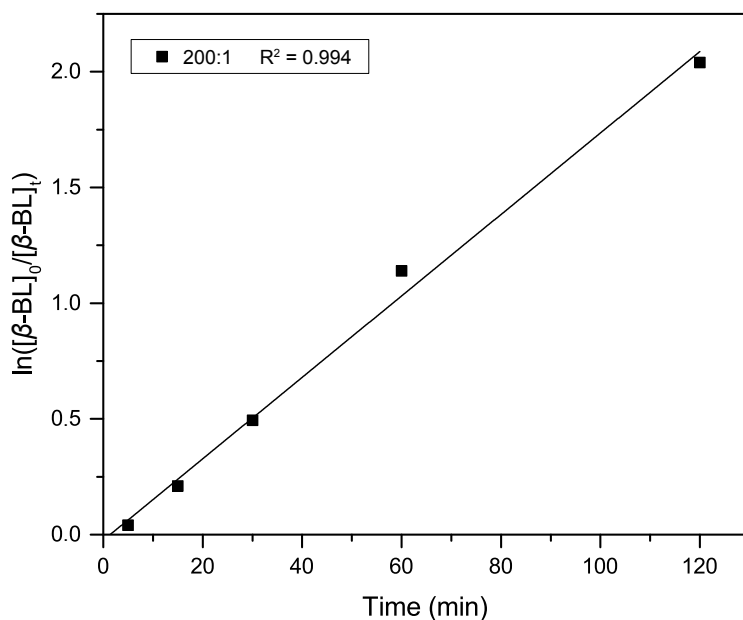
Figure S22. Semi-logarithmic plot of monomer concentration over time for the ROP of β-BL mediated by complex **1** (activated for 24 h in PO prior to addition of β-BL). $k_{obs} = 0.018 \pm 0.001$ min^{-1}. Conditions: $[\beta\text{-BL}]_0 = 2.0$ M, $[\beta\text{-BL}]/[\textbf{1}] = 200/1$, T = rt.

S20

Analysis of Polymer Microstructure
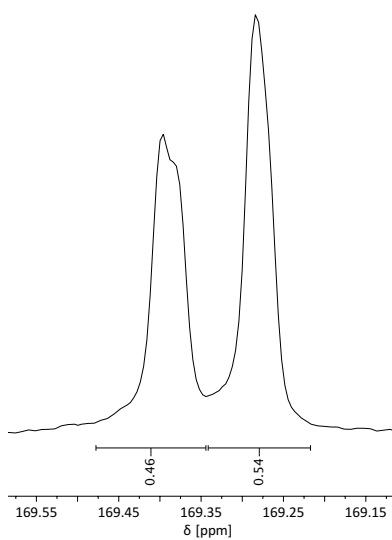
Figure S23. Representative ^{13}C{^{1}H} NMR spectrum (carbonyl region) of PHB produced by ROP of β-BL using **2** (P_m = 0.54).
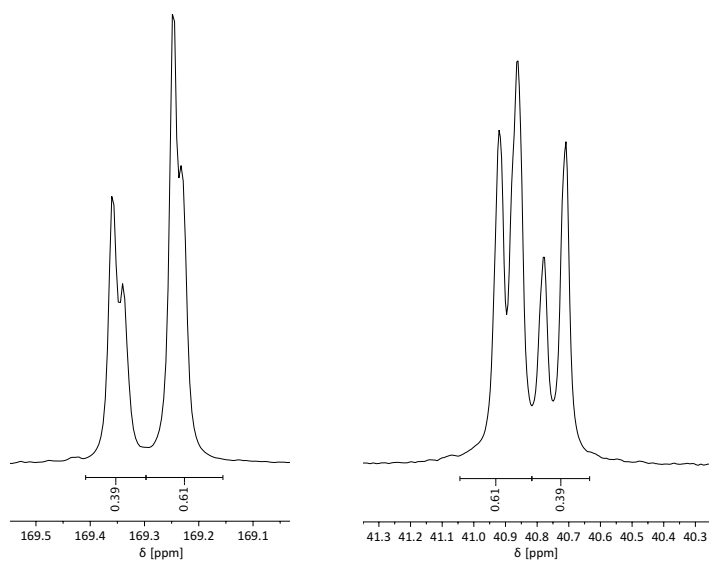
Figure S24. ^{13}C{^{1}H} NMR spectrum of PHB produced by ROP of β-BL using **3** (P_m = 0.61). Left: carbonyl region, right: methylene region.

S21
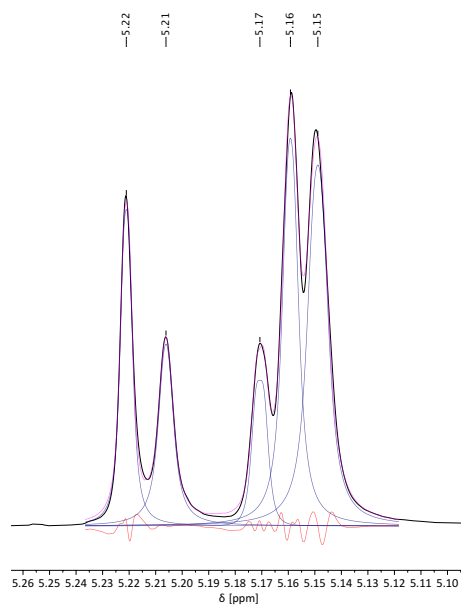
Figure S25. Representative peak deconvoluted $^1\text{H}\{^1\text{H}\}$ NMR spectrum (methine region) of PLA produced by ROP of *rac*-LA using **2** ($P_r = 0.62$).
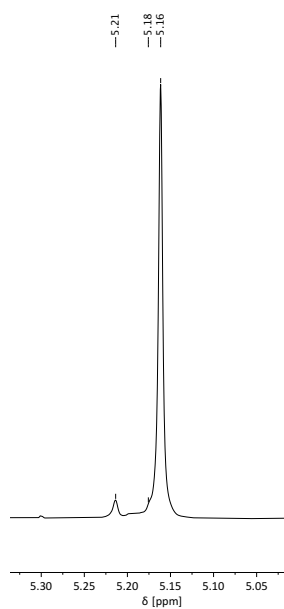
Figure S26. Peak deconvoluted $^1\text{H}\{^1\text{H}\}$ NMR spectrum (methine region) of PLA produced by ROP of unpurified *L*-LA using **2** ($P_m = 0.97$; Table 2, entry 11).

S22
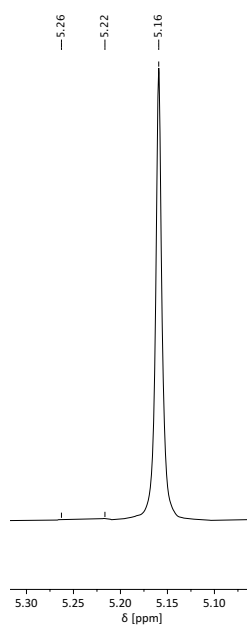
Figure S27. Peak deconvoluted ^{1}H{^{1}H} NMR spectrum (methine region) of PLA produced by ROP of unpurified *L*-LA using **2** ($P_m = 0.99$; Table 2, entry 12).
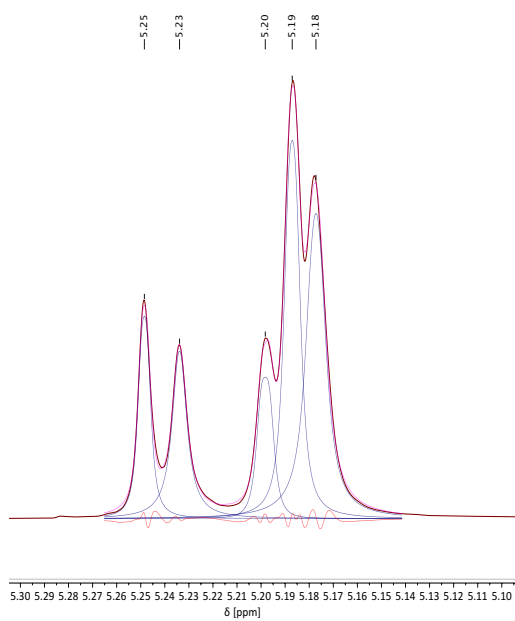
Figure S28. Peak deconvoluted ^{1}H{^{1}H} NMR spectrum (methine region) of PLA produced by ROP of *rac*-LA using **3** ($P_r = 0.57$).

S23

Polymer End-Group Analysis

End-group analysis of oligomeric PHB produced by **2** ([β-BL]/[**2**] = 20/1) was carried out using ESI-MS and ^{1}H NMR measurements. The ESI-MS spectrum consisted of three series of molecular ion peaks with the major series (red squares) corresponding to linear PHB with ^{t}BuO/H chain ends and Na$^+$ (Figure S27). The respective series with K$^+$ was also observed (orange triangles). The third population corresponded to linear PHB with crotonyl chain ends (blue circles). Although the formation of crotonyl chain ends in ROP of β-BL is a well-known phenomenon, we consider that the side reaction is not caused by the catalyst during ROP but is in fact occurring during the ionization of the oligomeric sample in the ESI-MS measurements. This is also supported by end-group analysis using NMR spectroscopy (Figure S28). The identical sample of oligomeric PHB used for ESI-MS measurements showed no signals of crotonyl chain ends in the ^{1}H NMR spectrum but solely the corresponding methine proton (4.2 ppm) of linear PHB (Figure S28).

m/z = 1 + 86.09 n + 73.07 + 22.99   m/z = 1 + 86.09 n + 73.07 + 39.10   m/z = 69.04 + 86.09 n + 73.07 + 22.99
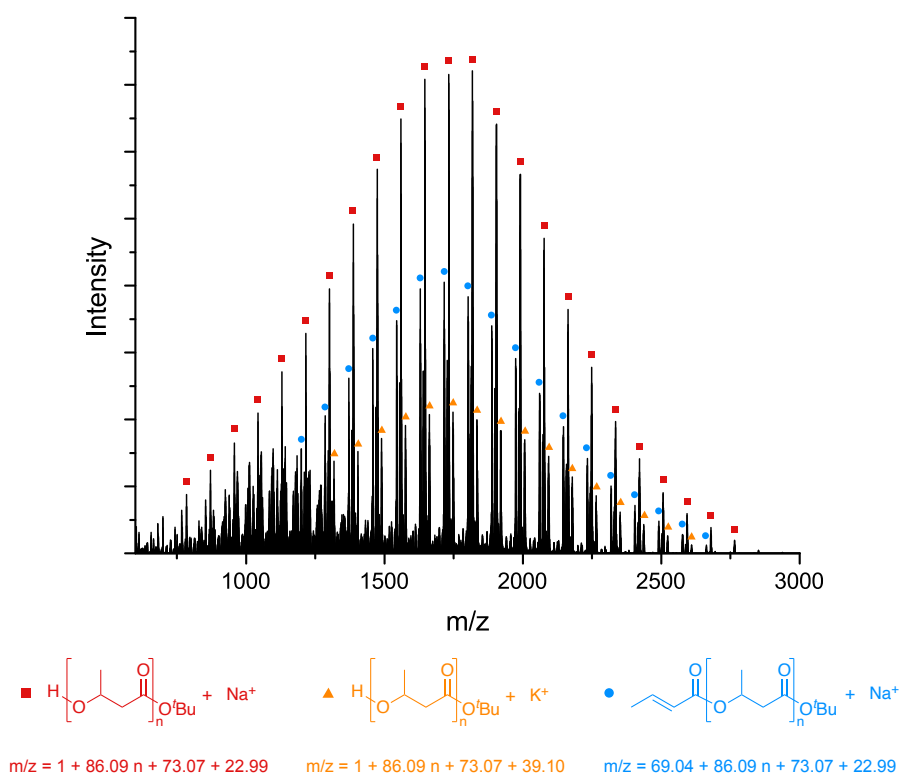
Figure S29. ESI-MS spectrum of PHB produced by **2** ([β-BL]/[**2**] = 20/1). For remarks on crotonyl chain ends see discussion above.

S24
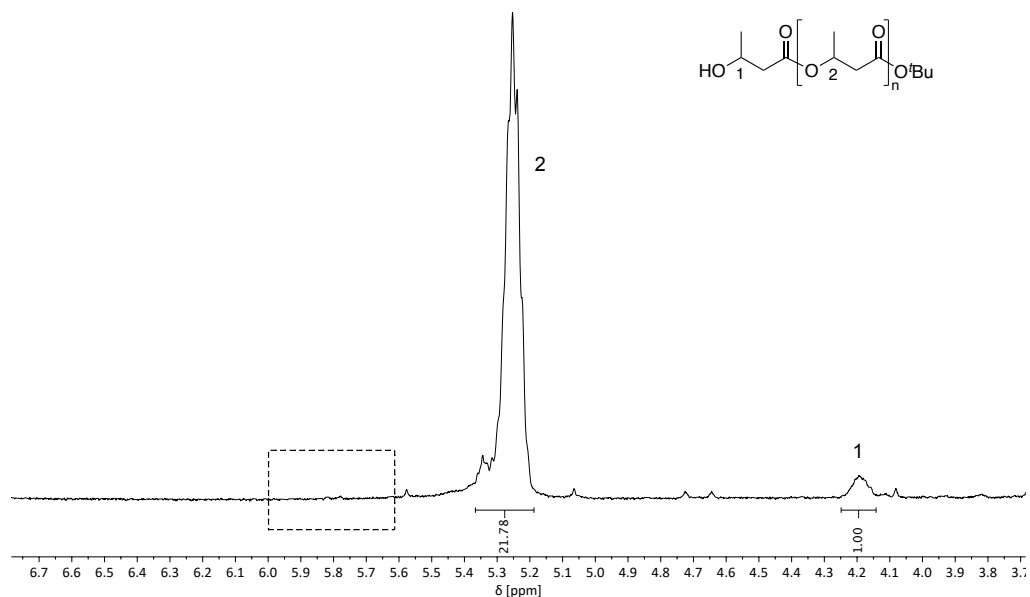
Figure S30. ^1H NMR spectrum (CDCl$_3$) of the methine region of PHB produced by **2** ([β-BL]/[**2**] = 20/1). The absence of signals corresponding to crotonyl chain ends is highlighted by the rectangle.

DOSY NMR Analysis of Compounds 2 and 3

DOSY NMR measurements were performed to elucidate the nuclearity of compounds **2** and **3** in solution under conditions relevant for polymerization runs. The molecular weight of the compounds was determined by using external calibration curves with normalized diffusion coefficients.[8] Toluene-d$_8$ was used as solvent and the diffusion coefficient of the residual solvent resonance used as an internal reference for calculations. An external calibration curve for dissipated spheres and ellipsoids was chosen (see ref. 8 for details). The observed diffusion coefficients of the analytes and the internal reference are given in Figures S29 and S30. A molecular weight of 450 g mol^{-1} and 642 g mol^{-1} was determined for compound **2** and **3**, respectively, indicating that both compounds are mononuclear in solution.

S25
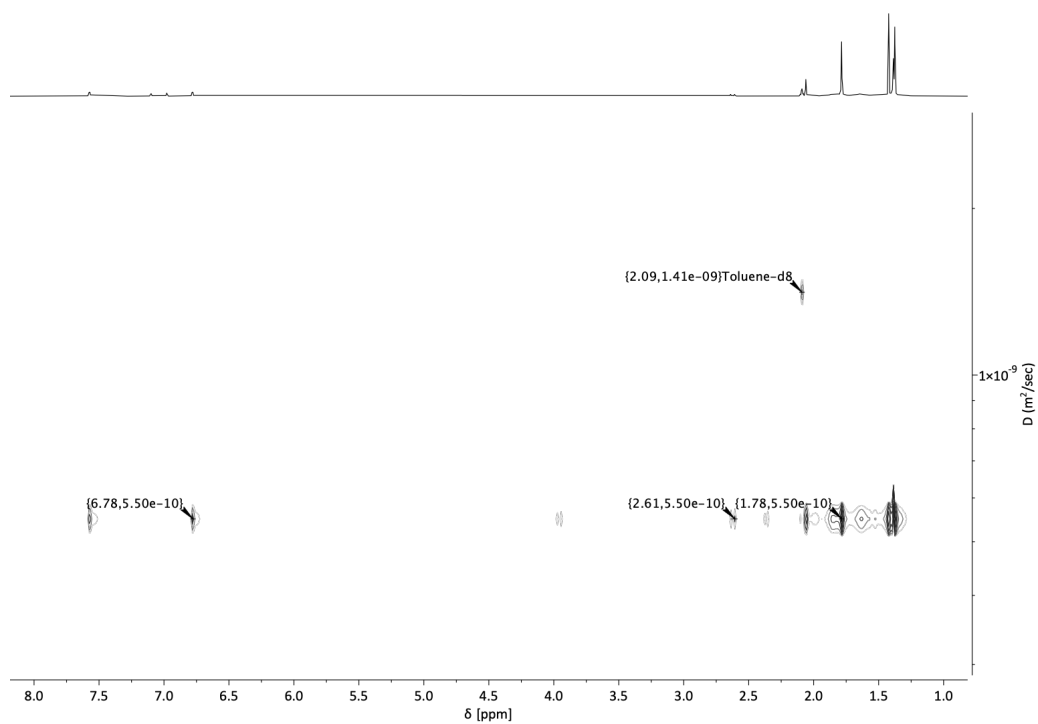
Figure S31. ^{1}H DOSY NMR of compound **2** in toluene-d$_8$ at room temperature.
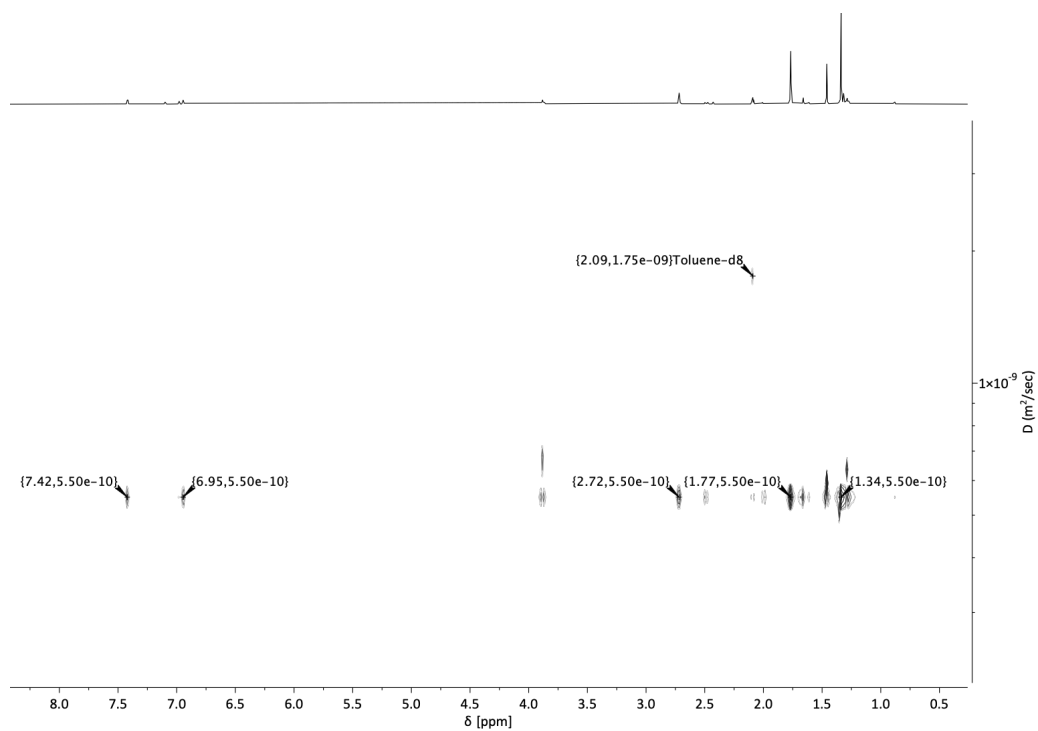
Figure S32. ^{1}H DOSY NMR of compound **3** in toluene-d$_8$ at room temperature.

S26

Representative GPC Traces
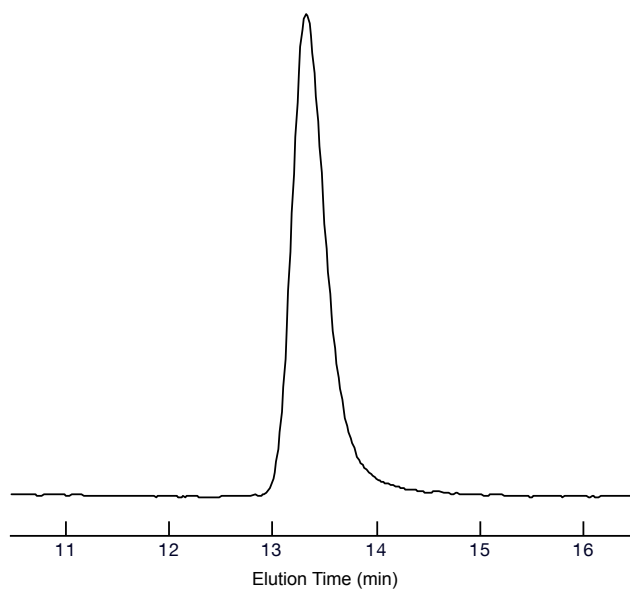
Figure S33. GPC trace of PHB by [β-BL]/[**2**] = 400/1 (M_n = 43.9 kg mol^{-1}, $Ð$ = 1.03).
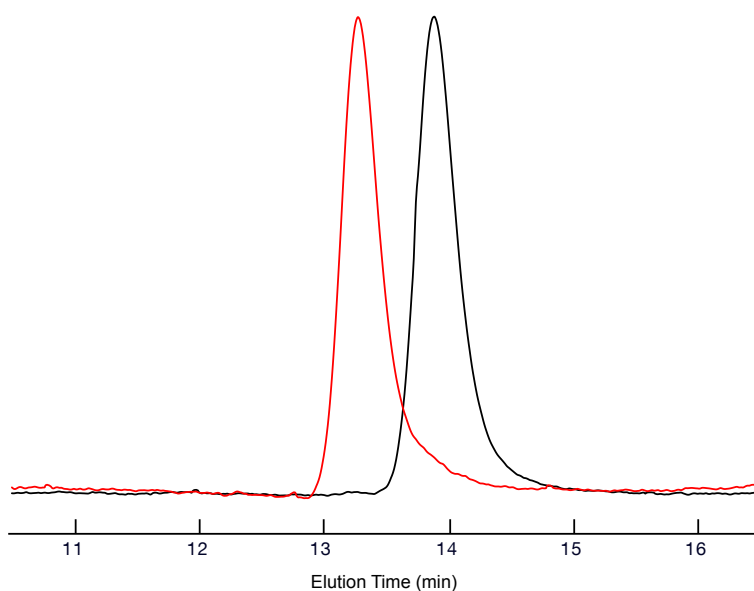
Figure S34. GPC traces of PHB of a chain extension experiment with catalyst **2**. Black: polymer after conversion of first 200 equiv of β-BL (M_n = 24.5 kg mol^{-1}, $Ð$ = 1.05). Red: polymer after conversion of second 200 equiv of β-BL (M_n = 48.0 kg mol^{-1}, $Ð$ = 1.06).

S27
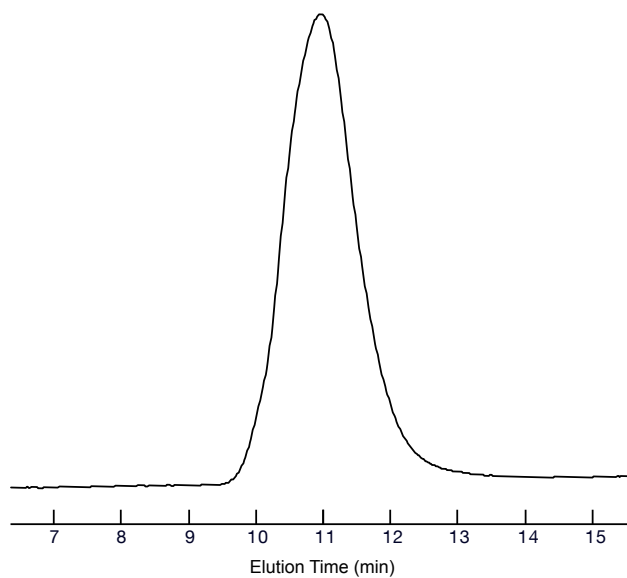
Figure S35. GPC trace of PεCL by [ε-CL]/[**2**] = 2000/1 ($M_{n,corr}$ = 318.8 kg mol^{-1}, Đ = 1.49).
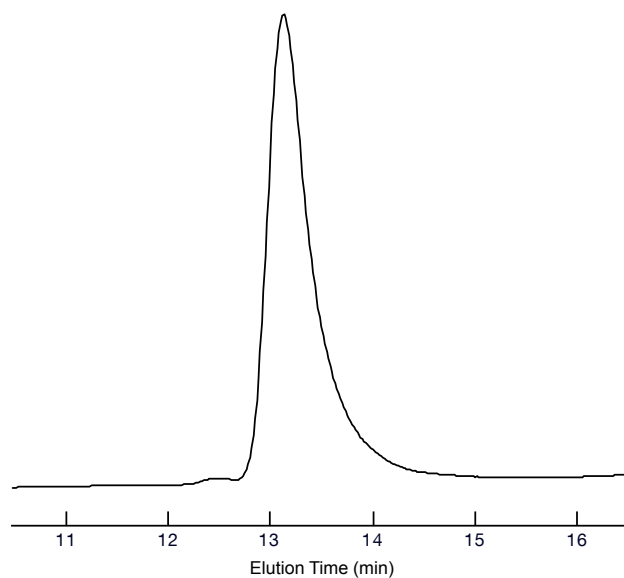
Figure S36. GPC trace of PεDL by [ε-DL]/[**2**] = 200/1 (M_n = 50.8 kg mol^{-1}, Đ = 1.13).

S28
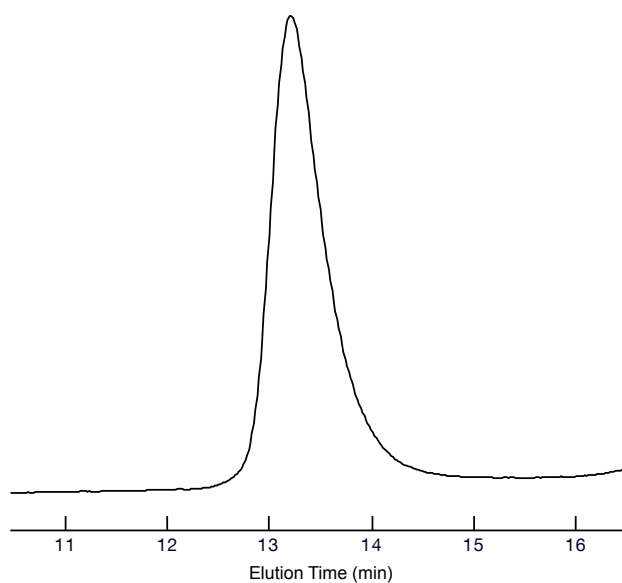
Figure S37. GPC trace of PLA by [*rac*-LA]/[**2**] = 500/1 ($M_{n,corr}$ = 26.8 kg mol^{-1}, $Đ$ = 1.15).
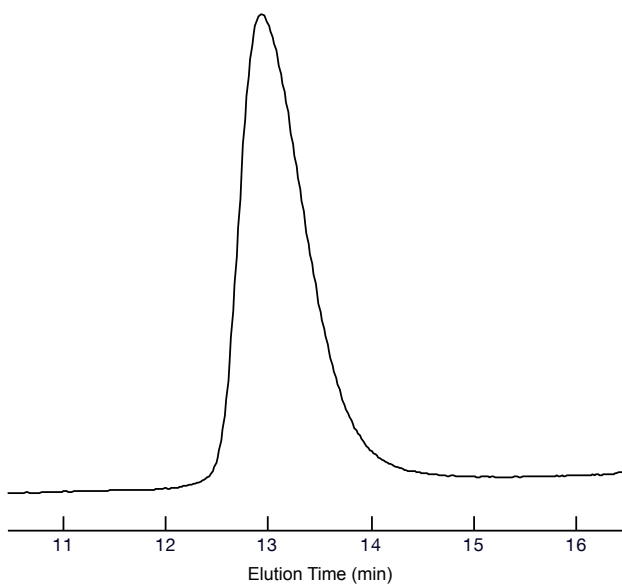
Figure S38. GPC trace of PLA by [*rac*-LA]/[**2**] = 1000/1, unpurified *rac*-LA used ($M_{n,corr}$ = 35.1 kg mol^{-1}, $Đ$ = 1.16).

S29
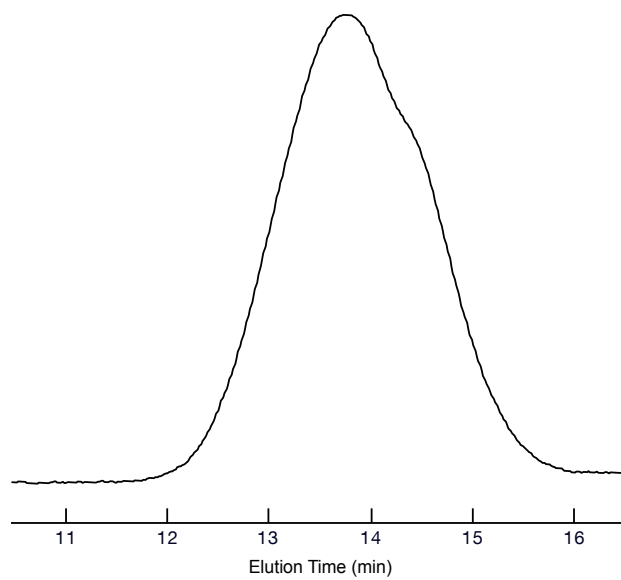
Figure S39. GPC trace of PγBL by [γ-BL]/[**2**] = 200/1 (M_n = 21.2 kg mol^{-1}, Đ = 1.80).

S30

3. X-Ray Crystallography

Single crystals of complex **2** were obtained by slow evaporation from a saturated toluene solution at room temperature and were measured following the details given below.
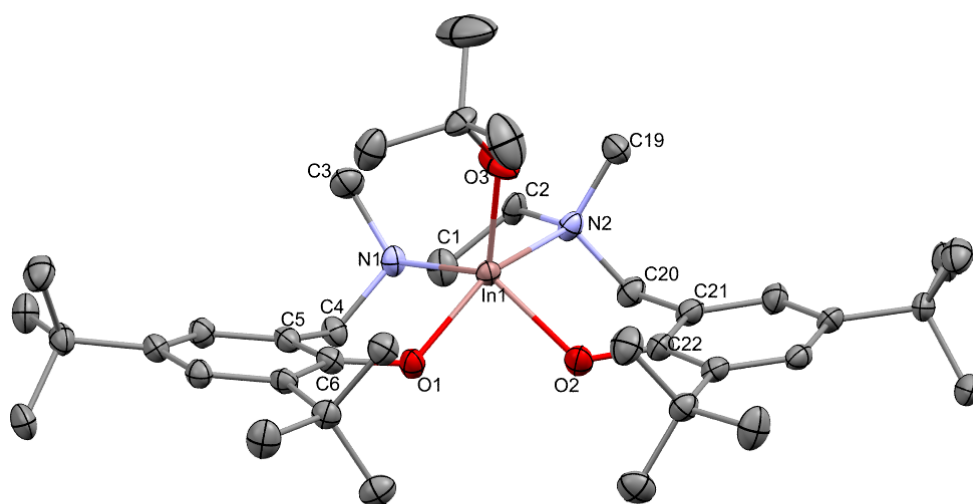
Figure S40. Molecular structure and numbering scheme of complex **2**: Displacement ellipsoids are drawn at the 50% probability level. Hydrogen atoms are omitted for clarity. Selected bond lengths and angles are given in Table S2.

General procedure

The X-ray data were collected on an X-ray single crystal diffractometer equipped with a CMOS detector (Bruker Photon-100), an IMS microsource with MoKα radiation (λ=0.71073Å) and a Helios mirror optic by using the APEX III software package.[9] The crystal was fixed on top of a microsampler using perfluorinated ether, transferred to the diffractometer and measured under a stream of cold nitrogen. A matrix scan was used to determine the initial lattice parameters. Reflections were corrected for Lorentz and polarization effects, scan speed, and background using SAINT.[10] Absorption corrections, including odd and even ordered spherical harmonics were performed using SADABS.[10] Space group assignments were based upon systematic absences, *E* statistics, and successful refinement of the structures. Structures were solved by SHELXT[11] (intrinsic phasing) with the aid of successive difference Fourier maps, and were refined against all data using with SHELXL2018[12] in conjunction with SHELXLE.[13] Methyl hydrogen atoms were refined as part of rigid rotating groups, with a C–H distance of 0.98 Å and Uiso(H)= 1.5·Ueq(C). Other H atoms were placed in calculated positions and refined using

S31

a riding model, with methylene and aromatic C–H distances of 0.99 and 0.95Å, respectively, and Uiso(H)= 1.2·Ueq(C). Non-hydrogen atoms were refined with anisotropic displacement parameters. Full-matrix least-squares refinements were carried out by minimizing $\Delta w(F_o^2\text{-}F_c^2)^2$ with the SHELXL[12] weighting scheme. Neutral atom scattering factors for all atoms and anomalous dispersion corrections for the non-hydrogen atoms were taken from *International Tables for Crystallography*.[14] Images of the crystal structures were generated with MERCURY.[15] Crystallographic data are also deposited at the Cambridge Crystallographic Data Centre (CCDC 2128903) and are available free of charge via www.ccdc.cam.ac.uk/structures/.

Table S2. Selected bond lengths (Å) and angles (°) for the X-ray crystal structure of complex **2**.

Bond Length		Bond Angle		Bond Angle	
In1-O1	2.082(3)	O1-In1-N1	86.7(1)	O2-In1-N2	85.2(1)
In1-O2	2.065(4)	O1-In1-O2	83.5(1)	O2-In1-O3	120.3(1)
In1-O3	1.987(3)	O1-In1-N2	148.5(1)	N1-In1-N2	77.8(1)
In1-N1	2.304(3)	O1-In1-O3	121.9(1)	N1-In1-O3	107.2(1)
In1-N2	2.375(4)	O2-In1-N1	129.0(1)	N2-In1-O3	89.1(1)

Table S3. Crystallographic data for complex **2** (CCDC 2128903).

Diffractometer operator: Daniel Henschel
scanspeed 9 s per frame
dx 30 mm
2287 frames measured in 15 data sets
phi-scans with delta_phi = 0.5
omega-scans with delta_omega = 0.5
shutterless mode

Crystal data

C₃₈H₆₃InN₂O₃	$F(000) = 754$
$M_r = 710.72$	
Triclinic, P	$D_x = 1.239$ Mg m⁻³
Hall symbol: -P 1	Melting point: ? K
$a = 11.4082 (16)$ Å	Mo $K\alpha$ radiation, $\lambda = 0.71073$ Å
$b = 13.035 (2)$ Å	Cell parameters from 9943 reflections
$c = 14.939 (2)$ Å	$\theta = 2.3–25.4°$
$\alpha = 66.497 (6)°$	$\mu = 0.66$ mm⁻¹
$\beta = 68.941 (6)°$	$T = 100$ K
$\gamma = 83.213 (7)°$	Clear fragment, colourless

S32

$V = \underline{1900.3\ (5)}$ Å³	$\underline{0.32} \times \underline{0.30} \times \underline{0.12}$ mm
$Z = \underline{2}$	

Data collection

Bruker Photon CMOS diffractometer	$\underline{6944}$ independent reflections
Radiation source: <u>IMS microsource</u>	$\underline{6024}$ reflections with $\underline{I > 2\sigma(I)}$
<u>Helios optic</u> monochromator	$R_{int} = \underline{0.072}$
Detector resolution: $\underline{16}$ pixels mm⁻¹	$\theta_{max} = \underline{25.4}°$, $\theta_{min} = \underline{1.8}°$
<u>phi– and ω–rotation scans</u>	$h = \underline{-13}\quad\underline{13}$
Absorption correction: <u>multi-scan</u> <u>*SADABS* 2016/2, Bruker, 2016</u>	$k = \underline{-15}\quad\underline{15}$
$T_{min} = \underline{0.634}$, $T_{max} = \underline{0.745}$	$l = \underline{-17}\quad\underline{17}$
$\underline{53587}$ measured reflections	

Refinement

Refinement on $\underline{F^2}$	Secondary atom site location: <u>difference Fourier map</u>
Least-squares matrix: <u>full</u>	Hydrogen site location: <u>inferred from neighbouring sites</u>
$R[F^2 > 2\sigma(F^2)] = \underline{0.042}$	<u>H-atom parameters constrained</u>
$wR(F^2) = \underline{0.105}$	$\underline{W = 1/[\Sigma^2(FO^2) + (0.0454P)^2 + 5.4852P]}$ <u>WHERE $P = (FO^2 + 2FC^2)/3$</u>
$S = \underline{1.00}$	$(\Delta/\sigma)_{max} \underline{< 0.001}$
$\underline{6944}$ reflections	$\Delta\varrho_{max} = \underline{0.87}$ e Å⁻³
$\underline{414}$ parameters	$\Delta\varrho_{min} = \underline{-0.85}$ e Å⁻³
$\underline{0}$ restraints	Extinction correction: <u>none</u>
$\underline{?}$ constraints	Extinction coefficient: $\underline{?}$
Primary atom site location: <u>iterative</u>	

S33

4. References

1. Min, K. S.; Weyhermüller, T.; Bothe, E.; Wieghardt, K., Tetradentate Bis(*o*-iminobenzosemiquinonate(1−)) π Radical Ligands and Their *o*-Aminophenolate(1−) Derivatives in Complexes of Nickel(II), Palladium(II), and Copper(II). *Inorg. Chem.* **2004,** *43*, 2922-2931.

2. Bloembergen, S.; Holden, D. A.; Bluhm, T. L.; Hamer, G. K.; Marchessault, R. H., Stereoregularity in synthetic *β*-hydroxybutyrate and *β*-hydroxyvalerate homopolyesters. *Macromolecules* **1989,** *22*, 1656-1663.

3. Aluthge, D. C.; Ahn, J. M.; Mehrkhodavandi, P., Overcoming aggregation in indium salen catalysts for isoselective lactide polymerization. *Chem. Sci.* **2015,** *6*, 5284-5292.

4. Save, M.; Schappacher, M.; Soum, A., Controlled ring-opening polymerization of lactones and lactides initiated by lanthanum isopropoxide, 1. General aspects and kinetics. *Macromol. Chem. Phys.* **2002,** *203*, 889-899.

5. Schneider, F.; Zhao, T.; Huhn, T., Cytotoxic heteroleptic heptacoordinate salan zirconium(iv)-bis-chelates - synthesis, aqueous stability and X-ray structure analysis. *Chem. Commun.* **2016,** *52*, 10151-10154.

6. Meppelder, G.-J. M.; Fan, H.-T.; Spaniol, T. P.; Okuda, J., Group 4 Metal Complexes Supported by [ONNO]-Type Bis(*o*-aminophenolato) Ligands: Synthesis, Structure, and α-Olefin Polymerization Activity. *Organometallics* **2009,** *28*, 5159-5165.

7. Beament, J.; Mahon, M. F.; Buchard, A.; Jones, M. D., Salan group 13 complexes – structural study and lactide polymerisation. *New J. Chem.* **2017,** *41*, 2198-2203.

8. Neufeld, R.; Stalke, D., Accurate molecular weight determination of small molecules *via* DOSY-NMR by using external calibration curves with normalized diffusion coefficients. *Chem. Sci.* **2015,** *6*, 3354-3364.

9. APEX suite of crystallographic software, APEX 3, version 2019.1-0, Bruker AXS Inc.: Madison, Wisconsin, USA, **2019**.

10. SAINT, Version 8.40a and SADABS Version 2016/2, Bruker AXS Inc.: Madison, Wisconsin, USA **2017**.

11. Sheldrick, G. M. SHELXT-2014/5, University of Göttingen: Göttingen, Germany, **2014**.

12. Sheldrick, G. M. SHELXL-2018/3, University of Göttingen: Göttingen, Germany, **2018**.

13. Huebschle, C. B.; Sheldrick, G. M.; Dittrich, B., SHELXLE. *J. Appl. Cryst.* **2011**, *44*, 1281.

14. Wilson, A. J. C., *International Tables for Crystallography, Vol. C*. Kluwer Academic Publishers: Dordrecht, Netherlands **1992**.

15. C. F. Macrae, I. Sovago, S. J. Cottrell, P. T. A. Galek, P. McCabe, E. Pidcock, M. Platings, G. P. Shields, J. S. Stevens, M. Towler and P. A. Wood, Mercury 4.0: from visualization to analysis, design and prediction. *J. Appl. Cryst.* **2020**, *53*, 226-235.

S34

10.2 Supporting Information for Chapter 5

Supporting Information

For

Simple and Rapid Access towards AB, BAB and ABAB Block Copolyesters from One-Pot Monomer Mixtures Using an Indium Catalyst

Jonas Bruckmoser, and Bernhard Rieger[*]

WACKER-Chair of Macromolecular Chemistry, Catalysis Research Center,
Department of Chemistry, Technical University of Munich
Lichtenbergstraße 4, 85748 Garching bei München, Germany.

[*]Corresponding Author; email: rieger@tum.de

Table of Contents

1. Experimental Section

1.1 Materials and Methods

All manipulations containing air- and/or moisture sensitive compounds were carried out under argon atmosphere using standard Schlenk or glovebox techniques. Glassware was flame-dried under vacuum prior to use. Unless otherwise stated, all chemicals were purchased from Sigma-Aldrich, TCI Chemicals or ABCR and used as received. Solvents were obtained from an MBraun MB-SPS 800 solvent purification system and stored over 3 Å molecular sieves prior to use. β-BL was treated with BaO, dried over CaH_2 and distilled prior to use. ε-CL, ε-DL and benzyl alcohol (BnOH) were dried over CaH_2 and distilled prior to use. Deuterated chloroform ($CDCl_3$) and toluene (C_7D_8) were obtained from Sigma-Aldrich and dried over 3 Å molecular sieves. Indium salan complex **1** and yttrium bisphenolate complex **Y1** were prepared according to literature procedures.[1, 2] 1,5,7-Triazabicyclo[4.4.0]dec-5-ene (TBD) and tin(II) 2-ethylhexanoate [$Sn(Oct)_2$] were purchased from Sigma-Aldrich and used as received. $Ti(O^iPr)_4$ was purchased from Alfa Aesar and distilled prior to use.

Nuclear magnetic resonance (NMR) spectra were recorded on a Bruker AV-III-500 spectrometer equipped with a QNP-Cryoprobe, AV-III-300 or AV-III-400 spectrometers at ambient temperature (298 K). ^1H and $^{13}C\{^1H\}$ NMR spectroscopic chemical shifts δ are reported in ppm relative to tetramethylsilane and were referenced internally to the relevant residual solvent resonances.

Polymer weight-average molecular weight (M_w), number-average molecular weight (M_n) and polydispersity indices ($Đ = M_w/M_n$) were determined *via* gel permeation chromatography (GPC) relative to polystyrene standards on a PL-SEC 50 Plus instrument from Polymer Laboratories. The analysis was performed at 40°C using THF as the eluent at a flow rate of 1.0 mL min^{-1}.

Differential scanning calorimetry (DSC) measurements were carried out with a DSC Q2000 from TA Instruments with a heating and cooling rate of 10 °C min^{-1}. T_g values were obtained from the second heating scan.

Thermal gravimetric analysis (TGA) was carried out with a TGA Q5000 from TA Instruments. Polymer samples were heated under argon atmosphere from ambient temperature to 600 °C with a heating rate of 10 °C min^{-1}.

1.2 General Polymerization Procedures

Copolymerization of ε-CL and β-BL

In a glove box, a 4 mL glass reactor was charged with ε-CL and β-BL. The respective amount of a stock solution of initiator **1** in toluene was injected into the monomer mixture, such that the overall concentration of ε-CL and β-BL was 2.0 M each. After 15 min, the polymerization was quenched by addition of 0.5 mL MeOH and conversion was determined by ^{1}H NMR spectroscopy of an aliquot. The mixture was precipitated into excess methanol, filtered, washed with additional methanol and dried under vacuum.

^{1}H NMR Kinetic Study of ε-CL and β-BL Copolymerization

In a glove box, a 4 mL glass reactor was charged with ε-CL (156 μL, 161 mg, 1.41 mmol) and β-BL (115 μL, 121 mg, 1.41 mmol). 0.33 mL of toluene-d$_8$ were added and 0.10 mL of a stock solution of initiator **1** in toluene-d$_8$ (0.028 M) were injected into the monomer mixture, such that the overall concentration of ε-CL and β-BL was 2.0 M each. The reaction mixture was transferred to a J-Young type NMR tube and ^{1}H NMR spectra were recorded at certain time intervals.

Copolymerization of ε-DL and β-BL via Route A (Diblock Copolymer)

In a glove box, a 4 mL glass reactor was charged with ε-DL (344 μL, 335 mg, 1.97 mmol) and β-BL (162 μL, 170 mg, 1.97 mmol). 0.25 mL of toluene were added and 0.23 mL of a stock solution of initiator **1** in toluene (0.042 M) were injected into the monomer mixture, such that the overall concentration of ε-CL and β-BL was 2.0 M each. After 3 h, the polymerization was quenched by addition of 0.2 mL MeOH and conversion was determined by ^{1}H NMR spectroscopy of an aliquot. The mixture was precipitated into excess pentane, filtered, washed with additional pentane and dried under vacuum.

Copolymerization of ε-DL and β-BL via Route B (Tetrablock Copolymer)

In a glove box, a 4 mL glass reactor was charged with ε-DL (344 μL, 335 mg, 1.97 mmol) and β-BL (81 μL, 85 mg, 0.98 mmol). 0.13 mL of toluene were added and 0.35 mL of a stock solution of initiator **1** in toluene (0.028 M) were injected into the monomer mixture. After 90 min, a small aliquot was removed from the reaction mixture for determination of conversion by ^{1}H NMR spectroscopy and β-BL (81 μL, 85 mg, 0.98 mmol) was added to the reaction mixture afterwards. The polymerization was allowed to continue for an additional 150 min and was eventually quenched by addition of 0.2 mL MeOH after a total

S3

polymerization time of 4 h. The final monomer conversion was determined by ^{1}H NMR spectroscopy of an aliquot. The mixture was precipitated into excess pentane, filtered, washed with additional pentane and dried under vacuum.

Copolymerization of ε-DL and β-BL via Route C without BnOH (Triblock Copolymer)

In a glove box, initiator **1** (7.0 mg, 9.9 μmol) was dissolved in 0.64 mL of toluene and ε-DL (344 μL, 335 mg, 1.97 mmol) was injected into the reaction, such that the overall concentration of ε-DL was 2.0 M. After 60 min, a small aliquot was removed from the reaction mixture for determination of conversion by ^{1}H NMR spectroscopy and β-BL (162 μL, 170 mg, 1.97 mmol) was added to the reaction mixture afterwards. The polymerization was allowed to continue for an additional 2 h and was eventually quenched by addition of 0.2 mL MeOH after a total polymerization time of 3 h. The final monomer conversion was determined by ^{1}H NMR spectroscopy of an aliquot. The mixture was precipitated into excess pentane, filtered, washed with additional pentane and dried under vacuum.

Copolymerization of ε-DL and β-BL via Route C with 2 eq. BnOH (Triblock Copolymer)

In a glove box, initiator **1** (7.0 mg, 9.9 μmol) was dissolved in 0.43 mL of toluene and 0.21 mL of a BnOH stock solution in toluene (0.092 M) was added. After stirring for 15 min at room temperature, ε-DL (344 μL, 335 mg, 1.97 mmol) was injected into the reaction, such that the overall concentration of ε-DL was 2.0 M. After 45 min, a small aliquot was removed from the reaction mixture for determination of conversion by ^{1}H NMR spectroscopy and β-BL (162 μL, 170 mg, 1.97 mmol) was added to the reaction mixture afterwards. The polymerization was allowed to continue for an additional 135 min and was eventually quenched by addition of 0.2 mL MeOH after a total polymerization time of 3 h. The final monomer conversion was determined by ^{1}H NMR spectroscopy of an aliquot. The mixture was precipitated into excess pentane, filtered, washed with additional pentane and dried under vacuum.

Copolymerization of ε-DL and β-BL via Sequential Addition

In a glove box, initiator **1** (8.0 mg, 11.3 μmol) was dissolved in 0.94 mL of toluene and β-BL (185 μL, 194 mg, 2.25 mmol) was injected into the reaction, such that the overall concentration of β-BL was 2.0 M. After 20 min, a small aliquot was removed from the reaction mixture for determination of conversion by ^{1}H NMR spectroscopy and ε-DL

(393 μL, 383 mg, 2.25 mmol) was added to the reaction mixture afterwards. The polymerization was allowed to continue for an additional 2 h and was eventually quenched by addition of 0.2 mL MeOH after a total polymerization time of 140 min. The final monomer conversion was determined by ^{1}H NMR spectroscopy of an aliquot. The mixture was precipitated into excess pentane, filtered, washed with additional pentane and dried under vacuum.

Kinetic Studies of ε-DL and β-BL Copolymerization

For kinetic studies, copolymerizations of ε-DL and β-BL were performed as described above. After certain time intervals, aliquots were taken from the reaction mixture, quenched with 0.4 mL hydrous CDCl$_3$ and conversion determined by ^{1}H NMR spectroscopy. The crude products were additionally analyzed by GPC.

Bulk Copolymerization of ε-DL and β-BL using TBD or Sn(Oct)$_2$

In a glove box, a glass reactor was charged with catalyst and a monomer mixture of ε-DL and β-BL (1:1) was added. The vial was sealed, removed from the glovebox and stirred for 24 h at 100 °C in a preheated aluminum block. The polymerization was quenched by addition of 0.2 mL MeOH and conversion was determined by ^{1}H NMR spectroscopy of an aliquot. The mixture was precipitated into excess pentane, filtered, washed with additional pentane and dried under vacuum.

S5

2. Polymerization Kinetics and Polymer Characterization Data

PHB-*co*-PDL

N(SiHMe₂)₂

^{t}Bu ^{t}Bu

OMe

^{t}Bu ^{t}Bu

Y1

Sn(Oct)₂

TBD

Ti(O^{i}Pr)₄
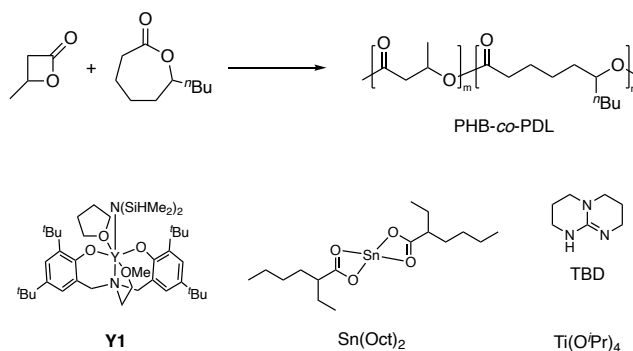
Figure S1. Copolymerization of *β*-BL and *ε*-DL, and chemical structures of additionally tested catalysts **Y1**, Sn(Oct)₂, TBD and Ti(O^{i}Pr)₄.

Table S1. Homopolymerization data for *β*-BL, *ε*-CL and *ε*-DL ROP using catalyst **1**, and copolymerization data using various catalysts [a]

Entry	Cat.	Monomer A	Monomer B	[A]/[B]/[I]	T (°C)	t (min)	Conv. A (%)[b]	Conv. B (%)[b]	M_n (theo) (kg mol⁻¹)[c]	M_n (GPC) (kg mol⁻¹)[d]	$Đ$[d]
1	**1**	*β*-BL	-	200:0:1	rt	15	97	-	16.7	21.2	1.05
2	**1**	*ε*-CL	-	500:0:1	rt	20 s	72	-	41.1	117.1	1.48
3	**1**	*ε*-DL	-	200:0:1	rt	120	90	-	30.6	50.8	1.13
4[e]	**1**	*ε*-DL	-	200:0:1	rt	15	21	-	7.2	n.d.	n.d.
5[e]	**1**	*ε*-DL	-	200:0:1	rt	60	73	-	24.9	n.d.	n.d.
6	**Y1**	*β*-BL	*ε*-DL	200:200:1	rt	120	>99	17	22.8	n.d.	n.d.
7	**Y1**	*β*-BL	*ε*-DL	200:200:1	rt	1440	>99	18	23.2	37.9	1.52
8	TBD	*β*-BL	*ε*-DL	200:200:1	100	1440	>99	0	17.0	n.d.	n.d.
9	Sn(Oct)₂	*β*-BL	*ε*-DL	130:130:1	100	1440	55	56	18.5	1.0	1.72
10	Ti(O^{i}Pr)₄	*β*-BL	*ε*-DL	200:200:1	100	1440	57	93	41.5	13.4	1.16

[a]Polymerizations were performed in toluene, except entries 8 and 9, which were performed in bulk. For homopolymerizations [M] = 2.0 M, for copolymerizations [*β*-BL] = [*ε*-DL] = 2.0 M. n.d. = not determined. [b]Conversion determined by ¹H NMR spectroscopy. [c]Theoretical molecular weights were determined from the [M]/[I] ratio and monomer conversion data. [d]Determined by GPC in THF at 40 °C relative to polystyrene standards. A correction factor of 0.56 was applied for PCL.[3] [e]1 equiv of BnOH added.

S6
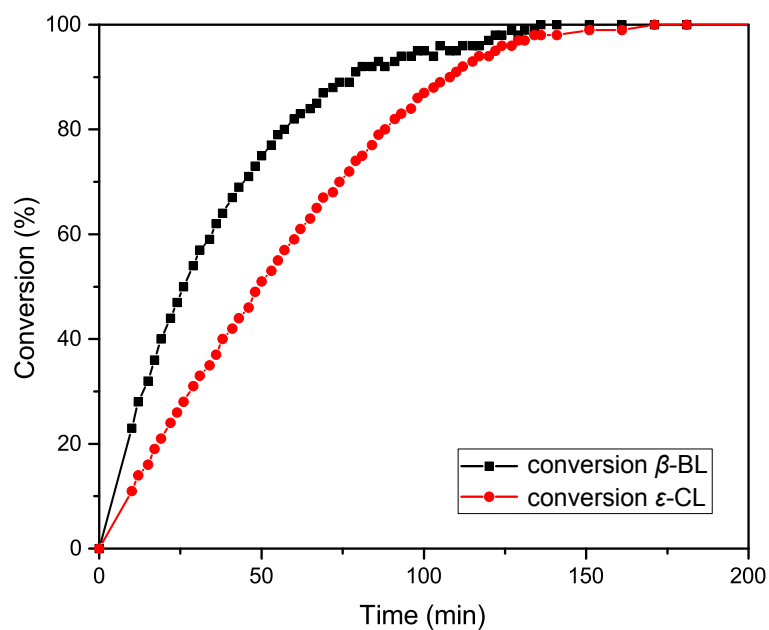
Figure S2. Conversion vs time plot for copolymerization of β-BL and ε-CL using **1** as catalyst ($[\beta$-BL]/$[\varepsilon$-CL]/[**1**] = 500/500/1, T = rt., $[\beta$-BL] = $[\varepsilon$-CL] = 2.0 M).
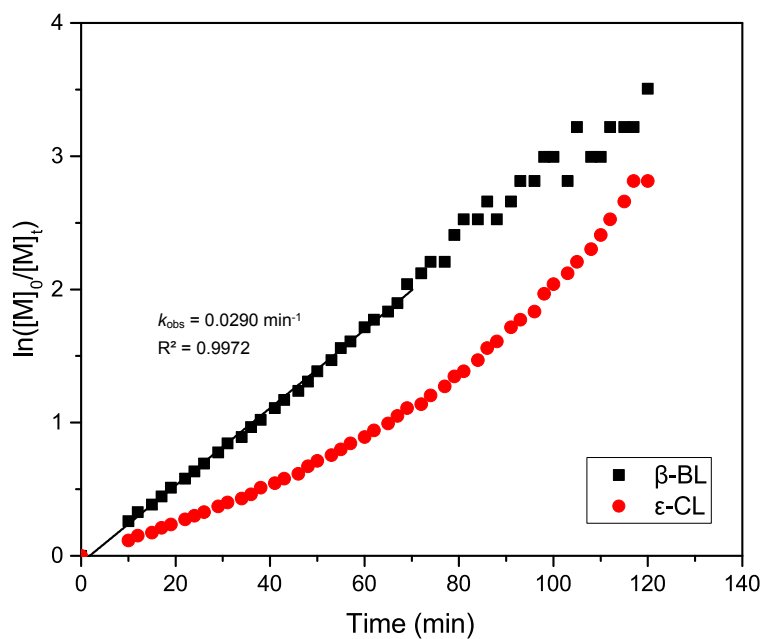
Figure S3. Semi-logarithmic plot of monomer concentration over time for the copolymerization of β-BL and ε-CL mediated by complex **1** ($[\beta$-BL]/$[\varepsilon$-CL]/[**1**] = 500/500/1, T = rt., $[\beta$-BL] = $[\varepsilon$-CL] = 2.0 M). Conversion of ε-CL does not follow a first-order behavior.

S7
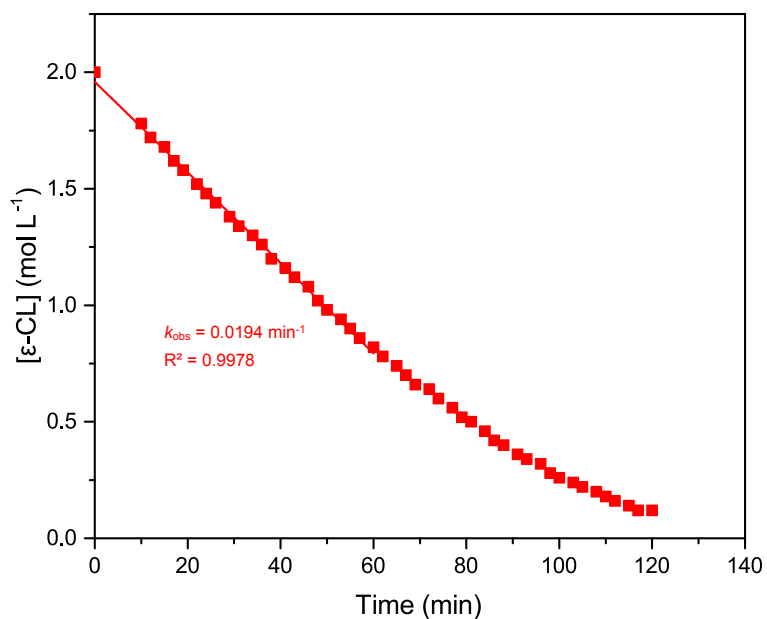
Figure S4. Monomer concentration vs time plot for copolymerization of β-BL and ε-CL mediated by complex **1** ($[\beta\text{-BL}]/[\varepsilon\text{-CL}]/[\mathbf{1}]$ = 500/500/1, T = rt., $[\beta\text{-BL}] = [\varepsilon\text{-CL}]$ = 2.0 M). β-BL data is not shown (see Figure S3).
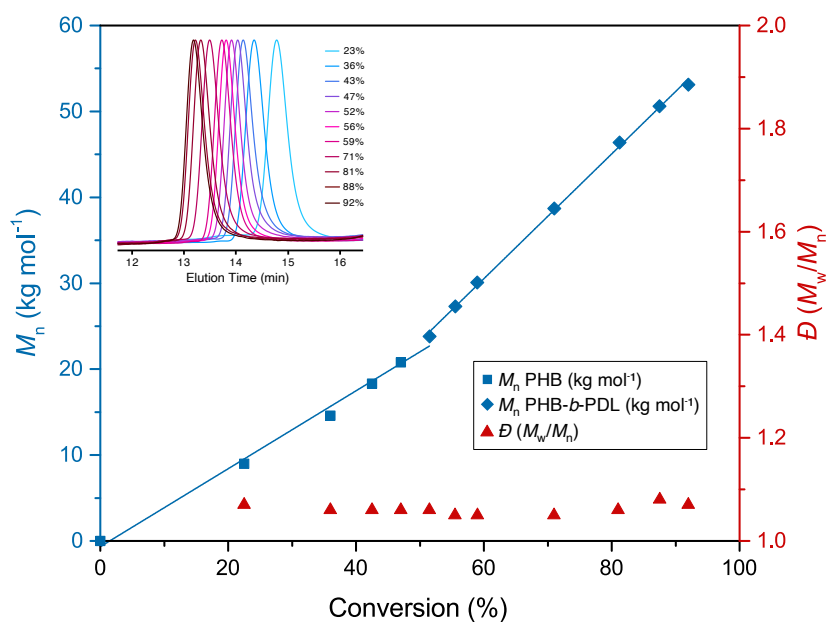
Figure S5. Evolution of molecular weight and dispersity with conversion for the copolymerization of β-BL and ε-DL mediated by catalyst **1**. Inset: GPC traces of the polymers at respective conversions.

S8

2.1 Analysis of the Causes of Bimodality in Triblock Copolymerization Experiments
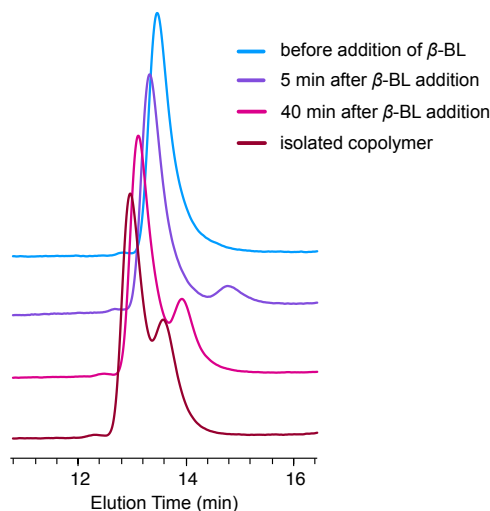
Figure S6. Evolution of GPC traces with time after addition of β-BL (200 equiv) to a polymerization of ε-DL (200 equiv) mediated by complex **1** without additional BnOH (addition of β-BL at 40% conversion of ε-DL).
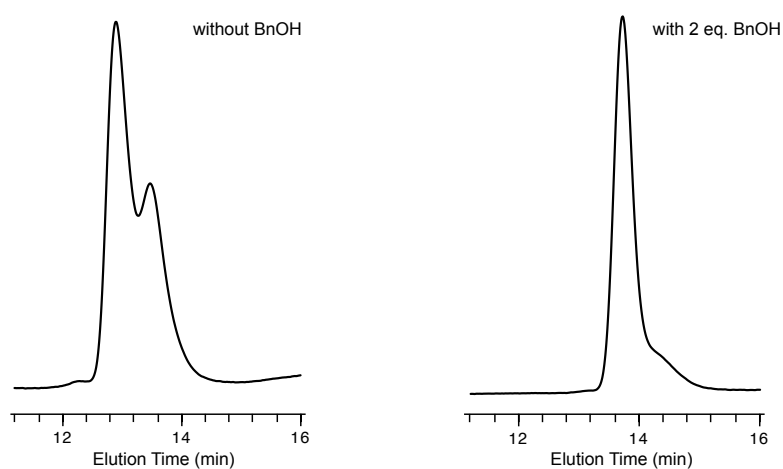
Figure S7. GPC traces of polymers obtained in triblock copolymer attempts with catalyst **1**. Without the addition of BnOH to the polymerization mixture a bimodal distribution is obtained (left), whereas a unimodal distribution is observed when **1** is activated *in situ* with 2 eq. of BnOH prior to the polymerization (right; $M_n = 23.8$ kg mol^{-1}, $Đ = 1.11$; Table 1, entry 8).

Triblock copolymer synthesis of ε-DL and β-BL *via* Route C was attempted. For this, 200 equiv of ε-DL were polymerized until 40% conversion using **1**, then, 200 equiv of β-BL were added to the reaction mixture, and the polymerization allowed to resume. Using this approach, polymers with bimodal distributions were obtained (Figure S7, left). GPC analysis of reaction aliquots revealed that the growing polymer chain was unimodal until β-BL was added (Figure S6, light blue curve). But from that point on, the emergence of a second

S9

unimodal polymer distribution with low molecular weight was observed in the GPC traces, which finally merged with the initial polymer distribution (Figure S6).

Both polymer distributions showed nearly identical molecular weight increase over the course of the polymerization. Initial distribution: $M_p = 39.2$ kg mol^{-1} (addition of β-BL), $M_p = 47.2$ kg mol^{-1} (+ 8.0 kg mol^{-1}, 5 min after β-BL addition), $M_p = 59.4$ kg mol^{-1} (+ 12.2 kg mol^{-1}, 40 min after β-BL addition), $M_p = 68.8$ kg mol^{-1} (+ 9.4 kg mol^{-1}, 120 min after β-BL addition). Arising distribution: $M_p = 0$ kg mol^{-1} (addition of β-BL), $M_p = 8.9$ kg mol^{-1} (+ 8.9 kg mol^{-1}, 5 min after β-BL addition), $M_p = 23.8$ kg mol^{-1} (+ 14.9 kg mol^{-1}, 40 min after β-BL addition), $M_p = 33.9$ kg mol^{-1} (+ 10.1 kg mol^{-1}, 120 min after β-BL addition).

These results show that the addition of β-BL monomer does not terminate initially growing polymer chains, but dormant catalyst species (resulting from incomplete initiation of ε-DL ROP) are activated by β-BL addition and initiate new polymer chains. Consequently, a mixture of PHB-b-PDL and PDL-b-PHB-b-PDL copolymers is formed. The poor initiation efficiency of catalyst **1** in ROP of ε-DL as cause of the bimodal polymer distributions in triblock copolymer attempts is further supported by the fact that similarly prepared tetrablock copolymers (where β-BL is present at the start of the polymerization, eventually resulting in complete initiation of catalyst) had unimodal polymer distributions.

Addition of 2 equiv of BnOH to a toluene solution of complex **1** prior to initiation of the polymerization resulted in a high initiation efficiency of **1** for the ROP of ε-DL. Thus, dormant catalyst species were almost completely absent when β-BL was added, resulting in strong suppression of the side reaction (Figure S7, right). Unimodal PDL-b-PHB-b-PDL copolymers were obtained using this approach.

S10

2.2 Mechanistic Considerations

A) Comparison of coordination ability
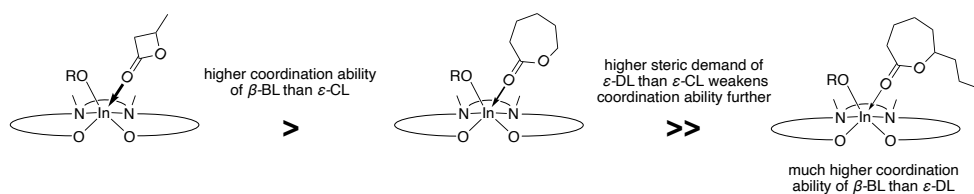
B) Correction of ε-DL misinsertion (steric differentiation)
(in the presence of β-BL)
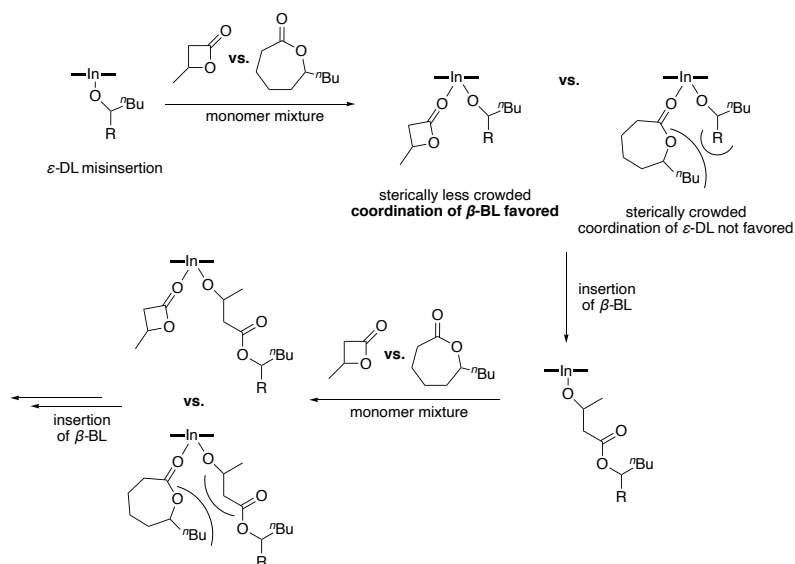
Figure S8. A) Proposed coordination ability of different monomers towards catalyst **1**. B) Correction of ε-DL misinsertion in the presence of β-BL in the one-pot monomer mixture. The ligand framework of **1** is only shown schematically.

S11

153

2.3 DSC Data of Polymers
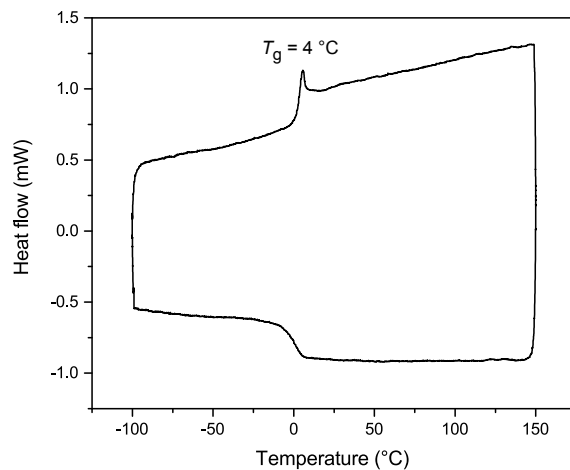
Figure S9. DSC curve (exo down) of PHB homopolymer ($M_n = 21.2$ kg mol^{-1}, $Đ = 1.05$).
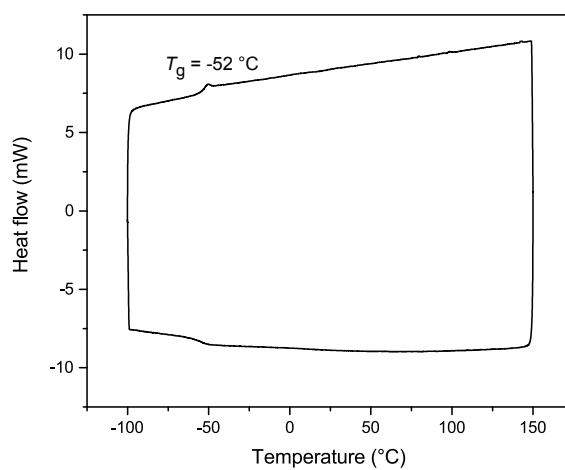
Figure S10. DSC curve (exo down) of PDL homopolymer ($M_n = 50.8$ kg mol^{-1}, $Đ = 1.13$).
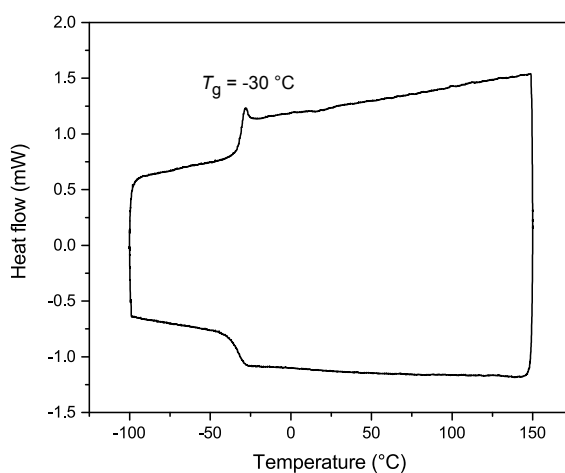
Figure S11. DSC curve (exo down) of PHB-*co*-PCL (Table 1, entry 1).

S12

154
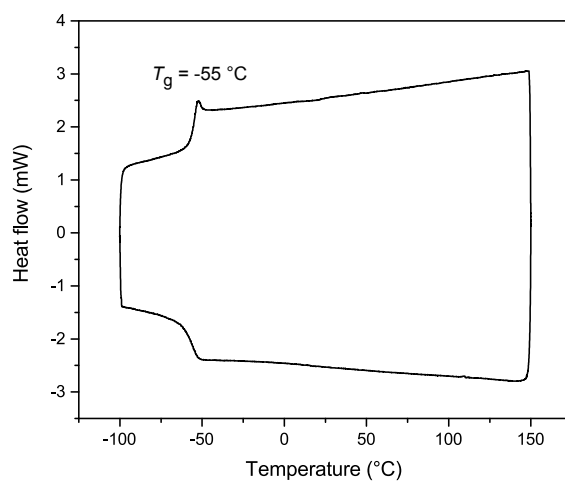
Figure S12. DSC curve (exo down) of PHB-*co*-PCL (Table 1, entry 2).
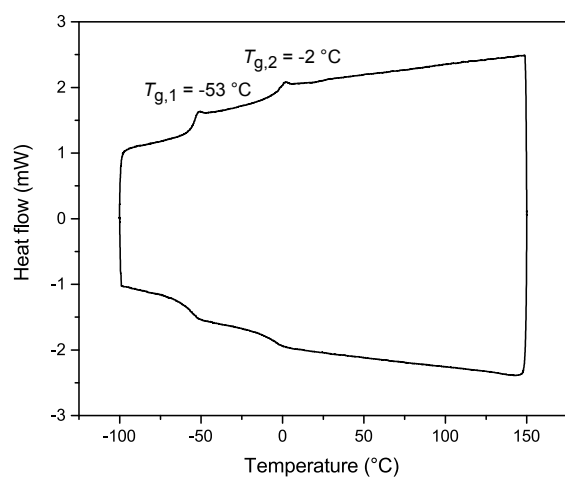
Figure S13. DSC curve (exo down) of PHB-*b*-PDL prepared *via* sequential addition (Table 1, entry 3).
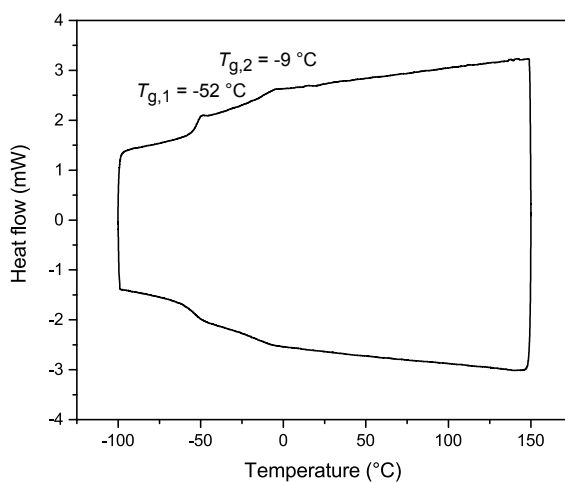
Figure S14. DSC curve (exo down) of PHB-*b*-PDL prepared from one-pot monomer mixture (Table 1, entry 4).

S13
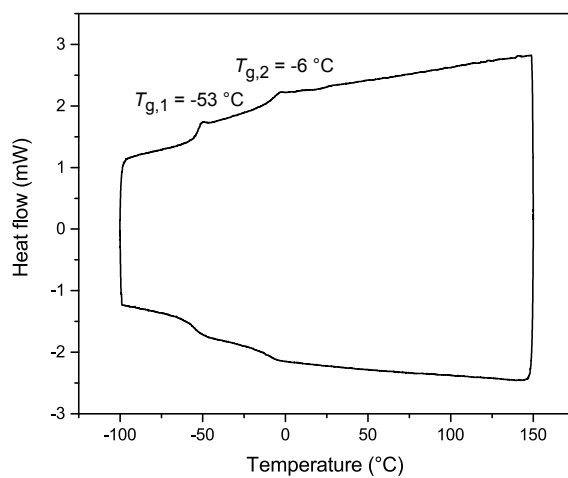
Figure S15. DSC curve (exo down) of PHB-*b*-PDL prepared from one-pot monomer mixture (Table 1, entry 5).
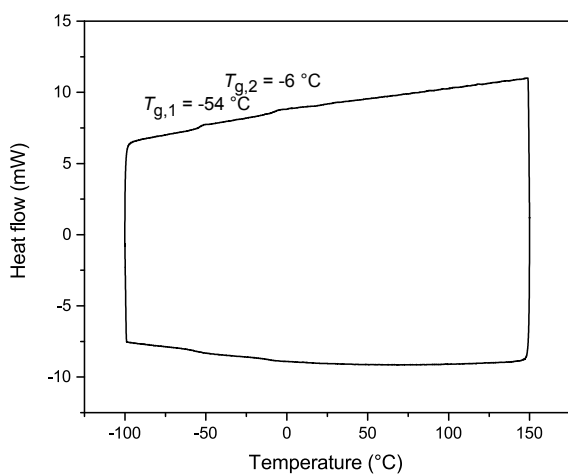
Figure S16. DSC curve (exo down) of PHB-*b*-PDL prepared from one-pot monomer mixture (Table 1, entry 6).
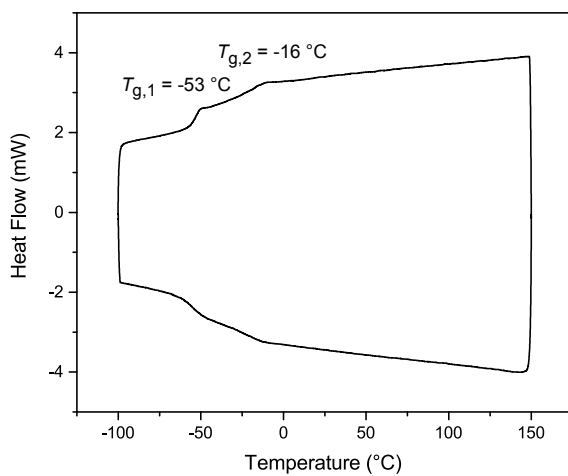
Figure S17. DSC curve (exo down) of PDL-*b*-PHB-*b*-PDL prepared from one-pot monomer mixture (Table 1, entry 8).

S14
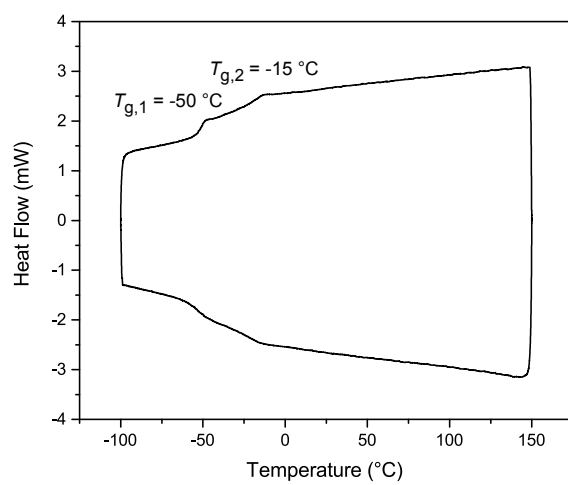
Figure S18. DSC curve (exo down) of PHB-*b*-PDL-*b*-PHB-*b*-PDL prepared from one-pot monomer mixture (Table 1, entry 9).
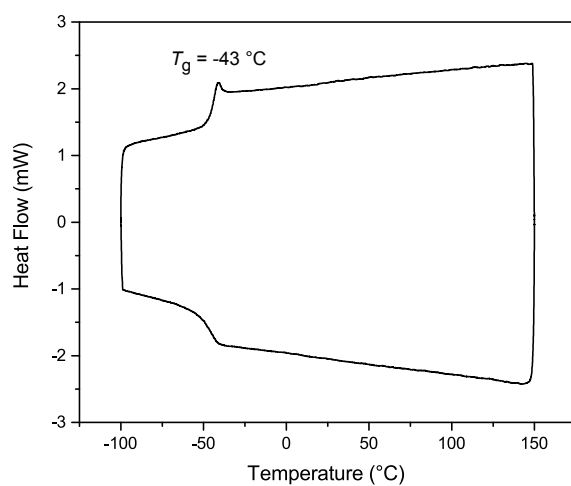
Figure S19. DSC curve (exo down) of PHB-*co*-PDL prepared from one-pot monomer mixture with Ti(O^{i}Pr)$_4$ (Table S1, entry 10).

S15

2.4 TGA Data of Polymers
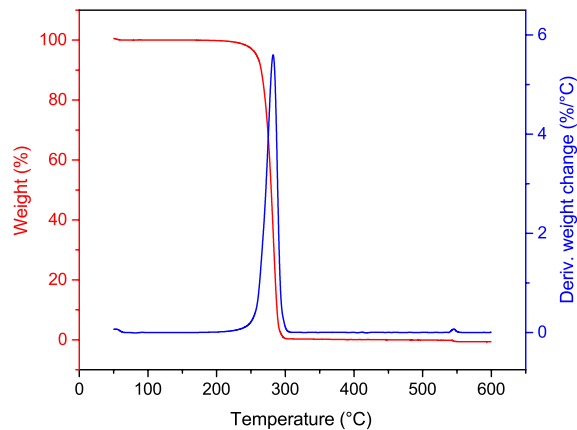
Figure S20. TGA curve of PHB homopolymer (M_n = 21.2 kg mol^{-1}, Đ = 1.05).
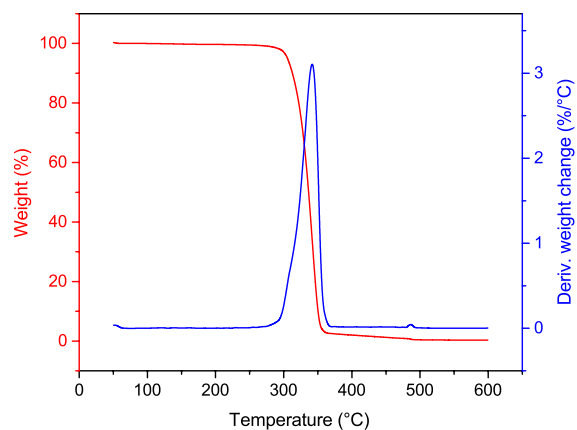
Figure S21. TGA curve of PDL homopolymer (M_n = 50.8 kg mol^{-1}, Đ = 1.13).
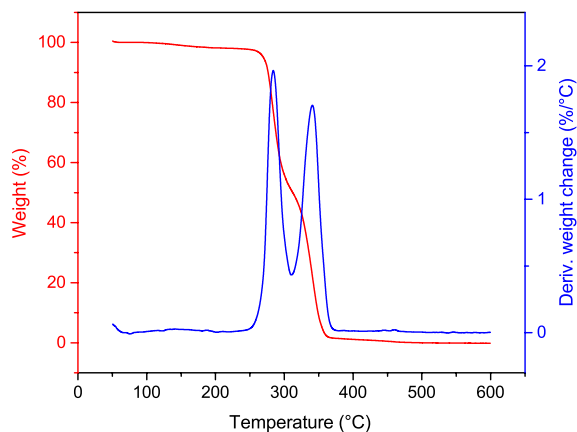
Figure S22. TGA curve of PHB-*b*-PDL prepared *via* sequential addition (Table 1, entry 3).

S16
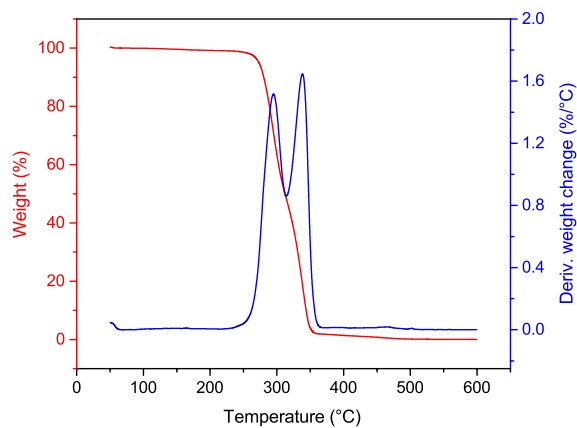
Figure S23. TGA curve of PHB-*b*-PDL prepared from one-pot monomer mixture (Table 1, entry 4).
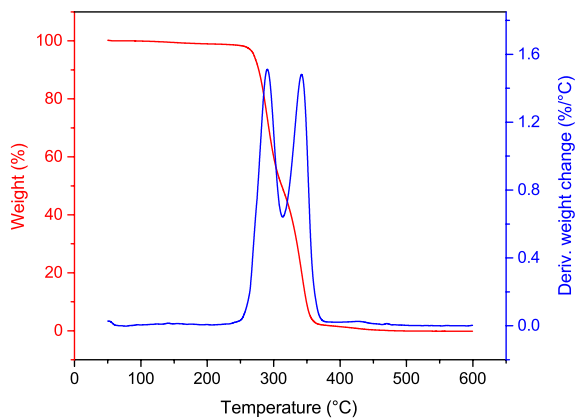
Figure S24. TGA curve of PHB-*b*-PDL prepared from one-pot monomer mixture (Table 1, entry 5).
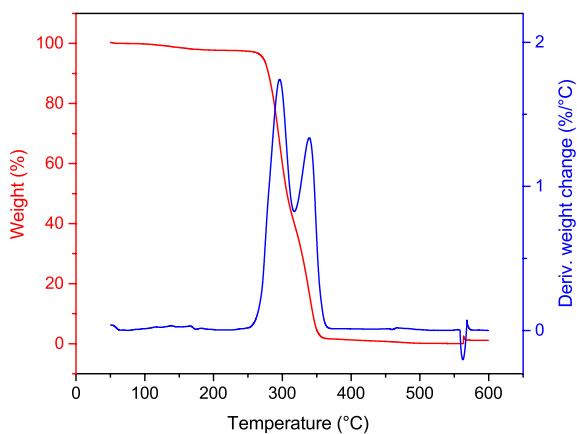
Figure S25. TGA curve of PHB-*b*-PDL prepared from one-pot monomer mixture (Table 1, entry 6).

S17
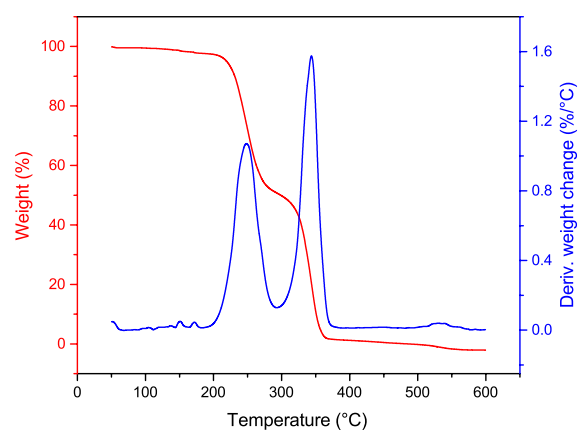
Figure S26. TGA curve of PHB-*b*-PDL-*b*-PHB-*b*-PDL prepared from one-pot monomer mixture (Table 1, entry 9).

2.5 DOSY NMR Spectra of Polymers
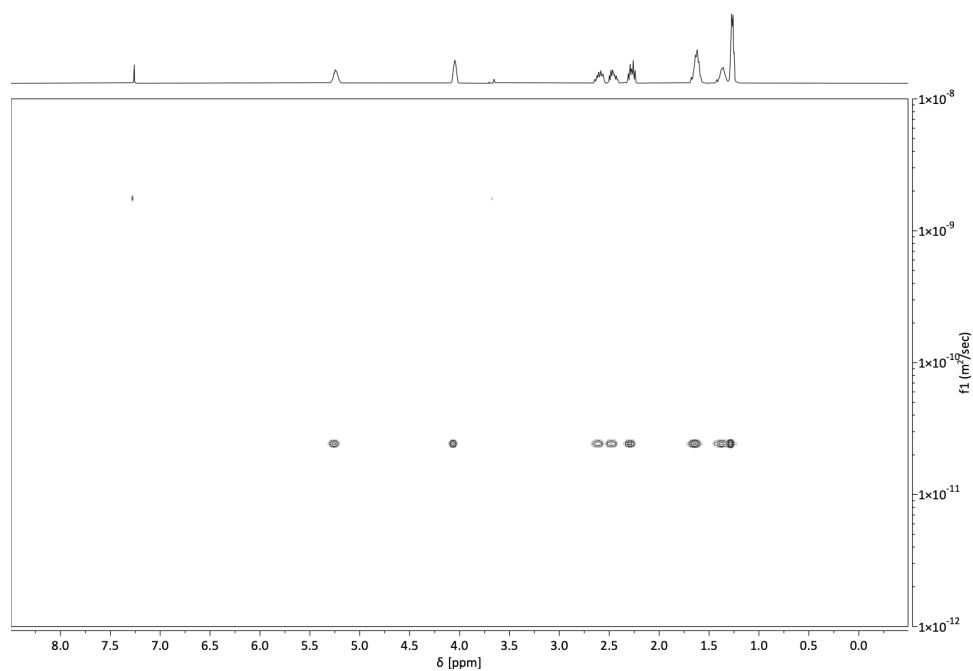
Figure S27. DOSY NMR spectrum (CDCl₃) of PHB-*co*-PCL (Table 1, entry 1).

S18
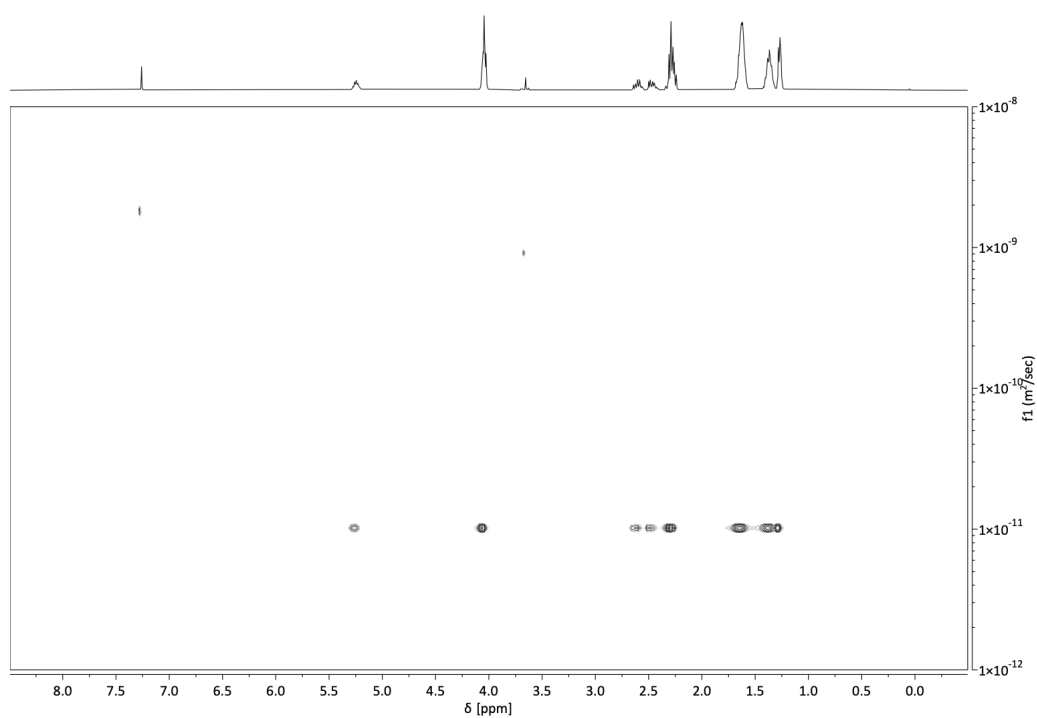
Figure S28. DOSY NMR spectrum (CDCl₃) of PHB-*co*-PCL (Table 1, entry 2).
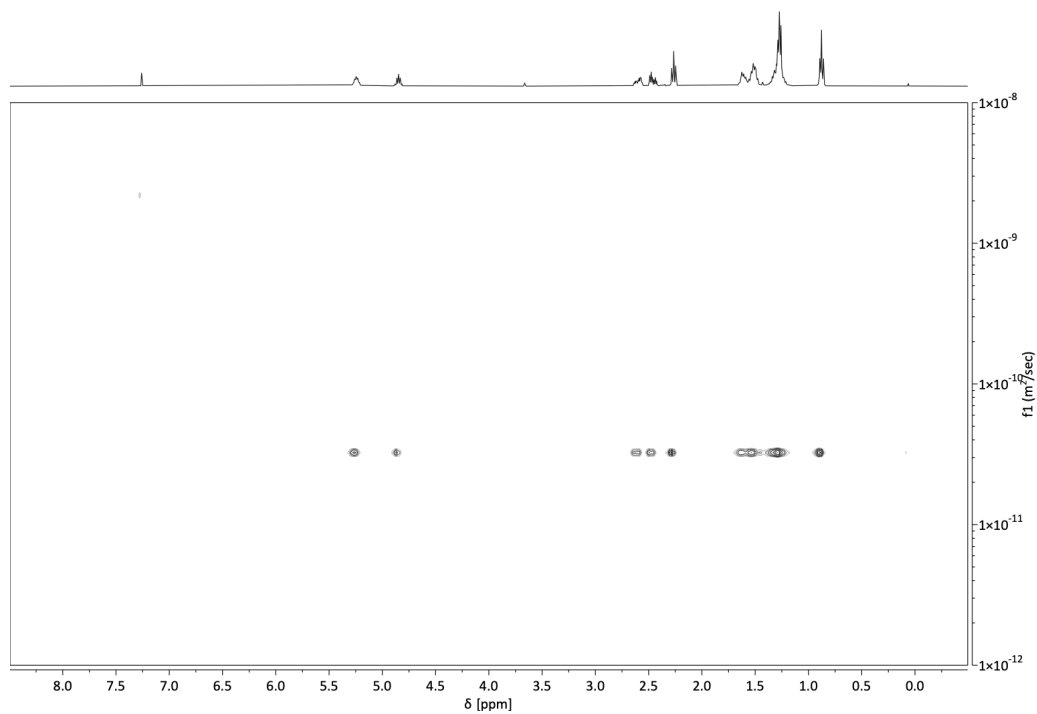
Figure S29. DOSY NMR spectrum (CDCl₃) of PHB-*b*-PDL prepared *via* sequential addition (Table 1, entry 3).

S19
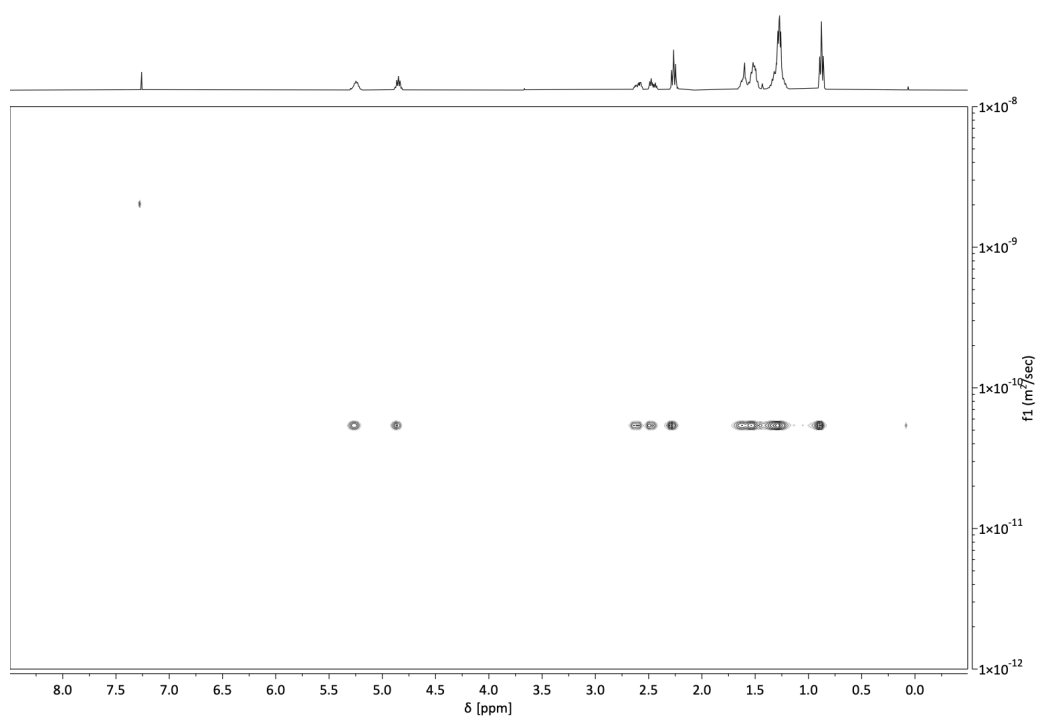
Figure S30. DOSY NMR spectrum (CDCl₃) of PHB-*b*-PDL prepared from one-pot monomer mixture (Table 1, entry 4).
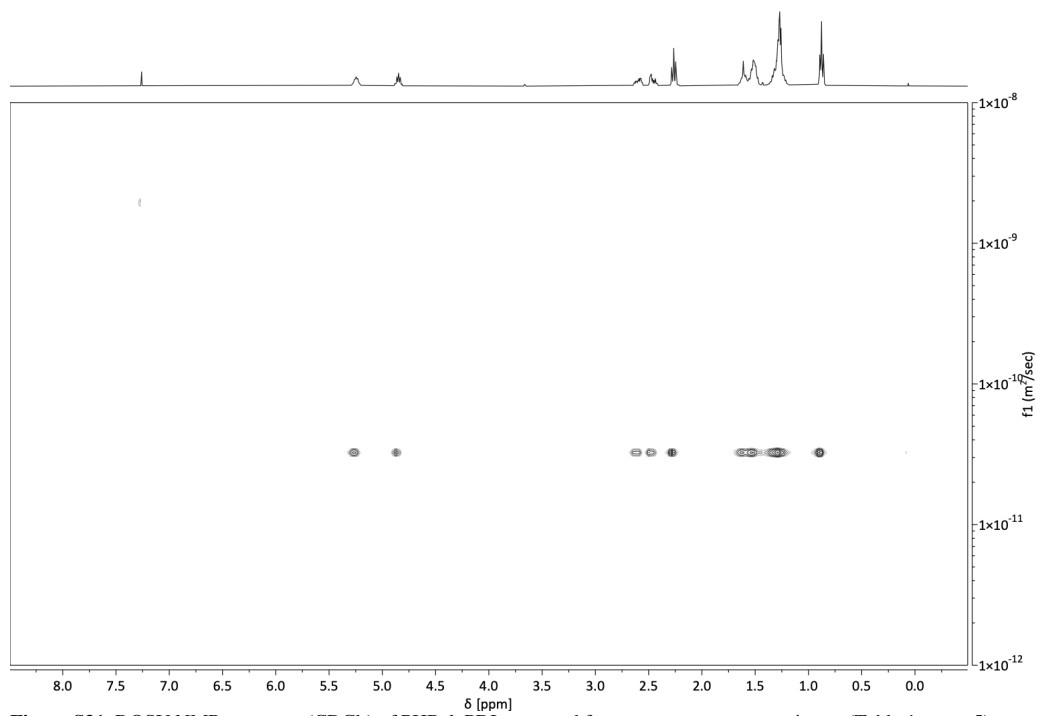
Figure S31. DOSY NMR spectrum (CDCl₃) of PHB-*b*-PDL prepared from one-pot monomer mixture (Table 1, entry 5).

S20

162
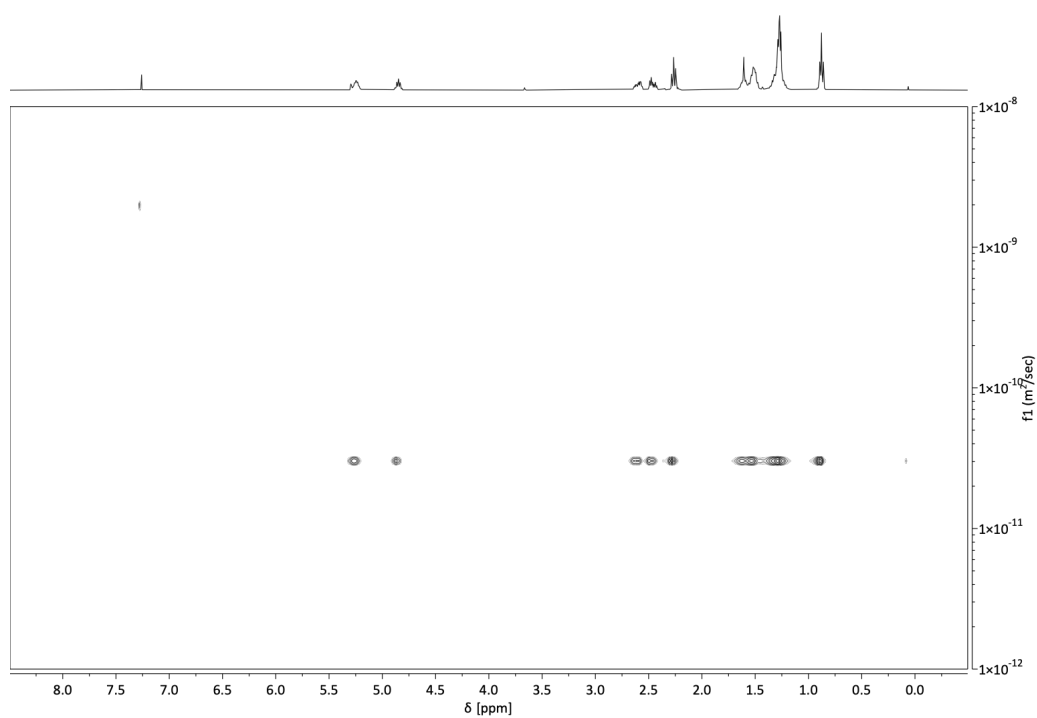
Figure S32. DOSY NMR spectrum (CDCl₃) of PHB-*b*-PDL prepared from one-pot monomer mixture (Table 1, entry 6).
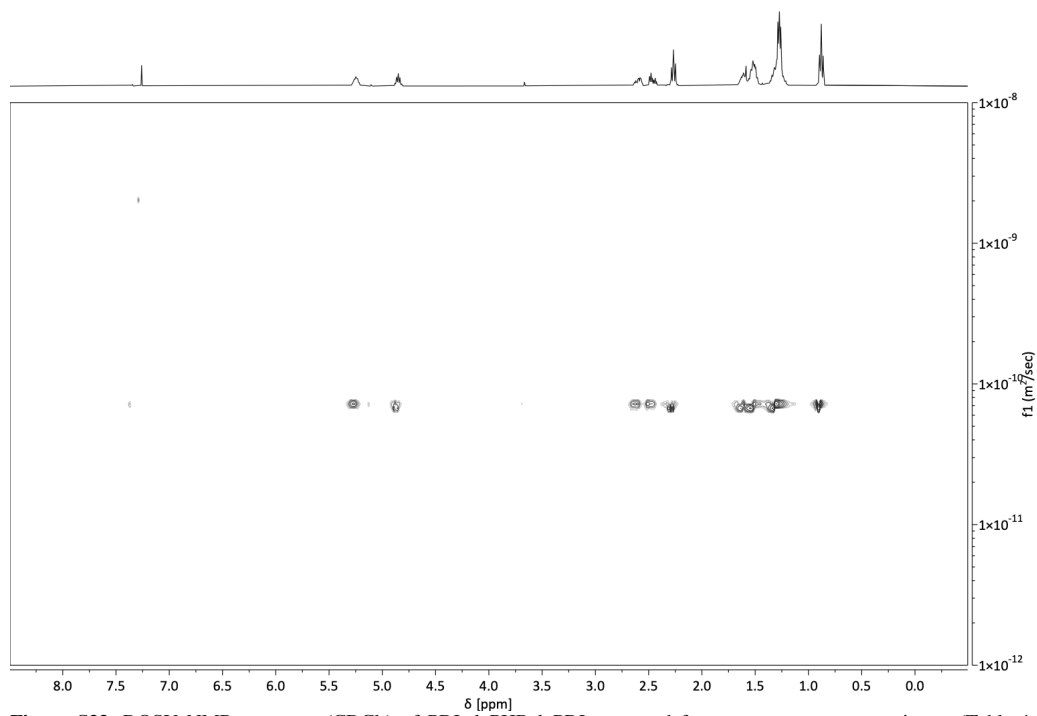
Figure S33. DOSY NMR spectrum (CDCl₃) of PDL-*b*-PHB-*b*-PDL prepared from one-pot monomer mixture (Table 1, entry 8).

S21
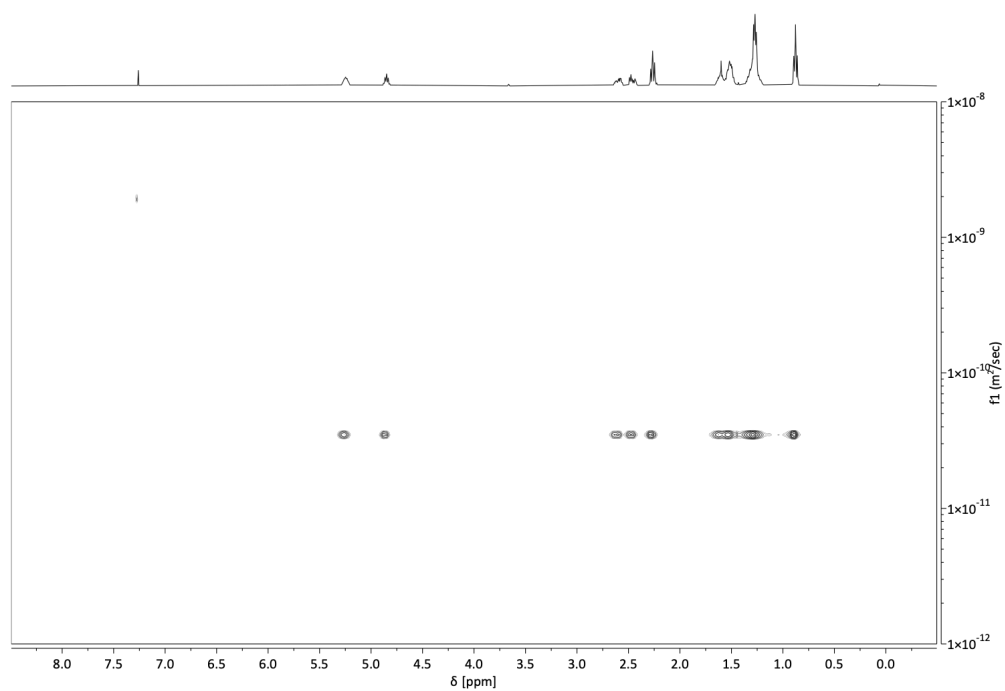
Figure S34. DOSY NMR spectrum (CDCl₃) of PHB-*b*-PDL-*b*-PHB-*b*-PDL prepared from one-pot monomer mixture (Table 1, entry 9).
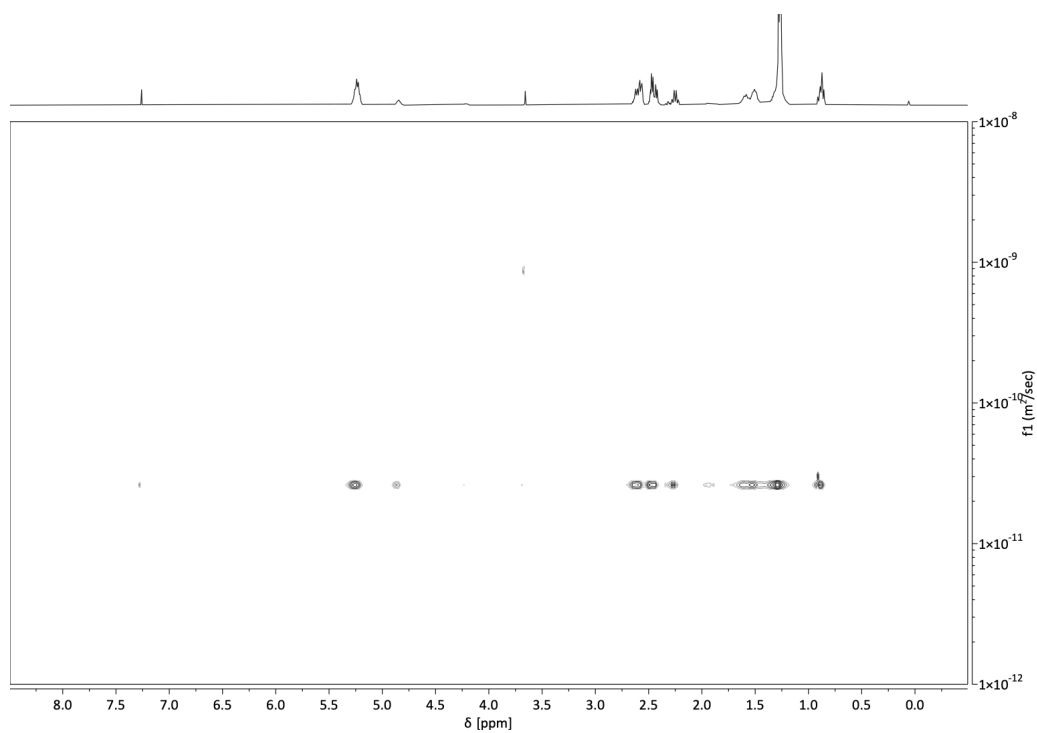
Figure S35. DOSY NMR spectrum (CDCl₃) of PHB-*co*-PDL prepared from one-pot monomer mixture with **Y1** (Table S1, entry 7).

S22

164
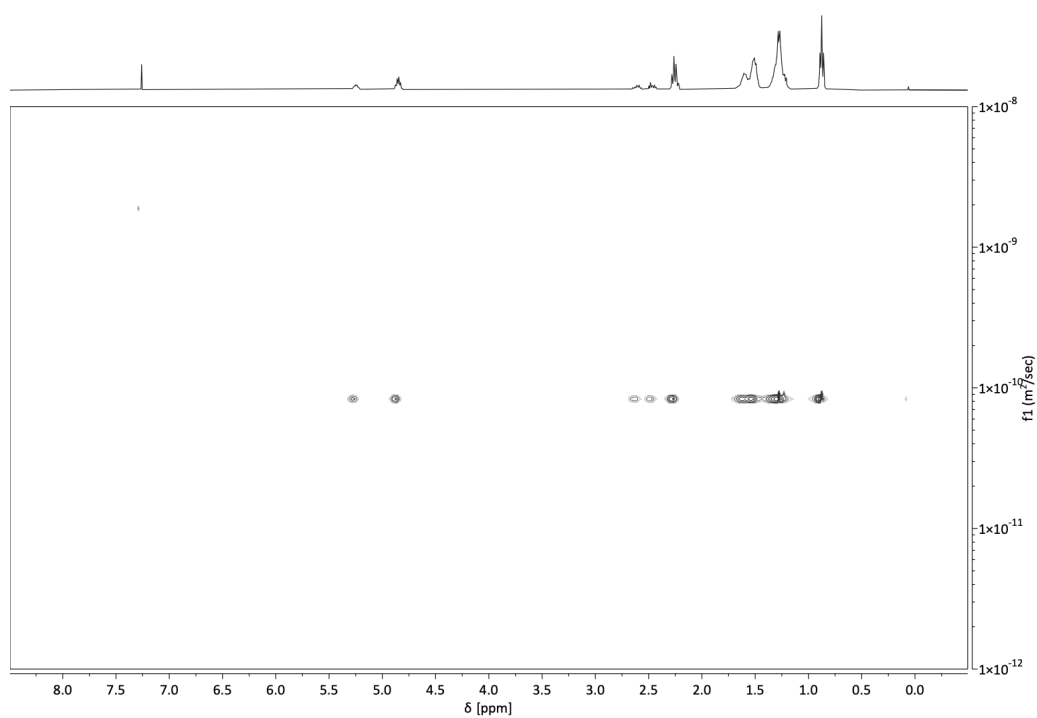
Figure S36. DOSY NMR spectrum (CDCl₃) of PHB-*co*-PDL prepared from one-pot monomer mixture with Ti(OⁱPr)₄ (Table S1, entry 10).
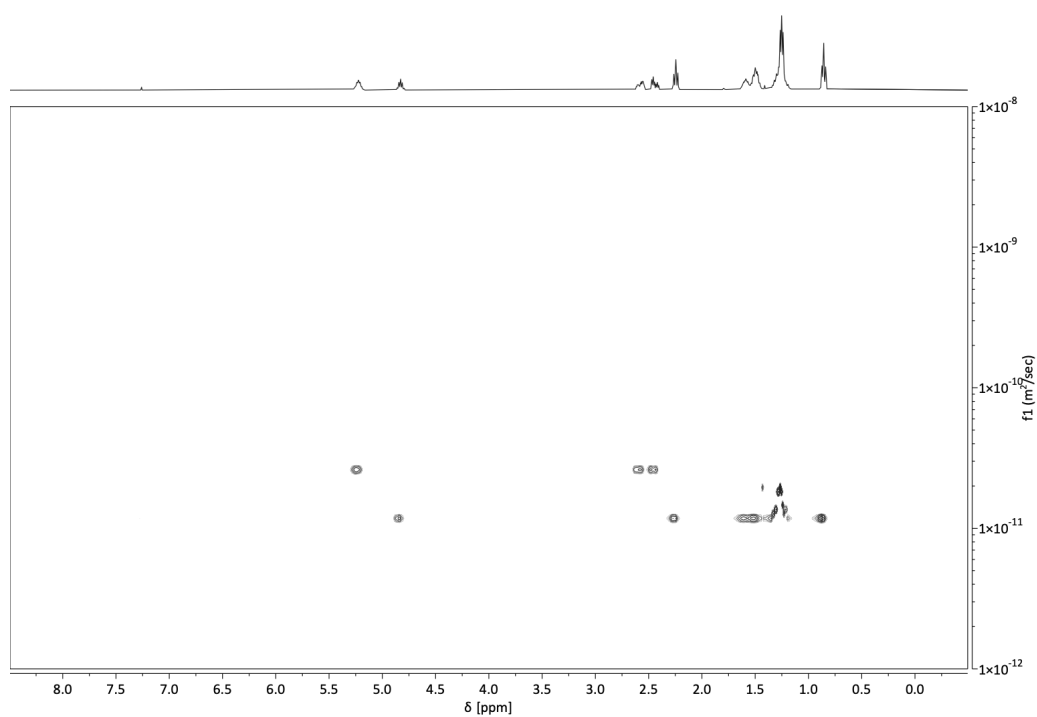
Figure S37. DOSY NMR spectrum (CDCl₃) of a blend of PHB homopolymer ($[\beta$-BL]/[**1**] = 200/1, M_n = 21.2 kg mol⁻¹) and PDL homopolymer ($[\varepsilon$-DL]/[**1**] = 200/1, M_n = 50.8 kg mol⁻¹).

S23

2.6 ^{1}H and ^{13}C NMR Spectra of Polymers
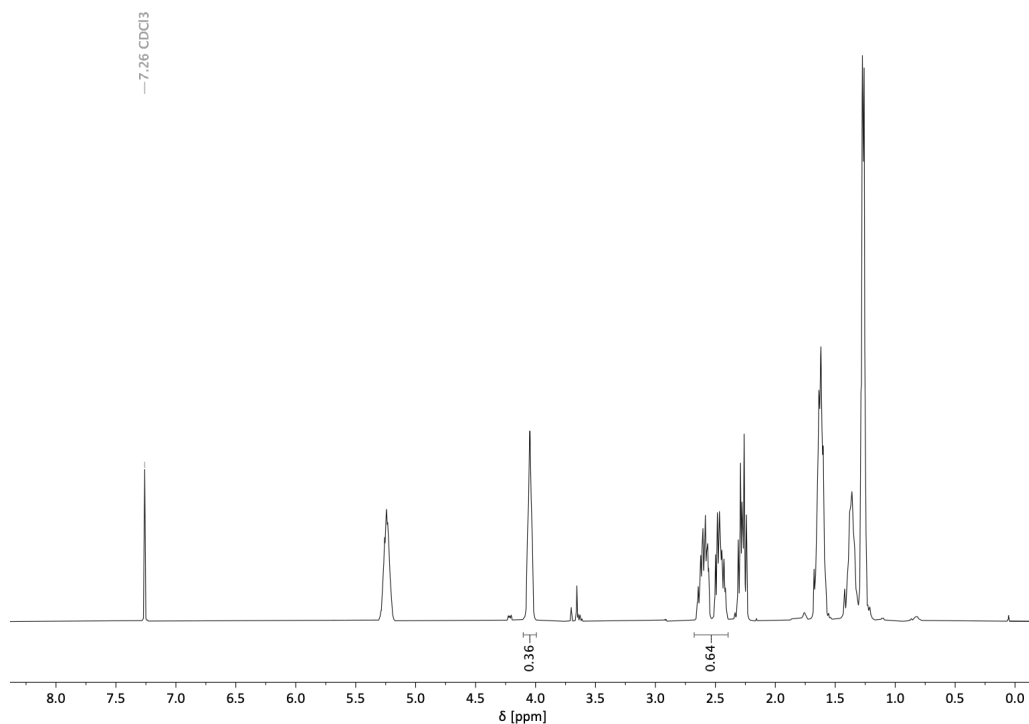
Figure S38. ^{1}H NMR spectrum (CDCl$_3$) of PHB-*co*-PCL (Table 1, entry 1).
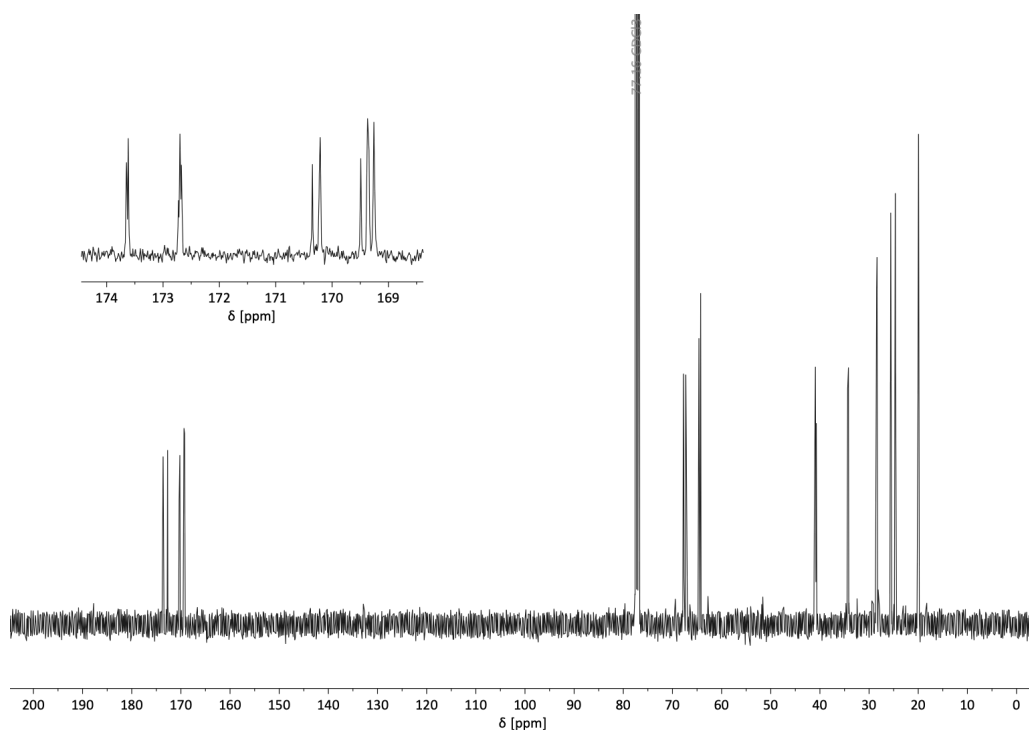
Figure S39. ^{13}C NMR spectrum (CDCl$_3$) of PHB-*co*-PCL (Table 1, entry 1).

S24

166
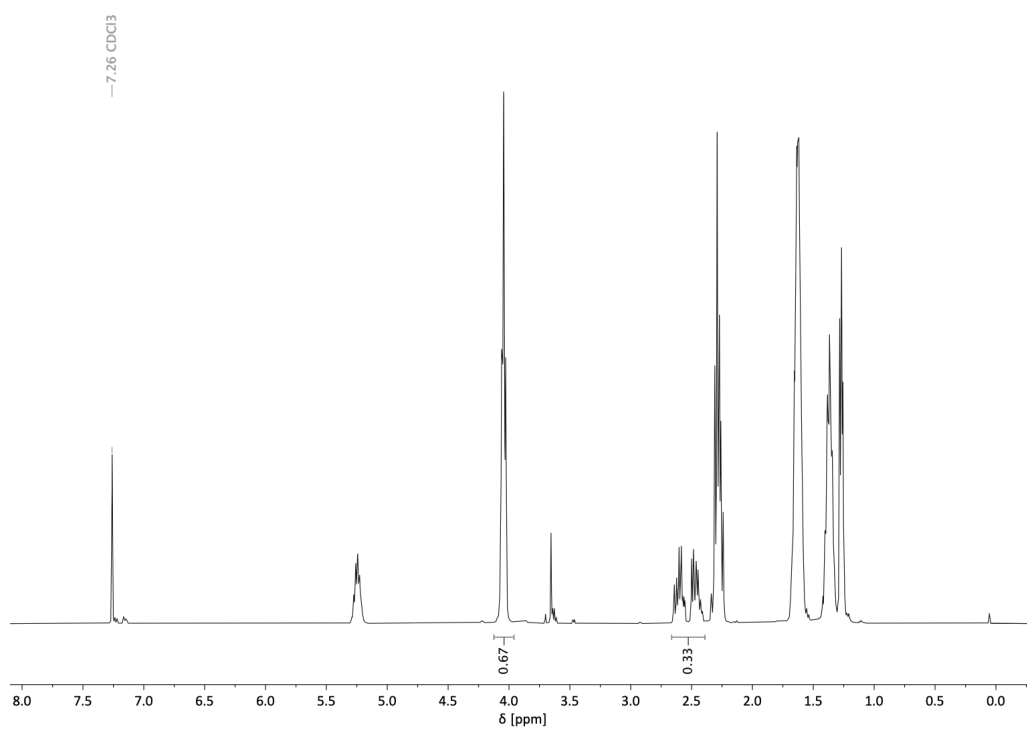
Figure S40. ^{1}H NMR spectrum (CDCl$_3$) of PHB-*co*-PCL (Table 1, entry 2).
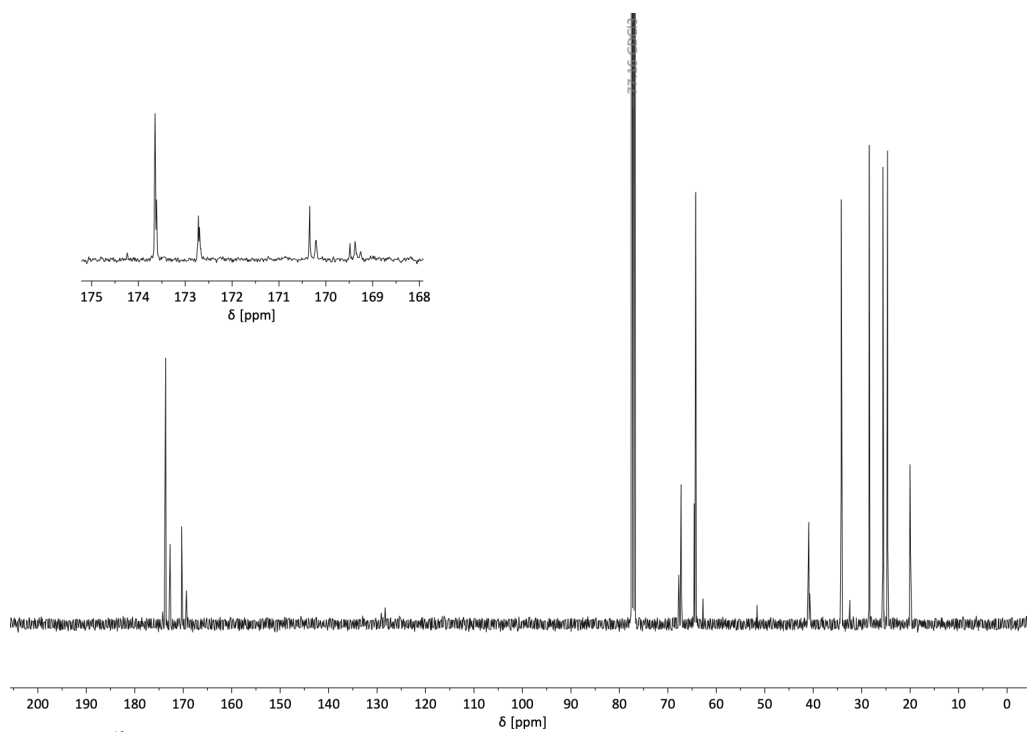
Figure S41. ^{13}C NMR spectrum (CDCl$_3$) of PHB-*co*-PCL (Table 1, entry 2).

S25
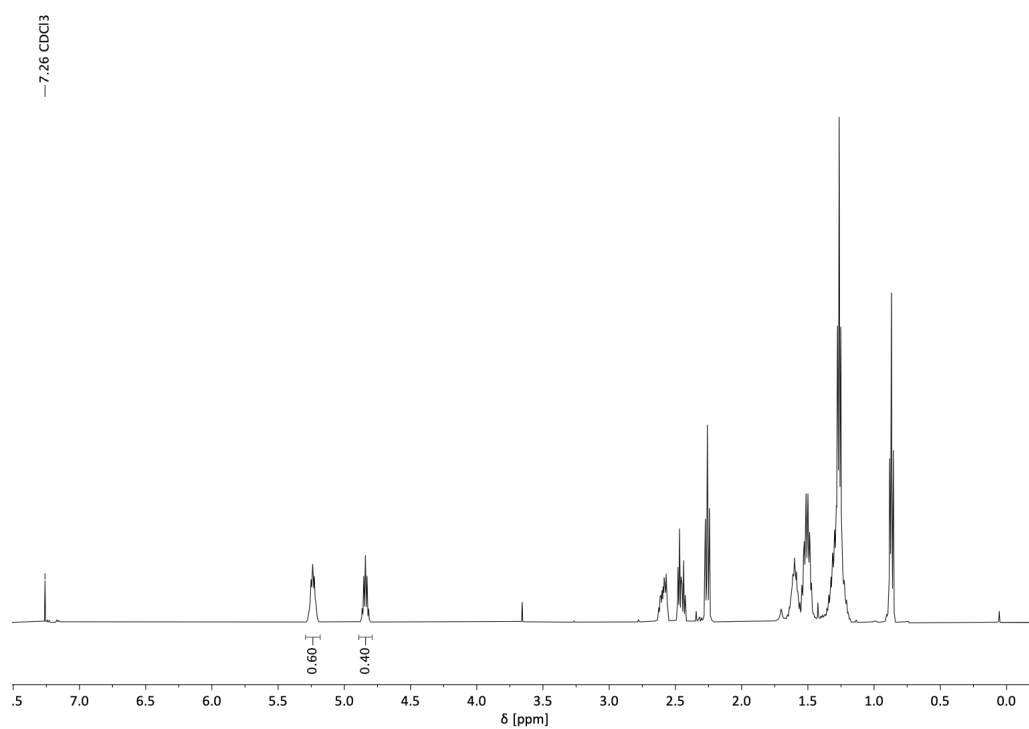
Figure S42. ^{1}H NMR spectrum (CDCl$_3$) of PHB-*b*-PDL prepared *via* sequential addition (Table 1, entry 3).
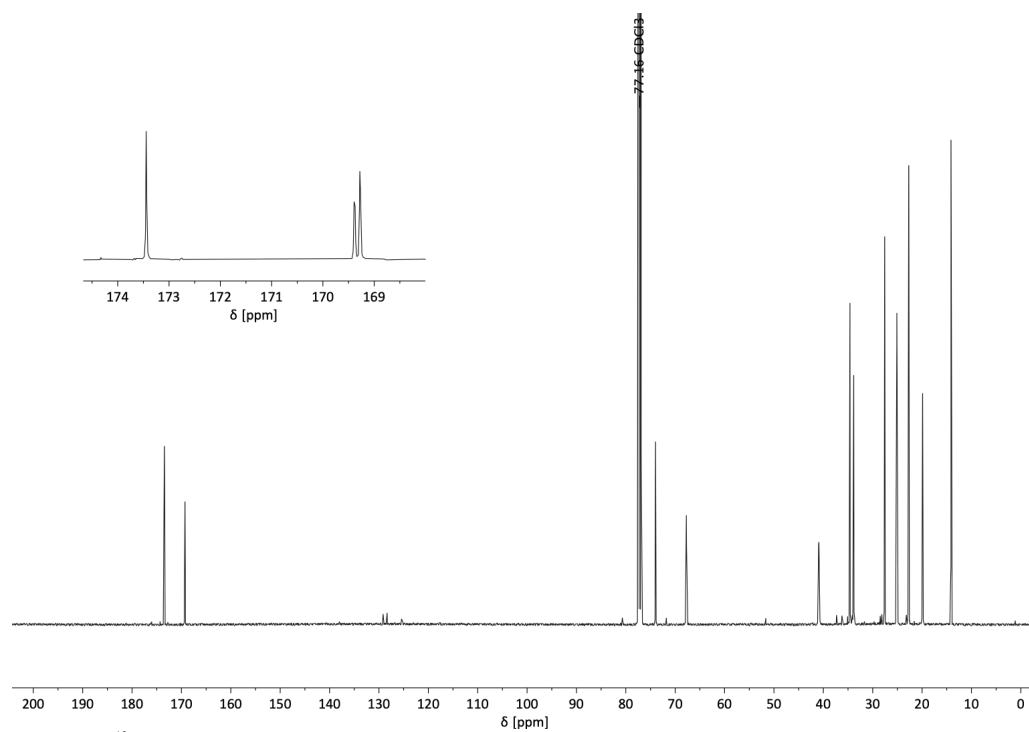
Figure S43. ^{13}C NMR spectrum (CDCl$_3$) of PHB-*b*-PDL prepared *via* sequential addition (Table 1, entry 3).

S26
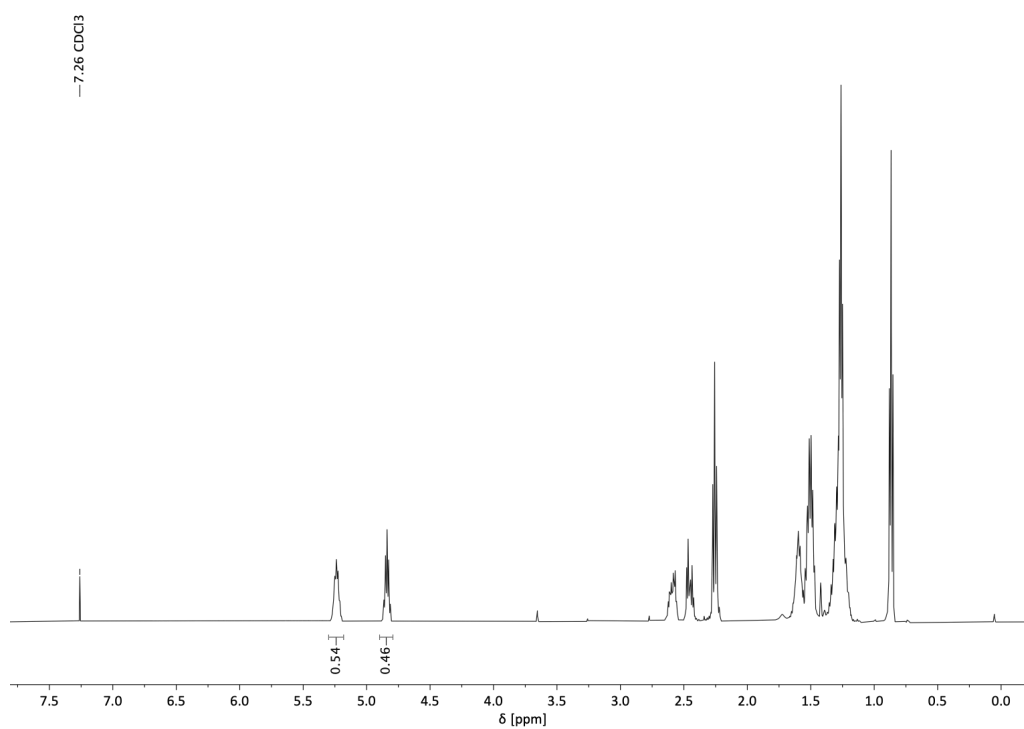
Figure S44. ^{1}H NMR spectrum (CDCl$_3$) of PHB-*b*-PDL prepared from one-pot monomer mixture (Table 1, entry 4).
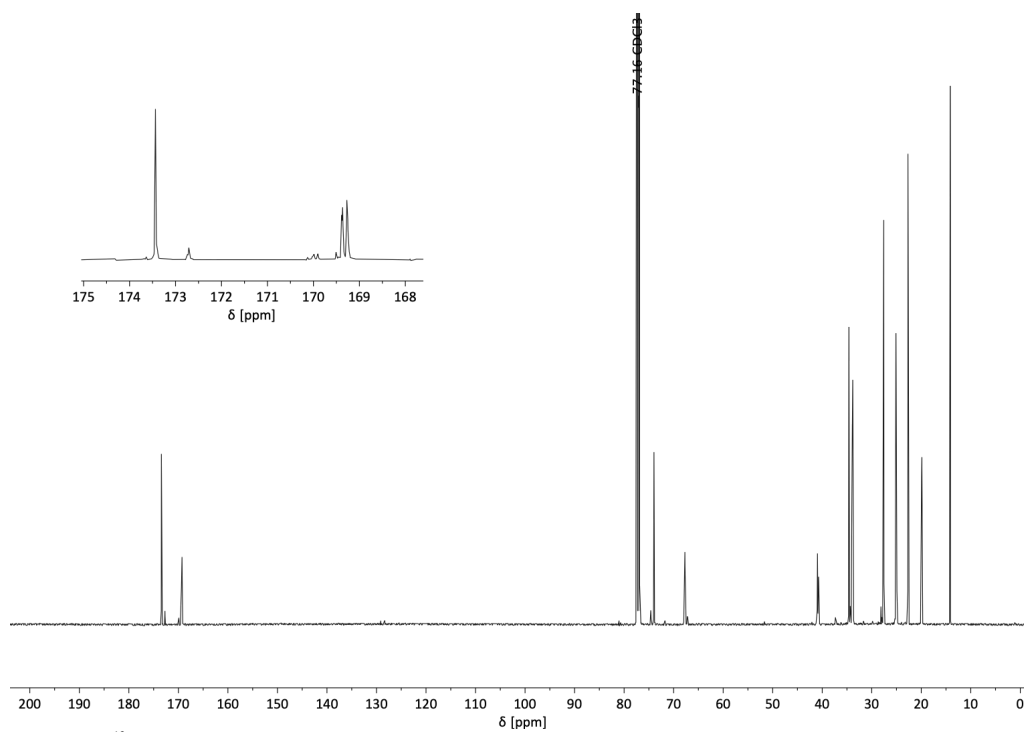
Figure S45. ^{13}C NMR spectrum (CDCl$_3$) of PHB-*b*-PDL prepared from one-pot monomer mixture (Table 1, entry 4).

S27
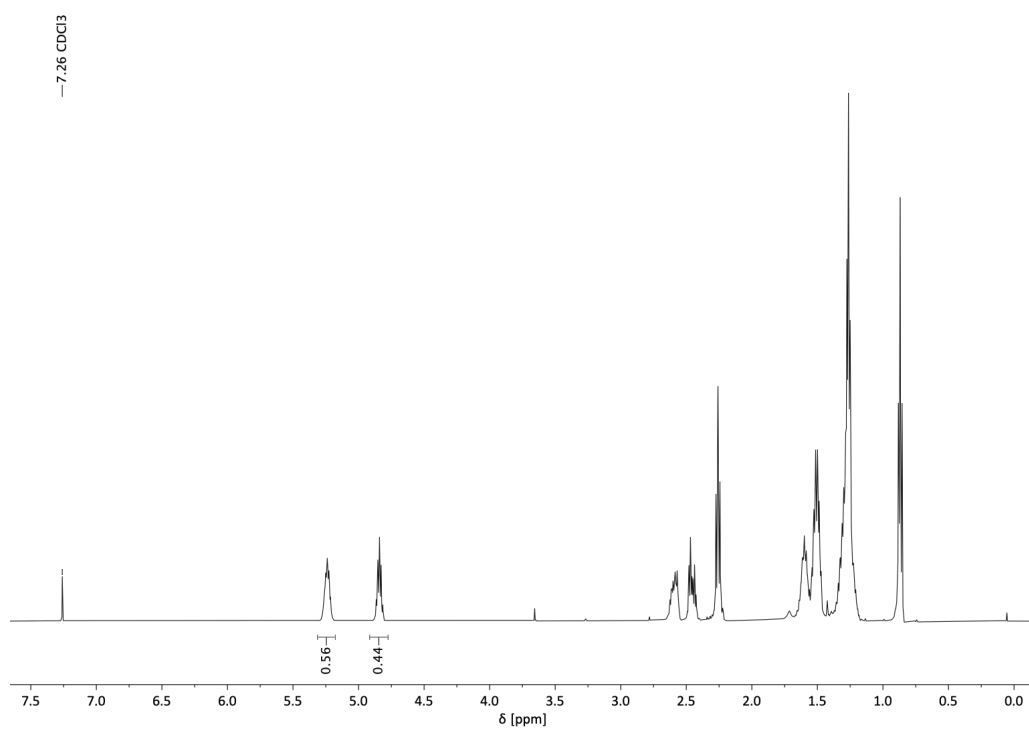
Figure S46. ¹H NMR spectrum (CDCl₃) of PHB-*b*-PDL prepared from one-pot monomer mixture (Table 1, entry 5).
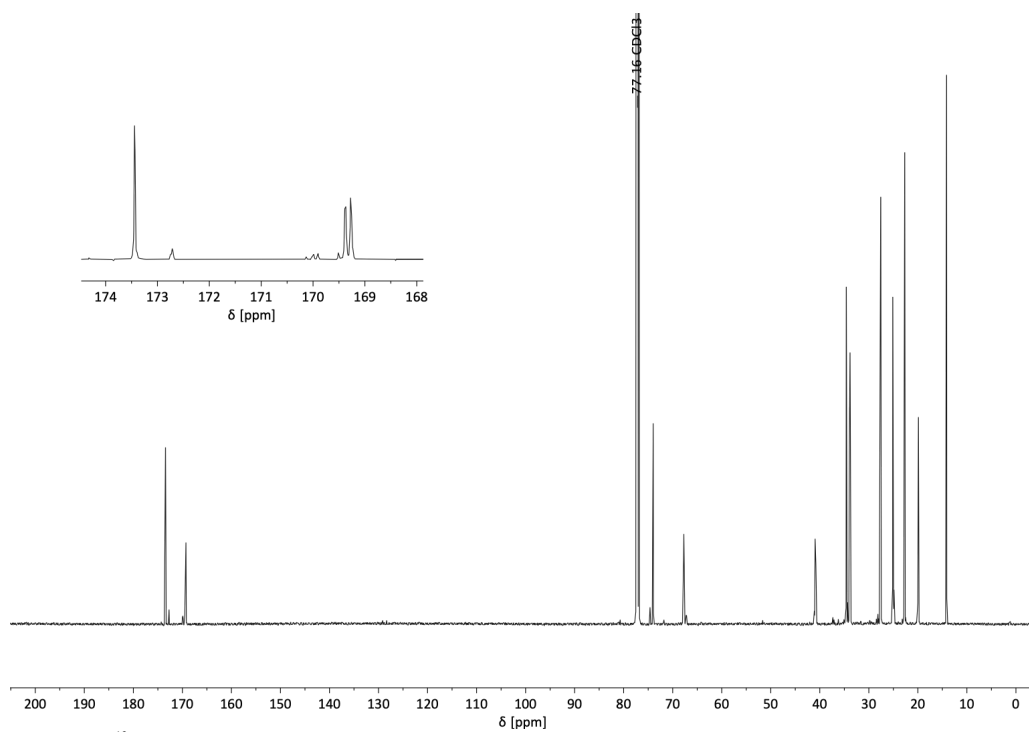
Figure S47. ¹³C NMR spectrum (CDCl₃) of PHB-*b*-PDL prepared from one-pot monomer mixture (Table 1, entry 5).

S28
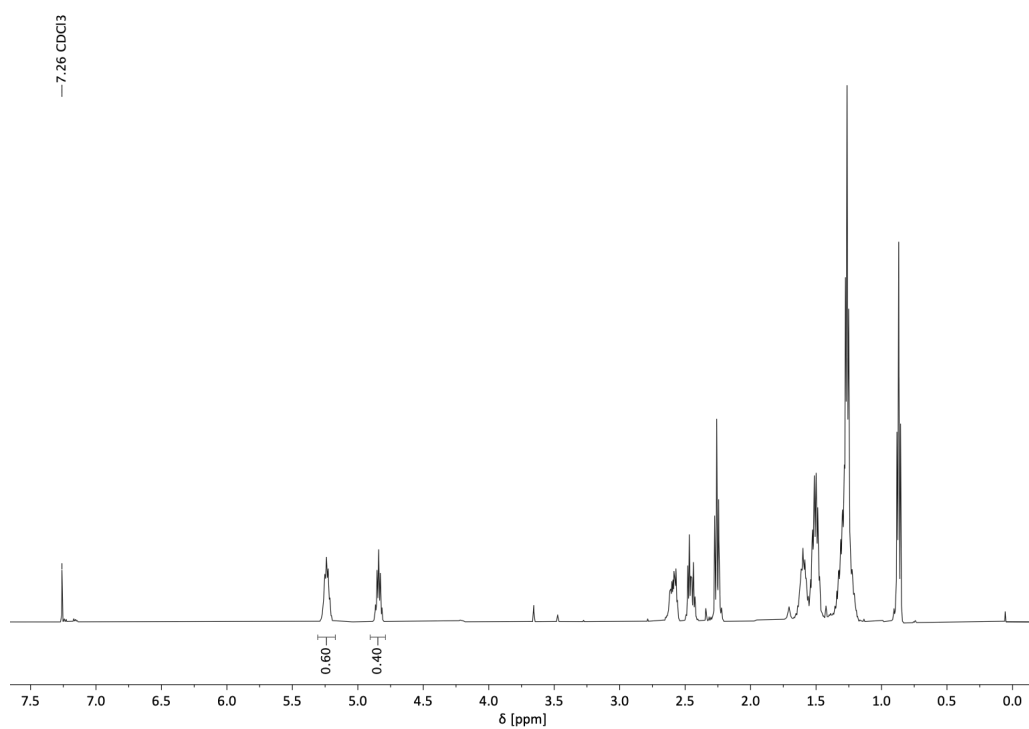
Figure S48. ^{1}H NMR spectrum (CDCl$_3$) of PHB-*b*-PDL prepared from one-pot monomer mixture (Table 1, entry 6).
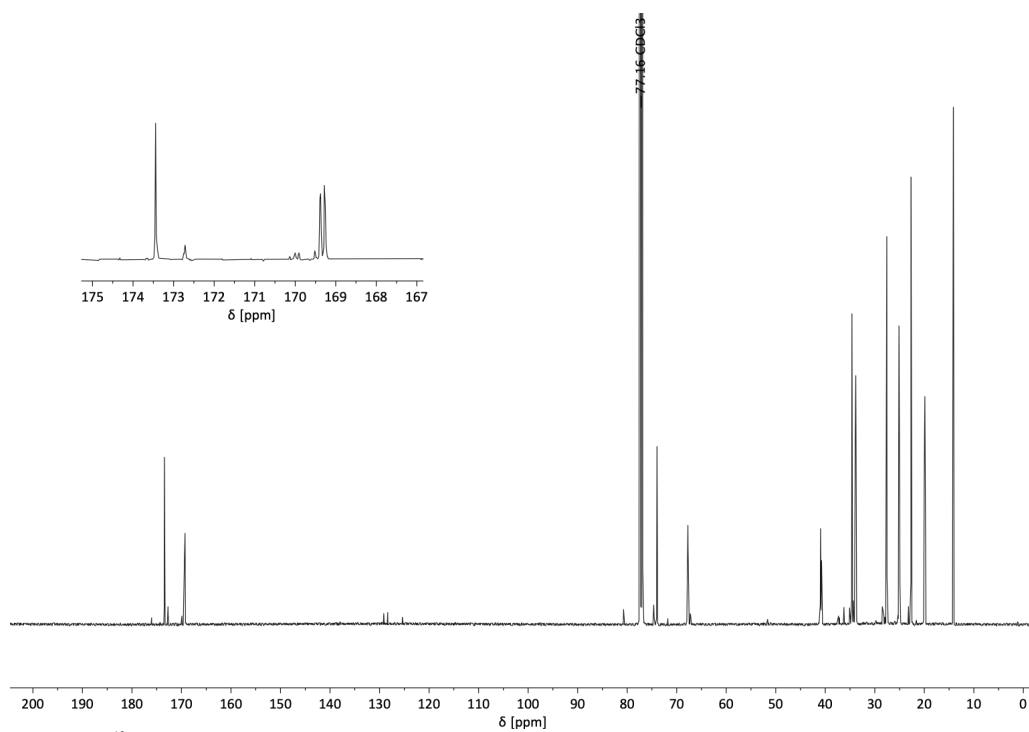
Figure S49. ^{13}C NMR spectrum (CDCl$_3$) of PHB-*b*-PDL prepared from one-pot monomer mixture (Table 1, entry 6).

S29

171
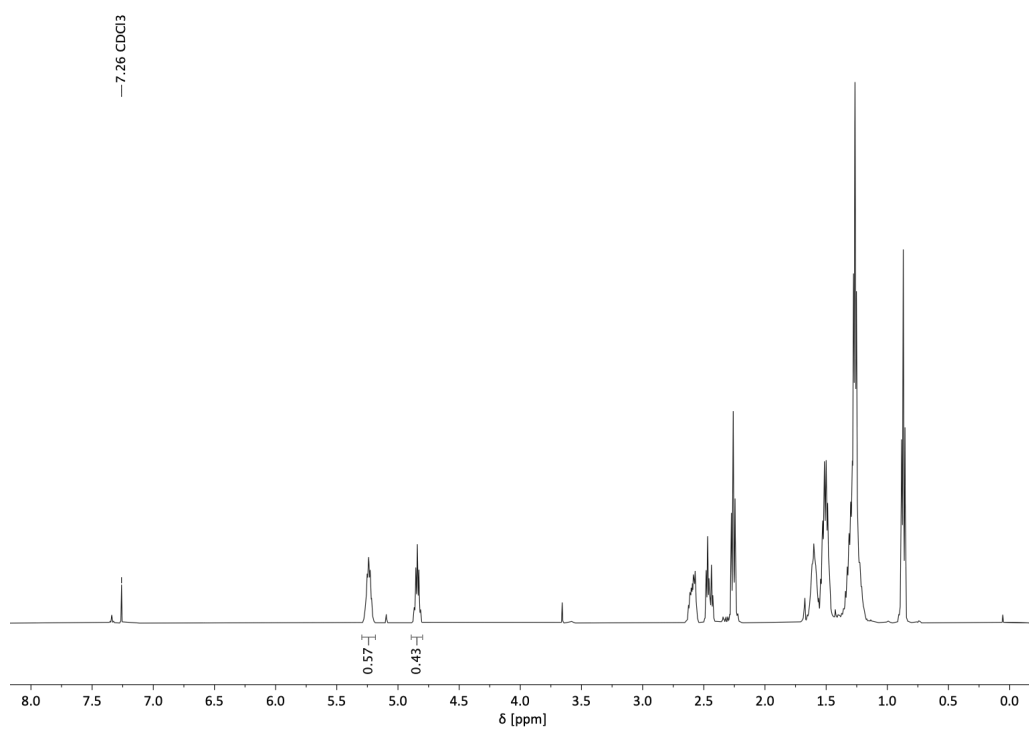
Figure S50. ¹H NMR spectrum (CDCl₃) of PDL-*b*-PHB-*b*-PDL prepared from one-pot monomer mixture (Table 1, entry 8).
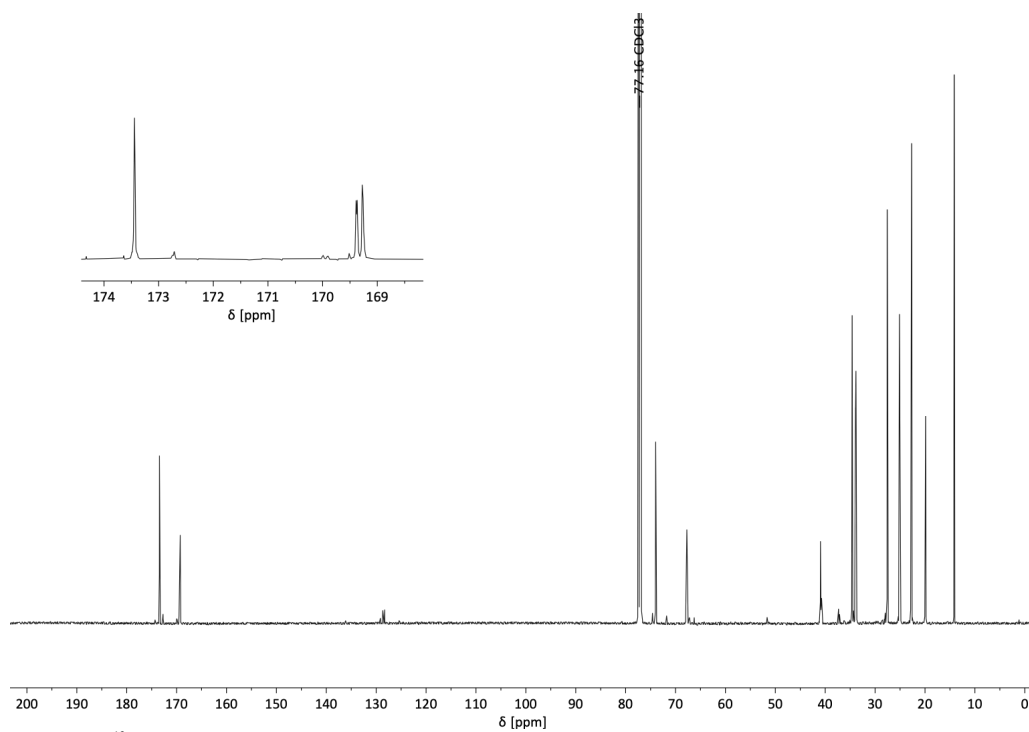
Figure S51. ¹³C NMR spectrum (CDCl₃) of PDL-*b*-PHB-*b*-PDL prepared from one-pot monomer mixture (Table 1, entry 8).

S30
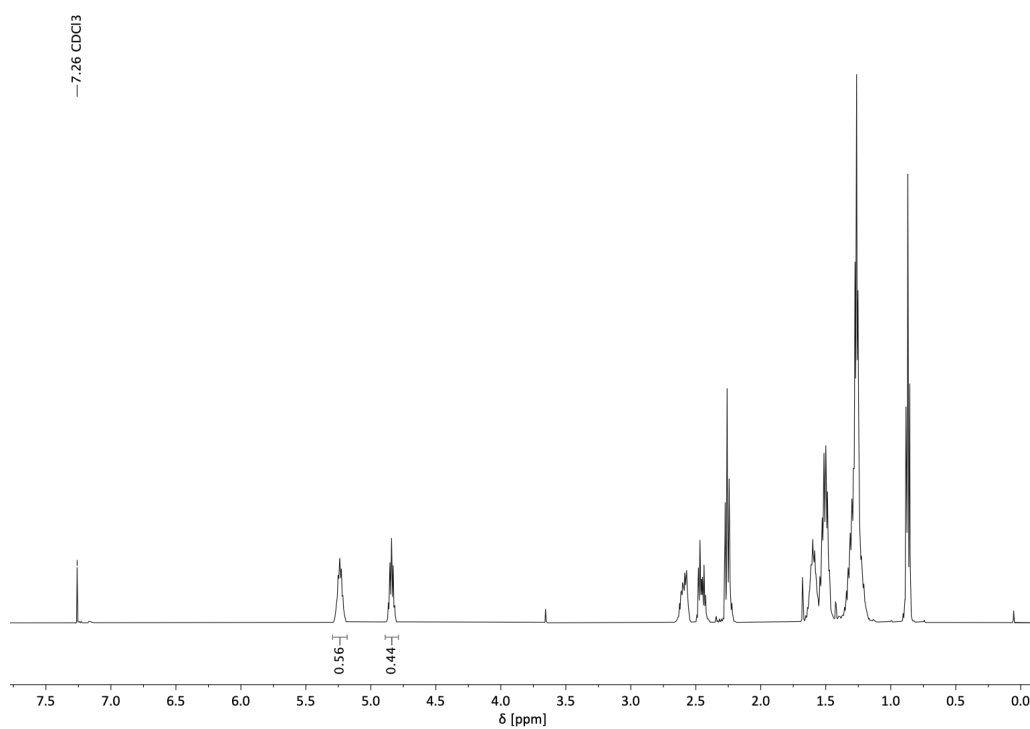
Figure S52. ¹H NMR spectrum (CDCl₃) of PHB-*b*-PDL-*b*-PHB-*b*-PDL prepared from one-pot monomer mixture (Table 1, entry 9).
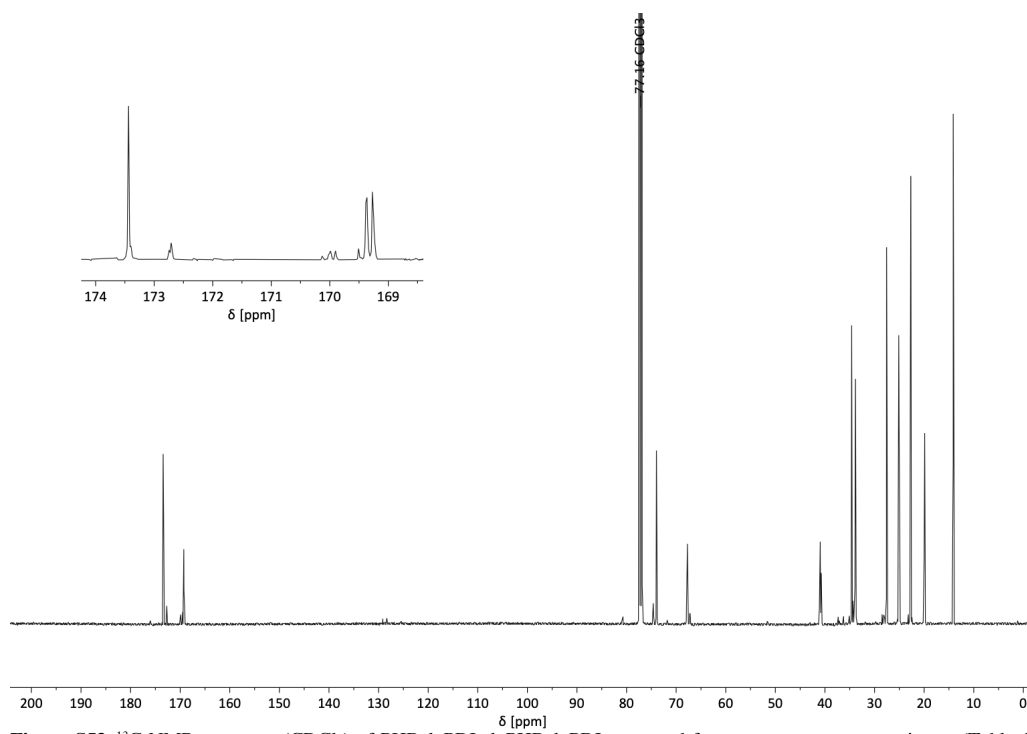
Figure S53. ¹³C NMR spectrum (CDCl₃) of PHB-*b*-PDL-*b*-PHB-*b*-PDL prepared from one-pot monomer mixture (Table 1, entry 9).

S31
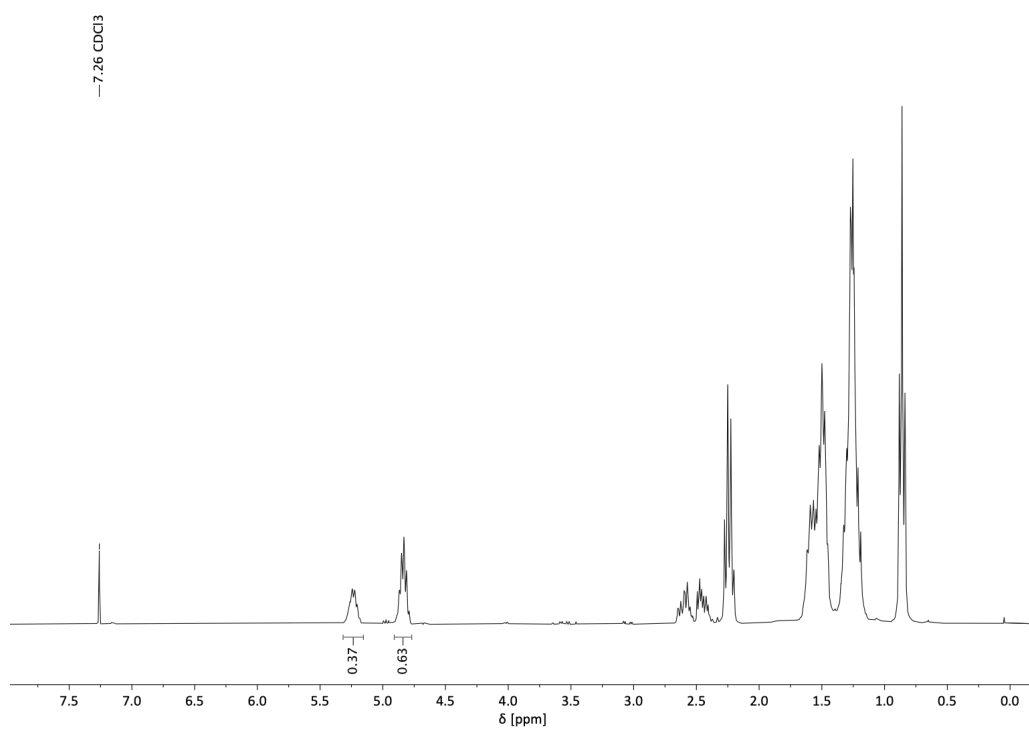
Figure S54. ^{1}H NMR spectrum (CDCl$_3$) of PHB-*co*-PDL prepared from one-pot monomer mixture with Ti(O^{i}Pr)$_4$ (Table S1, entry 10).
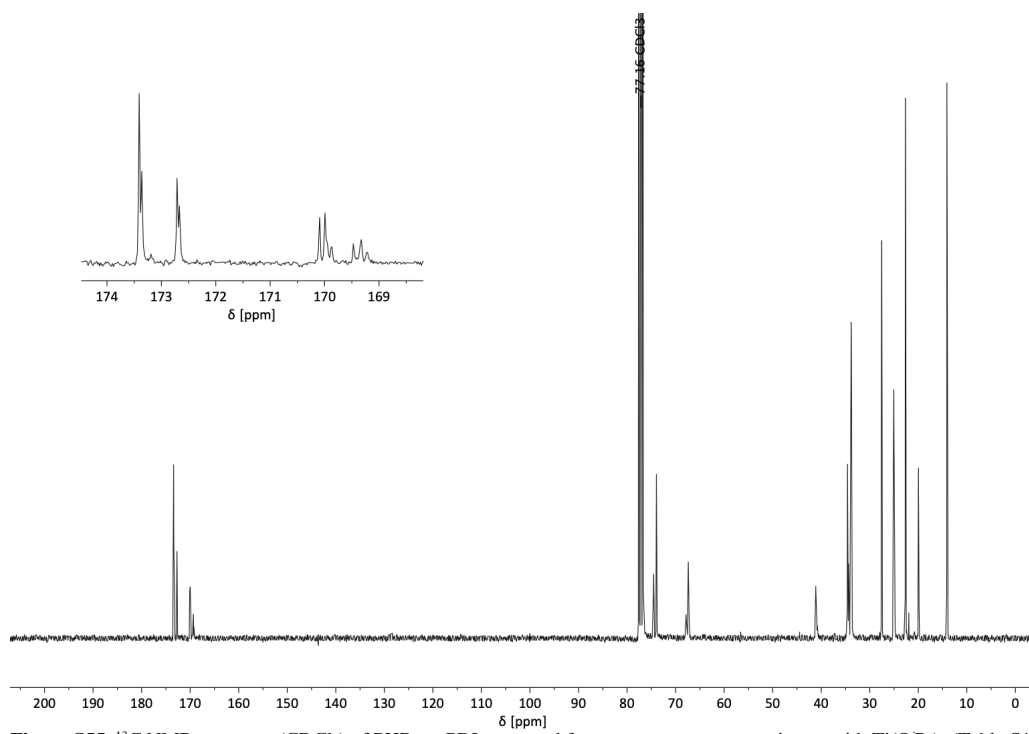
Figure S55. ^{13}C NMR spectrum (CDCl$_3$) of PHB-*co*-PDL prepared from one-pot monomer mixture with Ti(O^{i}Pr)$_4$ (Table S1, entry 10).

S32

2.7 GPC Traces of Polymers
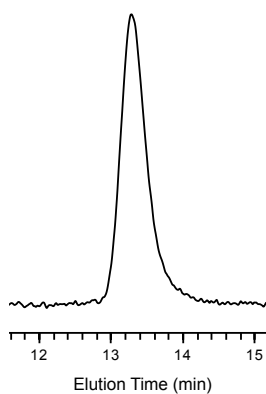
Figure S56. GPC trace of PHB-*co*-PCL (M_n = 48.6 kg mol^{-1}, $Đ$ = 1.07; Table 1, entry 1).
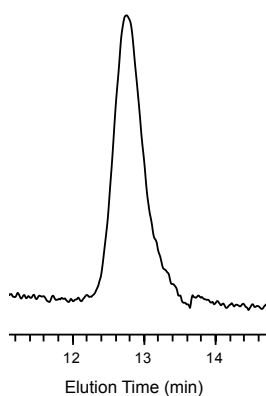
Figure S57. GPC trace of PHB-*co*-PCL (M_n = 88.9 kg mol^{-1}, $Đ$ = 1.07; Table 1, entry 2).
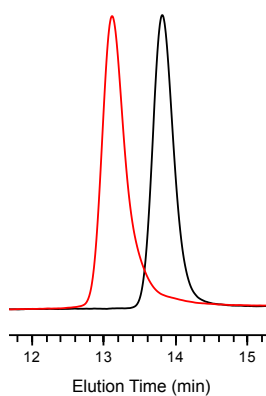
Figure S58. GPC trace of PHB-*b*-PDL (red trace, M_n = 51.0 kg mol^{-1}, $Đ$ = 1.08) prepared *via* sequential addition (Table 1, entry 3). Black trace: GPC trace of PHB block prior to ε-DL addition (M_n = 24.3 kg mol^{-1}, $Đ$ = 1.03).

S33
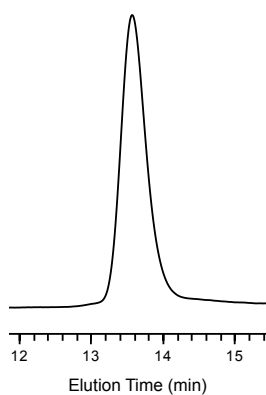
Figure S59. GPC trace of PHB-*b*-PDL prepared from one-pot monomer mixture (M_n = 31.8 kg mol^{-1}, Đ = 1.06; Table 1, entry 4).
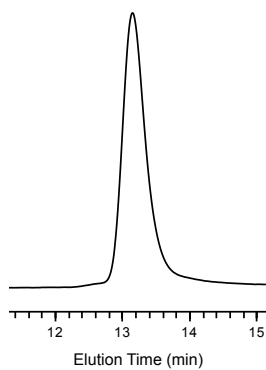
Figure S60. GPC trace of PHB-*b*-PDL prepared from one-pot monomer mixture (M_n = 49.7 kg mol^{-1}, Đ = 1.08; Table 1, entry 5).
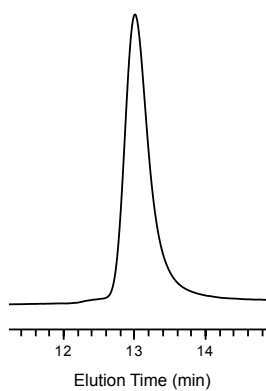
Figure S61. GPC trace of PHB-*b*-PDL prepared from one-pot monomer mixture (M_n = 58.9 kg mol^{-1}, Đ = 1.07; Table 1, entry 6).

S34
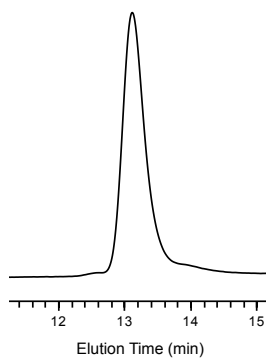
Figure S62. GPC trace of PHB-*b*-PDL-*b*-PHB-*b*-PDL prepared from one-pot monomer mixture (M_n = 50.2 kg mol^{-1}, Đ = 1.09; Table 1, entry 9).

2.8 Miscellaneous
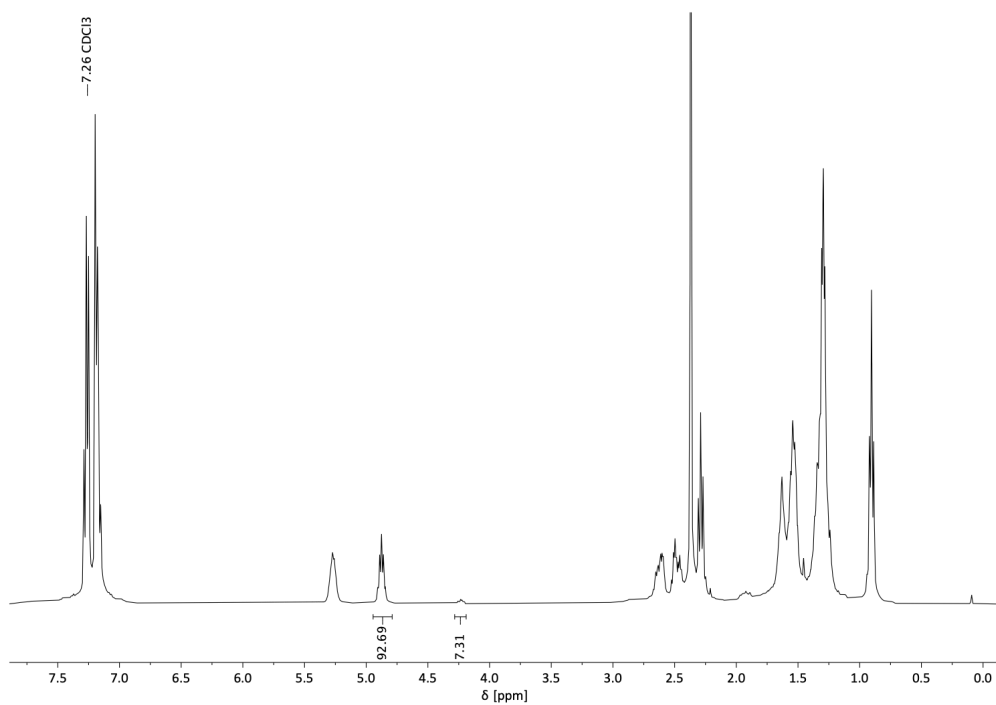
Figure S63. Representative ^{1}H NMR spectrum (CDCl$_3$) of an aliquot from the polymerization mixture for determination of *ε*-DL conversion.

S35
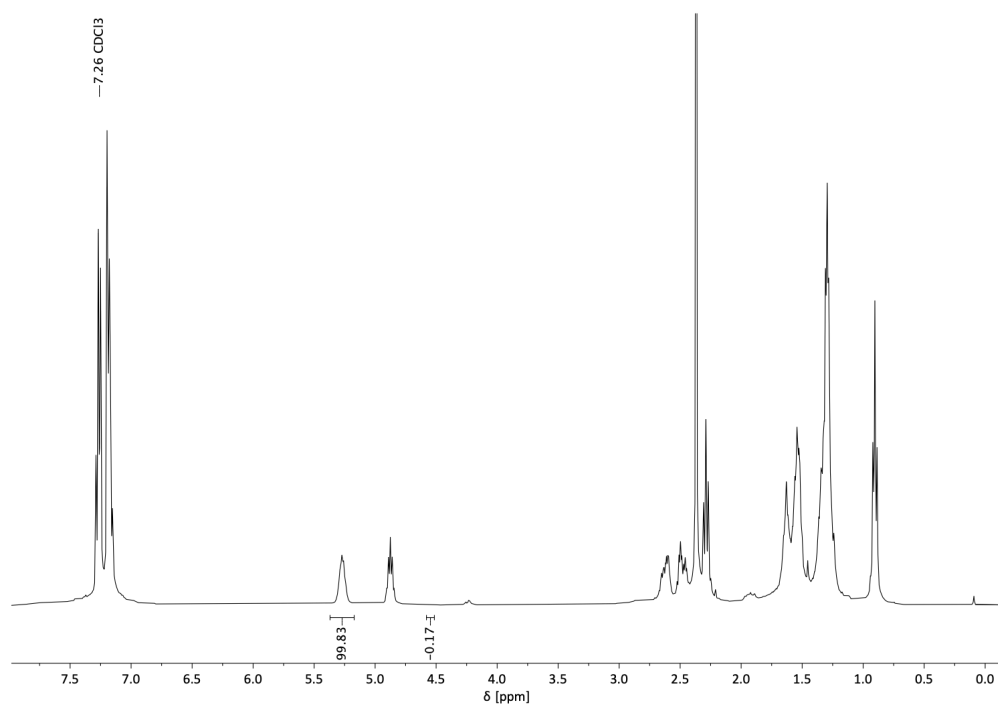
Figure S64. Representative ^{1}H NMR spectrum (CDCl$_3$) of an aliquot from the polymerization mixture for determination of β-BL conversion.

S36

3. References

1. Bruckmoser, J.; Henschel, D.; Vagin, S.; Rieger, B., Combining high activity with broad monomer scope: indium salan catalysts in the ring-opening polymerization of various cyclic esters. *Catal. Sci. Technol.* **2022,** *12*, 3295-3302.

2. Cai, C.-X.; Toupet, L.; Lehmann, C. W.; Carpentier, J.-F., Synthesis, structure and reactivity of new yttrium bis(dimethylsilyl)amido and bis(trimethylsilyl)methyl complexes of a tetradentate bis(phenoxide) ligand. *J. Organomet. Chem.* **2003,** *683*, 131-136.

3. Save, M.; Schappacher, M.; Soum, A., Controlled ring-opening polymerization of lactones and lactides initiated by lanthanum isopropoxide, 1. General aspects and kinetics. *Macromol. Chem. Phys.* **2002,** *203*, 889-899.

10.3 Supporting Information for Chapter 6

Supporting Information

For

Ring-Opening Polymerization of a Bicyclic Lactone – Polyesters Derived from Norcamphor with Complete Chemical Recyclability

Jonas Bruckmoser,[‡] Sebastian Remke,[‡] and Bernhard Rieger[*]

WACKER-Chair of Macromolecular Chemistry, Catalysis Research Center,
Department of Chemistry, Technical University of Munich
Lichtenbergstraße 4, 85748 Garching bei München, Germany.

[*]Corresponding Author; email: rieger@tum.de

Table of Contents

1. Experimental Section

1.1. Materials and Methods

All manipulations containing air- and/or moisture sensitive compounds were carried out under argon atmosphere using standard Schlenk or glovebox techniques. Glassware was flame-dried under vacuum prior to use. Unless otherwise stated, all chemicals were purchased from Sigma-Aldrich, TCI Chemicals or ABCR and used as received. Solvents were obtained from an MBraun MB-SPS 800 solvent purification system and stored over 3 Å molecular sieves prior to use. (±)-Norcamphor was purchased from Sigma-Aldrich. 2-Oxabicyclo[3.2.1]octan-3-one (norcamphor lactone, **NCL**) was prepared according to a literature procedure and sublimed twice prior to use.[1] Deuterated chloroform (CDCl$_3$) was obtained from Sigma-Aldrich and dried over 3 Å molecular sieves. Yttrium bisphenolate complex **Y1** was prepared according to a literature procedure.[2] Tin(II) 2-ethylhexanoate [Sn(Oct)$_2$], ZnEt$_2$ (1.0 M in hexanes), and La[N(SiMe$_3$)$_2$]$_3$ were purchased from Sigma-Aldrich and used as received. Ti(O^{i}Pr)$_4$ was purchased from Alfa Aesar and distilled prior to use.

Nuclear magnetic resonance (NMR) spectra were recorded on a Bruker AV-III-500 spectrometer equipped with a QNP-Cryoprobe or AV-III-400 spectrometers at ambient temperature (298 K). ^{1}H and ^{13}C{^{1}H} NMR spectroscopic chemical shifts δ are reported in ppm relative to tetramethylsilane and were referenced internally to the relevant residual solvent resonances.

Polymer weight-average molecular weight (M_w), number-average molecular weight (M_n) and polydispersity indices ($Đ = M_w/M_n$) were determined *via* gel permeation chromatography (GPC) relative to polystyrene standards on a PL-SEC 50 Plus instrument from Polymer Laboratories. The analysis was performed at ambient temperatures using chloroform as the eluent at a flow rate of 1.0 mL min^{-1}.

Elemental analyses were measured with a EURO EA instrument from HEKAtech at the Laboratory for Microanalysis, Catalysis Research Center, Technical University of Munich.

Gas chromatography measurements were carried out with an Agilent GC 7890B device equipped with an MS 5977A detector.

Differential scanning calorimetry (DSC) measurements were carried out with a DSC Q2000 from TA Instruments with a heating and cooling rate of 10 °C min^{-1}. T_g values were obtained from the second heating scan.

S2

Thermal gravimetric analysis (TGA) was carried out with a TGA Q5000 from TA Instruments. Polymer samples were heated under argon atmosphere from ambient temperature to 500 °C with a heating rate of 10 °C min^{-1}.

1.2 Monomer Synthesis
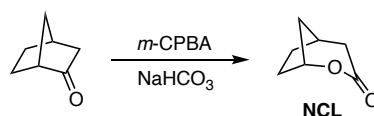
2-Oxabicyclo[3.2.1]octan-3-one (norcamphor lactone, **NCL**) was prepared according to a literature procedure.[1] ^{1}H NMR (400 MHz, CDCl$_3$): δ 4.86 (s, 1H), 2.71 (ddd, J = 15.5, 5.3, 2.6 Hz, 1H), 2.60 – 2.40 (m, 2H), 2.23 – 2.09 (m, 1H), 2.02 – 1.85 (m, 3H), 1.76 – 1.60 (m, 2H). ^{13}C{^{1}H} NMR (101 MHz, CDCl$_3$): δ 170.9, 81.1, 40.8, 36.0, 32.6, 32.0, 29.4. Anal. Calc. for C$_7$H$_{10}$O$_2$: C, 66.65; H, 7.99. Found: C, 66.75; H, 7.90%.

1.3 General Polymerization Procedures
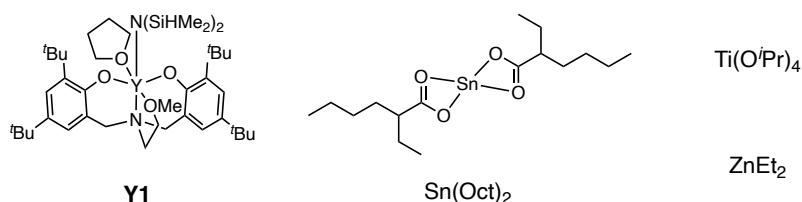
Figure S1. Catalysts used for the ROP of **NCL**.

*Polymerization of **NCL** under solvent conditions*

In a glove box, the required amount of catalyst (as specified in polymerization table 1) was loaded into a 1.5 mL vial and **NCL** (50 mg, 396 μmol) was added. To this mixture, toluene (100 mg, 115 μL) was added, the vial sealed, removed from the glovebox and placed in a pre-heated aluminum block at the desired polymerization temperature. The polymerization was quenched by addition of MeOH and conversion was determined by ^{1}H NMR spectroscopy of an aliquot. The mixture was precipitated into excess diethyl ether/pentane (1:1), filtered, washed with additional diethyl ether/pentane and dried under vacuum.

S3

*Bulk polymerization of **NCL***

In a glove box, the required amount of catalyst (as specified in polymerization table 1) was loaded into a 1.5 mL vial and **NCL** (50 mg, 396 μmol) was added. The vial was sealed, removed from the glovebox and placed in a preheated aluminum block at the desired polymerization temperature. The polymerization was quenched by addition of MeOH and conversion was determined by ^{1}H NMR spectroscopy of an aliquot. The mixture was precipitated into excess diethyl ether/pentane (1:1), filtered, washed with additional diethyl ether/pentane and dried under vacuum.

1.4 Depolymerization Procedures

*Depolymerization of **PNCL** under thermolysis conditions*

In a glove box, **PNCL** (10 mg, 79 μmol, M_n = 42.4 kg mol^{-1}) was loaded into a 1.5 mL vial. The vial was sealed, removed from the glovebox and placed in a preheated aluminum block at 220°C. The polymer was heated at this temperature for 4 h. Then, the vial was cooled to room temperature, 0.6 mL of CDCl$_3$ added, and the mixture analyzed by NMR spectroscopy and gas chromatography.

*Depolymerization of **PNCL** under chemolysis conditions*

In a glove box, La[N(SiMe$_3$)$_2$]$_3$ (2.5 mg, 4.0 μmol, 1.0 eq.) was loaded into a 4 mL vial and **PNCL** (25 mg, 198 μmol, 50 eq. per polymer repeating unit, M_n = 42.4 kg mol^{-1}) was added. Toluene (1.0 mL) was added, the vial sealed, removed from the glovebox and placed in a preheated aluminum block at 120°C. The depolymerization mixture was heated at this temperature for 3 h. Then, the catalyst was quenched by addition of 0.6 mL hydrous CDCl$_3$ and the mixture analyzed by NMR spectroscopy.

S4

2. Characterization Data of Monomer, Polymer and Depolymerizations
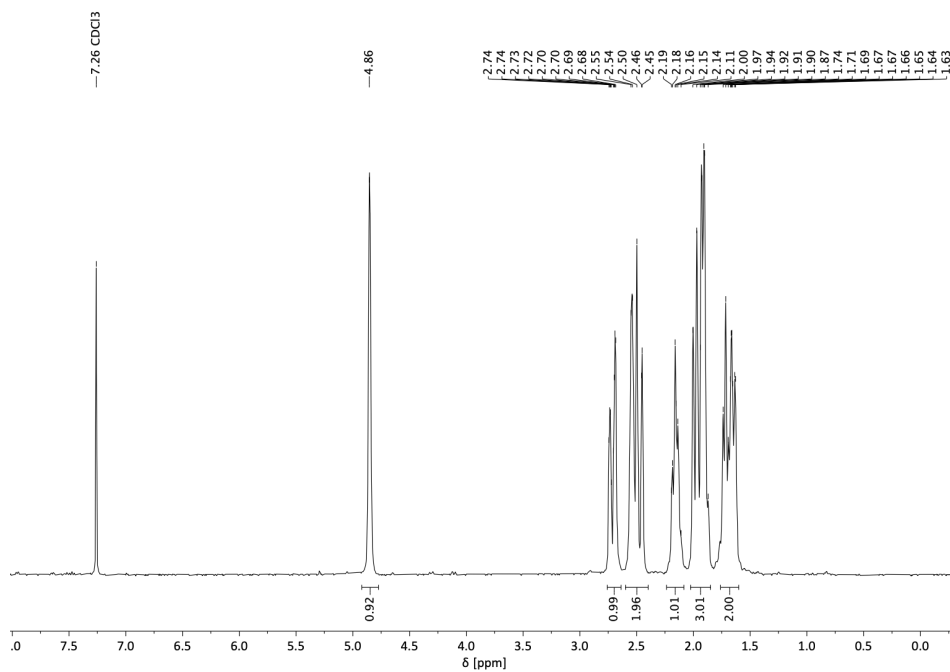
Figure S2. ^{1}H NMR spectrum (CDCl₃) of 2-oxabicyclo[3.2.1]octan-3-one (**NCL**).
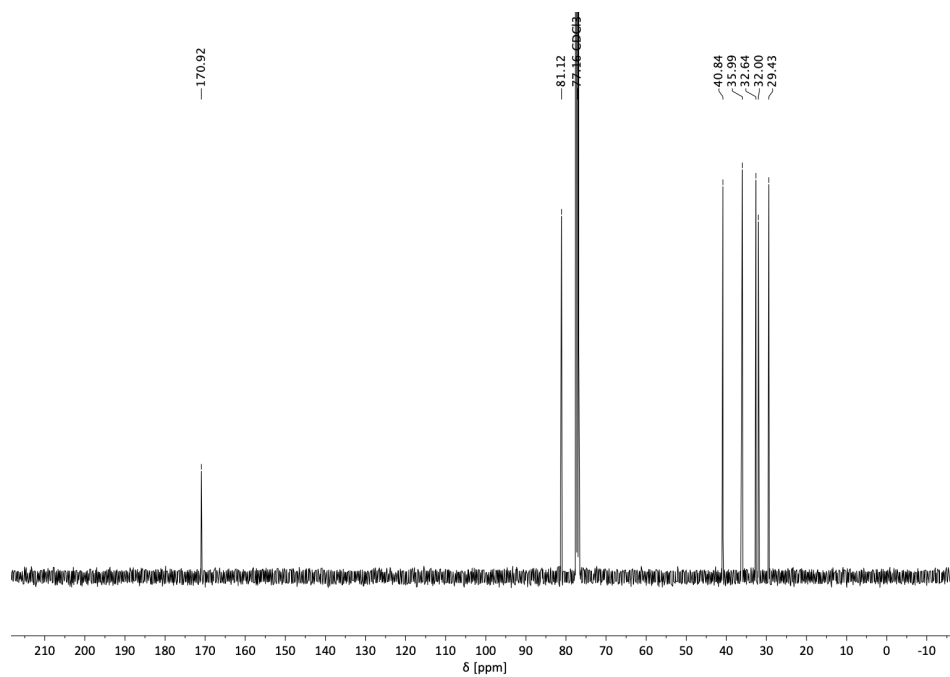
Figure S3. ^{13}C{^{1}H} NMR spectrum (CDCl₃) of 2-oxabicyclo[3.2.1]octan-3-one (**NCL**).

S5
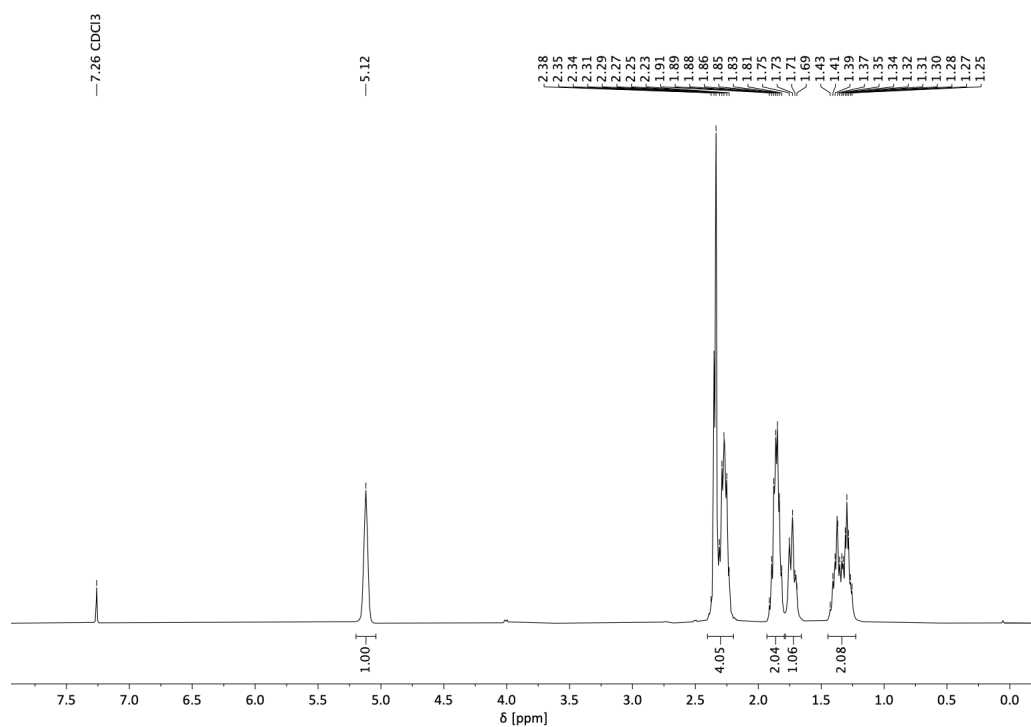
Figure S4. ^{1}H NMR spectrum (CDCl$_3$) of **PNCL**.
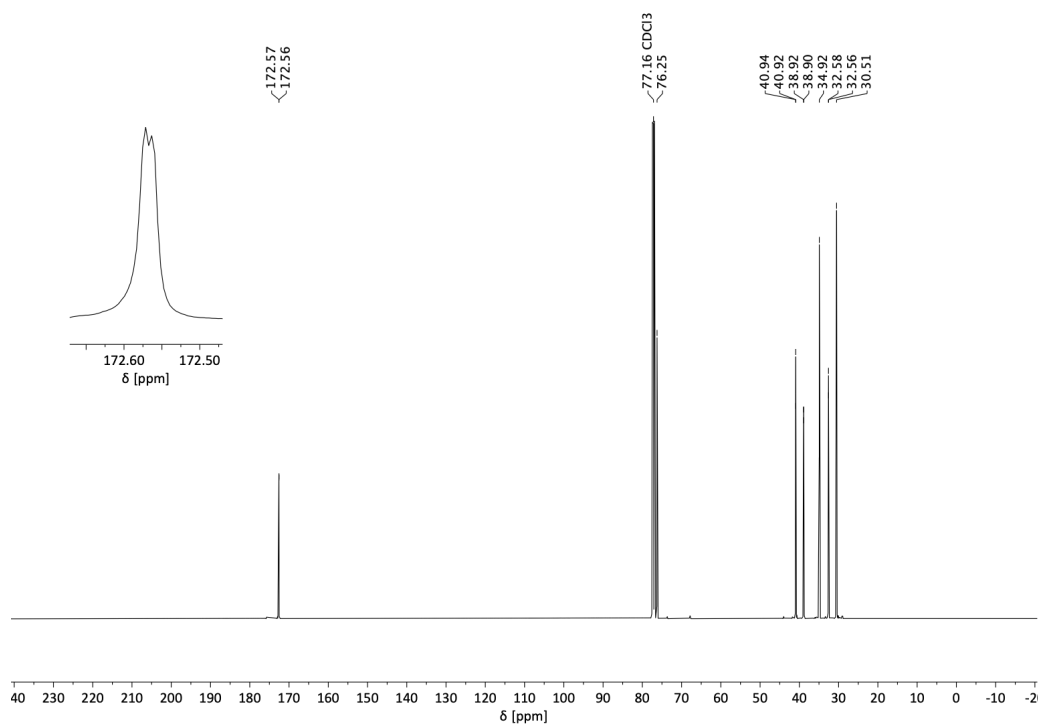
Figure S5. ^{13}C{^{1}H} NMR spectrum (CDCl$_3$) of **PNCL**. Inset: splitting of carbonyl signal.

S6
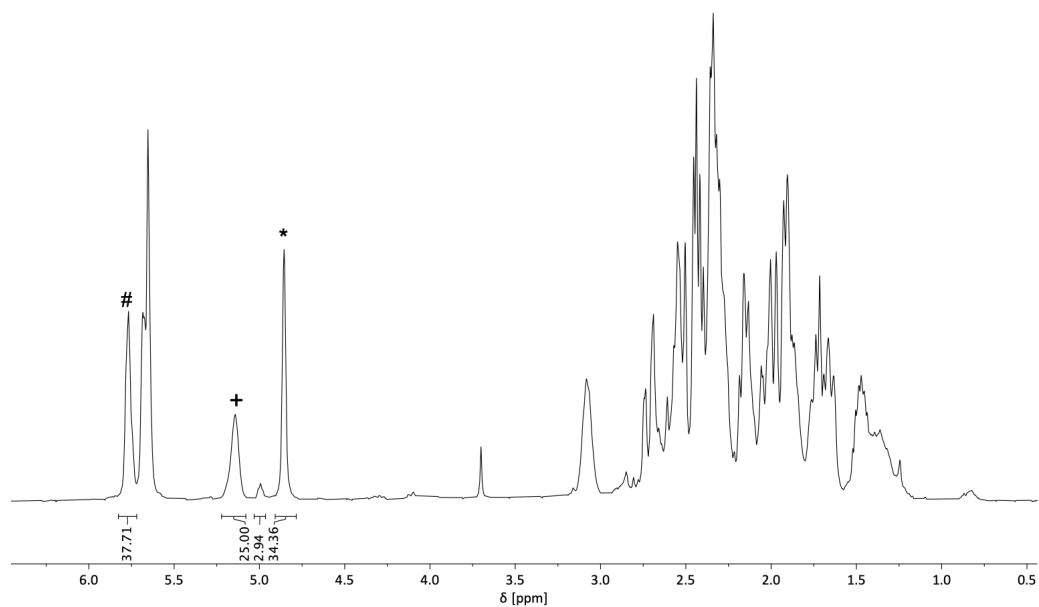
Figure S6. ^{1}H NMR spectrum (CDCl$_3$), depolymerization of **PNCL** at 280°C for 30 min. # 2-cyclopentene-1-acetic acid, + **PNCL**, * recovered monomer.
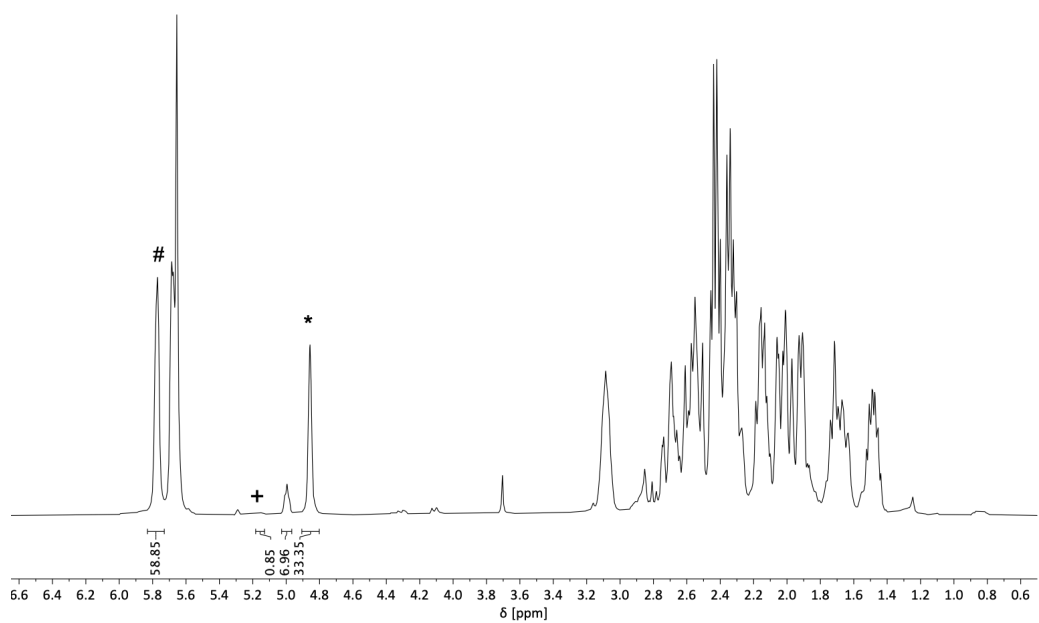
Figure S7. ^{1}H NMR spectrum (CDCl$_3$), depolymerization of **PNCL** at 280°C for 2 h. # 2-cyclopentene-1-acetic acid, + **PNCL**, * recovered monomer.

S7

186
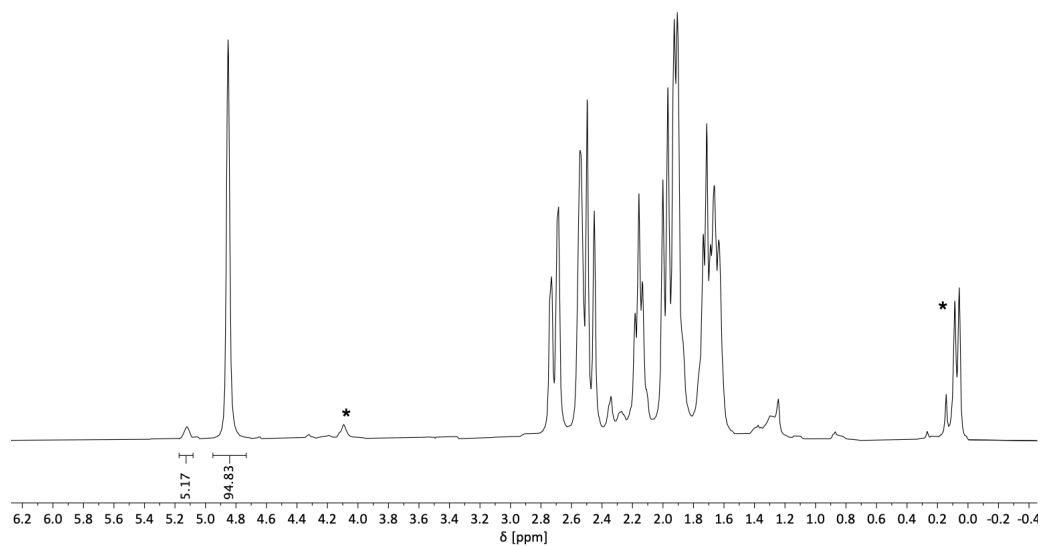
Figure S8. ^{1}H NMR spectrum (CDCl$_3$), bulk depolymerization of **PNCL** at 220°C for 2 h using La[N(SiMe$_3$)$_2$]$_3$ as catalyst. * quenched catalyst.
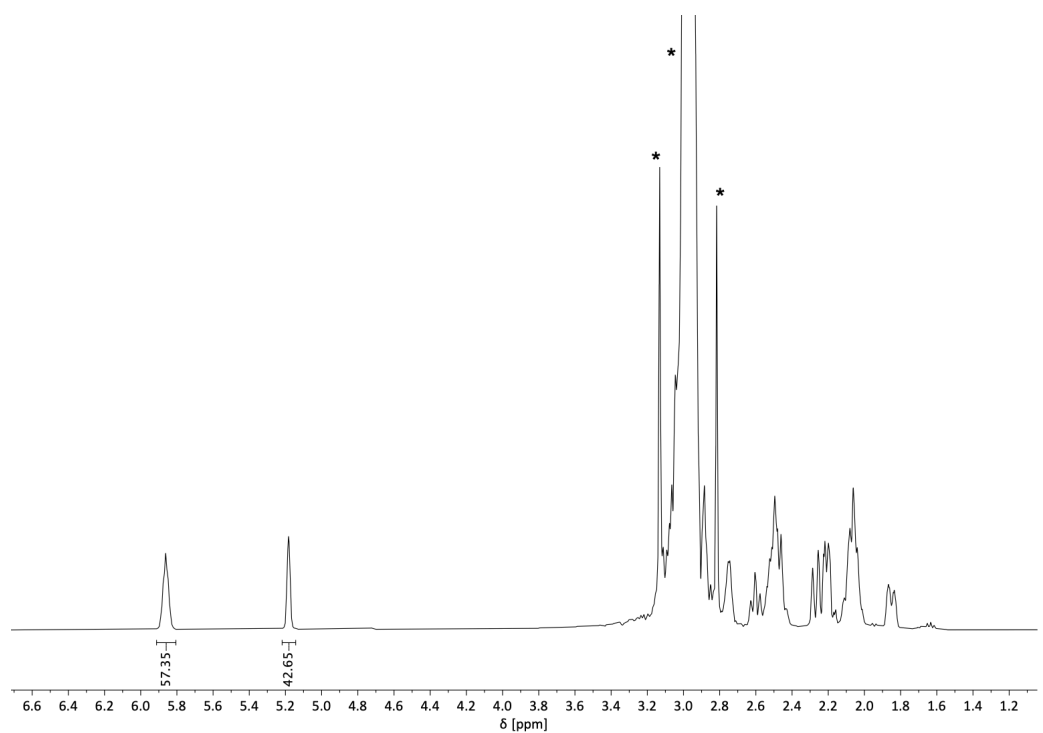
Figure S9. ^{1}H NMR spectrum (CDCl$_3$), depolymerization of **PNCL** in toluene (25 mg mL^{-1}) at 120°C for 3 h using La[N(SiMe$_3$)$_2$]$_3$ as catalyst. *toluene solvent and satellite signals.

S8
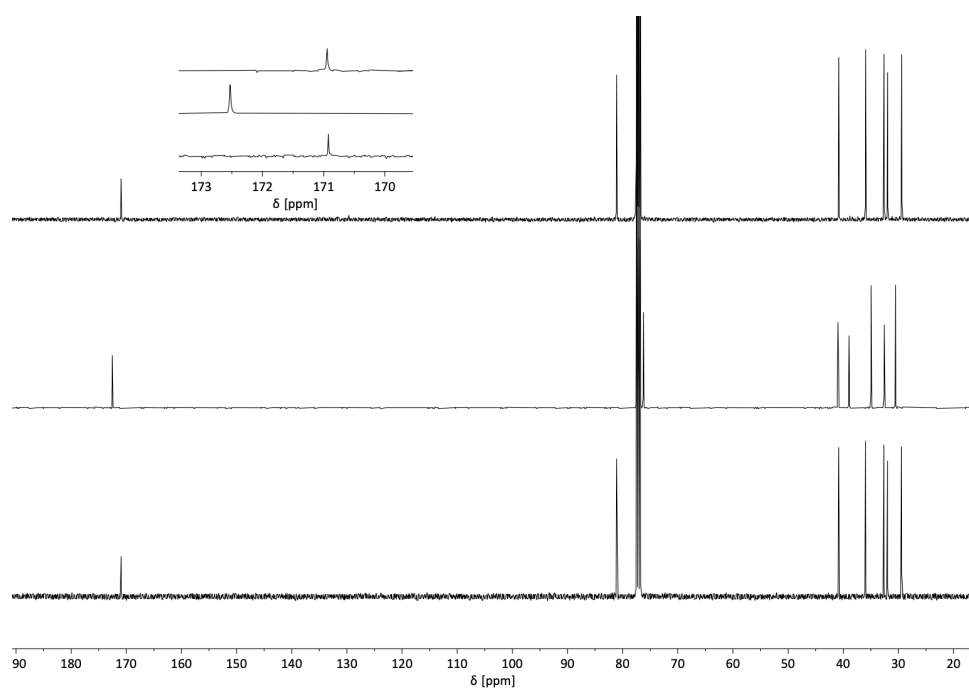
Figure S10. Comparison of $^{13}C\{^1H\}$ NMR spectra (CDCl$_3$) of pristine monomer (bottom), **PNCL** (middle), and recovered monomer from thermolysis of **PNCL** at 220°C (top). Inset: comparison of carbonyl region.
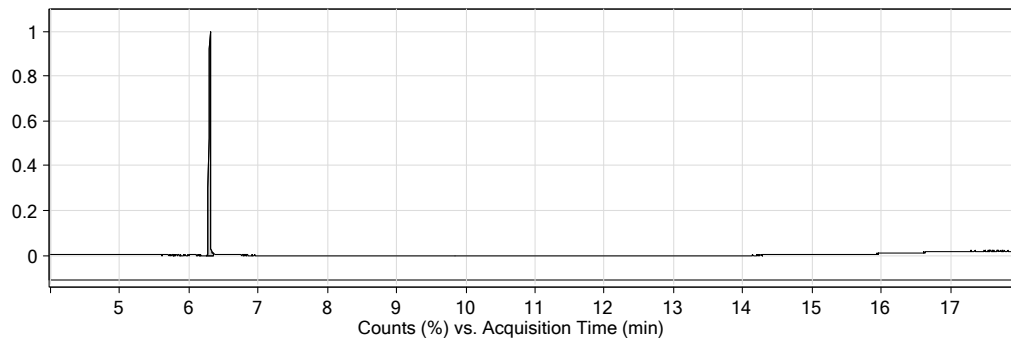
Figure S11. Gas chromatogram of the depolymerization mixture of **PNCL** at 220°C for 4 h.
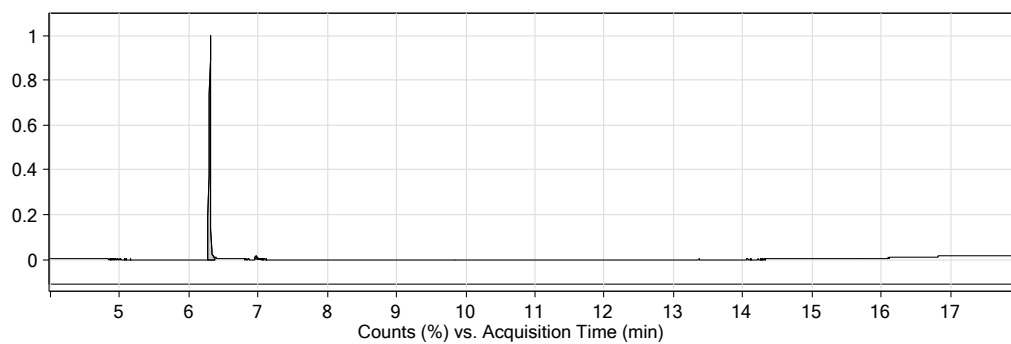
Figure S12. Gas chromatogram of the depolymerization mixture of **PNCL** at 220°C for 2 h using La[N(SiMe$_3$)$_2$]$_3$ as catalyst.

S9

Representative GPC Traces
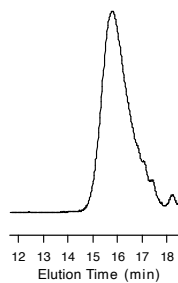
Figure S13. GPC trace of **PNCL** (M_n = 1.9 kg mol^{-1}, $Đ$ = 1.5; Table 1, entry 6).
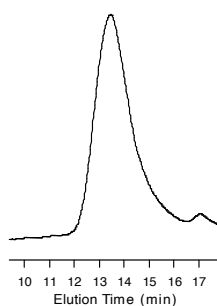
Figure S14. GPC trace of **PNCL** (M_n = 22.2 kg mol^{-1}, $Đ$ = 2.1; Table 1, entry 9).
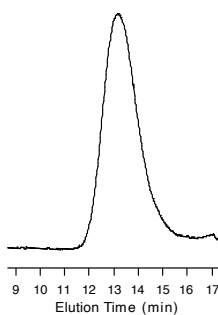
Figure S15. GPC trace of **PNCL** (M_n = 35.4 kg mol^{-1}, $Đ$ = 1.8; Table 1, entry 10).
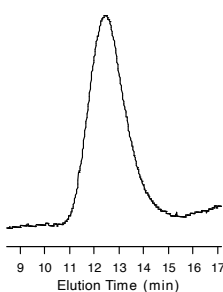
Figure S16. GPC trace of **PNCL** (M_n = 86.8 kg mol^{-1}, $Đ$ = 1.9; Table 1, entry 11).

S10

3. References

1. Tani, K.; Stoltz, B. M., Synthesis and structural analysis of 2-quinuclidonium tetrafluoroborate. *Nature* **2006,** *441*, 731-734.

2. Cai, C.-X.; Toupet, L.; Lehmann, C. W.; Carpentier, J.-F., Synthesis, structure and reactivity of new yttrium bis(dimethylsilyl)amido and bis(trimethylsilyl)methyl complexes of a tetradentate bis(phenoxide) ligand. *J. Organomet. Chem.* **2003,** *683*, 131-136.

S11

10.4 Supporting Information for Chapter 7

Supporting Information

For

High-Throughput Approach in the Ring-Opening Polymerization of *β*-Butyrolactone Enables Rapid Evaluation of Yttrium Salan Catalysts

Jonas Bruckmoser, and Bernhard Rieger[*]

WACKER-Chair of Macromolecular Chemistry, Catalysis Research Center,
Department of Chemistry, Technical University of Munich
Lichtenbergstraße 4, 85748 Garching bei München, Germany.

[*]Corresponding Author; email: rieger@tum.de

Table of Contents

S1

1. Experimental Section

Materials and Methods

All manipulations containing air- and/or moisture sensitive compounds were carried out under argon atmosphere using standard Schlenk or glovebox techniques. Glassware was flame-dried under vacuum prior to use. Unless otherwise stated, all chemicals were purchased from Sigma-Aldrich, TCI Chemicals or ABCR and used as received. Solvents were obtained from an MBraun MB-SPS 800 solvent purification system and stored over 3 Å molecular sieves prior to use. β-BL was treated with BaO, dried over CaH_2 and distilled prior to use. Deuterated chloroform ($CDCl_3$), benzene (C_6D_6), toluene (C_7D_8) and tetrahydrofuran (C_4D_8O) were obtained from Sigma-Aldrich and dried over 3 Å molecular sieves. $Y[N(SiHMe_2)_2]_3(THF)_2$, $La[N(SiHMe_2)_2]_3(THF)_2$ and catalyst **Y2** were prepared according to literature procedures.[1,2]

Nuclear magnetic resonance (NMR) spectra were recorded on a Bruker AV-III-500 spectrometer equipped with a QNP-Cryoprobe, AV-III-300 or AV-III-400 spectrometers at ambient temperature (298 K). ^1H and $^{13}C\{^1H\}$ NMR spectroscopic chemical shifts δ are reported in ppm relative to tetramethylsilane and were referenced internally to the relevant residual solvent resonances. The following abbreviations are used: br, broad; s, singlet; d, doublet; t, triplet; q, quartet; p, pentet; m, multiplet; AB, AB system.
The tacticity of PHB was determined by integration of the carbonyl region of the $^{13}C\{^1H\}$ NMR spectrum.[3]

Elemental analyses were measured with a EURO EA instrument from HEKAtech at the Laboratory for Microanalysis, Catalysis Research Center, Technical University of Munich.

Polymer weight-average molecular weight (M_w), number-average molecular weight (M_n) and polydispersity indices ($Đ = M_w/M_n$) were determined *via* gel permeation chromatography (GPC) relative to polystyrene standards on a PL-SEC 50 Plus instrument from Polymer Laboratories. The analysis was performed at 40°C using THF as the eluent at a flow rate of 1.0 mL min^{-1}.

S2

General Polymerization Procedures
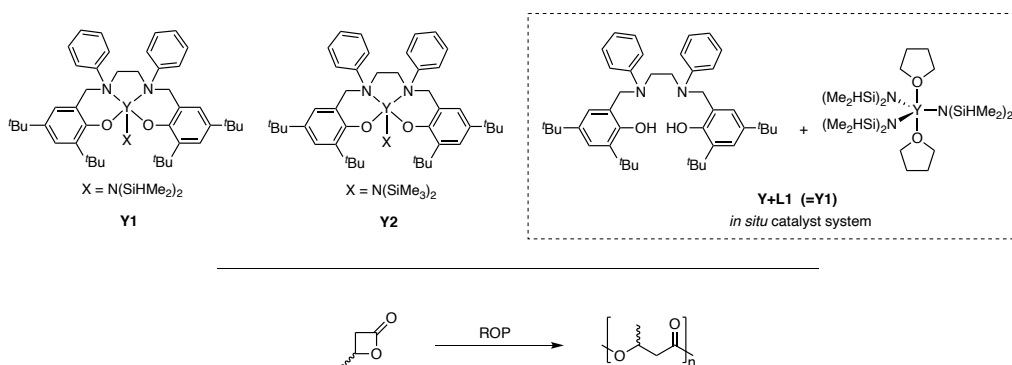
Scheme S1. Yttrium salan catalysts **Y1**, **Y2** and *in situ* catalyst system **Y+L1**. Bottom: ROP of β-BL.

Polymerization Procedure with Isolated Catalyst

In a glove box, initiator **Y1** (13.0 mg, 18.3 μmol) was dissolved in 1.55 mL of toluene and β-BL (300 μL, 315 mg, 3.66 mmol) was injected into the reaction, such that the overall concentration of β-BL was 2.0 M. After 15 min the polymerization was quenched by addition of 0.5 mL MeOH and conversion was determined by ^{1}H NMR spectroscopy of an aliquot. The mixture was precipitated into excess diethyl ether/pentane (1:1), filtered, washed with additional diethyl ether/pentane and dried under vacuum.

Polymerization Procedure with In Situ Generated Catalyst

In a glove box, a 4 mL glass reactor was charged with Y[N(SiHMe$_2$)$_2$]$_3$(THF)$_2$ (18.3 μmol) and the respective salan pro-ligand (18.3 μmol). 1.53 mL of toluene were added and the reaction mixture stirred for 1 h to generate the catalyst in situ. After that time, β-BL (300 μL, 315 mg, 3.66 mmol) was directly injected into this reaction mixture ([β-BL] = 2.0 M). After a respective time period, the polymerization was quenched by addition of 0.5 mL MeOH and conversion was determined by ^{1}H NMR spectroscopy of an aliquot. The mixture was precipitated into excess diethyl ether/pentane (1:1), filtered, washed with additional diethyl ether/pentane and dried under vacuum.

S3

Synthesis of Compounds

Synthesis of Precursors
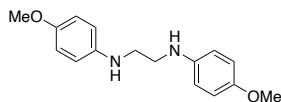
N,N'-Bis(4-methoxyphenyl)ethane-1,2-diamine

N,N'-Bis(4-methoxyphenyl)ethane-1,2-diamine was prepared according to a literature procedure.[4] Yield: 67%. ^{1}H NMR (400 MHz, CDCl$_3$): δ 6.83 – 6.76 (m, 4H, ArH), 6.68 – 6.61 (m, 4H, ArH), 3.76 (s, 6H, OMe), 3.58 (br s, 2H, NH), 3.34 (s, 4H, NCH$_2$). ^{13}C{^{1}H} NMR (101 MHz, CDCl$_3$): δ 152.5, 142.5, 115.1, 114.6, 55.9, 44.6.
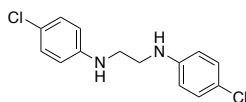
N,N'-Bis(4-chlorophenyl)ethane-1,2-diamine

N,N'-Bis(4-chlorophenyl)ethane-1,2-diamine was prepared according to a literature procedure.[4] Yield: 33%. ^{1}H NMR (400 MHz, CDCl$_3$): δ 7.17 – 7.11 (m, 4H, ArH), 6.63 – 6.55 (m, 4H, ArH), 3.84 (br s, 2H, NH), 3.37 (s, 4H, NCH$_2$). ^{13}C{^{1}H} NMR (101 MHz, CDCl$_3$): δ 146.6, 129.3, 122.7, 114.2, 43.5.
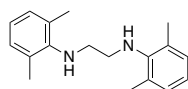
N,N'-Bis(2,6-dimethylphenyl)ethane-1,2-diamine

N,N'-Bis(2,6-dimethylphenyl)ethane-1,2-diamine was prepared according to a literature procedure.[5] Yield: 98%. ^{1}H NMR (400 MHz, CDCl$_3$): δ 7.01 (d, J = 7.5 Hz, 4H, ArH), 6.84 (t, J = 7.5 Hz, 2H, ArH), 3.40 (br s, 2H, NH), 3.22 (s, 4H, NCH$_2$), 2.32 (s, 12H, ArMe). ^{13}C{^{1}H} NMR (101 MHz, CDCl$_3$): δ 146.1, 129.6, 129.1, 122.2, 49.0, 18.7.

S4
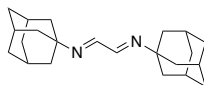
N,N'-Bis(adamantan-1-yl)ethane-1,2-diimine

N,N'-Bis(adamantan-1-yl)ethane-1,2-diimine was prepared according to a literature procedure.[6] Yield: 87%. ^{1}H NMR (400 MHz, CDCl$_3$): δ 7.93 (s, 2H, NCH), 2.14 (s, 6H, CH), 1.80 – 1.62 (m, 24H, CH$_2$). ^{13}C{^{1}H} NMR (101 MHz, CDCl$_3$): δ 158.0, 58.7, 42.9, 36.6, 29.6.
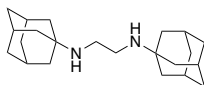
N,N'-Bis(adamantan-1-yl)ethane-1,2-diamine

N,N'-Bis(adamantan-1-yl)ethane-1,2-diimine (3.25 g, 10.0 mmol) was dissolved in CH$_2$Cl$_2$ (50 mL) and MeOH (50 mL). NaBH$_4$ (1.51 g, 40.0 mmol) was added portionwise and the resulting reaction mixture stirred overnight at room temperature. Subsequently, concentrated hydrochloric acid (1 mL) and H$_2$O (100 mL) were added and the mixture extracted with CH$_2$Cl$_2$ (50 mL). The aqueous phase was washed with CH$_2$Cl$_2$ (2×50 mL) and the solvent of the combined organic phases removed. Yield: 2.50 g (76%). ^{1}H NMR (400 MHz, CDCl$_3$): δ 2.66 (s, 4H, NCH$_2$), 2.05 (s, 6H, CH), 1.70 – 1.54 (m, 24H, CH$_2$). ^{13}C{^{1}H} NMR (101 MHz, CDCl$_3$): δ 50.4, 43.0, 41.4, 36.9, 29.7.
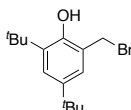
2-(Bromomethyl)-4,6-di-*tert*-butylphenol

2-(Bromomethyl)-4,6-di-*tert*-butylphenol was prepared according to a literature procedure.[7] Yield: 97%. ^{1}H NMR (400 MHz, CDCl$_3$): δ 7.34 (d, J = 2.6 Hz, 1H, ArH), 7.11 (d, J = 2.6 Hz, 1H, ArH), 5.28 (br s, 1H, OH), 4.59 (s, 2H, CH$_2$), 1.44 (s, 9H, C(CH$_3$)$_3$), 1.30 (s, 9H, C(CH$_3$)$_3$).

S5
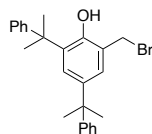
2-(Bromomethyl)-4,6-bis(2-phenylpropan-2-yl)phenol

2-(Bromomethyl)-4,6-bis(2-phenylpropan-2-yl)phenol was prepared according to a literature procedure.[8] Yield: 87%. ^{1}H NMR (400 MHz, CDCl$_3$): δ 7.38 – 7.24 (m, 11H, ArH), 7.12 (d, J = 2.4 Hz, 1H, ArH), 4.43 (s, 2H, CH$_2$), 1.72 (s, 6H, C(CH$_3$)$_2$), 1.60 (s, 6H, C(CH$_3$)$_2$).
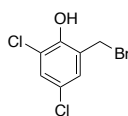
2-(Bromomethyl)-4,6-dichlorophenol

3,5-Dichloro-2-hydroxybenzaldehyde (3.82 g, 20.0 mmol) was dissolved in MeOH (100 mL). NaBH$_4$ (1.51 g, 40.0 mmol) was added portionwise and the resulting reaction mixture stirred for 2.5 h at room temperature. Subsequently, the solvent was removed, H$_2$O (100 mL) added and the mixture neutralized with glacial acetic acid. The mixture was extracted with CH$_2$Cl$_2$ (3×50 mL) and the solvent of the combined organic phases removed. The colorless oil was dissolved in CH$_2$Cl$_2$ (50 mL) and PBr$_3$ (0.95 mL, 2.71 g, 10.0 mmol) was added. The reaction mixture was stirred for 1 h at room temperature. H$_2$O (50 mL) was added, extracted with CH$_2$Cl$_2$ (3×30 mL), the combined organic phases washed with brine (30 mL) and the solvent removed. The residue was recrystallized from CH$_2$Cl$_2$ to give a colorless solid (3.31 g, 65%). ^{1}H NMR (400 MHz, CDCl$_3$): δ 7.30 (d, J = 2.5 Hz, 1H, ArH), 7.24 (d, J = 2.4 Hz, 1H, ArH), 4.84 (br s, 1H, OH), 4.50 (s, 2H, CH$_2$). ^{13}C{^{1}H} NMR (101 MHz, CDCl$_3$): δ 148.5, 129.7, 129.0, 126.8, 125.5, 121.0, 27.0.

S6

Synthesis of Salan Pro-Ligands

General Procedure A. The 4,6-substituted 2-(bromomethyl)phenol (20.0 mmol) was dissolved in 60 mL of dichloromethane and cooled to 0 C°. The respective diamine (10.0 mmol) and triethylamine (22.0 mmol) were added. The reaction mixture was stirred for 6 h at room temperature. Subsequently, water was added and the mixture extracted with dichloromethane (3×). The combined organic phases were dried over $MgSO_4$ and the solvent removed under reduced pressure. If required, the residue was further purified as described below.

General Procedure B. The 2,4-substituted phenol (40.0 mmol) was dissolved in 20 mL of methanol and 15 mL aqueous formaldehyde solution (37 wt.%) and the respective diamine (20.0 mmol) were added. The reaction mixture was refluxed overnight. After cooling to room temperature, the colorless precipitate was collected, washed with methanol and dried *in vacuo*. If required, the residue was further purified as described below.
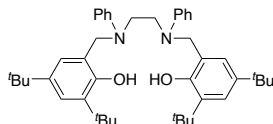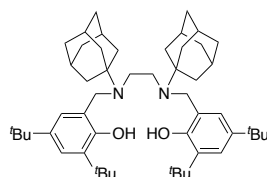

L1. Pro-ligand **L1** was prepared according to a literature procedure.[2] Yield: 63%. ^1H NMR (400 MHz, $CDCl_3$): δ 8.80 (br s, 2H, OH), 7.29 (d, J = 2.4 Hz, 2H, ArH), 7.21 – 7.09 (m, 4H, ArH), 7.02 – 6.69 (m, 8H, ArH), 4.25 (s, 4H, ArCH$_2$), 3.24 (br s, 4H, NCH$_2$), 1.41 (s, 18H, C(CH$_3$)$_3$), 1.26 (s, 18H, C(CH$_3$)$_3$). $^{13}C\{^1H\}$ NMR (101 MHz, $CDCl_3$): δ 153.5, 149.1, 141.7, 136.2, 129.4, 124.1, 123.7, 122.5, 121.3, 119.4, 58.3, 49.0, 35.0, 34.4, 31.8, 29.8. Anal. Calc. for $C_{44}H_{60}N_2O_2$: C, 81.43; H, 9.32; N, 4.32. Found: C, 81.17; H, 9.52; N, 4.37%.
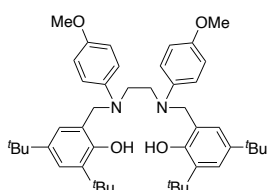
L2. Pro-ligand **L2** was prepared according to general procedure A. 2-(Bromomethyl)-4,6-di-*tert*-butylphenol and *N,N'*-bis(4-methoxyphenyl)ethane-1,2-diamine were used. Yield: 73%.

S7

^{1}H NMR (400 MHz, CDCl$_3$): δ 9.69 (br s, 2H, OH), 7.22 (d, J = 2.3 Hz, 2H, ArH), 6.93 – 6.81 (m, 4H, ArH), 6.81 – 6.64 (m, 6H, ArH), 4.11 (s, 4H, ArCH$_2$), 3.75 (s, 6H, OCH$_3$), 3.06 (s, 4H, NCH$_2$), 1.40 (s, 18H, C(CH$_3$)$_3$), 1.25 (s, 18H, C(CH$_3$)$_3$). ^{13}C{^{1}H} NMR (101 MHz, CDCl$_3$): δ 156.3, 153.9, 142.4, 141.2, 135.9, 123.8, 123.3, 122.8, 121.3, 114.6, 60.4, 55.6, 50.7, 35.0, 34.3, 31.8, 29.8. Anal. Calc. for C$_{46}$H$_{64}$N$_2$O$_4$: C, 77.92; H, 9.10; N, 3.95. Found: C, 77.72; H, 9.03; N, 3.94%.
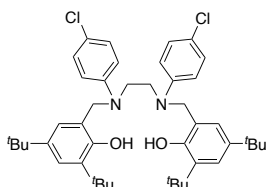
L3. Pro-ligand **L3** was prepared according to general procedure A. 2-(Bromomethyl)-4,6-di-*tert*-butylphenol and *N,N'*-bis(4-chlorophenyl)ethane-1,2-diamine were used. The reaction mixture was stirred overnight. The residue was recrystallized from tetrahydrofuran. Yield: 66%. ^{1}H NMR (400 MHz, THF-d$_8$): δ 7.88 (br s, 2H, OH), 7.27 (d, J = 2.3 Hz, 2H, ArH), 7.11 – 7.04 (m, 4H, ArH), 6.93 (d, J = 2.2 Hz, 2H, ArH), 6.71 – 6.65 (m, 4H, ArH), 4.36 (s, 4H, ArCH$_2$), 3.38 (s, 4H, NCH$_2$), 1.40 (s, 18H, C(CH$_3$)$_3$), 1.23 (s, 18H, C(CH$_3$)$_3$). ^{13}C{^{1}H} NMR (101 MHz, THF-d$_8$): δ 153.5, 148.9, 142.7, 137.5, 129.9, 125.2, 124.6, 123.8, 118.3, 54.8, 49.4, 35.8, 35.0, 32.2, 30.4. Anal. Calc. for C$_{44}$H$_{58}$Cl$_2$N$_2$O$_2$: C, 73.62; H, 8.14; N, 3.90. Found: C, 73.37; H, 8.30; N, 3.89%.
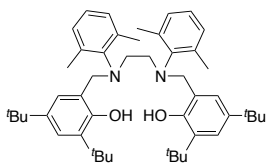
L4. Pro-ligand **L4** was prepared according to general procedure A. 2-(Bromomethyl)-4,6-di-*tert*-butylphenol and *N,N'*-bis(2,6-dimethylphenyl)ethane-1,2-diamine were used. Yield: 74%. ^{1}H NMR (400 MHz, CDCl$_3$): δ 9.08 (s, 2H, OH), 7.22 (d, J = 2.3 Hz, 2H, ArH), 6.99 – 6.90 (m, 6H, ArH), 6.78 (d, J = 2.3 Hz, 2H, ArH), 4.13 (s, 4H, ArCH$_2$), 3.00 (s, 4H, NCH$_2$), 2.16 (s, 12H, ArCH$_3$), 1.35 (s, 18H, C(CH$_3$)$_3$), 1.27 (s, 18H, C(CH$_3$)$_3$). ^{13}C{^{1}H} NMR (101 MHz, CDCl$_3$): δ 153.6, 147.0, 141.4, 136.1, 135.6, 130.3, 126.3, 124.2, 123.5, 122.0, 58.8, 52.4, 34.9, 34.3, 31.8, 29.7, 20.5. Anal. Calc. for C$_{48}$H$_{68}$N$_2$O$_2$: C, 81.77; H, 9.72; N, 3.97. Found: C, 81.78; H, 9.59; N, 4.04%.

S8
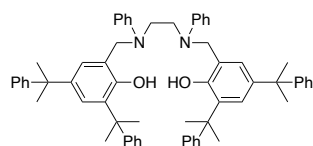
L5. Pro-ligand **L5** was prepared according to general procedure A. 2-(Bromomethyl)-4,6-bis(2-phenylpropan-2-yl)phenol and *N,N'*-diphenylethylenediamine were used. The reaction mixture was stirred overnight. The residue was recrystallized from acetone. Yield: 31%. ^{1}H NMR (400 MHz, CDCl$_3$): δ 7.24 – 7.06 (m, 26H, ArH), 6.87 – 6.81 (m, 2H, ArH), 6.72 (d, *J* = 2.4 Hz, 2H, ArH), 6.61 – 6.55 (m, 4H, ArH), 4.08 (s, 4H, ArCH$_2$), 3.02 (s, 4H, NCH$_2$), 1.64 (s, 12H, C(C*H*$_3$)$_2$Ph), 1.61 (s, 12H, C(C*H*$_3$)$_2$Ph). ^{13}C{^{1}H} NMR (101 MHz, CDCl$_3$): δ 152.0, 151.2, 150.3, 148.6, 141.3, 135.2, 129.1, 128.3, 128.0, 126.8, 126.2, 125.8, 125.7, 125.6, 124.7, 122.8, 120.9, 118.0, 55.4, 49.1, 42.6, 42.1, 31.2, 29.8. Anal. Calc. for C$_{64}$H$_{68}$N$_2$O$_2$: C, 85.67; H, 7.64; N, 3.12. Found: C, 86.43; H, 7.60; N, 3.28%.
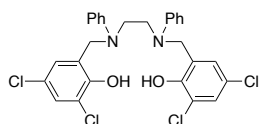
L6. Pro-ligand **L6** was prepared according to general procedure A. 2-(Bromomethyl)-4,6-dichlorophenol and *N,N'*-diphenylethylenediamine were used. The residue was recrystallized from acetone and subsequently washed with pentane. Yield: 48%. ^{1}H NMR (400 MHz, CDCl$_3$): δ 8.10 (br s, 2H, OH), 7.29 – 7.22 (m, 6H, ArH), 6.96 – 6.91 (m, 2H, ArH), 6.87 (d, *J* = 2.5 Hz, 2H, ArH), 6.86 – 6.81 (m, 4H, ArH), 4.34 (s, 4H, ArCH$_2$), 3.42 (s, 4H, NCH$_2$). ^{13}C{^{1}H} NMR (101 MHz, CDCl$_3$): δ 149.9, 147.6, 129.8, 128.2, 126.8, 125.7, 125.1, 121.4, 121.2, 117.1, 54.2, 48.9. Anal. Calc. for C$_{28}$H$_{24}$Cl$_4$N$_2$O$_2$: C, 59.81; H, 4.30; N, 4.98. Found: C, 59.98; H, 4.23; N, 5.13%.
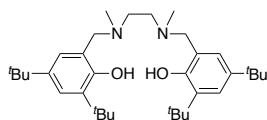
L7. Pro-ligand **L7** was prepared according to a literature procedure.[9] Yield: 87%. ^{1}H NMR (400 MHz, CDCl$_3$): δ 10.68 (br s, 2H, OH), 7.20 (d, *J* = 2.4 Hz, 2H, ArH), 6.80 (d, *J* = 2.4 Hz, 2H, ArH), 3.66 (s, 4H, ArCH$_2$), 2.63 (s, 4H, NCH$_2$), 2.26 (s, 6H, NCH$_3$), 1.40 (s, 18H, C(CH$_3$)$_3$), 1.27 (s, 18H, C(CH$_3$)$_3$). ^{13}C{^{1}H} NMR (101 MHz, CDCl$_3$): δ 154.3, 140.7, 135.8, 123.5, 123.1, 121.1, 62.9, 53.9, 41.8, 35.0, 34.3, 31.9, 29.8. Anal. Calc. for C$_{34}$H$_{56}$N$_2$O$_2$: C, 77.81; H, 10.76; N, 5.34. Found: C, 77.52; H, 11.03; N, 5.44%.

S9
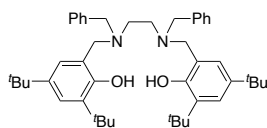
L8. Pro-ligand **L8** was prepared according to a literature procedure.[10] Yield: 60%. ^{1}H NMR (400 MHz, CDCl$_3$): δ 10.52 (br s, 2H, OH), 7.30 – 7.22 (m, 6H, ArH), 7.20 (d, J = 2.5 Hz, 2H, ArH), 7.18 – 7.11 (m, 4H, ArH), 6.80 (d, J = 2.5 Hz, 2H, ArH), 3.66 (s, 4H, ArCH$_2$), 3.50 (s, 4H, ArCH$_2$), 2.68 (s, 4H, NCH$_2$), 1.42 (s, 18H, C(CH$_3$)$_3$), 1.27 (s, 18H, C(CH$_3$)$_3$). ^{13}C{^{1}H} NMR (101 MHz, CDCl$_3$): δ 154.0, 140.9, 136.8, 135.8, 129.7, 128.7, 127.7, 123.8, 123.2, 121.2, 59.3, 58.2, 50.2, 35.0, 34.3, 31.8, 29.7. Anal. Calc. for C$_{46}$H$_{64}$N$_2$O$_2$: C, 81.61; H, 9.53; N, 4.14. Found: C, 81.24; H, 9.69; N, 4.29%.
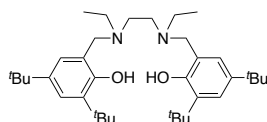
L9. Pro-ligand **L9** was prepared according to general procedure B. 2,4-Di-*tert*-butylphenol and *N*,*N'*-diethylethylenediamine were used. Yield: 83%. ^{1}H NMR (400 MHz, CDCl$_3$): δ 10.85 (br s, 2H, OH), 7.20 (d, J = 2.9 Hz, 2H, ArH), 6.80 (d, J = 2.8 Hz, 2H, ArH), 3.70 (s, 4H, ArCH$_2$), 2.66 (s, 4H, NCH$_2$), 2.55 (q, J = 7.1 Hz, 4H, NC*H*$_2$CH$_3$), 1.40 (s, 18H, C(CH$_3$)$_3$), 1.27 (s, 18H, C(CH$_3$)$_3$), 1.00 (t, J = 7.1 Hz, 6H, NCH$_2$C*H*$_3$). ^{13}C{^{1}H} NMR (101 MHz, CDCl$_3$): δ 154.4, 140.7, 135.7, 123.5, 123.0, 121.3, 59.1, 50.5, 47.9, 35.0, 34.3, 31.8, 29.7, 11.3. Anal. Calc. for C$_{36}$H$_{60}$N$_2$O$_2$: C, 78.21; H, 10.94; N, 5.07. Found: C, 78.26; H, 10.97; N, 4.96%.

L10. Pro-ligand **L10** was prepared according to general procedure B. 2,4-Di-*tert*-butylphenol and *N*,*N'*-bis(adamantan-1-yl)ethane-1,2-diamine were used. The residue was recrystallized from tetrahydrofuran. Yield: 11%. ^{1}H NMR (400 MHz, CDCl$_3$): δ 11.02 (br s, 2H, OH), 7.18 (d, J = 2.5 Hz, 2H, ArH), 6.81 (d, J = 2.4 Hz, 2H, ArH), 4.31 (br s, 2H, ArCH$_2$), 3.11 (br s, 2H, ArCH$_2$), 2.76 (br s, 2H, NCH$_2$), 2.07 (br s, 2H, NCH$_2$), 1.89 (s, 6H, CH), 1.61 – 1.47 (m, 12H, CH$_2$), 1.45 (s, 18H, C(CH$_3$)$_3$), 1.43 – 1.34 (m, 8H, CH$_2$), 1.25 (s, 18H, C(CH$_3$)$_3$), 1.24 – 1.17 (m, 4H, CH$_2$). ^{13}C{^{1}H} NMR (101 MHz, CDCl$_3$): δ 154.6, 140.7, 135.4, 123.8, 123.1,

S10

122.6, 55.9, 53.3, 50.2, 38.4, 36.4, 35.0, 34.3, 31.9, 29.9, 29.5. Anal. Calc. for $C_{52}H_{80}N_2O_2$: C, 81.62; H, 10.54; N, 3.66. Found: C, 81.74; H, 10.41; N, 3.75%.
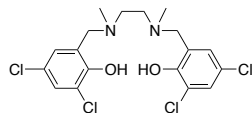
L11. Pro-ligand **L11** was prepared according to a literature procedure.[11] Yield: 72%. ^{1}H NMR (400 MHz, CDCl$_3$): δ 7.27 (d, J = 2.6 Hz, 2H, ArH), 6.87 (d, J = 2.6 Hz, 2H, ArH), 3.69 (s, 4H, ArCH$_2$), 2.70 (s, 4H, NCH$_2$), 2.32 (s, 6H, NCH$_3$). ^{13}C{^{1}H} NMR (101 MHz, CDCl$_3$): δ 152.6, 129.1, 126.9, 123.8, 123.6, 121.9, 61.3, 54.2, 42.0. Anal. Calc. for $C_{18}H_{20}Cl_4N_2O_2$: C, 49.34; H, 4.60; N, 6.39. Found: C, 49.47; H, 4.46; N, 6.34%.
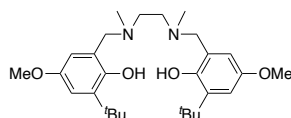
L12. Pro-ligand **L12** was prepared according to general procedure B. 2-*tert*-Butyl-4-methoxyphenol and *N,N'*-dimethylethylenediamine were used. Yield: 77%. ^{1}H NMR (400 MHz, CDCl$_3$): δ 10.34 (br s, 2H, OH), 6.79 (d, J = 3.1 Hz, 2H, ArH), 6.38 (d, J = 3.1 Hz, 2H, ArH), 3.74 (s, 6H, OCH$_3$), 3.63 (s, 4H, ArCH$_2$), 2.60 (s, 4H, NCH$_2$), 2.24 (s, 6H, NCH$_3$), 1.38 (s, 18H, C(CH$_3$)$_3$). ^{13}C{^{1}H} NMR (101 MHz, CDCl$_3$): δ 151.8, 150.7, 138.1, 122.4, 112.9, 111.2, 62.7, 55.8, 53.7, 41.6, 35.0, 29.5. Anal. Calc. for $C_{28}H_{44}N_2O_4$: C, 71.15; H, 9.38; N, 5.93. Found: C, 71.19; H, 9.33; N, 5.96%.
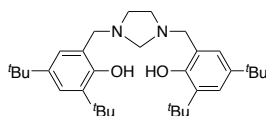
L13. Pro-ligand **L13** was prepared according to a literature procedure.[12] Yield: 20%. ^{1}H NMR (400 MHz, CDCl$_3$): δ 10.68 (br s, 2H, OH), 7.22 (d, J = 2.5 Hz, 2H, ArH), 6.83 (d, J = 2.6 Hz, 2H, ArH), 3.89 (s, 4H, ArCH$_2$), 3.52 (s, 2H, NCH$_2$N), 3.00 (s, 4H, NCH$_2$), 1.42 (s, 18H, C(CH$_3$)$_3$), 1.27 (s, 18H, C(CH$_3$)$_3$). ^{13}C{^{1}H} NMR (101 MHz, CDCl$_3$): δ 154.3, 140.9, 135.9, 123.5, 123.2, 121.0, 74.5, 59.4, 51.9, 35.0, 34.3, 31.8, 29.8. Anal. Calc. for $C_{33}H_{52}N_2O_2$: C, 77.90; H, 10.30; N, 5.51. Found: C, 77.51; H, 10.59; N, 5.65%.

S11
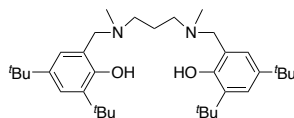
L14. Pro-ligand **L14** was prepared according to general procedure B. 2,4-Di-*tert*-butylphenol and *N,N'*-dimethyl-1,3-propanediamine were used. Yield: 49%. ^{1}H NMR (400 MHz, CDCl$_3$): δ 11.01 (br s, 2H, OH), 7.20 (d, *J* = 2.6 Hz, 2H, ArH), 6.80 (d, *J* = 2.6 Hz, 2H, ArH), 3.64 (s, 4H, ArC*H*$_2$), 2.46 (t, *J* = 7.6 Hz, 4H, NC*H*$_2$CH$_2$). 2.27 (s, 6H, NCH$_3$), 1.79 (p, *J* = 7.4 Hz, 2H, NCH$_2$C*H*$_2$), 1.41 (s, 18H, C(CH$_3$)$_3$), 1.27 (s, 18H, C(CH$_3$)$_3$). ^{13}C{^{1}H} NMR (101 MHz, CDCl$_3$): δ 154.4, 140.6, 135.6, 123.4, 123.0, 121.3, 62.5, 54.6, 41.4, 35.0, 34.3, 31.8, 29.8, 24.7. Anal. Calc. for C$_{35}$H$_{58}$N$_2$O$_2$: C, 78.01; H, 10.85; N, 5.20. Found: C, 78.30; H, 10.88; N, 5.16%.

Synthesis of Catalysts

Synthesis of Isolated Catalyst Y1
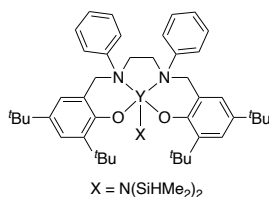
X = N(SiHMe$_2$)$_2$

Y1. A solution of Y[N(SiHMe$_2$)$_2$]$_3$(THF)$_2$ (299 mg, 475 μmol) in 5 mL of pentane was added to a suspension of **L1** (308 mg, 475 μmol) in 5 mL of toluene. Within minutes after addition, the reaction mixture became clear and was stirred for 3 h at room temperature. The reaction mixture was evaporated to dryness and the residue recrystallized from pentane to give a colorless solid (186 mg, 45%). ^{1}H NMR (400 MHz, C$_6$D$_6$): δ 7.51 (d, *J* = 2.6 Hz, 2H, ArH), 7.01 – 6.95 (m, 4H, ArH), 6.94 – 6.88 (m, 4H, ArH), 6.78 – 6.73 (m, 2H, ArH), 6.66 (d, *J* = 2.6 Hz, 2H, ArH), 5.11 – 5.00 (m, 2H, Si*H*Me$_2$), 3.77 (AB, *J* = 12.8 Hz, 4H, ArCH$_2$), 2.87 (br s, 4H, NCH$_2$), 1.75 (s, 18H, C(CH$_3$)$_3$), 1.33 (s, 18H, C(CH$_3$)$_3$), 0.43 (d, *J* = 2.9 Hz, 12H, SiH*Me*$_2$). ^{13}C{^{1}H} NMR (101 MHz, C$_6$D$_6$): δ 160.8, 148.0, 137.8, 137.1, 129.7, 126.6, 125.7, 124.6, 123.3, 123.0, 65.9, 52.6, 35.6, 34.2, 32.1, 30.4, 3.5.

NMR Experiment of *In Situ* Formation of Catalyst Y1

In a glove box, a vial was charged with Y[N(SiHMe$_2$)$_2$]$_3$(THF)$_2$ (6.3 mg, 10.0 μmol) and **L1** (6.5 mg, 10.0 μmol). 0.6 mL of toluene-d$_8$ were added, the reaction mixture stirred, and

S12

transferred to a J-Young-type NMR tube. ^{1}H NMR spectra were measured after certain time intervals. Within less than 30 min clean formation of **Y1** was observed. Longer reaction times did not show any further changes.
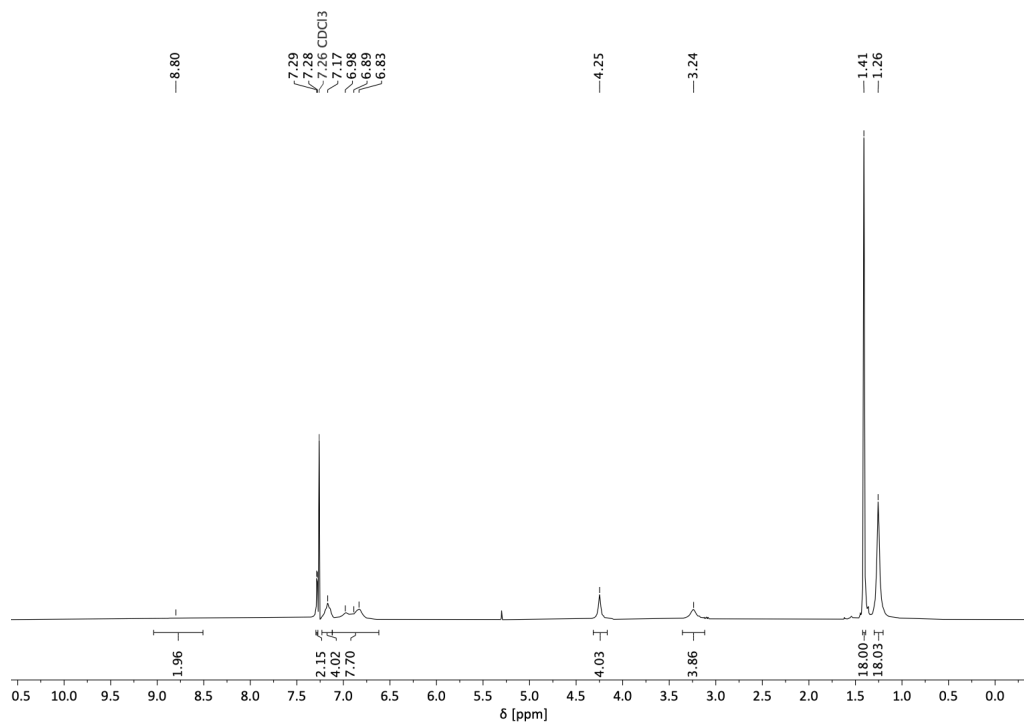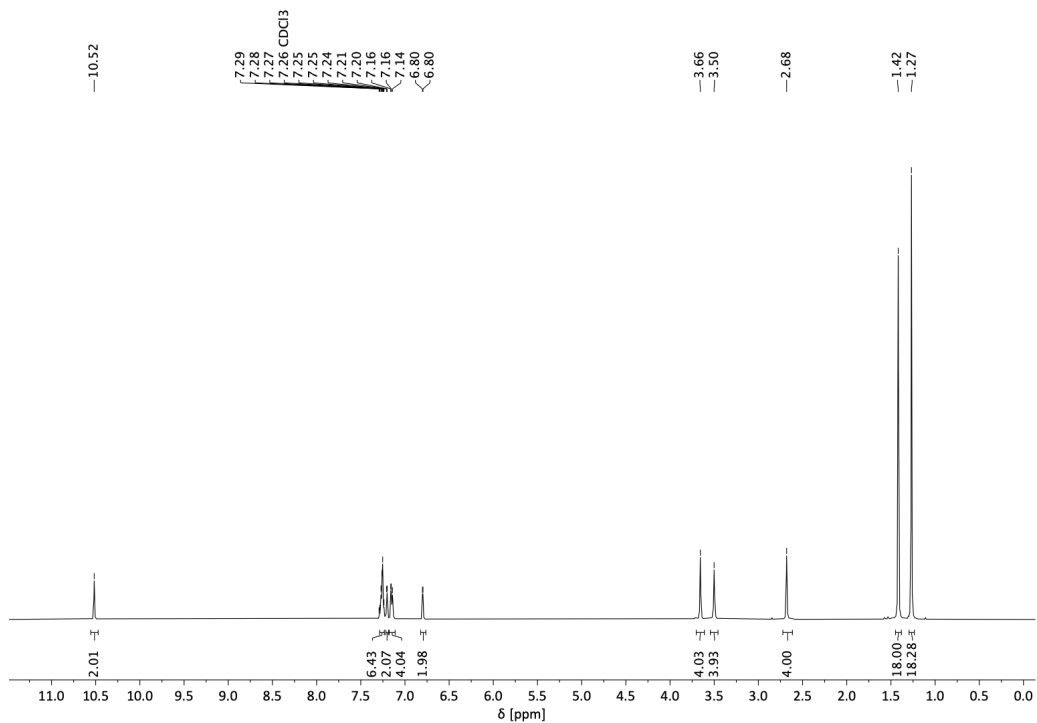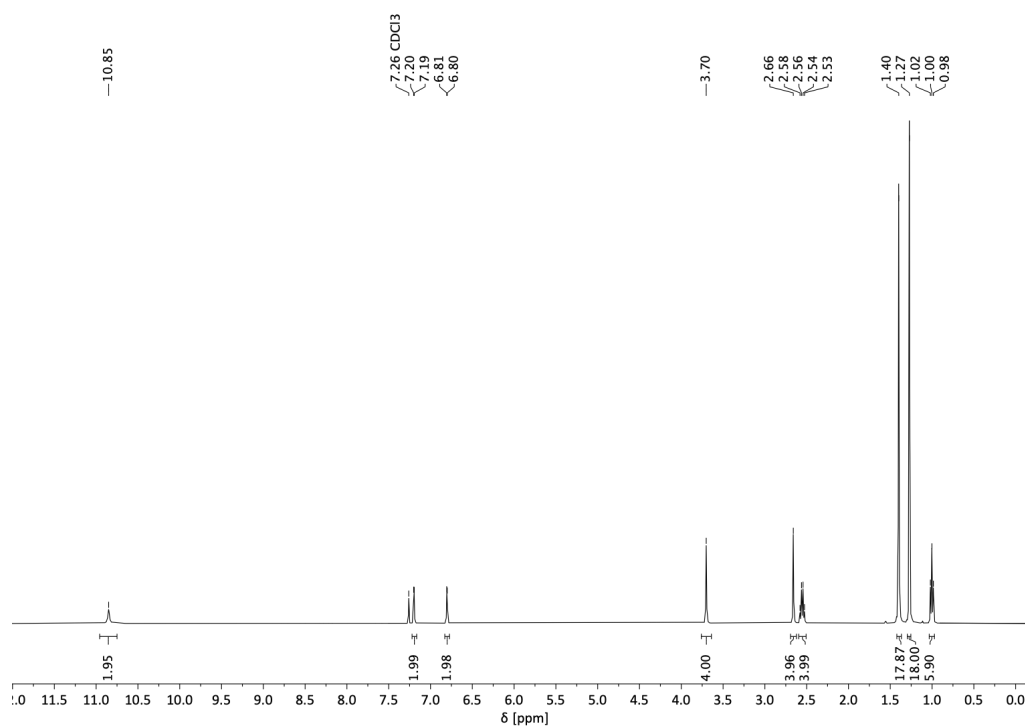
S13

NMR Spectra of Compounds

Figure S1. ^{1}H NMR spectrum (CDCl$_3$) of salan pro-ligand **L1**.

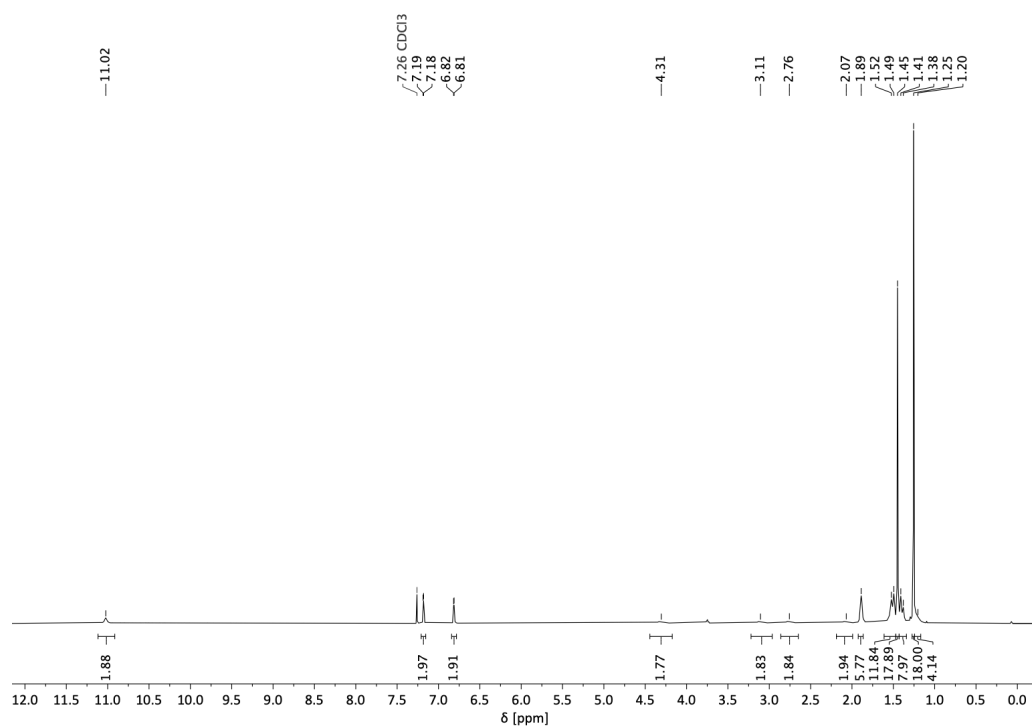**Figure S2.** ^{13}C{^{1}H} NMR spectrum (CDCl$_3$) of salan pro-ligand **L1**.

S14
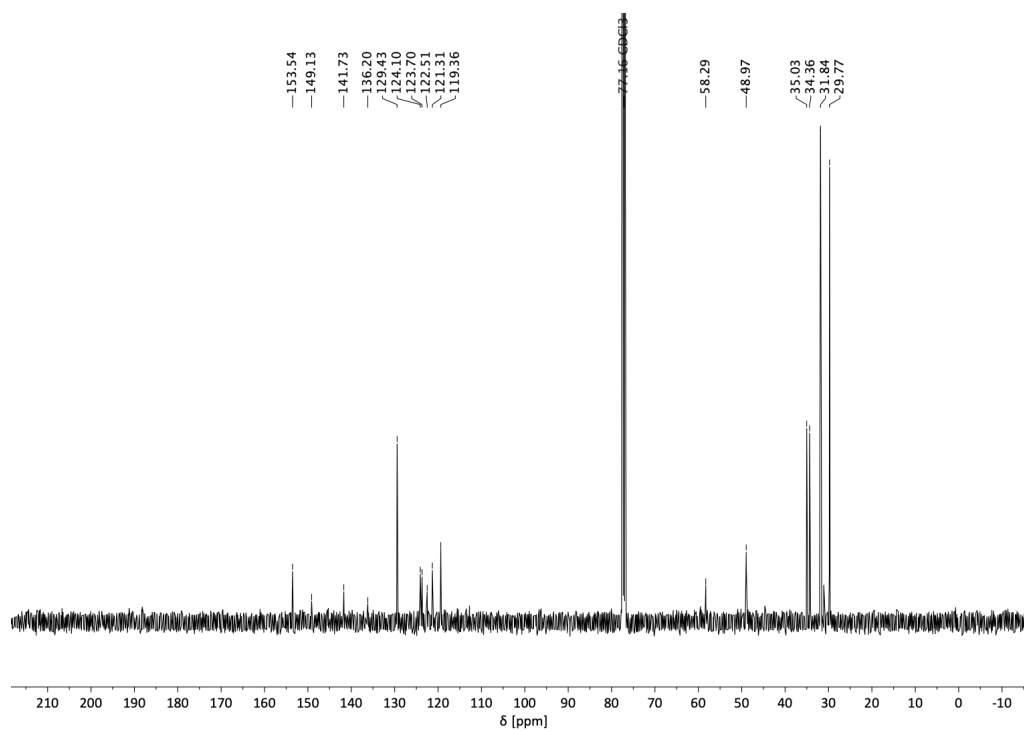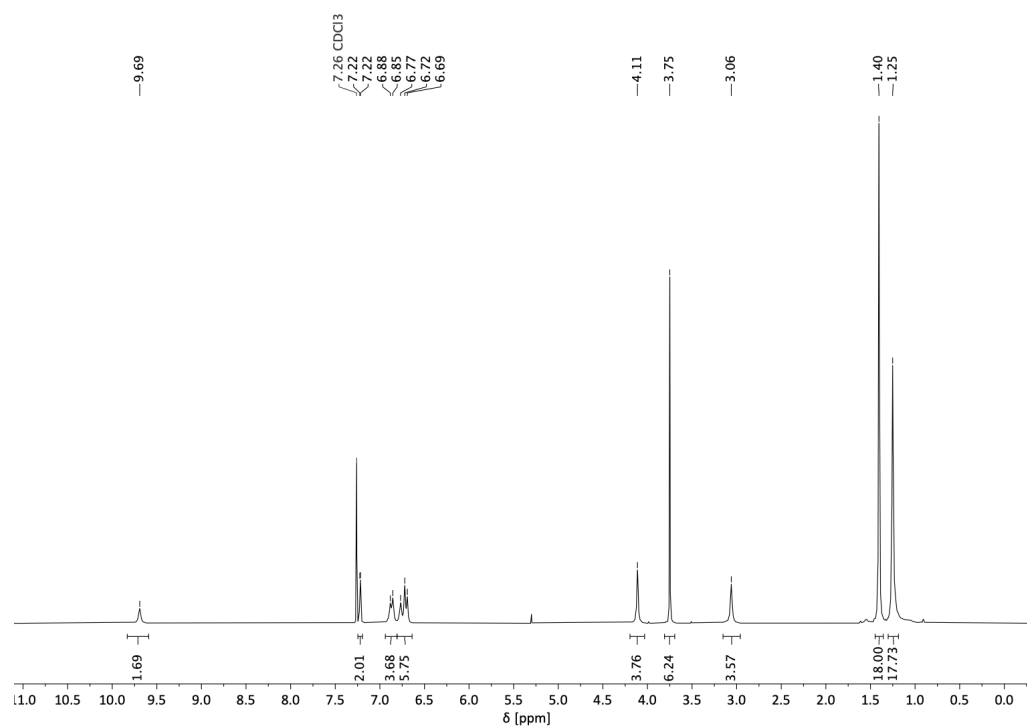
Figure S3. ^{1}H NMR spectrum (CDCl$_3$) of salan pro-ligand **L2**.
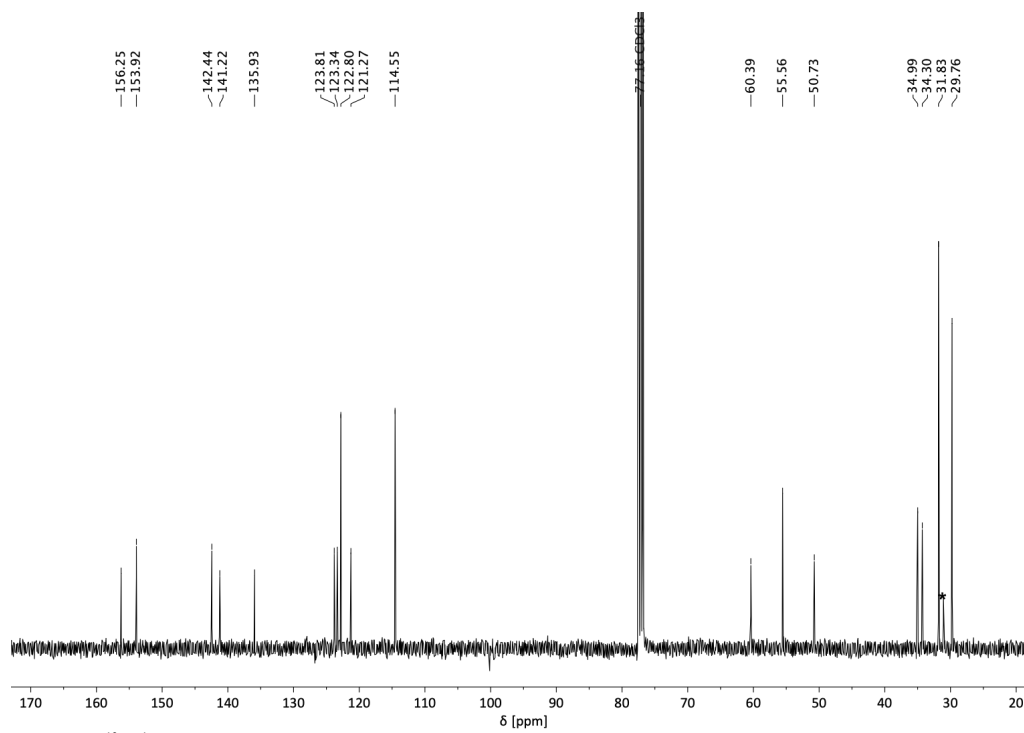
Figure S4. ^{13}C{^{1}H} NMR spectrum (CDCl$_3$) of salan pro-ligand **L2**, *=acetone.

S15
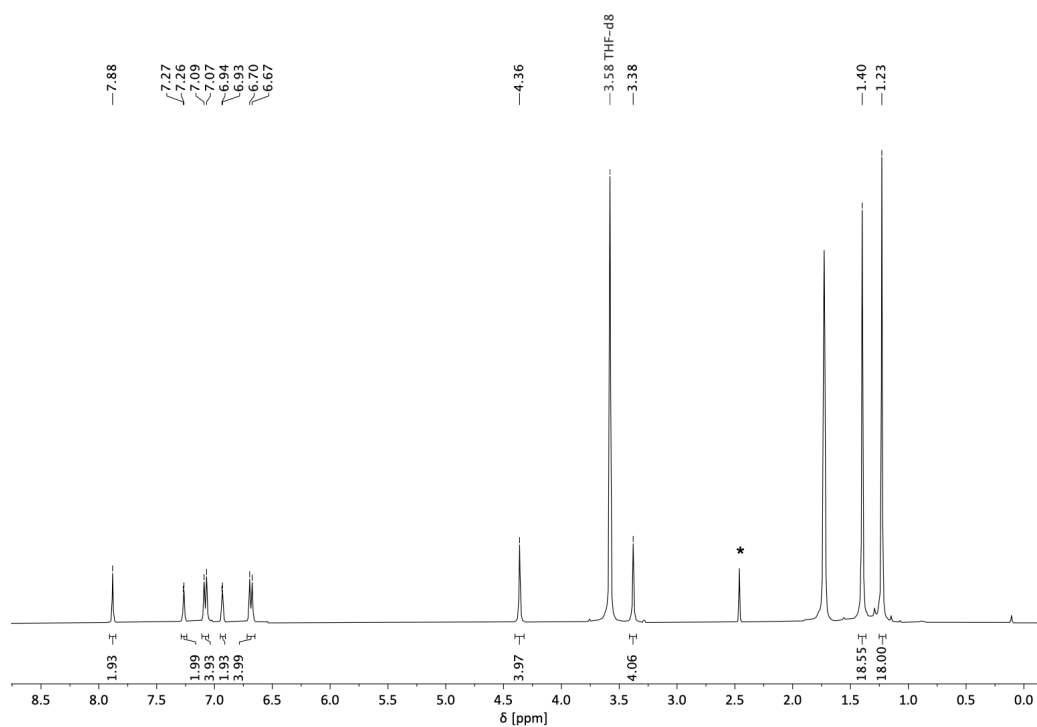
Figure S5. ^{1}H NMR spectrum (THF-d$_8$) of salan pro-ligand **L3**, *=H$_2$O.
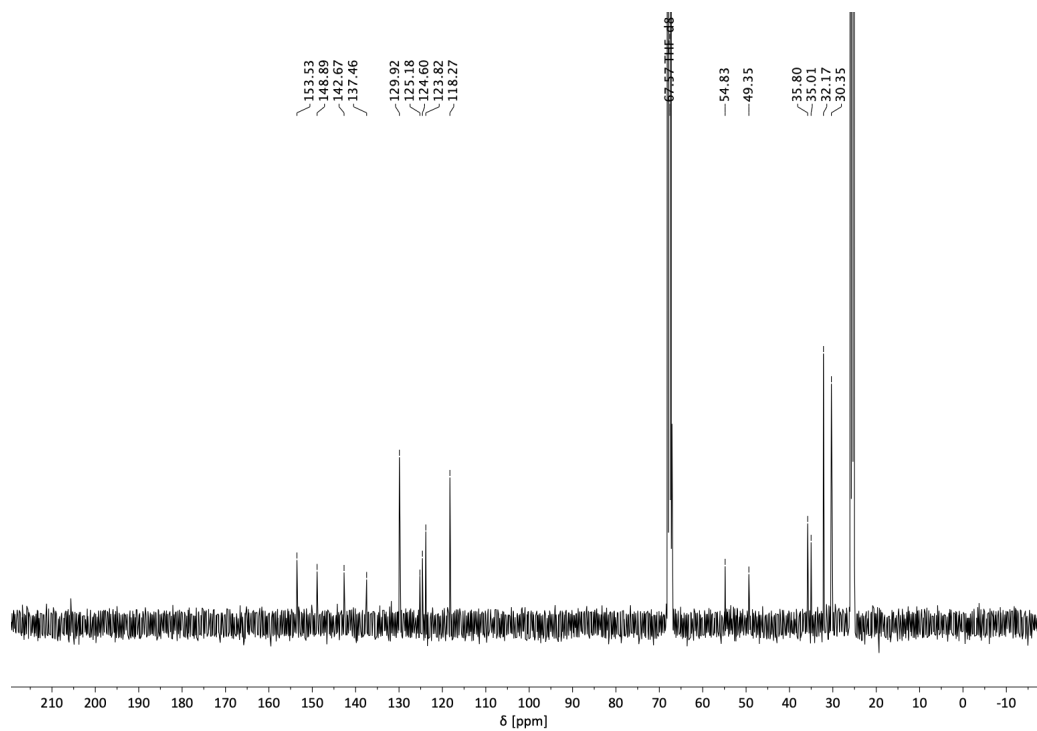
Figure S6. ^{13}C{^{1}H} NMR spectrum (THF-d$_8$) of salan pro-ligand **L3**.

S16
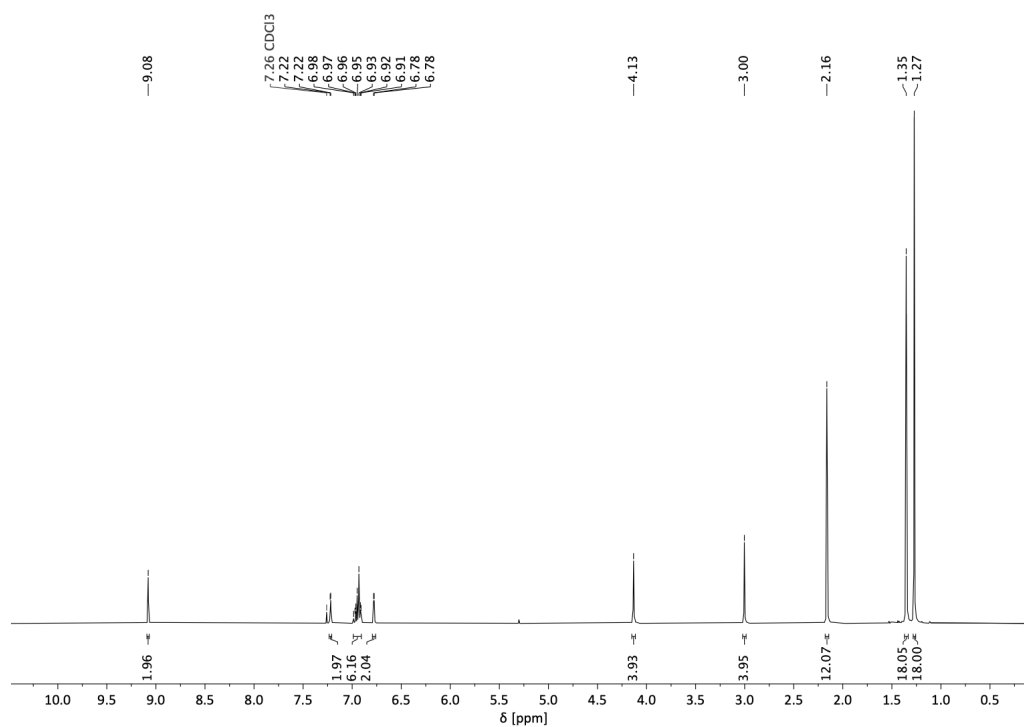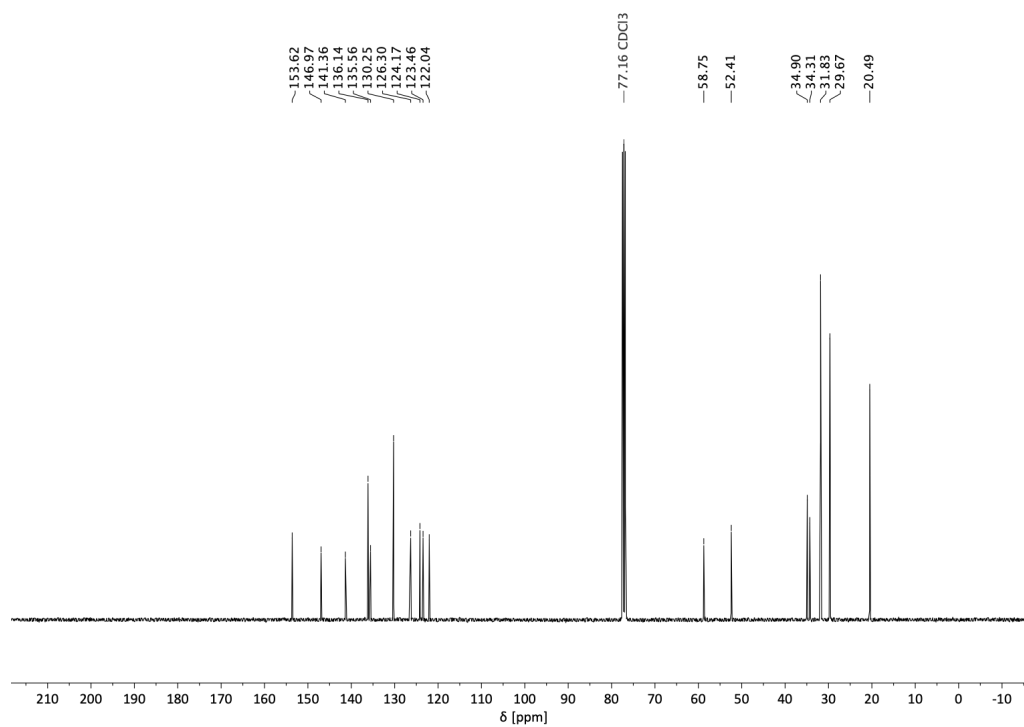
Figure S7. ^{1}H NMR spectrum (CDCl$_3$) of salan pro-ligand **L4**.

Figure S8. ^{13}C{^{1}H} NMR spectrum (CDCl$_3$) of salan pro-ligand **L4**.

S17
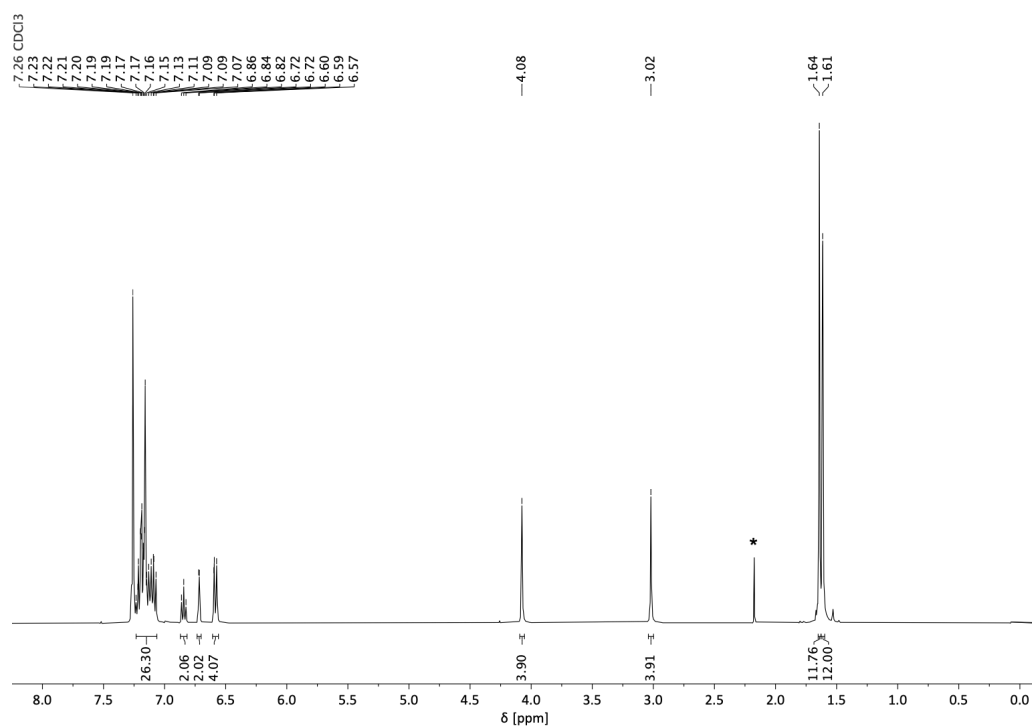
Figure S9. ^{1}H NMR spectrum (CDCl$_3$) of salan pro-ligand **L5**, * = acetone.
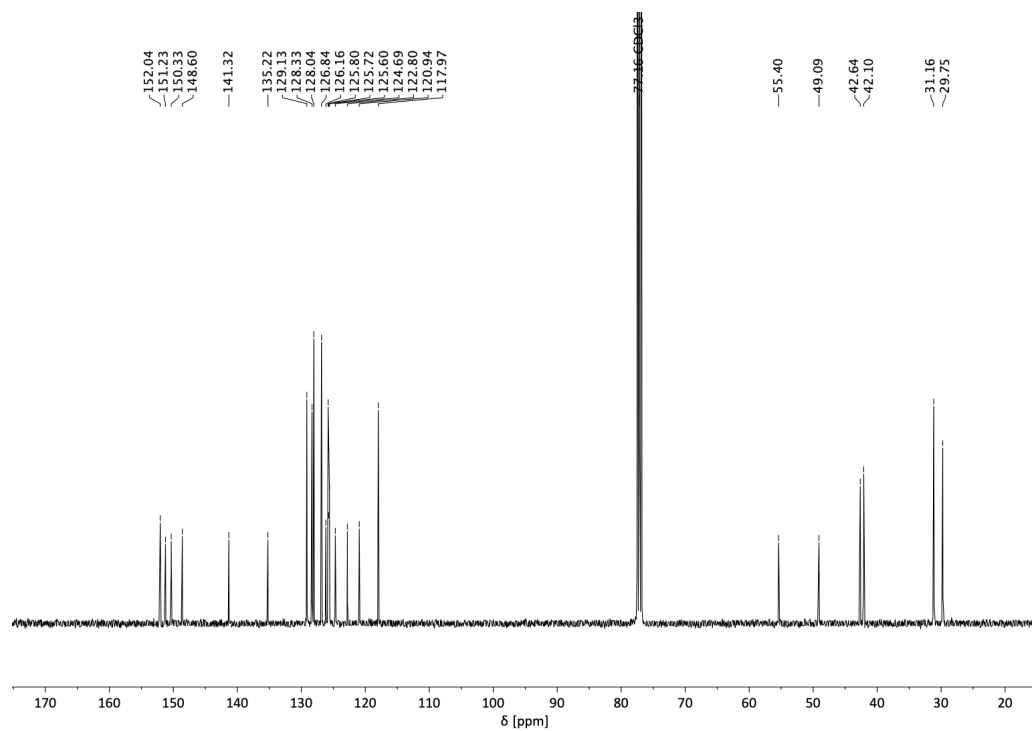
Figure S10. ^{13}C{^{1}H} NMR spectrum (CDCl$_3$) of salan pro-ligand **L5**.

S18
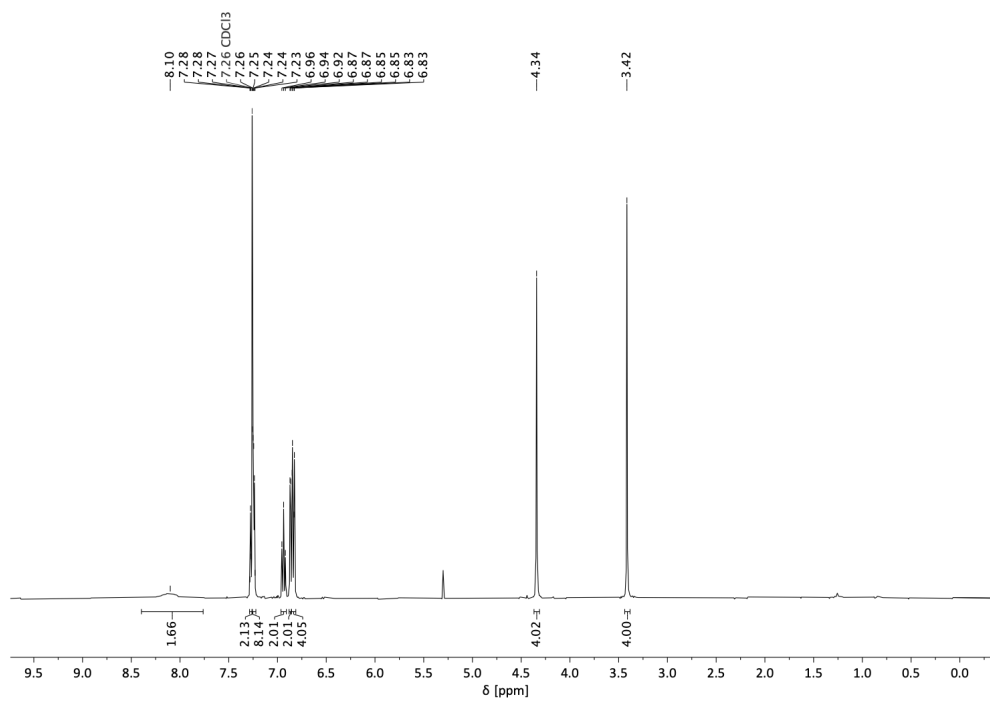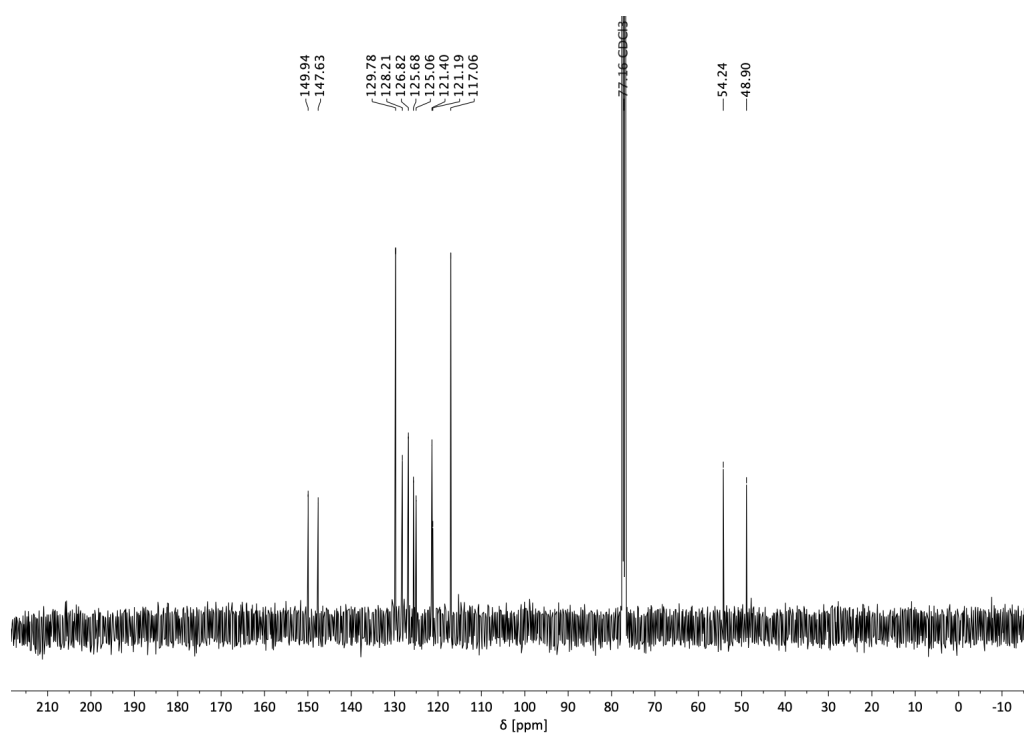
Figure S11. ^{1}H NMR spectrum (CDCl$_3$) of salan pro-ligand **L6**.

Figure S12. ^{13}C{^{1}H} NMR spectrum (CDCl$_3$) of salan pro-ligand **L6**.

S19
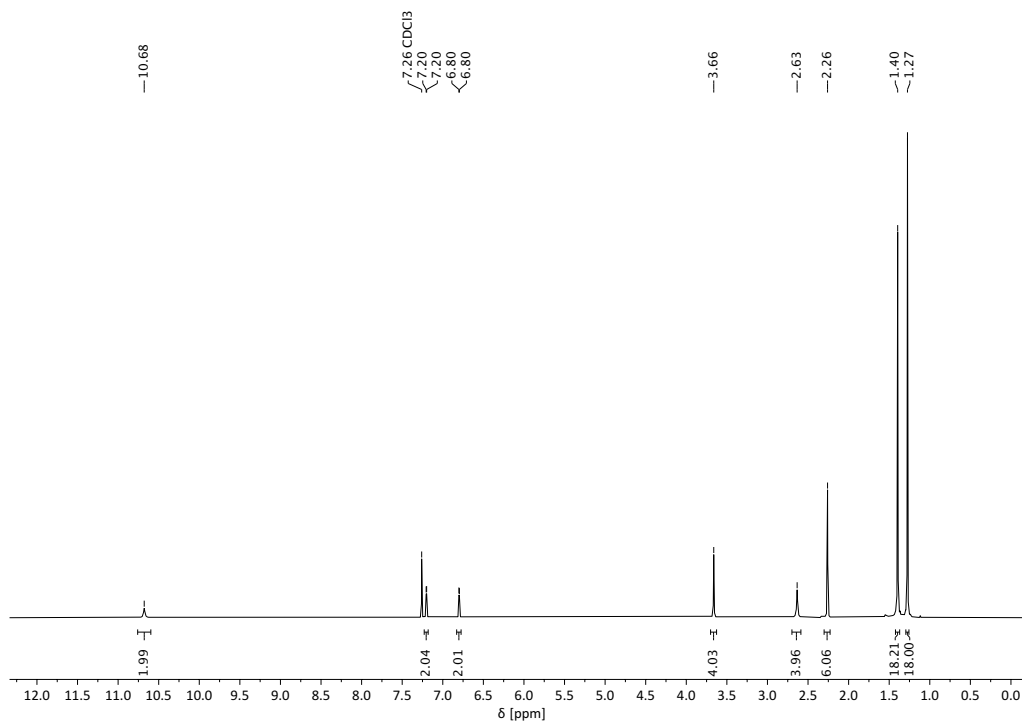
Figure S13. ^{1}H NMR spectrum (CDCl$_3$) of salan pro-ligand **L7**.
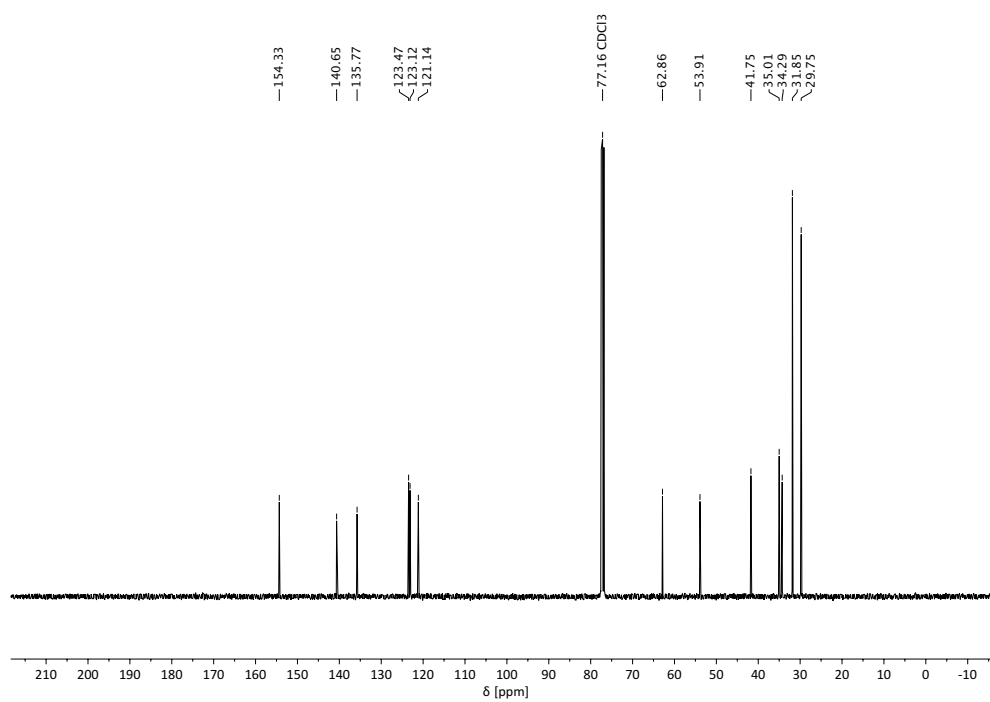
Figure S14. ^{13}C{^{1}H} NMR spectrum (CDCl$_3$) of salan pro-ligand **L7**.

S20

Figure S15. ^{1}H NMR spectrum (CDCl$_3$) of salan pro-ligand **L8**.
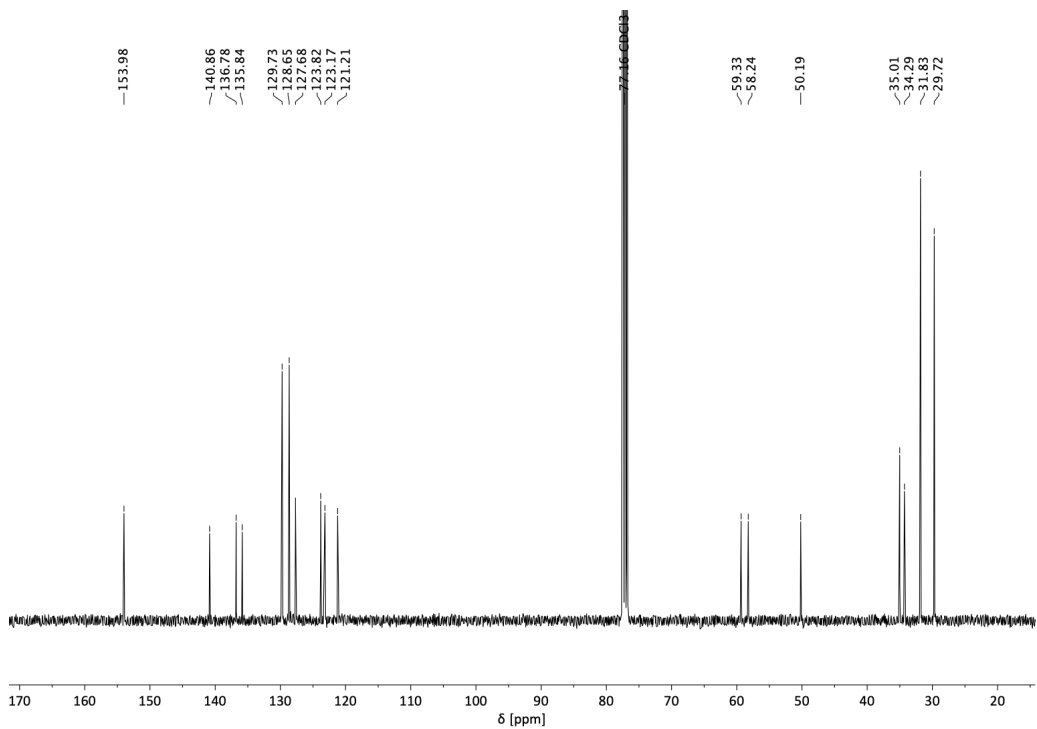
Figure S16. ^{13}C{^{1}H} NMR spectrum (CDCl$_3$) of salan pro-ligand **L8**.

S21

Figure S17. ^{1}H NMR spectrum (CDCl$_3$) of salan pro-ligand **L9**.
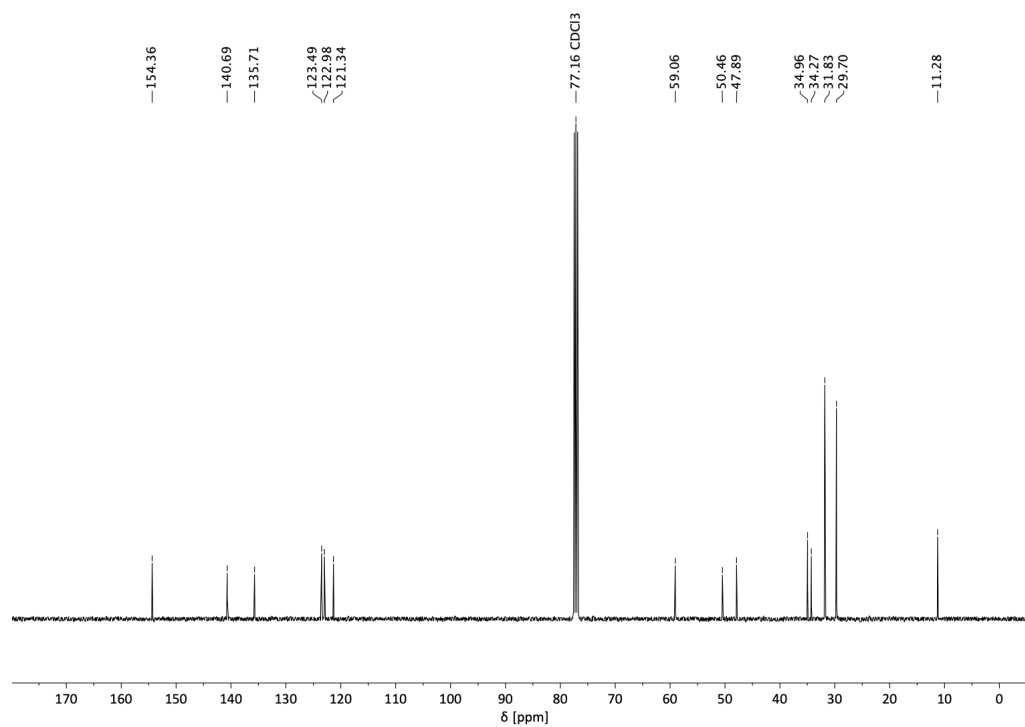
Figure S18. ^{13}C{^{1}H} NMR spectrum (CDCl$_3$) of salan pro-ligand **L9**.

S22

Figure S19. ^{1}H NMR spectrum (CDCl$_3$) of salan pro-ligand **L10**.
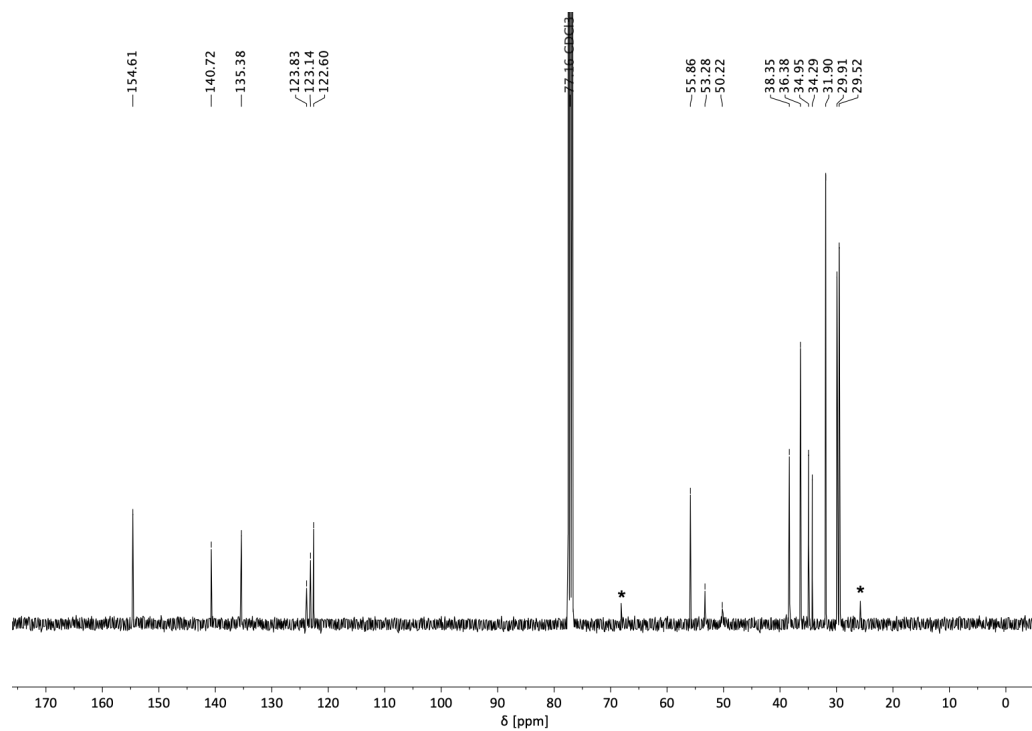
Figure S20. ^{13}C{^{1}H} NMR spectrum (CDCl$_3$) of salan pro-ligand **L10**, *=THF.

S23

213
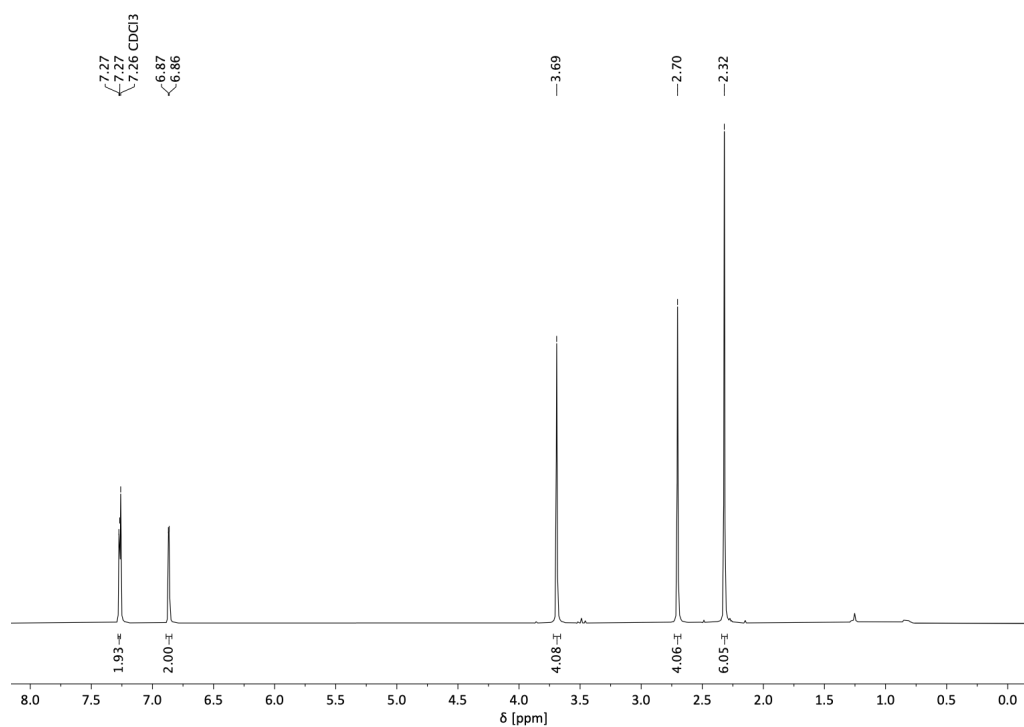
Figure S21. ¹H NMR spectrum (CDCl₃) of salan pro-ligand **L11**.
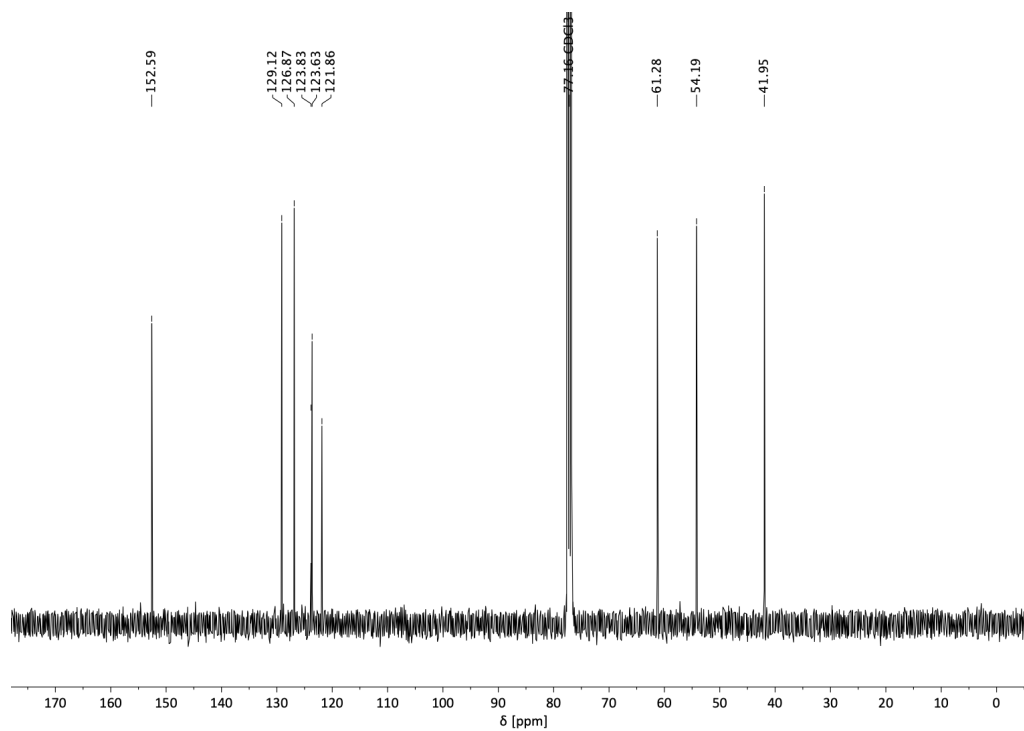
Figure S22. ¹³C{¹H} NMR spectrum (CDCl₃) of salan pro-ligand **L11**.

S24
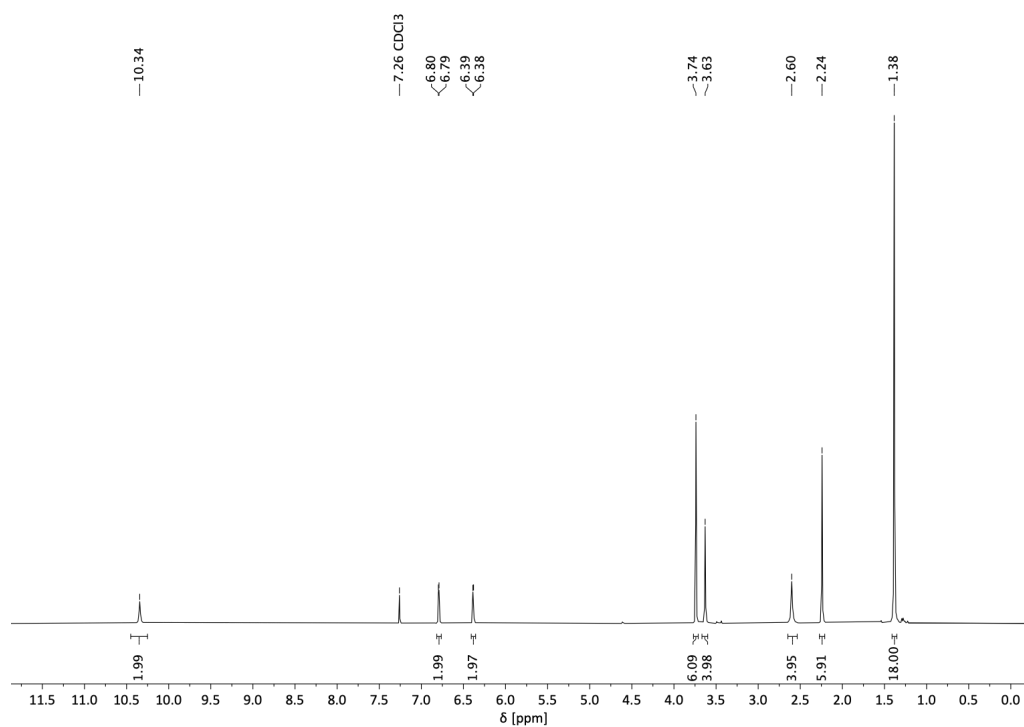
Figure S23. ^{1}H NMR spectrum (CDCl$_3$) of salan pro-ligand **L12**.
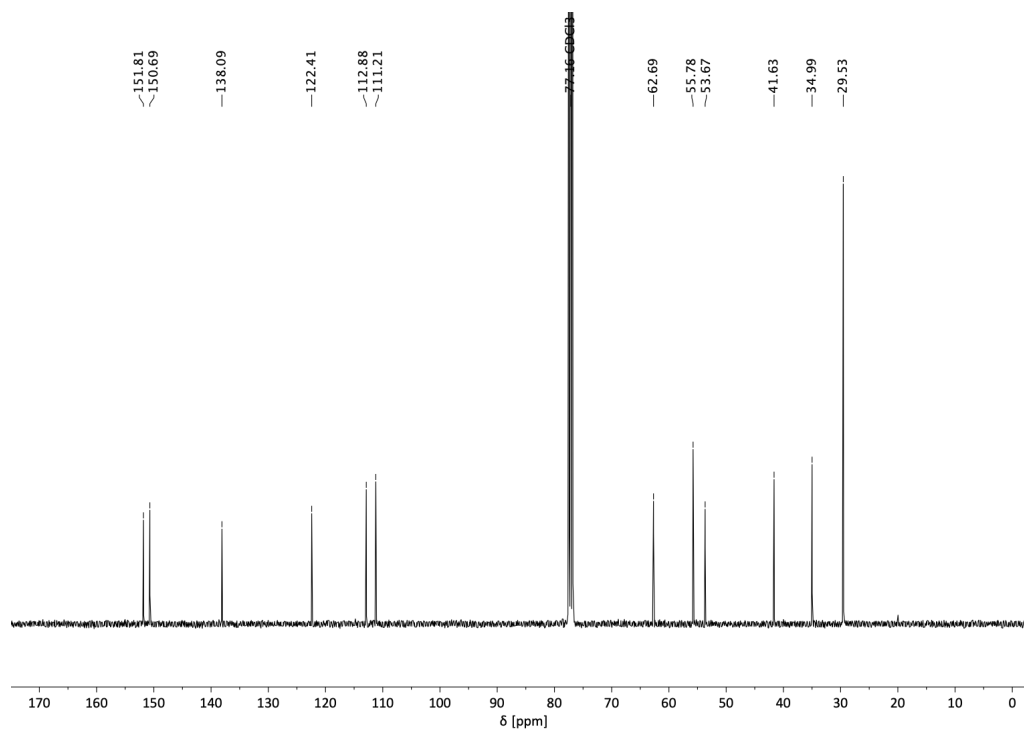
Figure S24. ^{13}C{^{1}H} NMR spectrum (CDCl$_3$) of salan pro-ligand **L12**.

S25
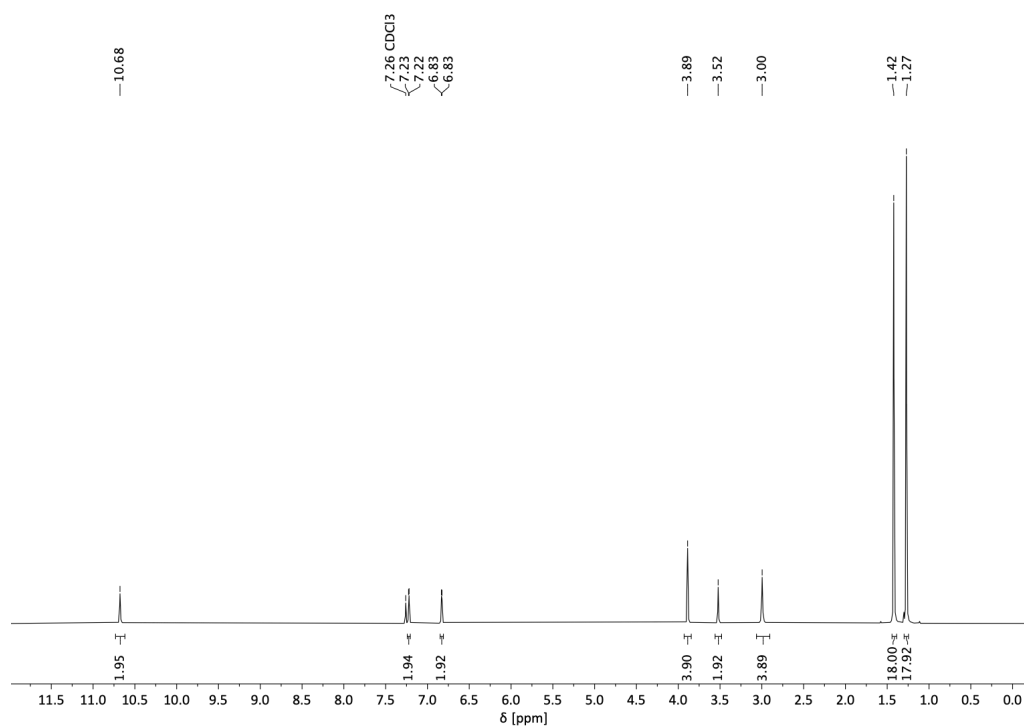
Figure S25. ^{1}H NMR spectrum (CDCl$_3$) of salan pro-ligand **L13**.
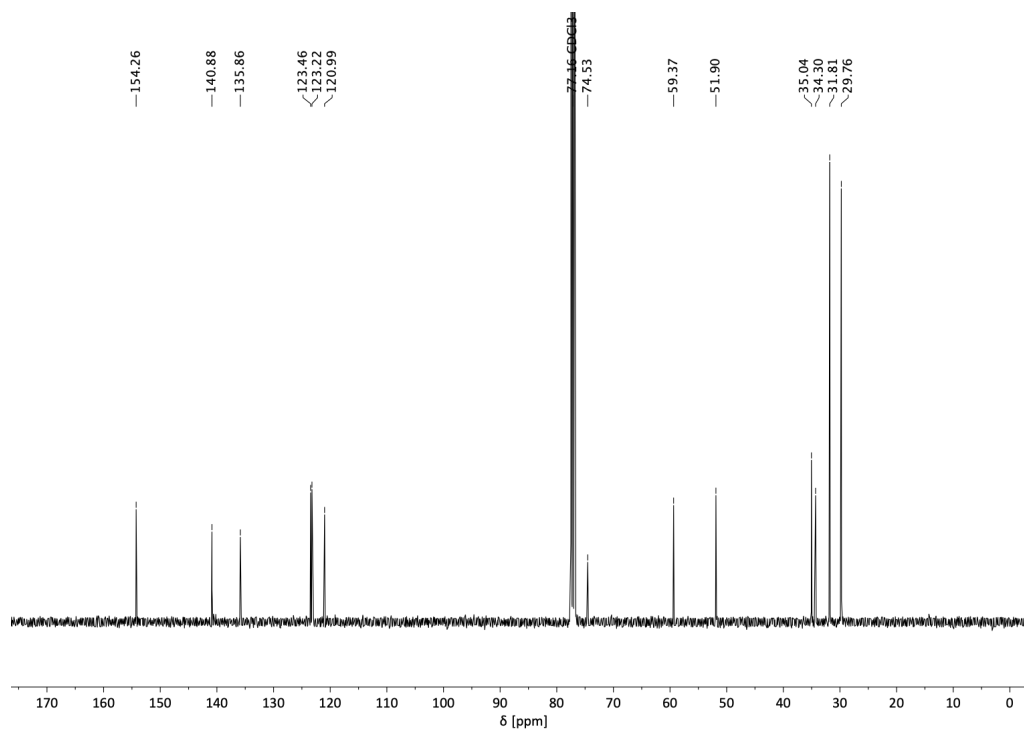
Figure S26. ^{13}C{^{1}H} NMR spectrum (CDCl$_3$) of salan pro-ligand **L13**.

S26
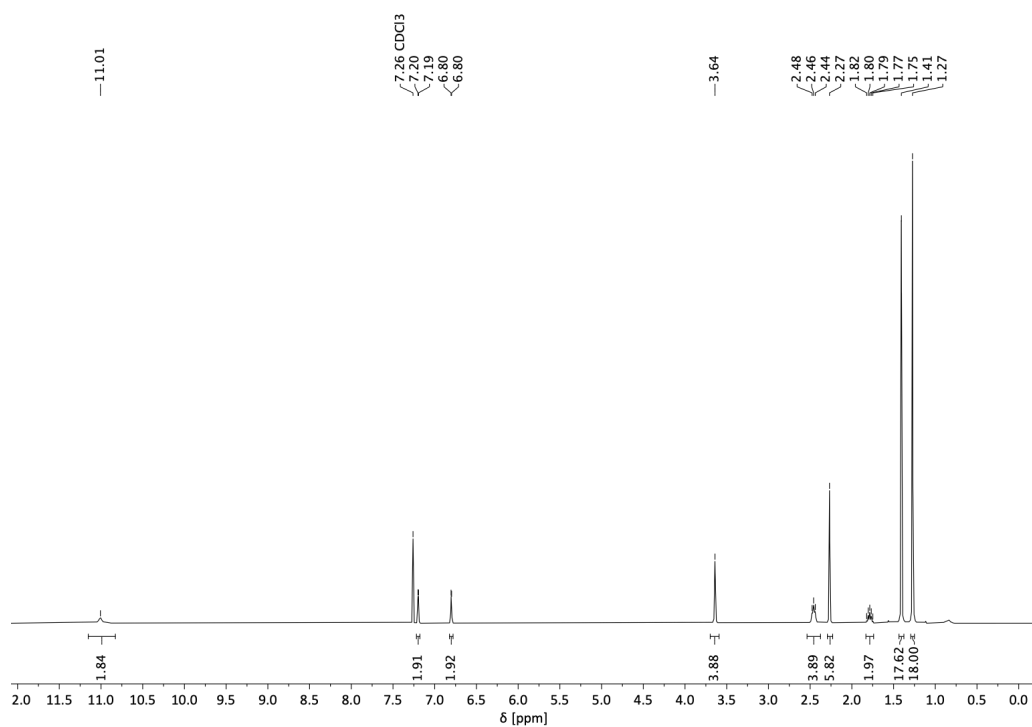
Figure S27. ^{1}H NMR spectrum (CDCl$_3$) of salan pro-ligand **L14**.
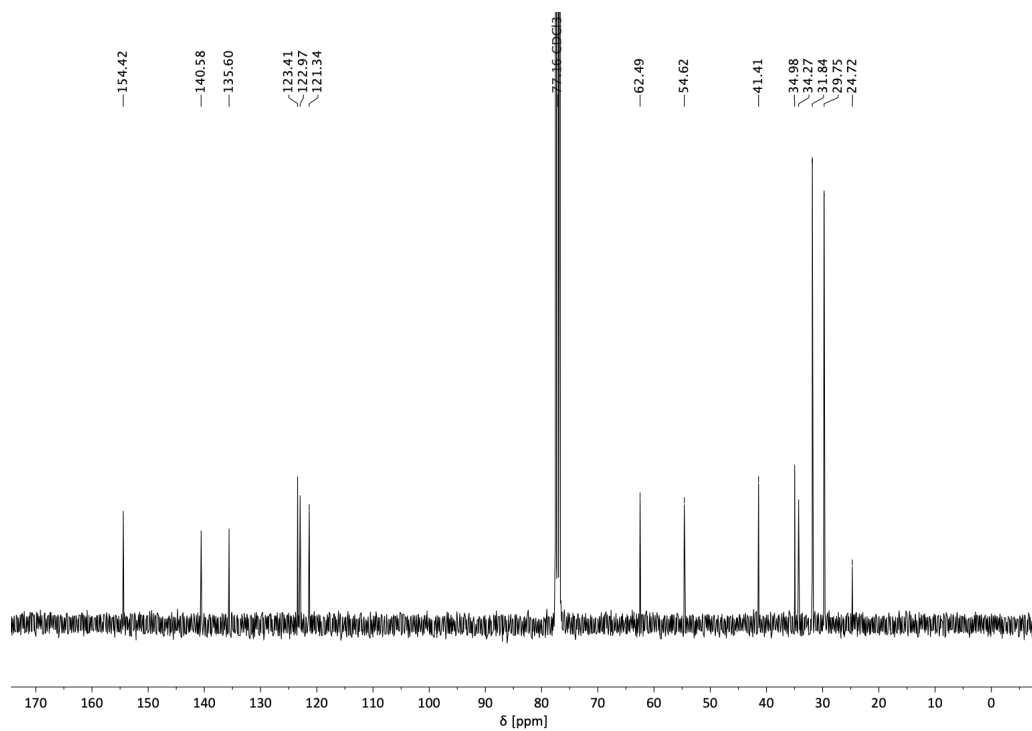
Figure S28. ^{13}C{^{1}H} NMR spectrum (CDCl$_3$) of salan pro-ligand **L14**.

S27

Figure S29. ^{1}H NMR spectrum (C$_6$D$_6$) of **Y1**.

Figure S30. ^{13}C{^{1}H} NMR spectrum (C$_6$D$_6$) of **Y1**.

S28
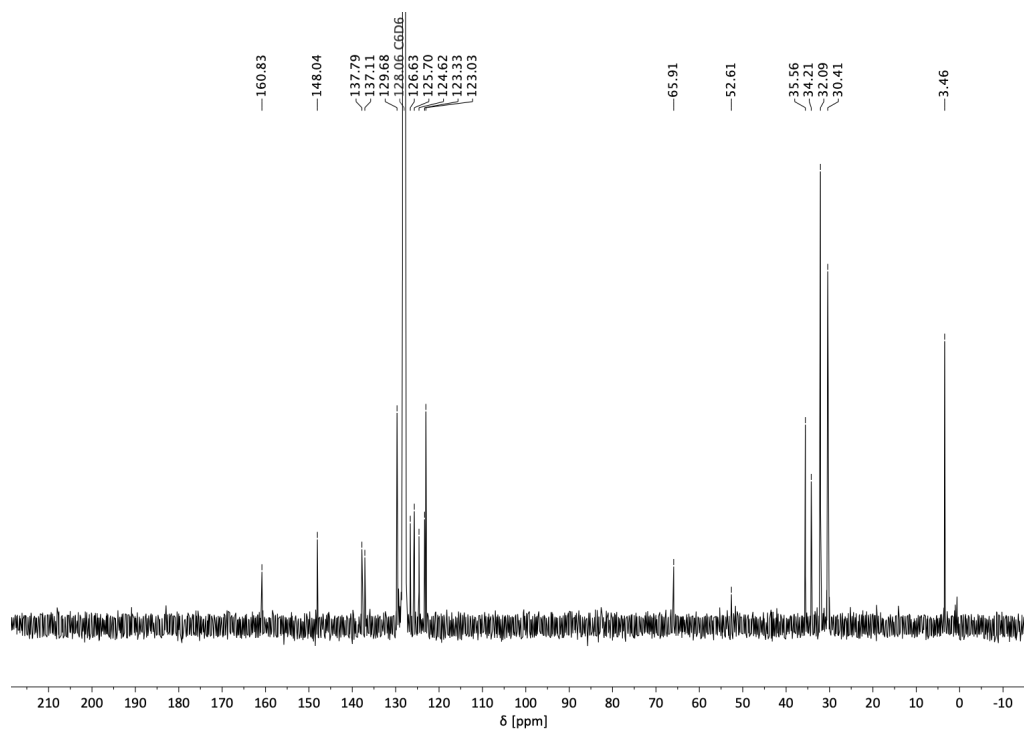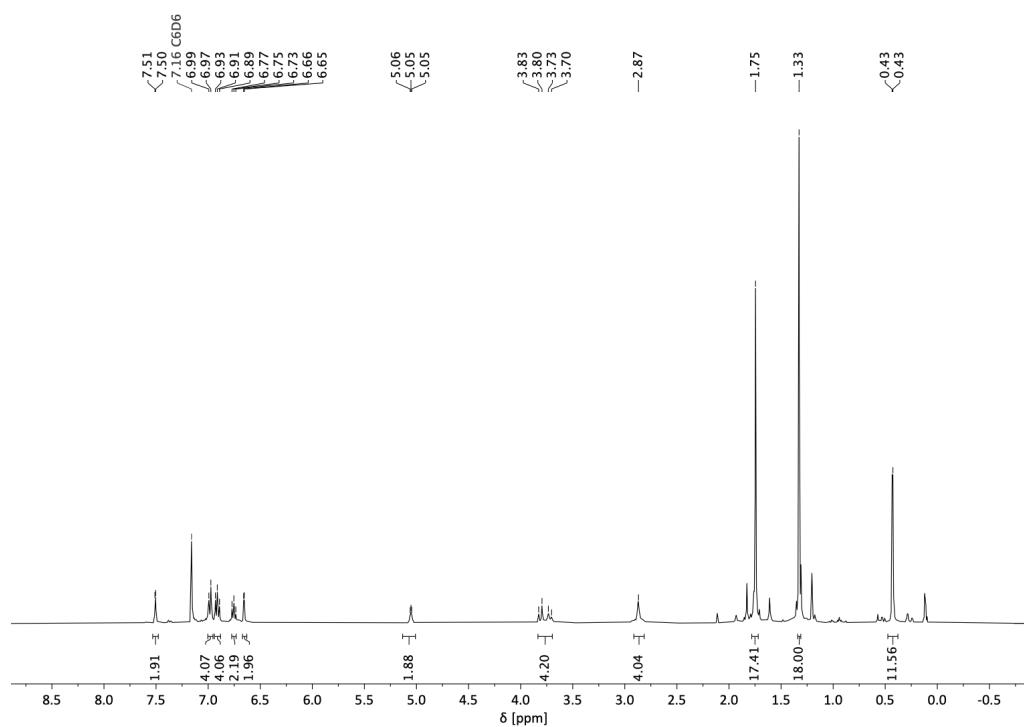
2. Polymer Characterization Data

^{1}H and ^{13}C{^{1}H} NMR Spectra of PHB
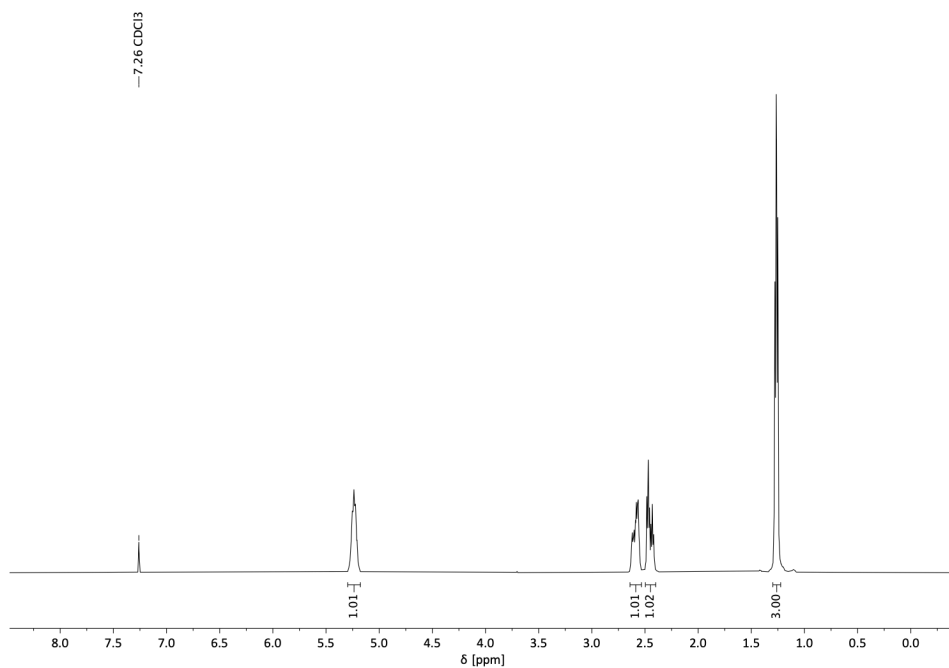
Figure S31. Representative ^{1}H NMR spectrum (CDCl$_3$) of PHB (produced by **Y+L14**).
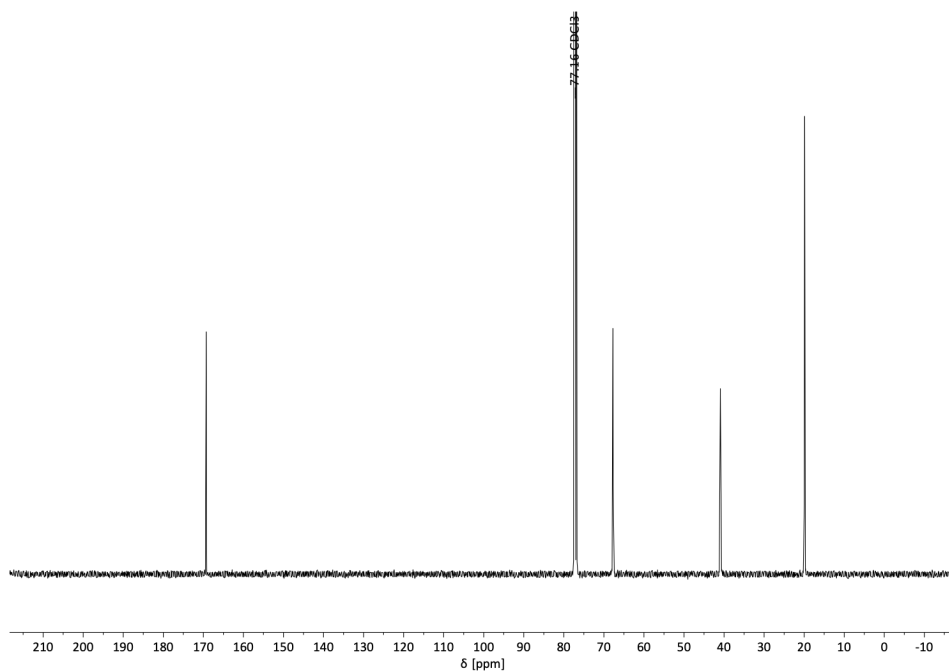
Figure S32. Representative ^{13}C{^{1}H} NMR spectrum (CDCl$_3$) of PHB (produced by **Y+L14**).

S29

Tacticity of PHBs Produced by *In Situ* Generated Catalysts
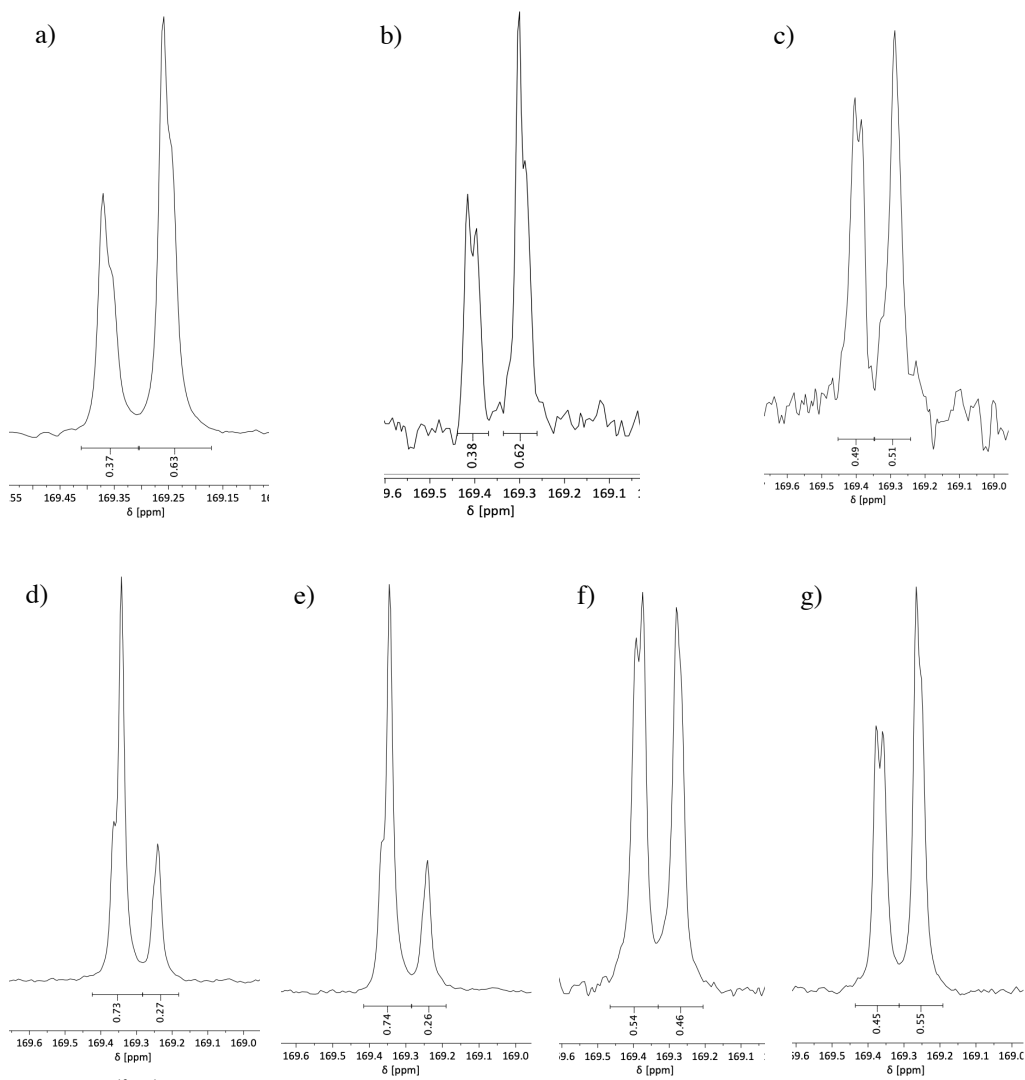
Figure S33. $^{13}C\{^1H\}$ NMR spectra (carbonyl region) of PHBs with variable tacticity produced by salan catalyst systems: a) **Y+L2** (Table 2, entry 2), b) **Y+L3** (Table 2, entry 3), c) **Y+L6** (Table 2, entry 6), d) **Y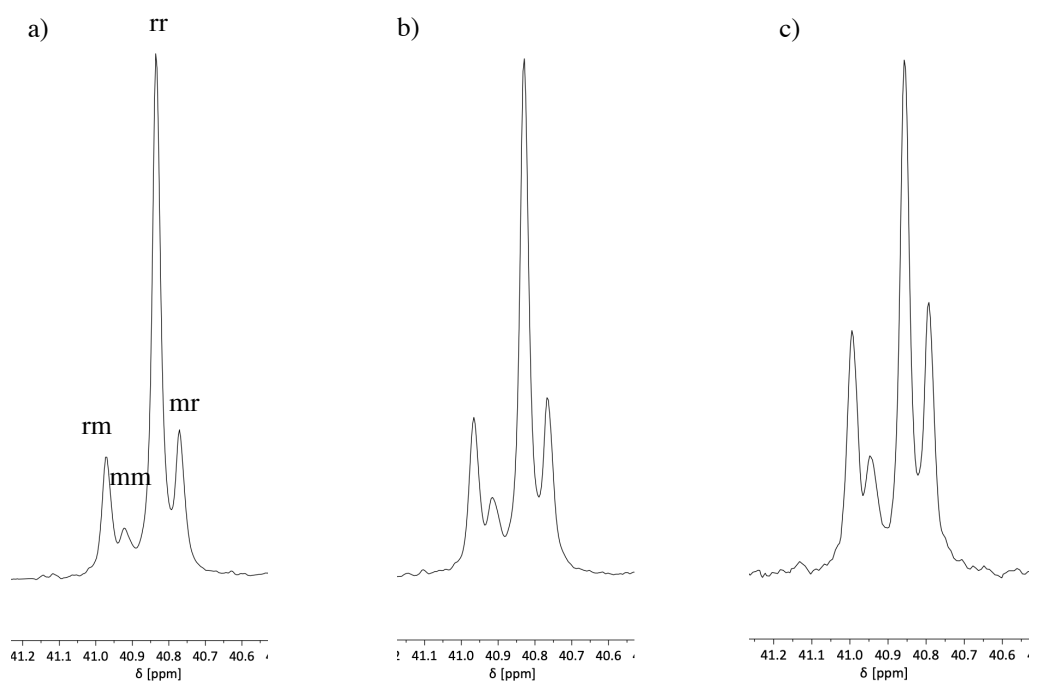+L8** (Table 2, entry 8), e) **Y+L12** (Table 2, entry 12), f) **Y+L13** (Table 2, entry 13), g) **Y+L14** (Table 2, entry 14).

S30
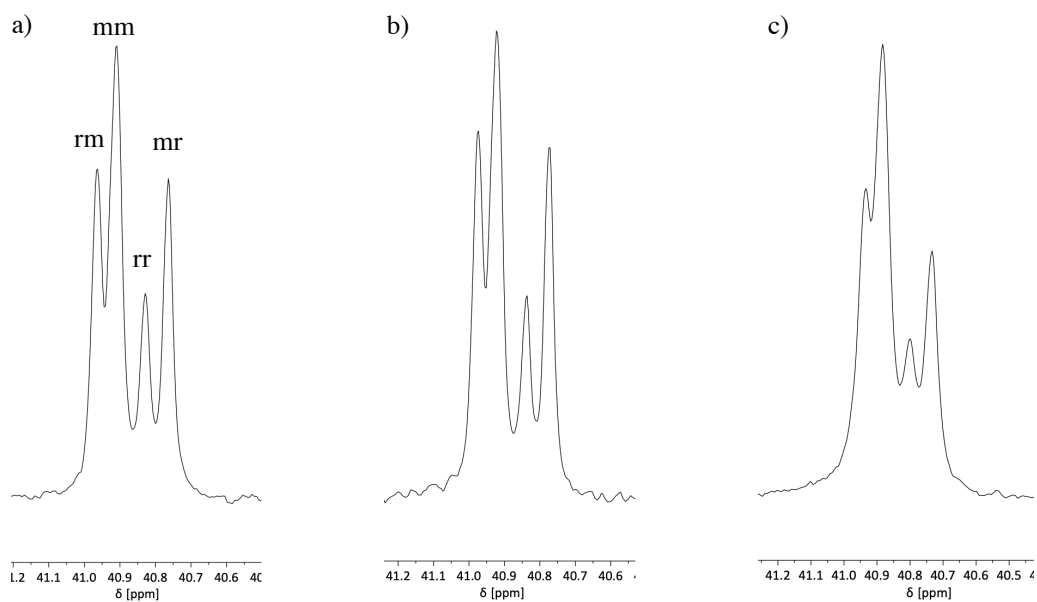
Figure S34. $^{13}C\{^1H\}$ NMR spectra (methylene region) of PHBs with an isotactic bias produced by salan catalyst systems: a) **Y+L1** (Table 2, entry 1), b) **Y+L2** (Table 2, entry 2), c) **Y+L5** (Table 2, entry 5).

Figure S35. $^{13}C\{^1H\}$ NMR spectra (methylene region) of PHBs with a syndiotactic bias produced by salan catalyst systems: a) **Y+L7** (Table 2, entry 7), b) **Y+L8** (Table 2, entry 8), c) **Y+L9** (Table 2, entry 9).
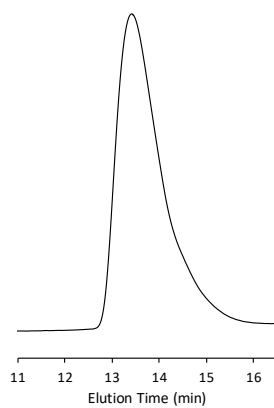
S31

Representative GPC Traces

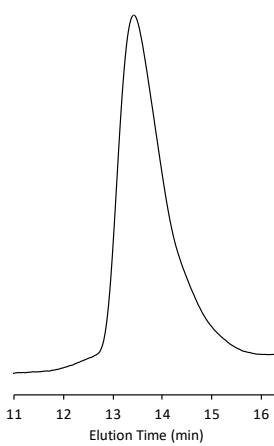**Figure S36.** GPC trace of PHB, M_n = 23.4 kg mol^{-1}, $Đ$ = 1.5 (Table 1, entry 3).

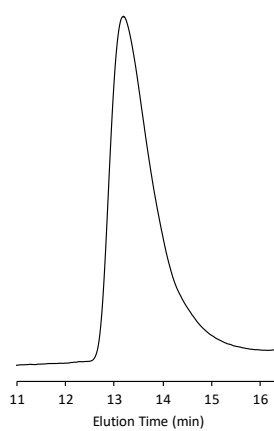**Figure S37.** GPC trace of PHB, M_n = 23.0 kg mol^{-1}, $Đ$ = 1.5 (Table 2, entry 1).

Figure S38. GPC trace of PHB, M_n = 29.8 kg mol^{-1}, $Đ$ = 1.4 (Table 2, entry 2).

S32

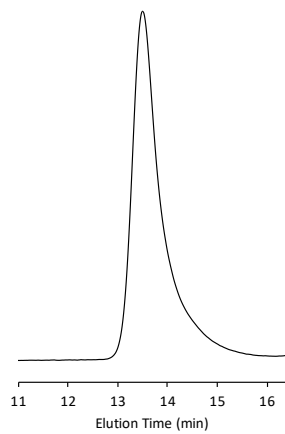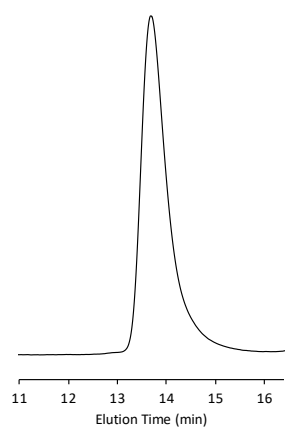**Figure S39.** GPC trace of PHB, M_n = 25.7 kg mol^{-1}, $Đ$ = 1.3 (Table 2, entry 9).

Figure S40. GPC trace of PHB, M_n = 23.2 kg mol^{-1}, $Đ$ = 1.2 (Table 2, entry 14).

S33

3. References

1. Anwander, R.; Runte, O.; Eppinger, J.; Gerstberger, G.; Herdtweck, E.; Spiegler, M., Synthesis and structural characterisation of rare-earth bis (dimethylsilyl) amides and their surface organometallic chemistry on mesoporous MCM-41. *J. Chem. Soc., Dalton Trans.* **1998**, 847-858.

2. Zhuo, Z.; Zhang, C.; Luo, Y.; Wang, Y.; Yao, Y.; Yuan, D.; Cui, D., Stereo-selectivity switchable ROP of rac-β-butyrolactone initiated by salan-ligated rare-earth metal amide complexes: the key role of the substituents on ligand frameworks. *Chem. Commun.* **2018,** *54*, 11998-12001.

3. Bloembergen, S.; Holden, D. A.; Bluhm, T. L.; Hamer, G. K.; Marchessault, R. H., Stereoregularity in synthetic β-hydroxybutyrate and β-hydroxyvalerate homopolyesters. *Macromolecules* **1989,** *22*, 1656-1663.

4. Buckley, B. R.; Neary, S. P., Thiadiazolidine 1-oxide systems for phosphine-free palladium-mediated catalysis. *Tetrahedron* **2010,** *66*, 7988-7994.

5. Papadaki, E.; Magrioti, V., Synthesis of pentafluorobenzene-based NHC adducts and their catalytic activity in the microwave-assisted reactions of aldehydes. *Tetrahedron Lett.* **2020,** *61*, 151419.

6. Thangavel, A.; Wieliczko, M.; Bacsa, J.; Scarborough, C. C., 1,4,7-Triazacyclononane ligands bearing tertiary alkyl nitrogen substituents. *Inorg. Chem.* **2013,** *52*, 13282-13287.

7. Konkol, M.; Nabika, M.; Kohno, T.; Hino, T.; Miyatake, T., Synthesis, structure and α-olefin polymerization activity of group 4 metal complexes with [OSSO]-type bis (phenolate) ligands. *J. Organomet. Chem.* **2011,** *696*, 1792-1802.

8. Altenbuchner, P. T.; Adams, F.; Kronast, A.; Herdtweck, E.; Pöthig, A.; Rieger, B., Stereospecific catalytic precision polymerization of 2-vinylpyridine via rare earth metal-mediated group transfer polymerization with 2-methoxyethylamino-bis(phenolate)-yttrium complexes. *Polym. Chem.* **2015,** *6*, 6796-6801.

9. Schneider, F.; Zhao, T.; Huhn, T., Cytotoxic heteroleptic heptacoordinate salan zirconium(iv)-bis-chelates - synthesis, aqueous stability and X-ray structure analysis. *Chem. Commun.* **2016,** *52*, 10151-10154.

10. Hormnirun, P.; Marshall, E. L.; Gibson, V. C.; White, A. J.; Williams, D. J., Remarkable stereocontrol in the polymerization of racemic lactide using aluminum initiators supported by tetradentate aminophenoxide ligands. *J. Am. Chem. Soc.* **2004,** *126*, 2688-2689.

11. Segal, S.; Goldberg, I.; Kol, M., Zirconium and titanium diamine bis (phenolate) catalysts for α-olefin polymerization: From atactic oligo (1-hexene) to ultrahigh-molecular-weight isotactic poly (1-hexene). *Organometallics* **2005,** *24*, 200-202.

12. Xu, X.; Yao, Y.; Zhang, Y.; Shen, Q., Synthesis, reactivity, and structural characterization of sodium and ytterbium complexes containing new imidazolidine-bridged bis (phenolato) ligands. *Inorg. Chem.* **2007,** *46*, 3743-3751.

10.5 Supporting Information for Chapter 8

Supporting Information

For

Highly Isoselective Ring-Opening Polymerization of *rac-β*-Butyrolactone: Access to Synthetic Poly(3-hydroxybutyrate) with Polyolefin-like Material Properties

Jonas Bruckmoser, Stefanie Pongratz, Lucas Stieglitz, and Bernhard Rieger[*]

WACKER-Chair of Macromolecular Chemistry, Catalysis Research Center,
Department of Chemistry, Technical University of Munich
Lichtenbergstraße 4, 85748 Garching bei München, Germany.

[*]Corresponding Author; email: rieger@tum.de

Table of Contents

S1

1. Experimental Section

Materials and Methods

All manipulations containing air- and/or moisture sensitive compounds were carried out under argon atmosphere using standard Schlenk or glovebox techniques. Glassware was flame-dried under vacuum prior to use. Unless otherwise stated, all chemicals were purchased from Sigma-Aldrich, TCI Chemicals or ABCR and used as received. Solvents were obtained from an MBraun MB-SPS 800 solvent purification system and stored over 3 Å molecular sieves prior to use. β-BL was treated with BaO, dried over CaH_2 and distilled prior to use. Deuterated chloroform ($CDCl_3$), benzene (C_6D_6), toluene (C_7D_8) and tetrahydrofuran (C_4D_8O) were obtained from Sigma-Aldrich and dried over 3 Å molecular sieves. Bacterial PHB was a gift from BASF SE (M_n = 247 kg mol^{-1}, $Đ$ = 2.3). $Y[N(SiHMe_2)_2]_3(THF)_2$ (**Y**) and $La[N(SiHMe_2)_2]_3(THF)_2$ (**La**) were prepared according to literature procedures.[1]

Nuclear magnetic resonance (NMR) spectra were recorded on a Bruker AV-III-500 spectrometer equipped with a QNP-Cryoprobe or AV-III-400 spectrometers at ambient temperature (298 K). ^1H and $^{13}C\{^1H\}$ NMR spectroscopic chemical shifts δ are reported in ppm relative to tetramethylsilane and were referenced internally to the relevant residual solvent resonances. The following abbreviations are used: br, broad; s, singlet; d, doublet; t, triplet; p, pentet; m, multiplet; AB, AB system. The tacticity of PHB was determined by integration of the carbonyl region of the $^{13}C\{^1H\}$ NMR spectrum.[2]

Elemental analyses were measured with a EURO EA instrument from HEKAtech at the Laboratory for Microanalysis, Catalysis Research Center, Technical University of Munich.

Electrospray ionization mass spectrometry (ESI-MS) was measured with a Thermo Fisher Scientific Exactive Plus Orbitrap in the positive mode in acetonitrile.

Polymer weight-average molecular weight (M_w), number-average molecular weight (M_n) and polydispersity indices ($Đ = M_w/M_n$) were determined *via* gel permeation chromatography (GPC) relative to polystyrene standards on a PL-SEC 50 Plus instrument from Polymer Laboratories. The analysis was performed at ambient temperatures using chloroform as the eluent at a flow rate of 1.0 mL min^{-1}.

Differential scanning calorimetry (DSC) measurements were carried out with a DSC Q2000 from TA Instruments with a heating and cooling rate of 10 °C min^{-1}. T_g and T_m values were obtained from the second heating scan.

Thermal gravimetric analysis (TGA) was carried out with a TGA Q5000 from TA Instruments. Polymer samples were heated under argon atmosphere from ambient temperature to 600 °C with a heating rate of 10 °C min^{-1}.

For specimen fabrication for stress-strain measurements, polymer had to be milled prior to compression molding. The polymer was ultracentrifugal-milled by using a Retsch ultra centrifugal mill ZM 200 (12-tooth rotor, sieve size 2.00 mm, trapezoid holes) at 12000 rpm. Specimens (dog-bone-shaped, 50 mm long, 4.0 mm wide, 1.0 mm thick; parameters were checked prior to stress-strain measurements) were obtained by compression molding of the solvent-free polymer on a Servitec Polystat 200 T at temperatures 10°C higher than each material's respective T_m in a two-part cycle: first, the polymer was equilibrated with no applied pressure for 4 min and subsequently pressurized at 200 bar for 3 min. The specimens were checked with regard to a homogeneous distribution. Stress-strain measurements were performed on a Zmart.Pro ZwickRoell machine with a strain rate of 5 mm min^{-1} and analyzed with testXpert II software.

General Polymerization Procedures

Polymerization Procedure Using In Situ Generated Catalysts

In a glove box, a 20 mL glass reactor was charged with a predetermined amount of Y[N(SiHMe$_2$)$_2$]$_3$(THF)$_2$ (1 eq.) and salan pro-ligand (1 eq., **L1 – L5**). The respective amount of toluene was added such that the overall monomer concentration after *rac-β*-BL addition is 2.0 M. The reaction mixture was stirred for 1 h at room temperature and then, *rac-β*-BL (equivalents as specified in the polymerization table) was added to this mixture. After stirring for a desired time period at room temperature, the polymerization was quenched by the addition of 0.5 mL of methanol. An aliquot sample was taken for determination of conversion by ^{1}H NMR spectroscopy. The quenched mixture was then precipitated into 20 mL of diethyl ether/pentane (1/1), filtered, washed with diethyl ether/pentane (1/1) and dried *in vacuo*.

*Polymerization Procedure at Low Temperatures Using Y+L2*

In a glove box, a 4 mL glass reactor was charged with Y[N(SiHMe$_2$)$_2$]$_3$(THF)$_2$ (11.5 mg, 18.3 μmol, 1 eq.) and salan pro-ligand **L2** (14.6 mg, 18.3μmol, 1 eq.). 1.53 mL of toluene was added such that the overall monomer concentration after *rac-β*-BL addition is 2.0 M. The reaction mixture was stirred for 1 h at room temperature. After that period, the reaction

S3

mixture was equilibrated at -35°C for 30 min and then, pre-cooled *rac-β*-BL (300 μL, 315 mg, 3.66 mmol, 200 eq.) was added to this mixture. After stirring for 60 min at -35°C, the polymerization was quenched by the addition of 0.5 mL of methanol. An aliquot sample was taken for determination of conversion by ^{1}H NMR spectroscopy. The quenched mixture was then precipitated into 20 mL of diethyl ether/pentane (1/1), filtered, washed with diethyl ether/pentane (1/1) and dried *in vacuo*.

Large Scale Polymerization Procedure

Large scale polymerization reactions were performed in a 250 mL double-walled Büchi steel autoclave equipped with a KPG- stirrer (Heidolph, 800 rpm), a temperature sensor, and a heating/ cooling jacket attached to a cryo-/thermostat unit (Julabo F-25-ME). In a glove box, Y[N(SiHMe$_2$)$_2$]$_3$(THF)$_2$ (48.8 mg, 77.4 μmol, 1 eq.) and salan pro-ligand **L2** (61.9 mg, 77.4 μmol, 1 eq.) were dissolved in 7.0 mL of toluene in a 20 mL glass vial. The reaction mixture was stirred for 1 h at room temperature. Subsequently, the catalyst solution was removed from the glove box and injected into an argon-flushed 250 mL double-walled Büchi steel autoclave containing *rac-β*-BL (9.5 mL, 10.0 g, 116 mmol, 1500 eq.) in 100 mL of toluene, and the polymerization was initiated. After stirring for 20 min at 25°C (active cooling with a Julabo F-25-ME cryo-/thermostat), the polymerization was quenched by the addition of 5 mL of methanol. Chloroform was added to dissolve the polymer and an aliquot sample taken for determination of conversion by ^{1}H NMR spectroscopy. The quenched mixture was then precipitated into 200 mL of diethyl ether/pentane (1/1), filtered, washed with diethyl ether/pentane (1/1) and dried *in vacuo*.

Synthesis of Salan Pro-Ligands
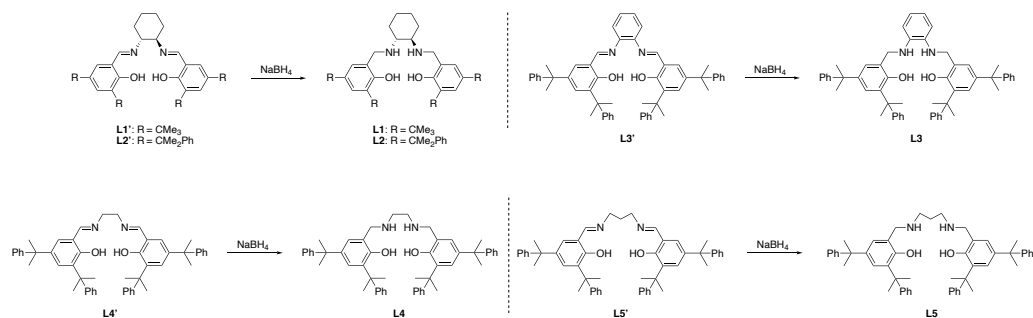
Synthesis of Salen Precursors L1'–L5'

Schiff base precursors **L1'** and **L2'** were prepared according to literature procedures.[3]

Schiff base precursors **L3'** was prepared according to a literature procedures but 3,5-dicumyl-salicylaldehyde was used instead of 3,5-bis(*tert*-butyl)salicylaldehyde, respectively.[3] 3,5-Dicumylsalicylaldehyde (15.0 mmol, 2.0 eq.) was dissolved in 100 mL of methanol, and 1,2-diaminobenzene (7.5 mmol, 1.0 eq.) and 0.1 mL of formic acid was added. The mixture was refluxed for 6 h. Subsequently, the reaction mixture was cooled to room temperature, the precipitate filtered and washed with methanol. Yield: 74%, orange solid. ^{1}H NMR (400 MHz, CDCl$_3$): δ 12.97 (s, 2H, OH), 8.44 (s, 2H, N=CH), 7.33 – 7.26 (m, 10H, Ar-H), 7.23 – 7.16 (m, 12H, Ar-H), 7.14 – 7.09 (m, 4H, Ar-H), 7.04 – 6.99 (m, 2H, Ar-H), 1.70 (s, 24H, C*Me*$_2$Ph). ^{13}C{^{1}H} NMR (101 MHz, CDCl$_3$): δ 164.8, 158.1, 150.8, 150.5, 142.7, 140.0, 136.6, 130.5, 128.8, 128.2, 127.9, 127.3, 126.9, 126.0, 125.8, 125.3, 120.3, 118.6, 42.6, 42.4, 31.0, 29.5.

Schiff base precursor **L4'** was prepared following an adopted literature procedure.[3] 3,5-Dicumylsalicylaldehyde (7.0 mmol, 2.0 eq.) was dissolved in 65 mL of ethanol, and ethylenediamine (3.5 mmol, 1.0 eq.) and 0.1 mL of formic acid was added. The mixture was refluxed for 45 min. Subsequently, the reaction mixture was cooled to room temperature, the precipitate filtered and washed with pentane. Yield: 81%, yellow solid. ^{1}H NMR (400 MHz, CDCl$_3$): δ 13.23 (s, 2H, OH), 8.19 (s, 2H, N=CH), 7.34 – 7.26 (m, 10H, Ar-H), 7.24 – 7.16 (m, 10H, Ar-H), 7.16 – 7.11 (m, 2H, Ar-H), 7.00 (d, J = 2.5 Hz, 2H, Ar-H), 3.68 (s, 4H, N-CH$_2$), 1.71 (s, 12H, C*Me*$_2$Ph), 1.66 (s, 12H, C*Me*$_2$Ph). ^{13}C{^{1}H} NMR (101 MHz, CDCl$_3$): δ 167.1, 157.7, 150.9, 150.8, 139.7, 136.1, 129.2, 128.2, 128.0, 127.9, 126.8, 125.8, 125.7, 125.2, 118.0, 59.7, 42.5, 42.2, 31.1, 29.5.

Schiff base precursor **L5'** was prepared according to the following procedure. 3,5-Dicumylsalicyl-aldehyde (10.0 mmol, 2.0 eq.) was suspended in 25 mL of methanol and 1,3-diaminopropane (5.0 mmol, 1.0 eq.) was added. The mixture was refluxed overnight. Subsequently, the reaction mixture was cooled to room temperature, the precipitate filtered and washed with methanol. Yield: 80%, yellow solid. ^{1}H NMR (400 MHz, CDCl$_3$): δ 13.37 (s, 2H, OH), 8.18 (s, 2H, N=CH), 7.34 – 7.26 (m, 10H, Ar-H), 7.24 – 7.09 (m, 12H, Ar-H), 6.99 (d, J = 2.5 Hz, 2H, ArH), 3.46 (t, J = 6.6 Hz, 4H, N-C*H*$_2$CH$_2$C*H*$_2$-N), 1.89 (p, J = 6.6 Hz, 2H, N-CH$_2$C*H*$_2$CH$_2$-N), 1.70 (s, 12H, C*Me*$_2$Ph), 1.66 (s, 12H, C*Me*$_2$Ph). ^{13}C{^{1}H} NMR (101 MHz,

S5

CDCl$_3$): δ 166.0, 157.9, 150.9, 150.8, 139.6, 136.2, 129.1, 128.2, 127.9, 127.8, 126.9, 125.8, 125.8, 125.2, 118.1, 56.8, 42.6, 42.3, 31.7, 31.1, 29.5.

**Synthesis of Salan Pro-Ligands L1–L5**

The synthesis of salan pro-ligands **L1** – **L5** followed a similar synthetic procedure and therefore the synthesis is described as a general procedure. For the synthesis of **L1** and **L2**, racemic Schiff base precursors were used.

General procedure for L1 – L5. The bis-imine type precursor (salen-type pro-ligand) (6.0 mmol, 1 eq.) was dissolved in 25 mL of tetrahydrofuran and 25 mL of methanol. The reaction mixture was cooled to 0°C and sodium borohydride, NaBH$_4$ (60.0 mmol, 10 eq.) was added portionwise. Subsequently, the reaction mixture was allowed to warm to room temperature and stirred for 3 h at this temperature. The solvent was removed under reduced pressure, the residue dissolved in dichloromethane (250 mL) and water (125 mL) was added. The phases were separated, and the organic layer washed with water (2×75 mL) and brine (1×75 mL). The organic layer was dried over Na$_2$SO$_4$, the solvent removed under reduced pressure and the residue further purified as described below.
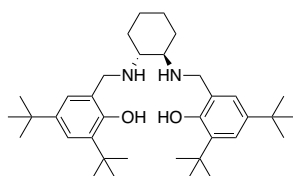

Salan pro-ligand **L1**: The residue was recrystallized from methanol/dichloromethane. Yield: 80%, colorless solid.

^{1}H NMR (400 MHz, CDCl$_3$): δ 10.64 (br s, 2H, OH), 7.21 (d, J = 2.5 Hz, 2H, Ar-H), 6.86 (d, J = 2.5 Hz, 2H, Ar-H), 3.97 (AB, J = 13.4 Hz, 4H, N-CH$_2$), 2.51 – 2.43 (m, 2H, Cy), 2.23 – 2.13 (m, 2H, Cy), 1.76 – 1.68 (m, 2H, Cy), 1.38 (s, 18H, ^{t}Bu), 1.28 (s, 18H, ^{t}Bu), 1.27 – 1.21 (m, 4H, Cy). ^{13}C{^{1}H} NMR (101 MHz, CDCl$_3$): δ 154.5, 140.8, 136.1, 123.3, 123.2, 122.5, 60.1, 51.0, 35.0, 34.3, 31.8, 30.9, 29.8, 24.3. Anal. Calc. for C$_{36}$H$_{58}$N$_2$O$_2$: C, 78.49; H, 10.61; N, 5.09. Found: C, 77.43; H, 10.33; N, 5.06%.

S6
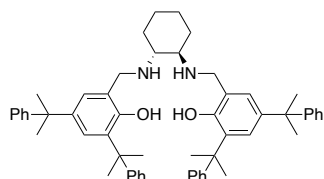
Salan pro-ligand **L2**: The residue was washed with methanol. Yield: 86%, colorless solid.

^{1}H NMR (400 MHz, CDCl$_3$): δ 10.38 (br s, 2H, OH), 7.31 – 7.23 (m, 10H, Ar-H), 7.20 – 7.08 (m, 10H, Ar-H), 7.05 – 6.99 (m, 2H, Ar-H), 6.64 (d, *J* = 2.5 Hz, 2H, Ar-H), 3.64 (AB, *J* = 13.5 Hz, 4H, N-CH$_2$), 1.87 – 1.79 (m, 2H, Cy), 1.71 (s, 6H, C*Me*$_2$Ph), 1.69 (s, 12H, C*Me*$_2$Ph), 1.68 – 1.63 (m, 2H, Cy), 1.57 (s, 6H, C*Me*$_2$Ph), 1.55 – 1.50 (m, 2H, Cy), 0.98 – 0.83 (m, 2H, Cy), 0.71 – 0.51 (m, 4H, Cy and NH). ^{13}C{^{1}H} NMR (101 MHz, CDCl$_3$): δ 154.0, 152.1, 151.7, 139.8, 135.4, 128.0, 127.6, 126.9, 125.9, 125.7, 125.5, 124.6, 124.3, 122.1, 58.0, 49.3, 42.6, 42.0, 31.3, 31.2, 30.9, 30.1, 28.0, 24.6. Anal. Calc. for C$_{56}$H$_{66}$N$_2$O$_2$: C, 84.17; H, 8.32; N, 3.51. Found: C, 83.89; H, 8.45; N, 3.55%.
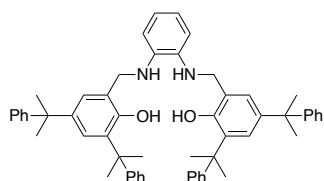

Salan pro-ligand **L3**: **L3** was prepared according to the general procedure but the stirring time of the reaction mixture was 4 h at room temperature. The residue was washed with methanol. Yield: 84%, yellow solid.

^{1}H NMR (400 MHz, CDCl$_3$): δ 7.31 – 7.27 (m, 10H, Ar-H), 7.23 – 7.15 (m, 10H, Ar-H), 7.14 – 7.08 (m, 2H, Ar-H), 6.95 (br s, 2H, OH), 6.92 (d, *J* = 2.4 Hz, 2H, Ar-H), 6.80 – 6.75 (m, 2H, Ar-H), 6.70 – 6.64 (m, 2H, Ar-H), 4.11 (s, 4H, N-CH$_2$), 3.40 (br s, 2H, NH), 1.71 (s, 12H, C*Me*$_2$Ph), 1.62 (s, 12H, C*Me*$_2$Ph). ^{13}C{^{1}H} NMR (101 MHz, CDCl$_3$): δ 152.1, 151.2, 150.4, 141.7, 136.9, 135.5, 128.4, 128.1, 126.9, 126.5, 125.8, 125.8, 125.7, 125.2, 123.8, 121.0, 114.0, 47.6, 42.7, 42.2, 31.2, 29.8. Anal. Calc. for C$_{56}$H$_{60}$N$_2$O$_2$: C, 84.81; H, 7.63; N, 3.53. Found: C, 84.76; H, 7.82; N, 3.37%.

S7

231
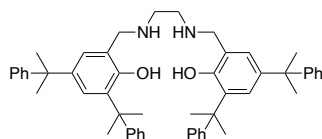
Salan pro-ligand **L4**: The residue was washed with methanol. Yield: 69%, off-white solid.

^{1}H NMR (400 MHz, CDCl$_3$): δ 10.37 (br s, 2H, OH), 7.33 – 7.27 (m, 8H, Ar-H), 7.24 (d, J = 2.6 Hz, 2H, Ar-H), 7.21 – 7.14 (m, 10H, Ar-H), 7.11 – 7.04 (m, 2H, Ar-H), 6.70 (d, J = 2.5 Hz, 2H, Ar-H), 3.71 (s, 4H, Ar-CH$_2$), 2.43 (s, 4H, N-CH$_2$), 1.70 (s, 12H, C*Me*$_2$Ph), 1.65 (s, 12H, C*Me*$_2$Ph). ^{13}C{^{1}H} NMR (101 MHz, CDCl$_3$): δ 154.0, 151.7, 151.5, 140.0, 135.4, 128.0, 127.7, 126.9, 125.8, 125.6, 125.5, 124.9, 124.9, 121.9, 53.1, 47.6, 42.6, 42.1, 31.2, 29.6.
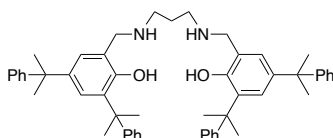
Salan pro-ligand **L5**: The residue was recrystallized from methanol. Yield: 51%, colorless solid.

^{1}H NMR (400 MHz, CDCl$_3$): δ 7.29 – 7.26 (m, 8H, Ar-H), 7.22 (d, J = 2.5 Hz, 2H, Ar-H), 7.20 – 7.14 (m, 10H, Ar-H), 7.10 – 7.04 (m, 2H, Ar-H), 6.70 (d, J = 2.5 Hz, 2H, Ar-H), 3.72 (s, 4H, Ar-CH$_2$), 2.40 (t, J = 6.8 Hz, 4H, N-C*H*$_2$CH$_2$C*H*$_2$-N), 1.68 (s, 12H, C*Me*$_2$Ph), 1.63 (s, 12H, C*Me*$_2$Ph), 1.39 (p, J = 7.0 Hz, 2H, N-CH$_2$C*H*$_2$CH$_2$-N). ^{13}C{^{1}H} NMR (101 MHz, CDCl$_3$): δ 154.2, 151.6, 151.5, 140.0, 135.4, 128.0, 127.8, 126.9, 125.8, 125.6, 125.4, 125.0, 124.9, 122.2, 53.3, 46.5, 42.6, 42.2, 31.2, 29.7, 29.5. Anal. Calc. for C$_{53}$H$_{62}$N$_2$O$_2$: C, 83.86; H, 8.23; N, 3.69. Found: C, 83.84; H, 8.21; N, 3.70%.
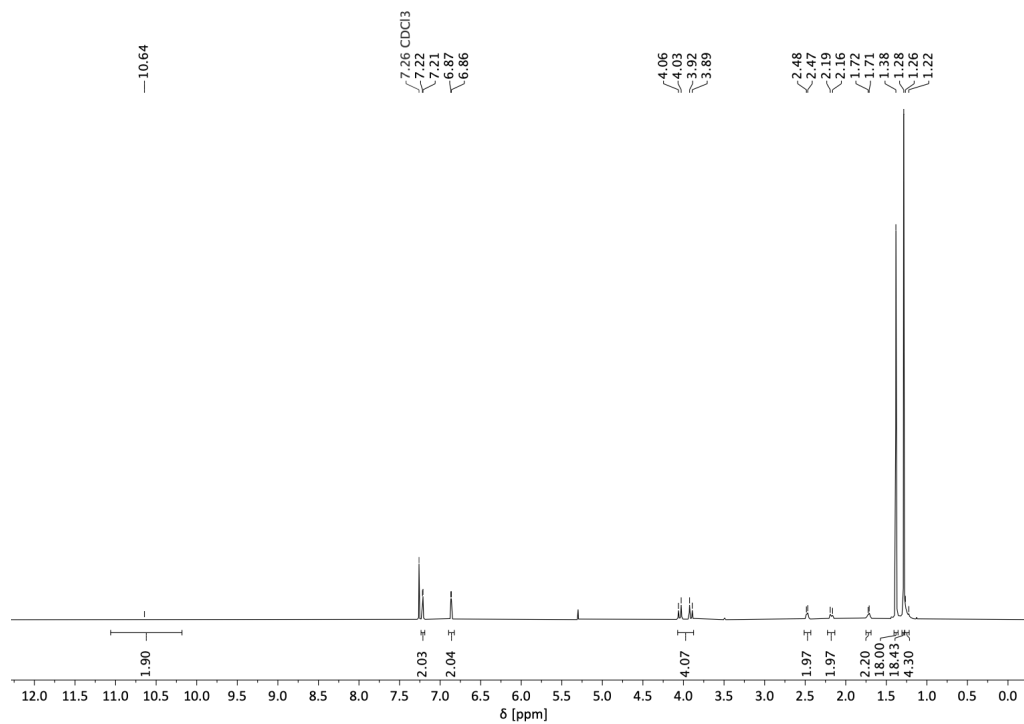
S8

NMR Spectra of Compounds

Figure S1. ^{1}H NMR spectrum (CDCl₃) of salan pro-ligand **L1**.

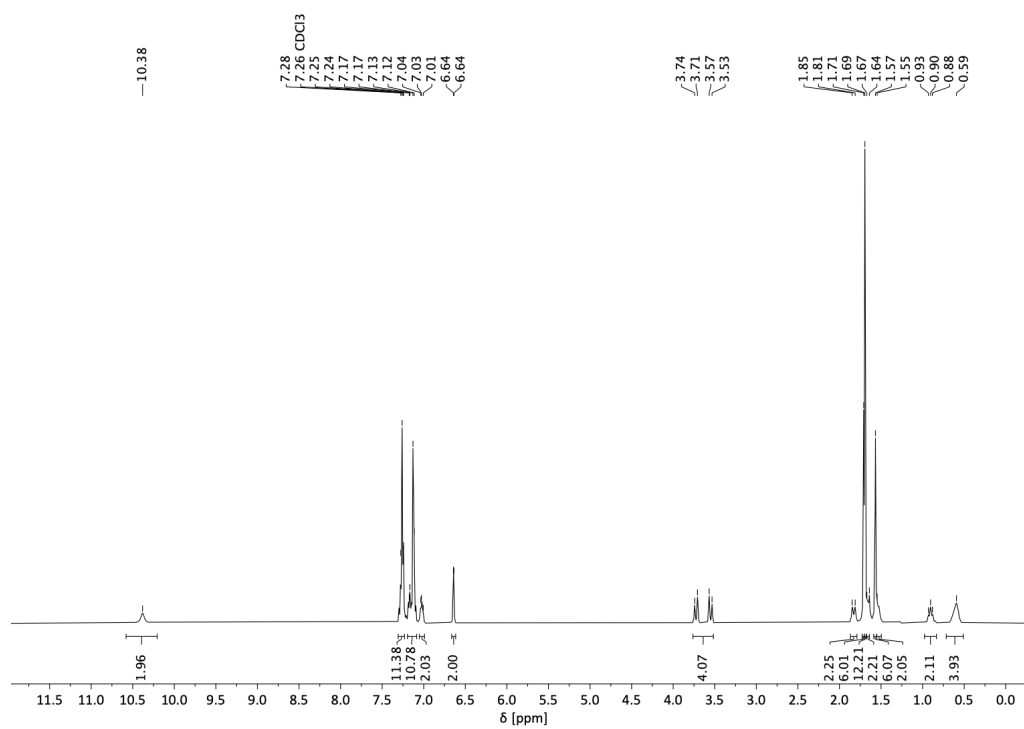**Figure S2.** ^{13}C{^{1}H} NMR spectrum (CDCl₃) of salan pro-ligand **L1**.

S9

Figure S3. ^{1}H NMR spectrum (CDCl$_3$) of salan pro-ligand **L2**.
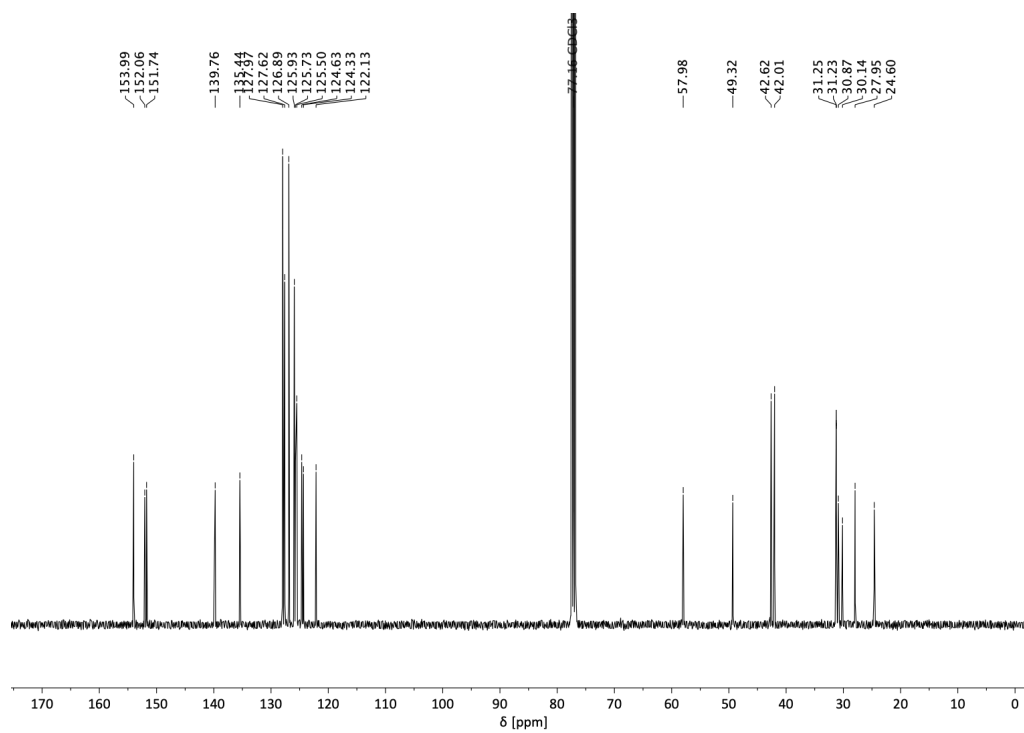

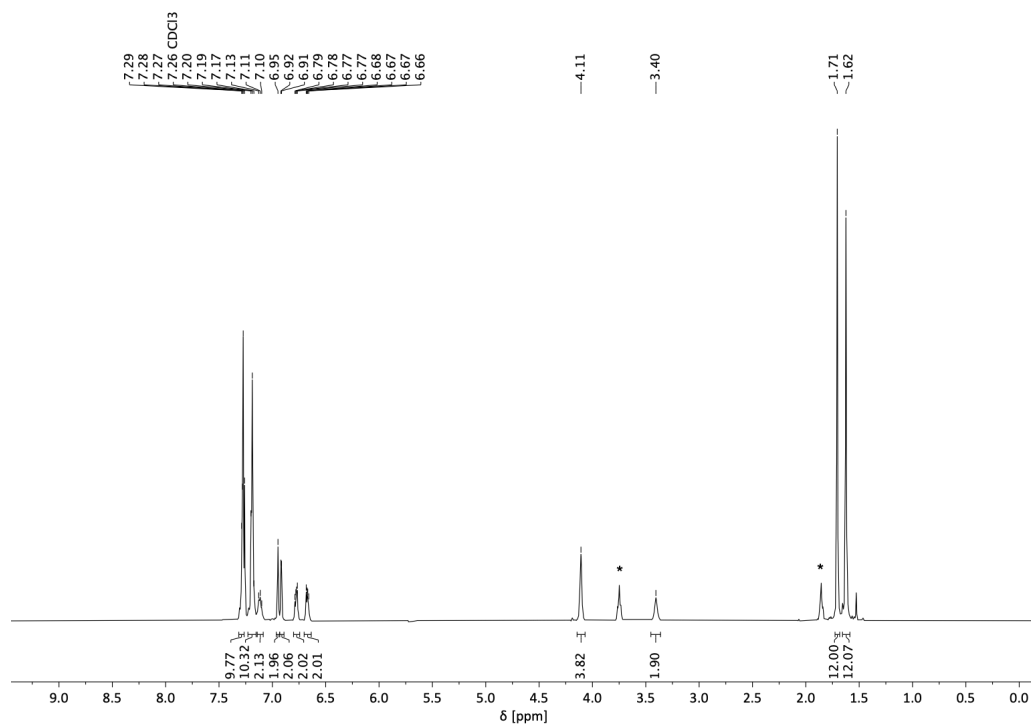**Figure S4.** ^{13}C{^{1}H} NMR spectrum (CDCl$_3$) of salan pro-ligand **L2**.

S10
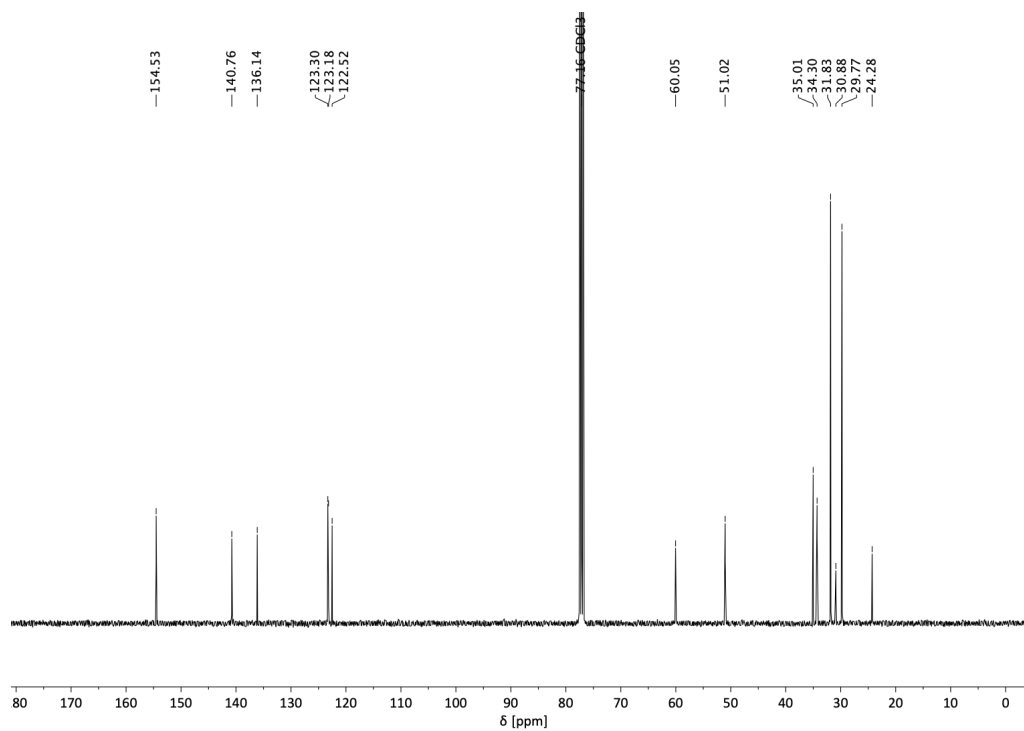
Figure S5. ^{1}H NMR spectrum (CDCl$_3$) of salan pro-ligand **L3**. * = THF.
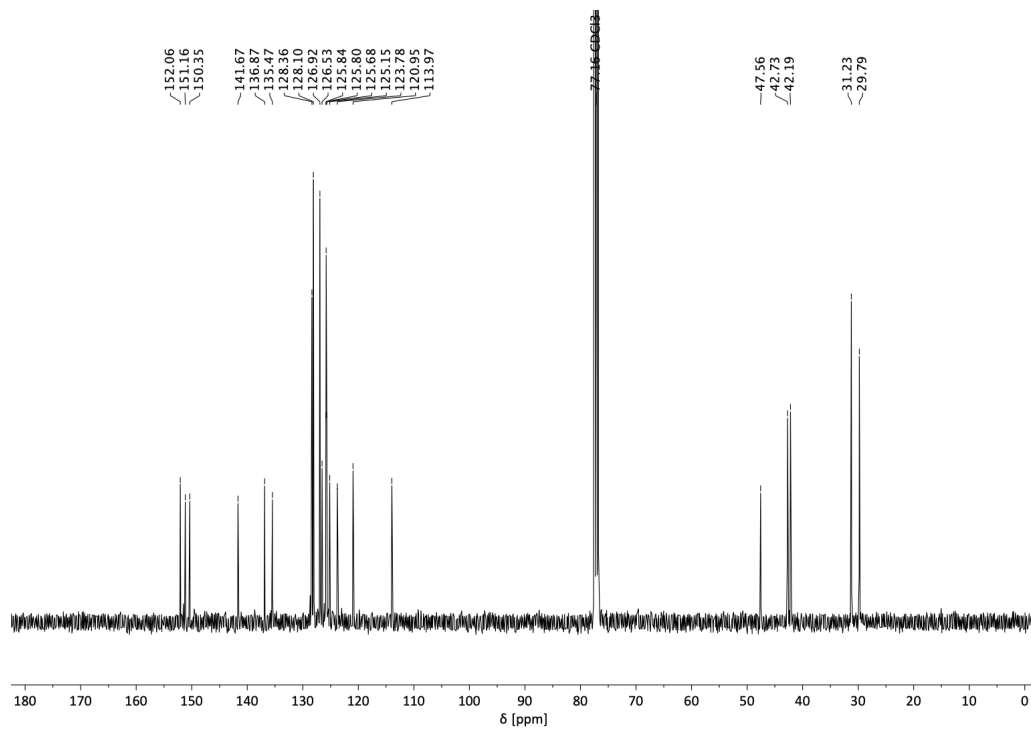
Figure S6. ^{13}C{^{1}H} NMR spectrum (CDCl$_3$) of salan pro-ligand **L3**.

S11

235

Figure S7. ^{1}H NMR spectrum (CDCl$_3$) of salan pro-ligand **L4**. * = CH$_2$Cl$_2$.
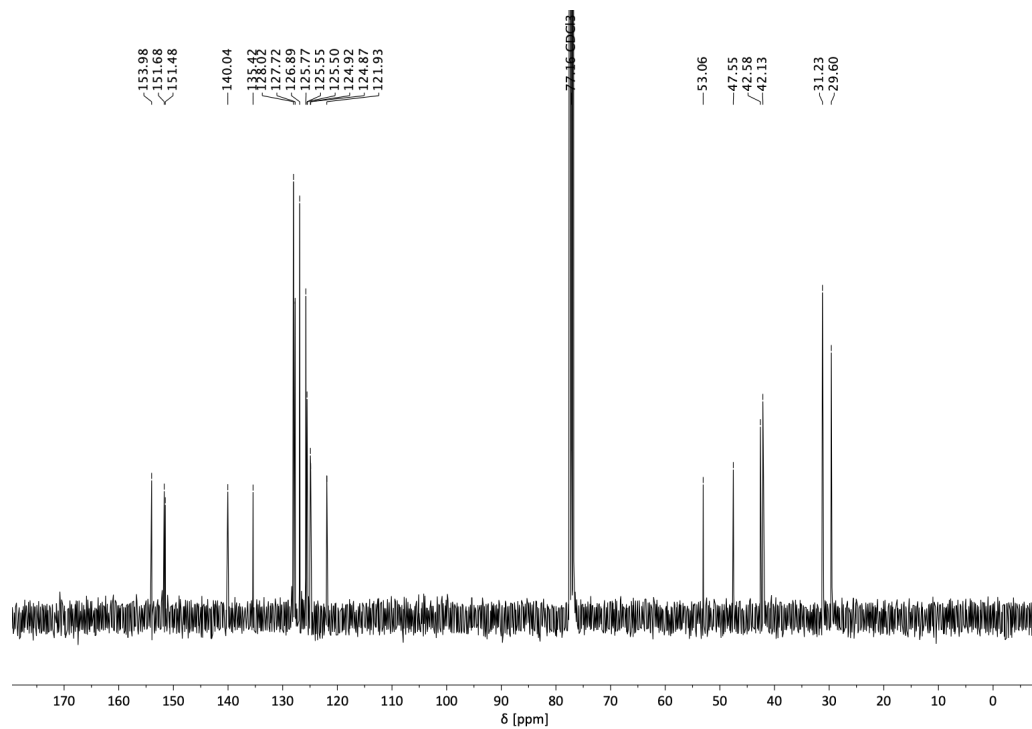
Figure S8. ^{13}C{^{1}H} NMR spectrum (CDCl$_3$) of salan pro-ligand **L4**.

S12

236

Figure S9. ^{1}H NMR spectrum (CDCl$_3$) of salan pro-ligand **L5**.

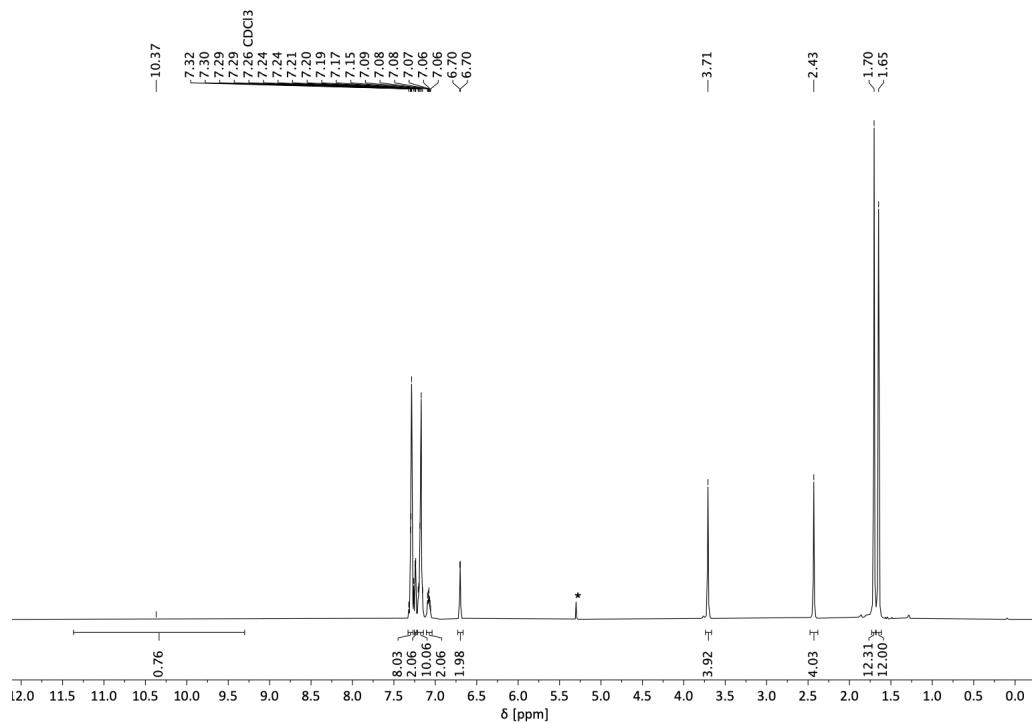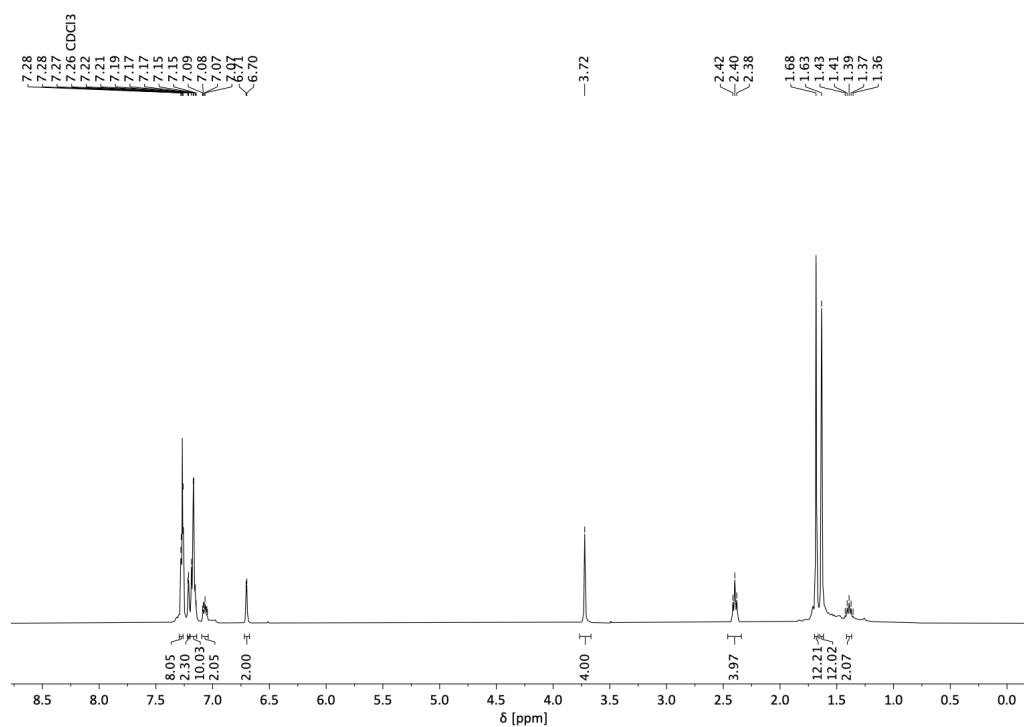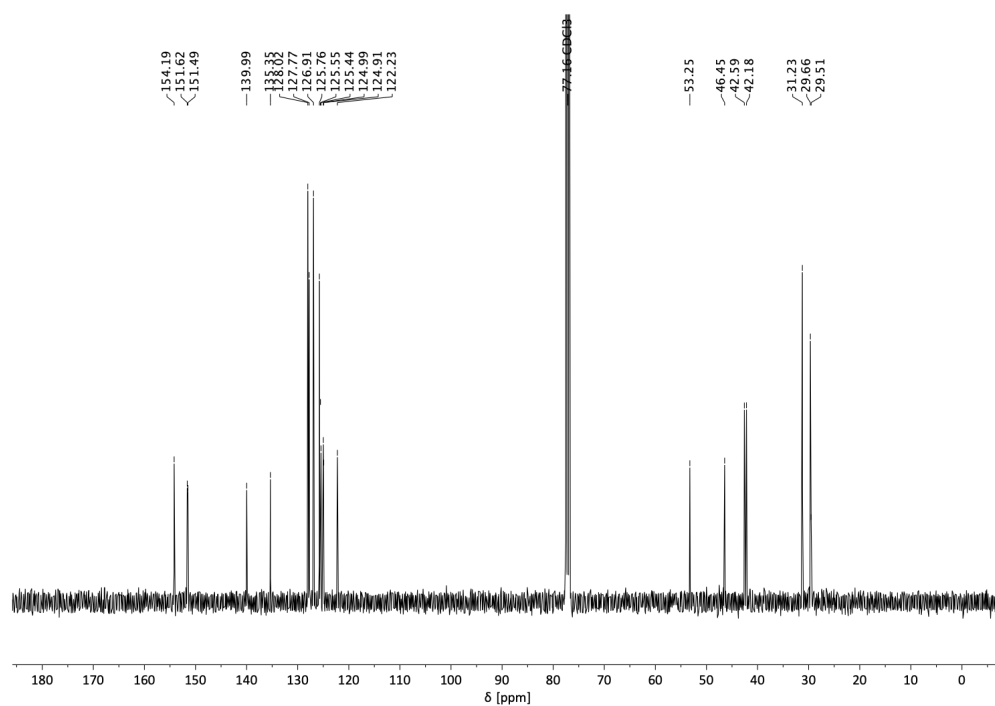
Figure S10. ^{13}C{^{1}H} NMR spectrum (CDCl$_3$) of salan pro-ligand **L5**.

S13

237

## 2. Polymerization Kinetics and Polymer Characterization Data

Additional Polymerization Data and Kinetics

Table S1. Additional polymerization data.[a]

entry	catalytic system	[M]/[cat]	time (min)	conv.[b] (%)	M_n [c] (kg mol^{-1})	$Đ$ [c]	P_m [d]
1	**Y**	200	1440	8	n.d.	n.d.	n.d.
2	**L2**	200	180	0	n.d.	n.d.	n.d.
3[e,f]	**Y+L2**	200	1	>99	40	1.9	0.83
4[e]	**Y+L2**	800	3	>99	118	2.2	0.83
5[e]	**Y+L2**	3000	10	85	445	1.8	0.75
6[e,g]	**Y+L2**	1500	20	>99	259	2.5	0.84

[a]Polymerizations were performed in toluene at room temperature, [β-BL] = 2.0 M. [b]Conversion determined by ^{1}H NMR spectroscopy. [c]Determined by GPC in CHCl$_3$ at room temperature relative to polystyrene standards. [d]Tacticity determined by ^{13}C NMR spectroscopy, integration of the carbonyl signal. [e]Catalyst was prepared *in situ* by treatment of **Y** with salan pro-ligand **L2** (1 eq.) in toluene at room temperature for 1 h prior to monomer addition. [f]*In situ* formation of catalyst for 24 h at room temperature. [g]Large scale polymerization in a 250 mL double-walled *Büchi* steel autoclave, 10.0 g of β-BL used, [β-BL] = 1.0 M. n.d. = not determined.

Table S2. Ring-opening polymerization of β-BL using *in situ* generated yttrium salen catalysts.[a]
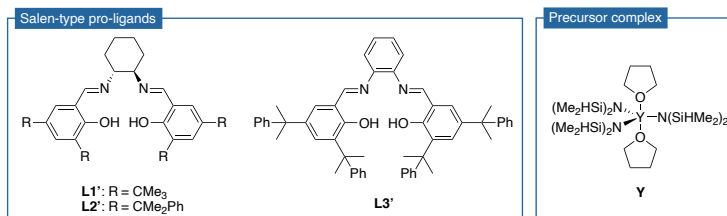
entry	catalytic system	[M]/[**Y+L'**]	t (min)	conv.[b] (%)	M_n [c] (kg mol^{-1})	$Đ$ [c]	P_m [d]
1	**Y+L1'**	200	1440	22	8	1.9	0.50
2	**Y+L2'**	200	1440	20	9	1.8	0.51
3	**Y+L3'**	200	1440	2	n.d.	n.d.	n.d.

[a]Polymerizations were performed in toluene at room temperature, [β-BL] = 2.0 M. Catalyst was prepared *in situ* by treatment of **Y** with salen pro-ligand **L'** (1 eq.) in toluene at room temperature for 1 h prior to monomer addition [b]Conversion determined by ^{1}H NMR spectroscopy. [c]Determined by GPC in THF at 40°C relative to polystyrene standards. [d]Tacticity determined by ^{13}C NMR spectroscopy, integration of the carbonyl signal. n.d. = not determined.

S14
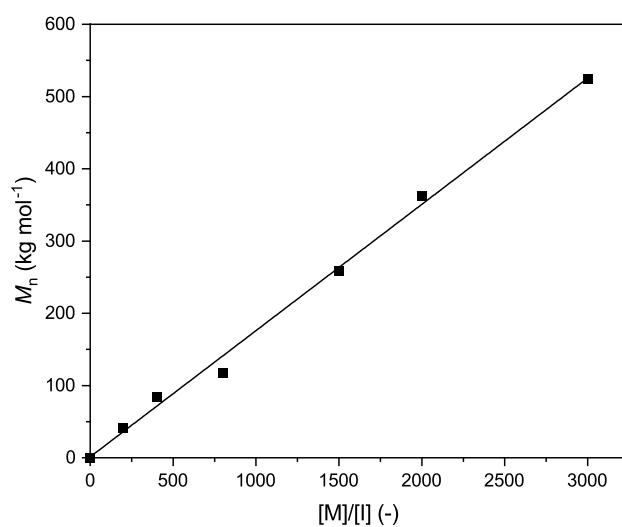
Figure S11. Plot of molecular weight vs. monomer-to-initiator ratio for the ROP of β-BL mediated by catalytic system **Y+L2**, $R^2 = 0.9959$. The runs at ratios of 2000/1 and 3000/1 did not achieve quantitative conversions, and thus, molecular weights used for the plot were adjusted by their conversions.
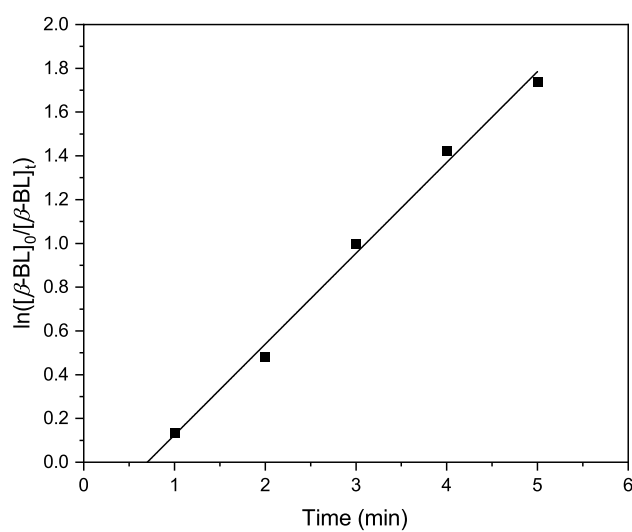
Figure S12. Semi-logarithmic plot of monomer concentration over time for the ROP of β-BL mediated by catalytic system **Y+L5**. $k_{obs} = 0.415 \pm 0.019$ min^{-1}, $R^2 = 0.9939$. Conditions: $[\beta\text{-BL}]_0 = 2.0$ M, $[\beta\text{-BL}]/[\textbf{Y+L5}] = 200/1$, T = rt.

S15
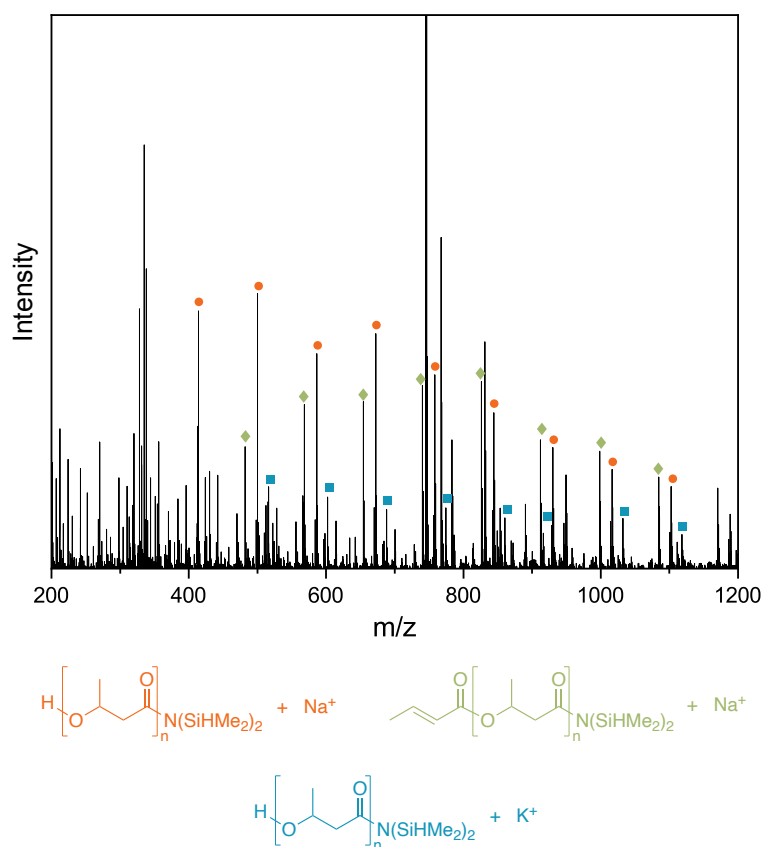
Figure S13. ESI-MS spectrum of PHB produced by **Y+L4** ([β-BL]/[**Y+L4**] = 5/1).

Photographs of Produced PHB and Polymerization Setup for Up-Scaling
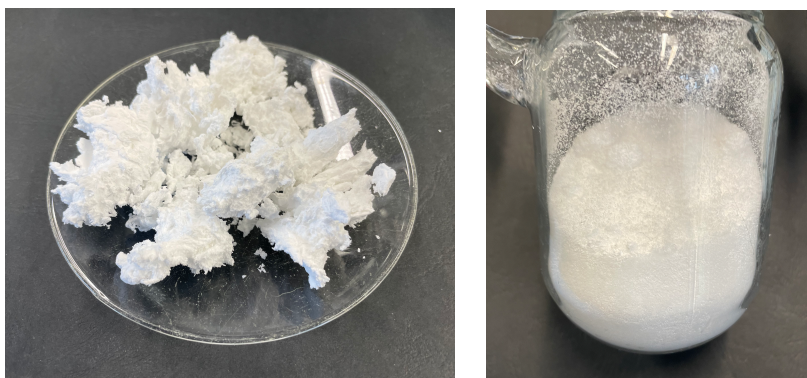
Figure S14. Photographs of PHB prepared from ROP of of β-BL mediated by catalytic system **Y+L2** (Table S1, entry 6). Polymer after precipitation (left) and ground polymer (right).

S16
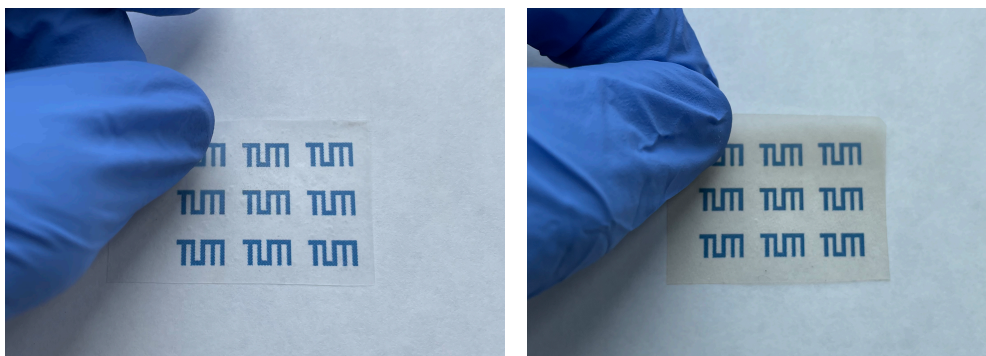
Figure S15. Photographs of polymer foils prepared by hot pressing of synthetic PHB with reduced isotacticity ($P_m = 0.84$, left) and bacterial PHB ($P_m = 1.00$, right).

Figure S16. Photograph of a 250 mL double-walled *Büchi* steel autoclave used for polymerization up-scaling.

S17

¹H and ¹³C{¹H} NMR Spectra of PHB
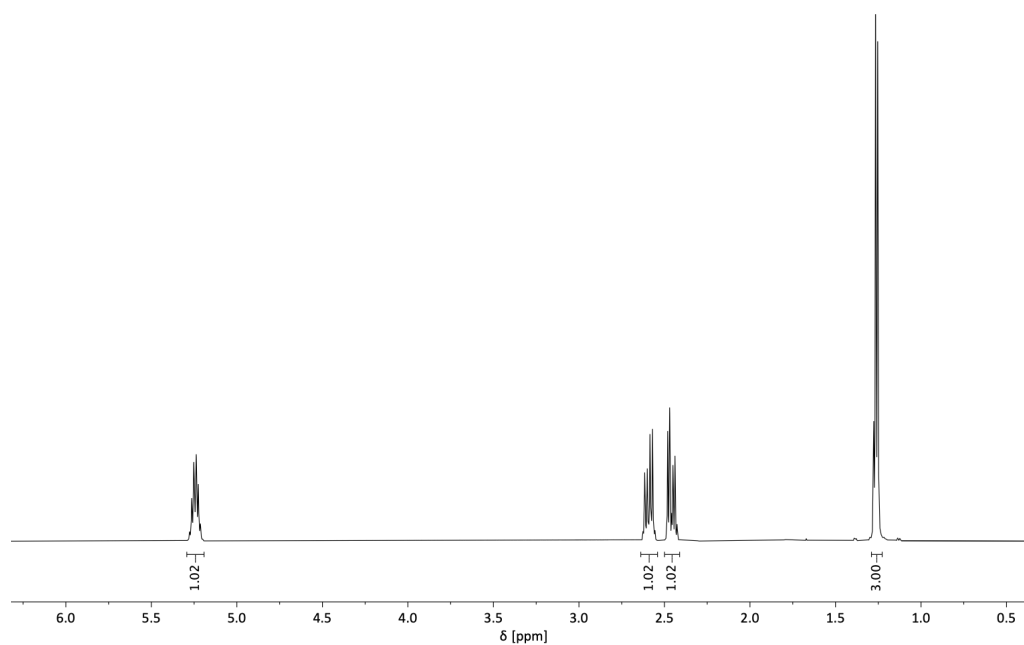
Figure S17. Representative ¹H NMR spectrum (CDCl₃) of PHB produced by **Y+L2** (Table 1, entry 2).
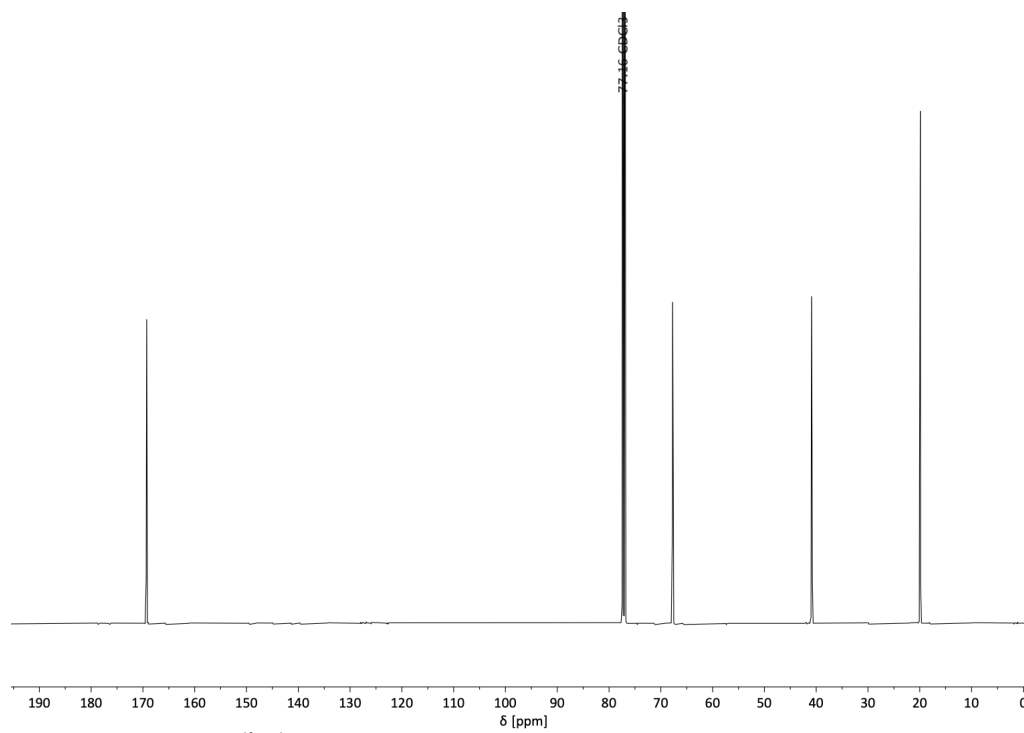
Figure S18. Representative ¹³C{¹H} NMR spectrum (CDCl₃) of PHB produced by **Y+L2** (Table 1, entry 2).

S18

Tacticity of PHBs Produced by *In Situ* Generated Catalysts
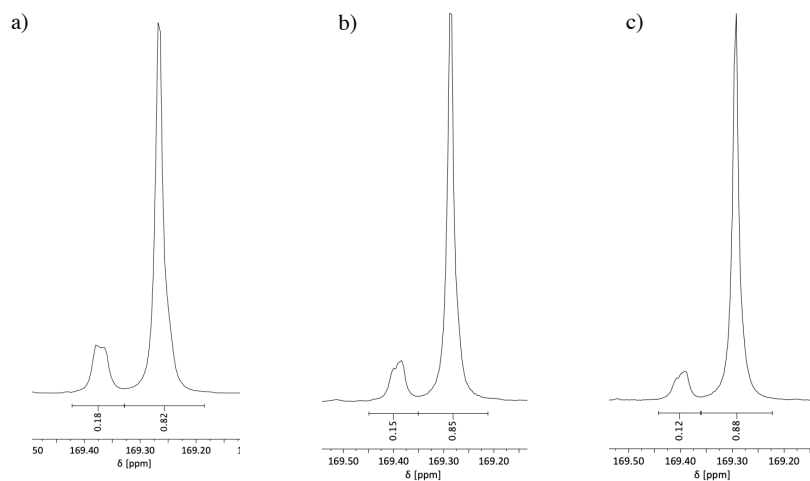
Figure S19. ^{13}C{^{1}H} NMR spectra (carbonyl region) of PHBs produced by *in situ* generated catalysts. a) **Y+L3** (Table 1, entry 6), b) **Y+L4** (Table 1, entry 7), c) **Y+L5** (Table 1, entry 8).
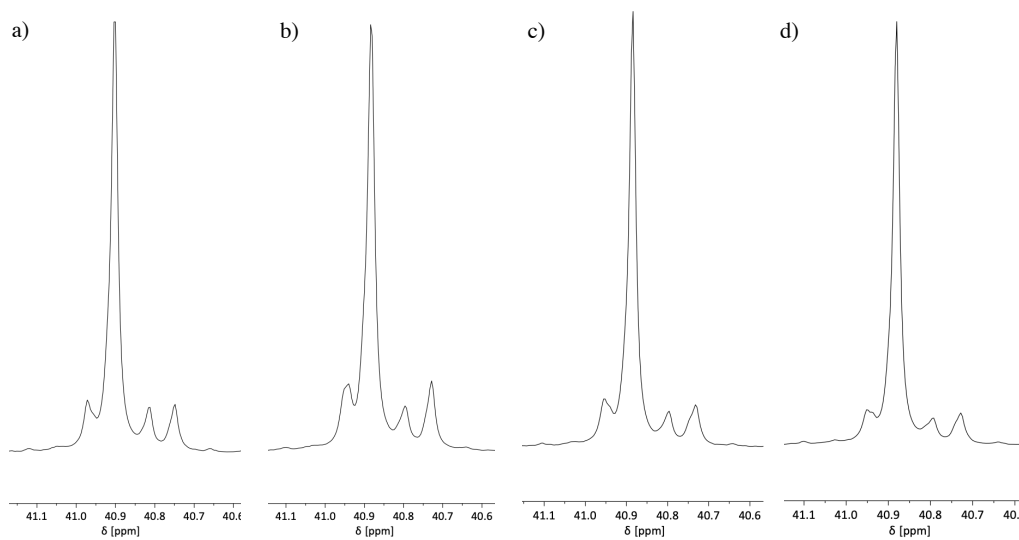
Figure S20. ^{13}C{^{1}H} NMR spectra (methylene region) of PHBs produced by *in situ* generated catalysts. a) **Y+L2** (Table 1, entry 4), b) **Y+L3** (Table 1, entry 6), c) **Y+L4** (Table 1, entry 7), d) **Y+L5** (Table 1, entry 8).

S19

243

Thermal Analysis of PHB
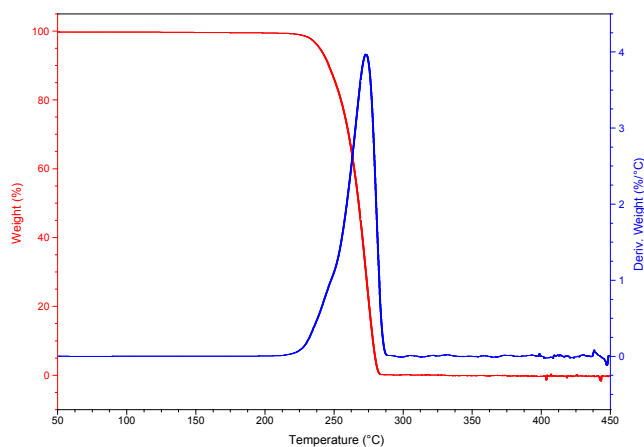
Figure S21. TGA curve of PHB (P_m = 0.84) prepared with catalyst system **Y+L2** (M_n = 290 kg mol^{-1}, $Đ$ = 2.0; Table 1, entry 4). $T_{d,5\%}$ = 239°C, $T_{d,max}$ = 273°C.
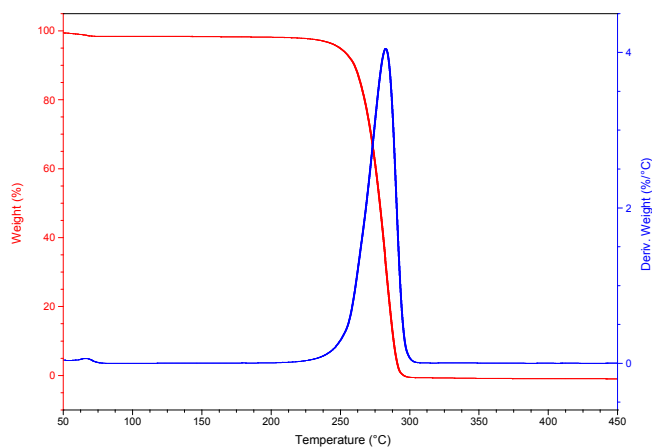
Figure S22. TGA curve of bacterial PHB (M_n = 247 kg mol^{-1}, $Đ$ = 2.3). $T_{d,5\%}$ = 249°C, $T_{d,max}$ = 282°C.
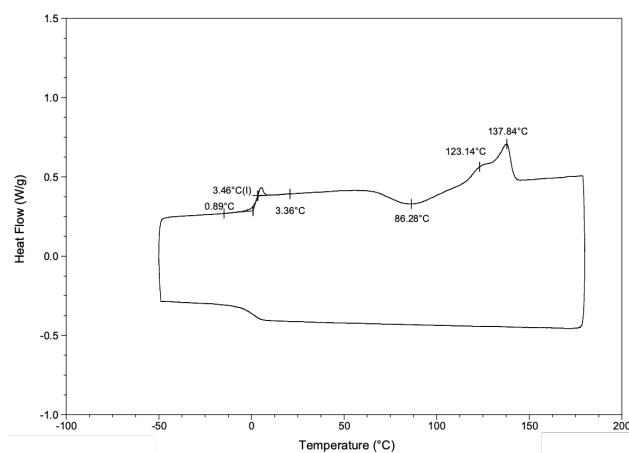
Figure S23. DSC curve (exo down) of PHB (M_n = 41 kg mol^{-1}, $Đ$ = 2.2; Table 1, entry 2).

S20
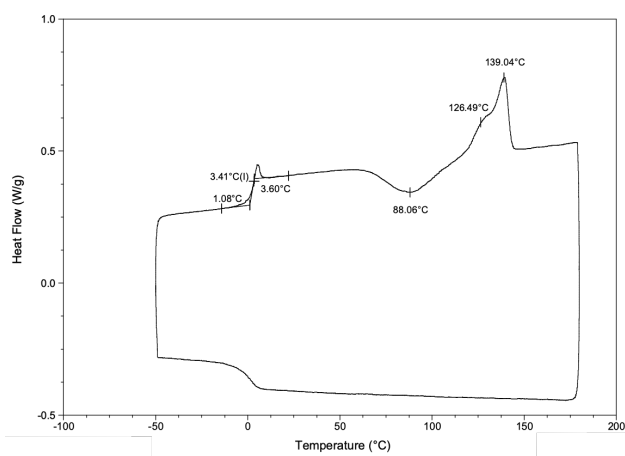
Figure S24. DSC curve (exo down) of PHB (M_n = 85 kg mol^{-1}, $Đ$ = 2.0; Table 1, entry 3).
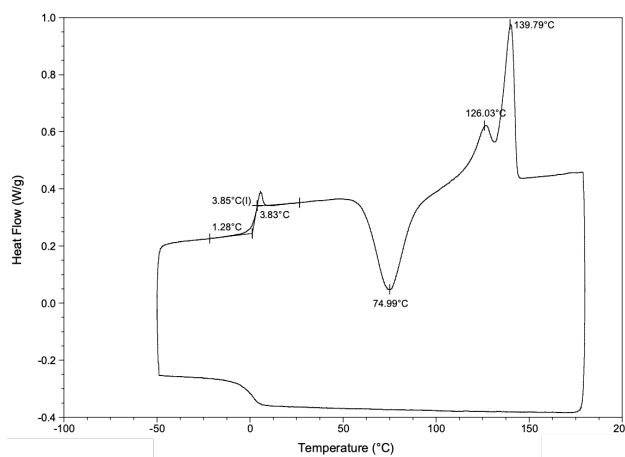
Figure S25. DSC curve (exo down) of PHB (M_n = 290 kg mol^{-1}, $Đ$ = 2.0; Table 1, entry 4).
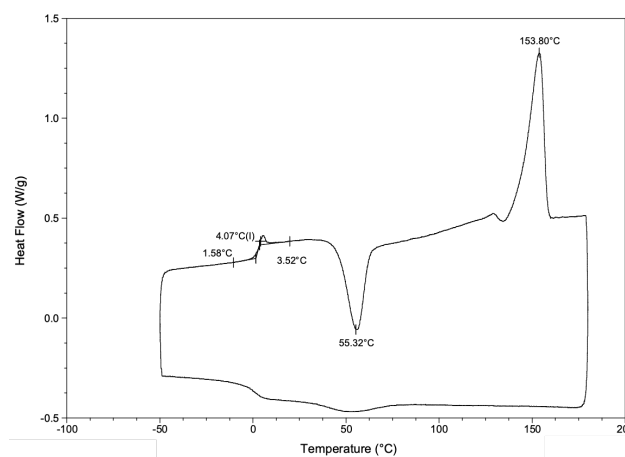
Figure S26. DSC curve (exo down) of PHB (M_n = 130 kg mol^{-1}, $Đ$ = 3.2; Table 1, entry 5).

S21

245
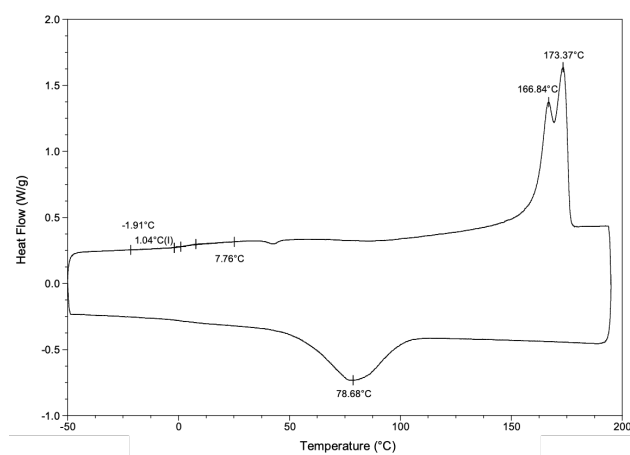
Figure S27. DSC curve (exo down) of bacterial PHB (M_n = 247 kg mol^{-1}, $Đ$ = 2.3).

S22

3. References

1. Anwander, R.; Runte, O.; Eppinger, J.; Gerstberger, G.; Herdtweck, E.; Spiegler, M., Synthesis and structural characterisation of rare-earth bis (dimethylsilyl) amides and their surface organometallic chemistry on mesoporous MCM-41. *J. Chem. Soc., Dalton Trans.* **1998**, 847-858.

2. Bloembergen, S.; Holden, D. A.; Bluhm, T. L.; Hamer, G. K.; Marchessault, R. H., Stereoregularity in synthetic β-hydroxybutyrate and β-hydroxyvalerate homopolyesters. *Macromolecules* **1989,** *22*, 1656-1663.

3. Tang, X.; Chen, E. Y., Chemical synthesis of perfectly isotactic and high melting bacterial poly(3-hydroxybutyrate) from bio-sourced racemic cyclic diolide. *Nat. Commun.* **2018,** *9*, 2345.

10.6 Licenses for Copyrighted Content

CCC Marketplace

This is a License Agreement between Jonas Bruckmoser, Technical University of Munich ("User") and Copyright Clearance Center, Inc. ("CCC") on behalf of the Rightsholder identified in the order details below. The license consists of the order details, the Marketplace Order General Terms and Conditions below, and any Rightsholder Terms and Conditions which are included below.

All payments must be made in full to CCC in accordance with the Marketplace Order General Terms and Conditions below.

Order Date	11-Nov-2022	Type of Use	Republish in a thesis/dissertation
Order License ID	1289083-1	Publisher	THE SOCIETY,
ISSN	1359-7345	Portion	Chart/graph/table/figure

LICENSED CONTENT

Publication Title	Chemical communications : Chem comm	Publication Type	Journal
		Start Page	8024
Article Title	Steric vs. electronic stereocontrol in syndio- or iso-selective ROP of functional chiral β-lactones mediated by achiral yttrium-bisphenolate complexes.	End Page	8031
		Issue	58
		Volume	54
		URL	http://www.rsc.org/Publishing/Journals/cc/Article.asp?Type=CurrentIssue
Author/Editor	ROYAL SOCIETY OF CHEMISTRY (GREAT BRITAIN)		
Date	01/01/1996		
Language	English		
Country	United Kingdom of Great Britain and Northern Ireland		
Rightsholder	Royal Society of Chemistry		

REQUEST DETAILS

Portion Type	Chart/graph/table/figure	Distribution	Worldwide
Number of Charts / Graphs / Tables / Figures Requested	1	Translation	Original language of publication
		Copies for the Disabled?	No
Format (select all that apply)	Electronic	Minor Editing Privileges?	Yes
Who Will Republish the Content?	Academic institution	Incidental Promotional Use?	No
Duration of Use	Current edition and up to 15 years	Currency	EUR
Lifetime Unit Quantity	Up to 499		
Rights Requested	Main product		

NEW WORK DETAILS

Title	Catalyst and Monomer Design for Simple Access toward Sophisticated Polyester Materials via Ring-Opening Polymerization	Institution Name	Technical University of Munich
		Expected Presentation Date	2023-02-28
Instructor Name	Prof. Dr. Bernhard Rieger		

ADDITIONAL DETAILS

Order Reference Number	N/A	The Requesting Person/Organization to Appear on the License	Jonas Bruckmoser, Technical University of Munich

REUSE CONTENT DETAILS

Title, Description or Numeric Reference of the Portion(s)	Scheme 1	Title of the Article/Chapter the Portion Is From	Steric vs. electronic stereocontrol in syndio- or iso-selective ROP of functional chiral β-lactones mediated by achiral yttrium-bisphenolate complexes.
Editor of Portion(s)	Carpentier, Jean-François; Guillaume, Sophie M; Hänninen, Mikko M; Ligny, Romain		
Volume of Serial or Monograph	54	Author of Portion(s)	Carpentier, Jean-François; Guillaume, Sophie M; Hänninen, Mikko M; Ligny, Romain
Page or Page Range of Portion	8024-8031		
		Issue, if Republishing an Article From a Serial	58
		Publication Date of Portion	2018-07-17

CCC

RightsLink

Home | Help ∨ | Live Chat | Jonas Bruckmoser ∨

Pre-Rate-Determining Selectivity in the Terpolymerization of Epoxides, Cyclic Anhydrides, and CO2: A One-Step Route to Diblock Copolymers

Author: Ryan C. Jeske, John M. Rowley, Geoffrey W. Coates

Publication: Angewandte Chemie International Edition

Publisher: John Wiley and Sons

Date: Jul 22, 2008

Copyright © 2008 WILEY-VCH Verlag GmbH & Co. KGaA, Weinheim

Order Completed

Thank you for your order.

This Agreement between Technical University of Munich -- Jonas Bruckmoser ("You") and John Wiley and Sons ("John Wiley and Sons") consists of your license details and the terms and conditions provided by John Wiley and Sons and Copyright Clearance Center.

Your confirmation email will contain your order number for future reference.

License Number	5402590794536		🖶 Printable Details
License date	Oct 05, 2022		

☑ Licensed Content

Licensed Content Publisher	John Wiley and Sons
Licensed Content Publication	Angewandte Chemie International Edition
Licensed Content Title	Pre-Rate-Determining Selectivity in the Terpolymerization of Epoxides, Cyclic Anhydrides, and CO2: A One-Step Route to Diblock Copolymers
Licensed Content Author	Ryan C. Jeske, John M. Rowley, Geoffrey W. Coates
Licensed Content Date	Jul 22, 2008
Licensed Content Volume	47
Licensed Content Issue	32
Licensed Content Pages	4

🗉 Order Details

Type of use	Dissertation/Thesis
Requestor type	University/Academic
Format	Electronic
Portion	Figure/table
Number of figures/tables	2
Will you be translating?	No

📄 About Your Work

Title	Catalyst and Monomer Design for Simple Access toward Sophisticated Polyester Materials via Ring-Opening Polymerization
Institution name	Technical University of Munich
Expected presentation date	Feb 2023

📁 Additional Data

Portions	Scheme 3, Figure 1

📍 Requestor Location

Requestor Location	Technical University of Munich Lichtenbergstrasse 4 Garching b. Muenchen, 85748 Germany Attn: Technical University of Munich

🗉 Tax Details

Publisher Tax ID	EU826007151

$ Price

Total	0.00 EUR

Would you like to purchase the full text of this article? If so, please continue on to the content ordering system located here: **Purchase PDF**
If you click on the buttons below or close this window, you will not be able to return to the content ordering system.

Total: 0.00 EUR

CLOSE WINDOW | ORDER MORE

CCC
RightsLink

🏠 Home   ❓ Help ⌄   ✉ Email Support   👤 Jonas Bruckmoser ⌄

ACS Publications
Most Trusted. Most Cited. Most Read.

Simple and Rapid Access toward AB, BAB and ABAB Block Copolyesters from One-Pot Monomer Mixtures Using an Indium Catalyst

Author: Jonas Bruckmoser, Bernhard Rieger
Publication: ACS Macro Letters
Publisher: American Chemical Society
Date: Sep 1, 2022

Copyright © 2022, American Chemical Society

PERMISSION/LICENSE IS GRANTED FOR YOUR ORDER AT NO CHARGE

This type of permission/license, instead of the standard Terms and Conditions, is sent to you because no fee is being charged for your order. Please note the following:

- Permission is granted for your request in both print and electronic formats, and translations.
- If figures and/or tables were requested, they may be adapted or used in part.
- Please print this page for your records and send a copy of it to your publisher/graduate school.
- Appropriate credit for the requested material should be given as follows: "Reprinted (adapted) with permission from {COMPLETE REFERENCE CITATION}. Copyright {YEAR} American Chemical Society." Insert appropriate information in place of the capitalized words.
- One-time permission is granted only for the use specified in your RightsLink request. No additional uses are granted (such as derivative works or other editions). For any uses, please submit a new request.

If credit is given to another source for the material you requested from RightsLink, permission must be obtained from that source.

BACK   CLOSE WINDOW

CCC
RightsLink

🏠 Home   ❓ Help ⌄   ✉ Email Support   👤 Jonas Bruckmoser ⌄

ACS Publications
Most Trusted. Most Cited. Most Read.

Ring-Opening Polymerization of a Bicyclic Lactone: Polyesters Derived from Norcamphor with Complete Chemical Recyclability

Author: Jonas Bruckmoser, Sebastian Remke, Bernhard Rieger
Publication: ACS Macro Letters
Publisher: American Chemical Society
Date: Sep 1, 2022

Copyright © 2022, American Chemical Society

PERMISSION/LICENSE IS GRANTED FOR YOUR ORDER AT NO CHARGE

This type of permission/license, instead of the standard Terms and Conditions, is sent to you because no fee is being charged for your order. Please note the following:

- Permission is granted for your request in both print and electronic formats, and translations.
- If figures and/or tables were requested, they may be adapted or used in part.
- Please print this page for your records and send a copy of it to your publisher/graduate school.
- Appropriate credit for the requested material should be given as follows: "Reprinted (adapted) with permission from {COMPLETE REFERENCE CITATION}. Copyright {YEAR} American Chemical Society." Insert appropriate information in place of the capitalized words.
- One-time permission is granted only for the use specified in your RightsLink request. No additional uses are granted (such as derivative works or other editions). For any uses, please submit a new request.

If credit is given to another source for the material you requested from RightsLink, permission must be obtained from that source.

BACK   CLOSE WINDOW

11 References

1. Abd-El-Aziz, A. S.; Antonietti, M.; Barner-Kowollik, C.; Binder, W. H.; Böker, A.; Boyer, C.; Buchmeiser, M. R.; Cheng, S. Z. D.; D'Agosto, F.; Floudas, G.; Frey, H.; Galli, G.; Genzer, J.; Hartmann, L.; Hoogenboom, R.; Ishizone, T.; Kaplan, D. L.; Leclerc, M.; Lendlein, A.; Liu, B.; Long, T. E.; Ludwigs, S.; Lutz, J. F.; Matyjaszewski, K.; Meier, M. A. R.; Müllen, K.; Müllner, M.; Rieger, B.; Russell, T. P.; Savin, D. A.; Schlüter, A. D.; Schubert, U. S.; Seiffert, S.; Severing, K.; Soares, J. B. P.; Staffilani, M.; Sumerlin, B. S.; Sun, Y.; Tang, B. Z.; Tang, C.; Théato, P.; Tirelli, N.; Tsui, O. K. C.; Unterlass, M. M.; Vana, P.; Voit, B.; Vyazovkin, S.; Weder, C.; Wiesner, U.; Wong, W. Y.; Wu, C.; Yagci, Y.; Yuan, J.; Zhang, G., The Next 100 Years of Polymer Science. *Macromol. Chem. Phys.* **2020,** *221,* 2000216.
2. Staudinger, H., Über Polymerisation. *Ber. Dtsch. Chem. Ges.* **1920,** *53,* 1073-1085.
3. Frey, H.; Johann, T., Celebrating 100 years of "polymer science": Hermann Staudinger's 1920 manifesto. *Polym. Chem.* **2020,** *11,* 8-14.
4. Mülhaupt, R., Hermann Staudinger and the origin of macromolecular chemistry. *Angew. Chem. Int. Ed.* **2004,** *43,* 1054-1063.
5. Staudinger, H.; Fritschi, J., Über Isopren und Kautschuk. 5. Mitteilung. Über die Hydrierung des Kautschuks und über seine Konstitution. *Helv. Chim. Acta* **1922,** *5,* 785-806.
6. Sturzel, M.; Mihan, S.; Mülhaupt, R., From Multisite Polymerization Catalysis to Sustainable Materials and All-Polyolefin Composites. *Chem. Rev.* **2016,** *116,* 1398-1433.
7. Geyer, R.; Jambeck, J. R.; Law, K. L., Production, use, and fate of all plastics ever made. *Sci. Adv.* **2017,** *3,* e1700782.
8. Ellen MacArthur Foundation. The new plastics economy: rethinking the future of plastics & catalysing action. https://www.ellenmacarthurfoundation.org/publications/the-new-plastics-economy-rethinking-the-future-of-plastics-catalysing-action. **2017**. Accessed on September 08, 2022.
9. Coates, G. W.; Getzler, Y. D. Y. L., Chemical recycling to monomer for an ideal, circular polymer economy. *Nat. Rev. Mater.* **2020,** *5,* 501-516.
10. Jambeck, J. R.; Geyer, R.; Wilcox, C.; Siegler, T. R.; Perryman, M.; Andrady, A.; Narayan, R.; Law, K. L., Plastic waste inputs from land into the ocean. *Science* **2015,** *347,* 768-771.
11. MacLeod, M.; Arp, H. P. H.; Tekman, M. B.; Jahnke, A., The global threat from plastic pollution. *Science* **2021,** *373,* 61-65.
12. Santos, R. G.; Machovsky-Capuska, G. E.; Andrades, R., Plastic ingestion as an evolutionary trap: Toward a holistic understanding. *Science* **2021,** *373,* 56-60.
13. Stubbins, A.; Law, K. L.; Muñoz, S. E.; Bianchi, T. S.; Zhu, L., Plastics in the Earth system. *Science* **2021,** *373,* 51-55.
14. Simon, N.; Raubenheimer, K.; Urho, N.; Unger, S.; Azoulay, D.; Farrelly, T.; Sousa, J.; van Asselt, H.; Carlini, G.; Sekomo, C.; Schulte, M. L.; Busch, P.-O.; Wienrich, N.; Weiand, L., A binding global agreement to address the life cycle of plastics. *Science* **2021,** *373,* 43-47.
15. Tschan, M. J. L.; Brulé, E.; Haquette, P.; Thomas, C. M., Synthesis of biodegradable polymers from renewable resources. *Polym. Chem.* **2012,** *3,* 836-851.
16. Delidovich, I.; Hausoul, P. J.; Deng, L.; Pfutzenreuter, R.; Rose, M.; Palkovits, R., Alternative Monomers Based on Lignocellulose and Their Use for Polymer Production. *Chem. Rev.* **2016,** *116,* 1540-1599.
17. Zhu, Y.; Romain, C.; Williams, C. K., Sustainable polymers from renewable resources. *Nature* **2016,** *540,* 354-362.
18. Winnacker, M., Pinenes: Abundant and Renewable Building Blocks for a Variety of Sustainable Polymers. *Angew. Chem. Int. Ed.* **2018,** *57,* 14362-14371.
19. Tang, X.; Chen, E. Y. X., Toward infinitely recyclable plastics derived from renewable cyclic esters. *Chem* **2019,** *5,* 284-312.

20.   Fagnani, D. E.; Tami, J. L.; Copley, G.; Clemons, M. N.; Getzler, Y. D. Y. L.; McNeil, A. J., 100th Anniversary of Macromolecular Science Viewpoint: Redefining Sustainable Polymers. *ACS Macro Lett.* **2020,** *10*, 41-53.

21.   Worch, J. C.; Dove, A. P., 100th Anniversary of Macromolecular Science Viewpoint: Toward Catalytic Chemical Recycling of Waste (and Future) Plastics. *ACS Macro Lett.* **2020,** *9*, 1494-1506.

22.   Thomas, C. M., Stereocontrolled ring-opening polymerization of cyclic esters: synthesis of new polyester microstructures. *Chem. Soc. Rev.* **2010,** *39*, 165-173.

23.   Rieger, B.; Künkel, A.; Coates, G. W.; Reichardt, R.; Dinjus, E.; Zevaco, T. A., *Synthetic biodegradable polymers*. Springer-Verlag, Berlin, Heidelberg, **2012**.

24.   Larrañaga, A.; Lizundia, E., A review on the thermomechanical properties and biodegradation behaviour of polyesters. *Eur. Polym. J.* **2019,** *121*, 109296.

25.   European Bioplastics. Bioplastics - Facts and Figures. https://docs.european-bioplastics.org/publications/EUBP_Facts_and_figures.pdf. **2021**. Accessed on September 08, 2022.

26.   Gabirondo, E.; Sangroniz, A.; Etxeberria, A.; Torres-Giner, S.; Sardon, H., Poly(hydroxy acids) derived from the self-condensation of hydroxy acids: from polymerization to end-of-life options. *Polym. Chem.* **2020,** *11*, 4861-4874.

27.   Tschan, M. J.; Gauvin, R. M.; Thomas, C. M., Controlling polymer stereochemistry in ring-opening polymerization: a decade of advances shaping the future of biodegradable polyesters. *Chem. Soc. Rev.* **2021,** *50*, 13587-13608.

28.   Dubois, P.; Coulembier, O.; Raquez, J.-M., *Handbook of ring-opening polymerization*. Wiley-VCH Verlag, Weinheim, **2009**.

29.   Carpentier, J. F., Discrete metal catalysts for stereoselective ring-opening polymerization of chiral racemic *β*-lactones. *Macromol. Rapid Commun.* **2010,** *31*, 1696-1705.

30.   Diaz, C.; Mehrkhodavandi, P., Strategies for the synthesis of block copolymers with biodegradable polyester segments. *Polym. Chem.* **2021,** *12*, 783-806.

31.   Wilson, J. A.; Ates, Z.; Pflughaupt, R. L.; Dove, A. P.; Heise, A., Polymers from macrolactones: From pheromones to functional materials. *Prog. Polym. Sci.* **2019,** *91*, 29-50.

32.   Martin Vaca, B.; Bourissou, D., O-Carboxyanhydrides: Useful Tools for the Preparation of Well-Defined Functionalized Polyesters. *ACS Macro Lett.* **2015,** *4*, 792-798.

33.   Agarwal, S., Chemistry, chances and limitations of the radical ring-opening polymerization of cyclic ketene acetals for the synthesis of degradable polyesters. *Polym. Chem.* **2010,** *1*, 953-964.

34.   Paul, S.; Zhu, Y.; Romain, C.; Brooks, R.; Saini, P. K.; Williams, C. K., Ring-opening copolymerization (ROCOP): synthesis and properties of polyesters and polycarbonates. *Chem. Commun.* **2015,** *51*, 6459-6479.

35.   Longo, J. M.; Sanford, M. J.; Coates, G. W., Ring-Opening Copolymerization of Epoxides and Cyclic Anhydrides with Discrete Metal Complexes: Structure-Property Relationships. *Chem. Rev.* **2016,** *116*, 15167-15197.

36.   Olsen, P.; Odelius, K.; Albertsson, A. C., Thermodynamic Presynthetic Considerations for Ring-Opening Polymerization. *Biomacromolecules* **2016,** *17*, 699-709.

37.   Xu, G.; Wang, Q., Chemically recyclable polymer materials: polymerization and depolymerization cycles. *Green Chem.* **2022,** *24*, 2321-2346.

38.   Lebedev, B. V., Thermodynamics of polylactones. *Russ. Chem. Rev.* **1996,** *65*, 1063-1082.

39.   Save, M.; Schappacher, M.; Soum, A., Controlled ring-opening polymerization of lactones and lactides initiated by lanthanum isopropoxide, 1. General aspects and kinetics. *Macromol. Chem. Phys.* **2002,** *203*, 889-899.

40.   Hong, M.; Chen, E. Y., Completely recyclable biopolymers with linear and cyclic topologies via ring-opening polymerization of *γ*-butyrolactone. *Nat. Chem.* **2016,** *8*, 42-49.

41.   Zhu, J.-B.; Watson, E. M.; Tang, J.; Chen, E. Y.-X., A synthetic polymer system with repeatable chemical recyclability. *Science* **2018,** *360*, 398-403.

42.   Zhu, J. B.; Chen, E. Y. X., Living Coordination Polymerization of a Six-Five Bicyclic Lactone to Produce Completely Recyclable Polyester. *Angew. Chem. Int. Ed.* **2018,** *57*, 12558-12562.

43.   Zhu, J. B.; Chen, E. Y., Catalyst-Sidearm-Induced Stereoselectivity Switching in Polymerization of a Racemic Lactone for Stereocomplexed Crystalline Polymer with a Circular Life Cycle. *Angew. Chem. Int. Ed.* **2019,** *58*, 1178-1182.

44.   Duda, A.; Penczek, S., Thermodynamics of L-lactide polymerization. Equilibrium monomer concentration. *Macromolecules* **1990,** *23*, 1636-1639.

45.   Ottou, W. N.; Sardon, H.; Mecerreyes, D.; Vignolle, J.; Taton, D., Update and challenges in organo-mediated polymerization reactions. *Prog. Polym. Sci.* **2016,** *56*, 64-115.

46.   Xu, J.; Wang, X.; Liu, J.; Feng, X.; Gnanou, Y.; Hadjichristidis, N., Ionic H-bonding organocatalysts for the ring-opening polymerization of cyclic esters and cyclic carbonates. *Prog. Polym. Sci.* **2022,** *125*, 101484.

47.   Nachtergael, A.; Coulembier, O.; Dubois, P.; Helvenstein, M.; Duez, P.; Blankert, B.; Mespouille, L., Organocatalysis paradigm revisited: are metal-free catalysts really harmless? *Biomacromolecules* **2015,** *16*, 507-514.

48.   Labet, M.; Thielemans, W., Synthesis of polycaprolactone: a review. *Chem. Soc. Rev.* **2009,** *38*, 3484-3504.

49.   Liu, Y.; Wu, J.; Hu, X.; Zhu, N.; Guo, K., Advances, challenges, and opportunities of poly(γ-butyrolactone)-based recyclable polymers. *ACS Macro Lett.* **2021,** *10*, 284-296.

50.   Batiste, D. C.; Meyersohn, M. S.; Watts, A.; Hillmyer, M. A., Efficient Polymerization of Methyl-ε-Caprolactone Mixtures To Access Sustainable Aliphatic Polyesters. *Macromolecules* **2020,** *53*, 1795-1808.

51.   Olsen, P.; Borke, T.; Odelius, K.; Albertsson, A. C., ε-Decalactone: a thermoresilient and toughening comonomer to poly(*L*-lactide). *Biomacromolecules* **2013,** *14*, 2883-2890.

52.   Schneiderman, D. K.; Hillmyer, M. A., Aliphatic Polyester Block Polymer Design. *Macromolecules* **2016,** *49*, 2419-2428.

53.   Della Monica, F.; Kleij, A. W., From terpenes to sustainable and functional polymers. *Polym. Chem.* **2020,** *11*, 5109-5127.

54.   Kränzlein, M.; Pongratz, S.; Bruckmoser, J.; Bratić, B.; Breitsameter, J. M.; Rieger, B., Polyester synthesis based on 3-carene as renewable feedstock. *Polym. Chem.* **2022,** *13*, 3726-3732.

55.   Tang, X.; Chen, E. Y., Chemical synthesis of perfectly isotactic and high melting bacterial poly(3-hydroxybutyrate) from bio-sourced racemic cyclic diolide. *Nat. Commun.* **2018,** *9*, 2345.

56.   Tang, X.; Westlie, A. H.; Watson, E. M.; Chen, E. Y.-X., Stereosequenced crystalline polyhydroxyalkanoates from diastereomeric monomer mixtures. *Science* **2019,** *366*, 754-758.

57.   Tang, X.; Westlie, A. H.; Caporaso, L.; Cavallo, L.; Falivene, L.; Chen, E. Y., Biodegradable Polyhydroxyalkanoates by Stereoselective Copolymerization of Racemic Diolides: Stereocontrol and Polyolefin-Like Properties. *Angew. Chem. Int. Ed.* **2020,** *59*, 7881-7890.

58.   Hiki, S.; Taniguchi, I.; Miyamoto, M.; Kimura, Y., Poly([R]-3-hydroxybutyrate-co-glycolate): A novel PHB derivative chemically synthesized by copolymerization of a new cyclic diester monomer [R]-4-methyl-1,5-dioxepane-2,6-dione. *Macromolecules* **2002,** *35*, 2423-2425.

59.   Amador, A. G.; Watts, A.; Neitzel, A. E.; Hillmyer, M. A., Entropically Driven Macrolide Polymerizations for the Synthesis of Aliphatic Polyester Copolymers Using Titanium Isopropoxide. *Macromolecules* **2019,** *52*, 2371-2383.

60.   Kim, H. J.; Reddi, Y.; Cramer, C. J.; Hillmyer, M. A.; Ellison, C. J., Readily Degradable Aromatic Polyesters from Salicylic Acid. *ACS Macro Lett.* **2020,** *9*, 96-102.

61.   Westlie, A. H.; Chen, E. Y. X., Catalyzed Chemical Synthesis of Unnatural Aromatic Polyhydroxyalkanoate and Aromatic–Aliphatic PHAs with Record-High Glass-Transition and Decomposition Temperatures. *Macromolecules* **2020,** *53*, 9906-9915.

62.   Li, J.; Liu, F.; Liu, Y.; Shen, Y.; Li, Z., Functionalizable and Chemically Recyclable Thermoplastics from Chemoselective Ring-Opening Polymerization of Bio-renewable Bifunctional α-Methylene-δ-valerolacton. *Angew. Chem. Int. Ed.* **2022,** *61*, e202207105.

63.   Worch, J. C.; Prydderch, H.; Jimaja, S.; Bexis, P.; Becker, M. L.; Dove, A. P., Stereochemical enhancement of polymer properties. *Nat. Rev. Chem.* **2019,** *3*, 514-535.

64. Muhammadi; Shabina; Afzal, M.; Hameed, S., Bacterial polyhydroxyalkanoates-eco-friendly next generation plastic: production, biocompatibility, biodegradation, physical properties and applications. *Green Chem. Lett. Rev.* **2015,** *8*, 56-77.

65. Kumar, M.; Rathour, R.; Singh, R.; Sun, Y.; Pandey, A.; Gnansounou, E.; Andrew Lin, K.-Y.; Tsang, D. C. W.; Thakur, I. S., Bacterial polyhydroxyalkanoates: Opportunities, challenges, and prospects. *J. Clean. Prod.* **2020,** *263*, 121500.

66. Abe, H.; Matsubara, I.; Doi, Y.; Hori, Y.; Yamaguchi, A., Physical properties and enzymic degradability of poly(3-hydroxybutyrate) stereoisomers with different stereoregularities. *Macromolecules* **1994,** *27*, 6018-6025.

67. Gogolewski, S.; Jovanovic, M.; Perren, S.; Dillon, J.; Hughes, M., The effect of melt-processing on the degradation of selected polyhydroxyacids: polylactides, polyhydroxybutyrate, and polyhydroxybutyrate-co-valerates. *Polym. Degrad. Stab.* **1993,** *40*, 313-322.

68. Westlie, A. H.; Quinn, E. C.; Parker, C. R.; Chen, E. Y. X., Synthetic biodegradable polyhydroxyalkanoates (PHAs): Recent advances and future challenges. *Prog. Polym. Sci.* **2022,** *134*, 101608.

69. Karasz, F. E.; Bair, H. E.; O'Reilly, J. M., Thermal properties of atactic and isotactic polystyrene. *J. Phys. Chem.* **1965,** *69*, 2657-2667.

70. Getzler, Y. D.; Mahadevan, V.; Lobkovsky, E. B.; Coates, G. W., Synthesis of β-lactones: a highly active and selective catalyst for epoxide carbonylation. *J. Am. Chem. Soc.* **2002,** *124*, 1174-1175.

71. Olah, G. A.; Goeppert, A.; Prakash, G. S., Chemical recycling of carbon dioxide to methanol and dimethyl ether: from greenhouse gas to renewable, environmentally carbon neutral fuels and synthetic hydrocarbons. *J. Org. Chem.* **2008,** *74*, 487-498.

72. Russo, V.; Tesser, R.; Santacesaria, E.; Di Serio, M., Chemical and Technical Aspects of Propene Oxide Production via Hydrogen Peroxide (HPPO Process). *Ind. Eng. Chem. Res.* **2013,** *52*, 1168-1178.

73. Tanahashi, N.; Doi, Y., Thermal properties and stereoregularity of poly(3-hydroxybutyrate) prepared from optically active *β*-butyrolactone with a zinc-based catalyst. *Macromolecules* **1991,** *24*, 5732-5733.

74. Hori, Y.; Suzuki, M.; Yamaguchi, A.; Nishishita, T., Ring-opening polymerization of optically active *β*-butyrolactone using distannoxane catalysts: Synthesis of high-molecular-weight poly(3-hydroxybutyrate). *Macromolecules* **1993,** *26*, 5533-5534.

75. Abe, H.; Doi, Y., Enzymatic and environmental degradation of racemic poly(3-hydroxybutyric acid)s with different stereoregularities. *Macromolecules* **1996,** *29*, 8683-8688.

76. Feghali, E.; Tauk, L.; Ortiz, P.; Vanbroekhoven, K.; Eevers, W., Catalytic chemical recycling of biodegradable polyesters. *Polym. Degrad. Stab.* **2020,** *179*, 109241.

77. Ariffin, H.; Nishida, H.; Shirai, Y.; Hassan, M. A., Highly selective transformation of poly[(R)-3-hydroxybutyric acid] into trans-crotonic acid by catalytic thermal degradation. *Polym. Degrad. Stab.* **2010,** *95*, 1375-1381.

78. Yu, J.; Plackett, D.; Chen, L. X. L., Kinetics and mechanism of the monomeric products from abiotic hydrolysis of poly[(R)-3-hydroxybutyrate] under acidic and alkaline conditions. *Polym. Degrad. Stab.* **2005,** *89*, 289-299.

79. Clark, J. M.; Pilath, H. M.; Mittal, A.; Michener, W. E.; Robichaud, D. J.; Johnson, D. K., Direct Production of Propene from the Thermolysis of Poly(*β*-hydroxybutyrate) (PHB). An Experimental and DFT Investigation. *J. Phys. Chem. A* **2016,** *120*, 332-345.

80. Li, Y.; Strathmann, T. J., Kinetics and mechanism for hydrothermal conversion of polyhydroxybutyrate (PHB) for wastewater valorization. *Green Chem.* **2019,** *21*, 5586-5597.

81. Melchiors, M.; Keul, H.; Höcker, H., Synthesis of highly isotactic poly[(R)-3-hydroxybutyrate] by ring-opening polymerization of (R,R,R)-4,8,12-trimethyl-1,5,9-trioxacyclododeca-2,6,10-trione. *Macromol. Rapid Commun.* **1994,** *15*, 497-506.

82. Melchiors, M.; Keul, H.; Höcker, H., Depolymerization of poly[(R)-3-hydroxybutyrate] to cyclic oligomers and polymerization of the cyclic trimer: an example of thermodynamic recycling. *Macromolecules* **1996,** *29*, 6442-6451.

83.   Yang, R.; Xu, G.; Lv, C.; Dong, B.; Zhou, L.; Wang, Q., Zn(HMDS)$_2$ as a versatile transesterification catalyst for polyesters synthesis and degradation toward a circular materials economy approach. *ACS Sustainable Chem. Eng.* **2020,** *8*, 18347-18353.

84.   Krall, E. M.; Klein, T. W.; Andersen, R. J.; Nett, A. J.; Glasgow, R. W.; Reader, D. S.; Dauphinais, B. C.; Mc Ilrath, S. P.; Fischer, A. A.; Carney, M. J.; Hudson, D. J.; Robertson, N. J., Controlled hydrogenative depolymerization of polyesters and polycarbonates catalyzed by ruthenium(II) PNN pincer complexes. *Chem. Commun.* **2014,** *50*, 4884-4887.

85.   Zhu, R.; Jiang, J.-L.; Li, X.-L.; Deng, J.; Fu, Y., A Comprehensive Study on Metal Triflate-Promoted Hydrogenolysis of Lactones to Carboxylic Acids: From Synthetic and Mechanistic Perspectives. *ACS Catal.* **2017,** *7*, 7520-7528.

86.   Song, X.; Liu, F.; Wang, H.; Wang, C.; Yu, S.; Liu, S., Methanolysis of microbial polyester poly(3-hydroxybutyrate) catalyzed by Brønsted-Lewis acidic ionic liquids as a new method towards sustainable development. *Polym. Degrad. Stab.* **2018,** *147*, 215-221.

87.   Yang, X.; Odelius, K.; Hakkarainen, M., Microwave-Assisted Reaction in Green Solvents Recycles PHB to Functional Chemicals. *ACS Sustainable Chem. Eng.* **2014,** *2*, 2198-2203.

88.   Lambert, S.; Wagner, M., Environmental performance of bio-based and biodegradable plastics: the road ahead. *Chem. Soc. Rev.* **2017,** *46*, 6855-6871.

89.   Chamas, A.; Moon, H.; Zheng, J.; Qiu, Y.; Tabassum, T.; Jang, J. H.; Abu-Omar, M.; Scott, S. L.; Suh, S., Degradation Rates of Plastics in the Environment. *ACS Sustainable Chem. Eng.* **2020,** *8*, 3494-3511.

90.   Cederholm, L.; Wohlert, J.; Olsen, P.; Hakkarainen, M.; Odelius, K., "Like Recycles Like": Selective Ring-Closing Depolymerization of Poly(L-Lactic Acid) to L-Lactide. *Angew. Chem. Int. Ed.* **2022,** *61*, e202204531.

91.   Li, H.; Shakaroun, R. M.; Guillaume, S. M.; Carpentier, J. F., Recent Advances in Metal-Mediated Stereoselective Ring-Opening Polymerization of Functional Cyclic Esters towards Well-Defined Poly(hydroxy acid)s: From Stereoselectivity to Sequence-Control. *Chem. Eur. J.* **2020,** *26*, 128-138.

92.   Tang, X.; Hong, M.; Falivene, L.; Caporaso, L.; Cavallo, L.; Chen, E. Y., The Quest for Converting Biorenewable Bifunctional α-Methylene-γ-butyrolactone into Degradable and Recyclable Polyester: Controlling Vinyl-Addition/Ring-Opening/Cross-Linking Pathway. *J. Am. Chem. Soc.* **2016,** *138*, 14326-14337.

93.   Kawalec, M.; Adamus, G.; Kurcok, P.; Kowalczuk, M.; Foltran, I.; Focarete, M. L.; Scandola, M., Carboxylate-induced degradation of poly(3-hydroxybutyrate)s. *Biomacromolecules* **2007,** *8*, 1053-1058.

94.   Dong, X.; Robinson, J. R., The role of neutral donor ligands in the isoselective ring-opening polymerization of rac-β-butyrolactone. *Chem. Sci.* **2020,** *11*, 8184-8195.

95.   O'Keefe, B. J.; Hillmyer, M. A.; Tolman, W. B., Polymerization of lactide and related cyclic esters by discrete metal complexes. *J. Chem. Soc., Dalton Trans.* **2001**, 2215-2224.

96.   Inoue, S., Immortal polymerization: The outset, development, and application. *J. Polym. Sci., Part A: Polym. Chem.* **2000,** *38*, 2861-2871.

97.   Ajellal, N.; Carpentier, J.-F.; Guillaume, C.; Guillaume, S. M.; Helou, M.; Poirier, V.; Sarazin, Y.; Trifonov, A., Metal-catalyzed immortal ring-opening polymerization of lactones, lactides and cyclic carbonates. *Dalton Trans.* **2010,** *39*, 8363-8376.

98.   Carpentier, J.-F., Rare-Earth Complexes Supported by Tripodal Tetradentate Bis(phenolate) Ligands: A Privileged Class of Catalysts for Ring-Opening Polymerization of Cyclic Esters. *Organometallics* **2015,** *34*, 4175-4189.

99.   Ajellal, N.; Lyubov, D. M.; Sinenkov, M. A.; Fukin, G. K.; Cherkasov, A. V.; Thomas, C. M.; Carpentier, J. F.; Trifonov, A. A., Bis(guanidinate) alkoxide complexes of lanthanides: synthesis, structures and use in immortal and stereoselective ring-opening polymerization of cyclic esters. *Chem. Eur. J.* **2008,** *14*, 5440-5448.

100.   Zhao, W.; Cui, D.; Liu, X.; Chen, X., Facile Synthesis of Hydroxyl-Ended, Highly Stereoregular, Star-Shaped Poly(lactide) from Immortal ROP of rac-Lactide and Kinetics Study. *Macromolecules* **2010,** *43*, 6678-6684.

101.   Wang, L.; Poirier, V.; Ghiotto, F.; Bochmann, M.; Cannon, R. D.; Carpentier, J.-F.; Sarazin, Y., Kinetic Analysis of the Immortal Ring-Opening Polymerization of Cyclic Esters: A Case Study with Tin(II) Catalysts. *Macromolecules* **2014**, *47*, 2574-2584.

102.   Xu, C.; Yu, I.; Mehrkhodavandi, P., Highly controlled immortal polymerization of *β*-butyrolactone by a dinuclear indium catalyst. *Chem. Commun.* **2012**, *48*, 6806-6808.

103.   Ebrahimi, T.; Aluthge, D. C.; Patrick, B. O.; Hatzikiriakos, S. G.; Mehrkhodavandi, P., Air- and moisture-stable indium salan catalysts for living multiblock PLA formation in air. *ACS Catal.* **2017,** *7*, 6413-6418.

104.   Bloembergen, S.; Holden, D. A.; Bluhm, T. L.; Hamer, G. K.; Marchessault, R. H., Stereoregularity in synthetic β-hydroxybutyrate and β-hydroxyvalerate homopolyesters. *Macromolecules* **1989,** *22*, 1656-1663.

105.   Poirier, V.; Roisnel, T.; Carpentier, J. F.; Sarazin, Y., Versatile catalytic systems based on complexes of zinc, magnesium and calcium supported by a bulky bis(morpholinomethyl)phenoxy ligand for the large-scale immortal ring-opening polymerisation of cyclic esters. *Dalton Trans.* **2009**, 9820-9827.

106.   Wang, H.; Guo, J.; Yang, Y.; Ma, H., Diastereoselective synthesis of chiral aminophenolate magnesium complexes and their application in the stereoselective polymerization of *rac*-lactide and *rac*-β-butyrolactone. *Dalton Trans.* **2016,** *45*, 10942-10953.

107.   Kerr, R. W. F.; Ewing, P. M. D. A.; Raman, S. K.; Smith, A. D.; Williams, C. K.; Arnold, P. L., Ultrarapid cerium(III)–NHC catalysts for high molar mass cyclic polylactide. *ACS Catal.* **2021,** *11*, 1563-1569.

108.   Rieth, L. R.; Moore, D. R.; Lobkovsky, E. B.; Coates, G. W., Single-site β-diiminate zinc catalysts for the ring-opening polymerization of β-butyrolactone and β-valerolactone to poly(3-hydroxyalkanoates). *J. Am. Chem. Soc.* **2002**, *124*, 15239-15248.

109.   Chamberlain, B. M.; Cheng, M.; Moore, D. R.; Ovitt, T. M.; Lobkovsky, E. B.; Coates, G. W., Polymerization of lactide with zinc and magnesium *β*-diiminate complexes: stereocontrol and mechanism. *J. Am. Chem. Soc.* **2001**, *123*, 3229-3238.

110.   Cross, E. D.; Allan, L. E. N.; Decken, A.; Shaver, M. P., Aluminum salen and salan complexes in the ring-opening polymerization of cyclic esters: Controlled immortal and copolymerization ofrac-β-butyrolactone andrac-lactide. *J. Polym. Sci., Part A: Polym. Chem.* **2013,** *51*, 1137-1146.

111.   Yuntawattana, N.; McGuire, T. M.; Durr, C. B.; Buchard, A.; Williams, C. K., Indium phosphasalen catalysts showing high isoselectivity and activity in racemic lactide and lactone ring opening polymerizations. *Catal. Sci. Technol.* **2020**, *10*, 7226-7239.

112.   Abbina, S.; Du, G., Zinc-Catalyzed Highly Isoselective Ring Opening Polymerization of rac-Lactide. *ACS Macro Lett.* **2014,** *3*, 689-692.

113.   Shaik, M.; Peterson, J.; Du, G., Cyclic and Linear Polyhydroxylbutyrates from Ring-Opening Polymerization of β-Butyrolactone with Amido-Oxazolinate Zinc Catalysts. *Macromolecules* **2018,** *52*, 157-166.

114.   Saha, T. K.; Ramkumar, V.; Chakraborty, D., Salen complexes of zirconium and hafnium: synthesis, structural characterization, controlled hydrolysis, and solvent-free ring-opening polymerization of cyclic esters and lactides. *Inorg. Chem.* **2011,** *50*, 2720-2722.

115.   Bakewell, C.; White, A. J.; Long, N. J.; Williams, C. K., Metal-size influence in iso-selective lactide polymerization. *Angew. Chem. Int. Ed.* **2014,** *53*, 9226-9230.

116.   Bakewell, C.; White, A. J.; Long, N. J.; Williams, C. K., Scandium and yttrium phosphasalen complexes as initiators for ring-opening polymerization of cyclic esters. *Inorg. Chem.* **2015,** *54*, 2204-2212.

117.   Nie, K.; Gu, W.; Yao, Y.; Zhang, Y.; Shen, Q., Synthesis and Characterization of Salalen Lanthanide Complexes and Their Application in the Polymerization of rac-Lactide. *Organometallics* **2013,** *32*, 2608-2617.

118.   Tian, T.; Feng, C.; Wang, Y.; Zhu, X.; Yuan, D.; Yao, Y., Synthesis of N-Methyl-o-phenylenediamine-Bridged Bis(phenolato) Lanthanide Alkoxides and Their Catalytic Performance for the (Co)Polymerization of rac-Butyrolactone and L-Lactide. *Inorg. Chem.* **2022,** *61*, 9918-9929.

119.   Le Roux, E., Recent advances on tailor-made titanium catalysts for biopolymer synthesis. *Coord. Chem. Rev.* **2016,** *306*, 65-85.

120.   Wang, B.; Wei, Y.; Li, Z. J.; Pan, L.; Li, Y. S., From $Zn(C_6F_5)_2$ to $ZnEt_2$-based Lewis Pairs: Significantly Improved Catalytic Activity and Monomer Adaptability for the Ring-opening Polymerization of Lactones. *ChemCatChem* **2018,** *10*, 5287-5296.

121.   Cai, C.-X.; Toupet, L.; Lehmann, C. W.; Carpentier, J.-F., Synthesis, structure and reactivity of new yttrium bis(dimethylsilyl)amido and bis(trimethylsilyl)methyl complexes of a tetradentate bis(phenoxide) ligand. *J. Organomet. Chem.* **2003,** *683*, 131-136.

122.   Cai, C. X.; Amgoune, A.; Lehmann, C. W.; Carpentier, J. F., Stereoselective ring-opening polymerization of racemic lactide using alkoxy-amino-bis(phenolate) group 3 metal complexes. *Chem. Commun.* **2004**, 330-331.

123.   Amgoune, A.; Thomas, C. M.; Ilinca, S.; Roisnel, T.; Carpentier, J. F., Highly active, productive, and syndiospecific yttrium initiators for the polymerization of racemic β-butyrolactone. *Angew. Chem. Int. Ed.* **2006,** *45*, 2782-2784.

124.   Wheaton, C. A.; Hayes, P. G.; Ireland, B. J., Complexes of Mg, Ca and Zn as homogeneous catalysts for lactide polymerization. *Dalton Trans.* **2009**, 4832-4846.

125.   Guillaume, S. M.; Carpentier, J.-F., Recent advances in metallo/organo-catalyzed immortal ring-opening polymerization of cyclic carbonates. *Catal. Sci. Technol.* **2012,** *2*, 898-906.

126.   Moore, D. R.; Cheng, M.; Lobkovsky, E. B.; Coates, G. W., Mechanism of the alternating copolymerization of epoxides and CO_2 using β-diiminate zinc catalysts: evidence for a bimetallic epoxide enchainment. *J. Am. Chem. Soc.* **2003,** *125*, 11911-11924.

127.   Cheng, M.; Moore, D. R.; Reczek, J. J.; Chamberlain, B. M.; Lobkovsky, E. B.; Coates, G. W., Single-site *β*-diiminate zinc catalysts for the alternating copolymerization of CO_2 and epoxides: catalyst synthesis and unprecedented polymerization activity. *J. Am. Chem. Soc.* **2001,** *123*, 8738-8749.

128.   Kernbichl, S.; Reiter, M.; Adams, F.; Vagin, S.; Rieger, B., CO_2-Controlled One-Pot Synthesis of AB, ABA Block, and Statistical Terpolymers from β-Butyrolactone, Epoxides, and CO_2. *J. Am. Chem. Soc.* **2017,** *139*, 6787-6790.

129.   Gruszka, W.; Walker, L. C.; Shaver, M. P.; Garden, J. A., In situ versus isolated zinc catalysts in the selective synthesis of homo and multi-block polyesters. *Macromolecules* **2020,** *53*, 4294-4302.

130.   Chuang, H.-J.; Chen, H.-L.; Huang, B.-H.; Tsai, T.-E.; Huang, P.-L.; Liao, T.-T.; Lin, C.-C., Efficient zinc initiators supported by NNO-tridentate ketiminate ligands for cyclic esters polymerization. *J. Polym. Sci., Part A: Polym. Chem.* **2013,** *51*, 1185-1196.

131.   Bruckmoser, J.; Henschel, D.; Vagin, S.; Rieger, B., Combining high activity with broad monomer scope: indium salan catalysts in the ring-opening polymerization of various cyclic esters. *Catal. Sci. Technol.* **2022,** *12*, 3295-3302.

132.   Dagorne, S.; Normand, M.; Kirillov, E.; Carpentier, J.-F., Gallium and indium complexes for ring-opening polymerization of cyclic ethers, esters and carbonates. *Coord. Chem. Rev.* **2013,** *257*, 1869-1886.

133.   Osten, K. M.; Mehrkhodavandi, P., Indium Catalysts for Ring Opening Polymerization: Exploring the Importance of Catalyst Aggregation. *Acc. Chem. Res.* **2017,** *50*, 2861-2869.

134.   Pietrangelo, A.; Hillmyer, M. A.; Tolman, W. B., Stereoselective and controlled polymerization of *D,L*-lactide using indium(III) trichloride. *Chem. Commun.* **2009**, 2736-2737.

135.   Pietrangelo, A.; Knight, S. C.; Gupta, A. K.; Yao, L. J.; Hillmyer, M. A.; Tolman, W. B., Mechanistic study of the stereoselective polymerization of *D,L*-lactide using indium(III) halides. *J. Am. Chem. Soc.* **2010,** *132*, 11649-11657.

136.   Thongkham, S.; Monot, J.; Martin-Vaca, B.; Bourissou, D., Simple In-based dual catalyst enables significant progress in *ε*-decalactone ring-opening (co)polymerization. *Macromolecules* **2019,** *52*, 8103-8113.

137.   Douglas, A. F.; Patrick, B. O.; Mehrkhodavandi, P., A highly active chiral indium catalyst for living lactide polymerization. *Angew. Chem. Int. Ed.* **2008,** *47*, 2290-2293.

138.   Quan, S. M.; Diaconescu, P. L., High activity of an indium alkoxide complex toward ring opening polymerization of cyclic esters. *Chem. Commun.* **2015,** *51*, 9643-9646.

139.   Myers, D.; White, A. J. P.; Forsyth, C. M.; Bown, M.; Williams, C. K., Phosphasalen Indium Complexes Showing High Rates and Isoselectivities in rac-Lactide Polymerizations. *Angew. Chem. Int. Ed.* **2017,** *56*, 5277-5282.

140. Ligny, R.; Hanninen, M. M.; Guillaume, S. M.; Carpentier, J. F., Steric vs. electronic stereocontrol in syndio- or iso-selective ROP of functional chiral β-lactones mediated by achiral yttrium-bisphenolate complexes. *Chem. Commun.* **2018,** *54,* 8024-8031.
141. Bouyahyi, M.; Ajellal, N.; Kirillov, E.; Thomas, C. M.; Carpentier, J. F., Exploring electronic versus steric effects in stereoselective ring-opening polymerization of lactide and β-butyrolactone with amino-alkoxy-bis(phenolate)-yttrium complexes. *Chem. Eur. J.* **2011,** *17,* 1872-1883.
142. Ajellal, N.; Bouyahyi, M.; Amgoune, A.; Thomas, C. M.; Bondon, A.; Pillin, I.; Grohens, Y.; Carpentier, J.-F., Syndiotactic-enriched poly(3-hydroxybutyrate)s via stereoselective ring-opening polymerization of racemic β-butyrolactone with discrete yttrium catalysts. *Macromolecules* **2009,** *42,* 987-993.
143. Spassky, N.; Wisniewski, M.; Pluta, C.; Le Borgne, A., Highly stereoelective polymerization of rac-(D,L)-lactide with a chiral schiff's base/aluminium alkoxide initiator. *Macromol. Chem. Phys.* **1996,** *197,* 2627-2637.
144. Hormnirun, P.; Marshall, E. L.; Gibson, V. C.; White, A. J.; Williams, D. J., Remarkable stereocontrol in the polymerization of racemic lactide using aluminum initiators supported by tetradentate aminophenoxide ligands. *J. Am. Chem. Soc.* **2004,** *126,* 2688-2689.
145. Bakewell, C.; Cao, T. P.; Long, N.; Le Goff, X. F.; Auffrant, A.; Williams, C. K., Yttrium phosphasalen initiators for rac-lactide polymerization: excellent rates and high iso-selectivities. *J. Am. Chem. Soc.* **2012,** *134,* 20577-20580.
146. Lyubov, D. M.; Tolpygin, A. O.; Trifonov, A. A., Rare-earth metal complexes as catalysts for ring-opening polymerization of cyclic esters. *Coord. Chem. Rev.* **2019,** *392,* 83-145.
147. Kramer, J. W.; Treitler, D. S.; Dunn, E. W.; Castro, P. M.; Roisnel, T.; Thomas, C. M.; Coates, G. W., Polymerization of enantiopure monomers using syndiospecific catalysts: a new approach to sequence control in polymer synthesis. *J. Am. Chem. Soc.* **2009,** *131,* 16042-16044.
148. Fang, J.; Tschan, M. J. L.; Roisnel, T.; Trivelli, X.; Gauvin, R. M.; Thomas, C. M.; Maron, L., Yttrium catalysts for syndioselective β-butyrolactone polymerization: on the origin of ligand-induced stereoselectivity. *Polym. Chem.* **2013,** *4,* 360-367.
149. Ebrahimi, T.; Aluthge, D. C.; Hatzikiriakos, S. G.; Mehrkhodavandi, P., Highly Active Chiral Zinc Catalysts for Immortal Polymerization of β-Butyrolactone Form Melt Processable Syndio-Rich Poly(hydroxybutyrate). *Macromolecules* **2016,** *49,* 8812-8824.
150. Agostini, D.; Lando, J.; Shelton, J. R., Synthesis and characterization of poly-β-hydroxybutyrate. I. Synthesis of crystalline DL-poly-β-hydroxybutyrate from DL-β-butyrolactone. *J. Polym. Sci., Part A: Polym. Chem.* **1971,** *9,* 2775-2787.
151. Teranishi, K.; Iida, M.; Araki, T.; Yamashita, S.; Tani, H., Stereospecific polymerization of β-alkyl-β-propiolactone. *Macromolecules* **1974,** *7,* 421-427.
152. Iida, M.; Araki, T.; Teranishi, K.; Tani, H., Effect of substituents on stereospecific polymerization of β-alkyl-and β-chloroalkyl-β-propiolactones. *Macromolecules* **1977,** *10,* 275-284.
153. Gross, R. A.; Zhang, Y.; Konrad, G.; Lenz, R. W., Polymerization of β-monosubstituted-β-propiolactones using trialkylaluminum-water catalytic systems and polymer characterization. *Macromolecules* **1988,** *21,* 2657-2668.
154. Jaimes, C.; Arcana, M.; Brethon, A.; Mathieu, A.; Schue, F.; Desimone, J., Structure and morphology of poly([R,S]-*β*-butyrolactone) synthesized from aluminoxane catalyst. *Eur. Polym. J.* **1998,** *34,* 175-186.
155. Wu, B.; Lenz, R. W., Stereoregular Polymerization of [R,S]-3-Butyrolactone Catalyzed by Alumoxane− Monomer Adducts. *Macromolecules* **1998,** *31,* 3473-3477.
156. Le Borgne, A.; Spassky, N., Stereoelective polymerization of β-butyrolactone. *Polymer* **1989,** *30,* 2312-2319.
157. Zintl, M.; Molnar, F.; Urban, T.; Bernhart, V.; Preishuber-Pflugl, P.; Rieger, B., Variably isotactic poly(hydroxybutyrate) from racemic β-butyrolactone: microstructure control by achiral chromium(III) salophen complexes. *Angew. Chem. Int. Ed.* **2008,** *47,* 3458-3460.

158. Reichardt, R.; Vagin, S.; Reithmeier, R.; Ott, A. K.; Rieger, B., Factors Influencing the Ring-Opening Polymerization of Racemic β-Butyrolactone Using CrIII(salphen). *Macromolecules* **2010,** *43*, 9311-9317.

159. Vagin, S.; Winnacker, M.; Kronast, A.; Altenbuchner, P. T.; Deglmann, P.; Sinkel, C.; Loos, R.; Rieger, B., New Insights into the Ring-Opening Polymerization of β-Butyrolactone Catalyzed by Chromium(III) Salphen Complexes. *ChemCatChem* **2015,** *7*, 3963-3971.

160. Vagin, S. I.; Reichardt, R.; Klaus, S.; Rieger, B., Conformationally flexible dimeric salphen complexes for bifunctional catalysis. *J. Am. Chem. Soc.* **2010,** *132*, 14367-14369.

161. Ajellal, N.; Durieux, G.; Delevoye, L.; Tricot, G.; Dujardin, C.; Thomas, C. M.; Gauvin, R. M., Polymerization of racemic β-butyrolactone using supported catalysts: a simple access to isotactic polymers. *Chem. Commun.* **2010,** *46*, 1032-1034.

162. Zhuo, Z.; Zhang, C.; Luo, Y.; Wang, Y.; Yao, Y.; Yuan, D.; Cui, D., Stereo-selectivity switchable ROP of rac-β-butyrolactone initiated by salan-ligated rare-earth metal amide complexes: the key role of the substituents on ligand frameworks. *Chem. Commun.* **2018,** *54*, 11998-12001.

163. Dong, X.; Brown, A. M.; Woodside, A. J.; Robinson, J. R., N-Oxides amplify catalyst reactivity and isoselectivity in the ring-opening polymerization of rac-β-butyrolactone. *Chem. Commun.* **2022,** *58*, 2854-2857.

164. Stirling, E.; Champouret, Y.; Visseaux, M., Catalytic metal-based systems for controlled statistical copolymerisation of lactide with a lactone. *Polym. Chem.* **2018,** *9*, 2517-2531.

165. Cameron, D. J.; Shaver, M. P., Aliphatic polyester polymer stars: synthesis, properties and applications in biomedicine and nanotechnology. *Chem. Soc. Rev.* **2011,** *40*, 1761-1776.

166. Södergård, A.; Stolt, M., Properties of lactic acid based polymers and their correlation with composition. *Prog. Polym. Sci.* **2002,** *27*, 1123-1163.

167. Tang, X.; Shi, C.; Zhang, Z.; Chen, E. Y. X., Toughening Biodegradable Isotactic Poly(3-hydroxybutyrate) via Stereoselective Copolymerization of a Diolide and Lactones. *Macromolecules* **2021,** *54*, 9401-9409.

168. Cohn, D.; Salomon, A. H., Designing biodegradable multiblock PCL/PLA thermoplastic elastomers. *Biomaterials* **2005,** *26*, 2297-2305.

169. Hillmyer, M. A.; Tolman, W. B., Aliphatic polyester block polymers: renewable, degradable, and sustainable. *Acc. Chem. Res.* **2014,** *47*, 2390-2396.

170. Badi, N.; Lutz, J. F., Sequence control in polymer synthesis. *Chem. Soc. Rev.* **2009,** *38*, 3383-3390.

171. Guillaume, S. M.; Kirillov, E.; Sarazin, Y.; Carpentier, J. F., Beyond stereoselectivity, switchable catalysis: some of the last frontier challenges in ring-opening polymerization of cyclic esters. *Chem. Eur. J.* **2015,** *21*, 7988-8003.

172. Teator, A. J.; Lastovickova, D. N.; Bielawski, C. W., Switchable Polymerization Catalysts. *Chem. Rev.* **2016,** *116*, 1969-1992.

173. Hu, C.; Pang, X.; Chen, X., Self-Switchable Polymerization: A Smart Approach to Sequence-Controlled Degradable Copolymers. *Macromolecules* **2022,** *55*, 1879-1893.

174. Jaffredo, C. G.; Carpentier, J.-F.; Guillaume, S. M., Poly(hydroxyalkanoate) Block or Random Copolymers of *β*-Butyrolactone and Benzyl *β*-Malolactone: A Matter of Catalytic Tuning. *Macromolecules* **2013,** *46*, 6765-6776.

175. Barouti, G.; Jarnouen, K.; Cammas-Marion, S.; Loyer, P.; Guillaume, S. M., Polyhydroxyalkanoate-based amphiphilic diblock copolymers as original biocompatible nanovectors. *Polym. Chem.* **2015,** *6*, 5414-5429.

176. Aluthge, D. C.; Xu, C.; Othman, N.; Noroozi, N.; Hatzikiriakos, S. G.; Mehrkhodavandi, P., PLA–PHB–PLA Triblock Copolymers: Synthesis by Sequential Addition and Investigation of Mechanical and Rheological Properties. *Macromolecules* **2013,** *46*, 3965-3974.

177. Yu, I.; Ebrahimi, T.; Hatzikiriakos, S. G.; Mehrkhodavandi, P., Star-shaped PHB-PLA block copolymers: immortal polymerization with dinuclear indium catalysts. *Dalton Trans.* **2015,** *44*, 14248-14254.

178. Kiriratnikom, J.; Robert, C.; Guerineau, V.; Venditto, V.; Thomas, C. M., Stereoselective Ring-Opening (Co)polymerization of *β*-Butyrolactone and *ε*-Decalactone Using an Yttrium Bis(phenolate) Catalytic System. *Front. Chem.* **2019,** *7*, 301.

179. Adams, F.; Pehl, T. M.; Kränzlein, M.; Kernbichl, S. A.; Kang, J.-J.; Papadakis, C. M.; Rieger, B., (Co)polymerization of (−)-menthide and β-butyrolactone with yttrium-bis(phenolates): tuning material properties of sustainable polyesters. *Polym. Chem.* **2020,** *11*, 4426-4437.

180. Jeffery, B. J.; Whitelaw, E. L.; Garcia-Vivo, D.; Stewart, J. A.; Mahon, M. F.; Davidson, M. G.; Jones, M. D., Group 4 initiators for the stereoselective ROP of rac-β-butyrolactone and its copolymerization with rac-lactide. *Chem. Commun.* **2011,** *47*, 12328-12330.

181. Walther, P.; Naumann, S., N-Heterocyclic Olefin-Based (Co)polymerization of a Challenging Monomer: Homopolymerization of *ω*-Pentadecalactone and Its Copolymers with *γ*-Butyrolactone, *δ*-Valerolactone, and *ε*-Caprolactone. *Macromolecules* **2017,** *50*, 8406-8416.

182. Doerr, A. M.; Burroughs, J. M.; Gitter, S. R.; Yang, X.; Boydston, A. J.; Long, B. K., Advances in Polymerizations Modulated by External Stimuli. *ACS Catal.* **2020,** *10*, 14457-14515.

183. Deacy, A. C.; Gregory, G. L.; Sulley, G. S.; Chen, T. T. D.; Williams, C. K., Sequence Control from Mixtures: Switchable Polymerization Catalysis and Future Materials Applications. *J. Am. Chem. Soc.* **2021,** *143*, 10021-10040.

184. Jeske, R. C.; Rowley, J. M.; Coates, G. W., Pre-rate-determining selectivity in the terpolymerization of epoxides, cyclic anhydrides, and CO_2: a one-step route to diblock copolymers. *Angew. Chem. Int. Ed.* **2008,** *47*, 6041-6044.

185. Romain, D. C.; Williams, C. K., Chemoselective polymerization control: from mixed-monomer feedstock to copolymers. *Angew. Chem. Int. Ed.* **2014,** *53*, 1607-1610.

186. Huang, Y.; Hu, C.; Zhou, Y.; Duan, R.; Sun, Z.; Wan, P.; Xiao, C.; Pang, X.; Chen, X., Monomer Controlled Switchable Copolymerization: A Feasible Route for the Functionalization of Poly(lactide). *Angew. Chem. Int. Ed.* **2021,** *60*, 9274-9278.

187. Li, C.; Dang, Y.-F.; Wang, B.; Pan, L.; Li, Y.-S., Constructing ABA- and ABCBA-Type Multiblock Copolyesters with Structural Diversity by Organocatalytic Self-Switchable Copolymerization. *Macromolecules* **2021,** *54*, 6171-6181.

188. Raman, S. K.; Raja, R.; Arnold, P. L.; Davidson, M. G.; Williams, C. K., Waste not, want not: CO_2 (re)cycling into block polymers. *Chem. Commun.* **2019,** *55*, 7315-7318.

189. Tang, J.; Li, M.; Wang, X.; Tao, Y., Switchable Polymerization Organocatalysis: From Monomer Mixtures to Block Copolymers. *Angew. Chem. Int. Ed.* **2022,** *61*, e202115465.

190. Yang, Z.; Hu, C.; Cui, F.; Pang, X.; Huang, Y.; Zhou, Y.; Chen, X., One-Pot Precision Synthesis of AB, ABA and ABC Block Copolymers via Switchable Catalysis. *Angew. Chem. Int. Ed.* **2022,** *61*, e202117533.

191. Ji, H. Y.; Wang, B.; Pan, L.; Li, Y. S., One-Step Access to Sequence-Controlled Block Copolymers by Self-Switchable Organocatalytic Multicomponent Polymerization. *Angew. Chem. Int. Ed.* **2018,** *57*, 16888-16892.

192. Liu, S.; Bai, T.; Ni, K.; Chen, Y.; Zhao, J.; Ling, J.; Ye, X.; Zhang, G., Biased Lewis Pairs: A General Catalytic Approach to Ether-Ester Block Copolymers with Unlimited Ordering of Sequences. *Angew. Chem. Int. Ed.* **2019,** *58*, 15478-15487.

193. Zhao, Y.; Wang, Y.; Zhou, X.; Xue, Z.; Wang, X.; Xie, X.; Poli, R., Oxygen-Triggered Switchable Polymerization for the One-Pot Synthesis of CO_2-Based Block Copolymers from Monomer Mixtures. *Angew. Chem. Int. Ed.* **2019,** *58*, 14311-14318.

194. Stosser, T.; Sulley, G. S.; Gregory, G. L.; Williams, C. K., Easy access to oxygenated block polymers via switchable catalysis. *Nat. Commun.* **2019,** *10*, 2668.

195. Stosser, T.; Mulryan, D.; Williams, C. K., Switch Catalysis To Deliver Multi-Block Polyesters from Mixtures of Propene Oxide, Lactide, and Phthalic Anhydride. *Angew. Chem. Int. Ed.* **2018,** *57*, 16893-16897.

196. Hu, C.; Duan, R.; Yang, S.; Pang, X.; Chen, X., CO_2 Controlled Catalysis: Switchable Homopolymerization and Copolymerization. *Macromolecules* **2018,** *51*, 4699-4704.

197.   Zhu, Y.; Romain, C.; Williams, C. K., Selective polymerization catalysis: controlling the metal chain end group to prepare block copolyesters. *J. Am. Chem. Soc.* **2015,** *137*, 12179-12182.

198.   Romain, C.; Zhu, Y.; Dingwall, P.; Paul, S.; Rzepa, H. S.; Buchard, A.; Williams, C. K., Chemoselective Polymerizations from Mixtures of Epoxide, Lactone, Anhydride, and Carbon Dioxide. *J. Am. Chem. Soc.* **2016,** *138*, 4120-4131.

199.   Sulley, G. S.; Gregory, G. L.; Chen, T. T. D.; Pena Carrodeguas, L.; Trott, G.; Santmarti, A.; Lee, K. Y.; Terrill, N. J.; Williams, C. K., Switchable catalysis improves the properties of CO_2-derived polymers: poly(cyclohexene carbonate-*b*-ε-decalactone-*b*-cyclohexene carbonate) adhesives, elastomers, and toughened plastics. *J. Am. Chem. Soc.* **2020,** *142*, 4367-4378.

200.   Leibfarth, F. A.; Mattson, K. M.; Fors, B. P.; Collins, H. A.; Hawker, C. J., External regulation of controlled polymerizations. *Angew. Chem. Int. Ed.* **2013,** *52*, 199-210.

201.   Chen, C., Redox-Controlled Polymerization and Copolymerization. *ACS Catal.* **2018,** *8*, 5506-5514.

202.   Wei, J.; Diaconescu, P. L., Redox-Switchable Ring-Opening Polymerization with Ferrocene Derivatives. *Acc. Chem. Res.* **2019,** *52*, 415-424.

203.   Gregson, C. K.; Gibson, V. C.; Long, N. J.; Marshall, E. L.; Oxford, P. J.; White, A. J., Redox control within single-site polymerization catalysts. *J. Am. Chem. Soc.* **2006,** *128*, 7410-7411.

204.   Broderick, E. M.; Guo, N.; Vogel, C. S.; Xu, C.; Sutter, J.; Miller, J. T.; Meyer, K.; Mehrkhodavandi, P.; Diaconescu, P. L., Redox control of a ring-opening polymerization catalyst. *J. Am. Chem. Soc.* **2011,** *133*, 9278-9281.

205.   Broderick, E. M.; Guo, N.; Wu, T.; Vogel, C. S.; Xu, C.; Sutter, J.; Miller, J. T.; Meyer, K.; Cantat, T.; Diaconescu, P. L., Redox control of a polymerization catalyst by changing the oxidation state of the metal center. *Chem. Commun.* **2011,** *47*, 9897-9899.

206.   Biernesser, A. B.; Li, B.; Byers, J. A., Redox-controlled polymerization of lactide catalyzed by bis(imino)pyridine iron bis(alkoxide) complexes. *J. Am. Chem. Soc.* **2013,** *135*, 16553-16560.

207.   de Vries, F.; Otten, E., Reversible On/Off Switching of Lactide Cyclopolymerization with a Redox-Active Formazanate Ligand. *ACS Catal.* **2022,** *12*, 4125-4130.

208.   Qi, M.; Dong, Q.; Wang, D.; Byers, J. A., Electrochemically Switchable Ring-Opening Polymerization of Lactide and Cyclohexene Oxide. *J .Am. Chem. Soc.* **2018,** *140*, 5686-5690.

209.   Hern, Z. C.; Quan, S. M.; Dai, R.; Lai, A.; Wang, Y.; Liu, C.; Diaconescu, P. L., ABC and ABAB Block Copolymers by Electrochemically Controlled Ring-Opening Polymerization. *J. Am. Chem. Soc.* **2021,** *143*, 19802-19808.

210.   Wang, X.; Thevenon, A.; Brosmer, J. L.; Yu, I.; Khan, S. I.; Mehrkhodavandi, P.; Diaconescu, P. L., Redox control of group 4 metal ring-opening polymerization activity toward L-lactide and ε-caprolactone. *J. Am. Chem. Soc.* **2014,** *136*, 11264-11267.

211.   Hong, M.; Chen, E. Y. X., Chemically recyclable polymers: a circular economy approach to sustainability. *Green Chem.* **2017,** *19*, 3692-3706.

212.   Lu, X. B.; Liu, Y.; Zhou, H., Learning Nature: Recyclable Monomers and Polymers. *Chem. Eur. J.* **2018,** *24*, 11255-11266.

213.   Martello, M. T.; Burns, A.; Hillmyer, M., Bulk Ring-Opening Transesterification Polymerization of the Renewable δ-Decalactone Using an Organocatalyst. *ACS Macro Lett.* **2012,** *1*, 131-135.

214.   Nishida, H.; Yamashita, M.; Endo, T.; Tokiwa, Y., Equilibrium polymerization behavior of 1,4-dioxan-2-one in bulk. *Macromolecules* **2000,** *33*, 6982-6986.

215.   Shi, C.; Li, Z.-C.; Caporaso, L.; Cavallo, L.; Falivene, L.; Chen, E. Y. X., Hybrid monomer design for unifying conflicting polymerizability, recyclability, and performance properties. *Chem* **2021,** *7*, 670-685.

216.   Yuan, J.; Xiong, W.; Zhou, X.; Zhang, Y.; Shi, D.; Li, Z.; Lu, H., 4-Hydroxyproline-Derived Sustainable Polythioesters: Controlled Ring-Opening Polymerization, Complete Recyclability, and Facile Functionalization. *J. Am. Chem. Soc.* **2019,** *141*, 4928-4935.

217. Shi, C.; McGraw, M. L.; Li, Z.-C.; Cavallo, L.; Falivene, L.; Chen, E. Y.-X., High-performance pan-tactic polythioesters with intrinsic crystallinity and chemical recyclability. *Sci. Adv.* **2020,** *6*, eabc0495.

218. Xiong, W.; Chang, W.; Shi, D.; Yang, L.; Tian, Z.; Wang, H.; Zhang, Z.; Zhou, X.; Chen, E.-Q.; Lu, H., Geminal Dimethyl Substitution Enables Controlled Polymerization of Penicillamine-Derived β-Thiolactones and Reversed Depolymerization. *Chem* **2020,** *6*, 1831-1843.

219. MacDonald, J. P.; Shaver, M. P., An aromatic/aliphatic polyester prepared via ring-opening polymerisation and its remarkably selective and cyclable depolymerisation to monomer. *Polym. Chem.* **2016,** *7*, 553-559.

220. Lizundia, E.; Makwana, V. A.; Larrañaga, A.; Vilas, J. L.; Shaver, M. P., Thermal, structural and degradation properties of an aromatic–aliphatic polyester built through ring-opening polymerisation. *Polym. Chem.* **2017,** *8*, 3530-3538.

221. Li, L.-G.; Wang, Q.-Y.; Zheng, Q.-Y.; Du, F.-S.; Li, Z.-C., Tough and Thermally Recyclable Semiaromatic Polyesters by Ring-Opening Polymerization of Benzo-thia-caprolactones. *Macromolecules* **2021,** *54*, 6745-6752.

222. Tu, Y. M.; Wang, X. M.; Yang, X.; Fan, H. Z.; Gong, F. L.; Cai, Z.; Zhu, J. B., Biobased High-Performance Aromatic-Aliphatic Polyesters with Complete Recyclability. *J. Am. Chem. Soc.* **2021,** *143*, 20591-20597.

223. Fan, H. Z.; Yang, X.; Chen, J. H.; Tu, Y. M.; Cai, Z.; Zhu, J. B., Advancing the Development of Recyclable Aromatic Polyesters by Functionalization and Stereocomplexation. *Angew. Chem. Int. Ed.* **2022,** *61*, e202117639.

224. Hall Jr, H., Polymerization and ring strain in bridged bicyclic compounds. *J. Am. Chem. Soc.* **1958,** *80*, 6412-6420.

225. Hall Jr, H., Mechanisms of Hydrolysis of Several Atom-Bridged Bicyclic Anhydrides, N-Methylimides, and Lactones. *J. Org. Chem.* **1963,** *28*, 2027-2029.

226. Ceccarelli, G.; Andruzzi, F.; Paci, M., Nmr spectroscopy of polyesters from bridged bicyclic lactones. *Polymer* **1979,** *20*, 605-610.

227. Zhou, T.; Guo, Y.-T.; Du, F.-S.; Li, Z.-C., Ring-opening Polymerization of 2-Oxabicyclo[2.2.2]octan-3-one and the Influence of Stereochemistry on the Thermal Properties of the Polyesters. *Chin. J. Polym. Sci.* **2022,** *40*, 1173-1182.

228. Fahnhorst, G. W.; Hoye, T. R., A Carbomethoxylated Polyvalerolactone from Malic Acid: Synthesis and Divergent Chemical Recycling. *ACS Macro Lett.* **2018,** *7*, 143-147.

229. Schneiderman, D. K.; Vanderlaan, M. E.; Mannion, A. M.; Panthani, T. R.; Batiste, D. C.; Wang, J. Z.; Bates, F. S.; Macosko, C. W.; Hillmyer, M. A., Chemically Recyclable Biobased Polyurethanes. *ACS Macro Lett.* **2016,** *5*, 515-518.

230. Li, C.; Wang, L.; Yan, Q.; Liu, F.; Shen, Y.; Li, Z., Rapid and Controlled Polymerization of Bio-sourced δ-Caprolactone toward Fully Recyclable Polyesters and Thermoplastic Elastomers. *Angew. Chem. Int. Ed.* **2022,** *61*, e202201407.

231. Aluthge, D. C.; Patrick, B. O.; Mehrkhodavandi, P., A highly active and site selective indium catalyst for lactide polymerization. *Chem. Commun.* **2013,** *49*, 4295-4297.

232. Pessoa, J. C.; Correia, I., Salan vs. salen metal complexes in catalysis and medicinal applications: Virtues and pitfalls. *Coord. Chem. Rev.* **2019,** *388*, 227-247.

233. Matsumoto, K.; Saito, B.; Katsuki, T., Asymmetric catalysis of metal complexes with non-planar ONNO ligands: salen, salalen and salan. *Chem. Commun.* **2007**, 3619-3627.

234. Gesslbauer, S.; Cheek, H.; White, A. J. P.; Romain, C., Highly active aluminium catalysts for room temperature ring-opening polymerisation of rac-lactide. *Dalton Trans.* **2018,** *47*, 10410-10414.

235. Marlier, E. E.; Macaranas, J. A.; Marell, D. J.; Dunbar, C. R.; Johnson, M. A.; DePorre, Y.; Miranda, M. O.; Neisen, B. D.; Cramer, C. J.; Hillmyer, M. A.; Tolman, W. B., Mechanistic Studies of ε-Caprolactone Polymerization by (salen)AlOR Complexes and a Predictive Model for Cyclic Ester Polymerizations. *ACS Catal.* **2016,** *6*, 1215-1224.

236. Beament, J.; Mahon, M. F.; Buchard, A.; Jones, M. D., Salan group 13 complexes – structural study and lactide polymerisation. *New J. Chem.* **2017,** *41*, 2198-2203.

237. Bruckmoser, J.; Rieger, B., Simple and Rapid Access toward AB, BAB and ABAB Block Copolyesters from One-Pot Monomer Mixtures Using an Indium Catalyst. *ACS Macro Lett.* **2022,** *11*, 1067-1072.

238. Zhang, Z.; Xu, X.; Li, W.; Yao, Y.; Zhang, Y.; Shen, Q.; Luo, Y., Synthesis of rare-earth metal amides bearing an imidazolidine-bridged bis(phenolato) ligand and their application in the polymerization of L-lactide. *Inorg. Chem.* **2009,** *48*, 5715-5724.

239. Luo, Y.; Li, W.; Lin, D.; Yao, Y.; Zhang, Y.; Shen, Q., Lanthanide Alkyl Complexes Supported by a Piperazidine-Bridged Bis(phenolato) Ligand: Synthesis, Structural Characterization, and Catalysis for the Polymerization of L-Lactide and rac-Lactide. *Organometallics* **2010,** *29*, 3507-3514.

240. Sinenkov, M. A.; Fukin, G. K.; Cherkasov, A. V.; Ajellal, N.; Roisnel, T.; Kerton, F. M.; Carpentier, J.-F.; Trifonov, A. A., Neodymium borohydride complexes supported by diamino-bis(phenoxide) ligands: diversity of synthetic and structural chemistry, and catalytic activity in ring-opening polymerization of cyclic esters. *New J. Chem.* **2011,** *35*, 204-212.

241. Li, W.; Zhang, Z.; Yao, Y.; Zhang, Y.; Shen, Q., Control of Conformations of Piperazidine-Bridged Bis(phenolato) Groups: Syntheses and Structures of Bimetallic and Monometallic Lanthanide Amides and Their Application in the Polymerization of Lactides. *Organometallics* **2012,** *31*, 3499-3511.

242. Pappalardo, D.; Bruno, M.; Lamberti, M.; Mazzeo, M.; Pellecchia, C., Ring-opening polymerization of ε-caprolactone and lactides promoted by salan- and salen-type yttrium amido complexes. *J. Mol. Catal. A: Chem.* **2013,** *379*, 303-308.

243. Pappalardo, D.; Bruno, M.; Lamberti, M.; Pellecchia, C., Ring-Opening Polymerization of Racemic β-Butyrolactone Promoted by Salan- and Salen-Type Yttrium Amido Complexes. *Macromol. Chem. Phys.* **2013,** *214*, 1965-1972.

244. Fagerland, J.; Finne-Wistrand, A.; Pappalardo, D., Modulating the thermal properties of poly(hydroxybutyrate) by the copolymerization of *rac-β*-butyrolactone with lactide. *New J. Chem.* **2016,** *40*, 7671-7679.

245. Beament, J.; Kociok-Kohn, G.; Jones, M. D.; Buchard, A., Bipyrrolidine salan alkoxide complexes of lanthanides: synthesis, characterisation, activity in the polymerisation of lactide and mechanistic investigation by DOSY NMR. *Dalton Trans.* **2018,** *47*, 9164-9172.

246. Liu, X.; Hua, X.; Cui, D., Copolymerization of Lactide and Cyclic Carbonate via Highly Stereoselective Catalysts To Modulate Copolymer Sequences. *Macromolecules* **2018,** *51*, 930-937.

247. Ouyang, H.; Yuan, D.; Nie, K.; Zhang, Y.; Yao, Y.; Cui, D., Synthesis and Characterization of Dinuclear Salan Rare-Earth Metal Complexes and Their Application in the Homo- and Copolymerization of Cyclic Esters. *Inorg. Chem.* **2018,** *57*, 9028-9038.

248. Zeng, T.; Qian, Q.; Zhao, B.; Yuan, D.; Yao, Y.; Shen, Q., Synthesis and characterization of rare-earth metal guanidinates stabilized by amine-bridged bis(phenolate) ligands and their application in the controlled polymerization of rac-lactide and rac-β-butyrolactone. *RSC Adv.* **2015,** *5*, 53161-53171.

249. Kerton, F. M.; Whitwood, A. C.; Willans, C. E., A high-throughput approach to lanthanide complexes and their rapid screening in the ring opening polymerisation of caprolactone. *Dalton Trans.* **2004,** 2237-2244.

250. Tani, K.; Stoltz, B. M., Synthesis and structural analysis of 2-quinuclidonium tetrafluoroborate. *Nature* **2006,** *441*, 731-734.

251. Bruckmoser, J.; Remke, S.; Rieger, B., Ring-Opening Polymerization of a Bicyclic Lactone: Polyesters Derived from Norcamphor with Complete Chemical Recyclability. *ACS Macro Lett.* **2022,** *11*, 1162-1166.